Eleonora Widzyk-Capehart ·
Asieh Hekmat · Raj Singhal *Editors*

Proceedings of the 27th International Symposium on Mine Planning and Equipment Selection— MPES 2018

Proceedings of the 27th International Symposium on Mine Planning and Equipment Selection—MPES 2018

Eleonora Widzyk-Capehart ·
Asieh Hekmat · Raj Singhal
Editors

Proceedings of the 27th International Symposium on Mine Planning and Equipment Selection—MPES 2018

Editors
Eleonora Widzyk-Capehart
AMTC
University of Chile
Santiago, Región Metropolitana, Chile

Asieh Hekmat
DIMET
University of Concepción
Concepción, VIII—Concepción, Chile

Raj Singhal
International Journal of Mining,
Reclamation and Environment
Calgary, AB, Canada

Organizing Committee

International Chairs

Dr. Raj Singhal, Canada
Dr. Uday Kumar, Sweden

MPES 2018 Chairs

Dr. Eleonora Widzyk-Capehart (University of Chile)
Dr. Asieh Hekmat (University of Concepción)

Technical Program Committee Chair

Dr. Nelson Morales

Co-chairs

Prof. Radoslaw Zimroz, Poland
Prof. Atac Bascetin, Turkey
Prof. Hideki Shimada, Japan
Prof. Morteza Osanloo, Iran
Prof. Cuthbert Musingwini, South Africa
Prof. Carsten Drebenstedt, Germany

International Organizing Committee

Prof. Ernest Baafi, Australia
Dr. Ian S. Lowndes, England
Prof. Sukumar Bandopadhyay, USA
Dr. Z. Bzowski, Poland
Prof. Carmen Neculita, Canada
Prof. Josee Duchesne, Canada
Dr. Lidia Gawlik, Poland
Prof. Ge Hao, China
Prof. Liu Mingju, China
Prof. Giorgio Massacci, Italy
Prof. Toyoharu Nawa, Japan
Dr. Antonio Nieto, USA
Dr. Bernadette O'Regan, Ireland
Prof. Kostas Fytas, Canada
Ms. M. Singhal, Canada
Prof. Svetlana Yefremova, Kazakhstan
Prof. A. B. Szwilski, USA
Andrea Brickey, USA
Prof. Bekir Genc, South Africa
Dr. Steven Rupprecht, South Africa
Dr. Enrique Jélvez, Chile
Dr. Alessandro Navarra, Chile
Prof. Xavier Emery, Chile
Prof. Edyta Brzychczy, Poland
Prof. Mauricio L. Torem, Brazil
Prof. Vladimir Kebo, Czech Republic
Prof. Gennady G. Pivnyak, Ukraine
Dr. Valentina Dentoni, Italy
Prof. Takashi Sasaoka, Japan
Dr. Gento Mogi, Japan
Dr. Mohan Yellishetty, Australia
Ms. Dr. Yanhua Fu, China
Prof. Celal Karpuz, Turkey
Dr. Joerg Benndorf, Netherlands
Prof. George N. Panagiotou, Greece
Prof. Nick Vayenas, Canada
Prof. Marilena Cardu, Italy
Dr. Sunniva Haugen, Norway–Sweden
Prof. Monika Hardygora, Poland
Prof. Rodrigo Pascual, Chile
Dr. Luis Garcia, Brazil
Dr. Vidal Torres, Brazil

Prof. Hani Mitri, Canada
Prof. Javier Ruiz-del-Solar, Chile
Prof. Marek Cała, Poland
Prof. Piotr Czaja, Poland
Dr. Eduardo Moreno, Chile
Dr. Marcos Goycoolea, Chile

Technical Review Committee

Foreword

Dr. Raj Singal   Prof. Uday Kumar

The International Symposium on Mine Planning and Equipment Selection (MPES) was started some 25 years ago. Since then, it has been held regularly becoming an internationally recognized event committed to technology transfer. It has been held in Turkey, Greece, Canada, Kazakhstan, Australia, South Africa, Czech Republic, Brazil, India, Australia, China, Ukraine, Poland, Germany, Sweden, and Italy. In 2018, MPES is being held in Chile for the first time.

The basic aim of MPES 2018 is to contribute to the development of highly productive methods and technologies for the various segments of the mining and mineral processing industries. Important themes of the 2018 symposium are: Economic and Technical Feasibility Studies, Reserve Estimation; Design, Planning and Optimization of Surface and Underground Mines; Planning under Uncertainty; Mine Development; Transition from Surface to Underground Mining; Mine Automation and Information Technology; Internet of Things in Mining; Drilling, Blasting, Tunneling and Excavation Engineering; Innovative Materials Handling Systems and Equipment; Mining Equipment Selection; Maintenance and Production Management for Mines and Mining Systems; Rock Mechanics and

Geotechnical Applications; and Research and Development to Improve Health, Safety and Productivity in Mines.

MPES 2018 derives its strength from the coalition of various worldwide institutions. It is organized by the Advanced Mining Technology Center, University of Chile and University of Concepción, Chile in collaboration with the Department of Mining, Metallurgical and Materials Engineering, Universite Laval; China University of Mining and Technology, Beijing; The National Technical University of Athens, Greece (NTUA); Dipartimento di Geoingegneria e Tecnologie Ambientali, Universita degli Studi di Cagliari, Italy; Western Australian School of Mines, Curtin University of Technology, Australia; International Journal of Mining, Reclamation and Environment; American Society for Mining and Reclamation; School of Mining and Petroleum Engineering, University of Alberta, Canada; Mining Engineering Department, Lulea University of Technology, Sweden; Faculty of Mining and Geology, VSB—Technical University, Ostrava, Czech Republic; Hokkaido University, Mineral Resources Engineering Department, Japan; Faculty Geoengineering, Mining and Geology, Wroclaw University of Technology, Poland; Department of Mining, Metals and Materials, McGill University; DIGET-Politechnico di Torino, Italy; School of Chemical, Environmental and Mining Engineering University of Nottingham, UK; Middle East Technical University Mining Engineering Department, Turkey; SASE, and Monash University Australia and Kyushu University, Fukuoka, Japan, and a few others.

The organization and success of such a symposium is due mainly to the tireless efforts of many individuals, the authors included. All members of the organizing committees and conference chairpersons have contributed greatly. The support of our plenary session speakers, invited speakers, and co-chairs is gratefully acknowledged. In addition, recognition is accorded to my co-editors and Chair Persons of this symposium, Dr. Eleonora Widzyk-Capehart and Dr. Asieh Hekmat, who together with their local organizing committee made MPES 2018 a success. I also wish to acknowledge the contribution of Mohini Singhal (my wife) who has been involved with MPES since its inception. She as a committee member of MPES organization and is an associate editor of the International Journal of Mining, Reclamation and Environment. She shares my workload and maintains the continuity of our work in my absence. We both are committed to make each symposium a successful one.

I, as the International Chair and Founder of this series of symposia would like to recognize the special contribution of Dr. Eleonora Widzyk-Capehart and Nelson Morales. Thanks are due to Springer whose editors have worked closely with us. They published the proceedings of our MPES 2013 held in Germany. We hopefully will work with them for our other symposia.

We are grateful to Dr. Patricio Aceituno, Dean, Facultad de Ciencias Fisicas y Matematicas, Universidad de Chile and Dr. Luis Moran T. Dean, Facultad de Ingenieria, Universidad de Concepción for accepting to hold this symposium under their tutelage.

This symposium provides a forum for the presentation, discussion, and debate of state-of-the-art and emerging technologies in the field of mining. The authors from over 20 countries with backgrounds in computer sciences, mining engineering, research, technology, and management representing government, industry, and academia concerned with mining and mineral production have contributed to these proceedings. The contents of this volume of proceedings will be of interest to engineers, scientists, consultants, and government personnel, who are responsible for dealing with the development and application of innovative technologies to the minerals industries.

Calgary, Canada   Dr. Raj Singhal
Luleå, Sweden   Prof. Uday Kumar
Chairs, International Organizing Committee

Preface

Dr. Eleonora Widzyk-Capehart   Dr. Asieh Hekmat

During most of Chile's history, from 1500 to the present, mining has been an important economic activity: sixteenth-century mining was oriented toward the exploitation of gold placer deposits using encomienda labour; after a period of decline in the seventeenth century, mining resurged in the eighteenth and early nineteenth century this time revolving chiefly around silver and, in the first half of the twentieth century, copper mining has come to the forefront.

The mining sector plays an important role in the Chilean economy: Chile is world's #1 copper, #2 lithium, and #3 molybdenum producer, making mining an economic engine of Chile, accounting for approximately 10% of GDP and 50% of Chilean exports. In 2017, Chile produced 5.3 million tons of copper, which represented 32% of world production. Chile's copper production comes primarily from porphyry copper deposits, which are rich in molybdenum, gold, and silver by-products. The massive Escondida mine, known as the world's largest copper mine, accounts for 5% of total global copper mine production.

In the midst of rising copper prices and predictions of an upcoming deficit in the market, Chile is still considered a primary target for exploration and the country expects $65 million in mining-related investment over the course of the next decade, with 90% of that dedicated to copper projects. Several new projects are expected to be exploration initiatives conducted by junior companies. With favorable jurisdiction, Chile has a long history of strong mining laws and being mining friendly, especially to foreign companies.

In this context, the 27th International Symposium on Mine Planning and Equipment Selection, MPES 2018, will provide opportunities for the scientists and the industry to share experiences and the latest advances in research and developments.

Contributions from MPES 2018 include economic and financial risk evaluations, methods, and technologies for design, planning, and optimization of surface and underground mines, mine development, equipment selection, drilling, blasting, tunneling and excavation engineering, maintenance and production management for mines and mining systems, rock mechanics and geotechnical applications, research, and development to improve health and safety in mines.

We present you with the *Proceedings of the 27th International Symposium on Mine Planning and Equipment Selection—MPES 2018*, from Santiago, Chile, which we hope would enable the holistic reflection and the practical application of "Mine planning and equipment selection" toward a sustainable future.

With Best Regards and Buena Suerte,

Chairs, MPES 2018 Organizing Committee

Santiago, Chile   Dr. Eleonora Widzyk-Capehart
Concepción, Chile   Dr. Asieh Hekmat

Acknowledgement

Contents

Lessons from Some Recent and Current Mine Planning Related Postgraduate Research Work at the University of the Witwatersrand

C. Musingwini

1 Introduction

The mine value chain is a series of interdependent stages starting from the exploration stage up to the closure and rehabilitation of a mining operation. Figure 1 is an illustration of the five commonly recognized stages comprising a mine value chain.

Mine planning, equipment and infrastructure maintenance, human resources, finance, engineering, and safety, health, environment and community are examples of service activities that are required to support the five broad stages [1]. Once exploration work has identified and delineated a mineral deposit to a point where Mineral Resources can be estimated and declared, mine design and planning are then undertaken to convert Mineral Resources to Mineral Reserves and set the basis for establishing a mining operation.

The South African Code for the Reporting of Exploration Results, Mineral Resources and Mineral Reserves (The SAMREC Code 2016) [2] defines a mine design as "*a framework of mining components and processes taking into account such aspects as mining methods used, access to the orebody, personnel and material handling, ventilation, water, power, and other technical requirements, such that mine planning can be undertaken*". The SAMREC Code 2016 [2] also defines mine planning as "*production planning and scheduling, within the mine design, taking into account such aspects as geological structures and mineralisation and associated infrastructure and other constraints*". Mine planning is intricately linked to valuation and optimization because a mine plan that is accepted for implementation must have been evaluated as being both technically and economically viable and robust through optimization. An optimized mine plan can be assumed to be a robust mine plan.

C. Musingwini (✉)
School of Mining Engineering, University of the Witwatersrand, Johannesburg, South Africa
e-mail: Cuthbert.Musingwini@wits.ac.za

| Exploration | Design & Planning | Construction | Production | Closure & Rehabilitation |

Fig. 1 The five broad stages comprising a generic mine value chain

Mine design and planning are critical to the mine value chain as they form the basis upon which performance targets are set. Therefore, mine plans should be adequately robust to ensure that actual performance can be as close as possible to planned outcomes both in the short and long term. However, this is often not the case as actual outcomes do not always align with planned targets, requiring reconciliation to be undertaken and plans to be adjusted accordingly. The non-achievement of performance targets has in recent years prompted financiers of mining projects to litigate against project proponents in some cases, claiming that they were misled into investing in projects that failed to deliver on promised outcomes. Newby et al. [3] mentioned such a case, where a shareholder class action lawsuit was filed against NovaGold over the Galore Creek copper-gold project in which costs had been revised to 127% of the initial estimates and the project was running 2½ years behind schedule. The failure to deliver actual outcomes that are close to or the same as planned targets is considered one of the top risks faced by the mining industry and requires mining companies to develop robust mine plans [4, 5]. This challenge emanates from the commonly used deterministic mine planning approached that fail to recognize that mining systems are stochastic in reality.

It is, therefore, necessary to have a paradigm shift from deterministic to stochastic mine planning. This requires more research to be undertaken on how to generate robust mine plans to improve confidence in achieving planned outcomes. Research findings from some of the mine planning related postgraduate research work that has recently been undertaken or is currently under way in the School of Mining Engineering at the University of the Witwatersrand are presented to share lessons that can be drawn towards closing the gap between planned and actual performance outcomes.

2 Examples of Recently Completed Research Work

Some of the recently completed postgraduate research work in the past 5 years in the School of Mining Engineering at the University of the Witwatersrand can be broadly classified into valuation aspects of mine planning and stochastic optimization approaches to mine planning. Examples of these completed research studies are summarized in the next sections.

2.1 Interfacing Valuation and Regular Financial Reporting

There exists some misalignment between the regular financial reporting done by mining companies and the valuation done at mine planning stages such as pre-feasibility study (PFS) and feasibility study stages. Valuation which is done during mine planning has a generally forward-looking performance perspective, while regular financial reporting which is done during the operational stage has a generally historical-looking performance perspective [6]. Regular reporting of financial performance is done in compliance with International Financial Reporting Standards (IFRS) or Generally Accepted Accounting Principles (GAAP) depending on the jurisdiction, while valuation is done following guidance from internationally recognized valuation codes such as the [6]:

– Code for the Technical Assessment and Valuation of Mineral and Petroleum Assets and Securities for Independent Expert Reports ("The VALMIN Code, 2015") which is used in the Australasia region.
– Standards and Guidelines for Valuation of Mineral Properties ("The CIMVAL Code, 2003") which is used in Canada.
– South African Code for the Reporting of Mineral Asset Valuation ("The SAMVAL Code, 2016") which is used in South Africa.
– Polish Code for the Valuation of Mineral Assets ("The POLVAL Code, 2008") which is used in Poland.
– Securities and Exchange Commission (SEC) Industry Guide 7 published in 1990 and used in the United States of America (US).

The misalignment between financial reporting and valuation contributes to the discrepancies that exist between planned and actual financial performance. Njowa and Musingwini [6] presented a framework to interface valuation and financial reporting in mine planning. The basic framework for interfacing valuation and regular financial reporting is illustrated in Fig. 2. The lesson that can be drawn from the research work is that by applying this framework it is possible to holistically model the valuation process by utilizing linkages from exploration results, through mineral project evaluation to financial reporting. In this way, it is possible to reduce the gap between regular financial reporting during the operational stage and valuation done during mine planning.

2.2 Stochastic Framework for Open-Pit to Underground Transition

The transition from open-pit mining to underground mining is often modeled as a deterministic process. However, deterministic approaches are inadequate for analyzing the open-pit to underground transition due to the dynamic nature of the transition indicators [7]. Opoku and Musingwini [7] presented a stochastic open-pit to under-
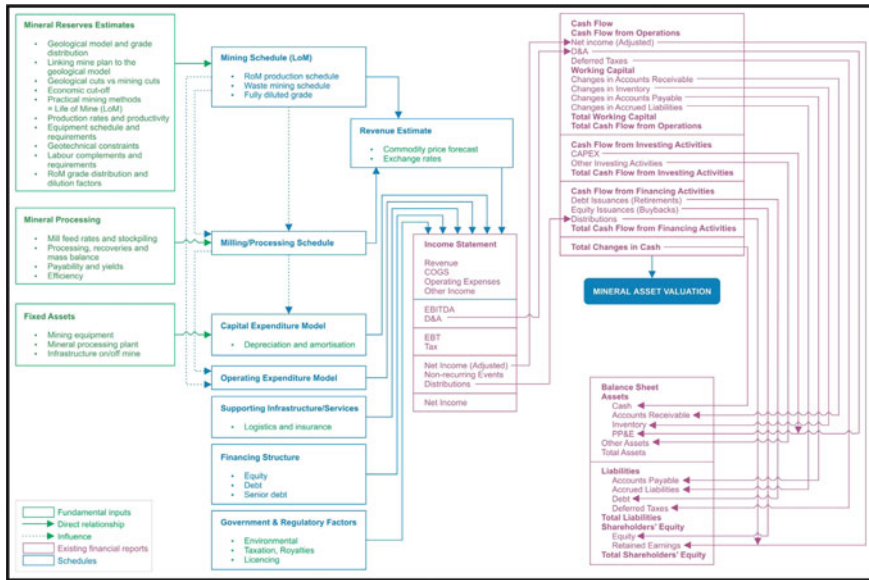
Fig. 2 A framework for linking financial reporting and valuation for developmental and producing mineral projects [6]

ground transition framework (Fig. 3) which was derived from an analysis of selected gold mines. The study's findings indicated that at a 95% confidence level, gold mines can prepare to transition from open-pit mining to underground mining. At this confidence level the gold price to cost per ounce ratio is just greater than 2.0; gold grade is between 4 and 9 g/t, stripping ratio is between 3 and 15 m^3/t, and net present value (NPV) is positive for the underground mining option. The lesson that can be drawn from this study is that it is possible through stochastic mine planning to improve confidence in the timing and placement of excavations.

2.3 Stochastic Cut-off Grade Optimization

Cut-off grade (CoG) is a parameter generally used to determine the quantities of material (ore and waste) mined, ore processed, and product produced and sold. Thus CoG inherently affects the cash flows produced from a mining operation, consequently affecting the NPV of a mining project at the mine planning or feasibility study stage. The CoG framework developed by Lane [8, 9] has been applied widely in mine planning. However, due to its deterministic construction it fails to capture the stochastic nature of the input variables. Therefore, it cannot guarantee the determination of an optimal CoG, hence there have been extensions to the original model to overcome some of the model's shortcomings. Githiria [10] therefore, extended
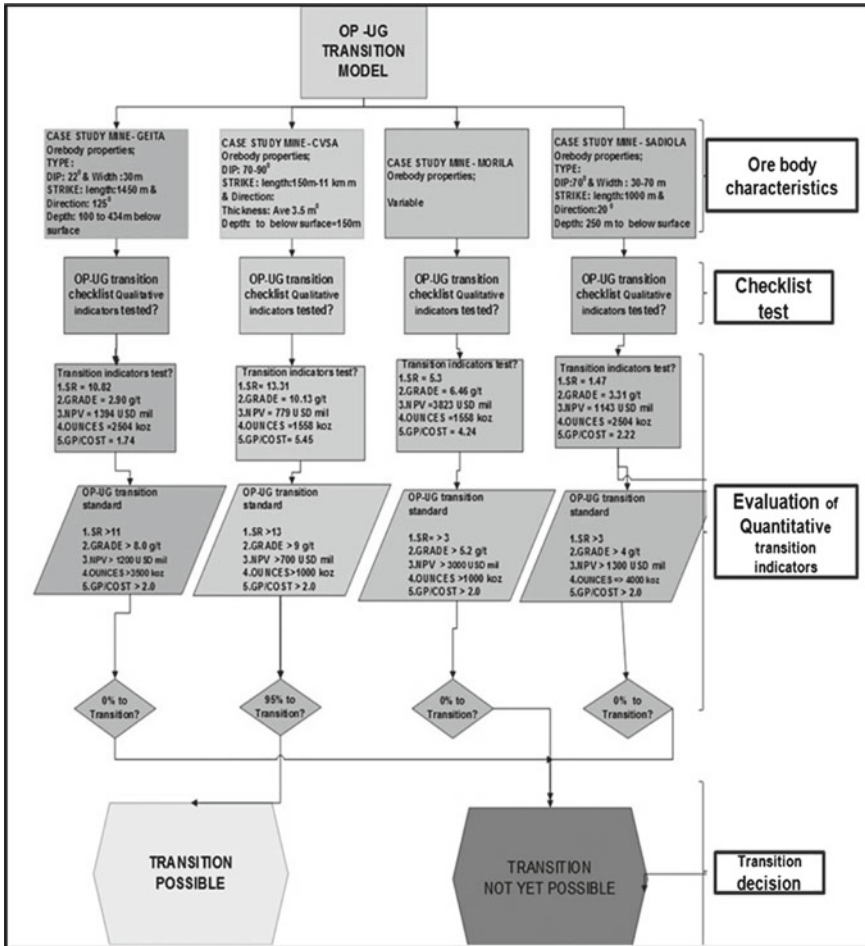
Fig. 3 A stochastic open-pit to underground transition framework for gold mines [7]

Lane's framework by simultaneously incorporating stochastic commodity prices and grade-tonnage realizations into the calculation procedure. The study concluded that the stochastic model generated improvements in NPV ranging between 7 and 186% over other models, thus demonstrating the value of using stochastic approaches to CoG optimization. The lesson that can be drawn from this study is that stochastic mine planning approaches enable the generation of more robust or superior mine plans than those produced from deterministic mine planning.

3   Examples of Current Research Work

Some of the current postgraduate research work being undertaken in mine planning related work is premised on a stochastic approach to underground stope design and development of a framework to improve both the temporal and spatial mine-to-plan compliance.

3.1   Probability Stope Design

The research work on probability stope design is planned to extend the work done by Whittle et al. [11] on probability (or stochastic) pit designs to underground mining environments. Whittle et al. [11] noted that the inherent assumption in the Lerchs-Grossmann (LG) algorithm used for open-pit optimization that block economic values (BEVs) are known with certainty, results in the LG algorithm failing to capture the variability in input parameters for open-pit optimization. In an actual mining operation the geological, technical and economic parameters are never known with certainty as they also change over time due to improved understanding of an operation or technical and economic conditions change. Whittle et al. [11] therefore extended the deterministic pit optimization approach to generate probability pits (Fig. 4). The different color shades in Fig. 4 indicate different probabilities attached to each pit limit with increasing probability towards the inner pit limits. The outer pit limits have lower probabilities but, are an indication of the extremities of the possible pit limits when pit limit determination input parameters change since they are dynamic. This approach ensures that mine planning is able to consider locating infrastructure outside of the probable pit limits, which is otherwise not possible under deterministic mine planning often resulting in the costly demolition or relocation of infrastructure. Again, this demonstrates the superiority of stochastic approaches over deterministic approaches to mine planning. A similar approach is being undertaken to optimize stope envelopes in underground mine planning through utilizing stochastic BEVs, as part of current postgraduate research work in mine planning in the School of Mining engineering at the University of the Witwatersrand. The envisaged lesson from this study is that stochastic mine planning helps to improve confidence in the placement and sizing of excavations.

3.2   Temporal and Spatial Mine-to-Plan Compliance

Mine-to-plan reconciliation tends to be undertaken and reported on an inter-temporal key performance indicators (KPIs) thus, failing address the spatial nature of mining operations. As such, temporal KPIs provide a false sense of achievement to mine management because performance against these KPIs could be positive, while actual
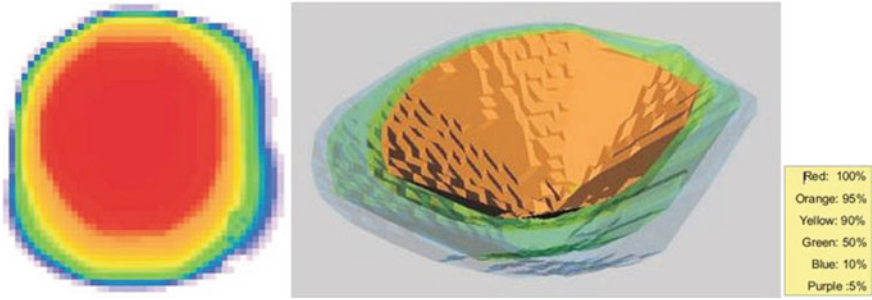
Fig. 4 Example of a probability pit design [11]

mining activities are not occurring in the correct spatial areas which is detrimental long-term KPIs that include technical operating mining flexibility advocated in the study by Musingwini et al. [12]. When temporal compliance is simultaneously evaluated together with spatial mine-to-plan compliance it is possible to align short-term KPIs that mining companies track on a weekly, monthly, quarterly, or annual basis to long-term value expected by (and often promised to) investors. It is against this background that research is currently being undertaken on the development and implementation of a combined temporal and spatial mine-to-plan compliance reconciliation framework. It is hoped that such a framework will ensure that short-term KPIs are achieved without compromising long-term KPIs. The envisaged lesson from this study is that a combined temporal and spatial mine-to-plan compliance framework aligns short-term mining activities to long-term KPIs.

4 Lessons Learnt

Mine planning is integral to the mine value chain and is intricately linked to valuation and optimization. Deterministic mine planning approaches fail to capture the stochastic nature of mine planning input variables resulting in actual outcomes deviating from planned outcomes. This challenge can be addressed when stochastic approaches are utilized in mine planning. This paper has demonstrated the value that can be created by a paradigm shift from deterministic to stochastic mine planning. Some of the lessons that can be drawn from the approaches discussed in this paper are:

– Stochastic mine planning approaches enable the generation of more robust mine plans;
– Stochastic mine planning assist in improving confidence in the timing, placement and sizing of excavations;

– It is possible to interface pre-feasibility and feasibility studies of mining projects with regular reporting of performance of the actual mining operations once the projects have progressed to the production phase;
– A combined temporal and spatial mine-to-plan compliance reconciliation framework can reduce detrimental impacts of short-term mining activities on long-term KPIs, hence ensure long-term value expected by (and often promised to) investors.

References

1. Musingwini, C.: Presidential address: Optimization in underground mine planning-developments and opportunities. J. South. Afr. Inst. Min. Metall. **116**(9), 809–820 (2016)
2. The South African Code for the Reporting of Exploration Results, Mineral Resources and Mineral Reserves (The SAMREC Code 2016). The Southern African Institute of Mining and Metallurgy and the Geological Society of South Africa, Johannesburg, (2016)
3. Newby, E., Fomeni, F.D., Ali, M.M., Musingwini, C.: A method for stochastic estimation of cost and completion time of a mining project. In: Proceedings of the Mathematics in Industry Study Group, pp. 13–20 (2010)
4. Gold Fields: Integrated Annual Report. Gold Fields (2015)
5. Price Waterhouse Coopers: Mine 2015—The gloves are off. Available online: http://www.pwc.com/gx/en/mining/publications/assets/pwc-e-and-m-mining-report.pdf (2015)
6. Njowa, G., Musingwini, C.: A framework for interfacing mineral asset valuation and financial reporting. Res. Policy **56**, 3–15 (2018)
7. Opoku, S., Musingwini, C.: Stochastic modelling of the open pit to underground transition interface for gold mines. Int. J. Min. Reclam. Environ. **27**(6), 407–424 (2013)
8. Lane, K.F.: Choosing the optimum cut-off grade. Colorado Sch. Min. Q. **59**(4), 811–829 (1964)
9. Lane, K.F.: The Economic Definition of Ore: Cut-off Grade in Theory and Practice. Mining Journal Books, London (1988)
10. Githiria, J.: A stochastic cut-off grade optimisation algorithm. Ph.D. Thesis, University of the Witwatersrand, Johannesburg (2018)
11. Whittle, G., Stange, W., Hanson, N.: Optimising project value and robustness. In: Project Evaluation Conference, Melbourne, The Australasian Institute of Mining and Metallurgy, pp. 147–155 (2007)
12. Musingwini, C., Minnitt, R.C.A., Woodhall, M.: Technical operating flexibility in the analysis of mine layouts and schedules. J. South. Afr. Inst. Min. Metall. **107**(2), 129–136 (2007)

Part I
Economic and Financial Risk Assessments

Economic Value Added Analysis for Mining Companies

T. Tholana and P. N. Neingo

1 Introduction

Every business including mining, exists to create optimum value for its various stakeholders. Even though the needs of all stakeholders are equally considered by mining companies, the creation of long-term sustainable shareholder value has increasingly been the major measure of success. However, mining companies operate in a challenging and constrained business environment characterized by turbulent global economic conditions. Access to capital is one of the constraints mining companies face. The scarcity of capital requires that when it is available, it must be allocated and managed effectively. The high cost of production, volatile and declining commodity prices force mining companies to focus on short-term strategies for survival, which may be in conflict to long-term value creation. Such short-term planning strategies many times ensure that shareholder value is not maximized [1]. The following are some of the short-term survival strategies by mining companies that destroy long-term value [1]:

- Chasing and mining high-grade areas without considering the long-term impacts.
- Avoiding necessary production delays to install critical infrastructure that will enable long-term sustainable production. Such short-term production disruptions will be necessary to support future production rate but are avoided for short-term benefits.
- Suspending or deferring exploration and capital projects which saves capital in the short-term but results in an operation without sufficiently developed mining areas to sustain optimum production rates.

T. Tholana (✉) · P. N. Neingo
School of Mining Engineering, University of the Witwatersrand, Johannesburg, South Africa
e-mail: tinashe.tholana@wits.ac.za

P. N. Neingo
e-mail: paskalia.neingo@wits.ac.za

These actions though beneficial in the short-term, may destroy value in the long-term. These actions are caused by wrong performance measures such as profit [1]. It was, therefore, suggested that EVA is an appropriate tool to measure value creation from the extraction of Mineral Resources [2]. It is the aim of this paper to compare profit and EVA for selected mining companies. This is to ascertain whether mining companies have been creating true economic value for shareholders (as measured using EVA) over and above the normal profit reported in income statements. To do the analysis, four major international mining companies were selected which are; BHP Billiton (BHP), Rio Tinto, CVRD-Vale (Vale) and Anglo American (Anglo). Major mining companies as opposed to junior companies were selected because they are well capitalized, have steady cash flows and their financial data is easily available on the public domain to enable a meaningful analysis. In 2006, the top four mining companies globally by market capitalization were BHP, Rio Tinto, Anglo and Vale [3]. However, over the years until 2017, the rankings of these companies have changed. As of year ending 2016, BHP and Rio Tinto have continued to be in the top four but, Vale and Anglo both slipped their positions to fifth and ninth, respectively [4]. Nevertheless, Vale and Anglo were selected for analysis to understand why their ranking declined from 2007 to 2017. Currently, in addition to BHP and Rio Tinto in the top four are Glencore Xstrata and China Shenhua Energy Company Limited. Xstrata and Glencore merged to form Glencore Xstrata in 2013 and therefore the new company's data is only available for the latter part of the analysis period. China Shenhua Energy is not geographically and commodity diversified; it focusses on coal mining only and its operations are only in China. Because of these reasons the two companies were excluded for analysis. The period 2007–2017 was selected as a suitable period that captures the performance of mining companies under varied economic and operational conditions.

2   Value Addition in Mining

Mining projects are capital intensive, thus, economically viable projects require capital injection from financiers who expect a return on their invested capital. In order to meet financiers' expectations effective management of upstream activities in the mining value chain results in value addition [5]. The concept of mining value chain recognizes that competitive advantage in mining can be derived from a sequential arrangement of value-adding activities in order to ensure that maximum value is generated from every dollar of capital invested [6, 7]. However, efforts to maximize this value are undermined by challenges that mining companies face such as volatile commodity prices, capital scarcity, low productivity, high production costs, and socioeconomic challenges. Also, mining involves the extraction of a wasting mineral resource whose value declines with each unit of extraction. This means that there is only a single opportunity available to maximize value from extracting the mineral resource. These challenges and the wasting nature of mineral assets neces-

sitate the need not only for value addition but also the need to measure, track and report this value.

There are several metrics used to measure the economic performance of a company such as profit, unit cost and several financial ratios. These metrics are considered traditional and have several pitfalls. The following are some of the pitfalls of using traditional metrics to evaluate or measure the performance of companies [8]:

– They ignore capital and its cost which may lead to overinvestment on projects with positive margins, profit, and productivity measure even though they may have inadequate returns.
– Traditional measures such as unit cost, utilization, and income that tend to promote overproduction to beyond demand. This appears to reduce unit cost but may also increase the cost of invested capital.
– They promote a chance of pursuing a project that destroys value while overlooking and rejecting a project that may create value.

Therefore, traditional measures are inappropriate for decision making. In addition to the pitfalls above, mining companies need to demonstrate profit growth because of the capital-intensive nature of the business and long lead times involved [9]. Given these pitfalls, a better value assessment tool is required such that the impact of operational decisions and/or delaying capital expenditure can be related to value added/destroyed. Analysis of financial performance of mining companies requires taking account of material reserves and production in addition to earnings [5]. Based on this argument, [5] defined two variables, namely, Total Shareholder Return (TSR) and Total Reserves Increment (TRI) to measure variations in company share price plus dividends and company Mineral Reserves plus production, respectively. These two measures combined take account of the entire mining value chain, attributing value addition to effective management of the underlying asset in mining, the mineral reserve. Garcia and Camus [5] then tested the performance of 14 companies based on TSR and TSI indices as shown in Fig. 1.

The results in Fig. 1 confirmed the hypothesis that leading companies surpass the average (the horizontal and vertical lines) for the sample [5]. However, Fig. 1 does not show the performance of companies year on year; it only shows an aggregated performance over that given 9 years. Therefore, TSR and TRI variables undermine the short-term operational and market challenges that may affect long-term value created. Literature is increasingly emphasizing the need to shift from traditional measurements such as profit to new metrics of measuring value created [10].

Market expectations are shifting towards profitable, integrated short-term and long-term growth under dynamic economic conditions and operational challenges [9]. To ensure both short-term survival and long-term value creation, MRM practice was developed. MRM is defined as "*an integrated activity which identifies, evaluates and provides an optimal extraction plan of the mineral resource, to produce a quality product which satisfies the business objectives of the company, and the requirements of the customer, in a dynamic environment…*" [2]. It is an important concept in mining that has been adopted by the global mining industry. Nevertheless, in a research by [2] on the application of MRM, it was concluded that its implementation has been met
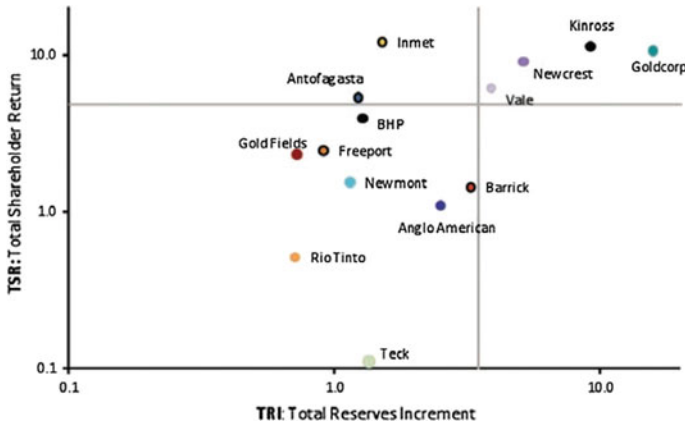
Fig. 1 TSR versus TRI for selected mining companies, 2000–2008 [5]

with marginal success. One of the reasons is inappropriate measures of the success of MRM which are short-term focused including profit and cost [2].

While traditional financial performance measures are commonly reported in financial statements, they have a common limitation. They do not incorporate the cost of invested capital which renders them inappropriate to give a reliable performance of a company. This resulted in the development of a better measure of the true value created or destroyed by a company called economic value add.

3 Economic Value Add

EVA is a concept that dates back to 1989 developed by Stern Stewart & Co as a financial performance measure that enables managers to see whether they are creating shareholder wealth. EVA is a copyright of Stern Stewart Inc. It is the net operating profit after taxes have been paid (NOPAT) minus a capital charge for the opportunity cost of all capital invested in a company or project [11]. NOPAT is the Earnings Before Interest and Taxes (EBIT) less Tax and can be expressed as [11]:

$$EVA = NOPAT - Cost\ of\ Capital * Invested\ Capital \qquad (1)$$

EVA, therefore, measures the surplus value created by a company on capital invested into a company or project. It is an estimate of true economic profit, or the amount by which earnings exceed or fail to meet the required minimum rate of return investors could get by investing in other securities of comparable risk [11]. If EVA is negative, shareholders wealth is being eroded and vice versa. EVA is, therefore, an indicator of a company's value growth in the future.

Since its development, it has been widely used by many companies to measure their performance. It was used to compare the performance of government-linked and non-government-linked companies in Malaysia [12]. In this research, it was found that government-linked companies tend to have lower EVA values than non-government linked companies. Several studies have also been done to prove that EVA is a better tool to assess company performance compared to traditional performance measures [10, 13–18].

4 Methodology

Data used in this paper was collected from the four companies' annual reports available on the public domain. The data was then used to calculate EVA using Formula 1. A cost of capital of 10% was assumed for all companies because the cost of capital is not reported in annual reports of the four companies. There are variations in calculation of invested capital. In this paper invested capital was calculated as in [7]:

$$
\begin{aligned}
\text{Invested capital} = \ &\text{Current assets} \\
&- \text{non-interest-bearing current liabilities} \\
&+ \text{Net property, plant and equipment} \\
&+ \text{Intangible assets} \\
&+ \text{Goodwill} \\
&+ \text{Other operating assets}
\end{aligned}
$$

5 EVA and Profit Analysis

Figure 2 shows a comparison of profit and EVA for the selected companies from 2007 to 2017. Data for Rio Tinto for the year 2007 was not available on the public domain. The analyses for each company are done after Fig. 2.

5.1 BHP Billiton

Figure 2a shows the profit and economic value added for BHP from 2007 to 2017. The years 2007 and 2008 were good years for the company in terms of both profit and EVA mainly because of the continued growth and demand for mineral commodities by emerging countries. Following the high demand and subsequently high commodity prices, the company announced an offer to acquire Rio Tinto in 2008 which later failed [20]. The onset of the global economic crisis (GEC) in the late 2008 until
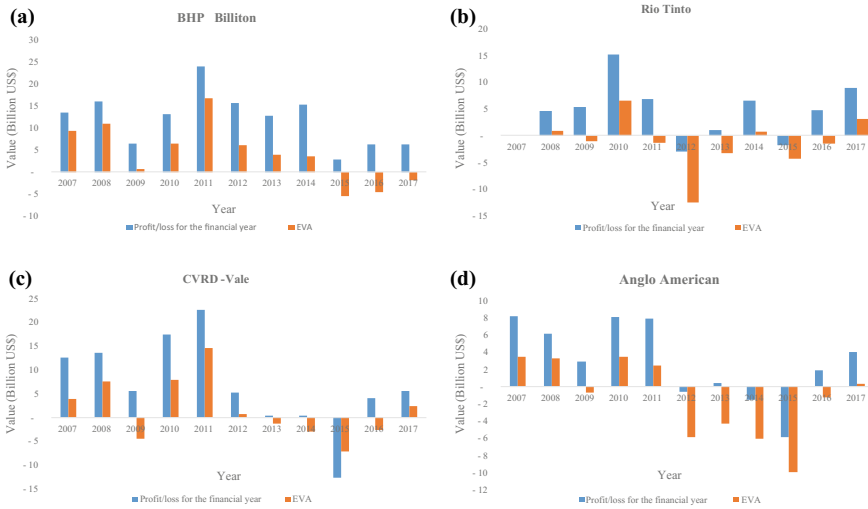
Fig. 2 A comparison of profit and EVA for the selected companies. **a** BHP Billiton, **b** Rio Tinto, **c** CVRD-Vale, and **d** Anglo American

mid-2010 resulted in a fall in profit and a significant decline in EVA, which means the company did not create as much shareholder value for the company compared to pre-GEC period. As commodity prices improved from mid-2010 both BHP's profit and EVA also improved.

From 2015 to 2017, even though the company made profits in the 3 years it did not create shareholder value. In 2014 BHP announced a demerger of a number of operations that formed the now South32 and in 2015 the demerger was completed [20]. The aim of the demerger strategy was for BHP to focus on "*high-quality aluminium, coal, manganese, nickel and silver assets*" [20]. From 2015 the company's strategy was to be more focused on large and long-life mineral assets with "*potential to unlock shareholder value by significantly simplifying the BHP Billiton Group and creating a new company specifically designed to enhance the performance of its assets*" [20]. The demerger has not proved to have added shareholder value as seen in Fig. 2a. The negative EVA for the three years can be attributed to the demerger. Since the demerger, it can be noted in Fig. 2a that even though EVA was negative it has been increasing year on year (2015–2017). Therefore, it is anticipated that the demerger strategy will create positive EVA in the long term.

5.2 Rio Tinto

Figure 2b shows the profit and economic value added for Rio Tinto from 2008 to 2017. In 2008 and 2009 the company's profits were relatively low and EVA was negative.

Like BHP this can be attributed to the 2008 GEC. As most commodities' prices improved from 2010 to 2011, profitability also improved. Generally, the profitability of Rio Tinto was low for most of the analysis except in 2010, 2011, 2014, and 2017 with low EVA in 2008 and 2014. In 2009, 2011, 2012, 2013, 2015, and 2016 the company did not create shareholder value even though it had made profits in some of these years (2009, 2011, 2013, and 2016). This performance can be attributed to the factors discussed below.

Since the early 2000s, the company has been implementing a significant growth strategy through acquisitions. In 2000, at the start of the minerals boom, Rio Tinto undertook US$4 billion worth of acquisitions—primarily Australian aluminum, iron ore, diamond, and coal assets. This strategy intensified and in 2007 the company acquired Alcan Inc. for US$38 billion to be the world's largest aluminum producer. In 2011, the company acquired the Riversdale coal asset in Mozambique for US$3.7 billion. The year 2012 also recorded a high capital expenditure of US$17.5 billion to support the company's iron ore operations in Australia and to develop the greenfield copper-gold project in Mongolia [21]. These acquisitions were done anticipating significant growth in the company. However, these efforts were offset by the significant weakening global economic and market conditions that resulted in significant impairment charges which ultimately destroyed shareholder value. It was stated that the Mozambican coal asset was sold for US$50m in 2014 following post-tax impairment charges of US$2.86 billion in 2013 and $470m in 2015 [22]. Over the period under analysis, 2012 is the worst year for Rio Tinto. This is attributed to total impairment charges of US$14.4 billion, primarily relating to the Alcan aluminum (US$11 billion) and its coal assets in Mozambique [21]. The company's chief executive officer lost his job in 2013 mainly due to these value destruction capital investment decisions [23].

5.3 CVRD-Vale

Figure 2c shows the profit and economic value added for Vale from 2007 to 2017. EVA rose to US$7.498 billion in 2008, a 93% increase over 2007, while profit rose by only 6.7%. These increments can be attributed to higher selling prices of the different products such as iron ore, iron ore pellets, manganese ore, ferroalloys, and potash offsetting lower selling prices for nickel and copper as well as lower sales volumes for aluminum and bauxite [24]. Weaker demand for various products including iron ore, ferroalloys, nickel as well as the lower prices resulted in lower volumes sold and consequently lower gross revenues [24]. The company further reported that Sudbury and Voisey Bay operations were shut down in the second half of 2009 due to labor strikes. These factors caused about 60% decrease in profit between 2008 and 2009 while EVA decreased from US$7.498 billion to negative US$4.563 billion. Due to the GEC, net operating profit after tax (NOPAT) reduced by about 72% and to sustain the business, capital invested increased by 27%.

In the last quarter of 2010 and the first quarter of 2011, floods and an earthquake negatively affected coal operations in Australia and sales of mining products in Japan, respectively [24]. Total operating costs and expenses increased by 36.8% from 2009 to 2010 [24]. The cost of goods sold was about 80% of the total operating costs and expenses. Despite the natural disasters and increased costs, profit rose to US$17.453 billion in 2010, a twofold increase over 2009 and EVA was also created to a value of US$7.922 billion in 2010. The profit rose because the company reported currency gains of US$102 million, net operating revenues increased by 94.3% due to higher prices of the major products. Moreover, there was a worldwide economic recovery and the demand for most products especially iron ore and iron ore pellets increased [24]. The recovery in demand and prices of iron ore and iron ore pellets accounted for 69% of the total increase in gross revenue. EVA increased mainly because the 355% increase in NOPAT offset the 18% increase in capital charge.

It was reported that the net operating revenues increased by 30.2% mainly due to: "*higher prices for the company's major products, especially for iron ore and other bulk materials; the increase in nickel volumes following the end of labor strikes and resumption of nickel production in Ontario and the inclusion of a full year of results for fertilizers compared to seven months in 2010*" [24]. The company continued to be highly reliant on iron ore and iron ore pellets. The sustained high demand and consequently higher prices for these two products accounted for about 70% of the increase in gross revenues. Although Fig. 2c shows increments in both profit and EVA from 2010 to 2011, during the same period the total operating costs and expenses also increased by 22.4% [24]. The largest contributors to increased costs as noted "*were the resumption of normal nickel operations in Ontario, the inclusion of a full year of the phosphate business acquired in 2010 and the start-up of Onça Puma*" [24].

In 2012, Vale's profit was 77% lower than that reported in 2011 while EVA was 94% lower than that created in 2011. Invested capital and consequently capital charge (on the basis of constant discount rate) decreased in 2012. The company recorded a 75.9% decrease in net income and attributed this decrease to various non-recurring items, lower prices of major products and slightly higher costs [24]. In 2013, net operating revenues increased marginally because higher volumes of base metals, iron ore, coal and higher prices of iron ore were partially offset by lower prices of base metals, fertilizers, metallurgical coal and lower volumes of iron ore pellets and fertilizers [24]. Although the company reported a profit of US$406 million as shown in Fig. 2c, under the conditions that prevailed, value was destroyed as EVA was negative US$1.288 billion. Invested capital in 2013 was only about 3% lower than that invested in 2012. Therefore, the negative EVA can be attributed to lower NOPAT which was affected by the factors that affected revenue.

In 2014, there was a decrease in the average price for iron ore and pellets which was partially offset by higher volumes of iron ore, iron ore pellets, and higher price for nickel [24]. Therefore, a decrease in both profit and EVA was observed, which can be attributed to the decrease in net operating revenues. Furthermore, the company also reported several non-recurring items including charges for impairment of some iron ore, coal, fertilizers and

nickel assets, foreign exchange and monetary losses [24]. Revenue continued on a downward trend and in 2015, a loss of US$12.62 billion was reported and for the period considered in this paper, 2015 also saw the lowest EVA of negative US$7.246 billion, i.e., most value was destroyed. The loss can be attributed to lower prices for major products as well as acquisitions and dispositions [24].

In 2016 and 2017, higher prices for iron ore fines and pellets and other products had the most impact on the 17.6 and 23.6% increases in net operating revenues from continuing operations, respectively [24]. Due to these increases, the company reported a positive profit but EVA remained negative. Profit generally increased between 2007 and 2011 with an exception in 2009 that can be attributed to the GEC. In years 2009, 2013, 2014, and 2014, profit was reported but value was destroyed. Vale has shown fluctuations between positive and negative EVA, thus, over the period of study, Vale created and also destroyed value. This necessitates the need to identify improvement opportunities within the company and also make better investment decisions.

5.4 Anglo American

Figure 2d shows the profit and economic value added for Anglo American from 2007 to 2017. In 2007 Anglo American reported a profit of US$8.172 billion as shown in Fig. 2d with a lower but positive EVA (US$3.435 billion). High earnings in 2007 were attributed to an increase in prices of platinum group metals (PGMs), lead, nickel, niobium and iron ore as well as higher volumes for copper, zin, and iron ore [25]. These together with higher earnings from De Beers offset a significant reduction in Australian coal contribution. In 2008, both profit and EVA decreased by 25% and 5%, respectively, because commodity prices decreased sharply in the second half of 2008. South African operations, mainly PGMs were faced with a 36% increase in costs, safety-related stoppages, electricity supply constraints, and commissioning delays at Mogalakwena North concentrator [25]. Despite the 2008 GEC, ferrous metals saw profit increasing to record levels due to increased volumes and operational efficiencies [25]. Overall, value was created in 2008 despite the factors that negatively affected several operations.

The impact of the GEC continued into 2009 as Anglo American reported a profit of US$2.912 billion, a 52% decrease over 2008 but positive due to rigorous cost reduction measures. Furthermore, value was destroyed as the company's EVA was negative US$736 million. The decline in profit was attributed to a sharp decrease in all commodity prices. Anglo American [25] confirmed this and stated that there was "*a 38% reduction in the platinum basket, an average 40% reduction in benchmark export iron ore, a 30% decline in average nickel and a more than 20% decline in export metallurgical coal*" [25]. In addition to lower commodity prices, a decline in global steel demand and coal export prices caused lower profits from Samancor, Metallurgical and Thermal coal [25]. While the company's profit declined due to various factors, value was destroyed as the capital invested rose to US$40.554 billion,

a 24% increase over 2008 due to increments in net working capital and tangible assets. Additional tangible assets to the value of US$5.563 billion inclusive of capital investment were added to the company's core commodity assets.

In 2010, Anglo American reported a profit and also created value for its shareholders. The company attributed its success to increased commodity prices and tightly controlled costs in addition to its ability to unlock value through asset optimization. Assets optimization and procurement initiatives unlocked a combined value of US$2.213 billion [25]. An additional value of US$1.304 billion was generated as the company completed disposals of Moly-Cop, AltaSteel, Skorpion zinc mine and an undeveloped coal asset in Australia. Asset optimization initiatives continued in 2011 and as such the company delivered both, profit and positive EVA though at slightly lower levels than in 2010.

Anglo American made a loss and also destroyed value in 2012 mainly because of lower commodity prices and higher costs. Invested capital increased mainly due to an increase in tangible assets. The platinum sector recorded an operating loss of US$120 million in 2012 from US$890 million profit in 2011 [25]. The sector which is mainly operating in South Africa faced lower volumes due to a 2-month illegal industrial action; a 21% increase in cash operating costs; and a 4% decline in productivity. All key commodities including PGMs made profits due to higher prices realized and/or increased sales volumes in 2013. For the year, the company made a profit and EVA improved slightly but remained negative. Between 2013 and 2016, Anglo American destroyed value as they undertook portfolio restructuring that saw them move from 65 to 45 to 16 core assets. In 2017, the company started creating value, with a calculated EVA of US$283 million and possibly marking the end of a tough restructuring period for the company.

6   Conclusion

Creation of long-term shareholder value is the aim of every business, mining included. The reporting of such value creation by companies is important to enable various stakeholders to analyze the performance of companies and be able to make informed decisions. Traditional performance measures are reported by mining companies including profit. However, the major limitation of such measures is that they ignore the cost of invested capital which means that these measures do not capture the true economic profit made by companies. EVA has proved to be the true measure of value that mining companies should measure and report on. This study found that even though profit was generated by mining companies in most of the analysis period, in contrast, EVA was not created. It was also found that cost-cutting measures improved profit without creating EVA. In addition to the traditional measures that are always reported by mining companies, EVA should also be reported to see whether the value is being created.

References

1. Hall, B.E.: Short-term gain for long-term pain -how focusing on tactical issues can destroy long-term value. J. South Afr. Inst. Min. Metall. **109**(3), 147–156 (2009)
2. MacFarlane, A.S.: Establishing a new metric for mineral resource management. J. South Afr. Inst. Min. Metall. **106**(3), 187–198 (2006)
3. Price Waterhouse Coopers Mine 2007—Riding the wave. Internet: https://www.pwc.co.za/en/assets/pdf/pwc-mining-review-07.pdf (Cited 5 May 2018) (2007)
4. Price Waterhouse Coopers Mine 2017—Stop Think… Act. Internet: https://www.pwc.co.za/en/assets/pdf/mine-2017.pdf (Cited 5 May 2018) (2007)
5. Garcia, J.M., Camus, J.P.: Value creation in the resource business. J. South Afr. Inst. Min. Metall. **111**(11), 801–808 (2011)
6. Vorster, A.: Planning for value in the mining value chain. J. South Afr. Inst. Min. Metall. **101**(2), 61–65 (2001)
7. Mauboussin, M.J., Callahan, D.: Calculating return on invested capital: how to determine ROIC and address common issues. Credit Suisse Global Financial Strategies (2014)
8. Pettit, J.: EVA & Production Strategy: Jonah is Back!. Stern Stewart & Co, New York (2000)
9. Prinsloo, J.J.: A comparative analysis of economic value created by South African mining companies in a growing platinum industry. University of Pretoria (2010)
10. Geyser, M., Liebenberg, I.E.: Creating a new valuation tool for South African agricultural co-operatives. Agrekon **42**(2), 106–115 (2003)
11. Stewart, G.B.: The Quest for Value: A Guide for Senior Managers. Harper Collins Publishers Inc., United States of America (1990)
12. Issham, I., Fazilah, A.S.M., Hwa, Y.S., Kamil, A.A., Ayub, A., Ayub, M.A.: Economic value added (EVA) as a performance measurement for government linked companies (GLCS) vs non-government linked companies (non-GLCS): evidence from bursa Malaysia (2008)
13. Tortella, B.D., Brusco, S.: The economic value added (EVA): an analysis of market reaction. Adv. Acc. **20**, 265–290 (2003)
14. Wainaina, G.J.: Economic value added (EVA) and market returns. The case of companies quoted on the Nairobi stock exchange. Unpublished master's thesis, University of Nairobi (2008)
15. Sharma, A.K., Kumar, S.: EVA versus conventional performance measures-empirical evidence from India. ASBBS Proceedings **19**(1), 804 (2012)
16. Shah, R., Haldar, A., Nageswara Rao, S.V.D.: Economic value added: corporate performance measurement tool (2015)
17. Maditinos, D., Sevic, Z., Theriou, N.A.: Review of the empirical literature on earnings and economic value added (EVA) in explaining stock market returns. Which performance measure is more value relevant in the Athens stock exchange (ASE)? In: Annual Conference of the Hellenic Finance and Accounting Association Thessaloniki, pp. 15–16 (2006)
18. Kramer, J.K., Peters, J.R.: An inter-industry analysis of economic value added as a proxy for market value. J. Appl. Finan. **11**(2), 41–49 (2001)
19. Ernst & Young LLP Getting ROIC right: how an accurate view of ROIC can drive improved shareholder value. Internet: https://www.newconstructs.com/wp-content/uploads/2017/10/EY_Proof-High-Quality-ROIC-Matters_NewConstructs-Materially-Better-1.pdf (Cited 6 May 2018) (2017)
20. BHP Billiton Annual Reports. Internet: https://www.bhp.com/investor-centre/annual-reporting-2017#Downloads, (Cited 5 May 2018) (2007–2015)
21. Rio Tinto Annual Reports. Internet: http://www.riotinto.com/investors/downloads-16678.aspx (Cited 5 May 2018) (2008–2017)

22. Business Day. Rio Tinto's calamitous $3.7bn Mozambique coal deal still haunts them, News article (2017)
23. Financial Post. Rio Tinto chief Albanese's downfall a cautionary tale of bad acquisitions (2013)
24. CVRD Vale. Annual Report. Internet: http://www.vale.com/en/investors/information-market/annual-reports/20f/pages/default.aspx (Cited 4 May 2018) (2007–2017)
25. Anglo American. Annual Reports. Internet: http://www.angloamerican.com/investors/annual-reporting/reports-library/report-2018 (Cited 20 April) (2007–2017)

Financial Risk Analysis of Optimized Ventilation System in the Gold Mine

S. Sabanov

1 Introduction

Costs for mine ventilation are typically increasing when mines expand to deep levels. Some underground mines in Kazakhstan still use continuously operating fans at its maximum capacity. This is not helping to save energy and costs that are in many cases very significant. However, mine safety is related to risks associated with a deficit of fresh air for mine gases dilution and their removal from the mine workings. The ventilation system in Kazakhstan's gold mine was in need of improvement for the reason of increased production from deep horizons. The main aim of this study was to analyze the financial risks associated with high-cost airflows in deep horizons of the gold mine.

The investigated mine uses sublevel caving method that produces ore utilizing conventional drill and blast method. The mine is serviced by one vertical Shaft#1 utilized as an intake airway and a ramp connected to an incline used as an exhaust. The mine uses blowing ventilation system with the fan 'VO-24K' arranged on the surface in Shaft#1. Auxiliary ventilation required to force air into blind headings use axial flow fans and flexible ventilation ducting. Fans located in the main access deliver air from the fresh side of the primary ventilation circuit without recirculating the blast fumes. The existing underground developments enable exhaust air to exit the mine through the ramp and further thought the incline. Shaft#1 is used for personnel transport. The incline commencing at the surface extends down to the ramp and joins major levels and generally services mining operations.

The mine operates in 2×10 h shifts per day, 7 days per week. There is a mid-shift lunch break to allow blasting to occur in the ore headings to maintain production efficiency.

S. Sabanov (✉)
School of Mining and Geosciences, Nazarbayev University, Astana, Kazakhstan
e-mail: sergei.sabanov@nu.edu.kz

Table 1 Kazakhstan mine ventilation requirements

Maximum air velocities	Requirements (m/s)
Cleaning and preparation drives (footwall drive)	4
Cross cuts, vent, main haulage ways, and main decline	8
Other places	6
Crossings and main vent shafts	10
Shafts for lifting persons	8
Shafts for lifting cargo	12
Shafts for lifting persons in emergency	15
Vent shafts and vertical development without ladders	No restriction

The mine ventilation network modelling has been undertaken to be compliant with Kazakhstan's mining regulations requirements for underground mine ventilation [1]. Table 1 shows the main mine ventilation regulations used to model the mine ventilation.

The airflow requirements for the mine have been calculated based on the underground equipment and the blast ventilation requirements.

Modelling of the ventilation network was limited to only the main ventilation network and did not consider abandoned closed mining areas. The ventilation network has been modelled at one stage to represent maximum mine air resistance towards later stage of mine life (7 years).

In this study, risk analysis used stochastic modelling applied to the optimized ventilation network to estimate risks of investment into Ventilation on Demand (VOD) system. VOD can influence power savings of fans by reducing wasted air in areas without mining activity, redistributing existing ventilation capacity and better control over the ventilation system. An accurate ventilation network model is needed to undertake the analysis, implement automatic ventilation controls and fans with sensors for air quantities and quality. VOD will need additional capital for remote airflow control using variable flow fans, in-flight adjustable blades, regulators with motorized louvers or sliding doors. The additional operating cost would be incurred for ongoing maintenance, moving, updating, adding and removing sensors and controls. The computer system will determine how much air is required to dilute contaminants below statutory levels. Target ventilation conditions need to be reached as people or equipment enter a drift, face area or other location. It has to be noted that the cost of ongoing maintenance must be significantly lower than savings in power cost to justify capital investment [2–4].

Stochastic modelling provided ranges of Internal Rate of Return (IRR) outcomes with confidence limits as well as mean values in each case. Risk is quantified by replacing single values with a probabilistic distribution and applying Monte Carlo simulation for each calculation. Decision-makers can view not only the mean outcome value but also the range of possible outcome range values. Monte Carlo simulation utilized the randomly select values from the probabilistic distribution. Software

'Palisade@Risk' was used to construct and analyze stochastic models in Microsoft Excel spreadsheets [5].

2 General Theory and Measurement Techniques

The determination of frictional pressure drop in mine airways may be obtained from the following relationship [6]:

$$P = f * L * \text{Per}/A * \rho * \upsilon^2/2 \quad \text{(Pa)} \tag{1}$$

where

f Chezy Darcy coefficient of friction
ρ Air density (kg/m^3)
Per   Airway perimeter (m)
υ Air velocity (m/s)
A Area (m^2)
L Length (m)

This is a form of the Chezy-Darcy (Darcy-Weisbach) equation applicable to circular and non-circular airways and ducts. The Chezy-Darcy coefficient of friction (dimensionless) varies with respect to Reynolds Number, the trend of which is plotted on the Moody diagram. The Chezy-Darcy equation was adapted by J. J. Atkinson to give the following, commonly used, Atkinson Equation [6]:

$$P = k * L * \text{Per}/A * \upsilon^2 \quad \text{(Pa)} \tag{2}$$

The k factor is a function of air density and is computed as the product of the Chezy-Darcy coefficient of friction and the air density, divided by a factor of two. Since the Chezy-Darcy coefficient of friction is dimensionless, the k factor has the units of density (kg/m^3). The Atkinson equation may be expressed in terms of the Atkinson resistance (R) for the airway, where [6]:

$$R = P/Q^2 = k * L * \text{Per}/A^3 \quad \left(\text{Ns}^2/\text{m}^8\right) \tag{3}$$

The first section of this equation, relating frictional pressure drop and quantity to resistance, is known as the Square Law. This important relationship is used to establish resistance from measured pressure and quantity data. The second section of the equation is used to determine resistance from typical k factors and known or proposed airway geometry. It should be noted that the frictional pressure drop term in the Square Law is directly proportional to air density, as is the k factor, which is the combination of the friction factor, air density and constants in the Chezy-Darcy equation. Hence, the k factor that is applied must be adjusted for actual mine air

density. The *k* factor is not constant for a given airway, but varies with Reynold's Number. However, in mine ventilation, it is normal to assume that the *k* factor is constant, regardless of the flow regime. This is because, for fully turbulent flow (which is typically the case in mine ventilation), the friction factor is a function only of the relative roughness of the airway. The relative roughness of the airway is defined as the height of the airway asperities (*e*) divided by the hydraulic mean diameter [6]:

$$d = 4A/\text{Per} \tag{4}$$

The selection of appropriate friction factors is a critical component of mine ventilation planning. Resistance values for future mine openings are determined by applying a suitable friction factor against proposed airway geometry. It is important to understand the source and specific conditions associated with the friction factors [6].

Regular measurements of airflow and pressure were undertaken. Resistances were evaluated from measured pressure and airflow data using the Square Law relationship (Eq. 3). The airflow surveys consisted of the measurement of mean air velocities and airway cross-sectional areas at the predetermined locations. A rotating vane anemometer attached to an extendible rod was used to traverse the airways for measurement of the mean air velocity [6].

The airway cross-sectional areas were measured using laser distance measurement with typically three width and three height measurements per cross section. Airway obstructions were measured, recorded and subtracted from the gross cross-sectional area. The air quantities at each station were computed as the product of the air velocity and the airway cross-sectional area. Frictional pressure drops were determined using the gauge-and-tube technique for all lateral airways and ramps. The gauge-and-tube (or trailing hose) method allows direct measurement of frictional pressure differentials using a digital manometer connected into a length of tubing, the ends of which are connected to the total pressure tappings of pitot-static tubes [6].

Measured airflow data used in computerized ventilation model for optimization of the mine ventilation networks [7].

3   Results and Discussions

3.1   Ventilation Financial Optimisation

Based on the latest mine ventilation system surveys, a computerized model was developed for simulation processes aimed to provide with sufficient amount of fresh air deep horizons. The principal objectives of the ventilation design were to remove the diesel fumes from mechanized mobile equipment and remove blasting fumes from the workings and provide for a reasonable re-entry period. Ventilation simulation has been carried out using 'Ventsim' software.
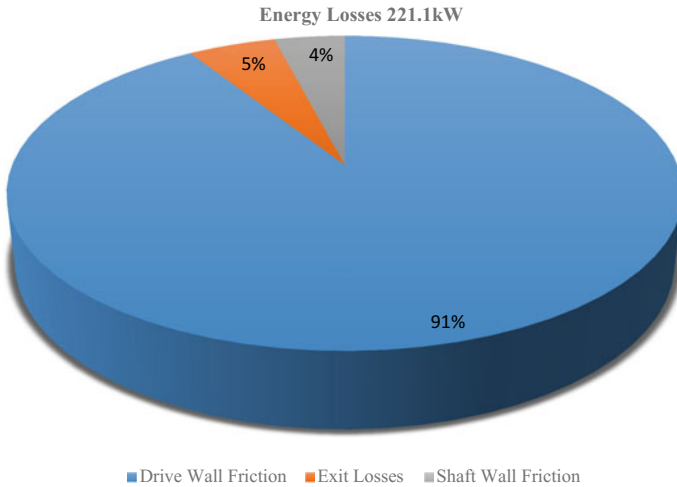
Fig. 1 Air pressure loss diagram

Calculated airflow requirements take into account the mining fleet. Accepted by Kazakhstan's mining regulations [1], the method of determining ventilation requirements considers that the removal of diesel fumes is based on a diesel dilution rate of 5 m^3/min/hp of diesel engine horsepower. Calculations used the entire fleet with their modelled availability and utilization. To support the proposed fleet in deep horizons, a primary circuit airflow was calculated to be 118 m^3/s.

Simulated intake from Shaft#1 delivered around 118 m^3/s of fresh air from the surface to the bottom of deep horizons. There were three regulators installed at the workshop level to control air movements to provide fresh air for the loading process and to place the refueling bay and welding bays under direct exhaust ventilation. A total of 18 m^3/s was exhausted directly to the return from the workshop level. The remaining fresh air from the Shaft#1 fed the production levels below. The ventilation system for the production areas did not reuse air, but instead exhausted the air from each footwall drive extremity after it was used in the ore drives.

Simulated network summary produced 272 airways with the total lengths of 12,744 m. The existing ventilation network was simplified by excluding closed airflows in abandoned mining areas. Results of the existing ventilation network simulation are listed and in Figs. 1 and 2.

Air pressure losses diagram is shown in Fig. 1. Air pressure losses were calculated to be approximately 221.1 kW from which 9.3 kW were losses incurred in Shaft#1 wall friction, 201.5 kW losses were in drives' wall friction, 10.2 kW in exit losses and 0.1 kW in shock losses (Fig. 1).

Input power electrical is 317 kW from which electric energy losses on pressure makes 19.6 kW and the fans efficiency losses—95.6 kW. Total pressure loss was about 1840 Pa as demonstrated in Fig. 2.
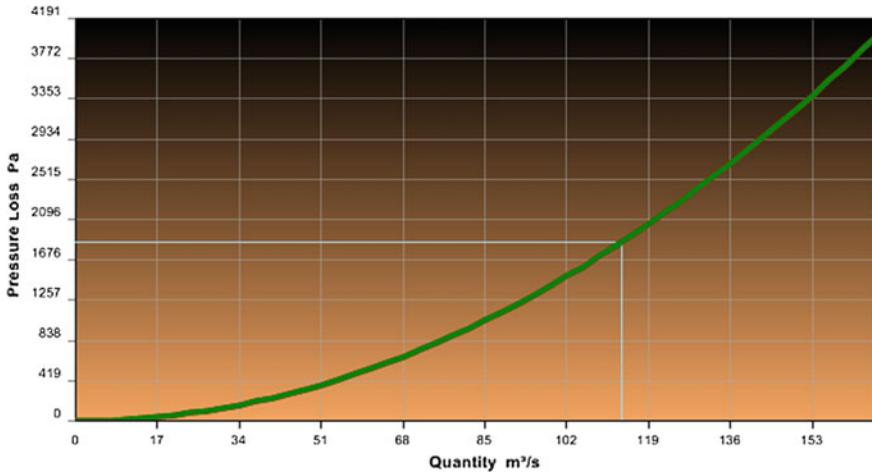
Fig. 2 Total pressure loss

3.2 Ventilation Financial Optimisation

Financial optimization was analyzed using 'Ventsim' software and showed that fourteen airways could be optimized. The optimization showed potential savings of approximately US\$ 355k for the following seven years. Optimized airways provided US\$ 595k in power savings (140 kW) discounted 10% and fans capital cost savings of about US\$ 124k. To achieve these savings, a capital investment will be required of about US\$ 366k for mining developments (increasing cross-sections for the existing incline, some areas of the ramp and other drifts). The most significant savings can be produced on the incline within a length of 450 m and on a part of the ramp within a length of 124 m. Financial simulation results propose to increase the incline cross-section by 3.7 m^2 to give potential annual power savings of about US\$ 70k and to increase cross-section by 5.2 m^2 for part of the ramp, which would generate annual power saving of about US\$ 38k.

The circuit illustrated in Fig. 3 is a screenshot from 'Ventsim' software after the financial simulation and with optimized airways cross-sections.

As a result of the financial ventilation optimization, the air pressure losses were made about 129.4 kW from which 9.3 kW losses were generated due to Shaft#1 wall friction, 115.4 kW losses due to drives' wall friction, 4.6 kW due to exit losses and 0.1 kW due to shock losses.

Input power electrical generated 207.8 kW from which the electric energy losses on pressure were 15.0 kW and the fan efficiency losses of 78.4 kW. Total pressure loss was about 1080 Pa.

In comparison with results for the existing ventilation network before the financial simulation, the energy losses for the optimized ventilation network were significantly decreased.

Fig. 3 Optimized ventilation network

Thus, the financial simulation estimated the optimum ventilation infrastructure size, where high-cost airflows were optimized by taking into consideration mining cost and ventilation operating costs.

3.3 Financial Risk Analysis

Preliminary estimations showed that VOD could save for the mine were about 23% of annual power cost. Savings resulted from improving ventilation system efficiency by reducing airflow in areas without mining activity and redistributing existing ventilation capacity. At the same time, there should be some capital investments based

Fig. 4 IRR distribution for the existing ventilation network

on variable speed fans, automated regulators, construction material, control system, communications, and tracking infrastructure. Financial model was produced taking into account capital and operational cost for options of the existing ventilation network and the optimized ventilation network with the implementation of VOD. The VOD capital cost was estimated at a conceptual level.

The optimized ventilation network with the implementation of VOD option demonstrated 3.1% higher IRR in comparison to the current ventilation network.

Stochastic modelling of investment analysis was examined. A major variability was in the electricity pricing. A triangle distribution was used for each price each year of the mine life. No escalation was applied to the price. After simulation of 1000 iterations, the existing ventilation network probability distribution of IRR value was between 10.8 and 16.2% at 90% confidence level and the mean was 13.6% (Fig. 4).

Optimzed ventilation network with VOD showed IRR value between 15.2 and 18.1% at 90% of confidence level and the mean was 16.7% (Fig. 5).

The optimized ventilation network with VOD gives probability distribution with a stronger confidence level of getting higher IRR than the existing ventilation network.

4 Conclusions

Mine ventilation system surveys were undertaken to develop a computerized model for simulation processes to provide with sufficient amount of fresh air deep horizons in the gold mine. Based on the completed computerized ventilation model, the financial simulation estimated optimum ventilation infrastructure size, where high-cost airflows were optimized by taking into consideration mining cost and ventilation
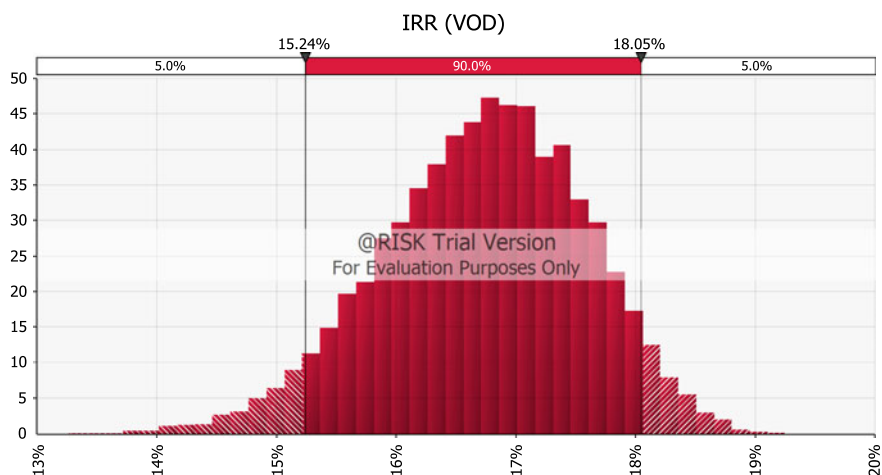
Fig. 5 IRR distribution for the optimized ventilation with VOD

costs. Results of ventilation financial simulation were used to analyze financial risks. Financial model was produced taking into account capital and operational cost for options of the existing ventilation network and the optimized ventilation network with use of VOD. The optimized ventilation network with VOD option demonstrates 3.1% higher IRR than the existing ventilation network option.

Stochastic modelling of investment analysis was undertaken and a major variability used was electricity pricing. A triangle distribution was used for each price each year of the mine life. As a result, the optimized ventilation network with VOD generated probability distribution with a stronger confidence level of getting higher IRR in comparison to the existing ventilation network. Financial risk analysis recommends implementing automated ventilation control for saving energy costs.

References

1. Kazakhstan mining regulations requirements for underground mine ventilation http://egov.kz/cms/en/law/list/P090001939_
2. Kocsis, C.: New ventilation design criteria for underground metal mines based upon the "life-cycle" airflow demand schedule (2009)
3. Paajanen, S., Trang, T.: NRG1-ECOTM—Impact on energy savings and air quality (2010)
4. Lyle, G., Bullock, K., Dasys, A., Hardcastle, S.: Ventilation on demand project. In: MDEC Conference (2010)
5. Palisade @Risk software, version 7.5 (2018)

6. Duckworth, I.J., Loomis, I., Prosser, B.: Fifteen years of resistance data collected at Freeport Indonesia. In: 14th United States/North American Mine Ventilation Symposium, 2012—Calizaya & Nelson© 2012, Department of Mining Engineering, University of Utah
7. Sabanov, S.: Determining ventilation system model inputs from field test work in the oil shale mine. In: The Australian Mine Ventilation Conference (2017)

Part II
Mine Development

Fundamental Study of Stope and Barrier Pillar Stabilities by Using Cut and Fill Method for Redevelopment of Rest Gold Mine, Myanmar

N. Naung, H. Shimada, T. Sasaoka, A. Hamanaka, S. Wahyudi and M. Pisith

1 Introduction

Mineral consumption is gradually increasing as the global standard of living increases and mineral demand will be largely concentrated in developing countries experiencing economic development progressively. This implies mineral extraction from greater depths both surface mining and underground mining. However, underground mining will become more important in coming decades as environmental issues make surface mining less attractive. After a period of mining, easily accessible shallow mineral resources are being mined out and the deposits of rest mine are left in deeper regions. Therefore, underground mining continues to progress into deeper levels in order to fulfill the mineral supply. Accordingly, stress condition in deeper mine will be greatly changed and the mining process would be more complicated when it is operated for the redevelopment of rest mine projects. Without doubt, the stability of underground openings is a major concern for the safety and productivity of mining operations. Mine development instability can result in production delays, loss of reserves, as well as damage to equipment, and injuries. Therefore, this paper outlines the fundamental study of stope and barrier pillar stabilities for the redevelopment of rest gold mine, National Prosperity Gold Production Group Limited (NPGPGL) underground gold mine in Myanmar, as a case study.

The instability of underground excavation depends on the behaviors of the surrounding rock mass. Different rock types have different characteristics parameters that influence their mechanical behaviors. Therefore, knowledge and understanding of rock mass condition are essential for the stability of underground excavations. The first step for describing rock mass is to examine rock mass properties determined by lithology, laboratory tests, and field observation data. The second step is to determine the geotechnical information of rock mass for the purpose of rock engi-

N. Naung (✉) · H. Shimada · T. Sasaoka · A. Hamanaka · S. Wahyudi · M. Pisith
Department of Earth Resources Engineering, Kyushu University, Fukuoka, Japan
e-mail: naung15r@mine.kyushu-u.ac.jp

neering design such as numerical modeling, analytical calculation, etc. Considering the importance of rock stability in stope opening, field observation for lithology, geology and mining system at NPGPGL underground gold mine was conducted, and laboratory experiments were carried out to get the physical properties of rock mass, and the fundamental study was carried out by using numerical simulations.

2 Case Study

2.1 Location

NPGPGL at Modi Taung is situated approximately 150 km southeast of Mandalay and 385 km north of Yangon, in the eastern part of the Yamethin Township, central Myanmar as shown in Fig. 1. The company is operating in the southern part of Block 10 area where the exploration works were previously conducted by Ivanhoe Myanmar Holding Ltd. (IMHL), a Canadian mining company, who acquired the exploration/mining lease from the government from August 1996 to August 2005. NPGPGL started this gold mine on September 2011 with total mine lease area of 24.71 km^2. The mine is located approximately 1300 m above sea level and it takes around three hours from Nay Pyi Taw, the capital city of Myanmar by car and the road conditions vary from sealed roads to off roads.

2.2 Regional Geology

Block 10 concession in central Myanmar has identified a 100 km^2 gold district, the Modi Taung—Nankwe district, with feature characteristic of slate-hosted mesothermal quartz–gold vein deposits as shown in Fig. 2. The deposit is hosted in the sedimentary units of the Mergui Group, which is composed of two dominant sedimentary formations. The lower part consists of massive to laminated mudstone, sandstone, rare limestones, and channel-fill pebbly wackes while the upper part includes several polymict conglomerates [1].

2.3 Host Rock Lithology of NPGPGL

Veins at Modi Taung gold mine are hosted by four main lithologies: mudstone, sandstone–siltstone, limey sandstone or limestone, and igneous intrusions. Mudstones are the predominant rock type in all vein system but sandstone occupies short segments, and veins tend to occur along the inclined interface between sandstone and mudstone. Their competence and hardness increase with depth from soft clay
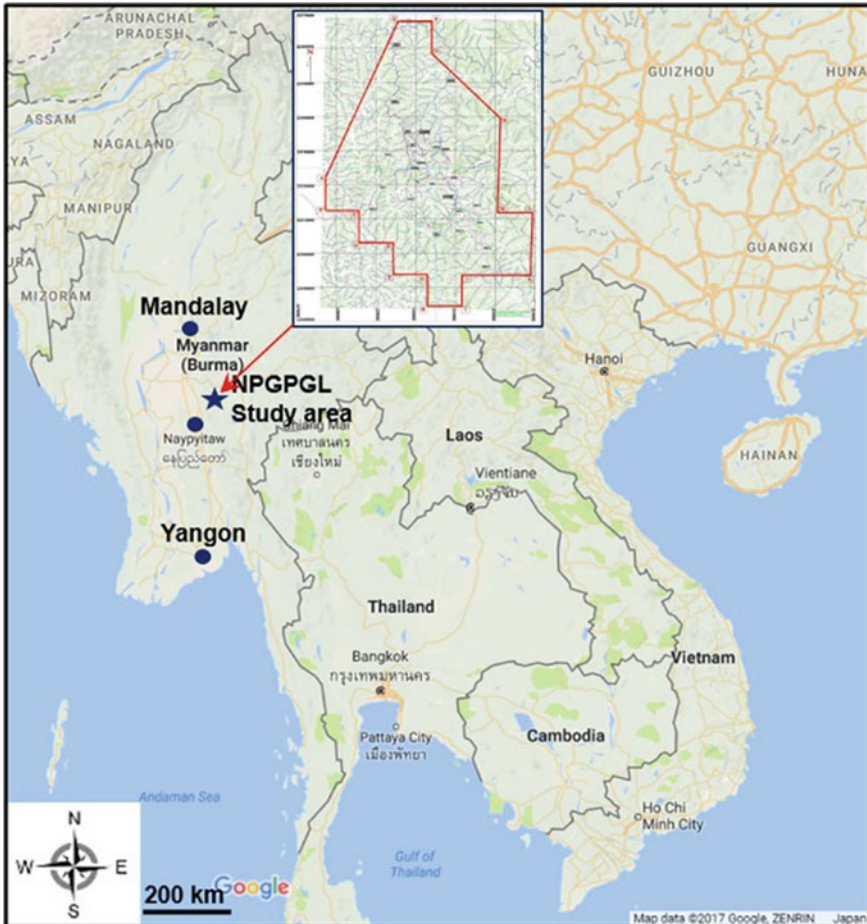
Fig. 1 Research mine site's location map

immediately beneath soil cover to a hard rock that is tough and competent with the exception of moderate hardness near and below the base of the oxide zone. Sandstone and siltstone are mostly silicified and cut by quartz stockworks, forming quartzite. They are mostly intensely fracture, and hence brittle. Ground conditions are poor in Shwesin vein system and within 60 m from the surface where partial oxidation has occurred [2].

At NPGPGL gold mine, Htongyi Taung and Sakangyi vein systems are hosted by mudstone, while in the Shwesin, Sakangyi and Momi Taung systems host rocks are predominantly mudstone or siltstone and the rest sandstone [1]. Veins in the east of the least area are dipping steeply to the west, while veins in the west are dipping steeply to the east. Vein width varies with elevation and ranges between centimeter and meter scale [3]. The detail geological structure of NPGPGL is shown in Fig. 3.
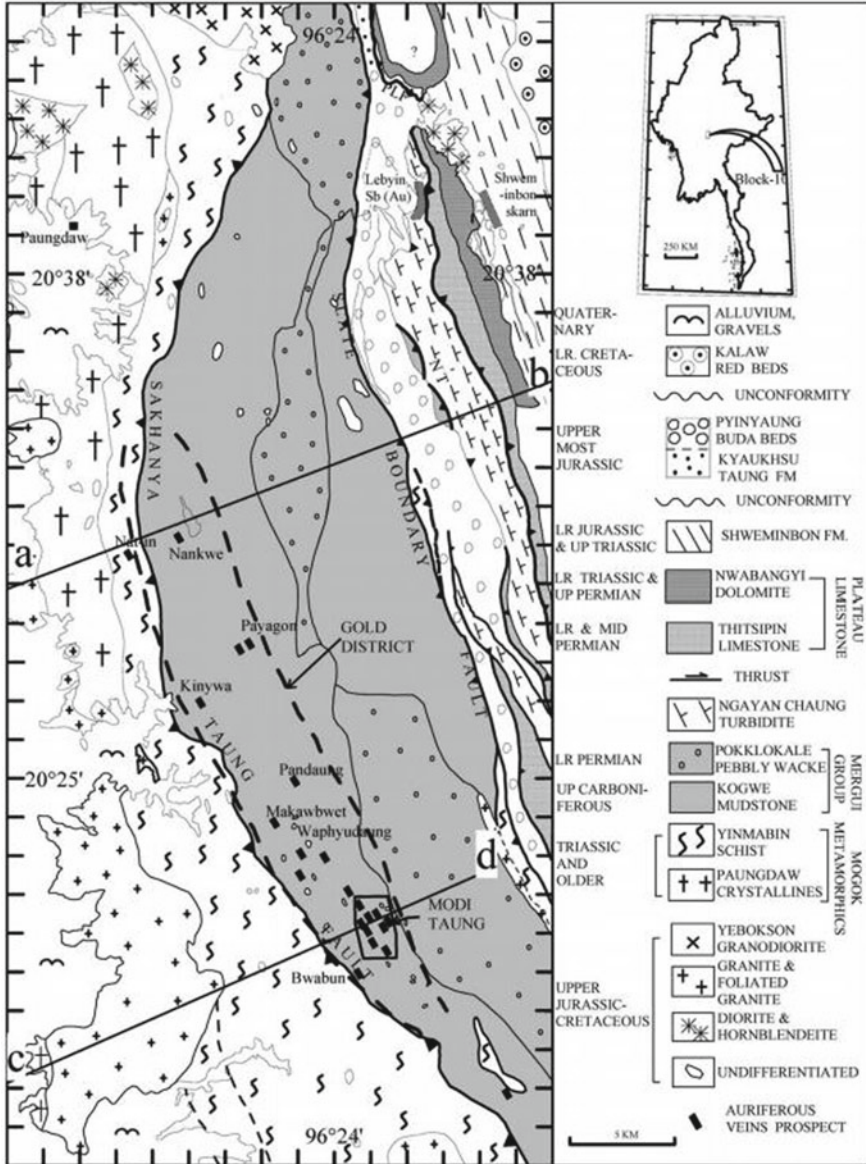
Fig. 2 Simplified geology map of Block 10 concession [1]
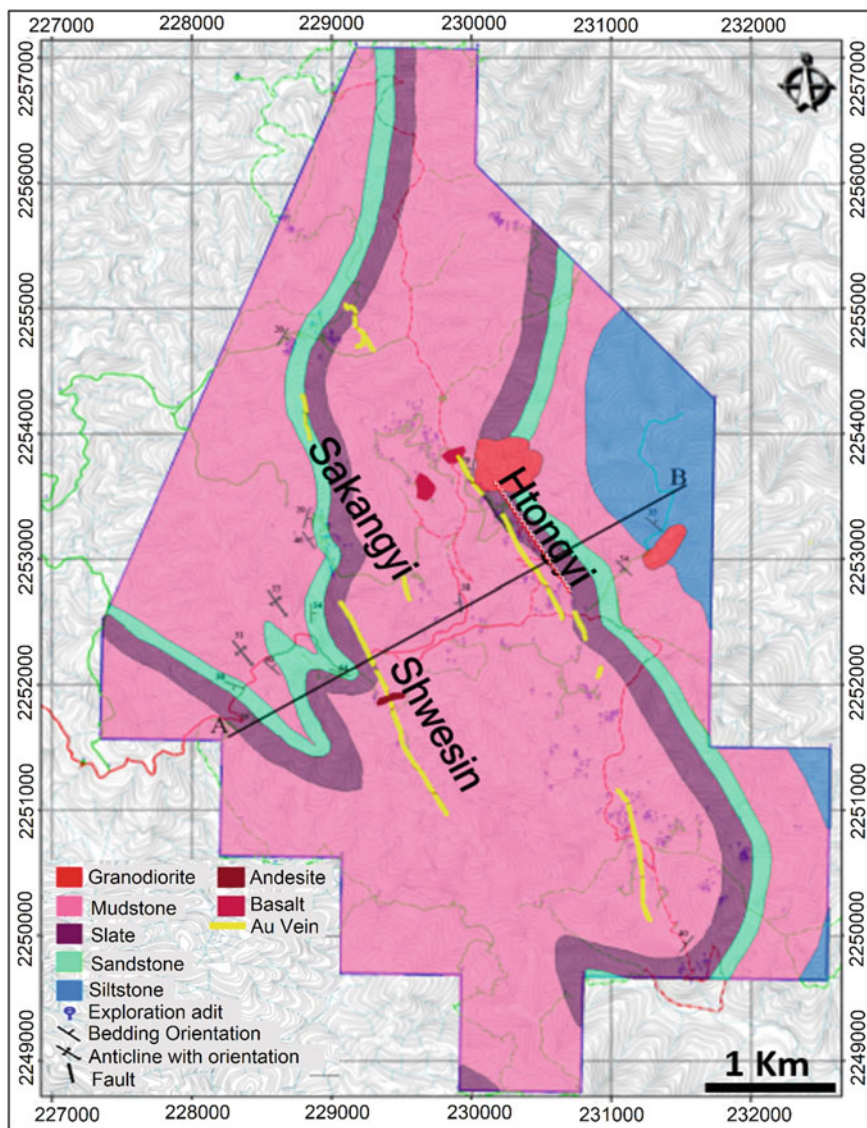
Fig. 3 Geological map of NPGPGL [3]

3   Field Observation

3.1   Rock Mass Condition

Currently, most of the shallow parts of NPGPGL are already mined-out and mining activities are going to continue to progress to deeper levels in order to fulfill the target ore production. Therefore, rock mass condition at deeper area should be investigated for the stability of underground excavations. From the borehole data, the RQD and depth from NPGPGL gold mine are shown in Fig. 4 and the correlation between RQD percentage and rock mass quality is shown in Table 1. Besides the RQD condition of the rock mass, some activities such as discontinuities, persistence, aperture, rock roughness, and weathering of rock are conducted to complete full estimation of rock mass condition. Furthermore, rock mass parameters that obtained from laboratory experiments are shown in Table 2 and the uniaxial compressive strength of intact host rock and vein from NPGPGL gold mine are 148 and 140 MPa, respectively.

According to these intact rock parameters, it can be seen that the rock mass strength from NPGPGL gold mine is strong. However, without the consideration of geological structure, rock mass properties are not properly applied for any form of analysis for the design of slopes and underground excavations. Regarding this case,
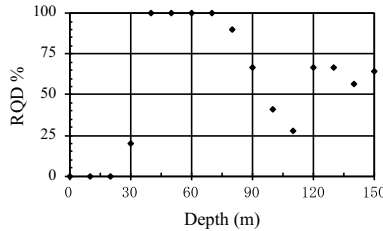
Fig. 4   Relation between RQD and depth of NPGPGL gold mine

Table 1   RQD classification index

RQD (%)	Rock mass quality
<25	Very poor
25–50	Poor
50–75	Fair
75–90	Good
90–100	Excellent

Table 2   Intact rock properties obtained from laboratory experiments

	ρ (kg/m^3)	E (MPa)	v (-)	σ_t (MPa)	φ (deg)	C (MPa)
Host rock	2717	19,000	0.25	10.4	58	18.5
Vein	2667	12,000	0.22	3.8	71	11.1

Fig. 5 Rock mass condition in underground tunnel showing joints and cracks

Table 3 Rock mass properties evaluated with geological conditions

	ρ (kg/m^3)	E (MPa)	v (-)	σ_t (MPa)	φ (deg)	C (MPa)
Hanging wall	2670	3786	0.23	0.035	42	0.904
Footwall	2717	3786	0.25	0.065	38	0.806
Vein	2667	3374	0.22	0.028	42	0.871

the Geological Strength Index (GSI) introduced by Hoek et al. [4] is very essential to estimate the rock mass strength for different geological conditions. From the field observation at NPGPGL gold mine, many cracks and joints within rock mass are found in underground tunnels and stopes as shown in Fig. 5. Additionally, heavy rainfall is one of the causes of weathering of the rock mass. The rate of water charge increases after periods of heavy rain which is common for this area. This meteoric water interacts with the surrounding rocks which result in weathering of host rocks, leading to strength reduction of host rocks. All of these conditions will give effect to the instability of underground excavations and should be paid attention in order to prevent the ground collapse.

Consideration of rock mass condition including several factors such as RQD, joint spacing, condition of joints, and weathering, the evaluation of NPGPGL rock mass properties from intact rock properties are shown in Table 3.
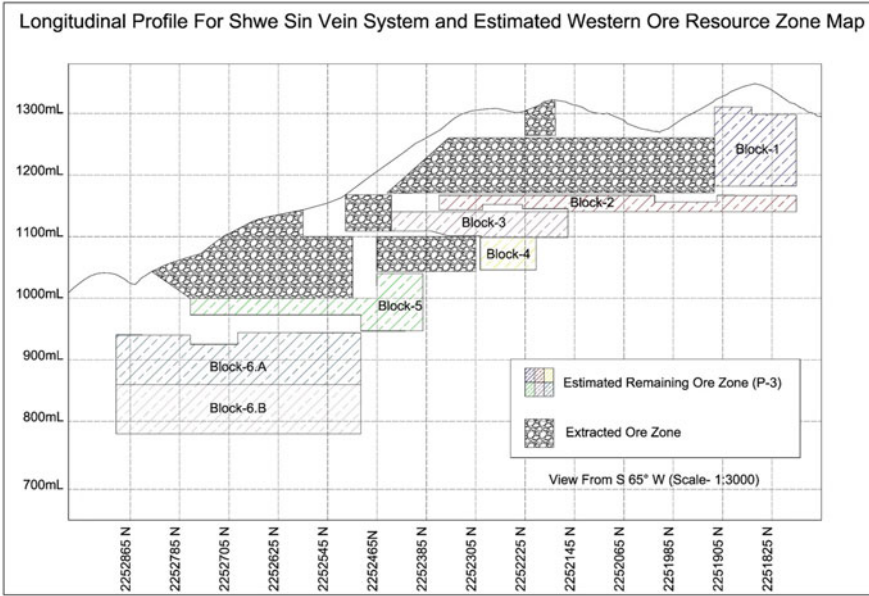
Fig. 6 Mine plan at Shwesin vein system. *Source* NPGPGL

3.2 Mining System

As described above, the accessible shallow area is already mined out at NPGPGL and the deposits of rest mine are left in deeper regions. Therefore, the company is planning to mine out the deeper area at Shwesin vein which is separated into 6 blocks, namely from block 1 to 6. The overall mine plan is illustrated in Fig. 6.

The company adopts open stope mining and overhand cut and fill method to extract the minerals at Shwesin vein system. The waste rocks from the excavation are only using to both fill the stope and provide permanent wall support for the lower mine out cavity. Vein width varies with elevation and ranges between centimeter and meter scale. Vein dipping is more than 50 degree, and Vein orientation within Shwesin vein system and vein widths with elevation at NPGPGL gold mine area are shown in Figs. 7 and 8 [3].

4 Numerical Modeling for NPGPGL Gold Mine

The stability of stope and barrier pillar for the redevelopment of rest gold mine in deeper regions at NPGPGL was carried out in different numerical models by using the FLAC3D code. FLAC3D is explicit finite difference code that is developed for analyzing stress and deformation of mining and tunneling problems conducted in
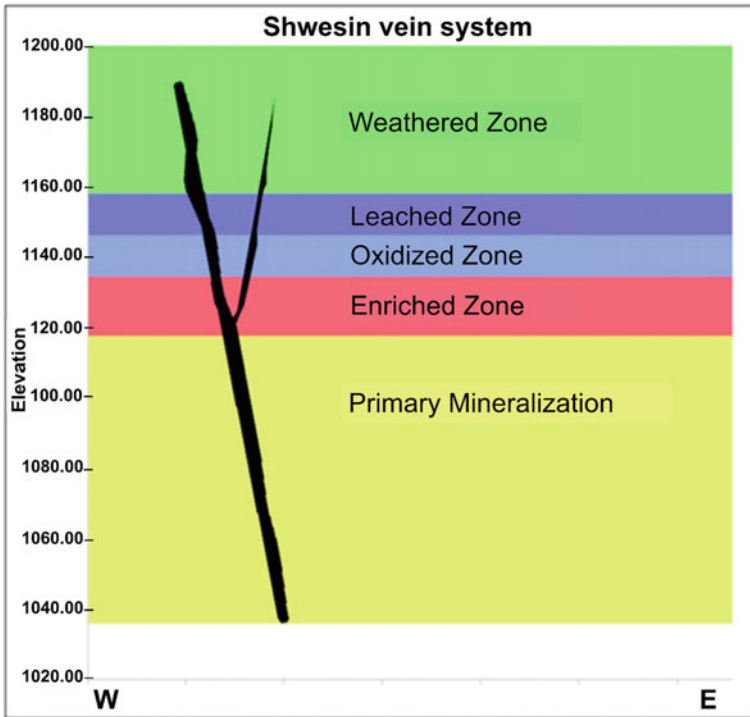
Fig. 7 Shwesin vein orientation system [3]
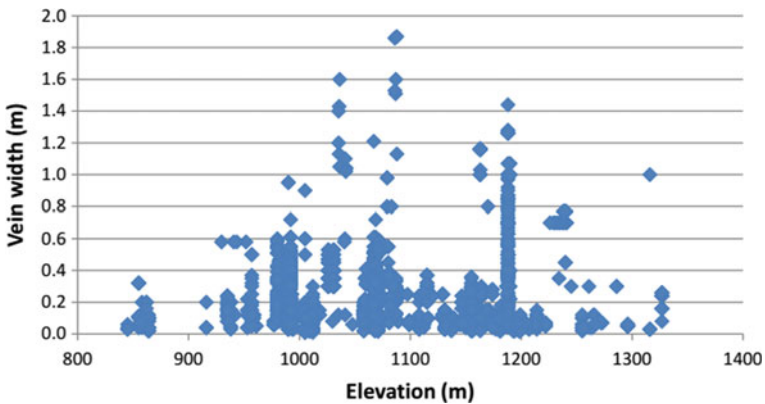
Fig. 8 Vein widths plotted against elevations at NPGPGL gold mine [3]

both soil and rock. In this paper, the numerical simulations were modeled in order to understand the failure conditions of new stope opening due to the effects of previous mined-out area, the stability analysis considering different barrier pillars size (2, 2.5,
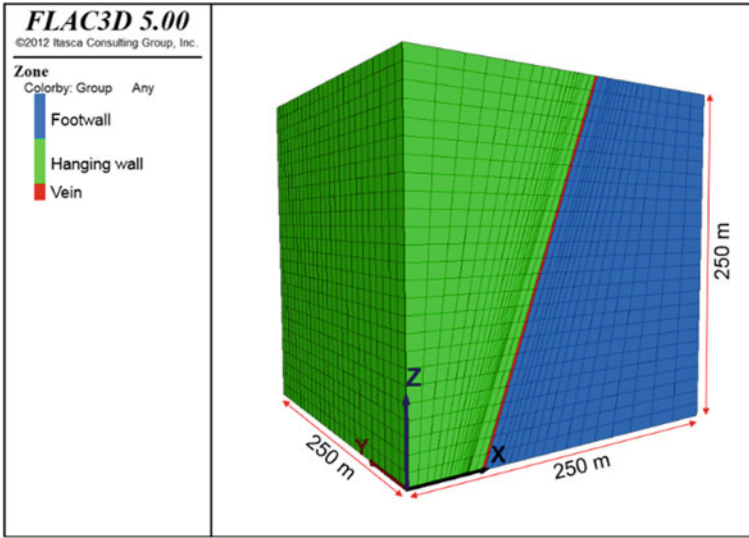
Fig. 9 Numerical model

3, 3.5 m) and various vein dips (60°, 70° and 80°). All the numerical models' size is 250 m × 250 m × 250 m as shown in Fig. 9. As described in host rock lithology of NPGPGL, the slaty mudstone is a dominant rock type in the NPGPGL gold mine, and therefore, the hanging wall and footwall are assigned as a homogenous model for simplification. The mechanical properties of host rock and vein are given in Table 3. Moreover, to obtain the more precise result of the rock failure distribution, the smaller mesh size was selected around the excavation area.

4.1 Case Study

In this research, the case study from Shwesin vein system at NPGPGL gold mine is presented for the overhand cut and fill mining from the lower slice of the vein of block 2 as shown in Fig. 10. Block 2 is the planned mine area with 24 m height that is assigned between adit 5 and adit 8 of the Shwesin vein. The previous mined-out area with 100 m height is overlaying above block 2 and the total overburden above block 2 is 150 m. This case study is investigated for the stability of the current stope opening in block 2 not only due to its own induced stress but also the effect of overlaying mined-out area. The stope dimension is 2.5 m in height and 2 m in width and the stoping sequence takes place from the lower slice to upwards direction. During the stope mining, the waste rocks from the excavation are used to fill the stope and it provides a working platform for the miners when the next slice is mined. For
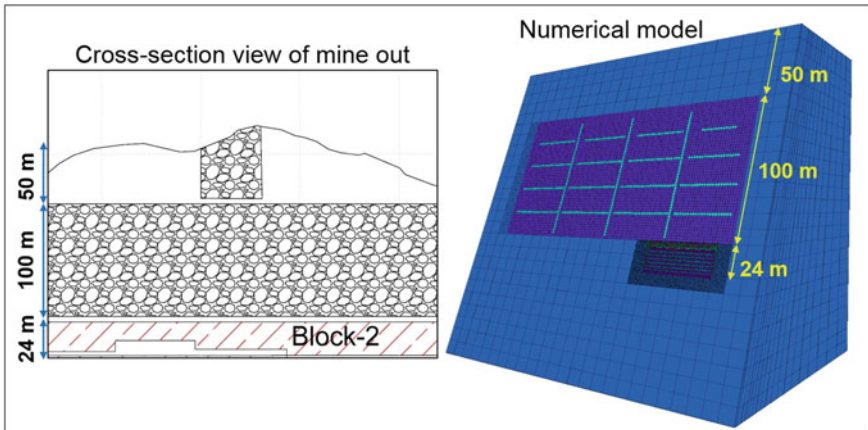
Fig. 10 Overhand cut and fill mine plan at Block 2 at Shwesin vein

preparing stope arrangements, steep compartment wooded raises are developed from the main roadway to provide ore/waste passes and manways.

4.2 Failure Evaluation Criterion

Mining objective is to recover as much ore as possible from the vein. However, men and machines work in the advancing stopes and their safety must be ensured. Potential hazards in the stopes are rock falls from the stope's roof and buckling failures in the hanging wall and footwall. In order to stabilize the stope, a failure criterion must be selected. A common problem in mine excavation engineering is estimating the stability of designed stope to achieve a minimum required value of Factor of Safety under which roof and wall are considered as unstable. A factor of safety of 1.3 would generally be considered for a temporary mine opening while a value of 1.5 to 2.0 may be required for a permanent excavation [5]. The selection of an appropriate factor of safety is based on engineering experience and field observation. In this research, the Mohr–Coulomb failure criterion is adopted as shown in Fig. 11 and elasto-plastic behavior of the rock mass is used.

The strength factor (factor of safety) is calculated by dividing the strength of rock mass by the induced stress of stoping activities to provide a basis of stability assessment as follows:

$$\text{Strenght factor} = \text{Rock mass strength/induced stress}$$
$$= \left\{ c \cos \varphi + \left[(\sigma_1 + \sigma_3)/2 \times \sin \varphi \right] \right\} / \left[(\sigma_1 + \sigma_3)/2 \right] \quad (1)$$
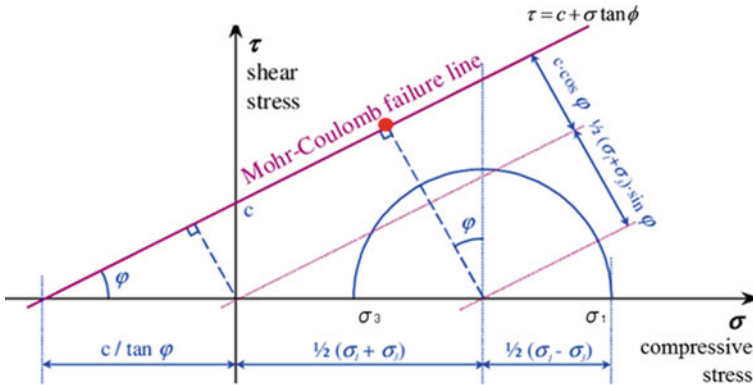
Fig. 11 Mohr-Coulomb failure criterion

Strength factor (safety factor) of 1.3 is adapted for temporary stope mining. The stope was considered to be in a stable condition when Mohr–Coulomb strength factor is greater than 1.3. On the other hand, the failure of stope is assumed to occur when the strength factor is less than 1, and the unstable condition was assigned between the strength factor value 1 and 1.3.

4.3 Result and Discussions

Redevelopment process of new open stoping under previous mining regions can affect in high levels of unplanned dilution around the stope room not only due to blast-induced over-break but also the stress redistribution of the overlaying mined-out regions. In general, no one can estimate the rock mass is stable or not without numerical simulations. Determining the tunnels and stopes are stable or unstable should be based on yield zones from numerical simulations. Thus, numerical simulations using FLAC3D have been observed to understand the effect of previous mined-out regions, the stability of barrier pillars with different heights and the failure condition of stope opening due to various vein dips. The explanations of failure terms given in the legend in FLAC3D are as follows:

– "none" indicates no-failure zone,
– "shear-n" indicates the region failed under shear loading and failure process is still in progress,
– "shear-p" indicates the region failed under shear loading and failure process is stopped due to lowered amount of shear forces,
– "tension-n" indicates the region failed under tensile loading, and failure process is still in progress,
– "tension-p" indicates the region failed under tensile loading, and failure process is stopped due to the lowered amount of tensile forces.
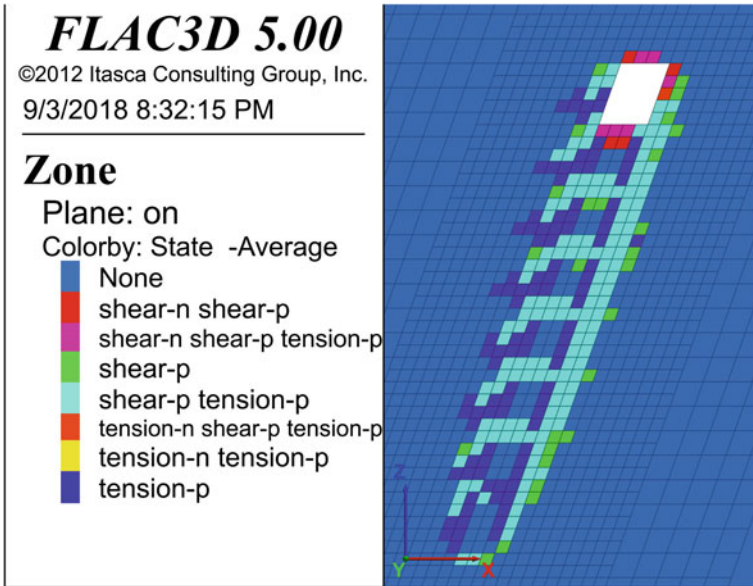
Fig. 12 Failure zone developed without previous mining effects

4.3.1 Effects of Previous Mined-Out Regions at Shwesin Vein System

First of all, numerical simulations are carried out with the aim to understand the failure zone and stability of stope due to the effects of previous mined-out regions. Stope mining activities from numerical simulations are modeled from the lower slice of the vein to upwards direction and the mined-out stope is backfilled by using waste rock from the excavation. Figure 12 shows the failure zone which occurred around the stope without previous mining effects and Fig. 13 shows the failure zone developed with previous mining effects. Based on the simulation results of Fig. 12, the failure zone around the stope is increasing steadily as the stope progressing move towards upper slices. These trends tell that failure zone of current stope is accumulated to the next stope. Compared with the failure condition with the previous upper mined-out effects as shown in Fig. 13, the failure characteristics of surrounding rock masses in Fig. 13 results are larger than those in Fig. 12. The statement can be drawn from these two results that the redistributed stresses from upper mined-out regions are surely propagated to the current stope mining activities. As a result, the development of failure zone of current stope room is increased not only due to its own induced stress but also the redistributed stresses of previous mined-out regions.

It can be clearly seen in Figs. 14 and 15 that show the increasingly unstable regions of current stope with the contour color code as mining activities continued into the upper slices. These results tell that decreasing strength factor makes increasing the unstable regions around the stope opening. Figure 16 proved this description that
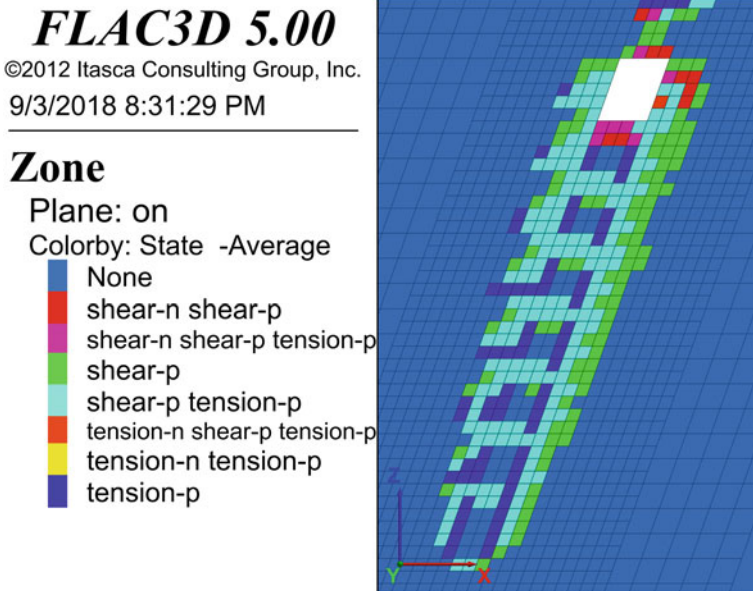
Fig. 13 Failure zone developed with previous mining effects

strength factor indicator is gradually decreasing as the mining steps increase. The monitoring point for these indicators is placed 0.5 m above the center of stope's roof. Additionally, it can also be seen that the instability of the barrier pillar at uppermost stope with the effects of previous mined-out regions became more severe when the stope mining reaches to the uppermost level (i.e. nearest stope to the upper mined-out regions). In this simulation, this barrier pillar is set to be 2 m between the final stope and upper mined-out regions. Therefore, the numerical simulations for the stability of barrier pillar are conducted to understand the possibility of unstable regions with different barrier pillars and determine the appropriate barrier pillar to avoid rock falls from the stope's roof.

4.3.2 Stability of Barrier Pillars with the Effects of Overlaying Mined-Out Regions

At Shwesin vein system from NPGPGL underground gold mine, the barrier pillar is broadly maintained 2 m between the top stope and overlaying mined-out regions. As explained in the previous section, the failure zone at the uppermost barrier pillar propagated to overlaying mined-out regions. Therefore, numerical simulations with different barrier pillar heights (2, 2.5, 3 and 3.5 m) were carried out in order to learn the stability of the barrier pillar of the top stope. Figure 17 shows that the failure condition of barrier pillar with different pillar heights and Fig. 18 indicates
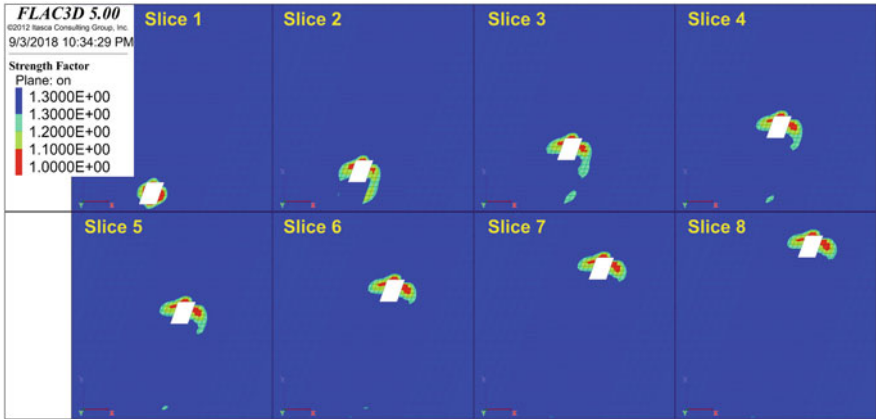
Fig. 14 Contour color of unstable area without the effect of previous mined-out regions
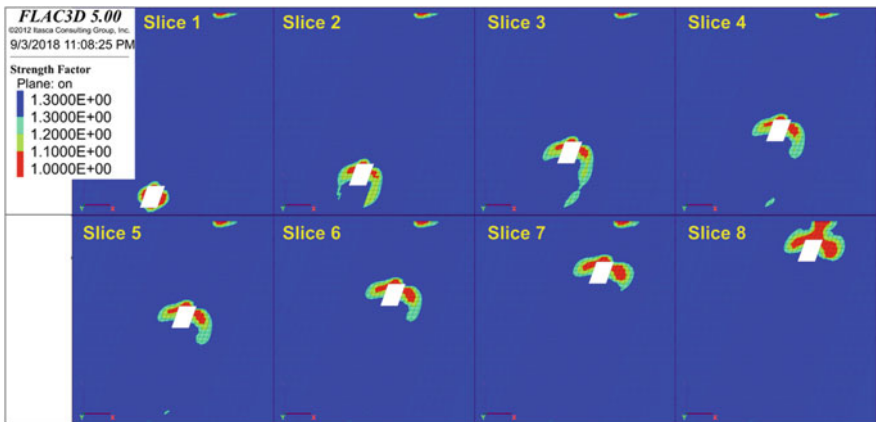
Fig. 15 Contour color of unstable area with the effect of previous mined-out regions

the unstable regions around the stope room shown by contour color code of strength factor. It can be seen that the failure zones and instability of top stope continue to the overlaying mined-out regions when the barrier pillar is set 2 m height, and decrease gradually when the barrier pillar increase to 2.5, 3 and 3.5 m height, respectively. According to these results, it can be seen that the unstable regions are still propagated to the upper mined-out failure zone when the barrier pillar height is set to 2.5 m height. However, this condition did not apply when the barrier pillars are 3 and 3.5 m height. Therefore, these results suggested that the barrier pillar between the top stope and overlaying mined-out regions should be maintained at least 3 m height in order to make sure to stabilize the stope and to prevent rock falls from the stope's roof and walls.
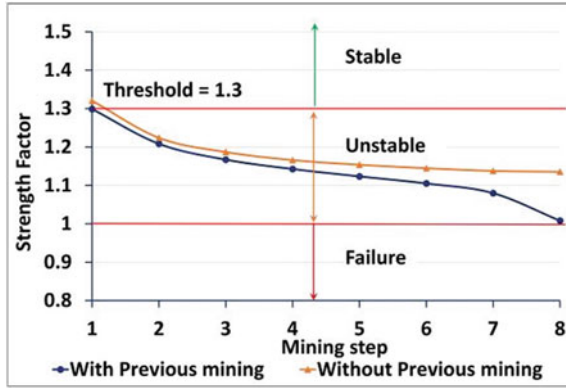
Fig. 16 Strength factor indicators at various mining steps
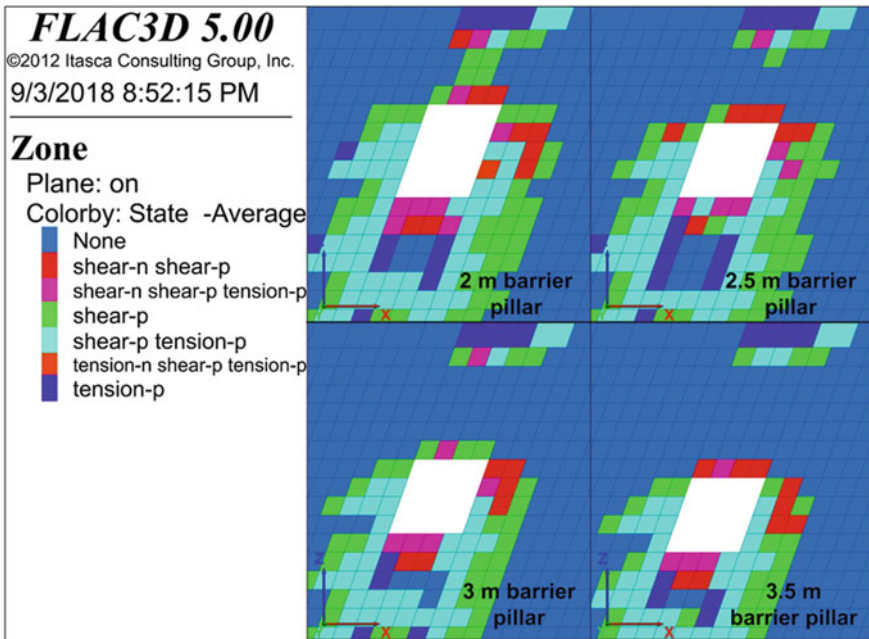
Fig. 17 Failure condition of barrier pillar with different pillar heights

4.3.3 Instability Due to the Effect of Various Vein Dips

Many mineral deposits can occur as steeply dipping narrow veins. As described above, vein dipping is more than 50° in this mine site. Numerical simulations with vein dip of 60°, 70° and 80° are carried out to understand stope and barrier pillar stability in various vein dips. The results of these simulations are given in Figs. 19
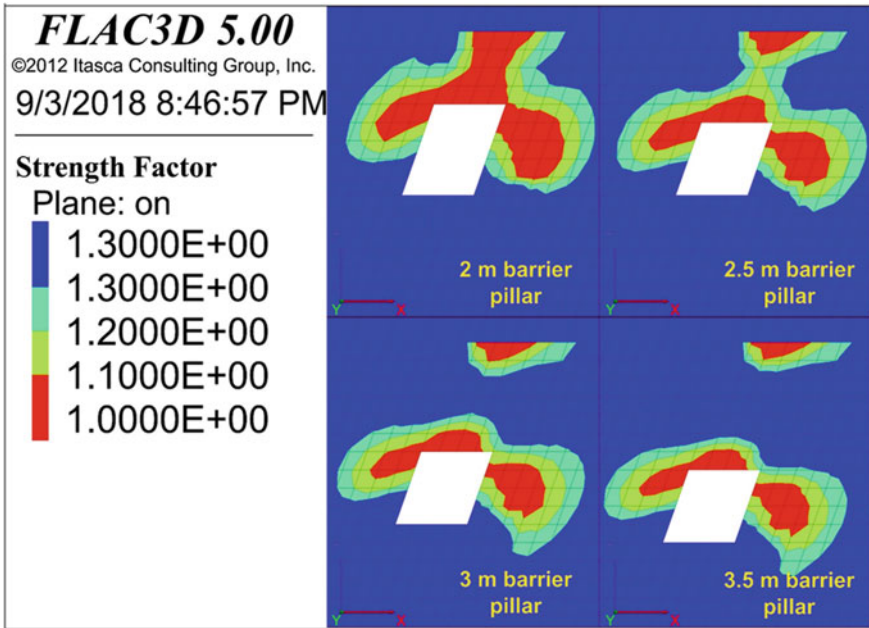
Fig. 18 Contour color of unstable area with different pillar heights
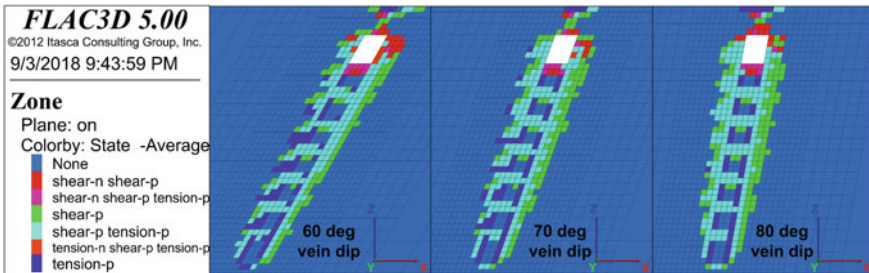
Fig. 19 Failure zones around the stope due to various vein dips

and 20. The result from Fig. 19 suggests that the failure conditions are more likely to occur with low vein dip, especially in hanging wall and footwall. On the other hand, the failure zones above the stope opening increase as the vein dip increase. Figure 20 shows the contour color code of unstable regions around the stope due to various vein dips. It can be seen clearly that the unstable regions are more severe in hanging wall and footwall with lower vein dip while the instability becomes more developed above the stope opening with steeper vein dip.
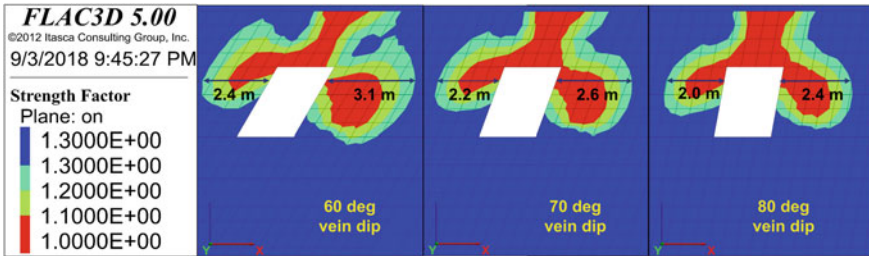
Fig. 20 Contour color of unstable regions around the stope due to various vein dips

5 Conclusion

As NPGPGL underground gold mine will continue to deeper regions for the redevelopment of rest gold deposit, the potential impacts from the overlaying mined-out regions to the new stope opening should be examined in order to stabilize the stope and barrier pillar in various mine conditions. Risk-index such as rock fracture, the effect of underground water, weathering and stress redistribution of the previous mined-out area, etc. will be subjected to the current stope mining activities. In this study, the stability of stope and barrier pillar of new opening under the effects of previous mined-out regions are investigated numerically with three-dimensional finite difference code software, FLAC3D. The analysis results indicated that the failure zone and instability of the surrounding rock mass of stope are increasing steadily as the stope progressing move towards upper slices and it will be propagated to the previous mine out regions. These conditions should be paid attention for underground mining under previous mining activities for the safety working environment. Additionally, the instability of the barrier pillar between the top stope and overlaying mined-out regions became more severe when the model is simulated with the effect of previous mined-out regions. This result suggested that the barrier pillar should be maintained at least 3 m height in order to make sure to stabilize the stope and to prevent rock falls from the stope's roof and walls. Furthermore, based on the simulations with various vein dips, the results highlight that the failure conditions especially in hanging wall and footwall are more likely to occur with low vein dip and it also increases above the stope opening as the vein dip increases. According to the above simulation results, suitable countermeasure arrangements is paramount to be prepared by considering the stability of stope mining activities under the effects of overlaying mined-out regions.

References

1. Mitchell, A.H.G., Ausa, C.A., Deiparine, L., Hlaing, T., Htay, N., Khine, A.: The Modi Taung-Nankwe gold district, Slate belt, central Myanmar: mesothermal veins in a Mesozoic orogeny. J. Asian Earth Sci. **23**, 321–341 (2004)
2. Ivanhoe Myanmar Holding Limited: Production sharing proposal, Modi Taung gold project, Myanmar. Unpublished (2003)
3. Erskine, T.R.: "Geology, Structure and Mineralisation Characteristics of the Modi Taung Gold Deposit, Myanmar", B.Sc Thesis. University of Tasmania, May (2014)
4. Marinos, V., Marinos, P., Hoek, E.: The Geological Strength Index: Applications and Limitations. Bulletin of Engineering Geology and the Environment **64**, 55–65 (2005)
5. Hoek, E., Kaiser, P.K., Bawden, W.F.: Support of underground excavations in hard rock. Taylor and Francis, p. 9 (2000)

Part III
Blasting and Fragmentation

Use of Geospatial Queries for Optimum Drilling and Blasting Practices in Surface Mining

M. Erkayaoglu

1 Introduction

Mining has an essential role in the sustainable development of the society as the demand for mineral reserves is continuously increasing. The equipment intensive nature of the mining industry is originated from the production cycle that depends on machines and manpower. Tracking the performance or the productivity of this equipment is of key importance for optimum production. Technology is a powerful potential for performance measurement and analysis as part of continuous improvement strategies [1]. Surface mining is responsible for the majority of the production of mineral reserves and relies on the efficient operation of mobile equipment. Data that represents the productivity and reliability of mobile equipment in surface mining has to be integrated into mine management.

Currently, the state-of-art techniques in data handling and visualization can be considered as being non-standard among the mining industry. Literature in this field is limited and a potential area that will be a popular research area for mining engineers and other disciplines in the near future. Although the amount and variety of data are considerably high due to the utilized equipment, the amount of data used in decision making is stated to be less than 1% [2]. This highlights the lack of data utilization in the industry and the lost opportunity related to production, maintenance, and safety. The IT infrastructure depends commonly on the type of equipment used on site and is improved when a new equipment, hardware, or system is integrated into the operation. The level of using technology varies between taking manual records and entering them to the existing IT infrastructure to more sophisticated and integrated data environments.

As the production in surface mining is conventionally starting from drilling and blasting, available technology, such as, high-precision GPS systems for operator

M. Erkayaoglu (✉)
Mining Engineering Department, Middle East Technical University, Ankara, Turkey
e-mail: emustafa@metu.edu.tr

guidance, and tracking drill hole accuracy can be used together with other operation-related data to achieve desired fragmentation on site [3]. A data source that has to be integrated into the drilling-related data in surface mining is blasting where explosive consumption could be tracked either manually or automatically in case bulk explosives are charged by trucks. Other technologies that are available on mobile equipment, such as the fleet management system, are also potential data sources of integration for a final objective of optimum drilling and blasting. The performance of drilling and blasting practices is commonly evaluated by fragmentation and this becomes crucial at surface metal mines due to the operation of a mineral processing plant. Various researchers investigated the impact of better fragmentation on the performance of downstream processes, in this case, mineral processing [4–7].

Therefore, the desired fragmentation can be considered as a demand from the mineral processing stage to the drilling and blasting stage of the production. The integration, analysis, and evaluation of different data sources are challenging as the systems installed on equipment will have different levels of granularity and even different nomenclature. In case the data sources can provide real-time data, the performance of the data integration layer will become a major bottleneck for the IT infrastructure. Data warehousing is a well-known solution to integrate different systems and extract information from it where execution times of the queries are critical. Geospatial queries are comparably faster when they are compared to the queries that are executed on relational data. The main advantage of using geospatial queries for drilling and blasting related data is that the drill holes can be represented as points that have a geospatial meaning. This enables to use built-in functions and grids that are available for geospatial queries and result in shorter execution times and some additional visual representations for reporting. This study introduces a systematic approach to integrate drilling and blasting related operational data collected either manually or automatically at a surface copper mine by using geospatial queries as part of integration in a data warehouse.

2 Methodology

The methodology followed in this study is based on data warehousing and the utilization of geospatial queries. The different types of data related to drilling and blasting were integrated into MS SQL Server and different Business Intelligence tools were developed for mine management purposes. As data sources related to different technologies had unique properties, the initial stage was to characterize all related sources of data. This stage has a major importance for integration as it guides the potential measures that will be used in developing management tools and reports. Once the data is characterized, possible integration points are identified and test queries are run. During this stage, the performance of queries is evaluated based on correctness and execution time. As the data used in this study was real-time, execution times of the queries and stored procedures were of major importance. For this purpose, drilling and blasting related data was converted into point data in MS SQL Server to

benefit from geospatial queries. Measures from different data sources were aggregated to set the level of granularity to a single blast hole that was represented by its coordinates. The available data in the mining industry has different characteristics and has to be handled accordingly especially for cases represented in real time.

2.1 Data Types in Mining Industry

The utilization of more operational data for decision-making has become an essential part of modern mine management. Increasing role of data led the mining industry to invest in technology to collect, integrate, and analyze data for generating information. The mining industry is dominated by relational and process type of data representing both mining and mineral processing operations.

Relational data is the basis of relational models in data warehousing where data is grouped into relations [8]. Fleet management systems (FMS) that provide operational information from all mobile equipment such as drilling rigs, haul trucks, shovels, and others can be considered as the main component of relational data in the mining industry. The operational cycles in mining can be represented by the time and location of the mobile equipment that is tracked by FMS. Other operational data such as, number of blast holes, tons hauled to a crusher or other measures can also be tracked by these systems and utilized for mine management. Enterprise systems that are used in corporate mining companies also have the capability to integrate asset management information and their mine planning software which can be monitored as a performance measure [9].

Equipment and machinery used in the mineral processing part of a mine operation generate a different type of data that is commonly represented by time series. SCADA systems and other process control environments display operational data of equipment in crushing and grinding, conveyors, other machines. This data is defined as process type of data and provides a timestamp and a value that is recorded very frequently. Examples of process type of data can be temperature, pressure, and humidity readings, the amount of power consumed, or whether the machine is working or not. In order to generate knowledge from this high-frequency data, it has to be characterized and measures have to be created. Integration of all types of data observed in the mining industry is of major importance for decision making and mine management.

3 Integration of Drilling and Blasting Data

Drilling and blasting related data is generated by different equipment and has to be integrated with other data sources for creating valuable metrics. In this study, a relational data warehouse was used as the semantic data layer and different business intelligence tools were developed.

3.1 Data Integration

In this study, the data used in geospatial queries was based on different data sources which are the equipment systems related to drilling and blasting. Data generated and provided by the drill monitoring system, reports of explosive loading, the drill and blast assessment system, and the fleet management systems were integrated. During this integration, the level of granularity was different for each of these systems. The drill monitoring system kept records for each blast hole, whereas the drill and blast assessment system data was based on every picture taken by the system during loading. These systems can be installed at different locations to track the fragmentation by using digital image analysis [10]. The different systems that provided data related to drilling and blasting are represented in Fig. 1.

As the aim was to improve the drilling and blasting process as a whole, all available and related data was integrated on each blast hole. These different systems had unique nomenclature to represent blast holes that were identified during data characterization. In order to create information from this data, geospatial queries were used.

3.2 Geospatial Queries

Geospatial data has been used in different systems especially in remote sensing and GIS applications as an interoperable source of information [11]. Similar to other types of data, geospatial data should also be integrated with other data sources and enabled to be used in a user-friendly way. Although database management systems have different functionalities focused on geospatial data, it is still crucial to meet the requirements while using industry-specific data. Data integration for modern mine management should utilize spatial data especially for drilling and blasting,

Fig. 1 Drilling and blasting related data sources used for integration
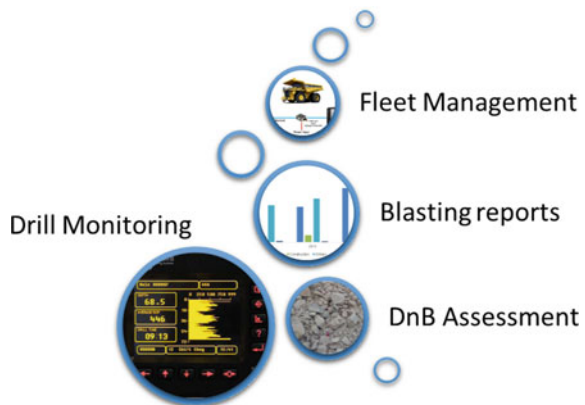
and therefore basic spatial data concepts are important to be understood before data integration [12].

Operational data in surface mining covers mostly relational data that can be considered to have geospatial meaning. Drilling operation is a geospatial data source that provides drill hole locations and other operational measures such as drilled depth, average penetration rate, and others. The locations provided by drill monitoring systems can be represented as points for exact locations. These points can be used to calculate measures such as spacing and burden in case they are integrated with the mine planning software from where the actual bench geometry can be exported as points. Each point representing the drill hole collar is recorded together with operational measures as bit on load, penetration rate, and revolutions per minute (rpm). This data was integrated and analyzed by using the geospatial functionality of MS SQL Server. The first step was the preparation of data for geospatial queries as functions such as shortest distance and others could only be executed on geospatial data specifically defined by a data type in MS SQL Server. All drill hole locations were represented by unique identifiers, known as spatial reference identifier (SRID) that combined the coordinates. Once the conversion was completed, it was possible to plot the drill hole locations by using the newly generated geospatial column in the fact table as shown in Fig. 2.
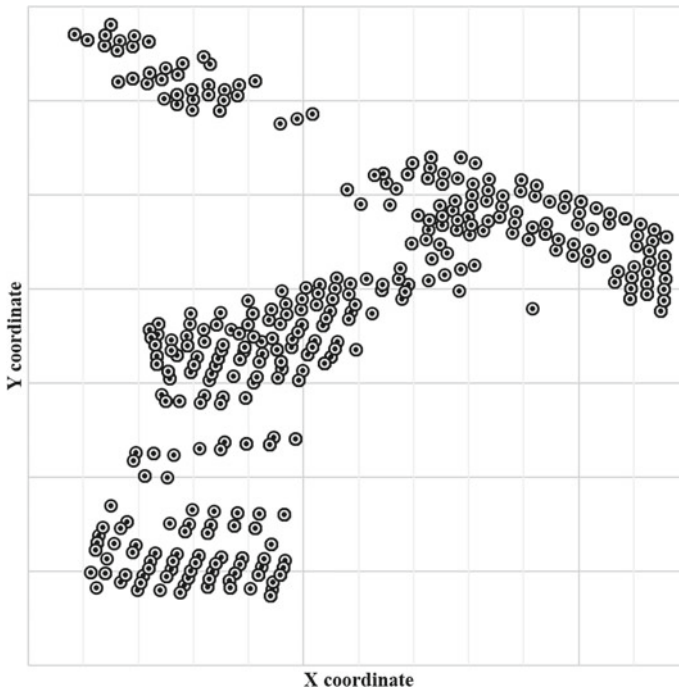
Fig. 2 Geospatial visualization of drill hole data in RDBMS

Geospatial indexing was used to define a grid for coordinates in which the geospatial query was executed. As real-time data was used in this study, a stored procedure to convert the coordinates of each drill hole was developed. In order to enhance the available information sourced from different systems, a nearest neighborhood algorithm was developed to identify the drill holes that are within a predefined perimeter for each individual drill hole. The table that stored the operational data related to drilling and blasting was updated to include the information of nearby drill holes. This also covered the data sourced from the blasting operation where explosive type, amount of explosive charged, and explosive density were combined for the nearest drill holes. As a result, each individual drill hole was represented by an aggregated information for all drill holes located within the nearest neighborhood algorithm. The distances between a drill hole and the nearest neighboring drill holes generated a new value that was used to calculate new measures. A representative data structure as seen in Fig. 3, illustrates the use of geospatial queries.

As a result, empirical approaches related to fragmentation commonly utilize a single value for blast geometry and are based on the assumption that all blast holes
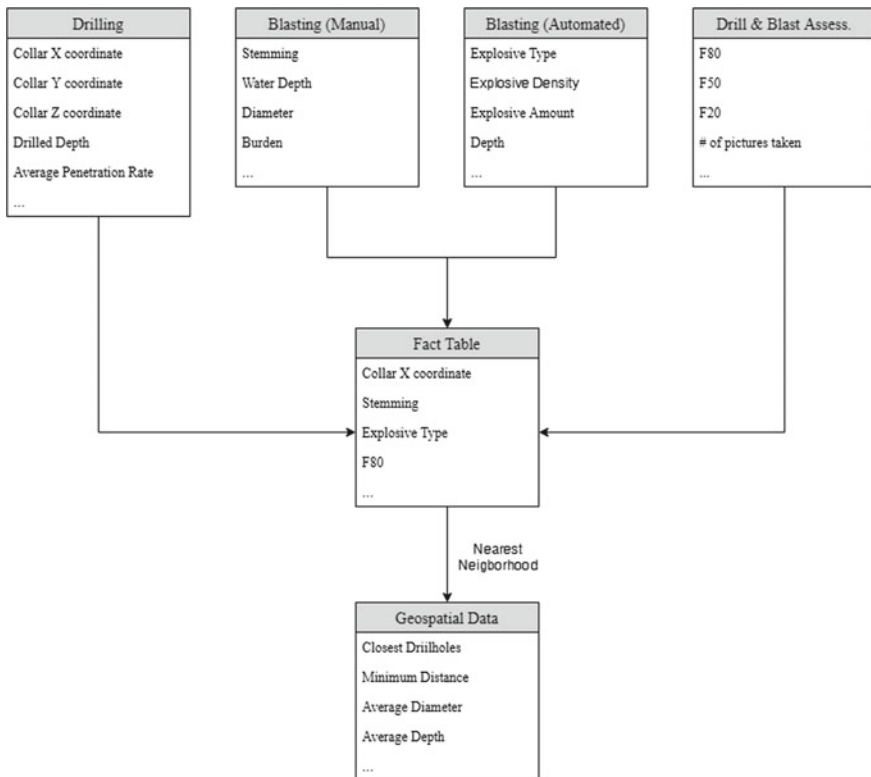
Fig. 3 Data structure of geospatial queries

in a round are drilled successfully as they are designed. However, it might be the case that there is a difference between the drill hole locations as they are designed and drilled. The information that was generated by geospatial queries was used to analyze the performance of drilling and blasting operations.

4 Data Analysis for Optimum Drilling and Blasting

The data that was used in geospatial queries in this study was utilized as the basis of evaluating the performance of drilling and blasting operations. Although most of the systems that were used as data sources were automated, the explosive consumption was recorded also by a manual entry document. Explosive consumption and blast hole design geometry data, manually prepared by field staff, are rather static when compared to real-time data sources such as drill navigation systems. The granularity of the manually collected data is also less than that of other data sources in the data warehouse. However, this data is valuable in validating and enhancing the data, as its content was not captured by any other system on site. Table 1 summarizes the available variables related to drilling and blasting in the data warehouse.

Table 1 Available variables related to drilling and blasting in the data warehouse

Drilling	Blasting (manual)	Blasting (automated)	Drill and blast assessment
Drilled hole count	Avg. subdrill per shot	Hole depth	Avg. of top size
Avg. pen. rate	Avg. plugged holes per shot	Stemming height	Avg. pictures taken per truck load
Number of re-drilled holes	Avg. diameter per hole	Hole diameter	Avg. of F80, F60, F20, etc.
Horizontal offset	Avg. spacing per hole	Explosives load height	Avg. of conveyed material on belt conveyors
Toe offset in X, Y, and Z	Avg. depth per hole	Water level	
Avg. duration to drill a hole	Avg. burden per hole	Explosives amount	
Collar offset in X, Y, and Z	Avg. stemming per hole		
# of holes with no design file	Avg. powder factor per hole		
Hole depth	Avg. depth per hole		
Actual avg. drilling rate	Rock density		
Collar coordinates in X, Y, Z			

The GPS coordinates recorded by the drill navigation systems provided exact locations of drilled blast holes on site. However, these drill hole locations are subject to controversy, as there are different sources for this data. Drill hole locations are first designed in mine planning software and then marked on site by surveying. Drill plans are uploaded to drilling machines and operators also consider survey marks. As a result, the drill navigation system collects GPS data while operating. The difference in these data sets indicates drilling accuracy, which can be visualized as shown in Fig. 4.

As seen in Fig. 4 the difference between the locations of drill holes as designed and as drilled is a major performance indicator for drilling operations. Visualizing data and providing an easy-to-use environment to drill down in the data layers is key to business improvement. Such accuracy metrics can also be considered as the basis for Quality Assurance/Quality Control (QA/QC) practices in drilling. Utilization of this data enabled a corrective action that benefited supervisors and operators. The discrepancy in drilling accuracy decreased and maintained its target value through daily data analysis. Another QA/QC benefit that data warehousing provided was related to explosive loading.

The amount of explosive loaded in blast holes has to be closely controlled for target fragmentation, environmental impacts, and stability concerns. Data related to explosive volume charged was extracted from available data sources and enhanced by using geospatial queries. The variation in explosive volume loaded in neighbor-
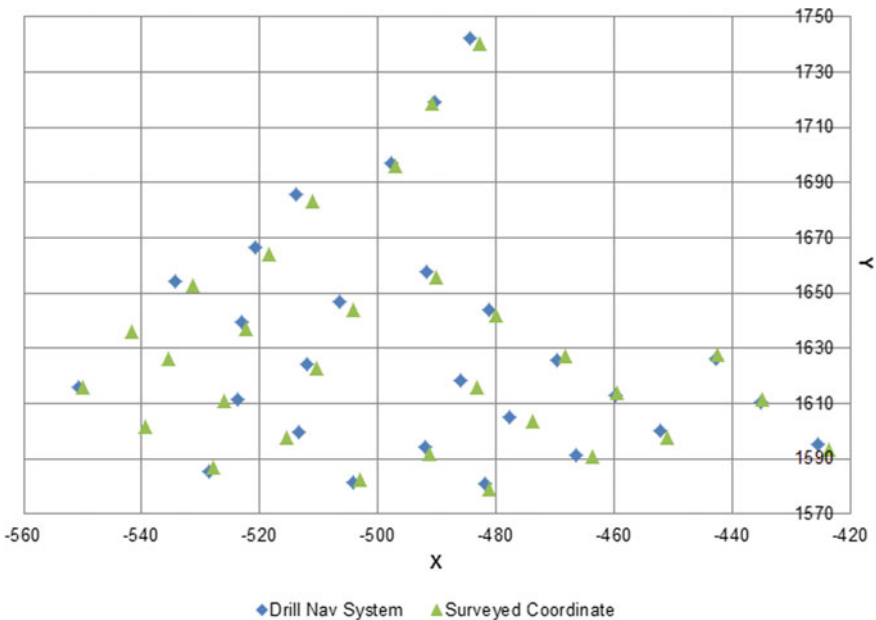
Fig. 4 Drilling accuracy
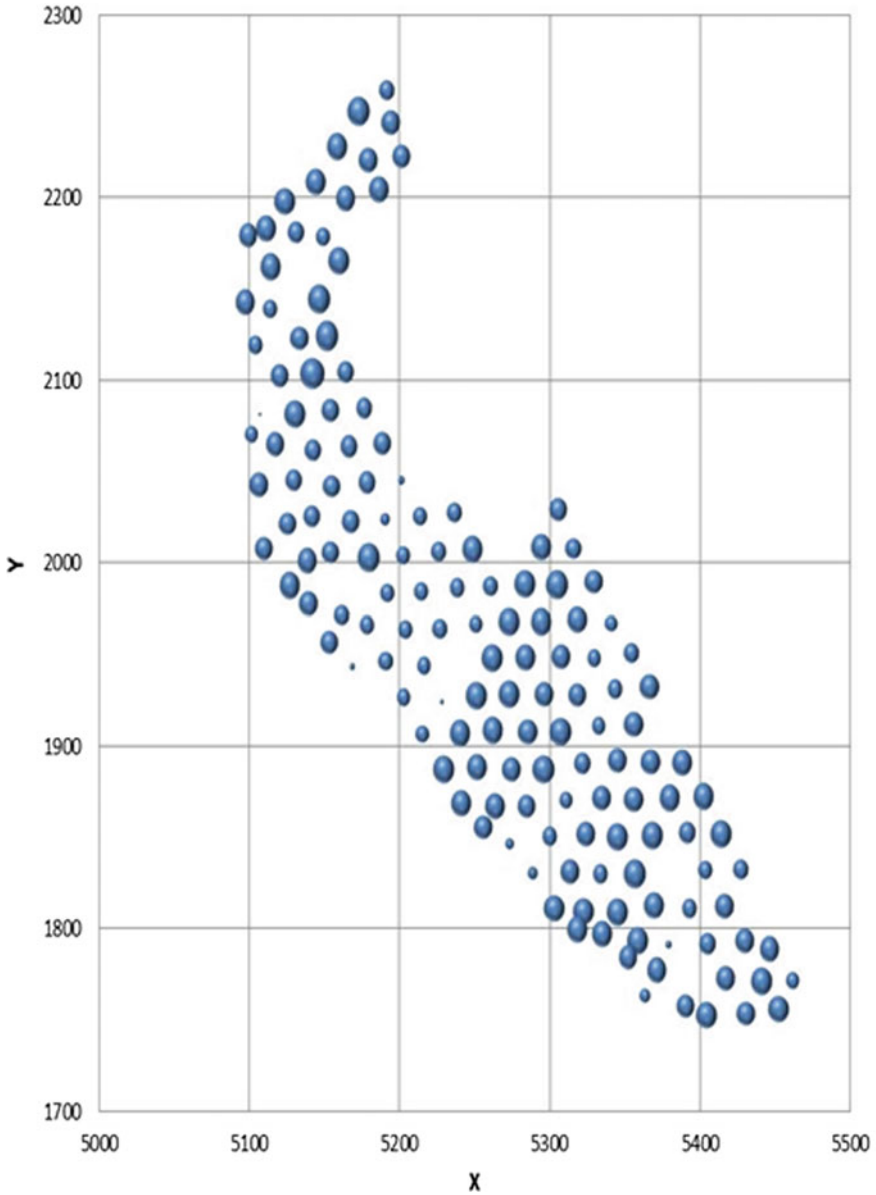
Fig. 5 Explosive volumes loaded in a single shot

ing blast holes indicates potential inefficiencies. Figure 5 shows that a single shot consisting of blast holes with the same design parameters produces inconsistencies in the amount of explosive.

This unbalanced distribution of explosives could have adverse effects such as fly rock, air shock, vibration, and over-size rocks. Nonuniform energy distribution can be considered as one of the major reasons of missing target fragmentation. The performance of downstream processes as digging, loading, haulage, and crushing is prone to be affected by uncontrolled explosive amounts.

5 Conclusion

Modern mines are equipped with different levels of technology that generate valuable operation-related data. The equipment intensive nature of the mining industry makes it a suitable environment to utilize data in decision making and management. This study focused on the drilling and blasting operations in an open-pit copper mine and introduced a management perspective that uses integrated and real-time data for the evaluation of drilling and blasting performance. Geospatial queries were developed to handle data generated by drill monitoring and explosive loading systems. This way, new measures and tools were created to track the success of drilling and blasting operations. Drilling accuracy was improved once the geospatial representation of drill holes were used as a performance measure. Similarly, engineers were provided with a valuable tool that can be used to drill down into the detail of the integrated data warehouse. The most considerable improvement was the 14% increase in mill throughput. This tool also enhanced the utilization of data in daily mine management. The systematic approach to integrate drilling and blasting related data collected either manually or automatically by using geospatial queries has the potential to improve efficiency. Although analyzing data by conventional ways might still provide similar results to a certain extent, the implementation of geospatial queries generates the same valuable information, by handling the amount and frequency of data in modern mines.

References

1. Rogers, W.P., Kahraman, M.M., Dessureault, S.: Exploring the value of using data: a case study of continuous improvement through data warehousing. Int. J. Min. Reclam. Environ. 1–11 (2017)
2. Durrant-Whyte, H., Geraghty, R., Pujol F., Sellschop, R.: How digital innovation can improve mining productivity, A. MacKenzie (2015)
3. Gokhale, B.V.: Rotary Drilling and Blasting in Large Surface Mines. CRC Press, Boca Raton (2011)
4. Dance, A., Mwansa S., Valery, W., Amonoo, G., Bisiaux, B.: Improvements in sag mill throughput from finer feed size at the Newmont Ahafo operation. CIM J. (2011)
5. Hawkes, P.: Using simulation to assess the impact of improvements in drill and blast on down stream processes. In: Mine to Mill, Brisbane, Australia (1998)

6. Kanchibotla, S.S., et al.: Exploring the effect of blast design on SAG mill throughput at KCGM. In: Mine to Mill Conference, Australasian Institute of Mining and Metallurgy, Brisbane, Australia (1998)
7. McKee, D.J.: Fragmentation and its impact on downstream processing. In: AusIMM Annual Conference—Resourcing the 21st Century (1997)
8. Codd, E.F.: A relational model of data for large shared data banks. Commun. ACM **13**(6), 377–387 (1970)
9. Kahraman, M.M., Dessureault, S.: Increasing adherence to mine plan through data integration and process change. Int. J. Min. Reclam. Environ. 1–14 (2017)
10. Kemeny, J., et al.: Analysis of rock fragmentation using digital image processing. J. Geotech. Eng. **119**(7), 1144–1160 (1993)
11. Albrecht, J.: Geospatial information standards. A comparative study of approaches in the standardisation of geospatial information. Comput. Geosci. 25(1), 9–24 (1999)
12. Aitichson, A.: Beginning Spatial with SQL Server 2008, pp. 3–12 (2009)

Prediction of Rock Fragmentation Based on a Modified Kuz-Ram Model

A. Hekmat, S. Munoz and R. Gomez

1   Introduction

In any mining project, drilling and blasting are the first basic operations that form part of an integrated system. They can influence the results of the subsequent operations in productivity as well as in costs, energy efficiency, and environmental emissions. An efficient blasting can be achieved by defining the relationship between blast design parameters and fragmentation. Many studies have been carried out to determine the impact of blast design parameters and fragmentation. These types of investigations are mostly accomplished by systematic study of blasting data at mines [1]. The size distribution of a blasted muck pile can be used to evaluate the stability of a waste dump, and optimize loading cycle times and crushing costs, among others. Furthermore, it is highly important to make a connection between rock blasting results and their impact on the downstream. Previous studies have been shown how rock fragmentation influence the loading efficiency [2], haulage productivity, fuel consumption [3], and crusher efficiency [4].

Several alternative procedures can be used to measure fragmentation. Methods of determining the size distribution of fragmented rock after blasting are grouped as direct and indirect methods. Sieving analysis of fragments is the only direct method. Although it is the most accurate technique compared to others, it is not practical because the implementation of this method is expensive and time consuming [5]. For this reason, indirect methods, which are observational, as well as empirical and digital

A. Hekmat (✉) · S. Munoz · R. Gomez
Department of Metallurgical Engineering, University of Concepción, Concepción, Chile
e-mail: ahekmat@udec.cl

S. Munoz
e-mail: sebastiamunoz@udec.cl

R. Gomez
e-mail: regomez@udec.cl

methods have been developed. The most popular method to quantify fragmentation is the determination of size distribution using digital image processing techniques. This method is cheap, less time consuming and does not interrupt production at site. Due to these reasons, it is preferred widely by explosives engineers and the second most reliable method after sieve analysis [6]. Several software suites such as SPLIT, WipFrag, GoldSize, FRAGSCAN, TUCIPS, CIAS, PowerSieve, IPACS, KTH, WIEP, etc. are commercially available to quantify size distribution [7, 8].

The other way to determine rock fragmentation is employing empirical models. A variety of modeling approaches ranging from purely empirical to rigorous numerical have been used to predict fragmentation from blasting. The most widely used model was developed by Cunningham [9], based on the size distribution curve of Rosin-Rammler and the average blast fragment size given by Kuznetsov [10], who estimates the average fragment size, X_{50}, based on explosive energy, powder factor and rock factor [9]. Larsson [11] proposed an equation to determine X_{50} with regards to drilling pattern, specific charge, and rock properties [11].

Even though digital imaging processing techniques are cheap and accurate, empirical models are quite successful due to the fact that they are simple, quick to calibrate and very easy to use [12]. Hitherto developed models to predict the blast fragmentation are mostly based on statistical analyses of field data. Hudaverdi et al. [13] gathered many blasts performed in different parts of the world to create a blast database [13]. Based on this database, a hierarchical cluster analysis was used to separate the blast data on the intact rock stiffness. The resulted database was applied to predict mean particle size of fragmented material based on neural network model [14]. Although the accuracy of artificial neural network method is more than regression analysis, multiple regression method is one of the easiest approaches to develop an empirical model of fragmentation prediction [15]. The cause of inaccuracy of the regression analysis might be due to the correlation linear assumption. Some studies also used Mont Carlo simulator to improve the former prediction methods such as Kuz-Ram or Larsson methods [16]. In this paper, the Kuz-Ram model is modified based on the results of image analysis in an iron mine of Iran.

2 Size Determination

The most popular method to quantify fragmentation is the determination of size distribution using digital image processing techniques which is the second most reliable method after sieve analysis. In this method, images acquired from muck pile, haul truck, leach pile, draw point, waste dump, stockpile, conveyor belt, etc. are delineated by using digital image processing techniques and size distribution of fragmented rocks is finally determined.

To estimate size distribution, images were taken from muck piles during loading. Having digitized images, the distribution of blasted rock was obtained by GoldSize software [2]. The basic steps are sampling the photos, processing the images and obtaining the size distribution curve of the blasted material (Fig. 1).
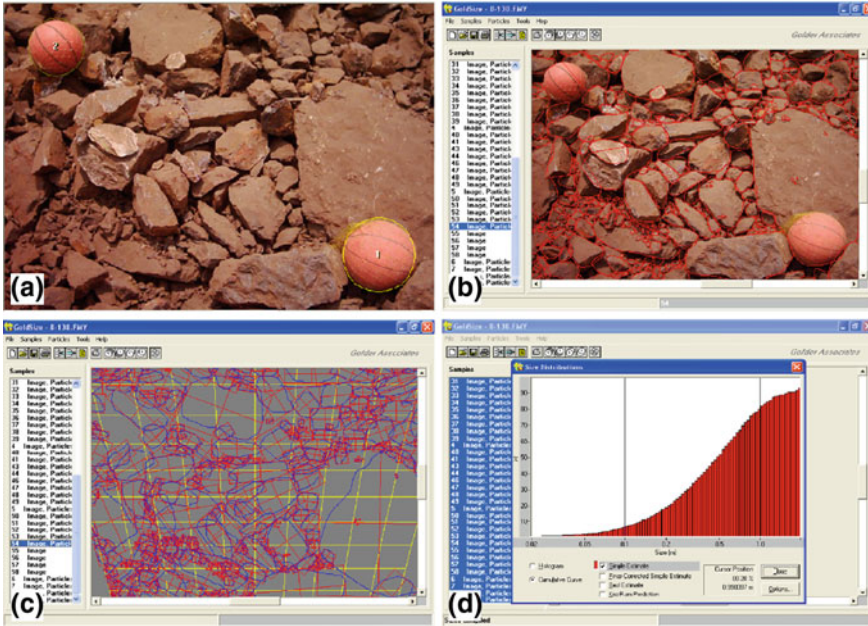
Fig. 1 Determination of rock size distribution using GoldSize software, **a** sampling the photos; **b** input images; **c** object contours; **d** image processing result [2]

Random sampling is done from the whole set of images assigned to a blast. Photos with bad quality or poor lighting are rejected manually. At least 20 photos per blast are selected for the analysis. Each photo contains a known object as scale. In this case, two balls of 25 cm diameter are used.

Fragmentation results of image analysis of different rock types existent at site are presented in Table 1. According to this study, the first blast pattern produced the largest X_{80}, with the least uniformity coefficient, whereby the uniformity coefficient of the last pattern is maximum as result of its minimum X_{80}.

3 Kuz-Ram Model

The Kuz-Ram model is probably the most popular model to predict fragmentation of blasted rock mass. It was developed by Cunningham [9] who modified Kuznetsov's equation for ANFO-based explosive to estimate average fragmented size (X_{50}) and combine it with the Rosin-Rammler equation to predict the entire size distribution. The Equations are written as [9]

$$X_{50} = \text{Fr}\left(\frac{Q}{V_o}\right)^{-0.8} Q^{0.167}\left(\frac{115}{E}\right)^{0.633} \tag{1}$$

Table 1 Results of rock size distribution in several blasted patterns in the mine

Blast no.	Rock type	X_{50} (cm)	X_{80} (cm)	Coefficient of uniformity
1	Oxide	48	114	0.80
2	Magnetite	44	74	1.02
3	Oxide	31	77	1.05
4	Oxide	27	78	1.07
5	Overburden	20	60	1.09
6	Magnetite	33	45	1.18
7	Oxide	26	98	1.23
8	Oxide	48	89	1.35
9	Oxide	26	52	1.54
10	Waste	27	54	1.83
11	Magnetite	21	34	2.10

$$R = 100 - e^{-0.693\left(\frac{x}{x_{50}}\right)^{n}} \tag{2}$$

where Fr is rock factor (7 for medium rock; 10 for hard, highly fissured rock and 13 for very hard rock); Q(kg) is the quantity of explosive in a blast hole; V_o (m^3) is rock volume broken by a blast hole (burden × spacing × bench height); E is relative weight strength of explosive (ANFO = 100; TNT = 115 and Slurry = 117); R represents the percentage passing smaller than x, x is rock size, and n is the uniformity coefficient.

The rock factor is calculated from an equation originally developed by Lilly in 1986 for blastability index [17]:

$$Fr = 0.06(RMD + JF + RDI + HF) \tag{3}$$

where Fr is the rock factor as mentioned above, RMD is the rock mass description, JF is the joint factor, RDI is the rock density index, and HF is the rock hardness factor.

Cunningham [18] further developed an equation to estimate the uniformity coefficient "n" of the Rosin-Rammler distribution curve from blast design parameters [18]:

$$n = \left(2.2 - 14\frac{B}{D}\right)\left[\frac{1 + \frac{S}{B}}{2}\right]^{0.5}\left(1 - \frac{W}{B}\right)\left(\frac{L}{H}\right) \tag{4}$$

where B is the blasting burden (m), S the blast hole spacing (m), D the blast hole diameter (mm), W the standard deviation of drilling accuracy (m), L the total charge length (m), and H the bench height (m).

Widely accepted, this equation is the starting point of any mining operation linked to blasting. Because of this, high correlation and good prediction capacity are required. Available fragmentation data obtained from digital image analysis are
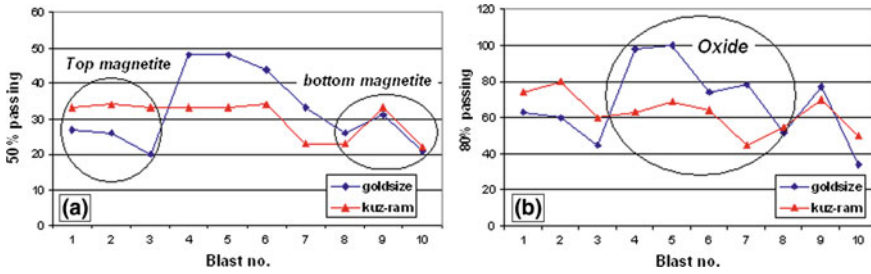
Fig. 2 Comparison of Kuz-Ram predicted size versus actual (GoldSize) data for mine site, **a** predicted X_{50}; **b** predicted X_{80}

used to examine whether the Kuz-Ram equation is satisfied. Figure 2a shows the 50% passing predicted by Kuznetsov's equation against the actual size at mine site. The comparison of actual X_{80} with the predicted value based on the Kuz-Ram model is also presented in Fig. 2b.

However, even though the Kuz-Ram model has been used widely for estimating blast fragmentation, it has some drawbacks. One of them is that the rock quality factor rating is based on subjective descriptions, such as massive, blocky or friable. With the same blasting pattern, various fragmentations will be obtained in a mine because of the variety of rock type and discontinuities. As represented by Fig. 2, the Kuz-Ram model overestimates the particle size in the top and bottom magnetite while for the oxide zone, the results of the Kuz-Ram model are less than the real size.

4   Data Analysis

To modify the Kuz-Ram prediction model based upon mine site conditions, two parameters of the Kuz-Ram equation, namely rock factor and uniformity coefficient, were investigated.

4.1   Rock Factor

In a research done by the authors, it was proved that Monte Carlo simulation is able to estimate the rock factor with acceptable accuracy. To estimate the rock factor by the Monte Carlo simulation technique, the size distributions of muck piles in several blasting patterns with different rock types were determined by applying the GoldSize software. Rock factor was then calculated by substituting the real average size in Eq. 1. Figure 3 shows the frequency histogram of rock types at mine site. The cumulative frequency (from 0 to 1) is also calculated in Fig. 3. The results obtained
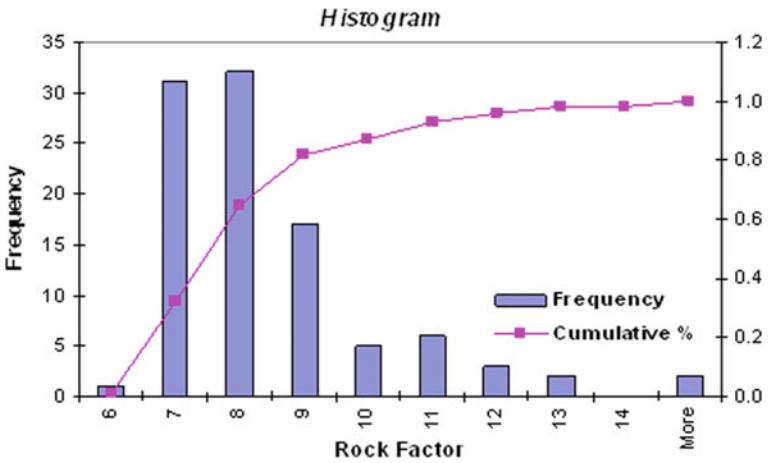
Fig. 3 Frequency histogram of rock factor
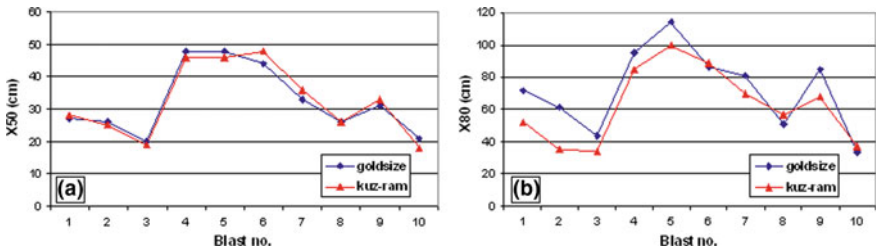
Fig. 4 Comparison of predicted size using Monte Carlo simulation versus actual data for mine site, **a** predicted X_{50}; **b** predicted X_{80}

from Fig. 3 show that the rock factor varies between 6 and 13 and the histogram represents a lognormal distribution function in the case of this iron mine. The results of Monte Carlo simulation show that the rock factor in three different materials of the mine varies as:

$5.5 \leq Fr \leq 7.0$	In top magnetite
$7.0 < Fr \leq 10$	In oxide
$10 < Fr \leq 14$	In bottom magnetite

Figure 4a shows the 50% passing predicted by Kuznetsov's equation using Fr obtained from Monte Carlo simulation. Despite X_{50}, 80% passing predicted have not a good correlation with the actual data as shown in Fig. 4b. The difference can be justified by the variety of the uniformity coefficient.

4.2 Uniformity Coefficient

The uniformity of fragmentation is expected to be fundamentally a function of pattern geometry, charging conditions and rock mass characteristics. Literature indicates that the uniformity index for blasted rock masses generally lies between values of 0.6 and 2.2 [19]. The larger the *n* value, the steeper the curve, i.e., the narrower the range of particle sizes in the given material. Values below 0.6 tend to indicate nonuniform breakage and fragmentation caused by the combination of blasting performance and other secondary effects such as structurally controlled failures, over break, back break, and/or poor stemming performance [20].

Figure 5 shows the uniformity factor obtained from Eq. 4 versus the real uniformity in the mine site. As shown in Fig. 5, Eq. 4 overestimates the uniformity factor. It is indicated from Fig. 5 that the Rosin-Rammler equation tends to represent more uniform distribution but the size distribution in the studied site is not uniform due to less performance of drilling and blasting.

The scatter plot between predicted and actual uniformity factor, "*n*" in Fig. 6, shows that there is a good correlation between them ($r^2 \geq 80\%$). Therefore, it is possible to "calibrate" a uniformity factor obtained from Eq. 4 using a factor to decrease the value calculated by the Kuz-Ram model. This factor is represented by Eq. 5:

$$n' = 5.3n - 7.8 \tag{5}$$

where n' is the modified uniformity factor and n is the normal uniformity factor obtained from Eq. 4. The coefficient of determination in Eq. 5 (r^2) is 0.89.
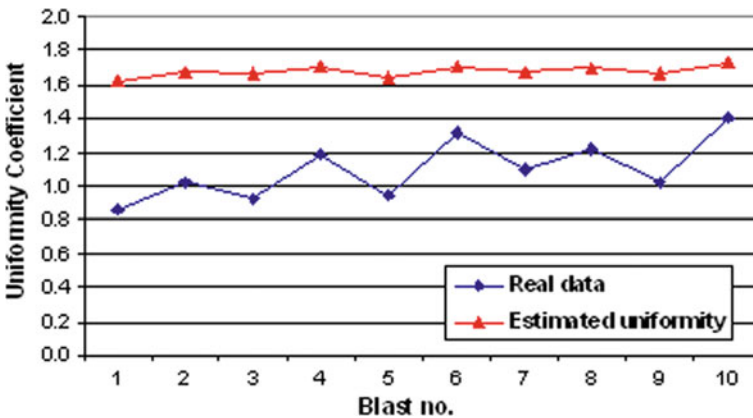
Fig. 5 Estimated uniformity coefficient versus actual data uniformity coefficient for mine
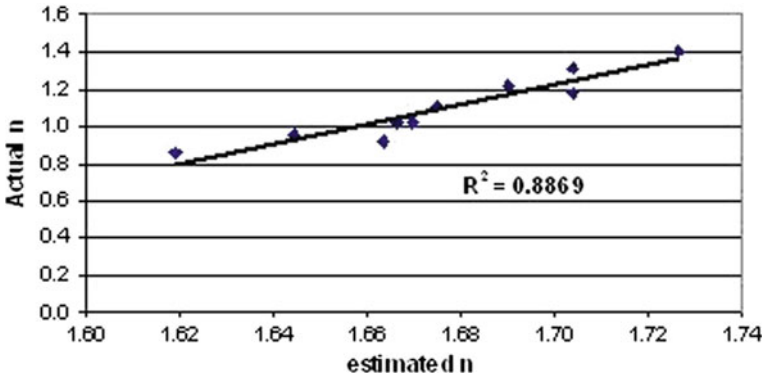
Fig. 6 Scatter plot of estimated uniformity coefficient versus actual uniformity coefficient for mine site
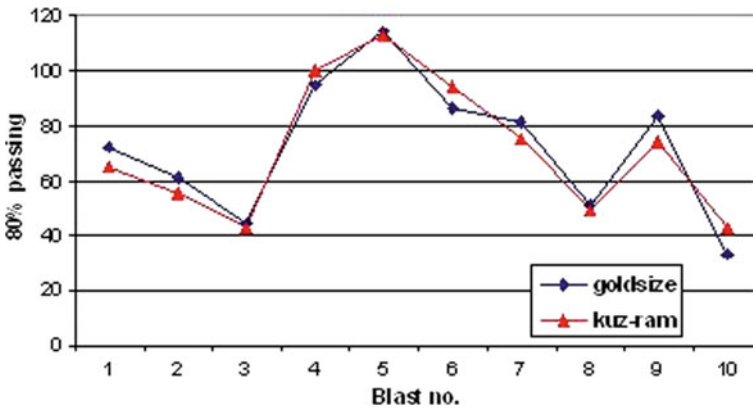
Fig. 7 Predicted X_{80} passing size after modification of n versus actual 80% passing size

5 Discussion

Using the modified uniformity factor, it is possible to have an accurate estimation of X_{80} in this mine. Figure 7 compares the recorded X_{80} with the predicted value based on the modified Kuz-Ram model. Figure 8 represents the cumulative distribution of two different blasting patterns before and after the implementation of the modified Kuz-Ram model. The cumulative size distribution in oxide rock shows that there is a significant difference in real and predicted data in fine materials especially for the particle size less than 30 cm. This is because of using a unique scale (two balls with 25 cm diameter) when taking the photographs from the blasted muck pile. Therefore, when digitizing the images by GoldSize software, the particles less than 25 cm were not completely designated. To overcome this obstacle, more photos were taken with different scales to cover all particles.
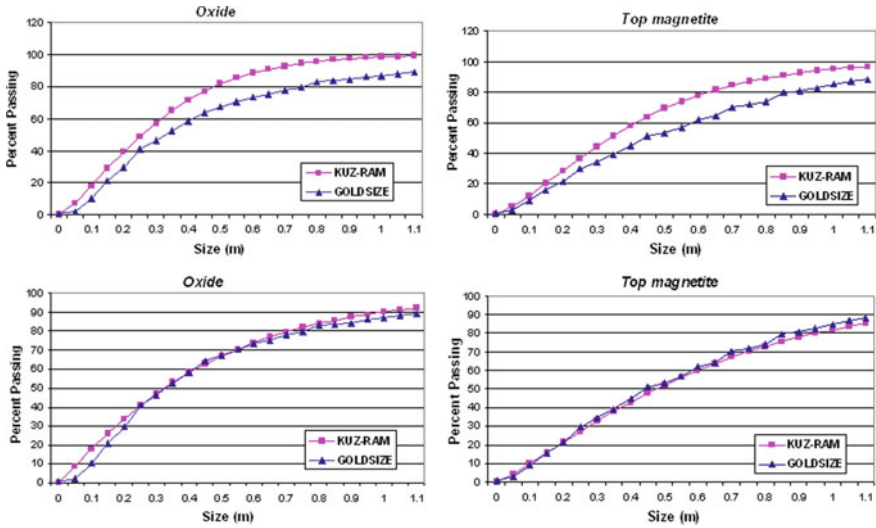
Fig. 8 Cumulative distribution before and after implementation of the modified Kuz-Ram model in different rock types; Top: before modification; Bottom: after modification

To determine the size distribution of top magnetite rock in Fig. 8, several scales were implemented to cover all sizes. It can be concluded from Fig. 8 that the difference in estimation of fine particles by the Kuz-Ram model and data obtained from GoldSize software is mainly because of the error produced by using unique scale in photos taken from blasted material for image analysis.

6 Conclusions

The Kuz-Ram fragmentation prediction model is the most widely studied and recognized in mining industries. It has been quite successful due to the fact that it is simple and quick to calibrate and also easy to use. In this paper, fragmentation results of image analysis and the Kuz-Ram prediction model were presented for three different materials in an iron mine of Iran.

Comparison of the cumulative size distribution of image analysis and the Kuz-Ram model shows that this model can predict the size distribution of blasted rock in the mine, but it required some modification to calibrate the model. The investigation of fragmentation in different rock types indicates that with the same blasting pattern, various fragmentations will be obtained in a mine because of the variety of rock types and discontinuities. The only parameter in the Kuz-ram model that considers the physical and geotechnical properties of rock is the rock factor (Fr). To have a good estimation of the rock factor, Monte Carlo simulation was used, and Fr was determined for three different materials present at site. Because of the good

correlation between the uniformity coefficients obtained from the Kuz-Ram model and the actual mine data, it is possible to "calibrate" a uniformity factor obtained from Eq. 4 using a factor to decrease the value calculated by the Kuz-Ram model (Eq. 5).

The results of model verification show that the modified Kuz-Ram model is able to predict rock fragmentation of blasted rock with an accuracy of 80% in the studied iron mine.

References

1. Singh, P.K., Roy, M.P., Paswan, R.K., Sarim, M.D., Kumar, S., Ranjan, J.R.: Rock fragmentation control in open cast blasting. J. Rock Mech. Rock Eng. **8**, 225–237 (2016)
2. Osanloo, M., Hekmat. A.: Prediction of shovel productivity in the Gol-e-Gohar iron mine. J. Min. Sci. 41(2), 177–184 (2005)
3. Soofastaei, A., Aminossadati, S.M., Kizil, M.S., Knights, P.: A comprehensive investigation of loading variance influence on fuel consumption and gas emissions in mine haulage operation. Int. J. Min. Sci. Technol. **26**(6), 995–1001 (2016)
4. Ouchterlony, F.: The Swebrec© function: linking fragmentaton by blasting and crushing. Min. Technol. **114**(1), 29–44 (2005)
5. Franklin, J.A., Kemeny, J.M., Girdner K.K.: Evolution of measuring systems: a review. In: Proceedings of the Fragblast-5 Workshop on Measurement of Blast Fragmentation, A.A. Balkema, Montreal, Quebec, Canada, pp. 47–52 (1996)
6. Higgins, M., BoBo, T., Girdner, K., Kemeny, J., Seppala, V.: Integrated software tools and methodology for optimization of blast fragmentation. In: Proceedings of the Twenty- Fifth Annual Conference on Explosives and Blasting Technique, Nashville, Tennessee, USA, 2, pp. 355–368 (1999)
7. Siddiqui, F., Shah, S., Behan, M.: Measurement of size distribution of blasted rock using digital image processing. J. King Abdulaziz Univ. Eng. Sci. **20**(2), 81–93 (2009)
8. Kemeny J., Girdner, K., BoBo, T.: New advances in digital image analysis software to quantify the size distribution of fragmented rock. In MINNBLAST, pp. 27–43 (1999)
9. Cunningham, C.V.B.: The Kuz-Ram model for prediction of fragmentation from blasting. In: Proceedings of the First International Symposium on Rock Fragmentation by Blasting, Lulea, Sweden, pp. 439–454 (1983)
10. Kuznetsov, V.M.: The mean diameter of the fragments formed by blasting rock. Sov. Min. Sci. **9**, 144–148 (1973)
11. Jimeno, L., Carcedo, F.: Drilling and Blasting of Rocks. A.A. Balkema, Rotterdam, Netherlands (1995)
12. Liu, Q.: Modification of the Kuz-Ram model for underground hard rock mine. In: Proceedings of 8th International Symposium of Rock Fragmentation by Blasting - FRAGBLAST Santiago, Chile, 8, pp. 185–192 (2006)
13. Hudaverdi, T., Kulatilake, P.H., Kuzu, C.: Prediction of blast fragmentation using multivariate analysis procedures. Int. J. Numer. Anal. Meth. Geomech. **35**(12), 1318–1333 (2010)
14. Kulatilake, P.H., Hudaverdi, T., Wu, Q.: New Prediction models for mean particle size in rock blast fragmentation. Geotech. Geol. Eng. **30**(3), 665–684 (2012)
15. Abbas Aghajani Bazzazi, E.I., Asadi, A.: Comparison between neural networks and multiple regression analysis to predict rock fragmentation in open-pit mines. Rock Mech. Rock Eng. 47(2), 799–807 (2013)
16. Mario, A., Ficarazzo, F.: Monte Carlo simulation as a tool to predict blasting fragmentation based on the Kuz-Ram model. Comput. Geosci. **32**(3), 352–359 (2006)

17. Lilly, P.A.: An empirical method for assessing rock mass blastability. In: Large Open Pit Mining Conference, pp. 41–44. The Auslmm/lE Aust. Newman Combined Group (1986)
18. Cunningham, C.V.B.: Fragmentation estimations and the Kuz-Ram model—four years. In: Proceedings of the Second International Symposium on Rock Fragmentation by Blasting, Keystone, CO, pp. 475–487 (1987)
19. Chung, S.H., Katsabanis, P.D.: An integrated approach for estimation of fragmentation. In: Proceedings of 6th International Symposium of Rock Fragmentation by Blasting - FRAGBLAST Johannesburg, South Africa: South African Institute of Mining and metallurgy, 6, pp. 231–219 (2001)
20. Onederra, I., Riihioja, K.: An alternative approach to determine the uniformity index of Rosin-Rammler based fragmentation models. In: 8th International Symposium of Rock Fragmentation by Blasting-FRAGBLAST, Santiago 8, pp. 193–199 (2006)

Neural Network Applied to Blasting Vibration Control Near Communities in a Large-Scale Iron Ore Mine

N. Torres, J. A. Reis, P. L. Luiz, J. H. R. Costa and L. S. Chaves

1 Introduction

The growing demand for minerals results in increased use of explosives for blasting in open pit mining [1]. Blasting is usually the main method used in hard rock mining to achieve rock breakage and fragmentation [2]. Blasting and fragmentation directly affects operational activities such as loading, hauling and mineral processing. Nevertheless, only 20–30% of the explosive energy is efficiently used in fragmentation and the remaining energy generates collateral effects that has potential environmental impacts such as ground vibration, air overpressure, dust generation, back break and fly rock [3].

Shi and Chen [4] considered the maximum charge per delay and the waveform interference by the delay blasting as important factors influencing the ground vibration and the final pit walls stability. Armaghani et al. [2] and Khandelwal and Singh [3] have obtained the maximum charge per delay as one of the main influencing factors on the resultant vibration velocity.

Several studies have been conducted using Artificial Neural Network (ANN) to predict blast-induced ground vibrations. Chakraborty et al. [5] studied multilayer perceptron networks to predict ground vibrations and compared it with different empirical models. Singh [6] applied feed-forward back propagation neural network to predict and control ground vibrations in mines. Khandelwal and Singh [7] predicted blast-induced ground vibration and frequency in open pit mines using ANN models and later [8] compared and evaluated ground vibration predictors using ANN models. Monjezi and Dehghani [9] applied ANN to evaluate the effects of blasting

N. Torres (✉) · J. H. R. Costa · L. S. Chaves
Instituto Tecnológico Vale (ITV), Belém, Brazil
e-mail: vidal.torres@itv.org

J. A. Reis · P. L. Luiz
Vale S.A., Rio de Janeiro, Brazil

pattern parameters on backbreak occurrence. Monjezi et al. [10] predicted backbreak formation using ANN.

The parameters that determine blast-induced ground vibrations can be divided into three groups: (1) Blast design parameters; (2) explosive parameters and (3) rock mass parameters [11]. Burden, spacing, hole depth, stemming, sub-drilling, maximum charge per delay and hole diameter are all blast design parameters. Explosive type, velocity of detonation (VOD), density, strength and specific charge are explosive parameters, and these are controllable. The third group consists of the rock mass parameters, such as Young's modulus, Poisson's ratio, P-wave velocity and Blastability Index, which are uncontrollable [11].

The Blastability Index, BI suggested by Lilly [12] can be calculated according to Eq. (1):

$$BI = 0.5 \times (RMD + JPS + JPO + RDI + S) \tag{1}$$

where: RMD is the rock mass description (powdery or friable $= 10$, blocky $= 20$ and massive $= 50$); JPS is the joint plane spacing (<0.1 m $= 10$, 0.1–1.0 m $= 20$, >1.0 m $= 50$); JPO is the joint plane orientation (horizontal $= 10$, dip out of face $= 20$, strike normal to face $= 30$, dip into face $= 40$); RDI is the rock density influence which is equal to $25d - 50$, where d is density; and S is the rock strength, equals to 0.05 times UCS, where UCS is the uniaxial compressive strength [12].

In the mining industry, the ground vibrations caused by blasting operations commonly have negative effect on adjacent populations, relative to possible infrastructure damage and human discomfort. Several countries have established limits for ground vibration to minimize infrastructure damage and human discomfort, including Brazil [13], Germany [14], Portugal [15], and the United States [16]. Therefore, it is essential to evaluate and control vibrations to avoid these undesirable effects.

This paper shows the development and application of an ANN to predict and control blast-induced vibrations at a community close to a large-scale open pit iron mine. The ANN was trained to predict the peak vector sum (PVS) using measured data obtained from mine blasting operations. The communities are frequently facing blast-induced ground vibration issues, therefore, ANN may be highly suitable to relate the blasting parameters and the vibration level.

2   Vibration Control Methodology

The method proposed by Navarro Torres et al. [17] involves the prediction of blast-induced ground vibrations through mathematical models and the vibration control through the adjustment of the maximum charge per delay by using delay blasting. The adapted method for the present work (Fig. 1) uses ANN to predict vibration velocity and the adequacy of the maximum charge per delay in a blast by the use of delay blasting to control the maximum resultant vibration, and is summarized in four steps:
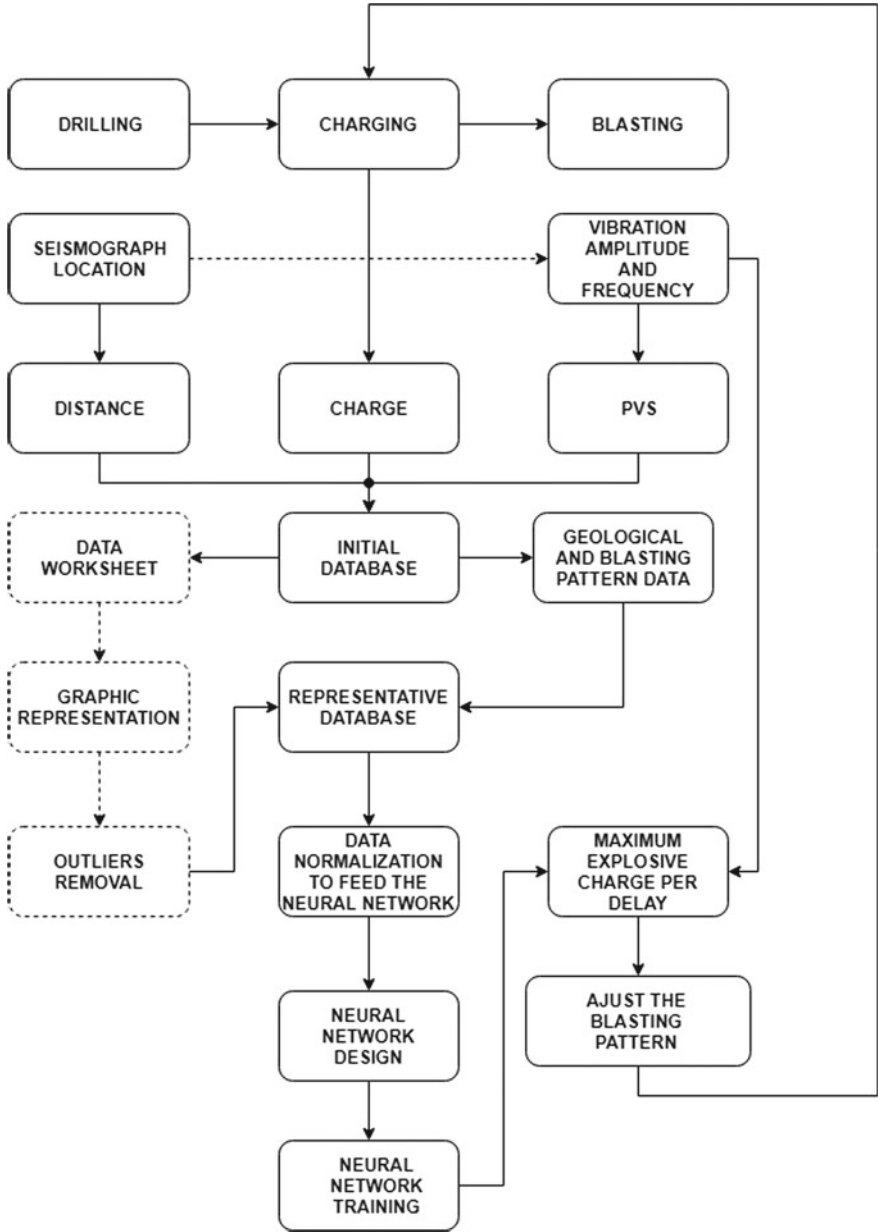
Fig. 1 Methodology proposed for blast-induced vibration and their control

(1) In situ blasting vibration monitoring to measure the PVS and the frequency
(f) caused by blasting, considering the maximum charge per delay (Q), the

distance between the blasting source and the position of the geophone (D), the blast design parameters (burden, spacing, hole depth, stemming, sub-drilling and powder factor), an explosive parameter (VOD) and rock mass parameters (blastability index, P-wave velocity, Young's modulus and Poisson's);

(2) Obtain the blasting vibration predictor by training an ANN with the monitoring data;

(3) Validate and test the ANN performance using new blasting data, and check the predictor's performance using all data set;

(4) Feed the ANN predictor with the data for a planned blasting in order to predict the expected vibration in a point and evaluate the adequacy of the planned maximum charge per delay to the desired vibration limits.

3 Artificial Neural Network

ANNs are computational techniques, which present a mathematical model inspired by the neural structure of intelligent organisms to acquire knowledge through experience. An artificial neural network consists of several processing units. These processing units are usually connected through communication channels associated with the given weight. These units are only operating on its local data, which are received by connections. The intelligent behavior of an ANN comes from the interactions between the network processing units [18].

The ability to "learn" associated with a neural network is one of the most important qualities of these structures. It is considered "learning" process that adapts the behavior and results in a performance improvement. In the context of ANNs, learning or training corresponds to the adjustment process of the free parameters of the network through a mechanism of presentation of environmental stimuli, known as standards (or data) input or training.

Figure 2 shows the network used in the Matlab® software to represent the ANN. The network has three layers, in which the hidden one has 15 neurons, the output layer has one neuron ($Y_k; k = 1$) and the input layer has 11 neurons ($X_i; i = 1, 2, 3 \ldots, 13$). The ANN architecture is showed in Fig. 3 and the connections are explained by Eqs. (4) to (10) [19]. The neuron j from the hidden layer is connected with all neurons from the input layer expressed by Eq. (2).

$$X_i = (X_1, X_2, \ldots, X_n) \tag{2}$$

The input values to the Net network's input layer are as defined in Eq. (3).

$$\text{Net}_j = \sum_{i=1}^{n} (X_i W_{ij} + \theta_j) \tag{3}$$
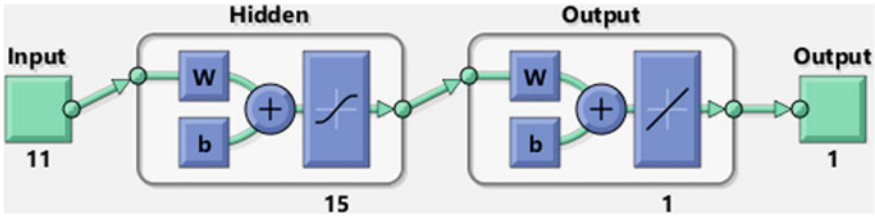
Fig. 2 Architecture of Neural Network in Matlab®
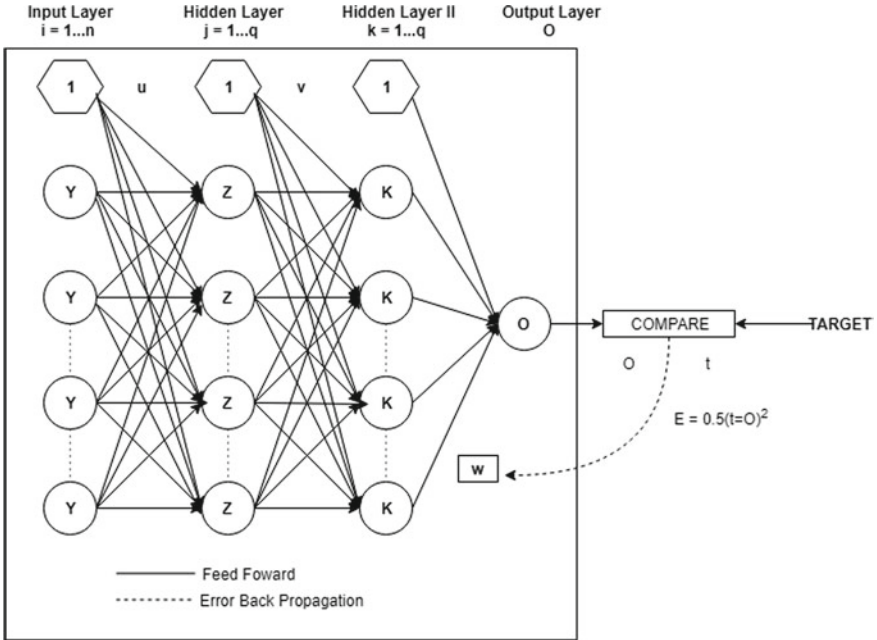
Fig. 3 Back-propagation neural network

where: X_i is the input value, W_{ij} is the weight of the connection between the neuron i from the input layer and the neuron j, from the hidden layer, θ_j is the fixed activation threshold of the neuron (bias) which may be used or not. As output from the hidden layer, each neuron from this network has a logistic activation function as Eq. (4).

$$\text{Out}_j = f\left(\text{Net}_j\right) = \frac{1}{1 + e^{-\left(\text{Net}_j + \theta_j\right)}} \tag{4}$$

The sum of the inputs of the k unit of the output layer is given by the following function expressed by Eq. (5).

$$\text{Net}_k = \sum_{j=1}^{m} S_j W_{jk} + \theta_k \tag{5}$$

where: S_j is the input value, W_{jk} is the weight of the connection between the neuron j from the input layer and the neuron k from the output layer, θ_k is the fixed activation threshold of the neuron (*bias*) which may be used or not. Therefore, the output of the k neuron is provided by the function (6).

$$\text{Out}_k = f(N_k) = \frac{1}{1 + e^{(N_k + \theta_k)}} \tag{6}$$

In the learning process, the ANN is presented to a data set corresponding to the input and the respective output. Using the weight of each connections and the fixed threshold from each neuron, the ANN calculates its' own solution comparing the obtained solution to the desired one. Thus, an error could be established as the Eq. (7).

$$e_k = t_k - \text{Out}_k \tag{7}$$

where: t_k is the target value. The function that determines the total error is the Mean Squared Error expressed by Eq. (8).

$$E = \frac{1}{p} \sum_{k=1}^{p} (t_k - \text{Out}_k)^2 \tag{8}$$

where: p is the number of neurons in the output layer. Figure 3 shows how the Input layer, Hidden Layer and Output Layer are connected. The ANN training consists in the process of optimizing the weight vector of the parameters. In other words, the training should identify a local or global minimum value. The steepest descent error surface is calculated using the following rule:

$$\nabla W_{jk} = -\gamma (\delta E / \delta w_{jk}) \tag{9}$$

where: $\gamma = $ learning rate parameter, and $E = $ error function. The update of weights for the $(n + 1)$ pattern is given as Eq. (10):

$$W_{jk}(n + 1) = W_{jk}(n) + \nabla W_{jk}(n) \tag{10}$$

The process is iterative for each pair of training values (set of input data and the target output values) and it is the same for the connections between the hidden and output layers. Each step of this iterative training process is called epoch. As long as the error not achieve the user specified goal, the number of epochs will increase until the network be trained [20].

Table 1 Input and output parameters for development of ANN

Input parameters	Range	Mean	Unit
Maximum charge per delay (MCPD)	800–2100	1463.5	kg
Distance	100–2000	954.3	m
Burden	4–4.4	4.17	m
Spacing	4.5–5.2	4.79	m
Hole depth	10.2–12.4	11.49	m
Stemming	5–5.8	5.28	m
Sub-drilling	0.4–1.1	0.70	m
Powder factor	0.96–1.76	1.34	kg/m^3
Velocity of detonation of explosive (VOD)	4000–6500	5315	m/s
Blastability index	58–63	60.6	–
P-wave	1600–3600	2552	m/s
Young's modulus	40–80	63.5	GPa
Poisson ratio	0.25–0.40	0.28	–
Peak vector sum (PVS)	0.19–15.8	1.34	mm/s

4   Case Study in Large Iron Ore Mine from Brazil

The case study was a large open pit iron mine located at the eastern portion of the Quadrilátero Ferrífero, at Minas Gerais state, Brazil, where the community was located about 500 m from the mining operation.

Monitoring systems were installed in different locations which includes: the vicinity of the open pit, the area between mining and the community, and in the community itself. The sum of 133 blast vibration events were used to feed the Neural Network. Vibration sources were from 10 production blasts using emulsion-type of explosive. The monitoring was performed using 20 geophones with natural frequency of 10 Hz and response on the range of 2–250 Hz, distributed in the monitoring area with distances from 100 to 2000 m from the vibration source. The determination of rock physic and mechanical properties follow the ISRM standards [21]. The vibration value used was the PVS that is the peak instant velocity of the vector sum of all the components.

Parameters, such as maximum charge per delay, burden, spacing, hole depth, stemming, sub-drilling, powder factor and velocity of detonation (VOD) were collected from the blast design. The distance was measured according to geophone's locations. A list of the parameters used as input and output to the network training is presented at Table 1.

A three-layer feedforward back-propagation neural network was design to estimate the PVS. The input layer has 13 neurons, the hidden layer has 15 neurons and the output layer has one neuron illustrated in Fig. 4. It was used logistic function as
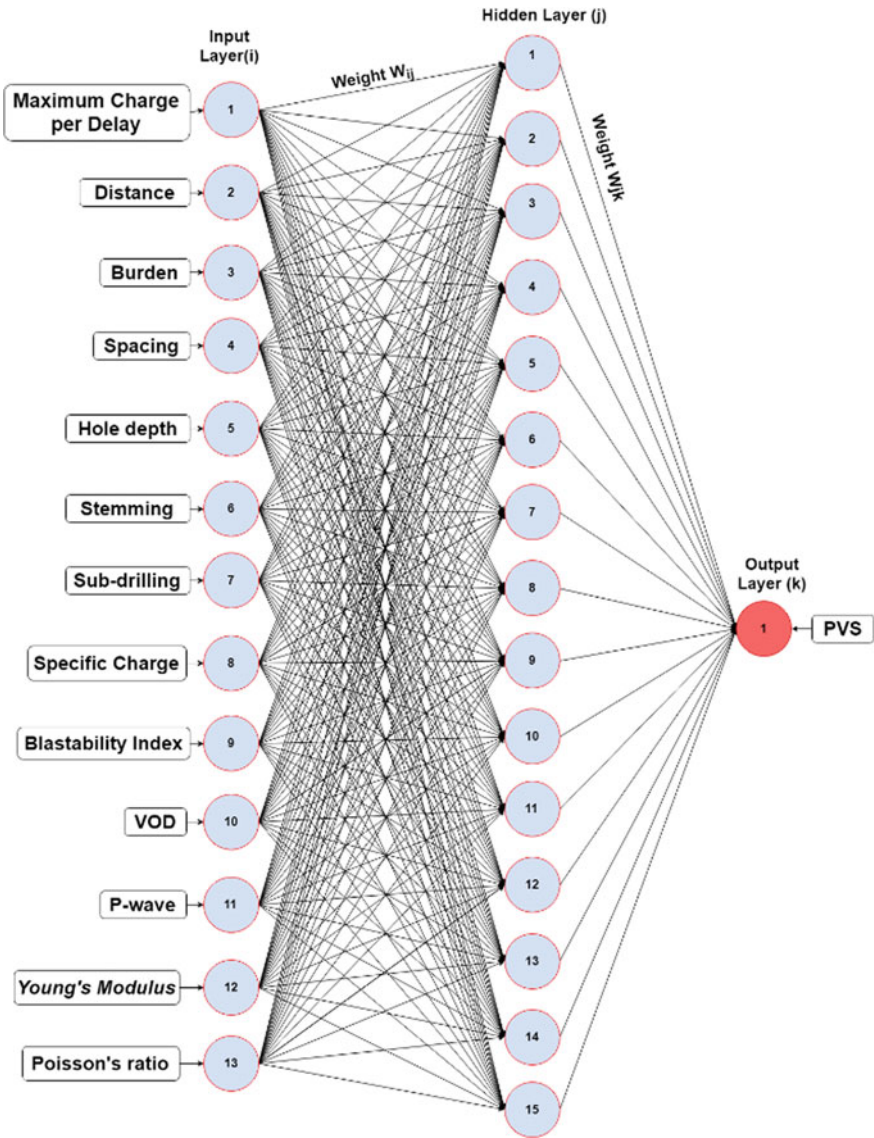
Fig. 4 Artificial neural network architecture

transfer function of the neurons and the Levenberg-Marquardt algorithm to train the
network [22].
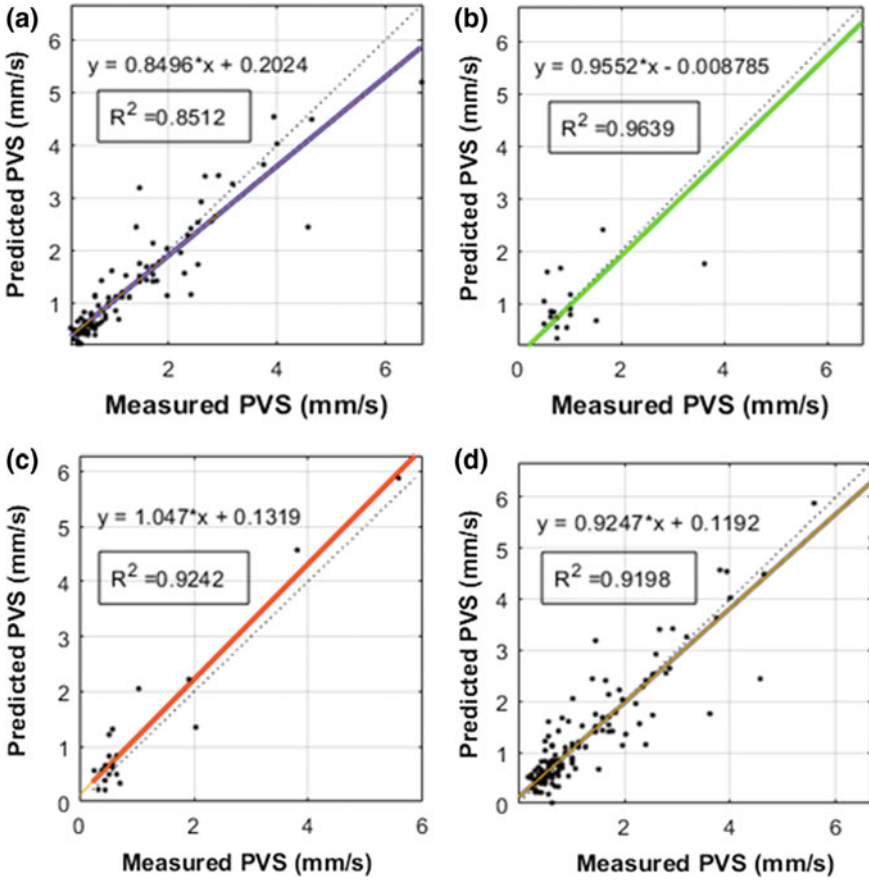
Fig. 5 Measured versus ANN predicted PVS **a** test stage, **b** all data set stage

5 Results and Discussion

The ANN was trained using 70% of the registered and measured data set, validated with 15% and tested with the remaining 15%. Figure 5 shows the comparison between the measured and the predicted PVS, in mm/s, for the data used at the three stages and for the entire data set. At the training stage, Fig. 5a, the resulting R squared (R^2) was 0.8512, at the validation stage, Fig. 5b, the R^2 obtained was 0.9639, at the test stage, Fig. 5c, the resulting R^2 was 0.9242 and considering the entire data set, Fig. 5d, the resulting R^2 was 0.9198.

R^2 is the main performance indicator to evaluate the ANN. R^2 is a statistical measure of how close the data are to the fitted regression line. It is also known as the coefficient of determination. The R^2 gives the relationship between the explained

variation and the total variation, and it ranges from 0 to 100%, providing a number to evaluate how well the model fits the data [23].

As illustrated by Fig. 5d, the vibration velocity (PVS) predicted by ANN is very close to the measured vibration when considering all data set, the R^2 of 0.9198 means a correlation of 91.98%, which indicates the reliability of the model. The developed ANN model has therefore a satisfying reliability on the prediction of blast-induced ground vibration. It may be used as an auxiliary tool for planning and controlling blasts for the mine located nearby the community in order to avoid infrastructure damage and neighborhood discomfort, assessing the environmental impacts caused by blasting by controlling the resultant ground vibrations. By predicting the vibration velocity in the community limits, the model provides more information for the blaster to take decisions related to the maximum charge to be detonated per delay.

6   Conclusions

A specific ANN was proposed to predict blast-induced ground vibration at a community near a large iron ore mine in the Quadrilátero Ferrífero region in Brazil. The specialty of the neural network consists of the use of blast design elements and rock properties in contrast with conventional predictors that are only based on maximum charge per delay and the distance between blasting and monitoring point. The conventional empirical predictors do not consider other influencing parameters.

Despite the complex correlation between input and output, the ANN obtained a good performance, showed by the high value of R^2. The ANN model can learn other hidden patterns that are not clear at the original data set. As long as the data set increases, the ANN can be updated and trained again to obtain better correlation results.

The ANN model may be used to predict the blast-induced ground vibration (PVS) before blasting, representing a valuable tool for evaluating the possible environmental effects of a blast in the surroundings of the mine. The model allows the blaster to stablish the maximum charge per delay and the amount of explosive to be used in order to control the ground vibrations, hence avoiding human discomfort and damage to nearby infrastructures from neighboring communities.

References

1. Álvarez-Vigil, A.E., Gonzalez-Nicieza, C., Gayarre, F.L., Álvarez-Fernández, M.I.: Predicting blasting propagation velocity and vibration frequency using artificial neural networks. Int. J. Rock Mech. Min. Sci. **55**, 108–116 (2012)
2. Armaghani, D.J., Hajihassani, M., Mohamad, E.T., Marto, A., Noorani, S.A.: Blasting-induced flyrock and ground vibration prediction through an expert artificial neural network based on particle swarm optimization. Arab. J. Geosci. **7**(12), 5383–5396 (2014)

3. Khandelwal, M., Singh, T.N.: Prediction of blast-induced ground vibration using artificial neural network. Int. J. Rock Mech. Min. Sci. **46**(7), 1214–1222 (2009)
4. Shi, X.Z., Chen, S.R.: Delay time optimization in blasting operations for mitigating the vibration-effects on final pit walls' stability. Soil Dyn. Earthq. Eng. **31**(8), 1154–1158 (2011)
5. Chakraborty, A.K., Guha, P., Chattopadhyay, B., Pal, S., Das, J.: A fusion neural network for estimation of blasting vibration. In: International Conference on Neural Information Processing, pp. 1008–1013. Springer, Berlin, Heidelberg (2004)
6. Singh, T.N.: Artificial neural network approach for prediction and control of ground vibrations in mines. Min. Technol. **113**(4), 251–256 (2004)
7. Khandelwal, M., Singh, T.N.: Prediction of blast induced ground vibrations and frequency in opencast mine: a neural network approach. J. Sound Vib. **289**(4–5), 711–725 (2006)
8. Khandelwal, M., Singh, T.N.: Evaluation of blast-induced ground vibration predictors. Soil Dyn. Earthq. Eng. **27**(2), 116–125 (2007)
9. Monjezi, M., Dehghani, H.: Evaluation of effect of blasting pattern parameters on back break using neural networks. Int. J. Rock Mech. Min. Sci. **45**(8), 1446–1453 (2008)
10. Monjezi, M., Rizi, S.H., Majd, V.J., Khandelwal, M.: Artificial neural network as a tool for backbreak prediction. Geotech. Geol. Eng. **32**(1), 21–30 (2014)
11. Kulatilake, P.H.S.W., Qiong, W., Hudaverdi, T., Kuzu, C.: Mean particle size prediction in rock blast fragmentation using neural networks. Eng. Geol. **114**(3–4), 298–311 (2010)
12. Lilly, P.A.: An empirical method of assessing rock mass blastability. The AusIMM (1986)
13. ABNT. NBR 9653. Guia para avaliação dos efeitos provocados pelo uso de explosivos nas minerações em áreas urbanas. Norma de Procedimento 13 (Guide for assessing the blasting effects in urban areas) (2005)
14. DEUTSCHE NORM (DIN 4150). Structural Vibration in Buildings e Effects on Structures (1986)
15. NP 2074-2015. Avaliaçao da influência de vibrações impulsivas em estruturas (Impulsive blasting-induced vibration in structures). Portugal, 17 (2015)
16. USBM (United States Bureau of Mines). Bureau of Mines report, 59. RI 8507 (1980)
17. Torres, V.N., Silveira, L.G., Lopes, P.F., de Lima, H.M.: Assessing and controlling of bench blasting-induced vibrations to minimize impacts to a neighboring community. J. Clean. Prod. **187**, 514–524 (2018)
18. Amnieh, H.B., Mozdianfard, M.R., Siamaki, A.: Predicting of blasting vibrations in Sarcheshmeh copper mine by neural network. Saf. Sci. **48**(3), 319–325 (2010)
19. Neaupane, K.M., Achet, S.H.: Use of backpropagation neural network for landslide monitoring: a case study in the higher Himalaya. Eng. Geol. **74**(3–4), 213–226 (2004)
20. Hudaverdi, T., Kuzu, C., Fisne, A.: Investigation of the blast fragmentation using the mean fragment size and fragmentation index. Int. J. Rock Mech. Min. Sci. **56**, 136–145 (2012)
21. Ulusay, R.: The ISRM Suggested Methods for Rock Characterization, Testing and Monitoring (2014)
22. Lourakis, M.I.: A Brief Description of the Levenberg-Marquardt Algorithm Implemented by Levmar. In: Matrix, vol. 3, no. 2 (August 2005)
23. Draper, N.R., Smith, H.: Applied Regression Analysis, vol. 326. Wiley, Hoboken (2014)

Part IV
Design, Planning and Optimization
of Surface and Underground Mines

Comparison of Different Approaches to Strategic Open-Pit Mine Planning Under Geological Uncertainty

G. Nelis, N. Morales and E. Widzyk-Capehart

1 Introduction

Strategic mine planning must gather and incorporate several sources of information: geology, geomechanical stability, financial, mineral processing, environmental, and others. These factors are often not well defined since they generally involve future behaviors, or their complete characterization is excessively expensive, such as, financial or equipment factors or geological factors, respectively. Therefore, the planner has to rely on estimation of these parameters to obtain the best production schedule possible for the mine operation. There is, however, no guarantee that these estimations will be correct, or even acceptable, when the mine operation is in progress. Bad estimation of some parameters could potentially lead to significant economic losses, which is highly detrimental for the mining project. Moreover, it could lead to wrong investment decision, which are very difficult to modify [1].

The incorporation of uncertainty during the strategic mine planning process has been a major topic of discussion in the last decade towards ensuring that the strategic decisions, such as mining sequencing, equipment fleet investment, and metal production per period consider the uncertainty during the process [2]. Since the deterministic approach in strategic mine planning is based on operational research techniques [3], the incorporation of uncertainty has followed the same approach, using stochastic optimization models to control the uncertainty.

Depending on the type of uncertainty selected to be addressed and how it is modeled, there has been a wide range of approaches to-date. Specifically, for geological

G. Nelis (✉) · N. Morales · E. Widzyk-Capehart
Advanced Mining Technology Center,
University of Chile, Santiago, Chile
e-mail: gnelis@delphoslab.cl

G. Nelis · N. Morales
Delphos Mine Planning Laboratory, Department of Mining Engineering,
University of Chile, Santiago, Chile

uncertainty, the traditional practice has been the use of a single estimate, based on a kriging technique, with the kriging variance as a measure of the precision of such estimation. However, it has been shown that, in some cases, the use of a single kriging estimate generates a production plan that is not achievable in the mine operation both in production targets and economical value [1]. More sophisticated techniques, such as geological simulation, rely on a different paradigm: they produce various possible scenarios, where a single block has a range of possible outcomes showing the local variability seen in real deposits. The use of stochastic techniques allows the mine planner to consider these different geological scenarios during the optimization process to obtain a reliable plan with a good performance for each simulation.

As there is no a unique approach to incorporate the uncertainty in the evaluation, various optimization models have been proposed based on different concepts of the strategic mine planning problem and the impact of the uncertainty. For example, the robust and risk averse approaches focus on obtaining a plan with an acceptable performance in the worst-case scenario to assure a minimum revenue with certain probability or minimizing a risk measure of the schedule [4–6]. In the neutral risk approaches, typically, an expected value over the different scenarios is optimized and no special weight is given to the bad outcomes.

The advantages and disadvantages of these models are not clear and there are no guidelines about which model ought to be used under certain conditions and which produces a higher value, a more reliable plan or other advantage to the mining operation.

This work focuses on comparing the performance of two risk neutral stochastic mine planning models. The first model is based on the minimization of the deviations from the production targets across every scenario and it was proposed in [7, 8]. They obtained a single mining sequence that incorporated the uncertainty as a penalty for not meeting the production targets in each geological scenario. This penalty was introduced as a cost in the objective function and the schedule aimed to maximize the expected value of the extraction while minimizing the deviations from the targets. This original formulation was extended to different cases: pushbacks selection under geological uncertainty incorporating penalties [9], mine design optimization based on simulated annealing [10], and joint multielement uncertainty for an iron deposit [11]. More recently, this approach was applied in mining complexes with multiple processing streams and transportation alternatives with blending constraints using metaheuristics such as simulated annealing and particle swarm optimization to obtain a solution [12, 13]. The results showed that this kind of formulation generates schedules with a lower deviation chance from the actual targets, with larger optimal pit limits and with NPVs up to 25% higher compared to the deterministic optimization techniques.

The second model is a multistage stochastic programming model proposed in [14]. This model defined different decision stages based on the information available about the uncertain parameters. In each stage, the decision made depended on the previous decisions, the information already gathered, and the probability distribution for the future outcomes. The multistage approach proposed in [14] considered different geological scenarios and incorporated extraction and processing decision that

could be modified in each period of the scheduling. The complexity of this model, however, forced the aggregation of blocks and scenarios to obtain a solvable problem. A similar approach was taken in [15] with a two-stage approach, where the first stage was the extraction decision for each period and the second-stage decision was the destination of each block which was different for each geological scenario, considering that in the short term, the blasthole information allowed the modification of the processing destination. This model was solved using a modified version of Bienstock-Zuckerberg algorithm [16] and a Toposort heuristic [17]. Another two-stage model was also proposed in [18], but the first and second stage were defined based on the availability of the blasthole information in the short term to evaluate the effect of gathering this information in advance. These models achieved higher NPVs in comparison to the deterministic optimization, which ranged from 1% up to 10% depending on the case.

2 Methodology

2.1 Minimization of Deviations

As different models can be used to minimize deviations from the production targets, in this paper, the variant found in [19] with a single mine, a single element, and without blending constraints was used in the analysis.

2.1.1 Definitions and Assumptions

Let B be the set of blocks, R the set of Resources, T the set of periods, and S the set of geological scenarios. Let us define $\bar{v}_{bt}$ as the expected value obtained if block $b \in B$ is extracted at period $t \in T$, r_{bs} the resource $r \in R$ of block $b \in B$ considering simulation $s \in S$, and $C_r^{u/l}$ as the upper and lower targets for resource r. The deviation cost from the upper or lower targets for resource $r \in R$ in scenario $s \in S$ is defined as $c_{rs}^{u/l}$ while f^t as the orebody risk discount rate.

2.1.2 Function Formulation

The decision variables for this model are

$$x_{bt} \begin{cases} 1 \text{ if block } b \in B, \text{ is extracted at period } t \in T \\ 0 \text{ otherwise} \end{cases} \tag{1}$$

$$d_{rst}^{u/l} = \text{deviation from target } C_r^{u/l} \text{ in scenarios at period } t \tag{2}$$

$$\max \quad \sum_{b \in B} \sum_{t \in T} \bar{v}_{bt} x_{bt} + \sum_{s \in S} \sum_{t \in T} \sum_{r \in R} f^t d_{rst}^{u/l} c_{rs}^{u/l} \tag{3}$$

$$\text{s.t.} \quad \sum_{b \in B} r_{bs} x_{bt} + d_{rst}^l \geq C_r^l \quad \forall t \in T, s \in S, r \in R \tag{4}$$

$$\sum_{b \in B} r_{bs} x_{bt} - d_{rst}^u \leq C_r^u \quad \forall t \in T, s \in S, r \in R \tag{5}$$

$$\sum_{b \in B} \left(\beta_{bs} - C_\beta^l \right) \alpha_{bs} x_{bt} + d_{\beta st}^l \geq 0 \quad \forall t \in T, s \in S, \alpha, \beta \in R \tag{6}$$

$$\sum_{b \in B} \left(\beta_{bs} - C_\beta^u \right) \alpha_{bs} x_{bt} - d_{\beta st}^u \leq 0 \quad \forall t \in T, s \in S, \alpha, \beta \in R \tag{7}$$

$$x_{it} \leq \sum_{p=1}^t x_{jp} \quad \forall t \in T, j \in \mathcal{P}(i) \tag{8}$$

$$\sum_{t \in T} x_{bt} \leq 1 \quad \forall b \in B \tag{9}$$

Equation (3) is the objective function. The first term addresses the maximization of the expected NPV of the extraction, while the second term discounts the deviation costs for every resource considered. The factor f discounts the value from deviations at different periods to introduce a geological risk profile on the schedule. Equations (4) and (5) represent the capacity deviation constraints for upper and lower targets, such as mining and processing limits. Equations (6) and (7) are blending deviations constraints, such as target metal grade or limits for contaminants. Equation (8) represents the precedence constraint to maintain the order in the extraction, where $\mathcal{P}(i)$ is the set of predecessors for each block i. Finally, Eq. (9) is the unicity constraint, where each block can be extracted only once.

This formulation is not exactly the same as the one proposed in [19] since the formulation in [19] incorporated dummy constraints to balance the deviation constraints. However, the results are indeed equivalent without those variables and imposed inequalities in the deviation constraints.

2.2 Two-Stage Stochastic Mine Planning Scheduling

The proposed two-stage stochastic model is based on [15]. The first stage decision considers only the extraction of each block, imposing the same schedule for every geological scenario. The second-stage decision selects the best destination for each scenario, aiming to maximize the NPV and fulfill the processing constraints. This two-stage decision framework is similar to the actual mining operation, where the destination decision can be changed in the short term. This model considers that the flexibility to make the long-term scheduling decision to obtain a higher NPV compared to the deterministic scheduling framework.

2.2.1 Definitions and Assumptions

Let B be the set of blocks, R the set of Resources, T the set of periods, and S the set of geological scenarios. Let us define $\bar{c}_{bt}$ as the extraction cost of $b \in B$ at period t, r_{bds} the resource $r \in R$ of block $b \in B$ considering simulation $s \in S$ if the block is sent to destination $d \in D$ associated with the second-stage decision, and $\overline{r_c}$ as the resources scenario-independent, associated with the first stage decision. Upper target for resource r is defined as C_r^u and the p_{btds} is the profit obtained if block $b \in B$ is sent to destination $d \in D$ in scenario $s \in S$ at period $t \in T$.

2.2.2 Model Formulation

The decision variables of this model are

$$x_{bt} \begin{cases} 1 \text{ if block } b \in B, \text{ is extracted at period } t \in T \\ 0 \text{ otherwise} \end{cases} \tag{10}$$

$$y_{btds} = \text{fraction of block } b \text{ sent to destination } d \text{ at period } t \text{ in scenario } s \tag{11}$$

$$\max \quad \sum_{b \in B} \sum_{t \in T} \bar{c}_{bt} x_{bt} + \frac{1}{|S|} \sum_{s \in S} \sum_{t \in T} \sum_{d \in D} p_{btds} y_{btds} \tag{12}$$

$$\text{s.t.} \quad \sum_{b \in B} \bar{r}_b x_{bt} \leq C_r^u \quad \forall t \in T, s \in S, r \in R \tag{13}$$

$$\sum_{b \in B} \sum_{d \in D} r_{bds} y_{btds} \leq C_{r'}^u \quad \forall t \in T, s \in S, r \in R \tag{14}$$

$$x_{bt} = \sum_{d \in D} y_{bdts} \quad \forall t \in T, s \in S, b \in B \tag{15}$$

$$x_{it} \leq \sum_{p=1}^{t} x_{jp} \quad \forall t \in T, j \in \mathcal{P}(i) \tag{16}$$

$$\sum_{t \in T} x_{bt} \leq 1 \quad \forall b \in B \tag{17}$$

Equation (12) is the objective function. The first term represents the cost of extraction while the second term is the expected profit obtained for processing decisions considering every geological scenario. Equation (13) represents the capacity constraints for the extraction, such as mining capacity. Equation (14) represents the capacity constraints for the processing of each block, associated with the second-stage variable. Equation (15) states the relation between x and y variables; a block can be processed only if it was extracted and every fraction of the block was processed. Equation (16) represents the precedence constraints while Eq. (17) the unicity constraints.

2.3 Comparison

Both models were implemented for the evaluation of the same deposit to obtain mining schedules under uncertainty. From these schedules, performance indicators were calculated, such as total ore and waste tonnage. In addition, a comparison between the different extraction decisions was performed to evaluate if different approaches would lead to different final pits.

The production plan was compared considering the deviations from the production targets for each scenario and the average ore and waste for each model to evaluate the mining and processing profile in each period.

An economic analysis was performed aiming to respond how these different methodologies achieved a higher NPV as compared to the traditional case.

3 Results

The study case was a copper porphyry deposit with 14,800 blocks. The scenarios were obtained using sequential Gaussian simulation on point support and later a reblock was performed to obtain the final block size. The scheduling and economic parameters for both cases are shown in Tables 1 and 2.

3.1 Scheduling Results

Table 3 shows a comparison of the value and the final pit for each model, with a deterministic schedule with the same parameters as reference. As expected, both

Table 1 Economic parameters

Mining cost	1.0	US$/ton
Processing cost	10	US$/ton
Deviation cost	0.1	US$/ton
Selling cost	0.5	US$/lb
Cu price	1.5	US$/lb
Cu recovery	90	%
Discount rate	10	%

Table 2 Scheduling parameters

Periods	5	
Scenarios	10	
Mining capacity	5.5	Mton/period
Processing target	4	Mton/period

Table 3 Reserves for each model

	Total tonnage [Mton]	Reported NPV [US$]	NPV increase (%)
Deviations	27.48	52,912,742	0.81
Two-stage	26.48	52,859,761	0.71
Deterministic	23.85	52,487,241	–
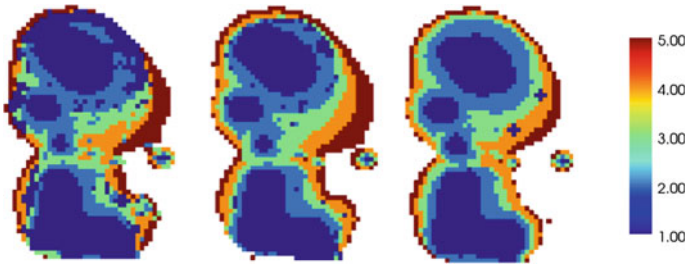
Fig. 1 Plan view of the schedules for different models. From left to right: deviations, two stage, deterministic

Fig. 2 Comparison of sequences between the stochastic models
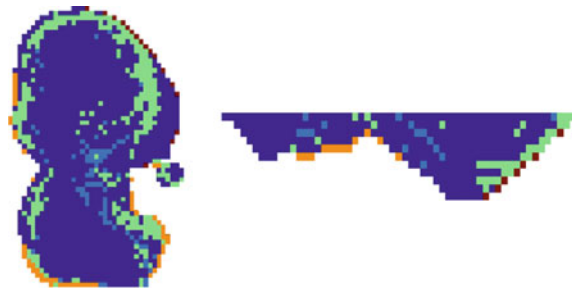
stochastic models achieved a higher NPV compared to the deterministic schedule. The difference between both models was small, both in terms of expected NPV and total tonnage, with the deviations model obtaining a larger and slightly more profitable final pit. Figure 1 shows a plan view of the schedules. The stochastic models generated a larger pit compared to the deterministic case, but the mining sequence was similar among them.

For a better visualization of the differences between both stochastic models, Fig. 2 shows the final pit limits with a color scale aimed to highlight the sequencing differences: the blue color represents the blocks that are extracted in the same period for both schedules; green color represents the blocks that are extracted in an earlier period in the minimization of deviations model, while the light blue represents blocks that are extracted earlier in the two-stage model. Orange blocks are extracted only in the minimization of deviations schedule, while dark red blocks are extracted only in the two-stage schedule.

Table 4 Sequence differences between both stochastic models

Category	Number of blocks
Same period	6618
Earlier in deviations	949
Earlier in two stage	634
Only in deviations	441
Only in two stage	125

The total magnitude of these differences is shown in Table 4, which shows the number of blocks for each category displayed in Fig. 2. The deviations model tended to extract more blocks earlier in the schedule. Also, it can be noticed that both schedules made different final pit decisions, with sets of blocks that are only extracted in one of the two models, which is an indication that both objective functions aimed for a different goal: minimizing the deviations in the first model and taking advantage of the change of destination policy in the second model, as it was detailed in Sect. 2.

The average production schedules for both models are shown in Fig. 3. The production profile was similar for both models except in period four, where the deviations model shows a higher average ore production. The dispersion of the ore production for both models is similar, with the maximum and minimum ore produced close to the average value, even for the two-stage model, which does not attempt to minimize these deviations explicitly. The average difference between the processing target and the ore scheduled across every period is 884 kton for the deviations model and 913 kton for the two-stage model. Most of this deviation comes from the last two periods since there is not enough ore to satisfy the production target.
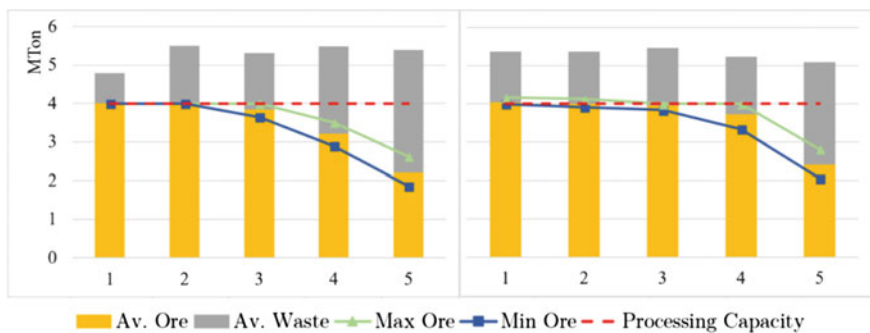
Fig. 3 Production schedules for two-stage model (left) and deviations model (right)

4 Discussion

The first relevant result is that both models achieve a higher NPV value compared to the deterministic schedule, with larger final pits limits as well, which was an expected result considering the related work. The magnitude of the NPV increase, however, was negligible for both models. The small increase could be related to the fact that this study case is a homogeneous copper porphyry with a single metal of interest. For a similar study case with low uncertainty, a similar result was found in [15] using a two-stage model with a negligible NPV increase. For the deviations model, however, a larger NPV increase was expected considering the previous works, where the increases in value ranged between 5 and 25%.

The final pit limits are similar for both models with a 95% of the reserves being common for both models while 80% of the blocks of the final pit are extracted in the same period for both models. Therefore, both models generate a similar pit and sequencing even when the formulations shown in Sect. 2 are different.

It is relevant, however, noting that the differences between the schedules reflect the different nature of both models. For example, Figs. 2, 3 and Table 3 show how the deviation model tends to extract the blocks in earlier periods compared to the two-stage models and how to process more mineral. This behavior is explained by the flexibility introduced by the deviations constraints since they allow to extract blocks faster if the deviation cost is compensated with a higher revenue. When considering the discount rate of the profit function, processing a block in an early period is more profitable than processing the same block later. With this trade-off, the deviations model produces a more aggressive extraction profile in the first periods to take advantage of the lower discount rate.

While the difference in NPV is negligible between both models, the difference in tonnage is not: the deviation model extracts 5% more ore and 3.8% more tonnage than the two-stage model. This difference is explained by the different formulations. The deviations model aims to extract a higher amount of ore to minimize the deviation cost, while the two-stage model extract less ore but with similar value since the objective function only considers the maximization of the expected NPV. The higher amount of ore could be beneficial depending on the strategic business model of the operation.

The analysis of the production schedules reveals that the deviation models surpass the processing targets in some scenarios at periods 1 through 4. While a minor excess of ore is manageable, in the short term, a surplus of mineral in every period generates additional handling cost with an impact on the final NPV. On the other hand, every scenario fulfills the maximum processing capacity in the two-stage model, where the ore target is a hard constraint in the model.

Finally, it is important to mention the selection process of the deviation cost. While the two-stage model does not introduce additional parameters for the schedule, the deviation model requires an additional discount rate and deviation costs for every resource considered. While the literature considers these as control parameters, as a way to introduce the risk profile of the mining engineering on the schedule, the deci-

sion of the best deviation cost, and the discount rate is not trivial. For tonnage deviations, the costs used on previous works range from 2 US$/unit [7] to 10,000 US$/unit [19]. For this work, a trial-and-error approach was used, trying to achieve a higher NPV with acceptable deviations, but this selection depends strongly on the study case. A deeper study of the impact of this cost and a recommended methodology to select it is necessary for future works.

5 Conclusion

The stochastic models compared in this work achieved similar NPV values for this study case but emphasizing different extraction strategies. Recommendations of which model is suitable depend on the strategic business plan since the deviations focused on processing more while the two-stage model focused on higher value. Both models achieved a higher value compared to the deterministic case, showing the advantages of stochastic frameworks in strategic mine planning. However, the increase was small in this study case. A comparison of these models in different, more complex orebodies is recommended to address their differences in a more challenging scenario.

References

1. Dimitrakopoulos, R., Farrelly, C.T., Godoy, M.: Moving forward from traditional optimization: grade uncertainty and risk effects in open-pit design. Trans. Inst. Min. Metall. Sect. A: Min. Technol. **111**, 82–88 (2002)
2. Dimitrakopoulos, R.: Stochastic optimization for strategic mine planning: a decade of developments. J. Min. Sci. **47**(2), 138–150 (2011)
3. Newman, A., Rubio, E., Caro, R., Weintraub, A.: A review of operations research in mine planning. Interfaces **40**(3), 222–245 (2010)
4. Espinoza, D., Lagos, G., Moreno, E., Vielma, J.: Risk averse approaches in open-pit production planning under ore grade uncertainty: an ultimate pit study. In: Proceedings of the 36th International Symposium on the Applications of Computers and Operations Research in the Mineral Industry (APCOM), pp. 492–501 (2013)
5. Espinoza, D., Goycoolea, M., Moreno, E., Muñoz, G., Queyranne, M.: Open pit mine scheduling under uncertainty: a robust approach. In: Proceedings of the 36th International Symposium on the Applications of Computers and Operations Research in the Mineral Industry (APCOM), pp. 433–444 (2013)
6. Amankwah, H., Larsson, T., Textorius, B.: Open-pit mining with uncertainty: a conditional value-at-risk approach. In: Optimization Theory, Decision Making, and Operations Research Applications, 31, pp. 117–139. Springer Proceedings in Mathematics & Statistics (2013)

7. Ramazan, S., Dimitrakopoulos, R.: Stochastic optimisation of long-term production scheduling for open pit mines with a new integer programming formulation. Australas. Inst. Min. Metall. Spectr. Ser. **14**, 359 (2007)
8. Dimitrakopoulos, R., Ramazan, S.: Stochastic integer programming for optimising long-term production schedules of open pit mines - methods, application and value of stochastic solutions. Trans. Inst. Min. Metall. Sect. A: Min. Technol. **117**(4), 155–160 (2008)
9. Albor Consuegra, F.R., Dimitrakopoulos, R.: Algorithmic approach to pushback design based on stochastic programming: method, application and comparisons. Trans. Inst. Min. Metall. Sect. A: Min. Technol. **119**(2), 88–101 (2010)
10. Albor Consuegra, F.R., Dimitrakopoulos, R.: Stochastic mine design optimisation based on simulated annealing: pit limits, production schedules, multiple orebody scenarios and sensitivity analysis. Trans. Inst. Min. Metall. Sect. A: Min. Technol. **118**(2), 79–90 (2009)
11. Benndorf, J., Dimitrakopoulos, R.: Stochastic long-term production scheduling of iron ore deposits: integrating joint multi-element geological uncertainty. J. Min. Sci. **49**(1), 68–81 (2013)
12. Goodfellow, R., Dimitrakopoulos, R.: Global optimization of open pit mining complexes with uncertainty. Appl. Soft Comput. **40**, 292–304 (2016)
13. Montiel, L., Dimitrakopoulos, R.: Optimizing mining complexes with multiple processing and transportation alternatives: an uncertainty-based approach. Eur. J. Oper. Res. **247**, 166–178 (2015)
14. Boland, N., Dimitrescu, I., Froyland, G.: A multistage stochastic programming approach to open pit mine production scheduling with uncertain geology. Optimization Online, http://www.optimization-online.org/DB_FILE/2008/10/2123.pdf. Visited 19 Apr 2018 (2008)
15. Moreno, E., Emery, X., Goycoolea, M., Morales, N., Nelis, G.: A two-stage stochastic model for open pit mine planning under geological uncertainty. In: Proceedings of the 38th International Symposium on the Application of Computers and Operations Research in the Mineral Industry (APCOM), pp. 13.27–13.33 (2017)
16. Bienstock, D., Zuckerberg M.: Solving LP relaxations of large-scale precedence constrained problems. In: Proc. 14th Conf. Integer Programming Combin. Optim. (IPCO). Lecture Notes in Computer Science, 6080, pp. 1–14 (2010)
17. Chicoisne, R., Espinoza, D., Goycoolea, M., Moreno, E., Rubio, E.: A new algorithm for the open-pit mine production scheduling problem. Oper. Res. **60**(3), 517–528 (2012)
18. Nelis, G., Morales, N.: Effect of information on the short-term scheduling in an open pit mine. In: Proceedings of the 5th International Seminar on Mine Planning (2017)
19. Leite, A., Dimitrakopoulos, R.: Stochastic optimization of mine production scheduling with uncertain ore/metal/waste supply. Int. J. Min. Sci. Technol. **24**, 755–762 (2014)

Use of Genetic Algorithms for Optimization of Open-Pit Mining Operations with Geological and Market Uncertainty

G. Franco-Sepulveda, G. P. Jaramillo and J. C. Del Rio

1 Introduction

Traditionally in the literature, there are several optimization models in which the inputs are assumed to be deterministic. The inputs include geological model (mineral available to extract), infrastructure, minerals market (sale prices), and operating scenarios (cutting laws, extraction capacity, among others). The results of this optimization models is a net present value (NPV) in which the value of the risk is zero.

The previous assumptions are far from reality once the operation of the mining project begins. For example, in [1], the copper price estimate for the technical report NI 43-101 of the Florence copper project was made at 3 USD/pound on February 28, 2017. However, while analyzing the price of the metal from that date until now, it was found that approximately 50% of the time the sale value was below the estimate made. It is in these situations when the mining companies begin to question and seek solutions to a problem that is sometimes unsolvable.

For this reason, this paper will address the management of inherent uncertainty with which to work in a mining project, specifically when estimating the amount of mineral resources available and with the prediction of prices of sale of the materials produced in the operation.

The papers discussed some previous works, where the geological and market uncertainty in the mining planning of some operations has been included; describes the stochastic optimization model implemented in the article and presents a case study.

G. Franco-Sepulveda (✉) · G. P. Jaramillo · J. C. Del Rio
Faculty of Mines, National University of Colombia, Bogotá, Colombia
e-mail: gfranco@unal.edu.co

2 Background

When including uncertainty in mining operations, several authors have developed research to address this issue. Boland et al. [2] proposes the open-pit mining production scheduling problem (OPMPSP) as an optimization problem that can be solved by making use of the mixed integer programming and the aggregation of the blocks that are inside the geological model of the deposit, this with the objective to reduce the number of decision variables within the problem as well as the number of restrictions of the same. Although the results obtained by implementing the proposed methodology managed to show improvements in the maximization of the NPV of the mining project, it does not manage to obtain a quantification of the risk which is subject to the same when considering all input data in a deterministic manner.

Dimitrakopoulos [3] proposes a new paradigm in mining planning that integrates stochastic simulation and optimization, where it takes these two elements to unite the uncertainty present in the design of the mine, the planning of the extraction and the valuation of projects and operations mining, using the simulated annealing algorithm in conjunction with the mixed integer programming and sequential simulation.

Dehghani et al. [4] through various methodologies to identify the possible scenarios in which the sale prices of minerals and operational costs will be found, achieve a financial evaluation in mining projects. The methodologies implemented by the authors were two: considering certainty in the sale price and operating costs, and adding uncertainty in both by Monte Carlo simulation, binomial tree method, and pyramid method, finding that in cases where uncertainty was considered, values of the NPV were lower than that found when it was not considered.

Montiel and Dimitrakopoulos [5] seek maximization of the NPV and minimize deviations from the objectives of the extraction, keeping in mind the uncertainty of the ore available in the deposit using the entire stochastic programming. This was done in a copper mine with concentrations of at least 10% in sulfides. The application of the method first analyzes the discount rates and for the stochastic integer programming the probability limits are calculated, observing that it does not matter if a high rate is used because the important changes were obtained with different mining strategies and different amount of mineral and waste.

In Costa and Suslick [6], the uncertainties of the sale prices of the minerals and the operating costs are considered in order to estimate the volatility to which the mining projects are exposed. Through this approach, the authors manage to provide a tool to the investors in charge of making strategic decisions within the companies, and to evaluate the financial viability of the projects.

Chatterjee et al. [7] through the implementation of the minimum cut network flow algorithm they manage to optimize the extraction phases and design the limit of the final pit taking into account the uncertainty of the sale prices of the ore. To create the different possible scenarios for this price, it used a spline smoothing algorithm in conjunction with Gaussian simulation, thus achieving an assessment of the economic benefits of each block within the geological model.

Although the previous works have a common integration of uncertainty when carrying out the optimization of the production scheduling, none integrated so much the geological and market uncertainty at the time to perform this task, leaving aside the full assessment of the risk to which a mining project is exposed. It is here where the methodology presented in this research contributes to the field of mining planning, since it manages these uncertainties simultaneously.

3   Stochastic Optimization Model

The following is a general explanation of the proposed model for the stochastic optimization of a polymetallic deposit of an open-pit operation based on the doctoral thesis [8], which consists of three stages: (1) estimation of the cutoff grade in each year of the mining operation, (2) definition of the production scheduling for the each of the blocks defined within the geological model, and (3) elaboration of the cash flow of the project in which the geological and economic uncertainty is included. It should be noted that those stages are usually optimized independently, while in this work, they are considered jointly.

The proposed optimization model begins with the extraction of the blocks in the mine, which once extracted are sent to a pre-classification process, where they are assigned to a specific stream: (1) the material with a concentration higher than the cutoff grade is sent directly to the mineral processing stage; (2) the material that has a marginal grade is taken to a stockpile in order to be processed later when market conditions are appropriate; and (3) the material that has a low grade is classified as waste and sent to the dumps. Once the material is classified and sent to the process, it goes through a process of size reduction for its subsequent selective flotation for each mineral of interest to the interior of the deposit to finally be refined and sold in the international market.

3.1   *Characteristics of the Proposed Optimization Model*

The main assumptions of the proposed model are:

– inclusion of geological uncertainty using distribution functions for each of the reservoir blocks and economic uncertainty when forecasting the future prices of the minerals of interest through the application of time series.
– inclusion of the complete production chain for a mining operation: Mine, mineral processing, dumps, stockpiles, tailings, refining and market.
– consideration of variation of the cutoff grade as a function of time.
– additional cutoff grade is included to support the decision of the quality of the material that should be sent to the stockpile for further processing.

– possible increases or decreases in the extraction capacity of the mine, in the different processes and refining.

For the application of the proposed model, the nomenclature proposed in [6] was followed, with which one of the following objective functions can be applied:

– Objective function 1: Maximize the expected value of the NPV of the operation.
– Objective function 2: Minimize the risk associated with the standard deviation of the NPV of the operation.
– Another objective function can be used by combining the above two objective funtions as follows.
– Objective 3 function: Maximize (objective function 1/objective function 2).

3.2 Mathematical Model

For the application of the proposed model, the following nomenclature was followed:

- i: index of the block inside the deposit $i = 1, 2, ..., N$
- p: process index $p = 1, 2, 3, 4$
- t: index of the period in which a block is extracted $t = 1, 2, ..., T$
- k: index of the mineral of interest $k = 1, 2, ..., m$
- $E(i, t)$: set of blocks above i that have not been extracted in period t.
- $\gamma(i, k)$: grade of ore k in block i. Specific distribution functions were used for each mineral type using Monte Carlo simulation
- $S(k, t)$: mineral sale price k in period t. Time series will be implemented for their forecast.
- T: time horizon in which the project will be evaluated.
- $m(i)$: cost of mining the block i.
- Cp(p): processing cost of the process p.
- CFLOT: cost of selective flotation.
- $r(k)$: cost of selective flotation of mineral k.
- f: fixed costs per period.
- FL: flotation capacity.
- CINCM/CDECM: cost of increasing or dismantling the capacity of the mine.
- CINCR/CDECR: cost of increasing or dismantling the refining capacity
- CINCC(p)/CDECC(p): cost to increase or dismantle the capacity of the process p.
- Cw: cost of sending waste to the dump.
- Cs: cost of sending material to stockpile.
- Csp: cost of sending material from stockpile to process.
- d: discount rate.
- Mo: initial capacity of mining.
- Co(p): initial capacity of the process p.
- Ro(k): initial refining capacity of mineral k.
- Qw: total capacity of the dump.

- Qs: total capacity of stockpile.
- $y(p)$: recovery factor of process p.
- yf: collective flotation recovery factor.
- yfs(k): selective flotation recovery factor of mineral k.
- $v(i)$: amount of material in block i.

On the other hand, the following decision variables are available within the model:

- $D(t)$: Deeper block that is extracted in t. This value defines which blocks are exploited in t.
- Sp(t): Amount of material in the stockpile that is sent to process in t.
- $\gamma_{cog}(k, t)$: cutoff grade of the mineral k in period t. As it is a polymetallic deposit, it is not a number but a decision rule type AND or OR.
- $\gamma s(k, t)$: cutoff grade of the mineral k in period t of the material sent to stockpile. As it is a polymetallic deposit, it is not a number but a decision rule type AND or OR.
- $\Delta M^{+}(t)$: increase in the capacity of the mine in year t.
- $\Delta M^{-}(t)$: decrease in the capacity of the mine in year t.
- $\Delta C^{+}(p, t)$: increase in the capacity of the process p in year t.
- $\Delta C^{-}(p, t)$: decrease in the capacity of the process p in year t.
- $\Delta R^{+}(t)$: increase in refining capacity in year t.
- $\Delta R^{-}(t)$: decrease in refining capacity in year t.

Other decision variables dependent on the above are presented below:

- $s(i, t)$: 1 if block i is sent to stockpile in period t, 0 otherwise.
- $w(i, t)$: 1 if block i is sent to dump in period t, 0 otherwise.
- pr(i, t): 1 if block i is sent directly to processing in period t, 0 otherwise.
- $x(i, t)$: 1 if block i is extracted in period t, 0 otherwise.
- g_s (k, t): grade of mineral k stored in the pile in period t. This varies as new material is stored.
- $Q(t)$: amount of material mined during period t.
- Qc(p, t): amount of material processed in process p during period t.
- Qr(t): amount of refined material during period t.
- $M(t)$: capacity of the mine in period t.
- $C(p, t)$: capacity of process p in period t.
- $R(t)$: refining capacity in period t.

The NPV of the operation can be expressed as follows:

$$NPV = \sum_{t}(1+d)^{-t}\left[\sum_{k}(S(k,t)\mathrm{yr}(k)\mathrm{Qr}(k,t) - r(k)\mathrm{Qr}(k,t)) - \mathrm{Qc}(t)C(1)\right.$$
$$- \mathrm{Qc}(t)\sum_{p>1} y(p-1)C(p) - \sum_{i} m(i)\mathrm{Qm}(i,t) - \mathrm{CEST}(t)$$
$$\left. - \mathrm{CPALM}(t) - f(t) - \mathrm{CINCRE}(t) - \mathrm{CDECRE}(t) - \mathrm{others}\right]$$
$$(1)$$

1	2	3	4	5	6
7	8	9	10	11	12
13	14	15	16	17	18
19	20	21	22	23	24

Fig. 1 Explanation of *D(t)*

Equations 2, 3, 4, and 5 expressed the total costs of increase or decrease the extraction capacity in the mine, in processes, in refining, of handling of sterile, and the stockpile, respectively.

$$\text{CINCRE}(t) = \text{CINCM} * \Delta M^+(t) + \sum_p \text{CINCC}(p)\Delta P^+(p, t) + \sum_k \text{CINCR}(k)\Delta R^+(k, t), \forall t \tag{2}$$

$$\text{CDECRE}(t) = \text{CDECM} * \Delta M^-(t) + \sum_p \text{CDECC}(p)\Delta P^-(p, t) + \sum_k \text{CDECR}(k)\Delta R^-(k, t), \forall t \tag{3}$$

$$\text{CEST}(t) = C_w \left(\sum_i w(i, t)v(i, t) + rw \right), \forall t \tag{4}$$

$$\text{CPALM}(t) = C_s \left(\sum_i s(i, t)v(i, t) \right) + \text{CspSp}, \forall t \tag{5}$$

To define the extraction constraints, the variable $D(t)$ is taken into account, which defines the blocks that are extracted in t, such that $x(i, t)$ $E(D(t), t)$ being $E(D(t), t)$ the upper cone blocks to the block $D(t)$ that have not yet been extracted in t. From this, in conjunction with the cutoff grade of the material that will be processed and the marginal cutoff grade for the material sent to the stockpile, the blocks that are sent to the process, stockpile or dump are defined by a decision rule. This is done in order to reduce the complexity of the problem by having only t block variables compared to the models generally found in the literature, where binary variables are defined for each block i and for each period t, requiring a lower computational cost which can increase the possibility of finding solutions closer to the optimum, as well as address larger problems or divide into a smaller size looking for an approach to the reality of mining planning. In Fig. 1, the decision variable $D(t)$ and the set $E(D(t),t)$ are exemplified illustratively.

For example, we have the following: D(1) = 8, D(2) = 20, and D(3) = 23, likewise E(D(1),1) = {1, 2, 3, 8}, E(D(2),2) = {4, 5, 7, 9, 10, 13, 14, 15, 20}, and E(D(3),3) = {6, 11, 12, 16, 17, 18, 23}. Thus, in Eq. (6), the exploitation restriction of the blocks is defined as a function of D(t).

$$x(i, t) = 1 \, if \, i \in E(D(t), t) \tag{6}$$

Then, if $x(i, t) = 1$, the decision rule described in [6] is applied according to the cutoff grade-defining if the block is sent to dump, stockpile, or process. For the next period t and for each block i, $E(i, t + 1)$ is updated, thus eliminating the blocks that have been mined in the previous periods. In the Eq. (7), the capacity of extraction of blocks in accordance with the capacity of maximum mining by period is restricted.

$$Qm(t) = \sum_i x(i, t)v(i) \leq M(t), \forall t \tag{7}$$

The distribution of each block is described in Eq. (8), where each block must be sent to dump, stockpile, or processing.

$$x(i, t) = w(i, t) + s(i, t) + \text{pr}(i, t), \forall t, i \tag{8}$$

The volume of the stockpile is updated with the material of the same plus the one that enters in period t and the material sent to processing in the same period. In Eq. (9), this update is shown.

$$IP(t) = IP(t - 1) + \sum_i s(i, t)v(i, t) - Sp(t) \leq Qs, \forall t \tag{9}$$

Once the amount of material entering the stockpile has been defined, the grade of the pile must be updated, assuming that the mixture of the material will have a weighted content due to the material previously stored and the new material. In Eq. (10), this process is detailed for each mineral k.

$$g_s(k, t) = \left(g_s(k, t - 1)IP(t - 1) + \sum_i \gamma(i, k)s(i, t)v(i)\right)\left(IP(t - 1) + \sum_i s(i, t)v(i)\right)^{-1}, \forall t, k \tag{10}$$

The amount of material that enters process 1 is the material extracted in t and complies with the decision rule for the cutoff grade, added to the material that comes from the stockpile. This sum of materials cannot exceed the capacity $C(1, t)$.

$$Qc(t) = \sum_i \text{pr}(i, t)v(i) + Sp(t) \leq C(1, t), \forall t \tag{11}$$

For the other processes, the recovery percentage of the previous process is taken into account.

$$\prod_q^{p-1} y(q)\left(\sum_i \text{pr}(i, t)v(i) + Sp(t)\right) \leq C(p, t), \forall t \tag{12}$$

For the collective flotation process, the amount of material entering this is the sum of the mineral that is recovered in the last process.

$$\text{Qr}(t) = \prod_p y(p) \left(\sum_i \text{pr}(i, t)(i) \sum_k \gamma(i, k) + \text{Sp}(t) \sum_k g_s(k, t) \right) \le \text{FL}(t), \text{ for all } t$$

(13)

Then, the material left over from this process becomes tailings.

$$\text{rw}(t) = \prod_q^{p-1} y(q)\text{Qc}(q) - \text{Qr}(t), \forall t$$

(14)

In each period, the amount of waste that is disposed of in the dump is updated.

$$W(t) = W(t - 1) + \sum_i w(i, t)v(i) + \text{rw}(t) \le \text{Qw}, \forall t$$

(15)

The amount of mineral material k that passes to selective flotation corresponds to the quantity that comes from the last process affected by the recovery factor of the same.

$$\text{QF}(t) = \text{yfs}(k) \prod_p y(p) \left(\sum_i \text{pr}(i, t)v(i)\gamma(k, t) + \text{Sp}(t)\gamma_s(k, t) \right) \le \text{RFS}(k, t), \forall t, k$$

(16)

$$M(t) = M(t - 1) + \Delta M^+(t) - \Delta M^-(t), \forall t$$

(17)

$$C(p, t) = C(p, t - 1) + \Delta C^+(p, t) - \Delta C^-(p, t), \forall t, p$$

(18)

$$R(t) = R(t - 1) + \Delta R^+(t) - \Delta R^-(t), \forall t$$

(19)

In the previous model, precedence and mining restrictions were not included, as it is traditionally done in the literature. This is because in the definition of $D(t)$ and the relation, it has with the matrix of $E(i, t)$ are implicit.

4 Study Case

Once the stochastic optimization model has been defined, we proceed to apply it to a hypothetical mine for a polymetallic deposit in which there are copper, gold and molybdenum minerals. In Table 1, the inputs on which the comparison of the solution obtained with the algorithm proposed in this research will be presented.

This study case has a model of 280 blocks (7 blocks on the x-axis, 8 blocks on the y-axis, and 5 blocks on the z-axis), with dimensions of 650, 390, and 224 m each.

The deterministic and stochastic inputs of the optimization model with their respective data and assumptions are described in [8]. The financial units of this model are given in American dollars.

Table 1 Parameters of model

Study case	
Total inversion	MUS$ 4200
Processing capacity	110 k TPD
Mine capacity	567 k TPD
Life of mine (LoM)	15 years
Refined copper (Cu)	225 k M pounds
Refined molybdenum (Mo)	49 k M pounds
Refined gold (Au)	40 k oz

Table 2 Correlation between the prices of metals

	Copper	Gold	Molybdenum
Copper	1	0.436	0.298
Gold	0.436	1	0.451
Molybdenum	0.298	0.451	1

Table 3 Forecast equations

Mineral	Forecast equation
Copper	$Y_t = 3.346 + 0.228\epsilon_{t-1} + \epsilon_t \ \epsilon_t = 0.203N_t$ $N_t \sim Normal(0, 1)$
Gold	$Y_t = 26.573 + \sigma_t N_t \ N_t \sim Normal(0, 1)$ $\sigma_t^2 = 2418.2 + 0.998(Y_{t-1} - 26.573)$
Molybdenum	$Y_t = \left[8.808 + e^{-0.264}(Y_{t-1} - 8.808)\right] +$ $5.901N_t\sqrt{\frac{1-e^{-2*0.264}}{2*0.264}} \ N_t \sim Normal(0, 1)$

To define the future sales prices of copper, molybdenum, and gold, the historical annual data of these were used from 1975 to 2016, this in order to make a time series adjusted by lots in which the correlation of the variation of metal prices with each other. In Table 2, this correlation is shown.

These correlations were made with the help of the software @RISK, which in turn made the forecast of the prices of metals through time series obtaining the following models, which can be consulted in [9]: RISK MA1 for the price of copper, RISK ARCH1 for the price of gold, and RISK BMMR for the price of molybdenum. Figure 2 shows the graphs that present the historical prices of minerals as well as their possible future scenarios.

In Table 3, the forecast equations for minerals are shown. In Table 3, Y_t is the forecast of the mineral sale price.

The optimization model was applied to the mine in a time horizon of 15 years. Figure 3 shows the results of this optimization for which the Palisade RISKOptimizer tool was implemented. For the execution of the genetic algorithm the following parameters were taken into account: population size of 50 individuals, each of which represents a different production scheduling and where those that present a better
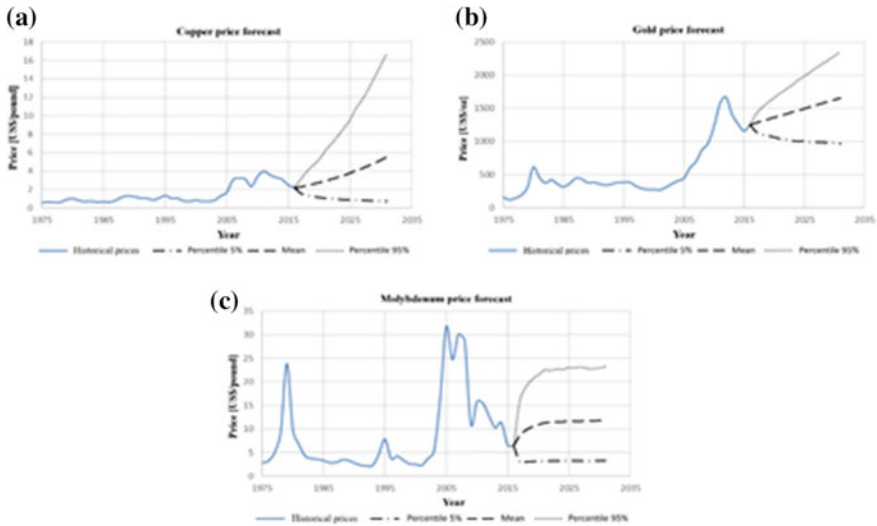
Fig. 2 **a** Copper price forecast. **b** Gold price forecast. **c** Molybdenum price forecast
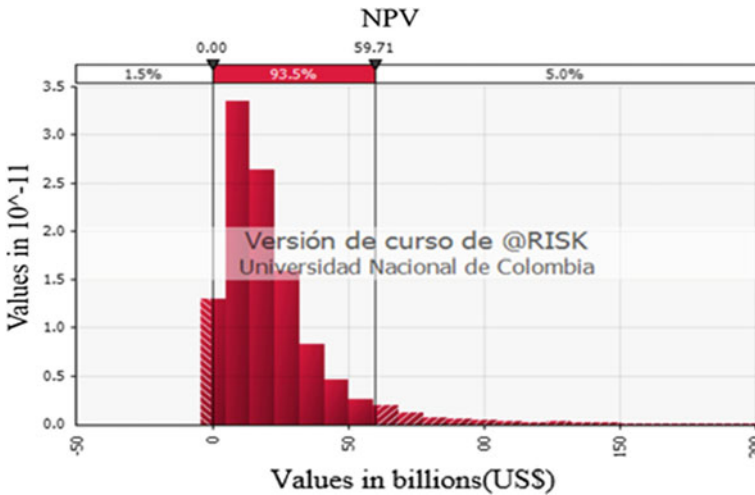
Fig. 3 *NPV* distribution function

fitness function (better VPN in this case) they will have a higher probability of reproducing, a crossover rate of 0.5, and a mutation rate of 0.1. It can be seen that the solution found by the algorithm has low chances of obtaining losses, which are 1.5%, providing financial security at the time of starting the operation of this mine.

However, we wanted to analyze what would happen if the life of mine were shorter; this will be done in order to establish what is the optimum amount of time in which the available mineral resource should be extracted, since we do not have the security
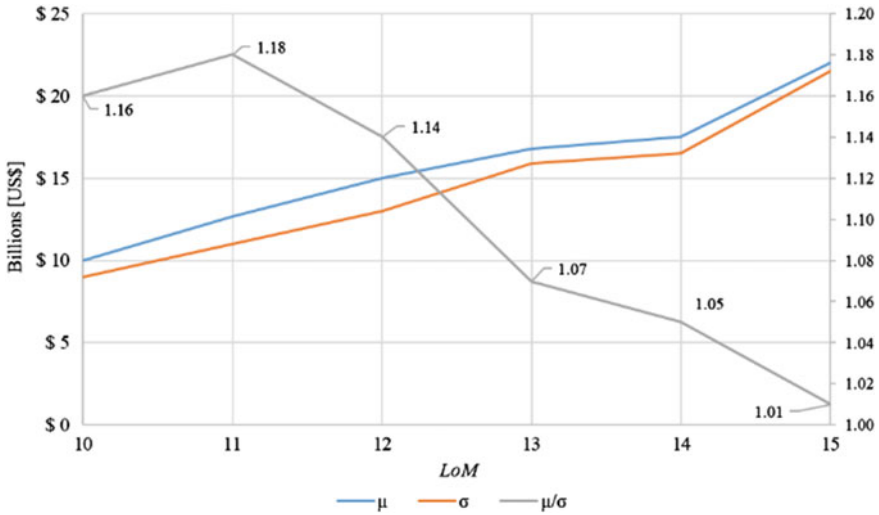
Fig. 4 Results for different years

of knowing if with the operative capacities that it is present in the mine can obtain a return of the capital invested in a shorter time. For this, additional optimizations were made with 10, 11, 12, 13, and 14 years, where the solution found was based on the model where a 15-year operation is considered. This was done with the objective of identifying if the uncertainty associated with the operation of the mine was reduced and in what proportion according to the expected value of the NPV.

Figure 4 shows that both the average NPV and its standard deviation increase as years are added to the LoM, however, the greater relationship between the expected value and its deviation is obtained in year 11, indicating that in the year where there will be a higher return associated with a level of risk is this. Therefore, the results shown below correspond to an operation with a LoM of 11 years.

It is observed that, in all the analyzed cases, a better result is obtained than in the base case [7], since when the uncertainties are not considered, a risk-free 1.7 billion NPV is obtained, while in the cases analyzed under the proposed model yields a much higher NPV, but with a high economic risk Figs. 5 and 6.

5 Conclusions

When analyzing the results obtained, it was observed that under the considerations with which the model was raised and the uncertainties taken into account, the production scheduling presents a low level of risk since its probability of obtaining losses is less than 2%. However, the uncertainty is high since compared to the average value of the NPV obtained is almost equal. On the other hand, if the inclusion of the uncer-

Processing cut-off grade
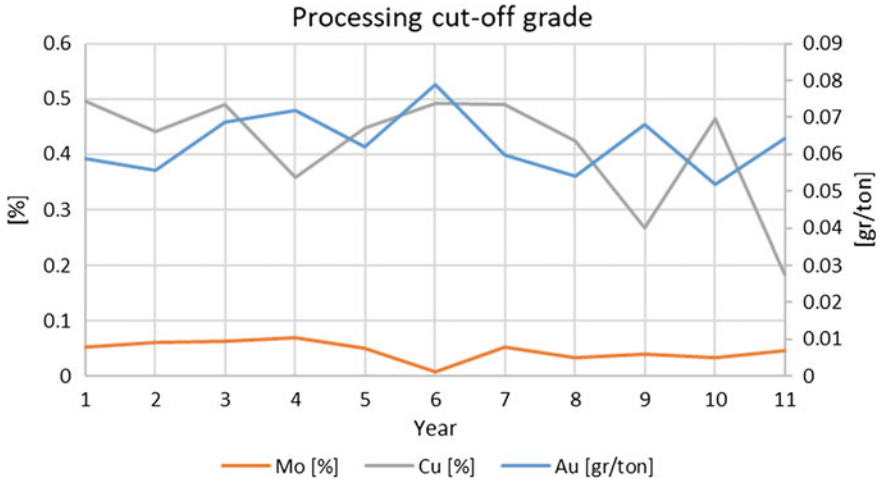
Fig. 5 Processing cutoff grade

Stockpile Cut-off grade
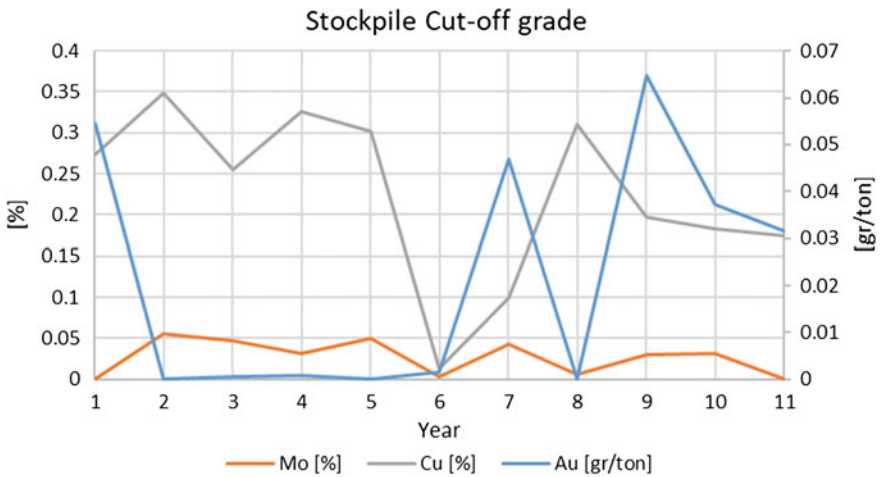
Fig. 6 Stockpile cutoff grade

tainty to which the mining project is exposed is not new given that in the literature, there are models that do it, the way in which they do it does not cover all of it since it is it works only with the average value, either for the price or the ore grades, or a finite and restricted series is made of the possible scenarios that may occur for these variables.

References

1. Taseko Mines Limited: NI 43–101 Technical report Florence copper project. Pinal County (2017)
2. Boland, N., Dumitrescu, I., Froyland, G., Gleixner, A.: LP-based disaggregation approaches to solving the open pit mining production scheduling problem with block processing selectivity. Comput. Oper. Res. **36**, 1064–1089 (2009)
3. Dimitrakopoulos, R.: Stochastic optimization for strategic mine planning: A decade of developments. Journal of Mining Science, 138–150 (2011)
4. Dehghani, H., Ataee, M., Esfahaniipour, A.: Evaluation of the mining projects under economic uncertaintis using multidimensional bionmial tree. Resour Policy **39**, 124–133 (2014)
5. Montiel, L., Dimitrakopoulos, R.: stochastic mine production scheduling with multiple processes: application at Escondida Norte, Chile. J Min Sci. 583–597 (2013)
6. Costa, G., Suslick, S.: Estimating the volatility or mining protects considering price and operating cost uncertainties. Resour Policy **31**(2), 86–94 (2006)
7. Chatterjee, S., Sethi, M., Asad, M.: Production phase and ultimate pit limit design under commodity price uncertainty. Eur. J. Oper. Res. **248**, 658–667 (2016)
8. Franco, G., Jaramillo, P., Branch, B.: Stochastic optimization model for open pit mining. Medellin (2017)
9. PALISADE.: Time series functions in guide for the use of @RISK, Ithaca, Palisade Corporation, 787–806 (2015)

Optimisation of Mining Block Size for Narrow Tabular Gold Deposits

C. Birch

1 Introduction

Key elements of the mine planning process are the geological block and mining block models [1]. These form the basis of the grade-tonnage curve, as well as the financial model [2]. The dimensions of the blocks for the geological block model are guided by the data spacing. The dimensions of the blocks in the mining block model are guided by the mining method and how selective the ore can be mined to minimise dilution [3]. It has been found that on some narrow tabular gold mines, the geological block model is used as the basis for the grade-tonnage curves and subsequent financial models [4]. Typically, narrow tabular gold mines have raise lengths of approximately 200 m with strike spacing between the raises of 150 m. The narrow tabular ore bodies are mined using conventional mining methods with individual panels typically 30–35 m in length. The sample spacing during the mining operation is typically on a 5–6 m grid. Boreholes ahead of the mining face are, however, very sparse, usually drilled from the development below the ore body. These would be closer to a 50 by 50 m grid. Observations by the author have noted that on some narrow tabular gold mines, the geology blocks (typically 15 by 30 m in size) are significantly smaller than the smallest mining block that is currently being mined (often the full 200 by 75 m block accessed by a raise line). The effect of this on the financial model is not clear.

This paper explores how differences in the mining block sizes affect the financial model. Monte Carlo simulation has been used to create a series of hypothetical, narrow tabular gold deposit databases with a range of average grades at either side of the assumed cut-off grade. EXCEL, as well as Leapfrog Geo, software is utilised to create geological block models with a range of sizes. Grade-tonnage curves are

C. Birch (✉)
School of Mining Engineering, University of the Witwatersrand,
Johannesburg, South Africa
e-mail: clinton.birch@wits.ac.za

created for each model and the assumed cut-off grade is applied to determine the resultant tonnes and average mining grade above cut-off grade. Financial models created by these are compared to determine how critical it is to have the mining block model dimensions similar to the smallest selective mining unit.

2 Selection of Block Size

Most of the available literature related to the selection of block sizes is focused on the geological block model rather than the mining block model except stating that the mining method should be taken into consideration. The dimensions of the blocks should be governed by both the mining method as well as the geology. The grade for the individual blocks can be assigned by a variety of methods including inverse distance squared or kriging. The layout of the blocks can be 2D or 3D depending on the nature of the deposit [5]. With the advent of computer technology, the model of the ore body usually consists of numerous small blocks to which the grades are assigned. The blocks size is usually uniform and the block boundaries are orientated to correspond with uniform coordinates and elevations regardless of the ore contacts [6]. If the block crosses the ore/waste boundary, then the block value would be a composite of the ore and waste samples. Although this approach is convenient, it does not take into account the way the ore body will be mined, especially where the mining operations follow the ore/waste contacts. The grade/tonnage curves produced by this approach may also be dangerously misleading [6]. Matomane researched the effect of changing block sizes on the resultant grade-tonnage curves. He identified that the average grade of the ore body [which is based on an Isobel Clark database (http://www.kriging.com/datasets/)] has an impact on whether small or large blocks are preferable as the cut-off grade was altered [7].

The SME Mining Engineering Handbook covers the creation and interpretation of geological models in extensive detail. It states that the purpose of geological modelling is to provide a clear picture of the three-dimensional geological relationships that impact on the geological resource. The improvements in computing technology have allowed for increasingly sophisticated models; however, these require superior data collection and interpretative work to provide these superior resource calculations. The SME Mining Engineering Handbook furthermore goes into detail regarding the block size selection and factors to be taken into account are the following:

– Block sizes need to take into account the computing time and disk storage restrictions;
– The block size should be one-half to one-fourth the average drillhole spacing. Smaller blocks sizes provide a minimal improvement in the estimation unless there are strong geological controls present;
– The block size must be at least one-half the size of the smallest geological feature to be modelled or these will be destroyed in the model;

– The block size may be related to the proposed mining method, for example in open-pit methods, the block height should correspond to the bench height;
– Most software allows for the selection of the block size and some allow for the rotation of the entire block model; and
– The rules are often contradictory and the best solution may be a compromise based on a case-by-case basis [3].

The ideal number of samples to base estimation on is usually in the order of between 10 and 20. More than 20 samples seldom improve the estimation whilst less than 10 samples may cause discontinuities in the estimated grade [3]. For this study, 200 samples are used in the Leapfrog Geo Model for the 1000 by 1000 m block of ground being evaluated. Each sample is 1 m thick and the grades have been assigned using Monte Carlo simulation following a lognormal distribution (mirroring a typical Witwatersrand gold deposit grade distribution). The positions of the samples have been distributed randomly through the hypothetical block.

3 Break-Even Grade, Cut-off Grade and Financial Optimisation

According to the SAMREC Code, mineral reserves or ore reserves are that portions of the mineral resource which is valuable, legally, economically and technically feasible to extract [8]. The commonly accepted method for determining if material forms part of the mineral reserve is to calculate a cut-off grade at the current economic conditions. The only material above this grade is then considered to have economic value and included in the mine plan. The material with a grade lower than the cut-off grade remains in the resource; although with rising commodity prices and/or lower mining costs, it may later be included in the mineral reserve.

3.1 Break-Even Grade

The break-even grade calculation is essentially very simple. It determines the grade required for a unit of ore to return a profit. It is essentially a volume break-even calculation where the volume is known (usually limited due to shaft capacity, mill capacity or some other physical constraint), and the unknown is the in situ grade of the commodity. The other parameters required are total fixed cost and unit variable cost. From these, the total unit cost can be obtained (typically expressed in US$/tonne). The other factors required for the break-even grade calculation is the mine recovery factor (MRF), which is the mine call factor (MCF), multiplied by the plant recovery factor (PRF). The commodity price is quoted in US$ (in troy ounce for gold and platinum). These are all estimates and subject to variation through the period in which the break-

even grade is used—and thus add to the financial risk to the investors if they change significantly. This can be expressed according to Eq. 1:

$$UTC = \left(\frac{TFC}{X}\right) + UVC \tag{1}$$

where UTC = Unit Total Cost [US$/tonne], TFC = Total Fixed Cost [US/tonne], X = Volume [tonne] and UVC = Unit Variable Cost [US$/tonne].

$$UR = G * MRF * P \tag{2}$$

where UR = Unit Revenue [US$/g], G = Grade [g/tonne], MRF = Mine Recovery Factor [%] and P = Price [US$/gram].

Thus, since unit revenue = unit total cost

$$G * MRF * P = \left(\frac{TFC}{X}\right) + UVC \tag{3}$$

$$G = \frac{\left(\left(\frac{TFC}{X}\right) + UVC\right)}{(P * MRF)} \tag{4}$$

For this case study, a gold price of US$1260/oz is assumed. The annual fixed costs for the mine are assumed to be US$50 million with the variable costs being US$80/tonne. The split between fixed and variable cost is 75:25. A feature of South African gold mines is that labour costs are typically 50% [9] of the total costs that results in a higher fixed cost to variable cost ration compared with more typical mining projects where a 50/50 split would be appropriate [10]. The mining cost is based on a hoisting/milling constraint of 200,000 tonnes/annum. The MRF used is 80.75% (85% MCF and 95% PRF). This cost excludes mineral resource royalty tax and income tax. The gold price, costs and production rate have been selected to give a break-even grade of 10 g/t. This is applied as the cut-off grade.

3.2 Cut-off Grade

The cut-off grade is an expansion of the break-even concept. Only blocks above break-even grade are mined—thus this becomes the cut-off grade. The cut-off grade is subject to variations over the life of the mine, however. The basics of the cut-off grade theory are described in Hall's 'Cut-off Grades and Optimising the Strategic Mine Plan' [14]. This book is a comprehensive study of the various techniques currently used in the mining industry. It includes various measures of value including optimising the discounted cash flow (DCF) and net present value (NPV) [11]. The DCF valuation method requires a mine design with good estimations of the expected tonnages and grades as well as costs (fixed and variable) and recoveries to be realised each year of production [12]. The mine's cost of capital is used as the discounting

rate of the cash inflows and outflows. The sum of these discounted cash flows is the (NPV). This discount rate is essentially the cost of capital and it is usually calculated by the weighted average cost of capital (WACC) which considers all the sources of capital required for a project (equity and debt). Real discount rates of 9–12% for mining projects are appropriate for South African mining projects [13]. This is equivalent to 14.5–17.6% at a 5% annual inflation rate for WACC in nominal terms. For this study, 10% has been assumed.

Lane describes in his book 'The Economic Definition of Ore' the economic principles of how cut-off grades are derived and how cut-off grades can be optimised at various stages of a mine's life [14]. Minnitt looked at how Lane's cut-off grade calculations were being adapted to Wits-type gold mines in 2004 [15] and found that the application of the NPV criterion for determining and optimising value in mining operations was limited. He considered NPVs at various points in the value chain (mining, processing and marketing) to determine a balanced cut-off grade. Both Lane and Minnitt consider the NPV calculated over the life of mine rather than short-term profitability as the primary measure of value. Krige and Assibey-Bonsu [16] considered how uncertainty affects the overall tonnage above cut-off grades for valuation purposes [16].

One of the commonly applied grade optimisation methods used by South African mining companies is to establish the break-even grade and apply this as the mining cut-off grade [17]. The estimation of the grades for each mining block is determined by sampling the mineral deposit and projecting the values into the area to be evaluated. Various techniques are used to do this including nearest neighbour, inverse distance squared and kriging. To determine if a mining block is classified as ore or waste, the estimated value is used for this classification. There is, however, a degree of uncertainty regarding the estimated value due to sampling spacing, deposit heterogeneity and method of estimation used. The author has established that the optimal cut-off grade should be lower than the break-even grade when the uncertainties of the grade estimation are considered [18]. For this study, the break-even grade is applied as the cut-off grade.

3.3 Financial Optimisation

Companies can use some sort of 'optimiser' program that utilises the block listing, as well as the basic inputs to calculate the cut-off grade. Every orebody is unique and thus should be considered individually for the determination of cut-off grades. The grade-tonnage curve is then automatically generated—indicating how much material is available above the cut-off grade. The average mining grade (AMG) is also then obtained. This is the average grade of the material above the cut-off grade and becomes the planning grade. For this study, the same approach is applied. The grade-tonnage curve is determined for each hypothetical orebody and block size combination. The tonnes above the cut-off grade (in all cases 10 g/t), as well as the AMG, are determined, and this becomes the basis for a cash flow model. The

Grade-Tonnage Curve
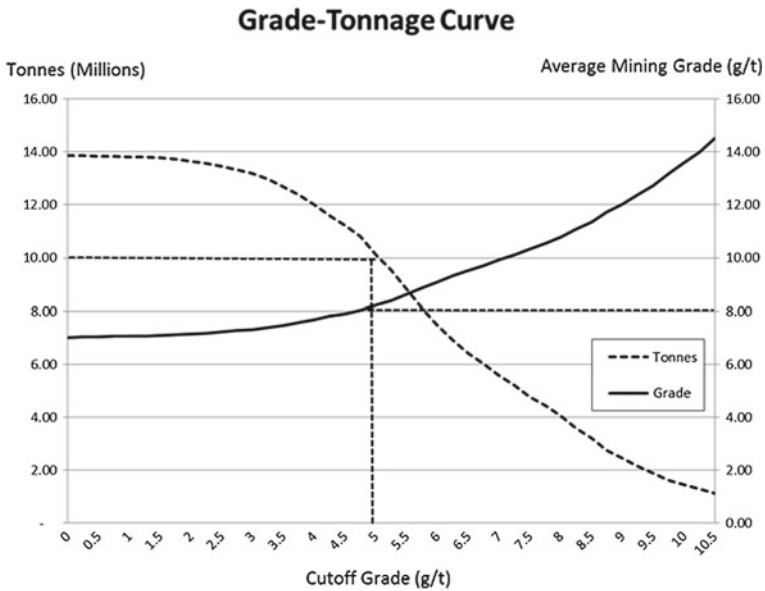
Fig. 1 Typical grade-tonnage curve with a cut-off grade of 5 g/t. The resultant tonnes above 5 g/t are 10.2 million tonnes and the average mining grade is 8.1 g/t

mining rate of 200,000 tonnes/annum is used to deplete the available tonnes, and the resultant profit, as well as the NPV at 10%, can be determined.

Using this block listing, companies declare their mineral resource and reserve into the public domain. This is usually as part of the annual report, but shareholders and potential investors require also at times when a competent person's report is prepared. Figure 1 shows a typical tabular gold deposit grade-tonnage curve.

4 Modelling Exercise

To investigate the impact that altering the mining block size has on the profit as well as the NPV, two approaches for this study were used. Both approaches use hypothetical ore bodies with a 1000 by 1000 m size along with a 1-m thickness. The density is 2.7 g/cm^3, which is typical for Witwatersrand gold deposits. The ore body model can be considered a 2D model. The mining is assumed to extract only the ore with no consideration for minimum mining widths and dilution. The first exercise utilises EXCEL and can be considered the 'theoretical' approach. The second exercise uses Leapfrog Geo and interpolates the grades into the blocks using the block modelling function. This approach is considered the more realistic approach and follows the methodology commonly found applied in South African gold mines.

	1	2	3	4	5	6	7	8	9	10
1	1.51	23.69	9.11	5.85	10.42	8.44	12.94	12.98	8.92	17.97
2	9.55	8.56	8.68	5.52	11.39	7.09	13.19	10.76	3.31	13.09
3	13.05	2.73	4.59	6.49	9.02	4.65	5.87	4.71	16.51	4.00
4	3.93	2.40	12.69	4.27	7.28	2.79	5.17	9.04	5.46	2.02
5	7.55	6.75	2.55	2.49	3.21	5.53	3.77	10.24	7.29	7.04
6	5.56	9.11	10.99	20.78	3.60	1.84	1.62	5.27	7.97	21.17
7	5.44	1.84	4.59	12.06	3.77	5.88	4.30	6.22	3.91	14.04
8	7.14	19.63	10.11	24.33	4.42	3.81	10.19	3.33	3.85	13.30
9	6.77	4.12	6.35	4.70	7.38	5.60	5.93	12.94	26.19	9.18
10	9.04	2.85	2.39	5.26	5.19	2.83	12.75	7.02	6.17	7.33

Fig. 2 A portion of the 10 by 10 m grid for the 8 g/t EXCEL model. 27% tonnes above cut-off grade with an average mining grade of 14.88 g/t

4.1 Grade Models

For both exercises, the grade model is based on the Isobel Clark CMGT dataset that represents a typical Witwatersrand gold deposit (http://www.kriging.com/datasets). The distribution profile is lognormal and Monte Carlo simulation (@Risk) has been used to create the hypothetical orebodies. For the study, these hypothetical ore bodies have average grades of 6, 8, 10, 12 and 14 g/t. The lognormal distributions were capped at the 95 percentile as well as not having negative grades. For the EXCEL Model, the grades were interpolated into a 10 by 10 m grid (effectively 10,000 samples). For the Leapfrog Geo model, 200 Collar, Survey and Assay files were created.

4.2 Block Models

Block sizes of 10 by 10, 20 by 20, 40 by 40, 100 by 100 and 200 by 200 m were selected which represent a total area of 1000 by 1000 m. The channel width assumed to be 100 cm. No dilution was included in the mining model. The density was assumed 2.7 g/cm^3. The total tonnage in the area is thus 2,700,000 tonnes.

	1	2	3	4	5	6	7	8	9	10
1	1.51	23.69	9.11	5.85	10.42	8.44	12.94	12.98	8.92	17.97
2	9.55	8.56	8.68	5.52	11.39	7.09	13.19	10.76	3.31	13.09
3	13.05	2.73	4.59	6.49	9.02	4.65	5.87	4.71	16.51	4.00
4	3.93	2.40	12.69	4.27	7.28	2.79	5.17	9.04	5.46	2.02
5	7.55	6.75	2.55	2.49	3.21	5.53	3.77	10.24	7.29	7.04
6	5.56	9.11	10.99	20.78	3.60	1.84	1.62	5.27	7.97	21.17
7	5.44	1.84	4.59	12.06	3.77	5.88	4.30	6.22	3.91	14.04
8	7.14	19.63	10.11	24.33	4.42	3.81	10.19	3.33	3.85	13.30
9	6.77	4.12	6.35	4.70	7.38	5.60	5.93	12.94	26.19	9.18
10	9.04	2.85	2.39	5.26	5.19	2.83	12.75	7.02	6.17	7.33

Fig. 3 A portion of the 20 by 20 m grid created by compositing and four 10 by 10 m blocks

4.3   The EXCEL Model

EXCEL was used to generate a 10 by 10 m grid. This then averaged for the 20 by 20, 40 by 40, 100 by 100 and 200 by 200 m grids. This was repeated for the 6, 8, 10, 12 and 14 g/t grade distributions. This approach is shown in Figs. 2, 3 and 4.

As can be observed in Figs. 2, 3 and 4, the creation of the larger block models for the EXCEL model is by simply averaging the individual grades from the smaller blocks. It is known that the variance of the grades decreases as the number of samples increases, the so-called volume-variance relationship [19]. This effect is clearly observed in the exercise as the values of the smaller blocks are averaged together as the larger blocks are created.

4.4   EXCEL Grade-Tonnage Curves

In total, 25 grade-tonnage curves created. The cut-off grade of 10 g/t is applied to each of these grade-tonnage curves. The resultant tonnes above cut-off grade as well as average mining grade were obtained for each of these. Examples of these grade-tonnage curves are shown in Figs. 5 and 6.

Fig. 4 A portion of the 20 by 20 m EXCEL model for the 8 g/t model. 21% tonnes above cut-off grade with an average mining grade of 11.78

As can be observed in Figs. 5 and 6, as the block size is increased, there is a significant change in the tonnes above the cut-off, as well as the average mining grade. For this example, the tonnes above cut-off reduce from 735,000 to 571,000 tonnes whilst the average mining grade drops from 14.88 to 11.78 g/t. Figures 7 and 8 show the results from all 25 grade-tonnage curves.

It can be observed in Fig. 7 that as the blocks get larger, the average grade above cut-off grade reduces. In Fig. 8, the percentage tonnes above cut-off grade reduce for the models where the average grade of the ore body is below the cut-off grade. Were the average grade of the ore body is above the cut-off grade, the percentage tonnes above cut-off grade increase as the block size increases.

4.5 EXCEL Cash Flow Model

The cash flow model utilises the following parameters to determine the gross revenue:

– Tonnes available above the cut-off grade
– Average mining grade above cut-off (g/t)
– Annual Production
– Mine call factor (MCF)

Grade-Tonnage Curve 10m by 10m Blocks - Cutoff grade 10g/t

Tonnes above cutoff grade: 735 000   Average mining grade: 14.88g/t
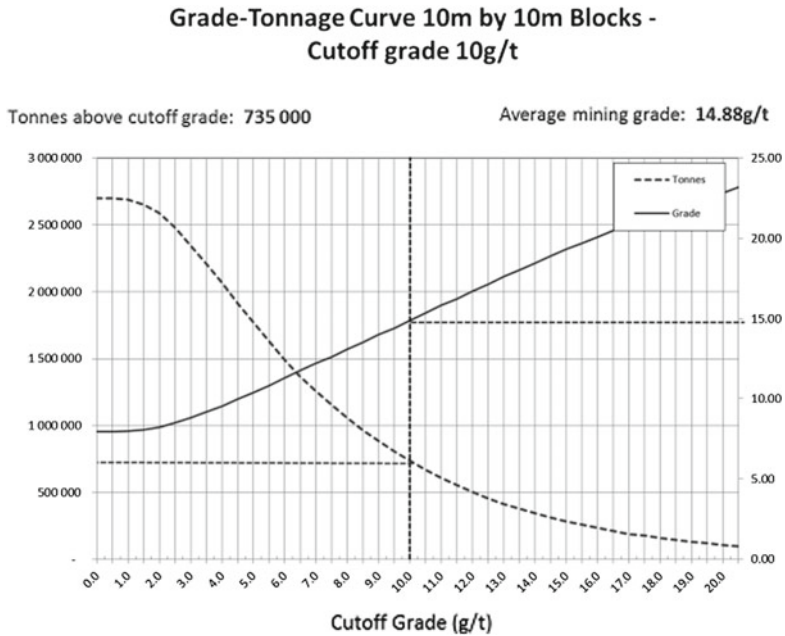
Fig. 5 The 10 by 10 m grade-tonnage curve for the 8 g/t EXCEL model

– Plant recovery factor (PCF)
– Gold Produced (Oz)
– Price (US$/Oz).

The costs are based on a 75:25 split between fixed and variable costs. The annual production, mine recovery factor (MRF), price and costs have been selected to give the selected cut-off grade of 10 g/t. For each grade-tonnage curve, the tonnage above cut-off grade and average mining grade are inserted into the model and the resultant profits as well as NPVs (at a discount rate of 10%) are determined. No separate CAPEX is included in the cash flow model and it is assumed the development costs are included in the fixed and variable costs used. For this exercise, the production rate is kept constant at 200,000 tonnes per annum irrespective of the block size. Thus, no distinction made for costs related to the selectivity. The results are tabulated in Table 1.

It can be clearly seen that in each case, the smaller block size results in higher profits as well as NPV. However, in reality, selectivity comes at a cost. It reduces mining rates (stopping and re-equipping stopes on a regular basis) and causes extra costs to be incurred by extra development. Added flexibility must also be factored into the mine design with spare faces being available to account for unexpected grade drops. These are more likely with small blocks than in the case of larger blocks that are subject to the volume-variance effect [19]. Sampling errors are also considered more critical [20]. To investigate the effect of this, the fixed and variable mining costs

Table 1 Cash flow results for the EXCEL model

Average = 6 g/t					
Block size	10 × 10	20 × 20	40 × 40	100 × 100	200 × 200
Average grade above cut-off	14.85	11.61	10.49		
Tonnes above cut-off	487,000	181,000	4000		
Profit ($ mil)	$86.71	$12.64	$5.33		
NPV ($ mil)	$73.02	$11.49	$4.84		
Average = 8 g/t					
Block size	10 × 10	20 × 20	40 × 40	100 × 100	200 × 200
Average grade above cut-off	14.88	11.78	10.68		
Tonnes above cut-off	735,000	571,000	160,000		
Profit ($ mil)	$113.05	$29.50	$13.75		
NPV ($ mil)	$92.10	$25.36	$12.50		
Average = 10 g/t					
Block size	10 × 10	20 × 20	40 × 40	100 × 100	200 × 200
Average grade above cut-off	15.55	12.48	11.13	10.48	10.18
Tonnes above cut-off	1,090,000	1,236,000	1,296,000	1,296,000	1,512,000
Profit ($ mil)	$212.99	$124.97	$61.98	$34.30	$24.56
NPV ($ mil)	$157.39	$87.51	$43.94	$24.31	$16.75
Average = 12 g/t					
Block size	10 × 10	20 × 20	40 × 40	100 × 100	200 × 200
Average grade above cut-off	16.26	13.30	12.18	11.90	11.90
Tonnes above cut-off	1,451,000	1,927,000	2,424,000	2,700,000	2,700,000
Profit ($ mil)	$337.44	$221.76	$210.77	$196.22	$196.22
NPV ($ mil)	$226.37	$139.70	$115.67	$105.16	$105.16
Average = 14 g/t					
Block size	10 × 10	20 × 20	40 × 40	100 × 100	200 × 200
Average grade above cut-off	17.13	14.58	14.01	13.98	13.98
Tonnes above cut-off	1,829,000	2,418,000	2,683,000	2,700,000	2,700,000
Profit ($ mil)	$479.90	$413.64	$384.69	$379.64	$379.64
NPV ($ mil)	$296.50	$226.76	$205.51	$203.46	$203.46

Grade-Tonnage Curve 20m by 20m Blocks - Cutoff grade 10g/t

Tonnes above cutoff grade: 571 000

Average mining grade: 11.78g/t
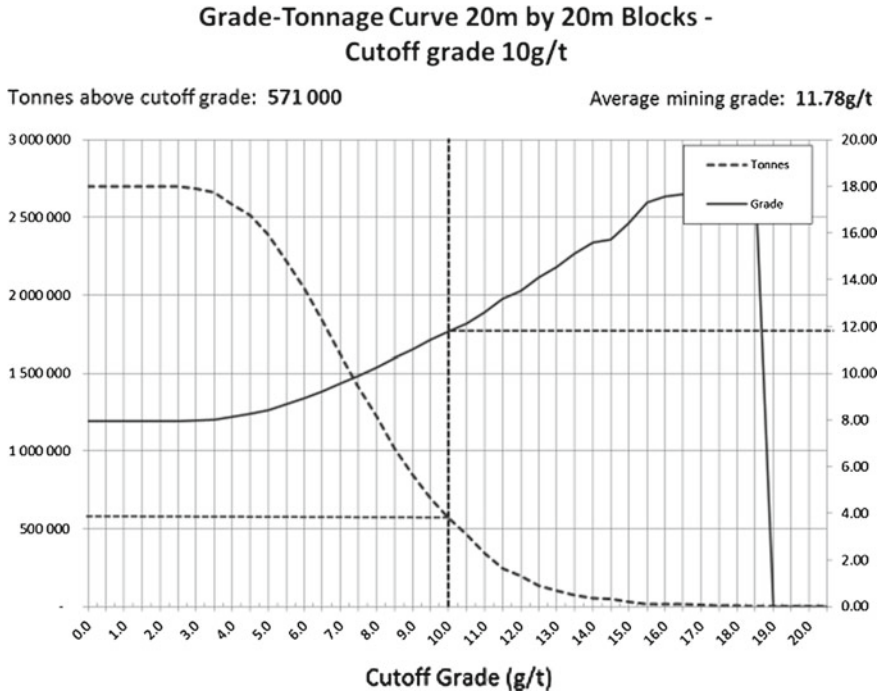
Fig. 6 The 20 by 20 m grade-tonnage curve for the 8 g/t EXCEL model

have kept constant but the mining rate adjusted to simulate the effects of selectivity. The cut-off grade kept at 10 g/t which are based on the planned 200,000 tonnes per annum. However as the block sizes become smaller, this mining rate is adjusted:

– For 10 by 10 m blocks, the mining rate reduced to 120,000 tonnes per annum.
– For 20 by 20 m blocks, the mining rate reduced to 140,000 tonnes per annum.
– For 40 by 40 m blocks, the mining rate reduced to 160,000 tonnes per annum.
– For 100 by 100 m blocks, the mining rate reduced to 180,000 tonnes per annum.
– For 200 by 2000 m blocks, the mining rate kept at the planned 200,000 tonnes per annum.

The profit results for the cash flow exercise are shown in Fig. 9 and the profit results of the adjusted cash flows are shown in Fig. 10.

There is a clear reversal in the cash flow results when the cost of selectivity is considered in the modelling exercise. For the low-grade ore bodies (6, 8 and 10 g/t where the average ore body grade is the same or below the cut-off grade), selectivity and small block sizes were shown increase the average mining grade, as well as the tonnes above cut-off grade in these cases. However, when the cost of selectivity is taken into account (by reducing the mining rate in this case), the model shows they cannot be mined economically. For the higher grade models (where the average ore

Average Grade Above Cut-off Grade
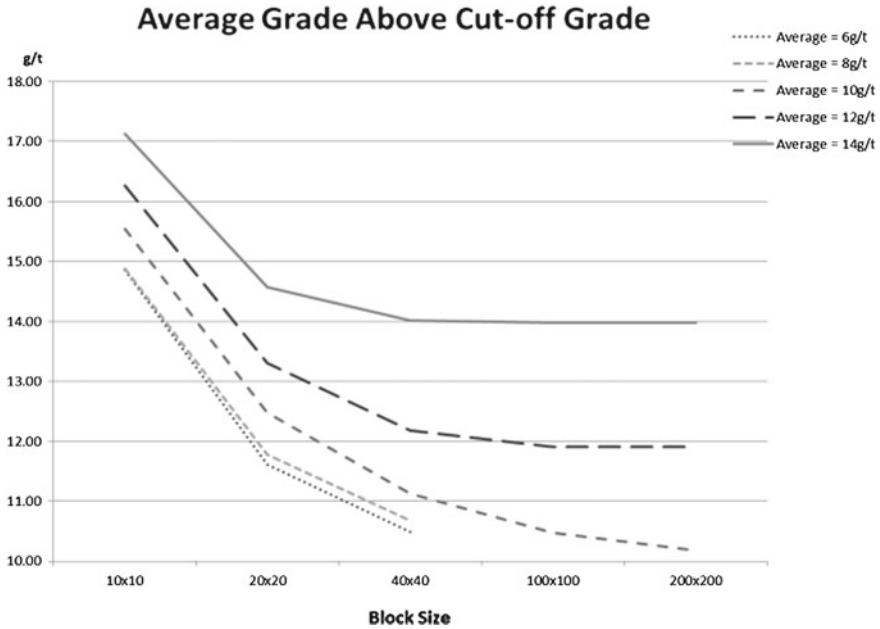
Fig. 7 The average grade above the cut-off for the 6, 8, 10, 12 and 14 g/t EXCEL models as the block sizes are altered

body is above the cut-off grade), the larger mining blocks and the mining efficiencies associated with them show increased profit and NPV.

4.5.1 Leapfrog Geo Grade Model

The EXCEL model can be considered the theoretical model. In an attempt to determine how altering the block sizes will affect the financial model in a more realistic scenario, Leapfrog Geo has been utilised. 200 simulated boreholes with random positioning through the 1000 by 1000 m area have been created. The Collar and Survey files are kept the same for all the models, with just the Assay file been altered to simulate the various average grades for the five ore bodies. This was achieved by using the same lognormal distribution profile and Monte Carlo Simulation (@Risk) approach used to create the EXCEL 6, 8, 10, 12 and 14 g/t hypothetical ore bodies.

Leapfrog Geo uses its own interpolation tool called FastRBF™. This can perform linear or spherical interpolants [21]. These are similar to the linear and spherical variogram models, which are used by other packages to perform kriging [21]. For this exercise, the interpolation was done using the linear interpolation tool (no significant differences were noted in the outputs for the purpose of this study when using the spherical tool). This meant that nuggets, sills and ranges were not required for the creation of the basic model. Due to the base model accuracy not being critical in the
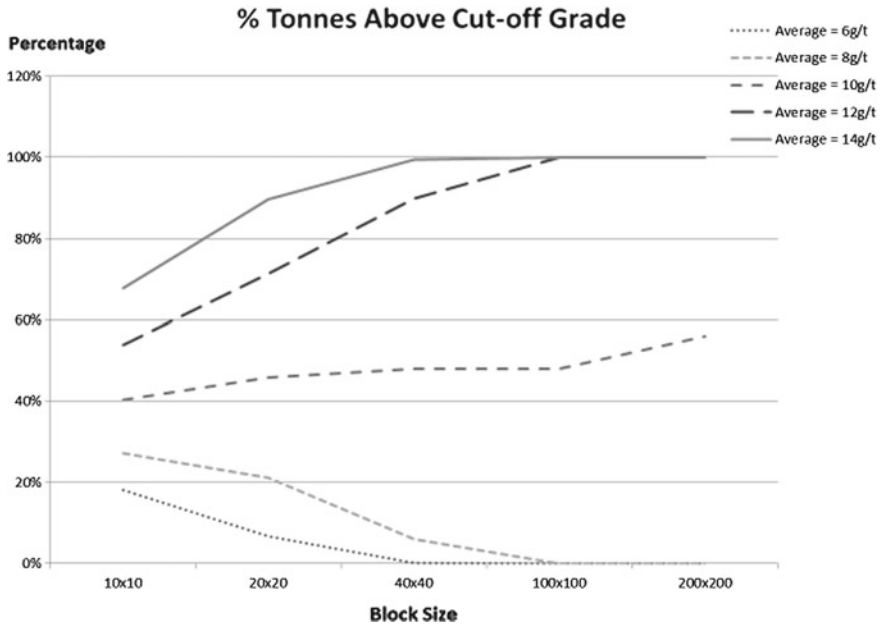
Fig. 8 Percentage tonnes above the cut-off for the 6, 8, 10, 12 and 14 g/t EXCEL Models as the block sizes are altered

study, this was considered acceptable. Figure 11 shows the base model created using the average 8 g/t database. In all the Leapfrog Geo models, the light grey areas/blocks are below the 10 g/t cut-off grade.

Figures 12, 13 and 14 show the 10 by 10, 40 by 40 and 100 by 100 block models for the 8 g/t model.

There is a clear correlation between the grades in the various models as the block sizes are altered. The same pattern is observed in the 10 by 10, 40 by 40 and 100 by 100 m models (Figs. 16, 17 and 18) created for the 14 g/t ore body model (Fig. 15).

The effect of altering the block size using Leapfrog Geo on the resultant grade-tonnage curves is completely different from results observed in the Excel model, as shown in Figs. 19 and 20.

The average grades and percentage tonnes above cut-off grades remain constant for the 10 by 10, 20 by 20, 40 by 40 and 100 by 100 m Leapfrog Geo models. It is only the 200 by 200 m model that shows any variation to this. This is markedly different from the theoretical EXCEL model. In reality, the Leapfrog Geo model is based on 200 sample points, whilst the EXCEL model has effectively 10,000 sample points (but representing the resolution that would require 100,000–200,000 sample points to generate). It is clear that the Leapfrog Geo model lacks the resolution to accurately put values into blocks smaller than approximately 100 by 100 m (based on the 10–20 samples in a block suggested by the SME Mining Engineering Handbook). Due to the lack of variation between the different block size models regarding average grades
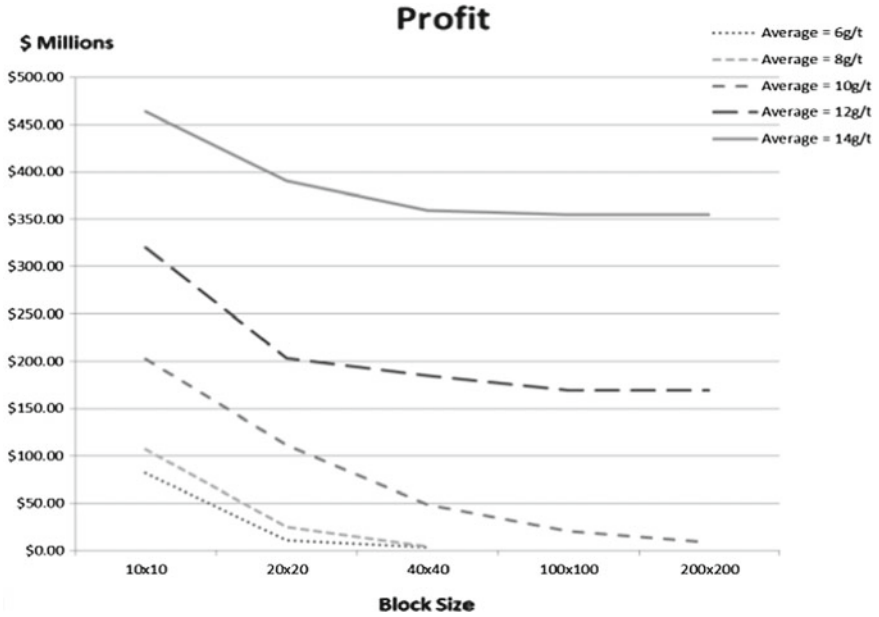
Fig. 9 Profit for each ore body related to the block size
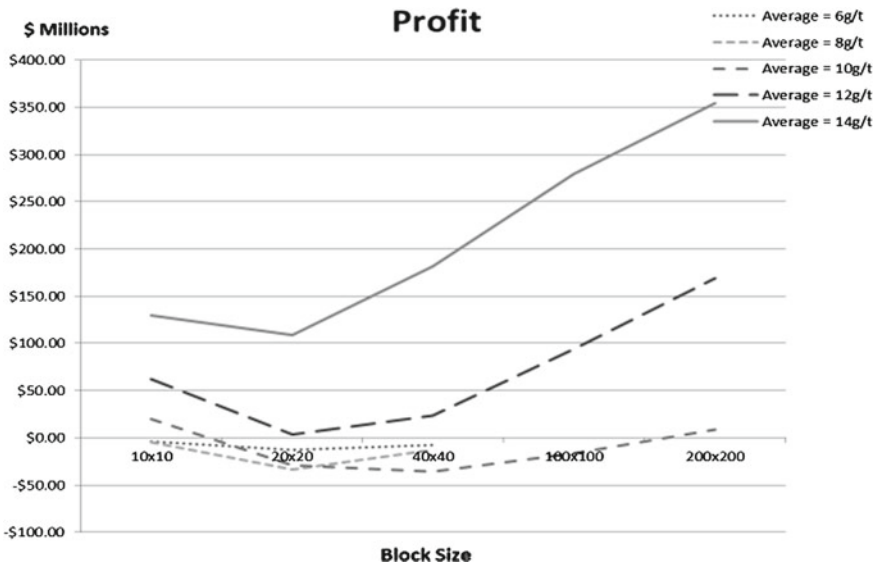
Fig. 10 Profit for each ore body related to block size when the cost of selectivity is considered
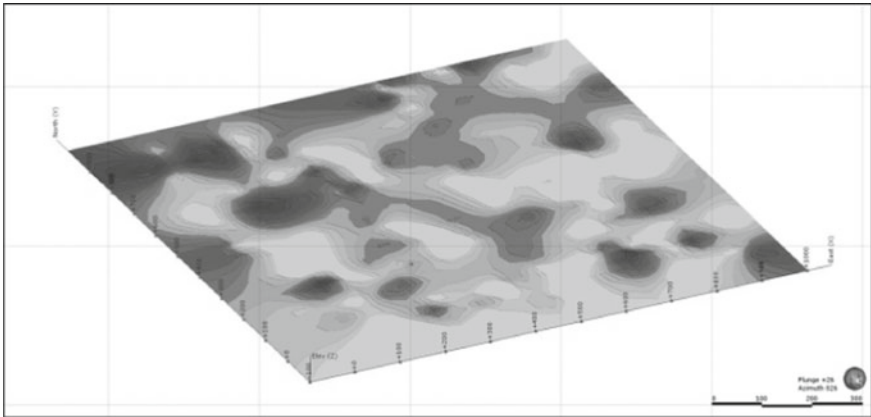
Fig. 11 The base 8 g/t model
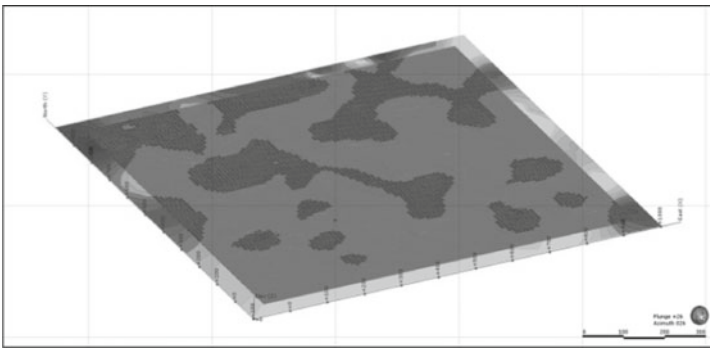
Fig. 12 10 by 10 m blocks for the 8 g/t model
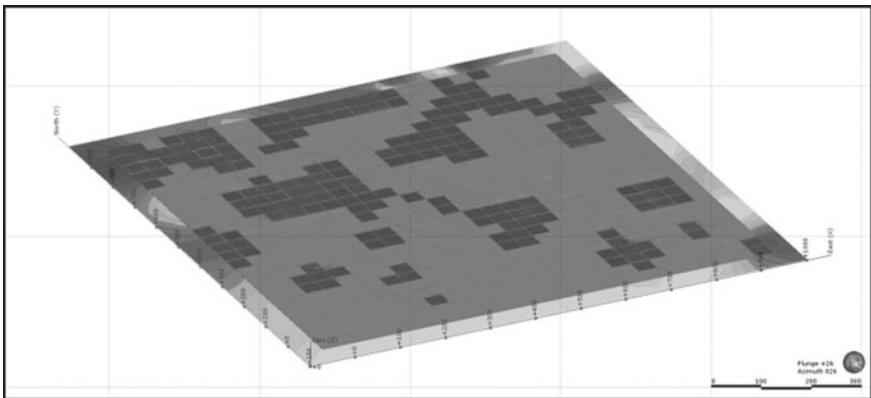
Fig. 13 40 by 40 m blocks for the 8 g/t model
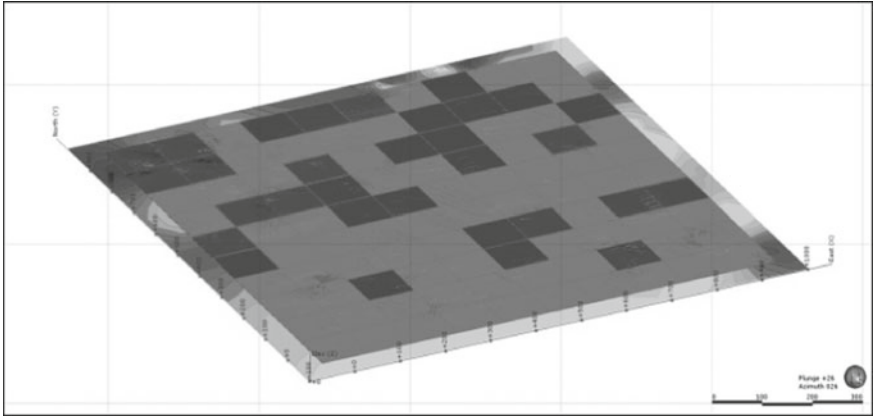
Fig. 14 100 by 100 m blocks for the 8 g/t model
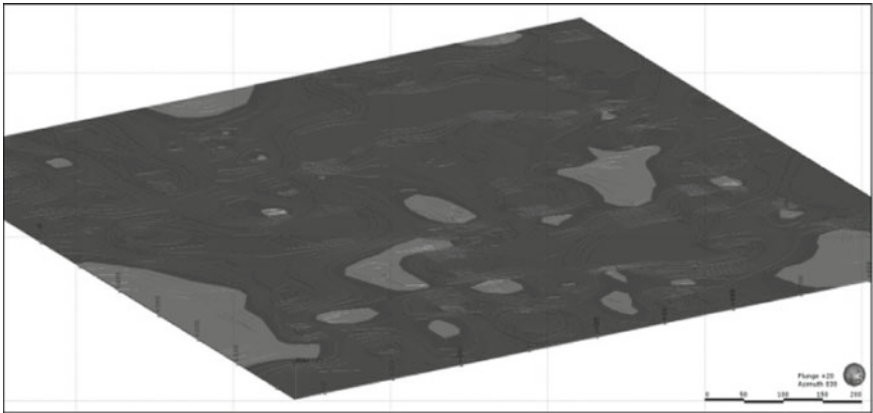
Fig. 15 14 g/t base model

and tonnages above cut-off grade, further financial modelling was not undertaken. The exercise could have been run with more samples, but this would have been considered unrealistic considering the nature of the orebodies being replicated (deep narrow tabular gold deposits) which tend to have sparse drilling intersections. Further samples would also have caused far slower modelling due to the limitations of the computer being utilised for the study.
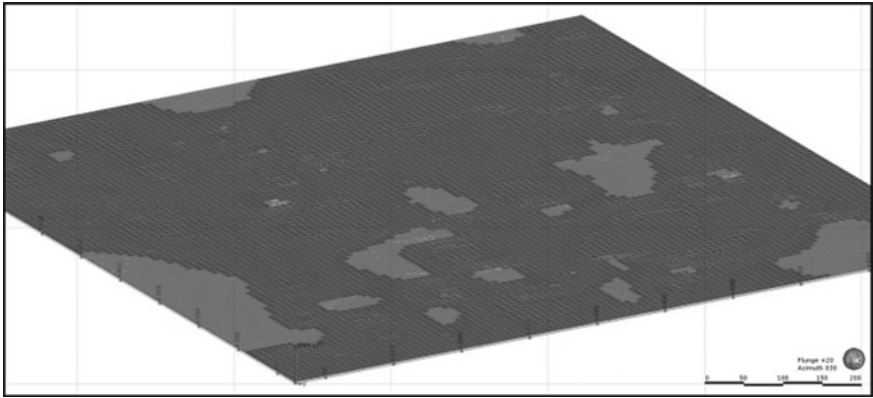
Fig. 16 10 by 10 m blocks for the 14 g/t model
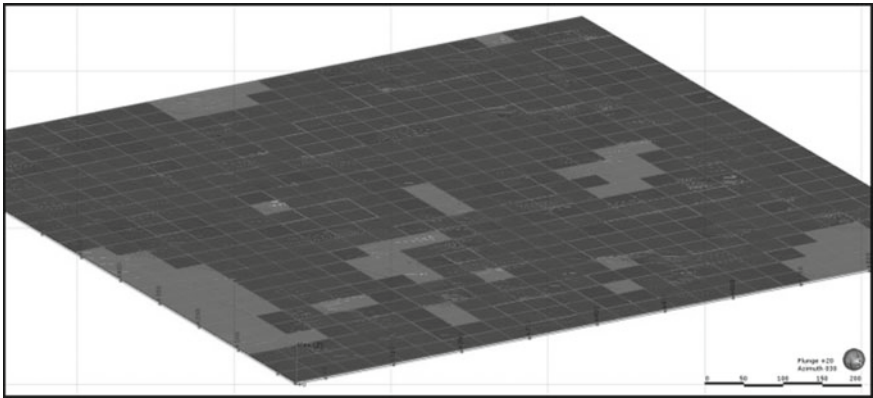
Fig. 17 40 by 40 m blocks for the 14 g/t model
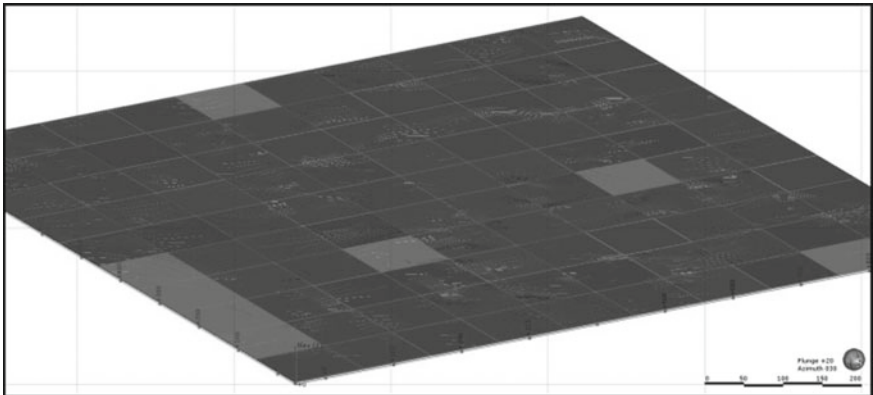
Fig. 18 100 by 100 m blocks for the 14 g/t model
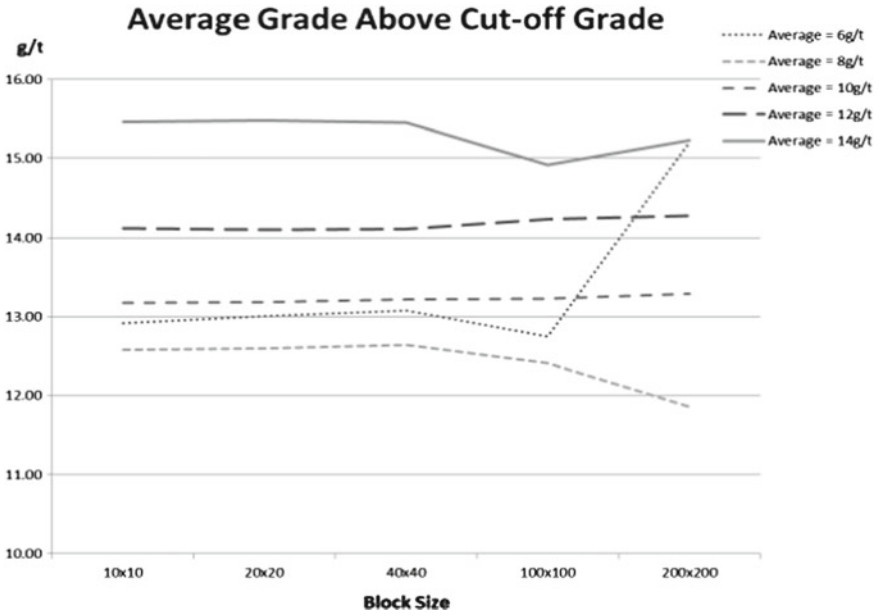
Fig. 19 Average grades above cut-off for the Leapfrog Geo model
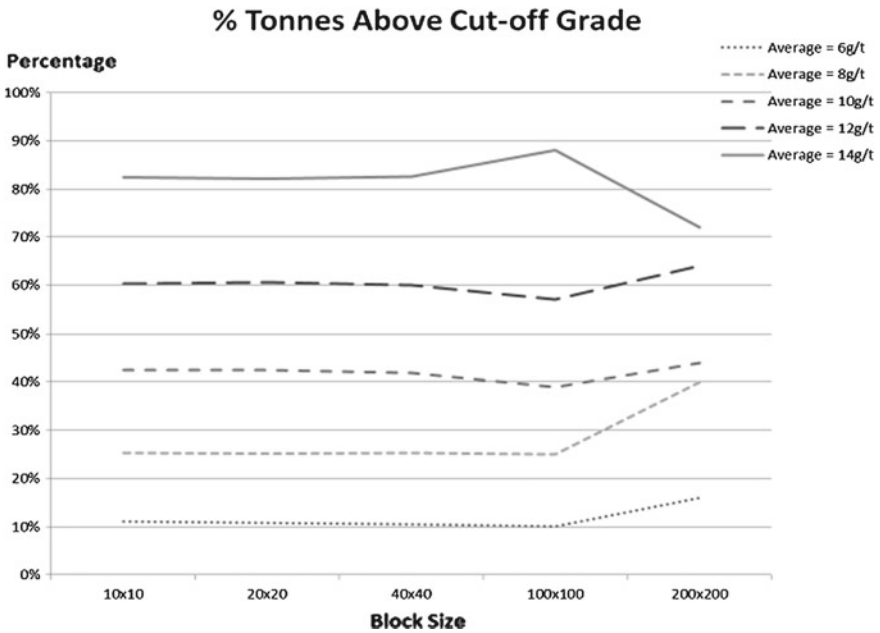
Fig. 20 Percentage tonnes above cut-off grade for the Leapfrog Geo model

5   Conclusions

This study shows that the findings from a theoretical study can be very different when attempted using a more realistic approach. When considering the findings from the EXCEL model the following conclusions can be made:

– Smaller blocks allow more selectivity and the average grade above cut-off grade is higher;
– Where the average grade of the ore body is less than the cut-off grade, then fewer tonnes above cut-off grade are found when smaller blocks are used. This is reversed when the average grade of the ore body is above the cut-off grade where larger blocks result in higher tonnages;
– If the cost of selectivity not considered, then mining smaller blocks is financially optimum irrespective of the average grade of the ore body; and
– When the cost/efficiency effect of selectivity is considered, then larger blocks are optimum when the average grade of the ore body is above the cut-off grade. However, with the low-grade ore bodies, selectivity is critical and the cost of selectivity can result in these not being economical to mine.

When the more realistic Leapfrog Geo modelling approach is considered, the sample spacing will dictate the size of the smallest blocks. Realistic data spacing in the narrow tabular ore bodies considered in this study is unlikely to give block sizes smaller than 100 by 100 m. Although the model may appear to have a high resolution when viewed visually, in reality, the small blocks cannot be considered a true reflection of their individual grades. They are effectively just splitting the underlying composited model into smaller units without showing their true grade variability. Trying to identify potential smaller high-grade blocks to mine selectively without sufficient data is not possible. The SME Mining Engineering Handbook guide of between 10 and 20 samples in a block to give a reliable estimation is a good measure in determining the smallest realistic block [3].

References

1. SRK Consulting: Block Modelling [Online]. Available: https://www.srk.ru/en/block-modelling (2018)
2. Ronald, E.: Rules of Thumb for Geological Modeling—SRK presentation at SME 2018 [Online]. Available: www.na.srk.com/en/na-rules-thumb-geological-modeling (2018)
3. Hartman, H.L., Britton, S.G., Gentry, D.W., Karmis, M., Mutmansky, J.M., Schlitt, W.J., Singh, M.M.: SME Mining Engineering Handbook, 2nd edn. Society for Mining, Metallurgy, and Exploration, Inc., Littleton, United States (1992)
4. Birch, C.: New systems for geological modelling-black box or best practice? J. South Afr. Inst. Min. Metall. **114**(12), 993–1000 (2014)
5. Annels, A.E.: Mineral Deposit Evaluation. A Practical Approach. Chapman & Hall, Cardiff (2012)
6. Stone, J.G., Dunn, P.G. Ore Reserve Estimates in the Real World, 2nd edn. Society of Economic Geologists Special Publication Number 3, Littleton, United States (2002)

7. Matomane, O. The Effect of Changing Block Sizes on Grade-Tonnage Curves, Unpublished BSc (Eng) Final Year Report, Johannesburg, (2017)
8. SAMCODE: The South African Mineral Codes, July 2009 [Online]. Available: http://samcode.co.za/downloads/SAMREC2009.pdf (2013)
9. Savant, R.: Overview of Mining Costs—CPM Group 2012 [Online]. Available: http://www.goldconvention.in/iigc2012/presentation/CPM%20Group%20Overview%20of%20Mining%20Costs%20RS.pdf (2018)
10. Poxleitner, G.: Operating Costs for Mines—SRK Consulting (Canada) [Online]. Available: https://www.srk.com/sites/default/files/file/GPoxleitner_OperatingCostEstimationForMiners_2016.pdf (2018)
11. Hall, B.: Cut-off Grades and Optimising the Strategic Mine Plan, Spectrum Series, 20 edn. The Australasian Institute of Mining and Metallurgy, Carlton Victoria, Australia (2014)
12. Border, S.: Optimisation of Cut-off Grades During Design of Underground Mines. Sydney (1991)
13. Smith, G.L., Pearson-Taylor, J., Anderson, D.C., Marsh, A.M.: Project valuation, capital investment and strategic alignment—tools and techniques at Anglo Platinum. The Journal of The Southern African Institute of Mining and Metallurgy **107**, 67–74 (2007)
14. Lane, K.F.: The Economic Definition of Ore. Mining Journal Books Limited, London (1988)
15. Minnitt, R.: Cut-off grade determination for the maximum value of a small Wits-type gold mining operation. The Journal of The South African Institute of Mining and Metallurgy, 277–283 (2004)
16. Krige, D., Assibey-Bonsu, W.: Use of direct and indirect distributions of selective mining units for estimation of recoverable resource/reserves for new mining projects. In: APCOM '99 Symposium (1999)
17. Birch, C.: Impact of the South African mineral resource royalty on cut-off grades for narrow, tabular Witwatersrand gold deposits. The Journal of The Southern African Institute of Mining and Metallurgy **116**, 237–246 (2016)
18. Birch, C.: Optimization of cut-off grades considering grade uncertainty in narrow, tabular gold deposits. The Journal of the Southern African Institute of Mining and Metallurgy **117**(2), 149–156 (2017)
19. Marques, D., Costa, J.: Analysis of the dispersion variance using geostatistical simulation and blending piles. The Journal of The Southern African Institute of Mining and Metallurgy **118**(8), 599–604 (2014)
20. Minnitt, R.: Sampling: the impact on costs and decision making. The Journal of The Southern African Institute of Mining and Metallurgy **107**(7), 451–462 (2007)
21. Spragg, K.: Leapfrog Interpolation Basics, 2013 [Online]. Available: http://blog.leapfrog3d.com/2013/05/08/leapfrog-interpolation-basics/ (2018)

Methodology to Optimize and Sequence the Semiautomated Ramp Design in Underground Mining

S. Montané, P. Nancel-Penard and N. Morales

1 Introduction

The mining industry market competitiveness forces the companies to continuously seek cost reduction strategies to improve the profit. On the other hand, there are few investigations about optimization of the design of access routes in underground mining.

De Smith [6] focused on the analysis of the gradient and on the curvature restrictions for road forms and lengths to find optimal routes. The study contemplated three steps for the selection of the optimal route:

– initial alignment of the route subject to a preset range of gradient restrictions,
– horizontal smoothing of the route to find objectives of curvature and smoothness of horizontal route, and
– vertical smoothing of the route to achieve similar objectives, with a minimum of cut/fill in the vertical plane.

Ghaffariyan [7] developed a study to determine optimal path spacing, where the best solution found was based on a modification of the shortest path algorithm. The objective of the study was to apply a mixture of integral programming and network analysis to optimize the route.

S. Montané (✉) · P. Nancel-Penard · N. Morales
DELPHOS Mine Planning Laboratory and AMTC, University of Chile, Santiago, Chile
e-mail: smontane@delphoslab.cl

P. Nancel-Penard
e-mail: pierre.nancel@amtc.cl

N. Morales
e-mail: nelson.morales@amtc.cl

S. Montané · N. Morales
Department of Mining Engineering, University of Chile, Santiago, Chile

References [1–4] proposed the creation of an optimization tool that allowed obtaining the best alternative for the construction of ramps, shafts, and tunnels to minimize the associated costs. Their work was based on Steiner's networks, where nodes are established that represent the places through which one must necessarily pass, given the design of the mine. These nodes must be joined by sections (ramp/gallery) that have associated costs corresponding to the development of the section and the cost for the transit of ore through it. Brazil et al. [5] developed some software to obtain the design of ramp using his algorithms.

In this paper, we present a methodology to assist the ramp design in underground mining, minimizing both development and operational costs. The methodology considers an optimization model that obtains an initial ramp design, which is subsequently, refined to arrive at the final configuration. A sequencing of ramps' construction is generated using the UDESS software. The general sequencer model Universal Delphos Sequencer and Scheduler (UDESS) seeks to maximize the NPV of the scheduling, subject to resource constraints and precedencies, to generate a Gantt chart of development of activities.

2   Optimization Model

The proposed methodology contemplates the creation of a mathematical model to solve a problem of minimization of costs of the ramp route, granting access to production levels via tunnels in a straight line called crosscut to extract the mineral. The mathematical model considers predefined starting point and the height for the connection between the crosscuts and the ramp.

The optimization model uses the following input parameters; the values of the parameters depend on the case to which the methodology is applied:

- a guiding form from which the ramp is generated, which defines the available space and the final form. A tolerance border is established for the location of the solution
- the quantity and location of the access points to production levels, with the associated tonnage to be extracted from each level
- the maximum tolerable slope in the construction of the ramp that the equipment can operate
- development costs of ramps and crosscuts
- operational costs of ramps and crosscuts
- direction of the ramp (clockwise or counterclockwise)
- starting point of the ramp
- cost of ventilation.

In addition, a penalty is established in the optimization model whereas the curved sections generated during the modeling are "punished", because they are more complicated to construct operationally. These considerations were established after meetings with experienced consultants.

Similarly to the design of ramps in open-pit mines [8], the methodology consists of precomputing shortpaths at block level for each level of the mine within a predefined boundary and using the mathematical model to determine, which are the best shortpaths to assemble to generate the full ramp.

The nomenclature for the proposed mathematical modeling is as follows:

B	The block model
K	The maximum level at which the ramps can begin
B_k	The set of blocks of level k, $k \in \{0, 1, \ldots, K\}$, level 0 is lower level, K is ramp top level
b_{startk}	The starting block of the ramp
F	The defined boundary of blocks where ramps can pass
E	The set of the access points
E_k	The set of the access points for the production level k
$\hat{k}_e$	The level of the connection of the crosscut starting from e with the ramp
$\hat{k}$	The minimum level for the connection of the crosscut, that start from the lower access point with the ramp
I_k	The set of indexes i of all precomputed paths of level k
s_k^i	The ith precomputed path of level k
o_k^i	The first block of s_k^i
f_k^i	The last block of s_k^i
$b_{e,k}^i$	The block of s_k^i nearest to the access point e
l_k^i	The approximation of length of s_k^i
$l_{e,k}^i$	The approximation of length of $(f_k^i, b_{e,k}^i)$
c_k^i	The value equal to 1 if s_k^i is a curve, else equal to 0
C_{H1k}	The haulage cost of all the mine production for 1 meter of ramp that must pass on level k
C_{H2e}	The haulage cost of the production of the access point e for one meter of ramp
C_{Te}	The haulage cost of the production of the access point e for 1 meter of crosscut
C_{RD}	The cost of development of 1 m of ramp
C_{CD}	The cost of development of 1 m of crosscut
C_{VD}	The cost of ventilation of development of 1 m of tunnel
V_T	The cost of ventilation that corresponds to the haulage
P_{RD}	The penalization of 1 m of curve tunnel development

The variables of the problem are defined as follows:

$$y_b = \begin{cases} 1 \text{ if block } b \text{ belongs to ramp,} \\ 0 \text{ otherwise.} \end{cases}$$

$$x_k^i = \begin{cases} 1 \text{ if all blocks of level k of } s_k^i \text{ are part of the ramp of level } k \\ \quad \text{and } f_k^i \text{ is the first block of the ramp of level } k-1 \\ 0 \text{ otherwise.} \end{cases}$$

Domain definition of variable y is F, domain definition of index k of variable x is $\{1, 2, \ldots, K\}$, domain definition of index i of variable x is Ik.

Therefore, the Single Ramp Underground Design Problem (SRUDP), can be formulated as follows:

$$(SRUDP) \quad \min \sum_{k=1}^{K} \sum_{i \in I_k} \left((C_{RD} + C_{VD}) \cdot \left(1 + P_{RD} \cdot c_k^i\right) + C_{H1k} \cdot (1 + V_T) \right) \cdot l_k^i \cdot x_k^i$$

$$- \sum_{e \in E} \sum_{i \in I_{\hat{k}_e}} C_{H2e} \cdot (1 + V_T) \cdot l_{e,k}^i \cdot x_k^i$$

$$+ \sum_{k=1 | \exists e \in E_k} \sum_{i \in I_k} (C_{CD} + C_{VD} + C_{Te} \cdot (1 + V_T)) \cdot \left\| eb_{e,k}^i \right\| \cdot x_k^i \tag{1}$$

s.t.

$$\sum_{i \in I_k | f_k^i = o_{k-1}^j} x_k^i \geq x_{k-1}^j \qquad (\forall k > 1, \ \forall j \in I_{k-1}) \tag{2}$$

$$\sum_{i \in I_k} x_k^i \leq 1 \qquad (\forall k \geq 1) \tag{3}$$

$$x_k^i \leq y_b \qquad (\forall k \geq 1, \ \forall b \in s_k^i) \tag{4}$$

$$\sum_{i \in I_k | b \in s_k^i} x_k^i \geq y_b \qquad (\forall b \in F) \tag{5}$$

$$\sum_{i \in I_K | o_K^i = b_{start}} x_K^i \geq 1 \tag{6}$$

$$\sum_{i \in I_{\hat{k}_e}} x_K^i \geq 1 \tag{7}$$

$$x_k^i = 0 \qquad \left(\forall k < K, \ \forall i \in I_k | \left\{ s_{k+1}^j | f_{k+1}^j = o_k^i \right\} = \emptyset \right) \tag{8}$$

The objective function (1) minimizes the overall development and operational costs of ramp sections in a level, crosscuts, and ramp connection between levels.

Constraint (2) ensures the connectivity between ramp paths. Constraint (3) states that there is at most one ramp per level. Constraint (4) ensures that for each chosen

path, all blocks in the path are part of the ramp. Constraint (5) states that ramp block belongs to an elected precomputed path. Constraint (6) states that the ramp will start from the defined start block. Constraint (7) forces the existence of a ramp to connect the lower crosscut. Constraint (8) prevents a no connected path from being an eligible path.

SRUDP model is equivalent to a shortest path problem to minimize the function cost (1) instead of the length of paths. The graph of connection of all precomputed paths is constructed. Each arc is associated with the cost that corresponds to the development of this tunnel part and the corresponding operational cost. The operational cost includes the haulage cost of material that goes through the arc, considering the crosscut development and operational costs, if the level of path corresponds to a fixed connection height $\hat{k}_e$. The shortest path problem can be solved very fast; however, the proposed methodology is addressing a more general problem because the optimal height of the crosscut connections with the ramp is not known in advance. To solve this more general problem, a heuristic approach that tries different heights of connection starting from horizontal crosscuts was made to approximate the optimal ones. The heuristic keeps the ones that improve the cost function starting from the higher crosscut, considering only a feasible connection boundary and preventing the intersection of crosscuts. The heuristic iterates while the value of the objective decreases.

3 Methodology and Performance

The procedure to use the heuristic optimization model requires a block model of the workspace, where the access points to production levels are identified and the shape and working space for the design of the ramp are defined. This block model must be in a text file format separated by tabs. The input values are defined as costs, slope, and tonnage to be extracted from production levels, direction, start point, and penalty of arcs.

To execute the modeling code, a server with a Xeon processor E5-2660v32 @2.6 GHz. 128 GB RAM with a CPU that has 20 threads was used. The execution time is approximately 2 min, although this depends on the amount of data within the block model. The outputs are the approximate total cost of the design and the points where the ramp passes. When these points are viewed, they are blocks, whose size varies depending on the resolution used. This design contemplates the original dimensions of the final design, its costs, and the tonnage associated with the development. This solution must be refined by the engineer in charge of the design, to transform the points into a triangulation that represents the real section of the gallery, using mining CAD software. The data flow of the methodology is summarized in Fig. 1.
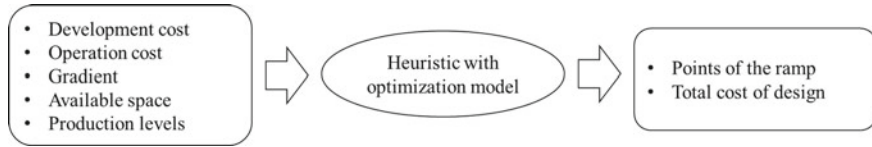
Fig. 1 Flowchart of methodology

Table 1 Developed meters and total cost for each zone

Zone	*Y* east	*Y* west lower	*Y* west higher
Long developed ramp (m)	1099	1136	1455
Long developed crosscuts (m)	979	522	443
Total cost (MUSD)	10.8	10.5	5.5

4   Case Study

A case study of a gold and silver mine operated by Bench & Fill was undertaken. The data used in this section was provided by a confidential prefeasibility study made in 2014, which includes from geostatistical study until final economic analysis.

The mine had two main sectors and three exploitation zones: *Y* east mine, *Y* west mine, and *V* mine. Production levels were separated by 12 m vertically. Some levels had a principal drift to connect crosscuts to access the extraction galleries, while in other levels, it was possible to access directly without using the drifts.

The methodology to design ramps was used in three zones: *Y* east, *Y* west lower, and *Y* west higher. The objective of the case study was to replicate as much as possible the original designs of the prefeasibility study and, therefore, each zone was considered independently of the others, it was expected to use the same space available and respect a gradient 13% proposed in the report of the project.

Y east zone had 26 production levels, but the design had to reach an access to 13 main drifts because in these levels, the drift system was implemented. In *Y* west lower zone, there were 11 drifts to access; therefore, there were 22 production levels. Finally, *Y* west higher zone did not have the drift system; there were 15 production levels to access directly.

4.1   Ramp Design Result

The results obtained with the application of the new methodology are shown in Table 1. Because there were three zones, the methodology was used three times and the time for execution required was about three minutes for each zone.

Figure 2 shows a comparison between designs obtained using the proposed methodology and designs obtained by prefeasibility study. In general, the designs are

Fig. 2 Comparison of designs
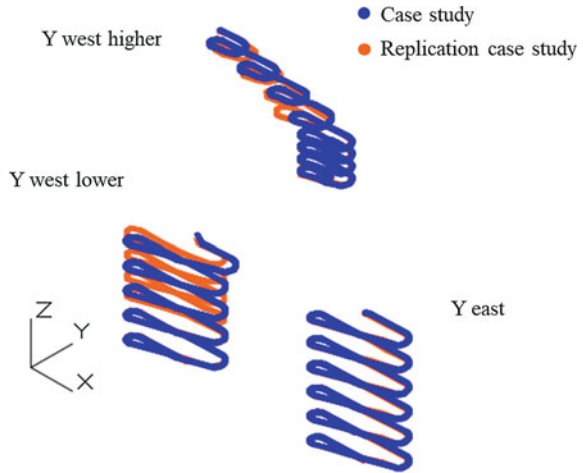
very similar in the three zones. The main difference is in Y west lower zone, where the upper half is different because the prefeasibility study design had two values of gradient: 13 and 15%, while the design obtained by methodology used a gradient of 13% only.

4.2 Sequencing Result

The UDESS tool was used to accomplish the sequencing of ramp and crosscuts construction and extraction of ore from production levels, through a maximization of NPV. Three types of activities were defined ramp sections, crosscut sections, and production levels, which had associated revenues and costs. In addition, three types of restrictions were set maximum tonnage extracted per period, effective hours of work, and availability of equipment for construction.

The sequencing of the three zones was considered as a single problem in UDESS and each sector was considered independent to each other. The exploitation of production levels was from the bottom-up. The problem considered by UDESS consisted of 467 activities and 728 precedencies and the execution time was 4.6 h. The result yielded an NPV of 1,041.8 MUSD, 13 years of ramp and crusher construction, and 18 years of ore extraction, as shown in Figs. 3 and 4.

In general, the results are consistent with the maximum extraction rates. The ramp-up lasted 3 years and the ramp-down 4 years, which are reasonable times for the scale of the project. The progress of development of ramps and crosscuts was related to the opening of production levels, which had precedence among them to extract the ore from the lower levels as a priority.
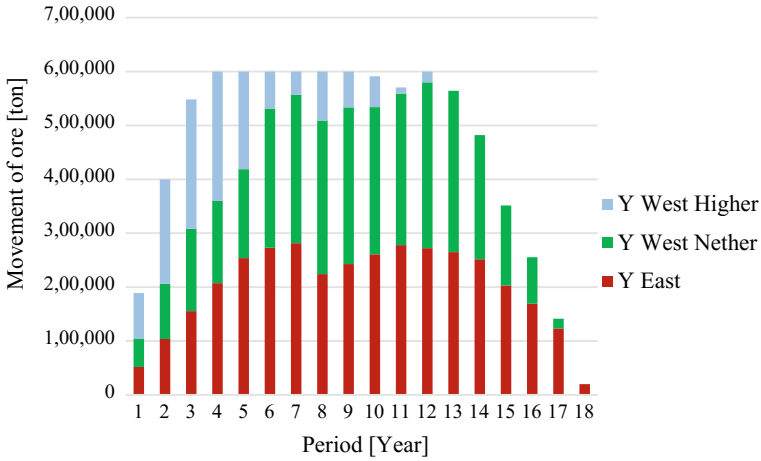
Fig. 3 Tonnage extracted per year obtained from UDESS
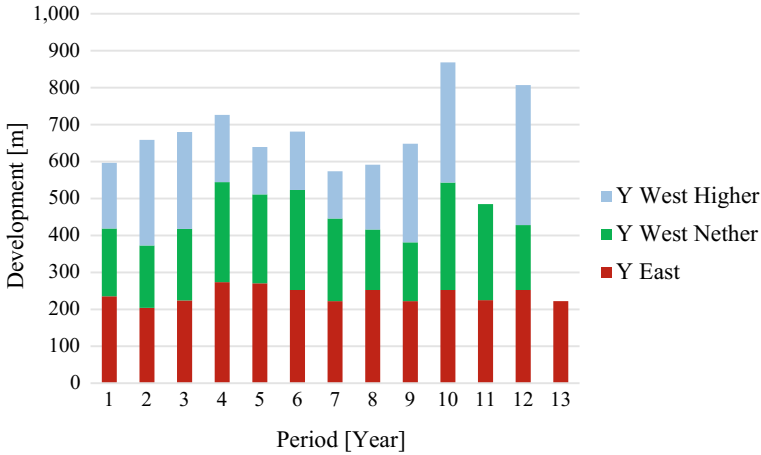
Fig. 4 Development per year obtained from UDESS

5   Conclusions

The designs made in the case study allowed to verify that the proposed model is capable of replicating the designs of the engineering study, which proves that this tool can provide feasible solutions for the industry.

The times required for the execution of the heuristic are prudent, between 1 and 3 minutes, depending on the case study. The complexity lies in a good establishment of the ramp guide form according to the conditions of each case.

On the other hand, the heuristic with optimization model is capable of delivering solutions that can assist in the design of ramps, facilitate the work of the engineer and deliver options with more objectivity.

For the construction sequencing, it is observed that the times needed are linked with the dimensions of the deposit and the amount of infrastructure needed. This scheduling is a good complement of ramp design because it allows to verify the times of the project from initial stages.

As future work, the construction of a heuristic which can obtain the ramp and crosscut design and, in addition, the sequencing of construction thereof, maximizing the NPV of the associated project, is proposed. The idea is to generate designs that involve some aspects of the production to include, from the beginning of the project, the costs of the infrastructure necessary for the operational stage.

References

1. Brazil, M., Lee, D.H., Rubinstein, J.H., Thomas, D.A., Weng, J.F., Wormald, N.C.: A network model to optimize cost in underground mine design. Trans.-South African Inst. Electr. Eng. **93**(2), 97–103 (2002)
2. Brazil, M., Lee, D.H., Rubinstein, J.H., Thomas, D.A., Weng, J.F., Wormald, N.C.: Optimization in the design of underground mine access. In: Uncertainly and Risk Management in Orebody Modelling and Strategic Mine Planning (2004)
3. Brazil, M., Thomas, D.A.: Network optimization for the design of underground mines. Networks **49**(1), 40–50 (2007)
4. Brazil, M., Grossman, P.A., Lee, D.H., Rubinstein, J.H., Thomas, D.A., Wormald, N.C.: Constrained path optimization for underground mine layout. In: World Congress on Engineering, pp. 856–861 (2007)
5. Brazil, M., Grossman, P., Rubinstein, J.H., Thomas, D.: Improving underground mine access layouts using software tools. Interfaces **44**(2), 195–203 (2013)
6. De Smith, M.J.: Determination of gradient and curvature constrained optimal paths. Comput.-Aided Civil Infrastruct. Eng. **21**(1), 24–38 (2006)
7. Ghaffariyan, M.R., Stampfer, K., Sessions, J., Durston, T., Kuehmaier, M., Kanzian, C.: Road network optimization using heuristic and linear programming. J. Forest Sci. **56**(3), 137–145 (2010)
8. Morales, N., Nancel-Penard, P., Parra, A.: An integer linear programming model for optimizing open pit ramp design. In: APCOM 2017 Proceedings, Session 11, pp. 9–16 (2017)

Production Scheduling in Sublevel Caving Method with the Objective of NPV Maximization

M. Shenavar, M. Ataee-pour and M. Rahmanpour

1 Introduction

Optimization of mineable reserve in open pit and underground mines is a critical issue. Optimization of mineable reserve in underground mines has received less attention than in open-pit mines. This is mostly due to the diversity of underground mining methods and complexity of underground mining parameters. Open-pit mining method has a great importance among surface mining methods, and there are many studies to optimize this method. Concurrently, optimization of ultimate mine limit and production planning in other surface mining methods has not improved so much, and studies on optimization and planning in these methods are very limited and primitive. Among underground mining methods, block caving, sublevel caving, sublevel stopping, cut and fill, and stope and pillar methods are usable for the mining of metallic reserves.

The true optimum solution is guaranteed for the pit limit optimization and several computer packages are available to the industry. However, only few algorithms have been developed for optimization of ultimate stope boundaries in underground mines [1].

Stope design affects the profit and safety of the operation. Stope design requires: (1) ore reserve model as input data, usually created by estimation or simulation using geostatistical tools and (2) the geotechnical constraints, including the hanging wall

M. Shenavar (✉) · M. Ataee-pour
Department of Mining and Metallurgical Engineering, Amirkabir University of Technology, Tehran, Iran
e-mail: mortezashenavar@gmail.com

M. Ataee-pour
e-mail: map60@aut.ac.ir

M. Rahmanpour
School of Mining, College of Engineering, Technology of Tehran, Tehran, Iran
e-mail: mrahmanpour.m@gmail.com

and footwall angles, stope dimensions, in situ stress tensor, rock strength, and local geological structures. The general procedure of stope optimization is to decide which parts of an ore reserve are included in the stope and which are not, such that, under some geotechnical constraints, the resulting stope produces the maximum possible profit [2]. Several approaches have been developed for stope optimization [1, 3]. Dynamic programming and branch and bound technique were used to optimize a stope in two-dimensional (2D). However, these methods fail to produce realistic stopes for complex three-dimensional (3D) deposits that cannot be simplified in 2D. Some 3D techniques were also reported, including mathematical morphology tools, floating stope [3], maximum value neighborhood method [1], and octree division. Bai et al. [2] has developed a stope optimizer based on graph theory [2]. Recently, some models are developed for underground mine reserve optimization under grade uncertainty [4].

Production scheduling defines the tonnages and grades to be mined throughout the mine life. The scheduling problems are usually complex due to the nature and variety of the constraints. A production schedule must provide a mining sequence that takes into account the physical limitations of the mine and, to the extent possible, meets the demanded quantities of each material at each time period throughout the mine life [5].

In underground mining, various models have been developed to optimize the production planning. In general, none of these models have been commercialized. Most of them are short-term planning models with the aim of minimizing production deviations from the existing manual non-optimized long-term program [6–16]. Some of these models are formulated for a specific mining operation and they must be modified before applying on other cases [17, 18]. Some models do not have real optimal solutions, which are some expert-oriented search-based methods [19–22]. In the process of developing these models for underground mining production scheduling, various objective functions are presented such as profit maximization [23], and project time minimization [24]. Recently, some models have been developed with objective function of NPV maximization for long-term production scheduling.

The economics of today's mining industry is such that the major mining companies are increasing the use of massive mining methods. Among the available underground mining methods, caving methods are favored because of their low-cost and high production rates. Caving methods are underground bulk mining method and are expected to continue in the foreseeable future. One of these methods is block caving, which has gained its popularity due to its low operating cost and high productivity [5].

In this paper, a two-dimensional mathematical model is presented to sublevel caving production scheduling, and it is applied on a hypothetical block model and a real thin-layer deposit.

2 Materials and Methods

In this research, production scheduling model is developed for sublevel caving method and it is applied on Golbini bauxite mine of Iran. In this regard, floating stope optimizer is used for reducing the number of blocks.

2.1 Floating Stope Optimizer

Floating stope is a technique implemented in the DATAMINE package (Mineral Industries Computing Limited) to determine the optimal limits (boundaries) of an ore reserve, which may be economic to be extracted by underground mining methods. The general concept of floating stope approach was outlined in 1995 as a search-based and heuristic approach, analogous to Moving Cone method for pit limit optimization.

The term floating stope is derived from the technique of floating a minimum stope shape through the ore body and evaluates the grade of material inside the stope at any position. In that regard, two envelopes will be created. The maximum envelope is the union of all possible economic stope positions, while the minimum envelope is found by taking the union of all best grade stope positions for every ore block in the ore body. The envelopes provide a limit for the engineer to design final stope positions, with the recommendation that the minimum envelope should be used as the guide in the first instance. In this research, the maximum envelope is used as the ultimate stope boundary as a guide for the production scheduling optimization model.

By using this optimizer, the numbers of blocks in the block model are reduced. It selects the blocks that have the potential to be mined by defining a mining envelope. In that regard, the blocks that are not selected by the envelope, are removed from the block model. This will considerably reduce the number of blocks that improves the running time.

2.2 Sublevel Caving Mining Method

Sublevel caving is one of the most advanced mining methods. This method is usually undertaken when mining the ore body through an open pit is no longer economically viable. In sublevel caving, mining starts at the top of the ore body and develops downwards. Ore is mined from sublevels spaced at regular intervals throughout the deposit (Fig. 1). A series of ring patterns is drilled and blasted from each sublevel, and the broken ore is mucked out after each blast. Sublevel caving can be used in ore bodies with very different properties and it is an easy method to mechanize. This method is normally used in massive, steeply dipping ore bodies with considerable strike length. In this method, dilution and ore-loss are usually high.
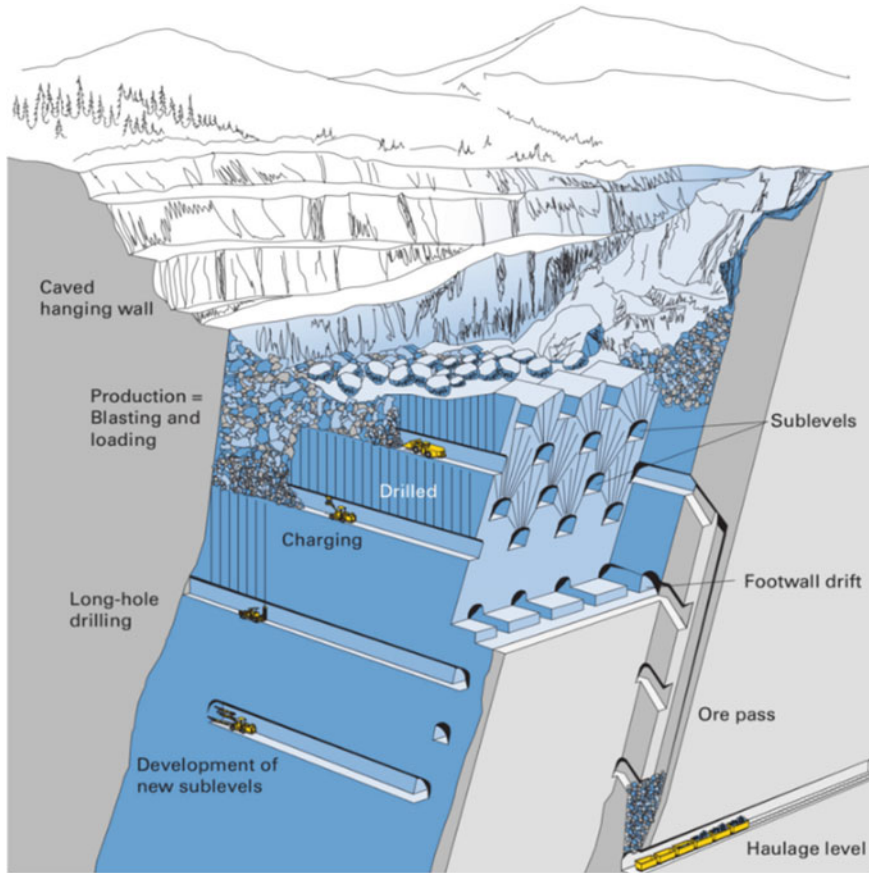
Fig. 1 Sublevel caving method

2.3 Golbini Bauxite Mine of Iran

Bauxite includes the oxides and hydroxides of iron and aluminum and silica. Golbini bauxite mine is located in the North of Iran. Considering the main faults, Golbini is divided into eight mining zones. Here, one of the Golbini zones with more than 3 million tons of bauxite is selected to study and apply the production scheduling optimization model.
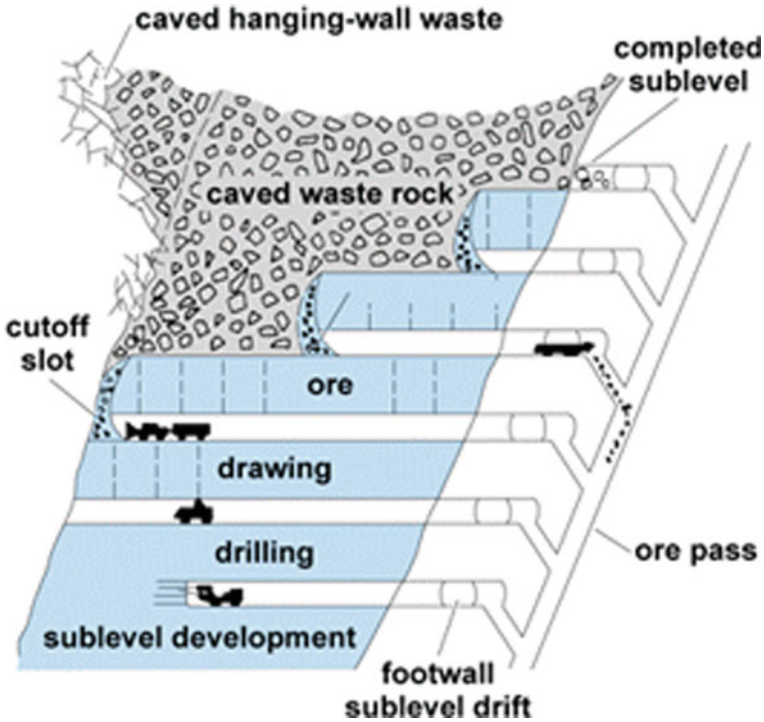
Fig. 2 Sublevel caving sequencing

Table 1 A hypothetical block model

$1.00	$2.00	$2.00	$1.00	$3.00	$2.00	$1.00	$2.00	$1.00	$1.00
$1.00	$2.00	$2.00	$4.00	$3.00	$2.00	$1.00	$2.00	$1.00	$2.00
$2.00	$3.00	$4.00	$5.00	$3.00	$2.00	$2.00	$1.00	$1.00	$1.00
$2.00	$4.00	$6.00	$4.00	$3.00	$2.00	$3.00	$2.00	$2.00	$1.00

3   Problem Definition

In sublevel caving method, mining starts at the top of the ore body and progresses downwards in a safe sequence as shown in Fig. 2. For production scheduling different objectives are available, but in this study, NPV maximizing is the objective of production scheduling. For better understanding, a two dimensional-block model is considered as an example and the procedure is explained (Table 1).

The presented block model (Table 1) can be mined from left to right or vice versa. Considering an annual capacity of eight blocks, the NPV of mining the blocks from left-to-right and right-to-left direction is shown in Fig. 3.

As shown in Fig. 3, different NPVs are achievable for various mining sequences, so it shows that the production scheduling with objective of maximization NPV

Fig. 3 Five-year scheduling of the hypothetical block model (*Y*: year, *P*: profit)

is applicable for sublevel caving method. This example shows the importance of production scheduling in reaching the objectives (NPV maximization) and satisfying the mining constraints. In order to optimize the mining sequence, a 2D mathematical model is presented that is suited for sublevel caving operations.

4 Mathematical Model

Long-term production scheduling plan of sublevel mining method is formulated within an IP framework. The objective is to maximize the NPV of the mining process. The objective function of the model is given in Eq. 1.

$$\sum_{i=1}^{I} \sum_{j=1}^{J} \sum_{t=1}^{T} \frac{\text{BEV}_{ij}}{(1+d)^t} \times x_{ijt} \tag{1}$$

where I is the number of blocks in horizontal direction, J is the number of blocks in vertical direction, T is the number of scheduling periods, BEV_{ij} is the economic value of B_{ij} (the block located in horizontal location i and vertical location j), d is discount rate, and x_{ijt} is the decision variable, representing that B_{ij} to be extracted in period t.

Two sets of constraints are taken into consideration. The first set is related to reserve and production capacity and the second set deals with the sequence of blocks extraction in horizontal and vertical directions. The constraints are given in Eqs. 2 through 5.

$$\sum_{t=1}^{T} x_{ijt} \leq 1 \quad \forall i = (1, \ldots, I), \ j = (1, \ldots, J) \tag{2}$$

$$\sum_{i=1}^{I} \sum_{j=1}^{J} x_{ijt} P_{ij} = ppy \quad \forall t \in T \tag{3}$$

$$x_{i+1jt'} \leq x_{ijt} \quad \forall i = (1, \ldots, I); \ j = (1, \ldots, J); \ t, t' \in T; \ t' \leq t \tag{4}$$

$$x_{i-2j+1t'} \leq x_{ijt} \quad \forall i = (1, \ldots, I); \ j = (1, \ldots, J); \ t, t' \in T; \ t' \leq t \tag{5}$$

where production per year *ppy* is the annual production capacity. In this model, constraint (2) is the reserve constraint and ensures that each block to be mined ones. Constraint (3) controls production capacity and it ensures that the number of blocks that must be mined each year does not exceed the predetermined capacity. Constraints (4) and (5) are the most important technical and operational constraints in sublevel caving method and are related to the sequence of blocks extraction. Horizontal block extraction sequencing is considered in Constraint (4) and vertical block extraction sequence is considered in Constraint (5). It should be noted that the actual level distances depend on geomechanical constraints.

Overall, the procedure that leads to an optimal production schedule has five steps which are as follows.

Step 1   Generate a geological block model
Step 2   Generate an economic block model
Step 3   Optimize stope boundaries using floating stope optimizer
Step 4   Determine the maximum envelope and remove the unnecessary blocks from the block model
Step 5   Determine the maximum NPV and the optimal mining sequence by using Eqs. 1–5

5   Results and Discussion

In this section, the presented IP model (Eqs. 1–5) is generated using MATLAB programming platform. The model is applied on the presented hypothetical block

1	2	3	4	5	6	7	8	17	25
9	10	11	12	13	18	19	26	27	28
14	15	16	20	21	29	30	33	34	35
22	23	24	31	32	36	37	38	39	40

Fig. 4 Production sequencing for achieving maximum NPV
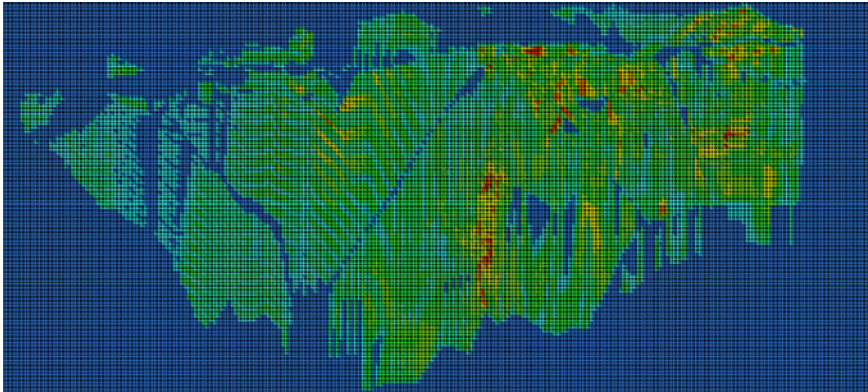
Fig. 5 Optimized stope layout economic block model

model (Table 1) and the maximum NPV is determined. Maximum achievable NPV for the hypothetical block model is 74.58$ and the optimum mining sequencing is shown in Fig. 4. As shown in the Fig. 4, the optimum mining sequencing is in left-to-right direction and varies with previous manual scheduling. Thus, maximum NPV is achievable for sublevel caving method with this model.

For better presentation, the presented approach is applied on Golbini bauxite mine of Iran. It is a layer deposit and its hanging wall is suitable for caving. As stated, considering the main faults, Golbini is divided into eight mining zones. Here, one of the Golbini zones with more than 3 million tons of bauxite is selected to study and apply the production scheduling optimization model. The reserve model is projected into a 2D vertical block model.

Using floating stope optimizer, stope boundaries are optimized. The block model of maximum envelope of the optimized stope layout with 2.1 million tons of bauxite (25,000 blocks with dimension of 5 m × 5 m × thickness of the layer) is shown in Fig. 5.

Once the optimized stope layout is determined, the unnecessary blocks are removed from the block model. The resulting block model is shown in Fig. 6. In this case, the production schedule is optimized for an operating period of 8 years. It is assumed that all the reserve will be mined within this time period. The presented IP model is applied on this block model and the optimum production schedule and min-
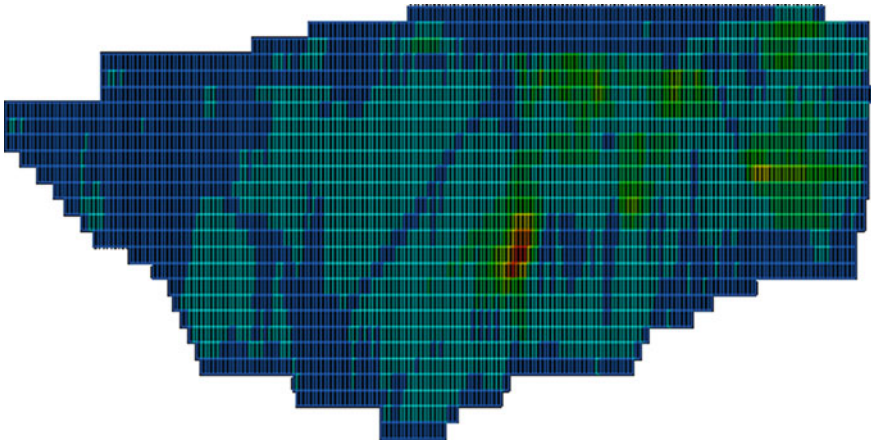
Fig. 6 The applicable economic block model
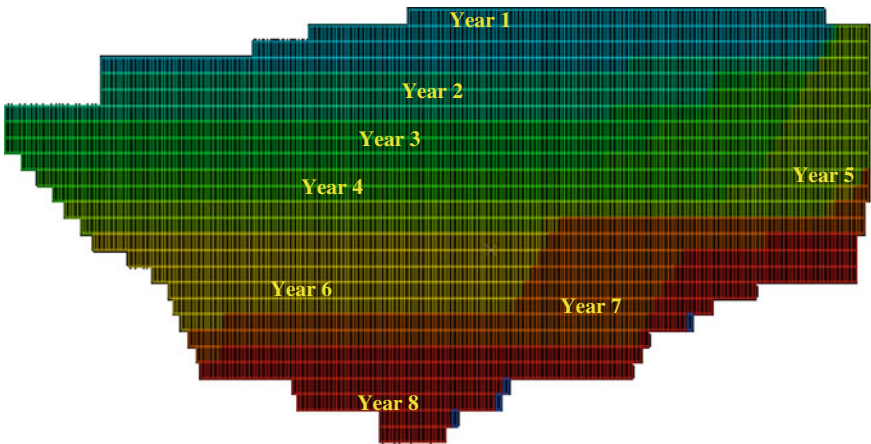
Fig. 7 Eight-year production scheduling

ing sequence is determined. The resulting mining sequence that leads to the highest NPV is shown in Fig. 7.

6 Conclusion

In this paper, a mathematical IP model is formulated with respect to technical constraints that are present in sublevel mining methods. Consideration of these constraints will lead to a practical mining sequence that maximizes the NPV of the mining operation. The model is applied on a hypothetical example to show the improvement

in NPV that the model causes with respect to conventional hand methods. Due to the large number of blocks (or decision variables), application of the model in real cases is somehow limited. In order to pass this issue, a minable stope envelope is determined by using floating stope algorithm, prior to the application of the model. In that regard, the blocks that are not selected by the envelope, are removed from the block model. This will considerably reduce the number of blocks that improves the running time. The presented procedure is applied on a 2D representation of a real bauxite deposit. The results show that an optimal and practical mining sequence is achievable.

References

1. Ataee-pour, M.: A critical survey of the existing stope layout optimization techniques. J. Min. Sci. **41**(5), 447–466 (2005)
2. Bai, X., Marcotte, D., Simon, R.: A heuristic sublevel stope optimizer with multiple raises. J. Southern African Inst. Mining Metall. **114**, 427–434 (2014)
3. Alford, C.: Optimization in underground mine design. APCOM **25**, 213–218 (1995)
4. Shenavar, M., Ataee-pour, M., Rahmanpour, M.: Evaluating mineable reserve in presence of grade uncertainty using floating stope optimizer in underground mines. In: 6th International Conference on Computer Applications in the Minerals Industries (CAMI), Turkey (2016)
5. Pourrahimian, Y.: Mathematical programming for sequence optimization in block cave mining. Doctor of Philosophy Thesis, Department of Civil and Environmental Engineering, Edmonton, Alberta (2013)
6. Williams, J.K., Smith, L., Wells, P.M.: Planning of underground copper mining. In: 10th International Application Symposium on the Application of Computer in the Mineral Industrial (APCOM), Johannesburg, South Africa, pp. 251–254 (1973)
7. Gillenwater, E.L.: An integrated model for production planning and scheduling in underground coal mining. Doctor of Business dissertation, University of Kentucky (1988)
8. Subhash, C., Sarin, J., Hansen W.: The long-term mine production scheduling problem. J. IIE Trans. **37**(2) (2005)
9. Chanda, E.K.C.: An application of integer programming and simulation to production planning for a strati form ore body. Mining Sci. Tech. **11**(2), 165–172 (1990)
10. Jawed, M.: Optimal production planning in underground coal mines through goal programming: a case study from an Indian mine. In: Elbrond, J., Tang, X., (eds.) Proceeding of 24th International Application of Computer and Operation Research in the Mineral Industry, (APCOM) Symposium, CIM, Montréal, pp. 44–50 (1993)
11. Winkler, B.: System for quality oriented mine production planning with MOLP. In: Proceeding of 27th International Application of Computer and Operation Research in the Mineral Industry, (APCOM) Symposium, Royal School of Mines, London, pp. 53–59 (1998)
12. Topal, E.: Advanced underground mine scheduling using mixed integer programming. Ph.D. thesis, Colorado School of Mines, Colorado (2003)
13. Rahal, D., Smith, M., Van G., Hout, A., Johannides, V.: The use of mixed integer linear programming for long-term scheduling in block caving mines. In: Camisani-Calzolari, F. (ed.) Proceeding of 31st International Application of Computer and Operation Research in the Mineral Industry, (APCOM) Symposium, SAIMM, Cape Town, South Africa, pp. 123–131 (2003)
14. Rubio, E., Diering, E.: Block cave production planning using operation research tools. In: Karzulovic, A., Alfaro, M. (eds.) Proceeding of MassMines in Chile, pp. 141–149 (2004)
15. Kuchta, M., Newman, A., Topal, E.: Implementing a production schedule at LKAB's Kiruna Mine. Interfaces **34**(2), 124–134 (2004)

16. Newman, A., Kuchta, M.: Using aggregation to optimize long-term production planning at an underground mine. Eur. J. Oper. Res. **176**(2), 1205–1218 (2007)
17. Carlyle, W.M., Eaves, B.C.: Underground planning at stillwater mining company. Interfaces **31**(4), 50–60 (2001)
18. McIsaac, G.: Long-term planning of an underground mine using mixed-integer linear programming. CIM Bull. **98**(1089), 1–6 (2005)
19. Fava, L., Saavedra-Rosas, J., Tough, V., Haarala, P.: Heuristic optimization of scheduling scenarios for achieving strategic mine planning targets. In: The 23rd World Mining Congress, Canada (2013)
20. O'Sullivan, D., Newman, A.: Optimization-based heuristics for underground mine scheduling. Eur. J. Oper. Res. **241**(1), 248–259 (2015)
21. Magda, R.: Mathematical model for estimating the economic effectiveness of production process in coal panels and an example of its practical application. Internat. J. Prod. Econom. **34**(1), 47–55 (1994)
22. Whitchurch, K., Cram, A.A., Ozawa, N., Koizumf, K.: Underground and open-cut coal scheduling using expert systems. In: 26th APCOM Proceedings, pp. 339–346 (1996)
23. Epstein, R., Gaete, S., Caro, F., Weintraub, A., Santibañez, P., Catalan, J.: Optimizing long term planning for underground copper mines. In: Proceeding of Copper 2003-Cobre 2003, 5th International Conference, Santiago, Chile, CIM and the Chilean Institute of Mining, vol. 1, pp. 265–279 (2003)
24. Schulze, M., Zimmermann, J.: Scheduling in the context of underground mining. In: Operations Research Proceedings (2010)

Generation of a Monthly Mining Development Plan for Underground Mines Using Mathematical Programming

V. Rojas, T. González and N. Morales

1 Introduction

Mine planning optimization is well developed and widely used in open-pit mining as the mining operation progresses outwards with the deepening of the pit. Underground mining is much more complex as, throughout the life cycle of the mine, the directions of growth depend, among other factors, on the extraction method [1] and specific characteristics of the mineral deposit often requiring a unique design; therefore, creating generic optimization algorithms is more difficult [2]. This complexity does not allow for the developed algorithms to be applied across all underground and, thus, a heuristic approach must be considered. The main differences between algorithms and heuristics, both considered *step-by-step procedures*, is that optimization algorithms iterate until finding an optimal solution while heuristics iteration make a trade-off between the quality of the solution and the calculation time.

According to Musingwini [3], there are different algorithms and heuristics that are applicable to the mine planning problem, for example, the simplex algorithm for linear programming problems formulated by Dantzig or the dynamic programming algorithm used by [4] applicable in open-pit mining in the determination of the final pit.

In underground panel caving operation, the development plans are created by expert mine planners, who use common criteria and historical data to build these plans. There are no defined methodologies that would allow to optimize the available resources and, most importantly, to analyze possible scenarios for the execution of these plans. This approach often leads to noncompliance of the development plan

V. Rojas (✉) · T. González · N. Morales
DELPHOS Mine Planning Laboratory, AMTC, University of Chile, Santiago, Chile
e-mail: vrojas@delphoslab.cl

V. Rojas · T. González · N. Morales
Mining Engineering Department, University of Chile, Santiago, Chile

with the established period for the execution of the mine development. Therefore, the development of methodologies that would allow to plan more efficiently, ensuring an optimal result (or close) given the specific mine conditions would minimize the noncompliance and lead to more optimal use of the resources during the mine development stage.

In this paper, a methodology is proposed to address the time optimization problem for underground mine development, minimizing the execution time and considering operational, geotechnical, and deadline constraints.

2 Methodology

2.1 UDESS—A Mathematical Programming Model

UDESS is a mathematical programming model developed at the Delphos Mine Planning Laboratory, University of Chile [5], where a mixed-integer programming model of activity sequencing is used. The application of this model to the mine development optimization sought to minimize the execution time of the mining development plan, subject to precedence constraints between activities, operational constraints, and deadline milestones of certain development activities. The outcome of this model is a Gantt chart of the activities of the development plan.

The main characteristics of the model are as follows. Let us consider a set of periods $t = \{1,\dots, T\}$, a set of activities $i = \{1,\dots, A\}$ that must be scheduled, $r = \{1, \dots, R\}$ a set of resources that can be consumed by starting, ending and development of each activity i, and that have certain availability in each period t. Each activity i has a cost/benefit v_i associated with its development, and v_{i+} and v_{i-} associated to its start and end, with a minimum and maximum rate ($v_{\min}^i$, $v_{\max}^i$) that limits the progress of each activity during each period t. Finally, each activity i has associated a set of predecessor activities given by $P(i)$.

The decision variables of this model are:

- p_{it}: Percentage of progress of activity i in period t (continuous variable whose value is $p_{it} = [0, 1]$)
- s_{it}, e_{it}: Start and end variables, respectively, for activity i (binary variable, whose value is 1 if activity i starts/ends in period t or before, 0 otherwise)
- k_{iPt}: Variable that establishes relations of precedence between the successor activity i and a group of preceding activities $P \in P(i)$ (binary variable, whose value is 1 if all the activities of the group $P \subseteq P(i)$ are completed in period t, 0 otherwise)
- τit: Time consumed by activity i in period t and its predecessors.

The set of main constraints is given by:

- Operational resource constraint: Each activity can consume $\lambda i, r$ amount of a resource r during its development. This constraint limits the resources consumed in each period (given by $R_{r\min,t}$, $R_{r\max,t}$, respectively) for all activities

- Progress limit constraint: It is possible to require for each activity i a minimum or maximum rate of progress in period t (limits given by $b - i, t, b + i, t$, respectively)
- Range resource constraint: Activities are required to have a minimum (R_{rm}) and maximum (R_{rM}) consumption of a resource r during a certain time interval ($[t_{rmin}, t_{rmax}]$)
- Starting resource capacity constraint: It is possible to model that activities consume a resource r when initiating or finishing their progress (given by $\lambda + ir$ and $\lambda - ir$, respectively), which must be in a certain range given by $[S_{rmin,t}, S_{rmax,t}]$ for the beginning, and $[Er_{min,t}, Er_{max,t}]$ for the end of the activity
- Activity incompatibility constraint: It is possible to model that a certain set of activities cannot start during a certain time interval
- Starting period constraint: It is possible to force the start of a set of activities C between certain interval given by $[tC_{min}, tC_{max}]$
- Precedencies: Each activity i has a set of precedencies $P(i)$ that can be divided into groups $P \subseteq P(i)$. Precedencies can be generated as type "and", in which all groups of the set $P(i)$ must be completed before starting activity i, or as type "or", where it is required that at least one of the groups $P \subseteq P(i)$ must be completed to start activity i.

2.2 Mine Development Optimization Methodology

The proposed methodology takes the mine development plan (prepared by the experts of the mine operation) as a base plan or input to the UDESS model. The base plan consists of various activities such as horizontal and vertical developments, infrastructure construction, and installation subject to various constraints, precedencies, and milestones.

The activities are discretized to avoid unique advance face if the activities are extensive in development. The activities are related to each other by precedencies constraints (see Sect. 2.1), which determine the order in which each activity is executed and have different attributes and consume different types of resources. The constraints of the case study, including operational, deadline, and resource consumption constraints, are identified before the optimization heuristics is applied to solve the optimization problem to find an optimal scheduling of activities and the associated Gantt chart.

3 Case Study

The methodology was applied in an underground operation located in Chile. The operation had nine underground panel caving mines and one open-pit mine, which together represented an average annual production of 142,000 tpd.
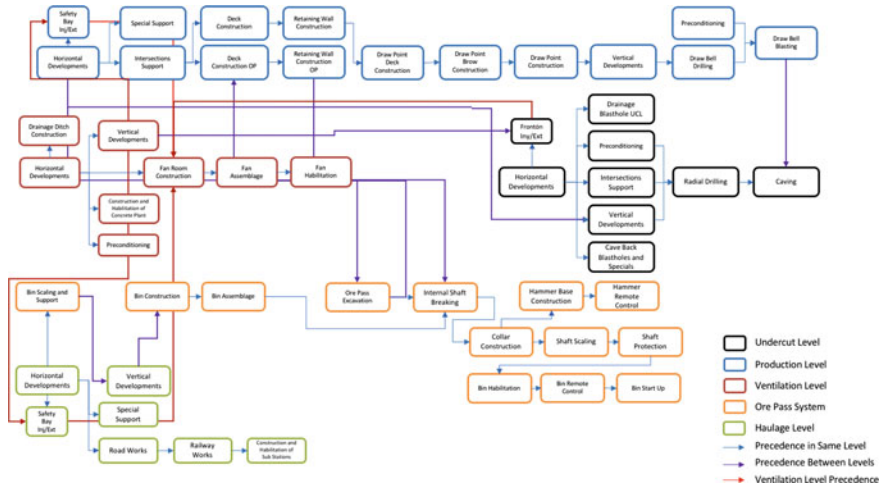
Fig. 1 Construction sequence of a conventional panel caving mine

The mine had four productive sectors, of which only one was considered, and four levels: sinking, production, ventilation, and hauling, where trains were used as a transport system for ore to the surface.

3.1 Construction Sequence of the Mine

Construction sequence of the extraction method was considered in modeling of the mine development plan. Figure 1 shows the construction sequence of the mine considering four levels: undercut, production, ventilation, and haulage as well as the ore pass systems.

3.2 Mine Development Plan

To fulfill the production goals, both in projects currently in execution and in future projects, a proper planning of mining development must be carried out for different time horizons.

The long-term plan had a time horizon ranging from 6 to 50 years and, in relation to mine development, it provided global figures required to comply with the production plans.

The medium-term plan had a time horizon of 1–5 years. This delivered the annual volumes of works required to comply with the production plans.

Table 1 Main results of the mine modeling with mathematical programming

Level	Activities	Precedencies	Constraints
Undercut level	210	417	409
Production level	775	1489	812
Ore pass systems	153	258	39
Haulage level	140	232	64
Ventilation level	162	286	68
Total	1440	2682	1392

The short-term plan had a time horizon of 1 year and its main function was to deliver the volumes of works considered during the annual period in the budgets allocated for the mining development.

The monthly short-term plan had a time horizon of 1 year and provided the growth guidelines for each sector and the monthly requirements for the incorporation of the area as well as incorporation of all the milestones of mining development to assure sustainability and continuity of production. It indicated when some of the main milestones had to be developed; the details of the activities to be developed monthly were added afterward.

4 Results

4.1 Mine Modeling

Table 1 shows the main outcomes of the implementation of the mine development plan within the optimization model.

The development of the activities and their precedence relationships can be modeled as precedencies of the "and" type and the "or" type. Of a total of 2682 precedencies, 1834 correspond to precedencies of the "and" type, while 848 correspond to precedencies of the "or" type.

4.2 Main Activities

Most of the activities focused on sinking and production levels, thus, the most relevant results for these levels are shown providing a good representation of the outcome for the rest of the mine. The activity with most volume of work in both levels corresponds to horizontal developments and, as shown in Fig. 2, the mathematical model is able to schedule all the plan activities leaving a small volume of activities to be carried out toward the final periods. The results for the rest of the activities in all levels are
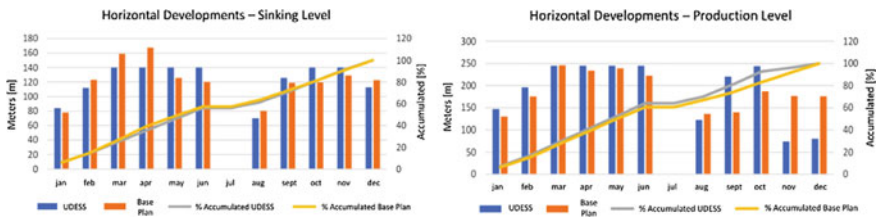
Fig. 2 Horizontal developments for undercut and production levels for the base development plan and the UDESS development plan

analogous, that is, all the activities of the development plan are scheduled within the 12-month horizon, respecting all constraints and leaving more time available toward the final periods.

5 Analysis

5.1 Modeling

The original activities presented in the development plan were taken and a discretization of these was carried out. For example, considering an activity of horizontal development of 100 m, this activity was discretized or divided into five smaller activities of 20 m each. The discretization for the modeling was made based on the discretization used by the expert planners of the operation for the construction of the plan, which complied with the operational requirements of the mine.

The advantage of the methodology applied to this case study was that most of the commercial scheduling software only use "and" type precedencies, thus the generated plans are more rigid in terms of possible outcomes. The mathematical model provides greater flexibility to the activity scheduling by incorporating type "or" precedencies, allowing the generation of plans that are closer to the operational reality.

5.2 Base Development Plan Versus UDESS Development Plan

The model scheduled all the activities associated with the program for the 12-month period (January–December 2017), which corresponds to the time horizon of the program.

The results obtained in scheduling the activities vary with respect to the original program, in many cases leading to important differences in sequencing and scheduling. This is mainly explained by analyzing the objective function that UDESS is
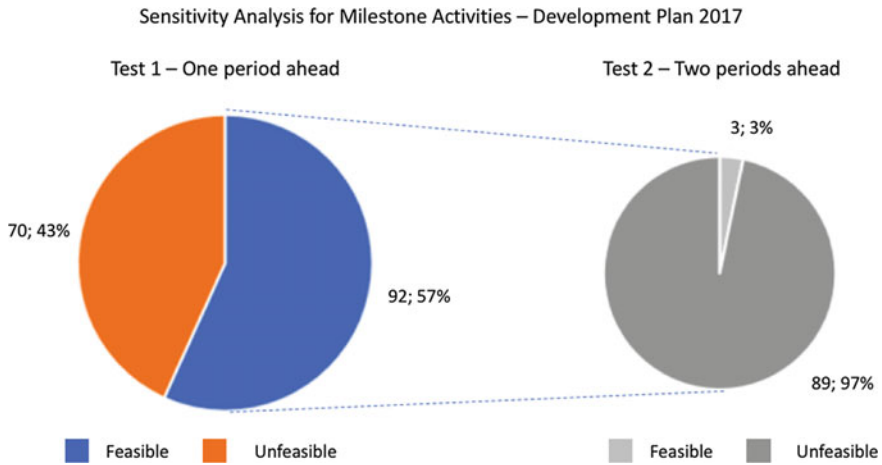
Fig. 3 Sensitivity analysis results for milestones and activities

using, which minimizes the total execution time of the plan, therefore, whenever possible, the software tries to advance the development works.

5.3 Milestones

In addition to being operationally feasible, the development plan must comply with a series of milestones in each level of the mine. The schedule given by UDESS fulfills all the milestones required, as shown in Table 2. When comparing both plans, it can be observed that the original plan does not meet the required deadlines established for three of the milestones required which results in 84% compliance.

5.4 Sensitivity Analysis

A sensitivity analysis was carried out, considering the scheduling of the mining development plan activities considering advancing the activities by 1 month. Those activities in which the rescheduling was possible, a new reschedule to advance the activities by 2 months was tested.

The results indicate that 57% of the activities of the plan accept the 1-month rescheduling. Of this 57%, only 3% of activities can be scheduled 2 months beforehand, as shown in Fig. 3. This result indicates that the plan has a good degree of flexibility to carry out the scheduling of activities, considering the multiple constraints of the problem.

Table 2 Comparison between base plan fulfillment and UDESS plan fulfillment

Milestone	Deadline	Fulfillment base plan	Fulfillment UDESS plan
Finishing special gallery south of crosscut access 4 at UCL	February	✓	✓
Connection ditch-53/crosscut-45at PL	February	✓	✓
Finishing special hydrocracking at PL	February	✓	✓
Finishing wall construction between ditches 49 and 50 at PL	February	✓	✓
Crosscuts 25 and 27 connections at UCL	March	✓	✓
Crosscut access 6-ramp connection al UCL	March	✗	✓
Total connection ditch-54/crosscut-27 to 59 at PL	April	✓	✓
Finishing special fortification at IZ	April	✗	✓
Enabling electrical station in crosscut-46 at VL	April	✓	✓
Finishing special fortification at Hw PL	May	✓	✓
Finishing constructions in crosscut-51 to 53 at north of ditch-49 PL	June	✓	✓
Total enabling injection crosscut-41 at VL	June	✗	✓
Enabling crosscut-38 at Block 1	June	✓	✓
Total fortification of crosscut-54 at PL	July	✓	✓
Connection ditch-54/crosscut-63/crosscut-1 at PL	August	✓	✓
Total enabling of extraction crosscut-46 at VL	December	✓	✓
Total enabling of crosscut-38	December	✓	✓
Finishing bin assembly in crosscut-43 at HL	December	✓	✓
Finishing labors inside shaft in crosscut-43 at PL	Various	✓	✓

6   Conclusions

The comparison of development plans created by experts and using new methodology identified multiple improvement opportunities. It was possible to reassign or add more activities in certain periods, where a large number of activities was not being developed, redistributing the available resources for greater efficiency or reducing the number of resources used.

Both plans scheduled all the activities within the established maximum period of one year (12 months), however, the due dates for milestones were not the same. While the expert schedule complied with 84% of the established due dates, the development plan built in UDESS complied with 100% of them.

The ability to model precedencies, such as type "and" and type "or", allowed the optimization model greater flexibility and, therefore, brought the results closer to the reality of the mine operation.

The results obtained from the sensitivity analysis established that there were improvement opportunities in scheduling since the original plan had certain gaps that had not been considered. In addition, UDESS provided the capacity and flexibility to test various development scenarios, a capacity that is nonexistent at present time due to the way in which the programs are built by the experts.

It was shown that an effective modeling methodology was created and validated in a real-case scenario adding value to the process of mine planning.

References

1. Alford, C., Brasil, M., Lee, D.: Optimisation in Underground Mining. Chapter 30 (2006)
2. Newman, A.M., Rubio, E., Caro, R., Weintraub, A., Eurek, K.: A review of operations research in mine planning. Interfaces **40**(3), 222–245 (2010)
3. Musingwini, C.: Optimization in underground mine planning-developments and opportunities. J. South Afr. Inst. Min. Metall. **116**(9), 809–820 (2016)
4. Lerchs, H., Grossman, I.F.: Optimum design of open-pit mine. Trans. CIM LXVII, 47–54 (1965)
5. Rocher, W., Rubio, E., Morales, N.: Eight-dimensional planning: construction of an integrated model for the mine planning involving constructability. In: Proceedings 35th International Symposium on Application of Computers in the Minerals Industry, pp. 393–406 (2011)

Optimization of Coal Production Rate as a Function of Cut-Out Distance

A. Anani, W. Nyaaba and A. Hekmat

1 Introduction

Room and pillar mining is the dominant underground mining method which is used to mine coal deposits. Even with the increasing demand for more alternative energy sources, coal still contributes to about 29% of the energy used worldwide [1]. However, productivity in underground mines is far less than its surface counterpart. In order to maximize coal production rate, many innovations in technology have been developed over the past decades for increased safety, which increases advance rate, geotechnical design innovations for maximum recovery, and continuous equipment for maximum production rate. The continuous mining system revolutionized underground coal production; however, their utilization is typically below 50% of its available time [2, 3]. This can be attributed to several factors including traveling time in and out of cut faces (the section where coal is produced), shift changing, moving cables, changing picks, waiting for roof bolter, breakdowns, belt delays, availability of power supply, and waiting for a shuttle car [2, 4]. Over the years, many researchers have focused on optimizing room and pillar design parameters for stability and maximum recovery [5, 6]. However, the rate at which coal is produced

A. Anani (✉)
Department of Mining Engineering, Department of Construction Engineering and Management, Pontificia Universidad Catolica de Chile, Santiago, Chile
e-mail: angelina.anani@ing.puc.cl

W. Nyaaba
Department of Mining and Nuclear Engineering, Missouri University of Science and Technology, Rolla, USA
e-mail: wnwt9@mst.edu

A. Hekmat
Department of Metallurgical Engineering, Universidad de Concepción, Concepción, Chile
e-mail: ahekmat@udec.cl

is heavily influenced by mine support systems such as fleet size, layout design, coal haulage, production sequence, ventilation, and labor [2, 7].

The continuous miner (CM) production cycle includes cutting and loading the haulage equipment typically shuttle cars, waiting on the shuttle cars, and moving from cut to cut. The amount of time the CM spends waiting for the haulage equipment can be minimized by matching the CM to an optimal fleet size given the operational constraints. The time the CM spends traveling from one cut to the other can take up to 10% of its available time [8]. However, minimizing CM travel time can be difficult due to the restrictive spaces in room and pillars mines. The time the CM spends traveling in a shift can be minimized by optimizing the width of the production panel and increasing the amount of time it spends cutting and loading the coal. The latter can be achieved by mining the maximum length at each cut face subject to geotechnical, ventilation, and safety constraints thus maximizing CM utilization. This can be considered as a constrained optimization problem with the form:

$$
\begin{aligned}
&\text{Min } f(x) \\
&\text{Subject to } g_i(x) = c_i \text{ for } i = 1, \ldots, n \\
&h_j(x) \geq d_i \text{ for } j = 1, \ldots, m
\end{aligned}
\tag{1}
$$

where $f(x)$ is the objective function, $g(x)$ is the equality constraint and $h(x)$ is the inequality constraint, x is the decision variable.

The objective function $f(x)$ is to maximize the CM utilization (for cutting and loading coal) or coal production rate subject to mining constraints such as:

– the CM follows a specific mining sequence
– the CM can only load one shuttle car at a time
– the maximum cut length (cut-out distance) cannot exceed 12.2 m (40 ft)
– a maximum of two shuttle cars can dump in the conveyor feeder breaker, etc.

The decision variables could be fleet size, panel width, and cut distances. The nature of the optimization problem makes it nonlinear and implicit and is therefore malleable to be solved using simulation-based optimization methods. The concept of optimizing support systems in room and pillar mines is not novel. Research can be found that optimizes the CM production sequence [2], selecting the best scheme for mining a coal panel [9], determining the optimal panel width for maximum production rate [7], matching CM to an optimal fleet size [10], and equipment dispatch as a function of CM duty cycles [11]. Although researchers point out the potential impact of CM travel times and the potential effect of cut-out distance on coal production rate [2, 12], there is no work, to the best of the authors' knowledge that optimizes the CM utilization as a function of the cut-out distance. This research uses computer simulation to solve the CM utilization optimization problem previously defined.

2 Simulation

Computer simulation has been widely used to solve mine planning problems. These applications are more prominent in mine surface operations [13, 14] compared to underground mining [7, 15]. The most common use is found in the optimization of material extraction and haulage systems with objectives such as to maximize production, equipment utilization, minimize fuel usage, equipment selection, and dispatch, and determination optimal design parameters [7, 13, 16]. The prominent use of simulation is as a result of its ability to solve implicit and complex optimization problems. Simulation can easily characterize the stochastic nature of mining systems, an aspect difficult to achieve with traditional mathematical optimization methods.

For the CM utilization and production rate problem, the authors solve the optimization problem as a discrete event simulation using Arena® optimization software. The approach used follows the general simulation methodology proposed in the literature [17].

3 Problem Definition and System Specifications

The objective of the simulation is to develop a discrete event model of a room and pillar material extraction and haulage system capable of evaluating the effect of cut-out distance on CM utilization and coal production rate, the optimal fleet size, and panel width. Consequently, the model should be able to determine the optimal fleet size, panel width, and cut-out distance for maximum CM utilization. The case study used in this research is based on a coal mining system in the midwestern region of the United States. The mine extracts the coal using a supersection approach, which involves two continuous miners mining a single coal panel. The conveyor belt feeder on which the coal is dumped and later taken to the surface is located at the center of the panel and fed by shuttle cars from both CMs. In the current mining system, each continuous miner has been assigned two 10.9 tonnes shuttle cars. The average payload is 8.6 tonnes per load. The dimensions of the rooms and pillars are 12 and 6 m, respectively.

4 Data Collection

The input and output data for the model were collected by observing shifts at the mine. For the optimization model, the input data collected to characterize the system included haulage travel (to and from the cut face to the change-out (CO) point and the change-out to the belt feeder) and dumping times for the shuttle cars, payload data, the CM traveling and loading times, and the dimensions of the cut. The width of the panel was also implemented as an input based on the cut sequence. The variables
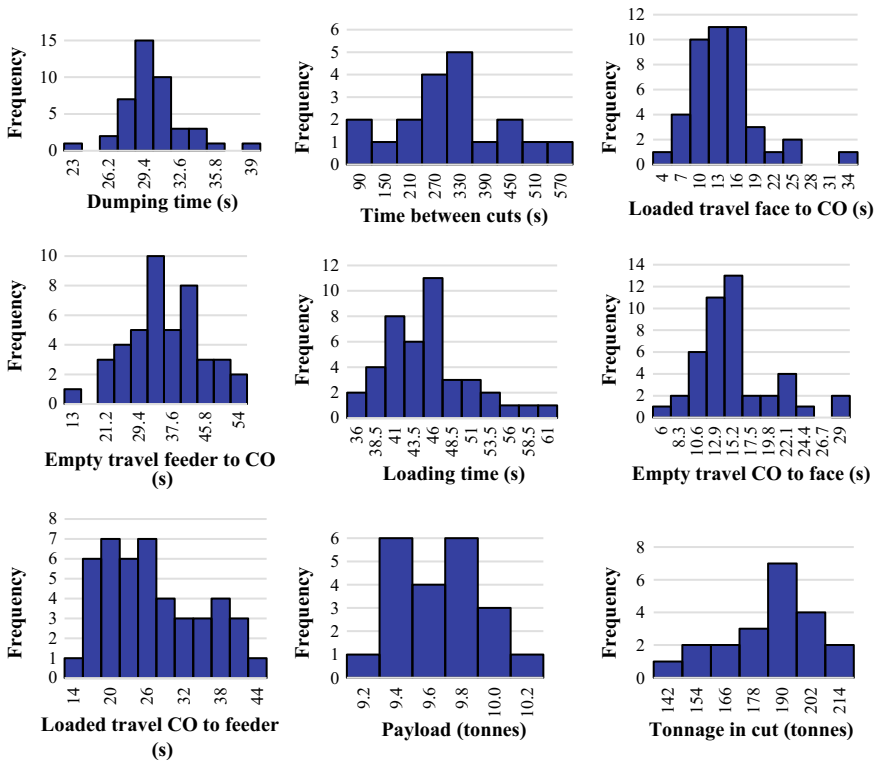
Fig. 1 Histogram plot of input data

are modeled as a distribution that characterizes their uncertainties (Fig. 1). Arena®
input analyzer tool was used to statistically fit the collected data. The production data
from the studied shifts are collected to validate the model.

5 Model Logic and Construction

The model logic follows the activities in a coal room and pillar production system.
The continuous miner follows a production sequence, which entails creating entries
and crosscut in a systematic pattern. An example of such sequence is shown in Fig. 2
for an 8-entry panel width. At each cut face, the CM cuts and loads the coal on to a
shuttle car. The shuttle cars are loaded on a first-in, first-out basis. The coal is then
transported by the shuttle cars to the feeder breaker located at the center of the panel.
The shuttle cars also dump the coal on a first-in, first-out basis. The shuttle cars then
return to the change-out (CO) location and join the queue to be loaded by the CM.
This cycle is repeated until the CM mines out the maximum possible depth of coal
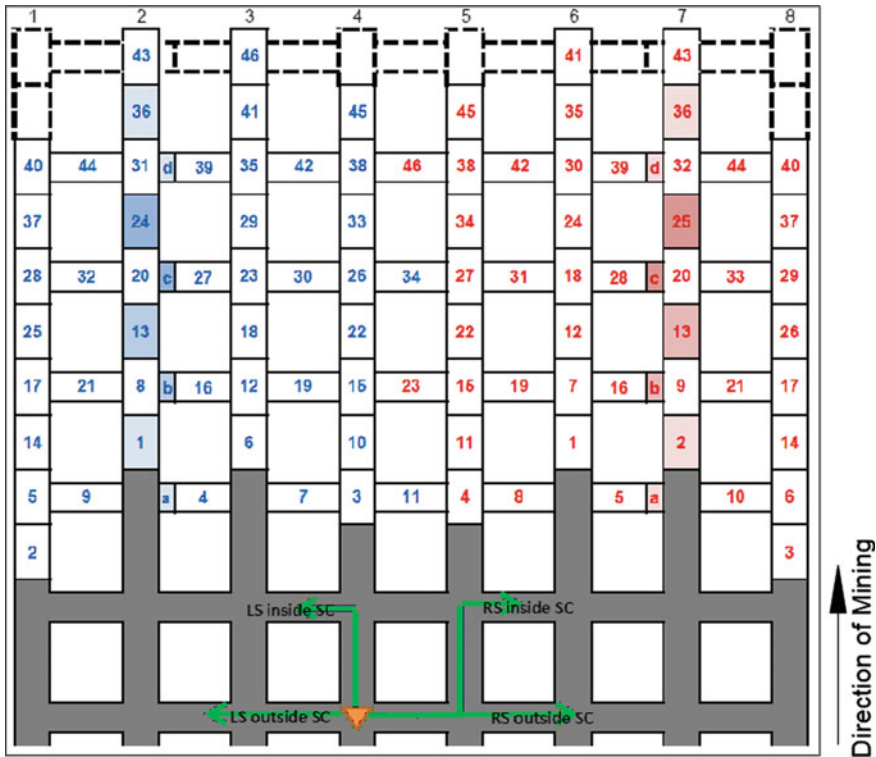
Fig. 2 CM cut sequence for an 8-entry panel width [2]

(cut-out distance) at each face given ventilation and geotechnical constraints. The CM then moves to the next cut in the sequence.

The Arena® process-orientated paradigm was used to construct this logic. Entities drive the simulation with time, activating each process such as loading, hauling, and dumping. The coal loads are model as entities. A process as defined in Arena® was used to model activities in the system and use resources to perform these activities. Thus, for activities such as loading, hauling, and dumping, the CM, shuttle cars, and feeder breaker are modeled as resources, respectively. The haulage units are modeled as a guided transporter, which ensures they cannot pass each other as is in the real system. The haulage routes were modeled as network links with which the transporters move from one location to the other.

Table 1 Validation results

	Simulation	Shift 1	% difference	Shift 2	% difference
Total production	1943.35	1852	4.93	1939	0.22
Number of loads	214	194	10.31	202	5.94

6 Model Validation and Verification

The constructed model was verified to ensure it behaves as intended. The verification process included the use of simple animation to determine if the entities followed the cut sequence as well as ensure the correct number of transporter units perform the task to which they are assigned. The output and internal values produced by the model such as queuing information, coal remaining in cut, and production data are evaluated to ensure they are within realistic values. The verified model was then validated using a trace-driven simulation approach by comparing the data collected from the studied shift to the simulation output. The data collect was from two 8-hour shifts in a 10-entry panel width. The results of the validation are summarized in Table 1.

The validation results show that the number of loads obtained by the simulation was 10.31 and 5.94% more than that recorded from the actual system for Shift 1 and Shift 2, respectively. The total amount of coal produced at the end of the shift was also higher than the actual system as shown in Table 1.

A consequence of this difference is that the model did not take into account specific delays such as scrubber inspection and bit changing. However, given the margin of error, the model was deemed valid and further used to analyze the system.

7 Experimental Analysis

7.1 Preliminary Analysis

Prior to solving the optimization problem using the valid model, a sensitivity analysis was conducted to determine, for the specific case study, the effect of CM travel times on coal production rate. Given the travel time data collected, the production data for an 11-entry panel with a fleet size of two was evaluated. The analysis was repeated with the travel time decreased in intervals of 10% (up to 50%). The results in Fig. 3 shows that the CM utilization and production rate increases with decreasing CM travel time. Currently, the CM travel time takes up 10.83% of an 8-hour shift. It is shown that a simple 10% decrease in travel time results in a 7.32% increase in production rate and 7.31% average increase in CM utilization when compared to current practices. A decrease in the overall CM cycle time can be achieved by maximizing the time
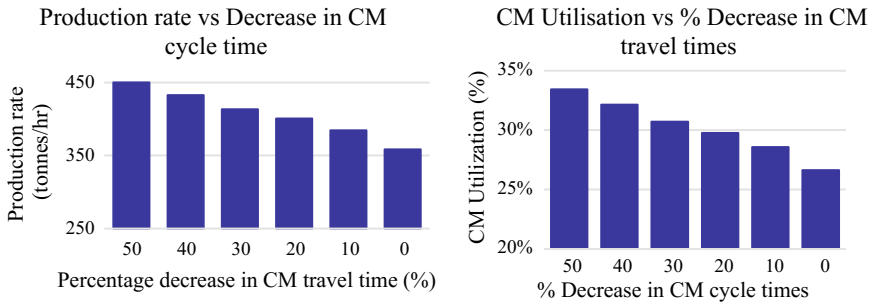
Fig. 3 Effect of CM travel times on CM utilization and production rate

Table 2 Experimental factors and their corresponding levels

Cut-out distance (m)	Fleet size (number of shuttle cars)	Panel width (number of entries)
9.14	2	8
10.06	3	9
10.67	4	10
11.28	5	11
12.19		12

the CM spends cutting and loading coal instead of traveling from cut to cut. Further experimental analysis was conducted to determine the optimal cut-out distance, panel width, and fleet size that maximizes CM utilization.

7.1.1 Optimization of CM Utilization and Production Rate

Three decision variables are considered in the experimental analysis (Table 2). These include the panel width, fleet size, and cut-out distance. Based on current practices at the mine, five levels of the panel width were evaluated. These included an 8-, 9-, 10-, 11-, and 12-entry panel widths. The volume of coal mined in each cut was a function of the cut-out distance calculated as the height (1.80 m), width (5.79 m), and depth (cut-out distance) of cut. The depth or cut-out distance is the distance from the last row of roof bolts to the mining face. The levels of cut-out distances selected were based on the historical data collected and geotechnical requirements.

Typically, the maximum recommended cut-out distance is approximately 12 m for safety and ventilation purposes. Lastly, four levels were selected for the fleet size based on practical feasibility. The number of shuttle cars was varied from two to five. The experimental analysis was run to determine values of the decision variables that maximize the objective function, in this case, CM utilization (and/or production rate). The analysis also answers the following questions:

– Does the cut-out distance affect the choice of optimal panel width?

– What is the effect of cut-out distance on CM utilization and production rate?
– Is there correlation between fleet size and cut-out distance?
– Is the current fleet size used by the mine truly optimal?

The design given the number of levels for each factor had 100 ($5^2 \times 4$) different experimental conditions. The simulation was run until the completion of the cut sequence. In order to compare all results within the same time frame, the simulation was run for 60 hours. The number of hours was selected to ensure that the production sequence was completed. The half-width was used to determine the number of replication to ensure reliability and statistical significance. As per Arena® statistical analysis, the number of replications of 150 was deemed adequate such that in 95% of repeated trials, the sample mean is reported as within the interval sample mean $\pm$ half-width.

8   Results and Discussion

This section discusses the relationship between the three factors evaluated and their effect on the production rate. The utilization of the CM is reflected by its rate of production.

8.1   Fleet Size Versus Panel Width

Figure 4 shows the relationship between fleet size and the panel width for each cut-out distance. For all panel widths, it can be seen that using a fleet size of three yields the highest production rate. The maximum production rate was obtained at the maximum cut-out distance specifically for the 11-entry panel. The lowest production rate was obtained when a fleet size of two was used for all panel width followed by a fleet size of five as a result of longer wait times by the CM and congestion due to excessive fleet in the system, respectively. Although production rate generally increases as the cut-out distance increases, it has no profound impact on the relationship between the fleet size and the panel width. Thus, a similar trend is observed for all cut-out distances.

8.2   Cut-Out Distance Versus Panel Width

Figure 5 shows the relationship between cut-out distance and panel width for various shuttle car fleet sizes. As expected, the production rate increases as the cut-out distance in each panel were increased for all fleet sizes. This is because the CM spends more time cutting and loading coal at maximized cut-out distances. Production rate
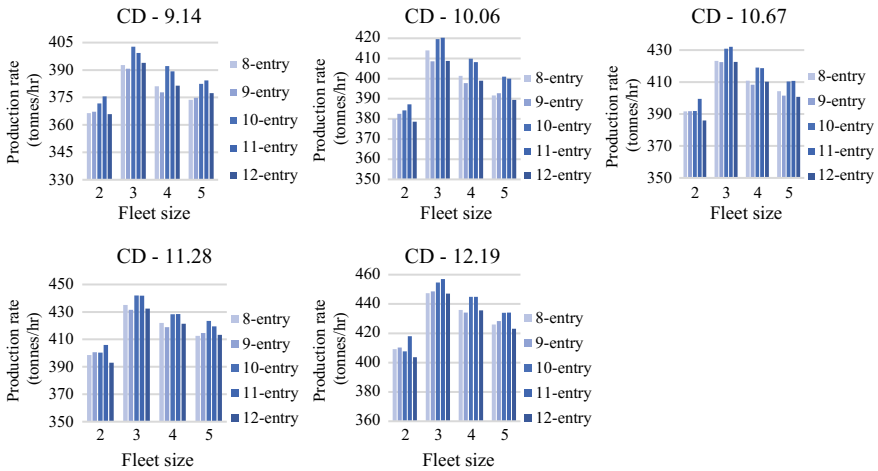
Fig. 4 The relationship between fleet size and panel width for each cut-out distance

using a fleet size of three for varying cut-out distance and panel width was generally higher than all other fleet sizes. The highest production rate for each fleet size is the 11-entry panel using the maximum cut-out distance of 12.19 m. The relationship between the cut-out distance and panel width varies for each fleet size. Take for example the production rate for the fleet size two (FS-2), travel time was higher in larger panels for the CM and shuttle cars. Inadequate fleet size in the system resulted in longer wait times by the CM in larger panels. As a result, the difference in production rate between larger and smaller panels is minimal at lower cut-out distances (9.14 and 10.06). However, as the time spent traveling is minimized by increasing cut-out distances, the benefits are much more evident in larger panels.

This is evident in the increase of the marginal differences in production rate between smaller and larger panels. On the other hand, as the fleet size increases factors such as congestion especially in smaller panels come into play resulting longer wait times for the shuttle cars. The optimum production rate was obtained by balancing factors such as traveling and waiting times. In this case, a combination of 11-entry panel, a fleet size of three, and cut-out distance of 12.19 yields the optimum solution as observed earlier.

8.3 Fleet Size Versus Cut-Out Distance

The results in Fig. 6 illustrates the effect of varying fleet size and cut-out distances on production rate. The production rate increases with cut-out distance for every fleet size. The overall production rate is higher for a fleet size of three in every panel width. Similar to previous observations, the optimal production rate of 457 tonnes/hr
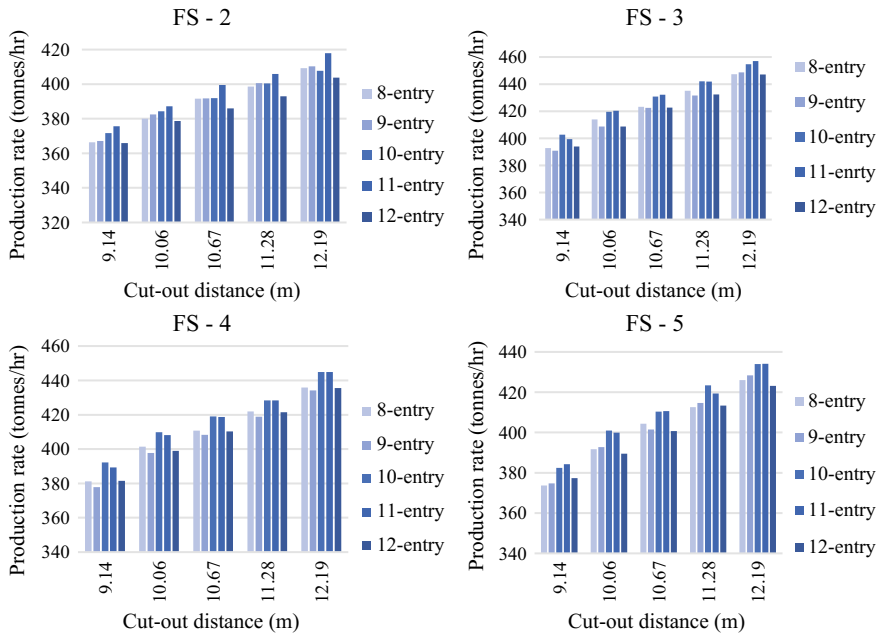
Fig. 5 The relationship between cut-out distance and panel width for various fleet sizes

is obtained in the 11-entry panel when the fleet size is three and the maximum cut-out distance is used. The production rate is heavily influenced by the width of the panel, which influences CM and the shuttle cars travel times. There is very little correlation between the cut-out distance and fleet size. The optimal fleet size for each panel width remains the same regardless of the cut-out distance. The overall increase in production rate is caused by minimizing the CM travel time and maximizing the time spent at each face not the increased amount of coal at each cut face. The distance traveled by the shuttle cars, therefore, remain the same regardless of the cut distance used.

9 Conclusion

A discrete event simulation of a room and pillar coal mining system was evaluated to determine the optimal decision for support systems needed to maximum CM utilization and production rate. Three factors were considered including the panel width, cut-out distance, and fleet size. It was determined that the optimal solution required the use of an 11-entry panel, cut-out distance of 12.19 m, and a fleet size of three. The results also show that regardless of the panel width and fleet size used maximum production is obtained at the longest cut-out distance. It is also
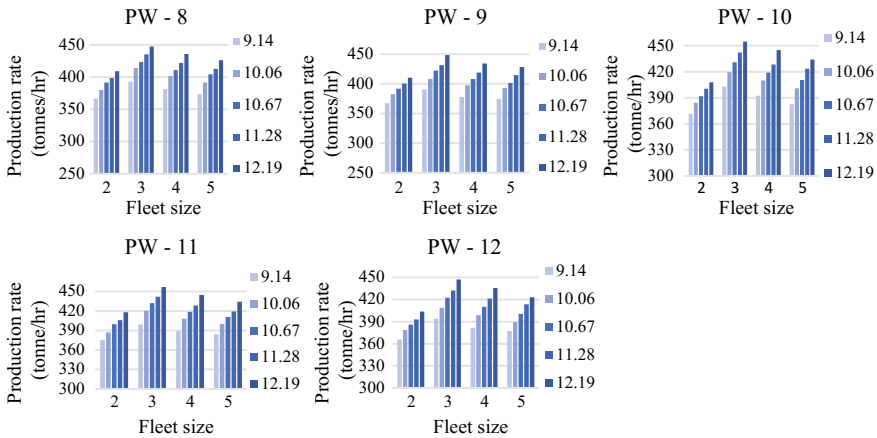
Fig. 6 The relationship between cut-out distance and panel width for various fleet sizes

determined that if the mine uses the maximum cut-out distance in all entry cuts, the production rate and CM utilization will increase by roughly 6%. This work has successfully proven, using a simulation that the utilization of continuous miners in an underground coal mine can be increased significantly by increasing the cut-out distance given production constraints.

References

1. IEA. Coal. Available from: https://www.iea.org/about/faqs/coal/ (2013, cited 2018, April 25)
2. Hirschi, J.C.A.: Dynamic programming approach to identifying optimal mining sequences for continuous miner coal production systems. Southern Illinois University at Carbondale (2012)
3. Sun, Y., Sidhom, J., Fourie, W.: Employing operational excellence to optimise underground haulage systems. In: SME Annual Conference & Expo 2017, Denver, Colorado, USA (2017)
4. Jemish, M., Bharti, S., Ramesh, K.: Applicability of continuous miner in room and pillar mining system: higher production and productivity with safety. In: International Conference on Deep Excavation, Energy Resource and Production: IIT Kharagpur, India DEEP16 (2017)
5. Ghasemi, E., Shahriar, K.: A new coal pillars design method in order to enhance safety of the retreat mining in room and pillar mines. Saf. Sci., 579–585 (2012)
6. Jaiswal, A., Shrivastva, B.K.: Stability analysis of the proposed hybrid method of partial extraction for underground coal mining. Int. J. Rock Mech. Mining Sci., 103–111 (2012)
7. Anani, A., Awuah-Offei, K., Hirschi, J.: Application of discrete event simulation in optimising coal mine room-and-pillar panel width: a case study. Mining Technol., 1–9 (2017)
8. Raghavan, V., Ariff, S., Kumar, P.P.: Optimum utilization of continuous miner for improving production in underground coal mines. Int. J. Sci. Res. Publ., 374 (2014)
9. Pereira, S.P, Costa, J.F.C.L., Salvadoretti, P., Koppe, J.: Mining simulation for room and pillar coal operation. J. Southern African Inst. Mining Metall., 473–447 (2012)
10. Suglo, R.S., Szymanski, J.: Computer simulation of underground room and pillar mining. In: Proceeding of Underground Operators' Conference, Kalgoolie, 13–14 November, pp. 1–4 (1995)

11. Anani, A., Awuah-Offei, K.: Incorporating changing duty cycles in CM-shuttle car matching using discrete event simulation: a case study. Int. J. Mining Miner. Eng., 96–112 (2017)
12. Mishra, D.P., Sugla, M., Singha, P.: Productivity improvement in underground coal mines—a case study. J. Sustain. Mining, 48–53 (2013)
13. Burt, C.N., Caccetta, L.: Equipment selection for surface mining: a review. Interfaces, 143–162 (2014)
14. Dindarloo, S.R., Osanloo, M., Frimpong, S.: A stochastic simulation framework for truck and shovel selection and sizing in open pit mines. J. Southern African Inst. Mining Metall., 209–219 (2015)
15. Park, S., Choi, Y., Park, H.S.: Optimization of truck-loader haulage systems in an underground mine using simulation methods. Geosyst. Eng., 222–231 (2016)
16. Awuah-Offei, K., Osei, B.A., Askari-Nasab, H.: Improving Truck-Shovel Energy Efficiency Through Discrete Event Modeling (2012)
17. Kelton, W.D., Sadowski, R.P., Sturrock, D.T.: Simulation With Arena, 4th edn (2010)

Analysis of the Impact of the Dilution on the Planning of Open-Pit Mines for Highly Structural Veined-Shaped Bodies

R. Amirá, N. Morales and A. Cáceres

1 Introduction

For the vein-shaped bodies, the dilution of the mineral resource causes greater economic impact than for the porphyry copper due to the higher amount of surface ore contact with waste that can be diluted during the operation.

According to Bertinshaw and Lipton [1], there exist four types of dilution:

1. By geometry: related to the size of shovel, bank. and shape of the mineral.
2. Due to uncertainty in the in situ contact: given by the lack of geological information.
3. By blasting: result of overbreak where it is also reduced waste.
4. Due to mining errors: due to errors in the operation, marking, and perforation.

Ebrahimi [2] defined two main types of dilution: internal dilution, which is difficult if not impossible to avoid, where lithology and the distribution of grades are important factors and external dilution, also called contact dilution, which refers to the waste outside of the mineralized body. The fundamental factors in the external dilution are the shape of the body, the techniques of drilling and blasting, and the scale of the operation and the size of the equipment.

The contact surface impacts mine planning as the material previously considered ore may become waste depending on the definition of the cut-off grade. Therefore, the quantification of this contact surface is essential to determine the possible dilution and to incorporate it in the mine planning. The study of the contact surface is intrinsically

R. Amirá (✉) · N. Morales
DELPHOS Mine Planning Laboratory, AMTC, DIMIN, Universidad de Chile,
Santiago, Chile
e-mail: ramira@delphoslab.cl

A. Cáceres
Geoinnova Association—GIS and Environment, Geoinnova, Chile
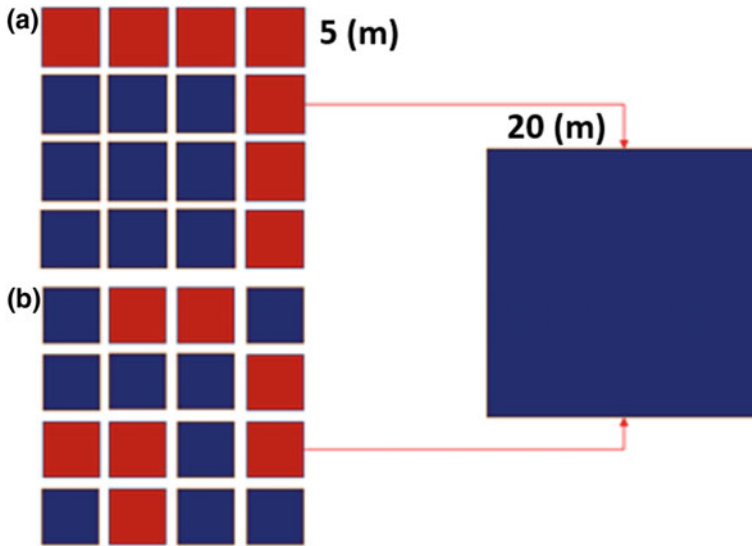
Fig. 1 Scheme of the internal dilution given by the two kinds of internal disposition of grades, ore blocks in blue and waste blocks in red: **a** regular distribution of ore, where the contact with waste is minimal and **b** irregular distribution of ore where the contact with waste is maximum

related to the size of the support used; the smaller it is, the larger the contact surface. Therefore, the size of the blocks must be considered in the analysis.

Vargas [3] defined planning as the ordering and scheduling of activities and resources of the mining operation to obtain the best possible result of the objective sought such as NPV, reserve, and life of the mine and operational continuity. In the planning, the geometric dilution is reflected in the change to a larger support unit, which results in the loss of selectivity of the extraction together with the incorporation of unwanted geological sections. In addition, the re-blocking decreases the recovery of the metal content as the size of blocks increase. Figure 1 shows an example of the change of support, where case (b) has a higher contact dilution income than case (a), with the same number of blocks in both cases.

Rossi and Deutsch [4] stated that a block size change brings with it several consequences; it is possible to reduce the block size to have the option to choose the blocks to be exploited better, increase the selectivity, or change to a larger support to reduce the number of blocks exploited. With the increase in block size, the softening of the grades implies a reduction of the variance, while the average does not vary.

This paper presents the outcome of the investigation to characterize and incorporate dilution in open-pit mining planning in structurally controlled high-grade deposits. A long-term strategic evaluation was carried out, using fixed economic parameters and considering the internal and contact dilution but not the operational dilution. The evaluation was made based on a block model of the copper deposit,
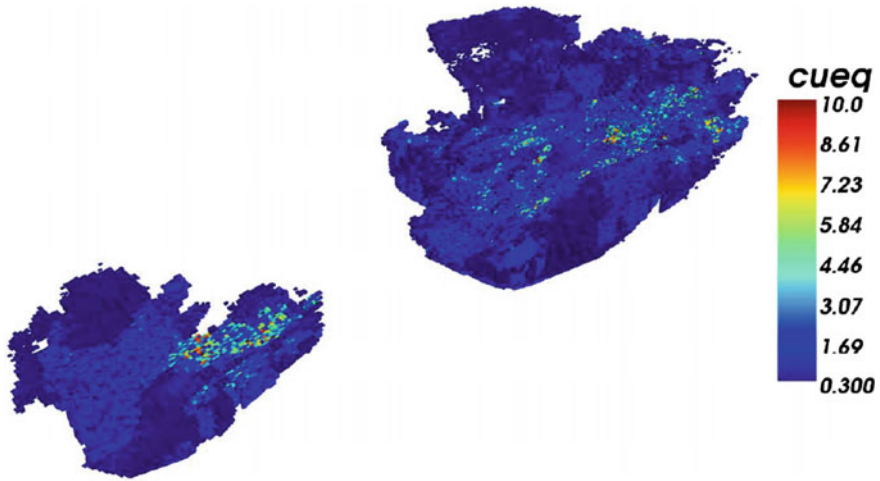
Fig. 2 Isometric view of the block model grades with a cut-off grade of 0.3 (%)

which consisted of a highly stratified vein-like body with 25,026,301 blocks, measuring 7.5 m × 5 m × 2.5 m each block.

2 Methodology

2.1 *Characterization of Geological Dilution by Contact*

A study of the neighborhood of each block was carried out identifying the blocks according to a cut-off grade threshold of 0.3 (%).

The categories shown in Fig. 2 defined in this study were as follows:

– ore in contact with ore (O-O): an ore block whose neighborhood consists only of blocks of ore (blue)
– ore in contact with waste (O-W): an ore block whose neighborhood consists of at least one block of waste (celestial)
– waste in contact with ore (W-O): a waste block whose neighborhood consists of at least one block of ore (yellow)
– waste in contact with waste (W-W): a waste block whose neighborhood consists only of waste blocks (red).

2.2 *Characterization of Internal Geological Dilution*

To study the internal dilution, four changes of support size were made with respect to the original model (C5), which had block dimensions of $7.5 \times 5 \times 2.5$ m, generating cases C10, C15, C20, and C30, where the dimensions of each block was multiplied by 2, 3, 4, and 6, respectively.

2.3 *Strategic Planning*

Valuation of the blocks using the grades was carried out according to fixed economic parameters, however, different sizes of the block have different costs. With this, a determined envelope was obtained with nested pits used to define the phases of the mine and a production plan with a corresponding NPV. For the mine planning, plans with different capacities of mine and plant were generated and fixed for the reminder of the study.

2.4 *Incorporation of CV in Mine Planning Due to Mixing Restrictions*

To study the impact of the internal distributions of the small blocks which make up the large blocks in a larger support, a calculation of the coefficient of variation (CV) was performed for each large block. This coefficient represents the variability of grades present within each large block; the higher it is, the greater the risk of dilution exists. Therefore, mixing restrictions were applied for the plans of each case studied consisting of each period sending blocks with CV average not exceed the maximum established to the plant.

3   Case Study

A cut-off grade of 0.3 (%) was established as a threshold between ore and waste. Figure 2 shows the grades present in the reserve of mineral.

The final pit had 4,688,153 blocks. The total ore tonnage was 180 (Mton), a 40 (%) of the reserve, with an average grade of 0.194 (%). Figure 3 shows the final pit for two different block sizes of 5 and 10 (m).

When considering the larger block sizes, the contact boundary between ore and waste was undoubtedly affected by the loss of information. To minimize this loss of information, the coefficient of variation (CV) of the grades for large blocks was calculated as follows:
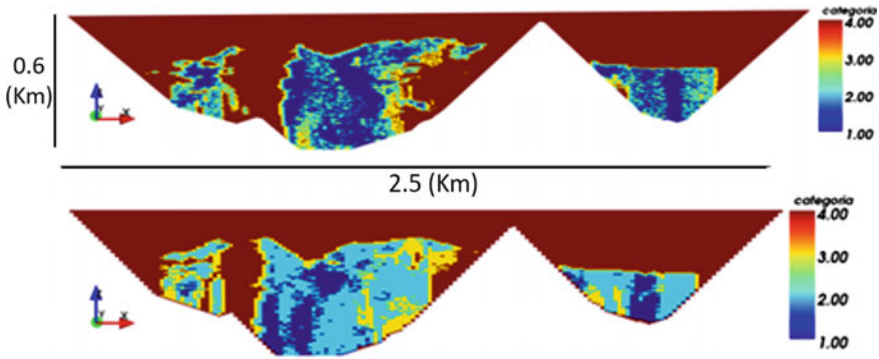
Fig. 3 View of the *X–Z* plane of the deposit categorized for the block size of 5 and 10 (m)

$$CV = \sigma / G \tag{1}$$

$$\sigma^2 = \frac{\sum (G - g_i)^2}{N - 1} \tag{2}$$

where G is the grade of the big block and σ is the variance applied to a large ore block, g_i is the grade of the small blocks i and N the number of small blocks.

4 Results

4.1 Categorization of Block Size

Table 1 shows the amount of ore and waste for each block size with their respective average grades. The considerable increase of the total ore by 44 (MTon) from C5 to C30 is explained by the incorporation of a large quantity of small waste blocks within the large ore block as observed directly from the reduction of total waste as the block size increases.

Table 1 indicates a 0.2 (%) reduction in the mean grade of the total ore verify by the addition of small waste blocks to the large ore blocks. Figure 4 shows the selectivity curve for the different block models, which compares the amount of fines obtained between the block sizes for different amounts of ore according to its cut-off grade. It can be noted that the amount of metal content is considerably reduced by the increase in block sizes, reaching 100 MTon, where the amount of metal content of C30 represents two-thirds of the amount of metal of C5. The magnitude of this difference between the curves is greater for the smaller blocks as seen in cases C5 and C10. This effect decreases with the increase in block size. The comparison between cases C15 and C20 can be observed, where the effect is smaller.

Table 1 Summary table of the amount of ore and waste with its average grade for each block size

	Tonnage (MTon)	Average grade (%)	Metal content (KTon)
C5			
Ore	180.33	1.01	1828.54
Waste	962.41	0.04	375.34
Strip ratio	5.34		
C10			
Ore	193.98	0.94	1827.26
Waste	948.760	0.04	370.02
Strip ratio	4.89		
C15			
Ore	211.77	0.86	1827.55
Waste	930.97	0.04	353.77
Strip ratio	4.40		
C20			
Ore	212.52	0.86	1817.01
Waste	930.22	0.04	353.48
Strip ratio	4.38		
C30			
Ore	224.42	0.80	1804.30
Waste	918.32	0.04	348.96
Strip ratio	4.09		
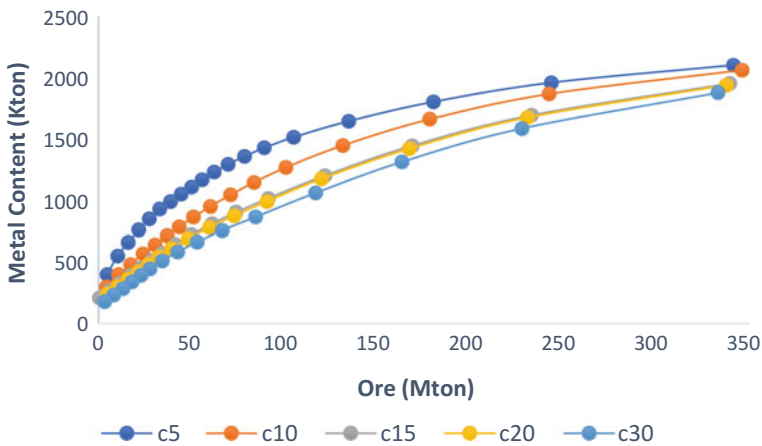
Fig. 4 Selectivity curve for each SMU

Figure 5a shows the percentages of the extreme categories O-O and W-W decrease while for the intermediate categories, O-W and W-O increase in a similar proportion. Figure 5b shows the increase of waste and the decrease of ore of small blocks. For
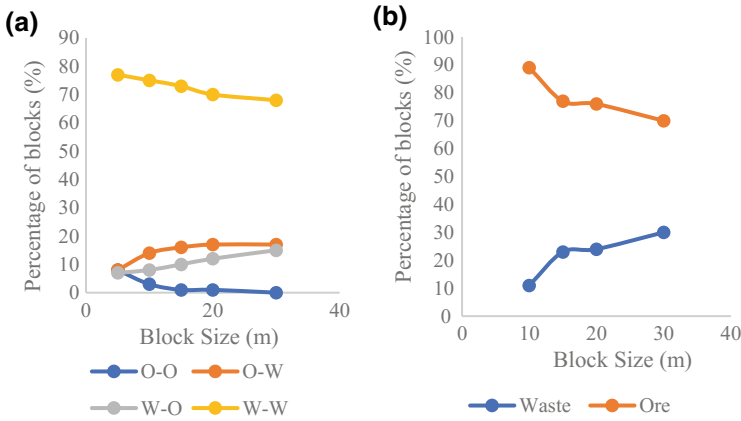
Fig. 5 **a** Proportions of the categories. **b** Ore and waste of small blocks in large blocks of ore present for each block size
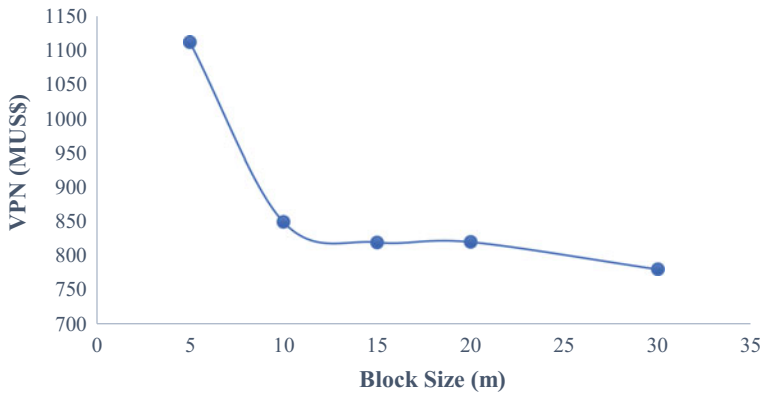
Fig. 6 NPV from the project according to the SMU

the small blocks, the amount of ore and waste material decreased and increased, respectively, up to 30 (%).

4.2 Strategic Planning

Figure 6 expresses the NPV obtained for the production plans for each case. There is an inverse relationship between the value of the project and the block size.

During the re-blocking, there is a difference of 20 (MTon) between C10 and 65 (MTon) for C30 between the amount of mineral of bigger blocks and the mineral of smaller blocks that composes it. This represents the conversion of 19 (%) from
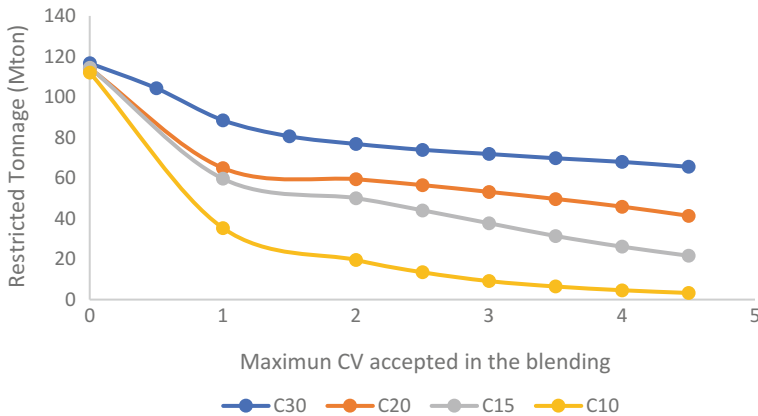
Fig. 7 Ore tonnage restricted by maximum CV

small waste blocks to ore and, thus, the loss of information when using SMU of larger size translates directly into a difference of the amount of ore sent to the plant and the mineral of small blocks that it really contains. This occurs because when working with a larger block size, waste support in contact with ore, it is considered to be ore and is processed as ore, resulting in poor utilization of the loading and processing equipment. In addition, the mixture produces a decrease in the grade punishing directly the fine obtained, with it the cash flows of each period and the final NPV of the project.

The direct translation of the loss of metal content is observed in a decrease of NPV reaching a difference of 291 (MUS\$) between the cases C5 and C30. Thus, the loss of information and the softening of grades decrease the value of the project itself by more than 25 (%).

Loss of information and quantity of waste within the block are often ignored in many current operations in the industry, a fundamental result being their consideration for the sale and purchase of new deposits, where, if the buyer does not ensure that the estimated SMU is adequate, the final result can have large variations or losses in the expected economic gains For the different block sizes, a blending restriction is applied for the coefficient of variability: if the CV required is 1, the average of the coefficients sent to be processed in a period must be less than or equal to 1.

For the different block sizes in the same CV and for smaller sizes, there was a smaller amount of restricted resources (Fig. 7). Thus, the variability increases with the block size. The average CV for each size C10, C15, C20, and C30 are 0.209, 0.621, 0.984, and 2.119, respectively, and thus, in addition to the loss of information, there is a significant increase in the variability within the block when changing to a larger support size.

Figure 8 shows the results obtained when applying the mixture restriction and achieving a direct comparison between the different SMU cases, which shows the NPV obtained for each size with an average CV allowed per period.
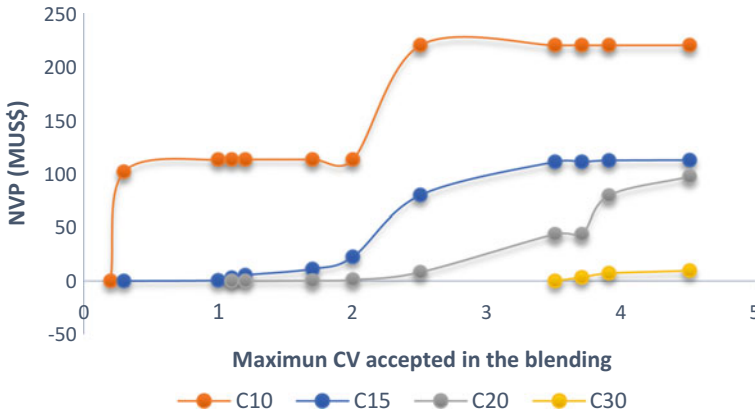
Fig. 8 NVP of the annual plans for different sizes within a restriction range

For all sizes, increasing the CV permitted per period increases the value of the project, unless the latter remains constant, because the NVP reaches the maximum achievable by applying a blending constrain.

The variability of blocks increases with block size. For example, for a block size of 10 m versus a block size of 30 m, the first achieves a value of 220 (MUS$) while the second obtains a value 0 for an average coefficient of variation of 2.5 for the entrance to the plant. The difference in the values obtained is the maximum allowed CV increases with the increase in the block size.

5   Conclusions

It is known that in the operation, block sizes are required that adapt to the operational requirements. Rarely, blocks sized of 2.5 m are used since the current equipment is larger and all the selectivity would be lost at the time of use. Therefore, the use of larger blocks has benefits by allowing an adequate operational geometry and minimum widths. In addition, the number of blocks is reduced and with it the number of components that make up the scheduling problem, so the resolution times decrease considerably. On the other hand, the metal content loss occurs, as shown by the selectivity curve and the quantification of the amount of ore and waste by size presented in this paper.

Another fact to highlight from the NPV obtained is the direct relationship between the range of feasible results and the SMU size. The smaller block sizes being those accept lower restrictions, while larger sizes give different results when the restriction is increased. As the block size is increased, the variation of NPV produced between different CV restrictions

becomes smaller. The effect of the variability has greater importance and economic impact in smaller blocks than in the cases with larger SMU size.

References

1. Bertinshaw, R., Lipton, I.: Estimating Mining Factors (Dilution and Ore Loss) in Open Pit Mines (2007)
2. Ebrahimi, A.: An Attempt to Standardize the Estimation of Dilution Factor for Open Pit Mining Projects (2013)
3. Vargas, M.: Modelo de planificación minera de corto y mediano plazo incorporando restricciones operacionales y de mezcla. Master's thesis in mining. Universidad de Chile, Chile (2011)
4. Rossi, M., Deutsch, C.: Mineral Resour. Estimation **2**(2), 12–18 (2014)

Modeling Optimum Mining Limits with Imperialist Competitive Algorithm

S. Javadzadeh, M. Ataee-pour and V. Hosseinpour

1 Introduction

After the feasibility studies determined the mineral profitability, the design must be done before production planning and exploitation. It is essential to determine ultimate pit limit (UPL) for design an open-pit mine. The UPL determination depends on mineral grade, income, and costs. Many algorithms have been proposed to determine the mine UPL. First UPL determination algorithm was proposed by Pana [1], based on the concept of a floating cone, and Lerch and Grossman using graph theory, dynamic programming [2] and corrected from of Korobov algorithm [3]. Over years, many algorithms have been developed for solving UPL determination problem. Major disadvantages of some of these algorithms were the speed of their resolution. The speed of computers has also greatly improved over time. However, smart and fast algorithms help to solve the engineering problems, and also mining industry uses these algorithms to solve mining problems. By matching mining problems with nature-inspired algorithms, researchers solved the problem and found an optimal solution. Smart algorithms such as genetic algorithms [4], ant colony [5], and bee colony [6] were implemented in solving UPL problem. Imperialist competitive algorithm (ICA) was developed by Atashpaz-Gargari and Lucas [7] to solving optimization problems that were inspired by human social evolution. The proposed algorithm is inspired by a social-political process and it is fast compared to the mentioned methods. ICA is simple for understanding and has high convergence speed to reach the optimal solution. ICA use a social-political evolutionary process in the creation of a powerful empire, in this case, the ultimate pit. In fact, this algorithm assumes optimal solution of the problem as a series of countries, tries to improve these solutions during the repetitive process, and eventually gives optimum solution of problem.

S. Javadzadeh · M. Ataee-pour (✉) · V. Hosseinpour
Department of Mining and Metallurgical Engineering, Amirkabir University of Technology, Tehran, Iran
e-mail: map60@aut.ac.ir

2   Materials and Methods

Each algorithm begins with a series of initial solutions for optimization, and in each algorithm, the same initial solutions are used in form of the country. Initial countries improve the solution for optimization problems. The ICA is designed in such a way that each country develops alone and finds the optimal solution to the problems. But it is possible to cooperate with colonial states of an empire with the colonial country of that empire so that the possibility of an acceptable solution can be increased.

3   Generating Initial Countries

Initial countries are the initial solutions that are introduced in the UPL problem as pit. Possible solution region must be specified before generating the initial solutions. As shown in Fig. 1, we have a 16×7 economic block model for the 1:1 slope and its possible solution zone shown in Fig. 2 with white blocks.

After we define the possible solution region, we determine the initial pits identified in the ICA as country. All pits determined stochastically and each pit known by its cone vertex. Pit vertexes should be in positive block values.

4   Initial Empires Establishment

In order to generate empires, countries must have already been generated at this stage. As mentioned, previously these countries are randomly selected from possible

i \ j	1	2	3	4	5	6	7	8	9	10	11	12	13	14	15	16
1	-3	0	-2	-4	-3	0	0	0	0	0	0	0	0	-3	-2	0
2	-6	-2	-6	-2	3	-1	0	0	0	0	0	2	1	2	4	-3
3	-8	-9	5	-4	2	2	-2	0	0	-2	3	3	-6	6	-5	-4
4	-7	-8	-8	4	5	6	-1	-3	-2	3	2	-4	-6	-7	-6	-10
5	-10	-9	-7	-6	-3	5	6	8	6	-3	-1	-6	-2	-3	-5	-6
6	-10	-6	-8	-6	-4	8	12	15	1	2	-2	-8	-4	-6	-8	-4
7	-9	-10	-7	-5	-2	2	10	6	-4	3	-1	-2	-3	-4	-6	-5

Fig. 1   Grade block model

i \ j	1	2	3	4	5	6	7	8	9	10	11	12	13	14	15	16
1	-3	0	-2	-4	-3	0	0	0	0	0	0	0	0	-3	-2	0
2	-6	-2	-6	-2	3	-1	0	0	0	0	0	2	1	2	4	-3
3	-8	-9	5	-4	2	2	-2	0	0	-2	3	3	-6	6	-5	-4
4	-7	-8	-8	4	5	6	-1	-3	-2	3	2	-4	-6	-7	-6	-10
5	-10	-9	-7	-6	-3	5	6	8	6	-3	-1	-6	-2	-3	-5	-6
6	-10	-6	-8	-6	-4	8	12	15	1	2	-2	-8	-4	-6	-8	-4
7	-9	-10	-7	-5	-2	2	10	6	-4	3	-1	-2	-3	-4	-6	-5

Fig. 2 Possible solution region

Table 1 Early pits (countries) with their cones vertex and profits

Pits	Pit 1	Pit 2	Pit 3	Pit 4	Pit 5	Pit 6	Pit 7	Pit 8	Pit 9
Profit	-13	6	-1	-5	-10	-2	-10	-17	-2
Cone vertex (i, j)	(4, 4)	(4, 10)	(2, 15)	(5, 8)	(4, 5)	(2, 13)	(4, 5)	(3, 3)	(2, 13)

solution region blocks. Selected countries are inverted cones which are based on are (positive) blocks. To determine candidate countries to become imperialist, we act as follows.

At first, all countries (Pits) are arranged, according to the amount of profit, from the maximum to the minimum. The number of imperialist countries that have already designated is chosen as imperialist. The number of initial countries for this model is nine, and the number of imperialists is three, as specified in Table 1 with their profits.

As mentioned, positive pits selected as the first countries are ranked on basis of the profit, and the first three will be as imperialist.

Pits number 1, 2, and 3 are selected as imperialists. However, in order to allocate countries to these imperialists, there are several ways to apply:

– Have the same chance for selecting countries.
– An imperialist country with more profits will take a higher share.

The designation of countries in the first method is that the probability of choosing is 1/3 and pits from number 9 to number 8 (Table 2) are chosen one by one and competing with three imperialists to take possession of it. Imperialist winner of this competition is determined by roulette wheel. In this method, all imperialists portion determined simultaneously. In addition, the winner imperialist identified by roulette wheel. For the allocation of other countries to these imperialists, the normalization cost of each imperialist is calculated using Eq. 1.

Table 2 Countries sorted by profit

Pits	Pit 2	Pit 3	Pit 6	Pit 9	Pit 4	Pit 5	Pit 7	Pit 1	Pit 8
Profit	6	−1	−2	−2	−5	−10	−10	−13	−17
Cone vertex (i, j)	(4, 10)	(2, 15)	(2, 13)	(2, 13)	(5, 8)	(4, 5)	(4, 5)	(4, 4)	(3, 3)

Table 3 Converting maximizing problem to minimization

Pits	Pit 2	Pit 3	Pit 6	Pit 9	Pit 4	Pit 5	Pit 7	Pit 1	Pit 8
Cost	−6	+1	+2	+2	+5	+10	+10	+13	+17
Cone vertex (i, j)	(4, 10)	(2, 15)	(2, 13)	(2, 13)	(5, 8)	(4, 5)	(4, 5)	(4, 4)	(3, 3)

$$C_n = \max\{c_i\} - c_n \tag{1}$$

where C_n is the normalized cost of the imperialist n. max C_i is also the highest cost among imperialist countries, and C_n is the cost of the imperialist n.

It needs to explain that in the minimization problems, the normalized cost and in the maximizing problems normalized profit can be calculated, or we can convert a maximization problem like a pit into minimization problem (multiplied by −1) and the normalized cost. We used the same second method in this paper (Table 3).

With the normalized cost, the normalized normal power of each imperialist is calculated using Eq. 2. Then colonial countries are divided among imperialists.

$$p_n = \left| \frac{C_n}{\sum_{i=1}^{N_{imp}} C_i} \right| \tag{2}$$

Thus, using Eq. 1, the normalized cost of each imperialist is calculated as follows:

$$C_1 = \max\{c_i\} - c_1 = 2 - (-6) = 8$$

$$C_2 = \max\{c_i\} - c_2 = 2 - 1 = 1$$

$$C_3 = \max\{c_i\} - c_3 = 2 - 2 = 0$$

Normalized power is calculated using Eq. 2 as follows:

$$p_1 = \left| \frac{C_1}{\sum_{i=1}^{N_{imp}} C_i} \right| = \left| \frac{8}{9} \right| = 0.89$$

$$p_2 = \left| \frac{C_2}{\sum_{i=1}^{N_{\text{imp}}} C_i} \right| = \left| \frac{1}{9} \right| = 0.11$$

$$p_3 = 0$$

From another standpoint, the normalized power of an imperialist is the colonial portion governed by imperialist. Thus, an imperialist that has a greater amount of probability is assigned more colonies. So, the number of primary colonies of an empire is calculated using Eq. 3:

$$N_{C_n} = \text{round}\{P_n \cdot N_{\text{col}}\} \tag{3}$$

where N_{C_n} is the number of colonies of an empire and N_{col} is the total number of colonial countries in the population of the original countries. Round is the function that assigns the closest integer to a decimal number.

The colonies of each imperialist are calculated using Eq. 3 as follows:

$$N_{C_1} = \text{round}\{P_1 \cdot N_{\text{col}}\} = 0.89 * 6 = 5$$

$$N_{C_2} = \text{round}\{P_2 \cdot N_{\text{col}}\} = 0.11 * 6 = 1$$

$$N_{C_3} = \text{round}\{P_3 \cdot N_{\text{col}}\} = 0 * 6 = 0$$

As shown in Eq. 3, the first five colonies devote to the first imperialist and the last colony (8th pit) is assigned to the second imperialist. The Third Empire does not receive any colony. After the colonists took their colonies, the policy of assimilating the colonies is applied.

5 The Assimilation Policy in the Imperialist Competitive Algorithm

The assimilation policy is implemented using Eqs. 4 and 5:

$$x \sim U(0 \cdot \beta \times d) \tag{4}$$
$$\theta \sim U(-\gamma \cdot \gamma) \tag{5}$$

where

x Colony toward imperialist movement unit
β A number greater than 1
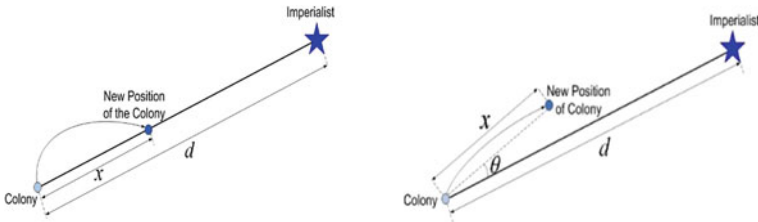
Fig. 3 The attraction policy in the Imperialist competitive algorithm [7]

d is the distance between colony and imperialist
θ In this figure, θ is a random number with uniform (ore any proper) distribution
γ A parameter adjusting the deviation from the original direction.

6   Implementation of the Assimilation Policy in the 2-D Ultimate Pit Model

In the ultimate pit limit, we cannot determine spatial destination for movement of colony toward imperialist. So we select a block of colony and a block of imperialist randomly. In next step we select a block from two random blocks (selected block must be positive) and all positive blocks between selected instants. For clarify this concept continue solving mention example (Fig. 3).

As mentioned in the establishment of the empires, the policy of assimilation is applied to the colonies. For better understanding, we solve the policy of assimilation to the colonies of the first imperialist. However, before solving, we need to point out that the positive blocks have the right to selection, which means that the probability of selecting nonpositive blocks is zero. Number 9 pit (with vertex 13, 2), which is the first colony of the empire 1 (with vertex 10, 4), has four blocks (Fig. 4).

The relevant probabilities are shown in Fig. 5.

Since the colony has a single member, the same member is selected, but to choose a member from the imperialists, we must use sampling methods. For this purpose, we used roulette wheel sampling method.

7   Combination Policy

Instead of individual developing and trying to reach the imperialist position to occupy the place of the imperialists, countries are working with each other to improve their empire. Imperialists will prevent the collapse of the empire. However, a country that fails to appear in a better empire will continue to be used by other empires. In this approach, stronger empires will try to improve the colony of the weakest empire. This

i\j	1	2	3	4	5	6	7	8	9	10	11	12	13	14	15	16
1	-3	0	-2	-4	-3	0	0	0	0	0	0	0	0	-3	-2	0
2	-6	-2	-6	-2	3	-1	0	0	0	0	0	2	1	2	4	-3
3	-8	-9	5	-4	2	2	-2	0	0	-2	3	3	-6	6	-5	-4
4	-7	-8	-8	4	5	6	-1	-3	-2	3	2	-4	-6	-7	-6	-10
5	-10	-9	-7	-6	-3	5	6	8	6	-3	-1	-6	-2	-3	-5	-6
6	-10	-6	-8	-6	-4	8	12	15	1	2	-2	-8	-4	-6	-8	-4
7	-9	-10	-7	-5	-2	2	10	6	-4	3	-1	-2	-3	-4	-6	-5

Fig. 4 Number 9 pit

i\j	7	8	9	10	11	12	13
1	0	0	0	0	0	0	0
2		0	0	0	0	0.33	
3			0	0	0.33		
4				0.33			

i\j	11	12	13	14
1		0	0	0
2			1	
3				
4				

Fig. 5 On the right, the likelihood of the first colony on the left is also likely to be monopolistic

Table 4 The position of the colonies after the application of the assimilating policy by roulette wheel method

Pits	Pit 2	Pit 3	Pit 6	Pit 9	Pit 4	Pit 5	Pit 7	Pit 1	Pit 8
Cost	−6	+1	+2	−5	+5	−17	−5	+8	+3
Cone vertex (i, j)	(4, 10)	(2, 15)	(2, 13)	(3, 11)	(5, 8)	(6, 7)	(3, 11)	(6, 10)	(2, 14)

policy also refers to the empire's recruiting, which will be discussed further. Since there is no combination policy operator in the original ICA algorithm, it is introduced in this paper. This operator causes to speed up the algorithm to reach the final solution. The process in which this policy works is that the imperialist, looks at its colonies, chooses, and combines each of the colonies, if the imperialist improves; the new imperialist is established by combination of imperialist and colony that improve it. Colonies search the possible solution region and improve their imperialists. We select Table 4 to continue the work.

Pits have turned into cost and the goal is to minimize them, so the first imperialist, known with vertex (4, 10), must be combined with pits that reduce its cost, and it gradually improves the problem and minimize it. In first composition, first imperialist

i \ j	1	2	3	4	5	6	7	8	9	10	11	12	13	14	15	16
1	-3	0	-2	-4	-3	0	0	0	0	0	0	0	0	-3	-2	0
2	-6	-2	-6	-2	3	-1	0	0	0	0	0	2	1	2	4	-3
3	-8	-9	5	-4	2	2	-2	0	0	-2	3	3	-6	6	-5	-4
4	-7	-8	-8	4	5	6	-1	-3	-2	3	2	-4	-6	-7	-6	-10
5	-10	-9	-7	-6	-3	5	6	8	6	-3	-1	-6	-2	-3	-5	-6

Fig. 6 A demonstration of the combined mode of the pit 4 with his imperialist

i \ j	1	2	3	4	5	6	7	8	9	10	11	12	13	14	15	16
1	-3	0	-2	-4	-3	0	0	0	0	0	0	0	0	-3	-2	0
2	-6	-2	-6	-2	3	-1	0	0	0	0	0	2	1	2	4	-3
3	-8	-9	5	-4	2	2	-2	0	0	-2	3	3	-6	6	-5	-4
4	-7	-8	-8	4	5	6	-1	-3	-2	3	2	-4	-6	-7	-6	-10
5	-10	-9	-7	-6	-3	5	6	8	6	-3	-1	-6	-2	-3	-5	-6
6	-10	-6	-8	-6	-4	8	12	15	1	2	-2	-8	-4	-6	-8	-4

Fig. 7 The combination of the first imperialist with his fifth colonial

examined with pit 9 (3, 11), because the pit 9 is within this imperialist the solution as initial imperialist. The next pit that combines is the pit 4 (5, 8), and as shown in Fig. 6, the pit 4 increases the cost and does not improve their imperialist, so it does not combine.

The next step is pit No. 5 (6, 7), which should be examined if its combination with the imperialist is better than the imperialist or not. As shown in Fig. 6, this combination reduces costs to −25, so this combination is accepted.

After updating the first imperialist, it should be checked for combining it with the number 7 (3, 11) and 1 (6, 10) pits. The combination of the first and seventh pits with the new imperialist, which combines number 2 (4, 10) and 5 (6, 7) pits, does not improve the solution to the problem. Therefore, the first empire solution is −25. After the first empire, second empire and combination of it with its colonies must be checked. As previously calculated, the only colony of the second empire is pit 8, although second imperialist and its colonies are not optimal pits, their combination gives a better solution (Figs. 7, 8 and 9).

Finally, the third empire without colonies will end the process of combination.

j / i	1	2	3	4	5	6	7	8	9	10	11	12	13	14	15	16
1	-3	0	-2	-4	-3	0	0	0	0	0	0	0	0	-3	-2	0
2	-6	-2	-6	-2	3	-1	0	0	0	0	0	2	1	2	4	-3
3	-8	-9	5	-4	2	2	-2	0	0	-2	3	3	-6	6	-5	-4

Fig. 8 Combine pit 8 with second imperialist

Fig. 9 Revolution operator to get out of the local optimum [7]

Local Optimum A

Optimum B
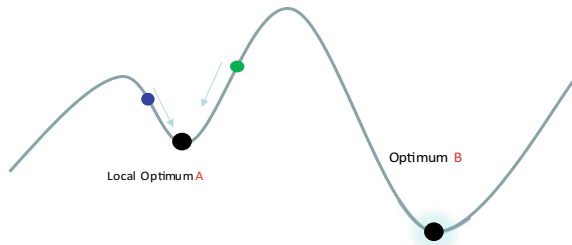
Table 5 First empire

Pits	Imperialist 1	Pit 9	Pit 4	Pit 5	Pit 7	Pit 1
Cost	−25	+4	+7	+8	+17	−65
Cone vertex (i, j)	(4, 10), (6, 7)	(2, 5)	(3, 5)	(6, 10)	(3, 13)	(7, 7)

8 Revolution Operator

Assimilation policy will not always lead to an optimal solution. Moving the colony towards imperialism may ultimately lead to a local optimal solution. Therefore, another operator called the revolution operator to bring that colony to the optimal position is needed.

In the imperialist competitive algorithm, revolution operator applies to the imperialists. This operator affects a small percentage of the colonies. However, in the case of the ultimate limit, the opposite is true of the implementation of the revolutionary operator for the colonial countries, so that the colony cone is randomly placed in one of the positive blocks. The rest of the above example continues with the application of the revolution operator on the colonies (Table 5).

The revolution operator occurs in such a way that for the entire positive blocks in the possible region, the equal probability is allocated. For placing the vertex of the cone, we use the Roulette wheel method for each pit because the problem is a discrete problem. In addition, there is a probability to select a block more than twice so the block that is already selected should be given a zero probability.

i \ j	1	2	3	4	5	6	7	8	9	10	11	12	13	14	15	16
2	-6	-2	-6	-2	3	-1	0	0	0	0	0	2	1	2	4	-3
3	-8	-9	5	-4	2	2	-2	0	0	-2	3	3	-6	6	-5	-4
4	-7	-8	-8	4	5	6	-1	-3	-2	3	2	-4	-6	-7	-6	-10
5	-10	-9	-7	-6	-3	5	6	8	6	-3	-1	-6	-2	-3	-5	-6
6	-10	-6	-8	-6	-4	8	12	15	1	2	-2	-8	-4	-6	-8	-4
7	-9	-10	-7	-5	-2	2	10	6	-4	3	-1	-2	-3	-4	-6	-5

Fig. 10 Positive blocks for the revolution

i \ j	1	2	3	4	5	6	7	8	9	10	11	12	13	14	15	16
					1/28							1/28	1/28	1/28	1/28	
			1/28		1/28	1/28					1/28	1/28		1/28		
				1/28	1/28	1/28				1/28	1/28					
						1/28	1/28	1/28	1/28							
						1/28	1/28	1/28	1/28	1/28						
						1/28	1/28		1/28							

Fig. 11 Probability of selecting positive blocks in the region

Table 6 Cumulative probability of positive blocks

1	2	3	4	5	6	7	8	9	10	11	12	13	14
0.04	0.07	0.11	0.14	0.18	0.21	0.25	0.29	0.32	0.36	0.39	0.43	0.46	0.50
15	16	17	18	19	20	21	22	23	24	25	26	27	28
0.54	0.57	0.61	0.64	0.68	0.71	0.75	0.79	0.82	0.86	0.89	0.93	0.96	1

As shown in Fig. 10, we have 28 positive blocks that are ready to welcome the revolution. Each block will compete with the probability of 1/28. To begin the revolution, we begin with the first empire of pit 9 and determine the victorious block using the roulette wheel (Figs. 11, 12 and 13).

The block cumulative probability is as per Table 6.

As mentioned in the assimilation policy, a random number is chosen that determines the winning block number; here its value is 0.0806. As stated above, in the assimilation policy, since this cumulative probability is greater than first two blocks

j / i	1	2	3	4	5	6	7	8	9	10	11	12	13	14	15	16
2					0							1/27	1/27	1/27	1/27	
3			1/27		1/27	1/27					1/27	1/27		1/27		
4				1/27	1/27	1/27					1/27	1/27				
5						1/27	1/27	1/27	1/27							
6						1/27	1/27	1/27	1/27	1/27						
7						1/27	1/27		1/27							

Fig. 12 Possibility of positive blocks to be selected for pit number four

Table 7 Cumulative probability for determining second block

1	2	3	4	5	6	7	8	9	10	11	12	13	14
0.04	0.07	0.07	0.15	0.19	0.22	0.26	0.30	0.33	0.37	0.41	0.44	0.48	0.52
15	16	17	18	19	20	21	22	23	24	25	26	27	28
0.54	0.57	0.61	0.64	0.68	0.71	0.75	0.79	0.82	0.86	0.89	0.93	0.96	1

Table 8 The first empire after the revolution

Pits	Imperialist 1	Pit 9	Pit 4	Pit 5	Pit 7	Pit 1
Cost	−25	+4	+7	+8	+17	−65
Cone vertex (i, j)	(4, 10), (6, 7)	(2, 5)	(3, 5)	(6, 10)	(3, 13)	(7, 7)

Table 9 The second empire after the revolution

Pits	Imperialist 2	Pit 8
Cost	−1	+2
Cone vertex (i, j)	(4, 10), (6, 7)	(2, 13)

and it is lower than first three blocks, so the third block selected to place the pit number nine in that block (2, 5) Fig. 12. Therefore, the probability of this block is zero to prevent it, selection for the second time and the probability of other blocks is 1/27

Cumulative probability is calculated again for determining second block (Table 7).

Random number generated to determine the winner block, that block 4 vertex placed in that winner block. The probability is 0.0806, which indicates that the 4th block must be selected, and in the next selection, the probability is zero for the other pits. The results are shown in Table 8.

For the second empire, revolution is like the first empire (Table 9).

Table 10 The third empire

Pits	Imperialist 3
Cost	+2
Cone vertex (i, j)	(2, 13)

And the Third Empire does not have any colony to use revolution operator for it (Table 10).

An operator after the revolutionary policy is the operator of recruitment. Because in the recruitment operator, the weak empire must give the weakest member, or the weakest colony, to one of the stronger empires, so we need to know weak empires. This can be calculated using the total cost of the empire, which is calculated using Eq. 6.

$$T_{cn} = \text{Cost}(\text{imperialist}_n) + \xi \ \text{mean}\{\text{Cost}(\text{colonies of empire}_n)\} \qquad (6)$$

This means that the imperialist cost directly affects the cost of the whole empires, but the colonies costs are a percentage of their average costs. This coefficient with a value of $\xi = 0.05$ has a better solution to most calculations [1]. For this example, we have

$$T_{c1} = -25 + 0.05 \times \frac{4 + 7 + 8 + 17 - 65}{5} = -25 - 1.45 = -26.4$$

$$T_{c2} = -1 + 0.05 \times 2 = -0.9$$

$$T_{c3} = 2$$

9 Recruitment

Once the cost of the empires was calculated, it is time to empires recruitment. The process of work is such that the weakest empire is determined using the expediency that calculated above and selected from among the colonies of the weakest colony that moves to a strong empire. Here, the weakest empire is the third empire. Which emperor wins to capture this member? Equation 7, the probabilities are calculated and determined by the victorious empire.

$$P_n \propto \exp\left(-\alpha \times \frac{\text{Total Cost}}{\max(\text{Total Cost})}\right) \qquad (7)$$

$$P_n = \frac{p_n}{\text{sum}(p)}$$

Table 11 First imperialist update after revolution and recruitment

Pits	Imperialist 1	Pit 9	Pit 4	Pit 5	Pit 7	Pit 1	Pit 6
Cost	−65	+4	+7	+8	+17	−65	+2
Cone vertex (i, j)	(7, 7)	(2, 5)	(3, 5)	(6, 10)	(3, 3)	(7, 7)	(2, 13)

Table 12 Second imperialist update after revolution and recruitment

Pits	Imperialist 2	Pit 8
Cost	−2	+4
Cone vertex (i, j)	(2, 14), (2, 15), (2, 13)	(2, 13)

In this case, α is equal to one.

$$P_1 \propto \exp\left(-1 \times \frac{-26.4}{2}\right) = 5.4 \times 10^5$$

$$P_2 \propto \exp\left(-1 \times \frac{-0.9}{2}\right) = 2.45$$

$$P_1 = \frac{5.4 \times 10^5}{5.4 \times 10^5} = 1 \quad \text{winner empire} = \text{empire 1}$$

$$P_2 = \frac{2.45}{5.4 \times 10^5} = 0 \quad \text{weakest empire} = \text{empire 2}$$

Here, we already know that the third empire is without colonies. So, the third imperialist will be transferred to winner imperialist. After the revolution and the transfer of the third imperialist, it is necessary to redefine the imperialist composition with its colonies. In Tables 11 and 12, the combination of the first and second imperialists is shown with their colonies.

Fig. 13 Solution
convergence figure
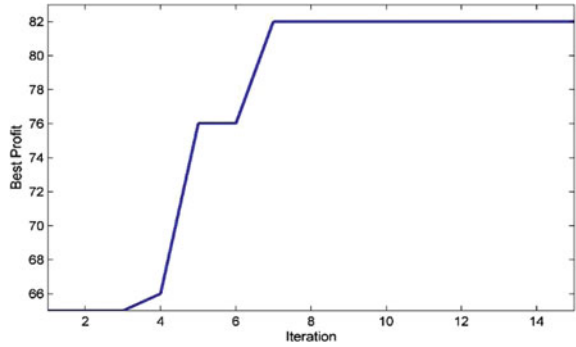
Fig. 14 Mine ultimate pit
limit
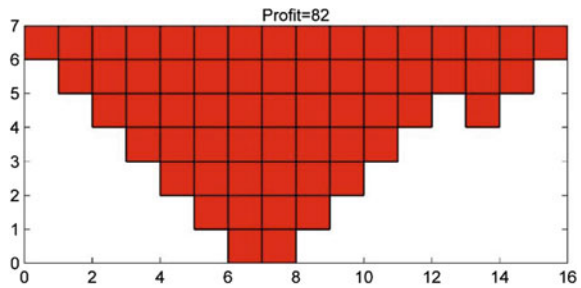
The algorithm's operation ends for the first cycle. This process continues for a number of iterations that are set before the start of the algorithm to obtain optimal or near optimal solution. The algorithm provides the following solution for 15 iterations.

As shown in the convergence Fig. 13, the optimum solution is obtained at the seventh iteration.

10　Verification

In order to validate the ICA, the block model of Fig. 1 was optimized using dynamic programming algorithm (2D Lerchs and Grossman). The steps for implementing the dynamic programming algorithm and the result are shown in Fig. 15. Comparing the results obtained from the ICA and dynamic programming in Figs. 14 and 15 indicates similarity of the solutions given by two algorithms.

In order to study the efficiency of the algorithm, the combination of the same model with the ten replications is obtained. Of course, the number of primary countries increased to 45, of which 15 were colonial.

0	0	0	0	0	0	0	0	0	0	0	10	26	65	72	72
-3	0	-2	-4	-3	0	0	0	0	0	10	26	65	72	72	82
-6	-5	-8	-8	-4	-4	0	0	0	10	26	65	75	74	82	79
-8	-17	-8	-18	-6	-3	-1	0	10	26	63	74	69	80	77	75
-7	-26	-28	-14	-14	1	-1	10	28	60	69	71	60	67	71	60
-10	-35	-44	-40	-10	2	13	30	59	64	70	66	58	55	53	48
-10	-43	-61	-62	-40	10	25	55	66	66	71	58	49	47	33	26
-9	-53	-76	-84	-60	-18	35	61	62	69	70	56	38	34	19	1
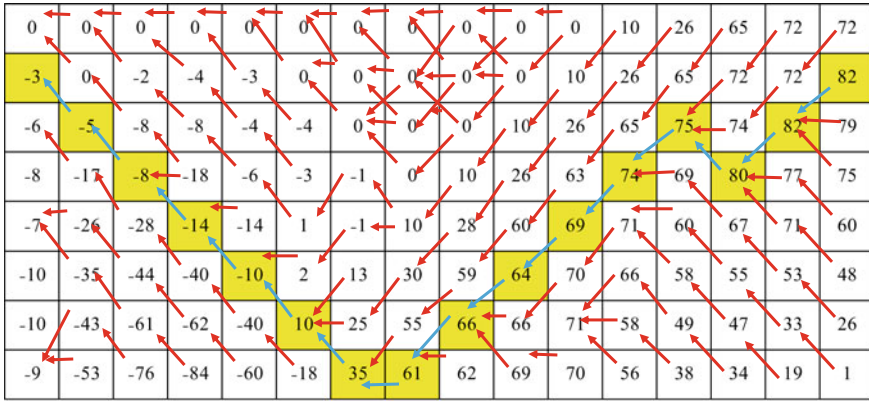
Fig. 15 Ultimate pit limit with dynamic programming algorithm

11 Conclusions

In this paper, the imperialist competitive algorithm was used to solve the ultimate limit optimization problem, and also a new operator was introduced that called combination operator of countries in each empire. The attitude of combination policy is that countries use peer-reviewed information to improve their empire and prevent it from falling. This attitude led to the rapid convergence of the problem. The result was compared with the result of dynamic programming method. Research in this field continues to be used to solve 3-D and real ultimate pit limits problems.

References

1. Pana, M.: The simulation approach to open pit design. In: Proceeding of the 5th Symposium on the Application of the Computers and Operations Research in the Mineral Industries (APCOM), Arizona, USA, pp. zz1–zz24 (1965)
2. Lerchs, H., Grossmann, I.F.: Optimum design of open pit mines. CIM Bull. **58**, 47–54 (1965)
3. Dowd, P.A., Onur, A.H.: Optimizing open pit design and sequencing: Proceedings of 23rdAP-COM symp., Tucson, Arizona, pp. 411–422 (1992)
4. Mirzaei Naseerabad, H., Khalou Kakaei, R.: Ultimate Optimum limit design in Open pit Mines Using Genetic Algorithm (persian). In 2nd Iranian Mining Conference, Tehran (2008)
5. Azimi, A.: Determination of the ultimate pit limit of open pit mines using optimization method of Ant Colony Algorithm (Persian). In Master thesis, Shahroud (2010)
6. Nowrouzi, G.E., Ataeepour, M.: Determination of the ultimate pit limit of the mine using an artificial bee colony optimization algorithm. In: 4th National Conference on Open Pit Mines, Kerman (2017)
7. Atashpaz-Gargari, E., Lucas, C.: "Imperialist competitive algorithm: an algorithm for optimization inspired by imperialistic competition," in Evolutionary computation, CEC. IEEE Congress on, pp. 4661-4667 (2007)

Application of Particle Swarm Optimization Algorithm to Optimize Stope Layout for Underground Mines

T. M. Mmola, A. S. Nhleko and J. M. Atherfold

1 Introduction

Mining projects have long turnaround times and require large start-up capital to build and operate. The objective of mine production is to maximize return on investment, which is derived from the extraction and sale of the mineral. The return on investment will depend on the physical location of the ore, the mining layout and extraction sequence, technical factors associated with the orebody, grade of the orebody, and the available mining methods [8]. It is in the early planning stages where a mine has the greatest level of flexibility to make decisions on these economic and technical criteria for operating a mine.

Thorough planning done in advance of constructing the mine lowers the risk of failure. Once the construction of the mine begins, the ability to alter the mine design diminishes exponentially as the mine matures [6]. Therefore, the mine engineer is required early on in a mining project to make long-term decisions that must optimize the cost efficiency and profitability of the mine operation.

The limited number of tested operations research (OR) techniques and the lack of tools and appropriate computer programs to address underground mine planning problems is an issue of concern to mining professionals [9]. This lack of software limits a company's capacity to develop underground mine plans that maximizes the net present value (NPV) of the project [1, 8]. There is a recognized need by

T. M. Mmola
School of Mining, Metallurgy and Chemical Engineering, University of Johannesburg, Johannesburg, South Africa

A. S. Nhleko (✉)
School of Mining Engineering, University of the Witwatersrand, Johannesburg, South Africa
e-mail: Sihesenkosi.Nhleko@wits.ac.za

J. M. Atherfold
School of Computer Science and Applied Mathematics, University of the Witwatersrand, Johannesburg, South Africa

the mining industry for improved software tools to support the planning, design and operation of underground mines [2]. The strategic planning tools could help to minimize the potential for suboptimal decisions being made at the outset of an operation by reviewing many different alternatives.

2 Background

In the mine design process of underground mines, the mining engineer must first select a mining method that is amenable to extracting the orebody and then decide on a cut-off grade for extracting the orebody. The next step is to create a stope design that maximizes the value of the mine. A stope is an underground production area from which ore is extracted from the surrounding rock mass [11]. The mine engineer will then design the access to the identified stopes. In addition, the mining engineer must sequence the extraction order of the stopes with the purpose to maximize economic ore recovery. Throughout this process, the mining engineer must consider the technical factors associated with the orebody and economic factors associated with the selected mining method [6]. Therefore, the design of the mine stopes, mainly their dimensions and location, is a critical aspect of the mine design process.

Historically, the mining engineer would design the stopes manually, which is a time-consuming process. Furthermore, the use of rules-of-thumb in determining the dimensions and locations of the stopes would be common practice. However, rules-of-thumb calculations do not always produce optimized designs. Since the subsequent introduction and proliferation of computers, the use of software applications with built-in algorithms that can automatically design and optimize the stope layout has increased. While this has reduced the time required for the stope design process, the literature indicates that none of the current algorithms are able to guarantee the optimum stope design [10]. Evolutionary algorithms and more specifically the particle swarm optimization (PSO) algorithm have been used successfully in a variety of industrial optimization problems. This begs the question: can the PSO algorithm generate an optimum 3D underground stope layout?

3 The Particle Swarm Optimization Algorithm

The PSO algorithm optimizes a problem by generating a population of particles, representing candidate solutions, and having each particle iteratively try to improve on its solution with regard to a given measure of quality. Each particle will evaluate its current solution quality against the personal best solution it has achieved so far and also the global best solution found by any particle in the population. Each particle moves in search of better solutions throughout the search space according to simple mathematical formulae that define the particle's position and velocity over time [7].

Parameter	Description	Value
ω_{max}	Maximum inertia coefficient	0.9
ω_{min}	Minimum inertia coefficient	0.4
K	Total number of iterations	100
c_1, c_2	Velocity coefficients	$c_1 = c_2 = 2$

Table 1 Selected PSO parameters based on literature review

To search for the optimal solution, the velocity and positions of each particle are updated by the following equations:

$$\begin{cases} v_i^d(k+1) = \omega v_i^d(k) + c_1 r_1 \left(P_{\text{best}}^d(k) - P_i^d(k) \right) + c_2 r_2 \left(g_{\text{best}}^d(k) - P_i^d(k) \right) \\ P_i^d(k+1) = P_i^d(k) + v_i^d(k+1) \end{cases}, \quad (1)$$

where c_1 and c_2 are acceleration constants regulating the relative velocities with respect to the personal best and global best positions, respectively; r_1 and r_2 are $N \times 1$ vectors of random numbers drawn from a uniform distribution in the interval $(0,1)$; and ω is an inertia parameter given by

$$\omega = \omega_{max} - \frac{\omega_{max} - \omega_{min}}{K} k, \quad (2)$$

where ω_{max} and ω_{min} are the initial and final weights, respectively, k is the iteration number and K is the total number of iterations.

The advantages of the PSO are that it is simple to code and it only requires the problem and a few parameters to solve [7]. We will look at the problem definition then encoding strategy and the parameters and then apply the PSO to an orebody.

3.1 Parameter Selection

One of the advantages of the PSO compared to other algorithms is the relatively few number of parameters that have to be tuned in the algorithm [7]. The parameter values used for this research were based on a literature survey of the existing research on parameter selection for the PSO algorithm [3, 5]. These parameters are indicated in Table 1.

The PSO is known to be very sensitive to the choice of parameters and parameter selection is one of the most important aspects in the PSO algorithm. It is accepted that generally the choice of the parameters will be problem dependent and that parameter hyper-tuning will be often required.

4   Model Details

As there was no readily available application to run the PSO on the stope boundary optimization problem (SBOP), it was necessary to code the SBOP and PSO algorithm from the ground up. The Python programming language was used for this purpose and the modeling strategy is discussed.

4.1   Problem Formulation and Modelling

The encoding of the problem is specified in two dimensions with the intention of clarifying the strategy for modelling the problem. It was assumed that the sublevel open stoping method would be used to mine the deposit and three constraints associated with this mining method, namely overlap constraint, level constraint, and uniqueness constraint, had to be considered in encoding the PSO algorithm. Figure 1 illustrates an example of a section of an orebody, and how the selected mine configuration is encoded such that it can be passed to the PSO algorithm.

In this trivial example, there are R rows and C columns in the orebody, representing the orebody extent. Each block represents a block in the orebody. The stope size is fixed at 3×2 blocks, and there are N possible stopes. The stopes selected in this particular configuration are marked in bold. The starting corner of each selected stope is marked with the number one, and the rest of the ore body is padded with zeros. The coordinates of all the ones in the ore body are then found, and stored in a set, as illustrated in Fig. 1. This set of coordinates forms one member of the population. Each member of the population is therefore an entire mine configuration. Figure 1 is an illustration of the encoding of the 2D SBOP. In 3D, the dimensionality of the problem is $N \times 3$.

Fig. 1 Encoding of a mine configuration
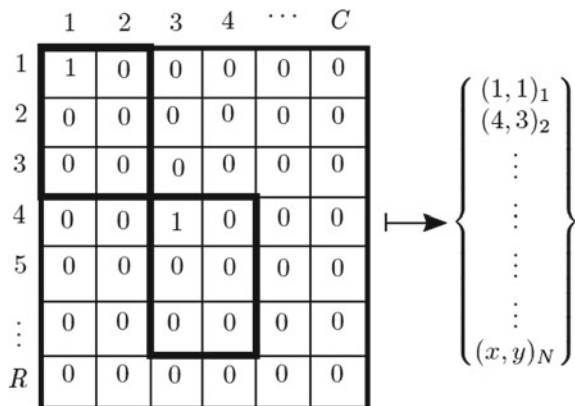
4.2 Fitness Evaluation

The PSO is initialized by generating random solutions, i.e. particles, which represent a specific mine layout. The number of stopes that may be used in the mine layout are predefined. Therefore, each particle will consist of the predefined number of stopes randomly selected from the set of all possible stopes.

The fitness of a particle is a direct function of the final value of the mine, i.e., the sum of the values of the selected stopes in the mine layout. The net smelter return (NSR) was used as the measure of value. Incorporated into the fitness evaluation are three important constraints; the level constraint, uniqueness constraint, and overlap constraint. The nature of these constraints is illustrated in Fig. 2.

The level violation indicates multiple stopes which have blocks on different mining levels. This is not allowed according to the design of the mine as each stope must lie within the defined level spacing. Uniqueness violation occurs when two stopes occur at the same location. Since a stope cannot be mined twice, the number or stopes needs to be explicitly specified in the model. Overlap violation occurs when stopes are overlapping. These stopes may or may not be on the same level. This incurs a penalty because stopes may not overlap, again because once a stope or a portion of it has been mined, it cannot physically be mined again. The fitness of the configuration is therefore taken to be the linear combination of the mine value, and the three penalties, i.e.,

$$\text{Fitness} = V_{\text{Mine}} - k_1 \times P_{\text{Level}} - k_2 \times P_{\text{Unique}} - k_3 \times P_{\text{Overlap}}, \tag{3}$$

where V_{Mine} is the calculated value of the mine configuration, P's are the penalties incurred by each respective constraint violation, and k's are constants, chosen large enough such that even if one penalty occurs, the fitness will indicate that the mine configuration will not be economically viable. This ensures that all economically viable configurations follow all the constraints. The goal of the algorithm is to maximize the fitness.
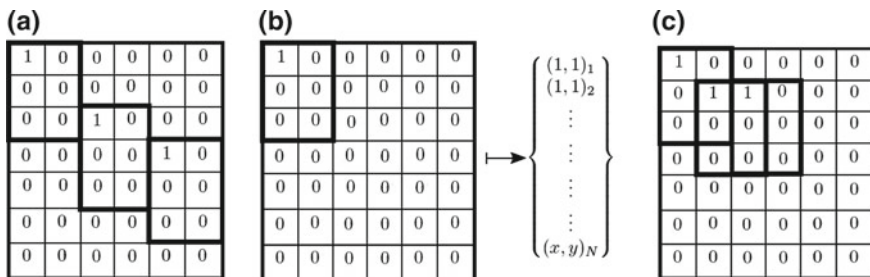
Fig. 2 Visual representation of **a** level constraint violation; **b** uniqueness constraint violation; and **c** overlap constraint violation

The experimental method utilizing PSO for the purpose of mine configuration optimization can be described as follows:

1. Initialize swarm size, maximum number of generations, and initial velocities and positions of each of the particles, where each particle represents a particular mine configuration.
2. Calculate the fitness of each member according to Eq. 3.
3. Update model parameters if necessary; the personal best position of each particle and the global best position at the current time step.
4. Update the velocity and positions of each particle according to Eq. 1.
5. The algorithm terminates when the maximum number of generations occurs. The output is an optimal mine configuration.

This method was conducted for a varying number of stopes of a fixed size. 20 experiments were conducted for each stope number. Figure 3 shows the flowchart for the mine configuration optimization.

Fig. 3 Flowchart of PSO algorithm
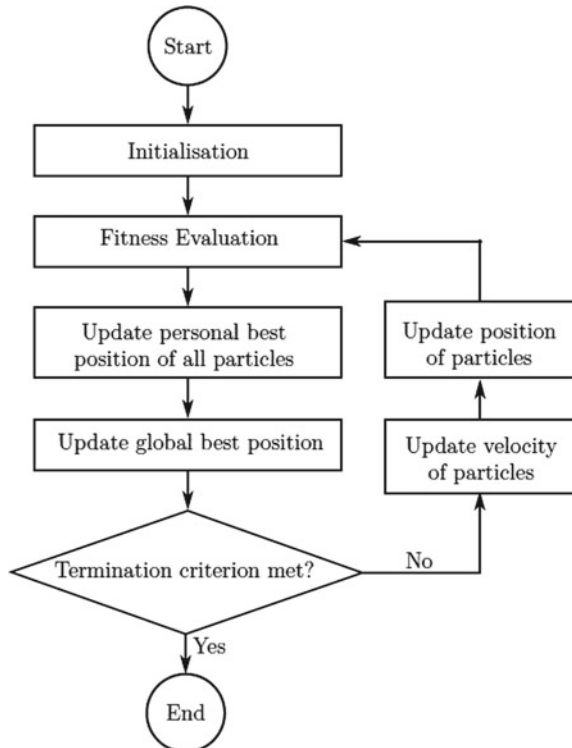
5 Experimental Results

The optimization of a mine configuration was attempted, using PSO as an optimization tool. Training data from a conceptual orebody was used to test the optimization algorithm, and the results are discussed.

The algorithm requires a regularized economic block model. The orebody model used in this study represents a theoretical gold deposit. The block model consists of 15,572 blocks of a uniform block size. The geological attributes assigned to each block are the gold grade and the rock density. The metal content per block was determined from these two attributes, taking into consideration the block size. An economical value, the Net Smelter Return (NSR), was calculated for each block based on assumptions of the mining costs, processing costs, logistical costs, and metal price. The economic block model data is summarized in Table 2.

The block model data was then imported into the Python script that was developed for this research. Then, the PSO algorithm optimization was run using a fixed stope size of 10 m × 10 m × 20 m along the *x*, *y*, and *z* axis, respectively.

Figure 4 shows the final results of all experiments. The maximum mine values are plotted as a function of the number of stopes. The maximum mine value found by the PSO algorithm is about 22,000 with 12 stopes.

Figure 5 shows how the mean and maximum fitness in the population change with iteration number from one of the experimental runs using 13 stopes. Figure 5a illustrates the convergence process of the algorithm. Convergence does not mean that the population has reached an optimum (local or global). Rather it means that the population has reached an equilibrium state, i.e., the particles converged to a point, which may not be an optimum point [4].

From Fig. 5a, the algorithm clearly converges to a maximum value within the 100 iterations. In this particular case, the maximum value is relatively small, at approximately 4400 and therefore this value is a local maximum, not the global maximum. The algorithm getting trapped in local maxima is the reason multiple experiments are run.

From Fig. 5b, the effect of the heavy penalties on the constraints violations can be observed. The mean mine value starts off at approximately −3,800,000, indicating a large number of constraints violations. The mean mine value then increases with the number of iterations to about 4000 as the violations are resolved.

Table 2 Summary of economic block model data

Attribute	Value
Number of blocks	15,572
Block sizes (*x*, *y*, *z*)	5 m × 5 m × 5 m
Rock density variation	$2.8 - 3.6$ t/m^3
Net smelter return variation	$0.6 - 301$ \$/t
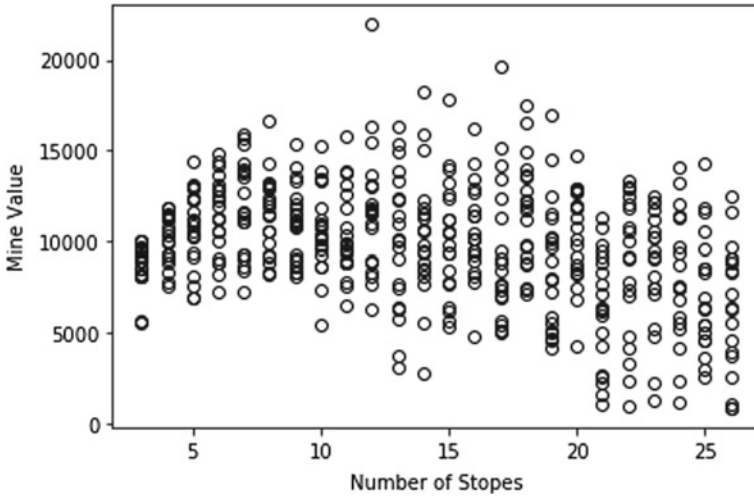
Fig. 4 Maximum mine values for all experiments
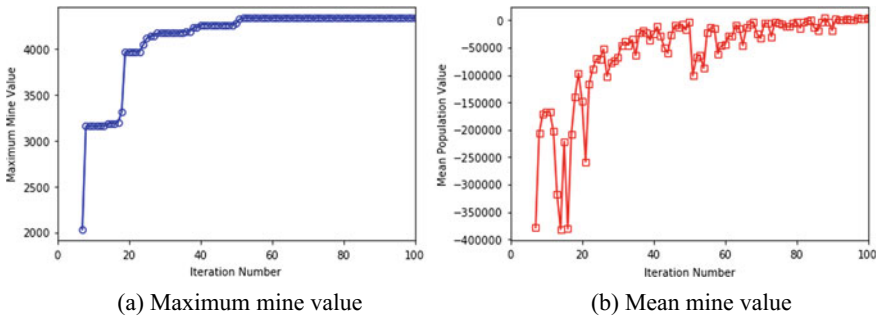
| (a) Maximum mine value | (b) Mean mine value |

Fig. 5 Results from an experimental run with 13 stopes

6 Conclusions

This paper proposes an approach to the SBOP in which the mine layout is optimized using the PSO algorithm. Such an approach has not previously been demonstrated as feasible for the SBOP. The reported experimental results show the convergence progress of the algorithm as well as the maximum mine value obtained by the optimization. Furthermore, the results indicate that the algorithm is able to handle the specified mining constraints associated with the SBOP. Moreover, the results indicate that a PSO approach is feasible, and warrants further investigation.

Further work is required to refine the algorithm, in particular, with respect to parameter selection. Since the PSO is not problem dependent, any other mining constraints, such as minimum pillar sizes, or mining parameters, such as variable

stope sizes, can be simply defined in the problem's objective function. The PSO algorithm will then run an optimization on the defined objective function.

References

1. Ataee-Pour, M.: A heuristic Algorithm to Optimise Stope Boundaries. University of Wollongong (2000)
2. Australian Minerals Industry Research Association International: AMIRA International Annual Report 2015–2016 (2016)
3. Clerc, M., Kennedy, J.: The particle swarm—explosion, stability, and convergence in a multi-dimensional complex space. IEEE Trans. Evol. Comput. **6**(1), 58–73 (2002)
4. Engelbrecht, A.P.: Computational Intelligence. Wiley, Chichester, UK (2007)
5. Engelbrecht, A.P.: Particle swarm optimization: global best or local best? In: Proceeding of 1st BRICS Congress on Computational Intelligence. BRICS-CCI 2013 vol. 1, pp. 124–135 (2013)
6. Kazakidis, V.: Operating Risk: planning for Flexible Mining Systems. University of British Columbia (2001)
7. Kennedy, J., Eberhart, R.: Particle swarm optimization. In: Proceedings of ICNN '95—International Conference on Neural Networks IEEE, pp. 1942–1948 (1995)
8. Little, J., Knights, P., Topal, E.: Integrated optimization of underground mine design and scheduling. J. South. African Inst. Min. Metall **113**(10), 775–785 (2013)
9. Musingwini, C.: Presidential address: optimization in underground mine planning-developments and opportunities. J. South. African Inst. Min. Metall **116**(9), 809–820 (2016)
10. Nhleko, A.S., Tholana, T., Neingo, P.N.: A review of underground stope boundary optimization algorithms. Resour. Policy. **56**, 59–69 (2018)
11. Sandanayake, D.S.S., Topal, E., Asad, M.W.A.: A heuristic approach to optimal design of an underground mine stope layout. Appl. Soft Comput. **30**, 595–603 (2015)

Open-Pit Mine Production Scheduling: Improvements to MineLib Library Problems

E. Jélvez, N. Morales and P. Nancel-Penard

1 Introduction

In open-pit mines, mineral is reached by digging material from the ground and then either processing or depositing it on stockpiles for later processing while waste material is deposited on dumps. To define which part of the mine should be extracted at each period of the lifetime of the mine, the terrain is modeled as a three-dimensional array of regular blocks and the planning horizon is discretized into time periods. For each block, estimations on the ore content, density, and other relevant attributes are constructed by using geostatistical methods [1].

The set of all blocks and their attributes form the so-called *block model*. Hence for each block, it is possible to specify: an extraction period, and a destination for processing, defining a *block scheduling*. The final value of a mine is, therefore, determined by the set of attributes and the block scheduling. The feasibility of a block scheduling for the open-pit method depends on accessibility and extraction constraints.

The extraction process must ensure the stability of the walls, which is expressed in terms of slope angles that must be satisfied at each moment (slope precedence constraints) as it follows the sequential extraction of blocks. In addition, there are certain limitations that are inherent to the process, for example, the amount of material to be transported and processed during each period is subject to lower and upper bounds given by transportation and plant capacity, respectively, which are usually expressed either in maximum tonnage or time available for transporting or processing. There exist other optional constraints (named general side constraints) that should be applied, including: (i) blending constraints, because the efficiency, feasibility (or even for regulatory reasons) of the plant process depends on the attributes of the

E. Jélvez · N. Morales · P. Nancel-Penard (✉)
Advanced Mining Technology Center & Delphos Mine Planning Laboratory & Department of Mining Engineering, Universidad de Chile, Santiago, Chile
e-mail: pierre.nancel@amtc.uchile.cl

combination of blocks that are processed at a given period and (ii) maximum vertical advance, among others.

Depending on the number of considerations included in the production scheduling model, Espinoza et al. summarized three specific problems [2]. First, the simplest problem in open-pit mine production planning is called Ultimate Pit (UPIT) Limit Problem and includes the selection of a subset of blocks that contains the maximum undiscounted value under slope precedence constraints. The time is not considered in this problem. Second, a generalized extension of the ultimate pit limit problem is the Constrained Pit Limit Problem (CPIT). This model incorporates temporal dimension, scheduling blocks for extraction over a fixed number of periods, maximizing discounted value under both slope precedence and capacity constraints, in which block destinations are fixed in advance. The Precedence Constrained Production Scheduling Problem (PCPSP) extends the last one mainly by considering multiple possible destinations for the blocks (therefore the model decides which one is the optimal choice) and respecting general side constraints, such as blending (where the quality of processed material is controlled).

Currently, a number of mine planning software developers are implementing the pseudoflow algorithm for UPIT (see [3, 4]) to compute both ultimate pit limit and nested pits, which were demonstrated to be more efficient than Lerchs and Grossmann algorithm [5].

While several open-pit block scheduling instances were published in MineLib [2], which presented good feasible solutions for CPIT and PCPSP by using the TopoSort algorithm presented in [6], other authors have proposed new methods and reported best-known solution when applied to CPIT instances of MineLib. Lamghari et al. [7] proposed a method to improve an initial feasible solution based on a local search algorithm called Variable Neighborhood Descent. Jélvez et al. presented an aggregation/disaggregation heuristic to generate good feasible solutions [8]. Liu and Kozan developed two new graph-based algorithms based on network flow graph and conjunctive graph theory, classified as topological ordering-based methods as well [9]. Samavati et al. outperform the TopoSort heuristic strengthening the LP relaxation of CPIT and generating better expected extraction times [10]. A similar approach was developed by [11]. Table 1 shows the best-known solutions for CPIT instances on MineLib expressed in terms of optimality gap.

PCPSP was first studied by Bienstock and Zuckerberg [12], who proposed a method based on Lagrangian relaxation to solve the linear relaxation of the PCPSP and reported a substantial computation time improvement with regards to the standard LP solvers. Espinoza et al. [2] also applied the TopoSort heuristic to PCPSP instances, but they did not generate a feasible solution on W23 (the only instance including blending constraints). Kenny et al. [13] reported improved solutions for some PCPSP instances by using a Greedy Randomized Adaptive Search Procedure, however the improvements do not include a feasible solution for W23 instance.

Most of the real instances of the CPIT and PCPSP in the mining industry are difficult to solve with block models containing large number of blocks for a time horizon that can be as long as several decades. This paper focuses on PCPSP, a new full-binary formulation and an improvement to the current best-known results for

Table 1 Current best-known solution on 11 CPIT instances available in MineLib library

CPIT instance	Source	GAP (%)
Newman	[10]	1.26
Zuck_small	[11]	0.71
KD	[11]	0.14
Zuck_medium	[11]	5.24
P4HD	[9]	0.08
Marvin	[11]	0.64
W23	[9]	0.19
Zuck_large	[8]	0.24
SM2	[7]	0.04
McLaughlin_lim	[10, 11]	0.06
McLaughlin	[8, 10, 11]	0.06

PCPSP instances on MineLib, which was made by means of a heuristic based on both a sliding time window and a linear relaxation to preselect a small subset of blocks to be scheduled within each time window. The approach includes blending constraints in its solution.

2 Mathematical Modeling

In this section, the main notation and the mathematical formulation of the optimization model used in this work are introduced. The formulation is referred to as the open-pit block scheduling problem (OPBSP). The only difference from the PCPSP is that the blocks cannot be split and sent to different destinations, hence this problem is fully binary and not mixed. However, the solutions are feasible for PCPSP as well.

2.1 Notation

Let us consider a set of blocks B. The elements of B (the blocks) are denoted by letters b, b' unless otherwise stated. The set of periods is denoted by T, hence the production is scheduled in periods $t = 1, \ldots, |T|$. There exists a set of destinations D (each destination is coded by a number, so the possible destinations for a block are $d = 1, \ldots, D$).

The net benefit perceived if a block $b \in B$ is sent to destination $d \in D$ at time period t is given by v_{bdt}. The block values will be denoted by $V(B, D, T) = (v_{bdt})_{b \in B, d \in D, t \in T}$ or simply V if there is no ambiguity. We consider two sets of attributes, namely A and $\tilde{A}$: A refers to the block attributes that participate in capacity constraints, like tonnage while $\tilde{A}$ relates to the attributes that are averaged (blending constraints),

such as grades or pollutant contents. The value of attribute $a \in A$ (or $\tilde{a} \in \tilde{A}$) in block b is denoted by g_{ba} (or $h_{b\tilde{a}}$), where $g_{ba} \geq 0$ (and similarly $h_{b\tilde{a}} \geq 0$) when the attributes denote tonnage and concentrations. Some constraints are applied on a subset of destinations $\delta \subseteq D$, for example, for processing. For each $a \in A$ and $\delta \subseteq D$, a minimum capacity (thus a demand) $L_{a\delta t} \in \mathbb{R}$ and a maximum capacity $U_{a\delta t} \in \mathbb{R} \cup \{+\infty\}$ are imposed. Similarly, for each $\tilde{a} \in \tilde{A}$, minimum $\tilde{L}_{a\delta t} \in \mathbb{R}$ and maximum $\tilde{U}_{\tilde{a}\delta t} \in \mathbb{R} \cup \{+\infty\}$ average values are allowed.

An attribute ton_b representing the tonnage of block b is used as a weight for computing averages. Due to stability requirements, slope constraints are given by one or several slope angles that define the maximum slopes that are possible in pit walls. The standard way to model these slope constraints is using precedencies as follows: for any given block b, there exists a set of other blocks (called predecessors) that must be mined before in order to gain access to block b. A very general way to encode this is by defining a set of arcs $P \subset B \times B$, where $(b, b') \in P$ means that block b' (predecessor of block b) has to be extracted in the previous or the same period that block b (successor of block b').

2.2 An Alternative Formulation for PCPSP Model: OPBSP

This subsection introduces a new formulation for PCPSP. The decision variables are related to the decision of whether to mine or not a given block, when to do so, and what destination is chosen for that block. The objective function is to maximize net present value. The constraints considered are: structural (related to the nature of the variables), precedence, capacity and general side (blending). For each block $b \in B$, destination $d \in D$ and period $t \in T$, the variable is defined in (1):

$$x_{bdt} = \begin{cases} 1 \text{ if block } b \text{ is to a destination } d' < d \text{ at period } t, \\ \quad \text{ or sent to any detination at some period } t' < t. \\ 0 \text{ otherwise} \end{cases} \quad (1)$$

To keep the notation simple, auxiliary variables Δx_{bdt} representing the exact notion of a block b sent to destination d at period t are defined:

$$\Delta x_{bdt} = \begin{cases} x_{bdt} & d = t = 1 \\ x_{bdt} - x_{bD(t-1)} & d = 1, t > 1 \\ x_{bdt} - x_{b(d-1)t} & d > 1 \end{cases} \quad (2)$$

For a block model B, precedence arcs P, set of destinations D, set of time periods T, block values $V = V(B, D, T)$, sets of capacity $C = C(B, A, D, T)$ and blending $\tilde{C} = \tilde{C}(B, A, D, T)$ constraints, an open-pit block scheduling problem **OPBSP**$\left(B, P, D, V, T, C, \tilde{C}\right)$ is defined as

$$\text{Max} \sum_{b \in B} \sum_{d \in D} \sum_{t \in T} v_{\text{bdt}} \Delta x_{\text{bdt}} \tag{3}$$

subject to

$$x_{\text{bDt}} \leq x_{\text{b'Dt}} \quad \forall (b, b') \in P, t \in T \tag{4}$$

$$\Delta x_{\text{bdt}} \geq 0 \quad \forall b \in B, d \in D, t \in T \tag{5}$$

$$\sum_{b \in B} \sum_{d \in \delta} g_{ba} \Delta x_{\text{bdt}} \leq U_{a\delta t} \quad \forall a \in A, \delta \subset D, t \in T \tag{6}$$

$$\sum_{b \in B} \sum_{d \in \delta} g_{ba} \Delta x_{\text{bdt}} \geq L_{a\delta t} \quad \forall a \in A, \delta \subset D, t \in T \tag{7}$$

$$\frac{\sum_{b \in B} \sum_{d \in \delta} h_{b\tilde{a}} ton_b \Delta x_{\text{bdt}}}{\sum_{b \in B} \sum_{d \in \delta} ton_b \Delta x_{\text{bdt}}} \leq \tilde{U}_{\tilde{a}\delta t} \quad \forall \tilde{a} \in \tilde{A}, \delta \subset D, t \in T \tag{8}$$

$$\frac{\sum_{b \in B} \sum_{d \in \delta} h_{b\tilde{a}} ton_b \Delta x_{\text{bdt}}}{\sum_{b \in B} \sum_{d \in \delta} ton_b \Delta x_{\text{bdt}}} \geq \tilde{L}_{\tilde{a}\delta t} \quad \forall \tilde{a} \in \tilde{A}, \delta \subset D, t \in T \tag{9}$$

$$x_{\text{bdt}} \in \{0, 1\} \quad \forall b \in B, d \in D, t \in T \tag{10}$$

Equation (3) presents the objective function, which is the discounted benefit from the extracted blocks over time horizon $|T|$. Equation (4) corresponds to the precedence constraints given by the slope angle and Eq. (5) means that the definition of the variables is satisfied. Moreover, Eqs. (6) and (7) limit the maximum and minimum resource consumption in each period, respectively. Equations (8) and (9) represent the blending constraints, and Eq. (10) establishes that all variables assume binary values.

The main difference between PCPSP (as presented in [2, 12]) and OPBSP relates to the fact that in OPBSP blocks cannot be split and thus a given extracted block is sent to only one destination. However, OPBSP solutions are feasible for PCPSP as well.

3 An Incremental Heuristic Based on Expected Time

Expected Time Incremental Heuristic (ETInc) is the proposed algorithm to approximate the solution of OPBSP and consists in a combination of an incremental heuristic that works on a subset of blocks and periods by using a sliding time window (as in [8]) plus expected extraction times computed from the linear relaxation of the problem as introduced in [6]. A more detailed version of this heuristic may be found in [14].

3.1 Incremental Heuristic Based on Sliding Time Window

The heuristic iteratively constructs a schedule for each period by solving the OPBSP for a time window $\tilde{T} = \{t, \ldots, \min(t + w - 1, |T|)\}$ limited to $w \leq |T|$ periods, starting from period $t = 1$ of the planning horizon, where w is an integer parameter used to determine the maximum length of the time window. Each time the OPBSP subproblem is solved, the variables x_{bdt} are fixed for the first w' periods of the incumbent time window, where w' is a parameter to be determined, the time window is moved forward by w' periods, and the OPBSP subproblem is solved for the new time window. The procedure stops when the last OPBSP subproblem corresponding to the period $t = |T|$ has been solved.

3.2 Block Preselection Using Expected Extraction Times

To solve each OPBSP subproblem, the heuristic preselects a subset $\tilde{B}$ of blocks based on a modified definition of the expected extraction time introduced by [6] according to the following procedure.

Let $\bar{x}^*_{\text{bDt}}$ be the solution of the LP relaxation of the original OPBSP. The expected extraction time E_b of block b is defined as

$$E_b = \sum_{t \in T} t \cdot \Delta \bar{x}^*_{\text{bDt}} + (T + 1)\left(1 - \bar{x}^*_{\text{bDt}}\right) \tag{11}$$

A subset of blocks $\tilde{B}$ not yet extracted at period t is defined for which expected time E_b is smaller than $\min(t + w - 1, |T|) + s$, where $s > 0$ is a continuous parameter to be determined representing a tolerance or additional margin in the selection. In this procedure, the expected times are used as a block preselection tool to reduce the size of the subproblems, they are not used to generate a sequence of blocks as in the TopoSort heuristic proposed by [6].

3.3 Expected Time Incremental Heuristic—ETInc

ETInc algorithm depends on three parameters:

1. w, which is the length of the sliding time window,
2. w', which is the number of periods to be fixed in the current solution of OPBSP subproblem, where $w' \leq w$, and
3. s, representing the tolerance parameter to select a subblock model $\tilde{B}$ based on expected extraction times.

The main steps of the ETInc algorithm can be described as follows:

Table 2 List of PCPSP instances from MineLib. ETInc parameters used in the experiments

PCPSP instance	ETInc parameters		
	w	w'	s
Newman	1	1	1.5
Zuck_small	6	1	0.5
KD	2	1	0.5
Zuck_medium	2	1	5.5
Marvin	5	1	0.5
W23	1	1	0.5
Zuck_large	4	1	0.5
SM2	1	1	0.5
McLaughlin_lim	2	1	0.5
McLaughlin	2	1	0.5

1. Select a new time window $\tilde{T}$ according to Sect. 3.1.
2. Select a subblock model $\tilde{B}$ according to Sect. 3.2.
3. Construct an auxiliary instance of OPBSP (or OPBSP sub-problem) by using $\tilde{B}$ and $\tilde{T}$ and solve it.
4. Select blocks for extraction.
5. If not finished, go to step 1.

4 Numerical Experiments

The datasets for all instances can be found at [2]. The list of 10 PCPSP instances on which the algorithm was applied and the parameters used are presented in Table 2. The computational resources consisted of a core i5-3570, 3.4 GHZ PC with 16 GB of RAM, and GUROBI 6.5.2 was used as optimization software.

4.1 Results and Discussion

The results obtained from the numerical experiments and a comparison with the corresponding best-known results for PCPSP instances from MineLib are presented in this section.

Table 3 shows the value of the solutions for the linear relaxation obtained for each instance of PCPSP, as reported in [2], and OPBSP, which were obtained by implementing the Bienstock-Zuckerberg (BZ for short) algorithm. From the theoretical point of view, these values should be equal, however, there are very small differences, being the largest relative difference for W23 smaller than 4×10^{-6}. This

Table 3 List of LP upper bounds obtained for PCPSP and OPBSP

PCPSP instance	LP solution value		
	PCPSP	OPBSP	Abs. difference
Newman	24,486,549	24,486,549	0
Zuck_small	905,878,172	905,878,194	22
KD	410,891,003	410,891,003	0
Zuck_medium	750,519,109	750,519,188	79
Marvin	911,704,665	911,704,801	136
W23	387,693,394	387,691,933	1461
Zuck_large	57,938,790	57,938,804	14
SM2	1,652,394,327	1,652,394,357	30
McLaughlin_lim	1,324,829,727	1,324,829,835	108
McLaughlin	1,512,971,680	1,512,971,772	92

Table 4 Current best-known solution on 10 PCPSP instances available in MineLib library

Instance name	Source	Gap (%)	Best-known OPBSP objective	Gap (%)
Newman	[13]	1.58	24,176,861	**1.26**
Zuck_small	[13]	1.64	897,453,456	**0.93**
KD	[2]	0.98	409,715,160	**0.29**
Zuck_medium	[13]	**3.00**	701,157,160	6.58
Marvin	[13]	1.61	905,829,721	**0.64**
W23	–	100.00	368,005,675	**5.08**
Zuck_large	[2]	1.04	57,534,355	**0.70**
SM2	[2]	0.12	1,651,599,491	**0.05**
McLaughlin_lim	[2]	0.24	1,322,283,576	**0.19**
McLaughlin	[2]	0.19	1,510,373,891	**0.17**

is explained because different stopping criteria of the implementations of the BZ algorithm were used. Therefore, the differences between LP upper bounds are small enough not affect the optimality gap defined as

$$\text{Gap} = (\text{LP upper bound} - \text{best-known solution objective})/\text{LP upper bound} \quad (12)$$

Table 4 shows the current best-known feasible solutions for each instance as reported in [2, 13] in terms of optimality gap, the objective values of the feasible solutions obtained using ETInc and their respective optimality gaps. All feasible solutions (except Zuck_medium instance) implemented to improve on the already existing values and particularly that for the instance W23, ETInc was able to produce a solution with 5.1% optimality gap for OPBSP, therefore, improving on the current trivial null solution.

5 Conclusions

A new full-binary formulation for the Precedence Constrained Production Scheduling Problem (PCPSP) was presented. In this formulation (OPBSP), the blocks cannot be partitioned, therefore, only one processing destination must be chosen for each block.

An algorithm (ETInc) that aims to produce good feasible solutions for OPBSP, and therefore for the PCPSP, was used. ETInc is similar to other algorithms proposed in the literature as it uses the solution of the linear relaxation as a guide to generate integer feasible solutions by constructing a ranking of blocks for extraction and by resorting to solutions for auxiliary instances. ETInc was applied to a publicly available library of instances included in MineLib, which consists of 10 different cases of variable size, obtaining better results for the 9 out of 10 cases.

Further research is required for the library of problems. For example, even though both formulations OPBSP and PCPSP accept lower bounds for capacity constraints, the library does not have this type of constraint. In this sense, it is a challenge to expand the number of case studies or instances available in MineLib to evaluate new models and compare new algorithms.

Additional research areas should consider the inclusion of the uncertainty in market and geology as well as the improvements in the computational time and memory footprint.

References

1. Chiles, J., Delfiner, P.: Geostatistics: modeling spatial uncertainty, vol. 497. Wiley, Hoboken (2009)
2. Espinoza, D., Goycoolea, M., Moreno, E., Newman, A.: Minelib: a library of open pit mining problems. Ann. Oper. Res. **206**(1), 93–114 (2013)
3. Hochbaum, D.: The pseudoflow algorithm: a new algorithm for the maximum-flow problem. Oper. Res. **56**(4), 992–1009 (2008)
4. Hochbaum, D., Orlin, J.: Simplifications and speedups of the pseudoflow algorithm. Networks **61**(1), 40–57 (2013)
5. Lerchs, H., Grossmann, I.F.: Optimum design of open-pit mines. Trans. Can. Inst. Min. **68**(1), 17–24 (1965)
6. Chicoisne, R., Espinoza, D., Goycoolea, M., Moreno, E., Rubio, E.: A new algorithm for the open-pit mine production scheduling problem. Oper. Res. **60**(3), 517–528 (2012)
7. Lamghari, A., Dimitrakopoulos, R., Ferland, J.: A hybrid method based on linear programming and variable neighborhood descent for scheduling production in open-pit mines. J. Glob. Optim. **63**(3), 555–582 (2015)
8. Jélvez, E., Morales, N., Nancel-Penard, P., Peypouquet, J., Reyes, P.: Aggregation heuristic for the open-pit block scheduling problem. Eur. J. Oper. Res. **249**(3), 1169–1177 (2016)
9. Liu, S., Kozan, E.: New graph-based algorithms to efficiently solve large scale open pit mining optimisation problems. Expert Syst. Appl. **43**, 59–65 (2016)

10. Samavati, M., Essam, D., Nehring, M., Sarker, R.: A methodology for the large scale multi-period precedence-constrained knapsack problem: an application in the mining industry. Int. J. Prod. Econ. **193**, 12–20 (2017)
11. Samavati, M., Essam, D., Nehring, M., Sarker, R.: A new methodology for the open-pit mine production scheduling problem. Omega (2017b) In press
12. Bienstock, D., Zuckerberg, M.: Solving LP relaxations of large-scale precedence constrained problems. In: Proceedings of the International Conference on Integer Programming and Combinatorial Optimization, pp. 1–14. Springer, Heidelberg (2010)
13. Kenny, A., Li, X., Ernst, A., Thiruvady, D.: Towards solving large-scale precedence constrained production scheduling problems in mining. In: Proceedings of the Genetic and Evolutionary Computation Conference, pp. 1137–1144. ACM, New York (2017)
14. Jélvez, E., Morales, N., Nancel-Penard, P., Cornillier, F.: A New Hybrid Heuristic for the Precedence Constrained Production Scheduling Problem: A Mining Application. Submitted paper

Part V
Mining Equipment Selection Innovative Materials Handling Systems and Equipment

Development of a Computer-Aided Dragline Selection Program

S. Akhundov and N. Demirel

1 Introduction

Removal of overburden in open cast coal mines to uncover coal seams is widely done by draglines. Draglines are highly advantageous over shovel truck system because of high productivity and low costs of process in open cast mines. They can handle overburden excavation, haulage, and dumping operations with single equipment which results in increase in mining productivity and decrease in mining costs.

Since, it is the most capital-intensive unit for a mining project, the selection of this equipment is one of the most important tasks and it should be made with utmost care. The way of selecting dragline requires consideration of geological properties of deposit, mining method to be applied, and the availability of resources and aspects of available technology offered on market. On selecting appropriate dragline equipment, all these factors have to be taken into account.

There are several stages should be completed before making a decision about the dragline to be invested on. Initially, based on the required production and stripping amounts required bucket capacity should be estimated. Then depending on the strip geometry and material properties, reach factor and operating radius figures should be calculated. Although there are some studies towards enhancing the selection process using computer simulations, interactive computer modeling to select draglines and to forecast their long-range productivities is still an emerging issue.

However, a tool or a model, which is specifically utilized for dragline selection, is not currently available. Manual process may involve human error and may yield wrong selection of equipment. However, using computerized tools gives an ability to see compatibility of other models and make this selection process quickly.

The main objective of this study is to develop a dragline selection and productivity prediction program by varying mine layout and dragline parameters to mini-

S. Akhundov · N. Demirel (✉)
Mining Engineering Department, Middle East Technical University, Ankara, Turkey
e-mail: ndemirel@metu.edu.tr

235

mize human error affecting the selection procedure. The elements of this objective are (i) conducting a comprehensive literature survey about conventional methods; (ii) reviewing and evaluating the dragline selection process with modern approach, (iii) develop a model to minimize human error in calculations and selection, and (iv) validate the developed program with a manual selection procedure. The main stages of methodology followed in the development of a Draglayout program are as follows:

– considering "Maximum suspended load" calculations based on required bucket capacity to reach expected production amount
– developing a computer program, this makes calculations and shows the list of dragline models with required parameters from the catalogues
– developing a new formula for calculating new approximate production amount based on selected dragline equipment's maximum suspended load
– developed new software also must calculate and draw the range diagram to see the whole picture better and let preview for acceptable changes on mine layout design
– discussion on finding best dragline equipment and mine layout design pair to reach best production rates.

   The developed program introduces a new automated tool for dragline equipment selection and provides further insight into equipment selection and mine design. Computerized systems are more accurate and fast which results in time saving. The study is expected to contribute to mining industry by providing a more flexible, user-friendly, and robust model for dragline selection. The scope of this study includes draglines therefore; the program cannot be used for selection of any other mining equipment.

2   Review of Previous Dragline Selection Models

The very first remarkable research on best suitable dragline equipment selection was held [1]. The author has developed a computer program to analyze the relationship between maximum usefulness factor and the pit geometry to select the parameters of suitable dragline equipment. The maximum usefulness factor was defined according to required bucket capacity and required reach of an equipment for stripping.

   Another research on simulating a dragline operation was reported in 1966 [2]. The authors have developed an analogue computer simulation model for investigation of the performance of different movements of the dragline. During the 1970s, the US Federal Government financed simulation models researches and computer programs in pit optimization and equipment selection. Many researchers and companies are involved in the program [3–6]. Developed computer programs were all based on single seam operations and software's could be run only on mainframe computers as expressed in [7]. Because of their hardware restrictions and poor graphical interfaces, these programs were not widely used [7].

Later in 1979, [8] reported a computer simulation method. They have modified conventional methods for reach and bucket capacity determination to a 3D approach to calculate optimum required dragline parameters. The authors claimed that the reach factor requirements for a dragline operation was underestimated with using conventional 2D approaches.

During the 1980s, many researchers worked on developing dragline operation and computer-aided dragline operation simulations. [9] reported a research on selecting a suitable size of the dragline. The authors used nonlinear analytical approach techniques to minimize the cycle time for overburden stripping and cost per ton of removed coal.

In 1990, it was reported that a new computer program that can calculate reach factor and bucket capacity considering factors such as the blasting effects on the swell factor and response angles [10].

Erdem and Çelebi [11] worked on developing computer-aided expert simulation system for dragline and method selection in surface coal mines. In this research author also worked on several problems that can occur in dragline selection. Research uses seven main surface stripping methods for modeling and simulating dragline selection and stripping process. Moreover, during research [11], several algorithms were developed on modeling and simulating production both single and tandem dragline systems. The dragline selection strategy of developed expert system based on forward changing algorithm. One of the recent researches on computer-simulated selection model of the walking dragline equipment for open cast stripping mine is held in 2003 [12]. They have developed a computer simulation model for simulating dragline stripping operation for the purpose of selecting the optimum dragline equipment, according to working face parameters results obtained again by the same simulation. Simulation process iterates till the convenient results are obtained.

3   Data and Methodology

In strip mine design using dragline as the major overburden removal unit, the production target has to be met first and then it will be possible to select a dragline which meets predefined production requirements. However, there might be situation in which existing dragline equipment may be required to be deployed. In such cases, the stripping methods and stripping geometry will be dependent on the dragline unit [2].

In order to identify the most compatible dragline to invest on, there are two important input variables to be determined [3]: (i) reach factor (RF) or operating radius of dragline, (ii) maximum suspended load (MSL). Operating radius, the total horizontal distance between crest of the highwall to the peak point of the spoil pile, determines how far the spoil pile can be located. It is the summation of reach factor and positioning as well (Fig. 1). If the reach of the dragline is not sufficient with respect to the depth of the overburden, then rehandling may be necessary to compensate the inadequate spoil pile. Since rehandling is an undesirable process

with increased operating cost, operating radius of dragline has a significant impact on the economic feasibility of a mine. The second important variable is maximum suspended load (MSL) and it can be defined as the maximum load that can be suspended from the boom sheave of the dragline and it includes dead weight of the bucket and payload. Besides these two variables, there are some other important characteristics to be determined before making the selection. These are maximum digging depth capability, maximum dumping height, stacking height. If there are several draglines operating in tandem, there will be some other factors that can affect selection.

The volume of spoil pile for a unit thickness and volume of overburden, spoil pile height (H), stacking height (SH), reach factor (RF), operating radius (OR), and positioning of dragline can be seen in a typical range diagram in Fig. 1. These variables are estimated based on the required coal production and stripping amounts using range diagrams.

Once the reach factor and maximum suspended load are determined then manufacture catalogues or selection charts are utilized to select the most compatible unit. The productivities of other options should be separately estimated again using range diagrams. This process is not efficient when several units are required to be compared with varying bench geometry and production conditions. Therefore, a systematic computerized tool is essential to increase the efficiency of dragline selection process.

Developing the Draglayout dragline selection program includes five stages: (i) creating a dragline database of commercially available models, (ii) developing algorithms for initial mine design geometry and interaction between dragline geometry and mine layout, (iii) generating a graphical user interface (GUI); and finally (iv) verifying the program.

Initial estimations and calculations of such parameters as dragline availability, dragline utilization, dragline operating hours, average duration of single cycle time,
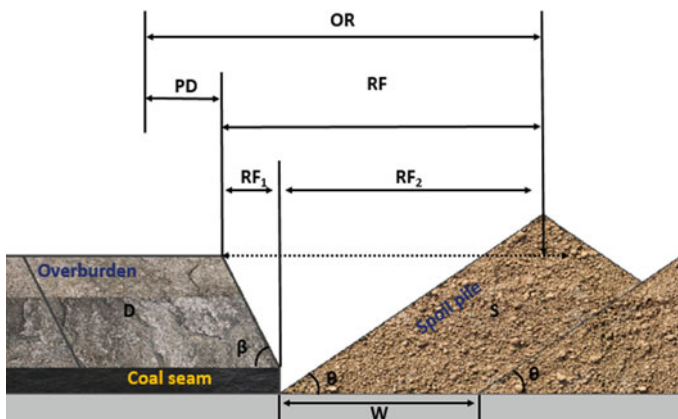
Fig. 1 Range diagram and geometry

estimated ore production, and recovery are taking. According to these parameters maximum, suspended load is calculated and an initial mine design geometry parameters are defined. In the third step according to previously calculated maximum suspended load and reach factor requirement available draglines from catalogues are choosing and last decisions on the mine geometry are holding. For the final step, best dragline is selecting from catalogues.

4 Draglayout Program

Draglayout program allows users to create a new project after entering input data and also to load an existing project. In order to create a new project, user data should be input to the program. These input data are grouped in three parts as bench geometry data, material characteristics data, and required stripping and/or production data. Main pane working tab is presented in Fig. 2.

Bench geometry is basically determined by the coal thickness, overburden thickness pit width, spoil angle, and pit angle. Program allows users to select different unit systems but SI unit system is set as default. Material characteristics data includes coal density, overburden density, swell factor, bucket fill factor, and specific weight of overburden. Required production data are scheduled operating time, dragline availability, dragline utilization cycle time of the dragline, required ore production and coal recovery. With Edit menu Draglayout offer, three additional options where entered data can be changed.

Draglayout software offers Multi Tabbed Pane interface in three working tab panes. These panes are main pane, plan view pane, and models pane. Main pane is available on start. After project created or loaded all usable information about the project is reachable from related sections. This screen tab is informational tab and
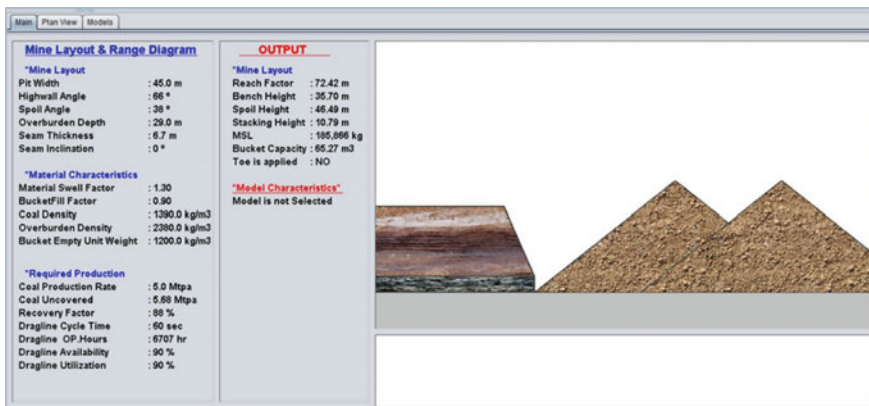
Fig. 2 Main pane working tab

includes only information, no changes on project can be done with this working tab pane. Plan view pane is not available on start. Only after project created or loaded will be available. From this, tab pane all geometrical parameters are available spinners and input areas are represented to enter a new data or change the previous entered data. Refresh button refers to affect and fix the new entered data to project. This button also works for reloading all working tab panes with one click. In case of changing input data, previous selected model removes itself. Models pane displays all suitable models from catalogue after implementing the program.

Selection takes place based on the computed maximum suspended load and reach factor values. Draglayout provides the most compatible model according to the required stripping amount. However, it also lists the models whose reach factors and maximum suspended loads are less/greater than the optimum ones. The user could find out the productivities associated with these models and answer certain what if questions in case of selection of these models. By clicking on the name of model from list, the Model Selection dialog will appear (Fig. 3). This dialog displays some important parameters of selected dragline model and also shows the results of production value which will prepare this model according to project details.

Visualizing is the last phase of main process cycle where graphing of range diagrams and geometry of bench is illustrated after the selection is done. Draglayout provides a link to the user interaction phase where it is possible to make changes on the selection criteria and other settings such as catalogue selection. In this phase, it is possible to go back and change all input data and parameters and run the calculations repeatedly (Fig. 4).
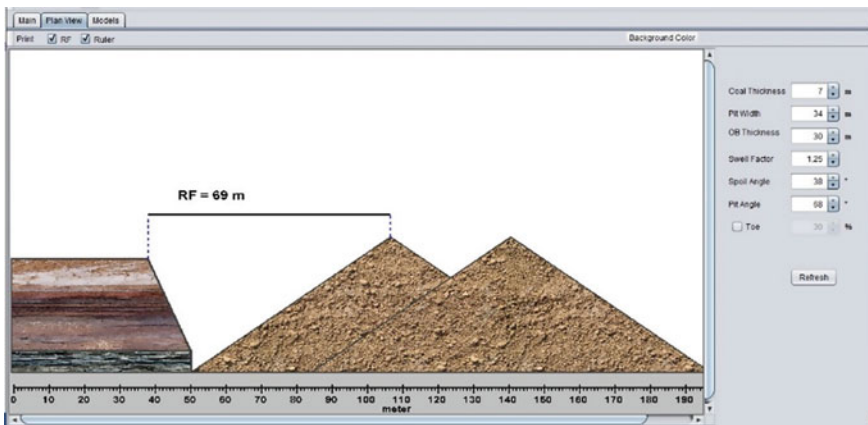
Fig. 3 Plan view working tab
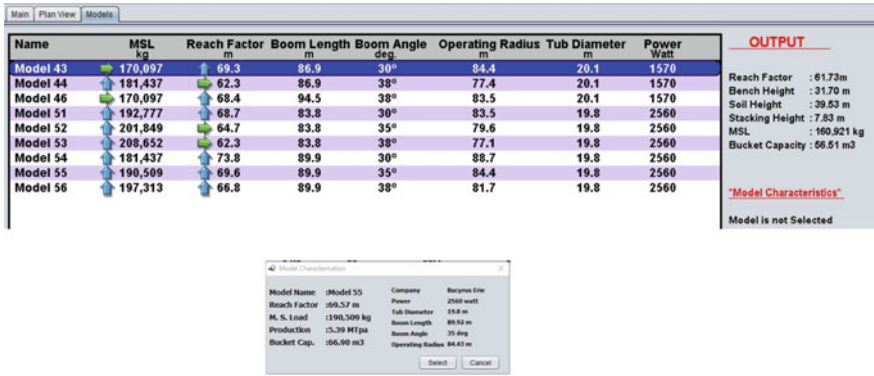
Fig. 4 Model selection dialog window

Table 1 Sample data for verification

Input parameter	Value
Operation time	8030 h/yr
Dragline availability	88%
Dragline utilization	90%
Density (bank)	1300 kg/m^3
Recovery	85%
Ore thickness	7 m
Swell factor	1.25
Bucket fill factor	88%
Annual production	5 M t
Cycle time	60 s
Overburden depth	30 m
Overburden density (bank)	2100 kg/m^3
Pit width	40 m
Pit slope angle	68°
Spoil pile angle	38°
Bucket empty unit weight	1100 kg/m^3
Dragline swing angle	120°

5 Verification of the Model

The developed program was verified using the sample data tabulated in Table 1. Dragline selection for the given production was done both using range diagrams and manual calculations and also the developed program Draglayout. Both ways yielded the same dragline model.
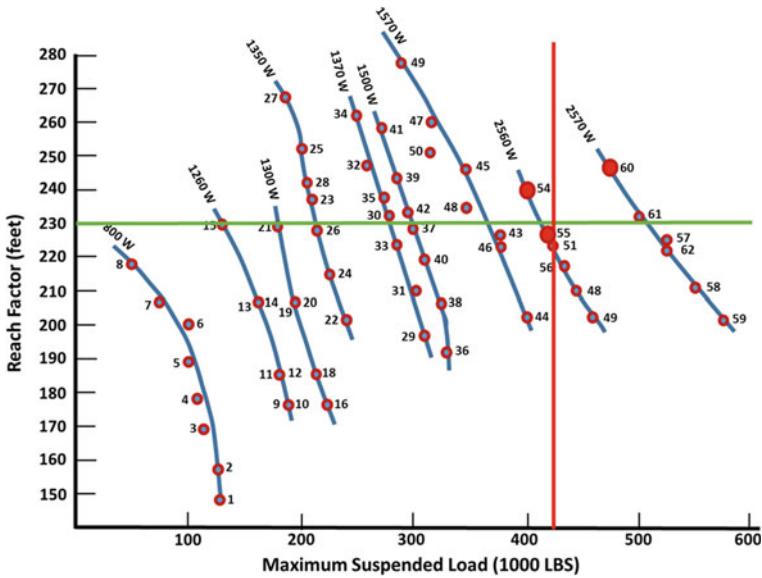
Fig. 5 Dragline selection chart provided by Model selection dialog window

Essential maximum suspended load and the reach factor were found to be 192,426 kg (423,337 lbs) and 70.12 m (230 ft), respectively. According to the obtained results, the most suitable dragline model was determined to be Model 51 as can be seen in Fig. 5.

When Draglayout program was run for the sample data, the outputs obtained were the same as the results obtained using conventional methods. Draglayout selected the same model, Model 51 as can be seen in the output window (Fig. 6).

According to the selected dragline models parameters, the approximate bucket capacity and the approximate production per year can be achieved with dragline model is calculated.

The calculations show that with this model of dragline the production of mine can be increased up to 0.18 Mt/yr. Validation shows that all calculated output results are approximately same with manually calculated results. Small differences on results observed because of rounding in manually calculating. Draglayout uses 8 bytes memory (13 digits) for storing each number which is a pretty big range, which makes results be more accurate. Moreover, Draglayout provides an easy graphical interface, fast calculation, menus to switch catalogues, and ability to make changes in design and run calculations repeatedly.

Fig. 6 Draglayout output window

6 Conclusions and Recommendations

The result of this study introduces a new approach to the dragline selection process and mine design. This thesis research is about automated dragline selection and developing computerized tool for this purpose, during the research process new convenient formulas and parameter were developed. Developed formulas for production, helps to calculate the approximate production according to load ability of dragline and it is providing an idea in selecting a dragline and other equipment. The rehandle amount causing of toeing is not taken an in consideration.

Developed Draglayout software is easy and useable tool for selecting dragline equipment. In order to make calculations easier, Draglayout provides to mining engineers working with different catalogues and gives ability in changing predesigned mine design. Also prove a friendly graphical interface to see full picture of designed mine layout. No doubt this ability will be improved in future and new useable functionalities will be added. Also, it is possible interactively go back to mine design and redesign mine layout for proper selection and design.

For this study, only catalogue installed to the developed software is a catalogue presented by Bucyrus Erie Co. For future developments and versions of Draglayout, it is possible to add new catalogues. For future improvements in software, it is also essentially important to add advanced stripping methods to the program.

References

1. Rumfelt, H.: Computer methods for estimating "Proper Machine Mass for Stripping Overburden". In: Mine Planning and Equipment Selection (2000)
2. Nikforuk, P.N., Zoerb, M.C.: Analogue computer simulation of a walking dragline. Society of Mining Engineering, AIME, New York (1966)
3. Stefanko, R., Ramani, R.V., Freko, M.R.: An Analysis of Strip Mining Methods and Equipment Selection, Prepared for Office of Coal Research United State Department of Interior, The Pennsylvania State University (1973)
4. Ford, Bacon and Davis Inc.: Surface Coal Mining Machinery and Equipment, National Technical Information Service, Washington D.C. (1975)
5. McDonnell Douglas Co.: Development of Operational Aids for Improved Dragline Utilization, Prepared for United States Department of Energy, Washington D. C. (1978)
6. Sadri, R.J., Lee, C.D.: Optimization of single and multiple seam dragline mines through simulation. In: 17th APCOM Symposium, Society of Mining Engineering, AIME, New York (1982)
7. Hamilton, B.W.: Dragline Pit Design and Sensitivity Analysis, MSc Thesis Collection, Department of Mining, Metallurgical and Petroleum Engineering, University of Alberta, Canada (1990)
8. Hrebar, M.J.: Preliminary Dragline Selection for Surface Coal Mining Operations, Mine Planning and Equipment Selection. Singhal and Vavra (eds.) Balkema, Rotterdam (1990)
9. Gibson, D.F., Mooney, E.L.: A mathematical programming approach to the selection of stripping technique and dragline size for area surface mines. In: Johnson, B., Barnes, R.J. (eds.) 17th International symposium on the Application of Computers and Operations Research in the Mineral Industry, Society of Mining Engineers, AIME, New York (1982)
10. Sharma, D.K., Singh, R.P.: A Computer Model for Dragline Selection in Open Cast Mine Planning, Mine Planning and Equipment Selection. Singhal and Vavra (eds.) Balkema, Rotterdam (1990)
11. Erdem, B., Çelebi, N.: Development of an Expert System for Dragline and Stripping Method Selection in Surface Coal Mines. METU Thesis Collection, METU, Ankara (1996)
12. Zhang, Y.D., Yang, Y.H., Li, K.M.: System simulation for dragline selection in open cast mines. In: Proceeding of Application of Computers and Operations Research in the Mineral Industries, South African Institute of Mining and Metallurgy, pp. 79–82 (2003)

Optimal Selection and Assignment of Loading Equipment for the Compliance of an Open-Pit Production Plan

H. González and N. Morales

1 Introduction

1.1 Motivation

Mine planning is a process in which, among other things, the volumes of material to be extracted at a given time and with a specific destination are defined. The decision on the material movements is a complex process with several stages which are present from the beginning of a project through selecting the blocks to be extracted in a block model to the last stage of the bench. However, the moment in which material extraction is conceptualized occurs in intermediate stages to those mentioned.

Material transport is a highly important process in the mining business, mainly due to the high costs associated with it [1]. This is a consequence of a large number of equipment involved in the operation, both for loading and transport; a high degree of mechanization and above all, the presence of this process throughout the life of the mine.

Removing the rock from the mine is not the same as extracting blocks in a model. Consideration should be given to aspects related to the mechanical equipment that will be used to extract the material and equipment that will move it from the mine to its destination. The decision about which equipment to use, how many and what type to buy, and where it should be operating has a strong impact on the value of the mining business. For these reasons, a model was created to determinate and evaluates various scenarios of material handling with different type and number of shovels.

The optimization of the equipment is strongly related to the optimization of the pit: improving the selection of equipment decreases mine costs and increases

H. González (✉) · N. Morales
DELPHOS Mine Planning Laboratory, AMTC, DIMIN, Universidad de Chile,
Santiago, Chile
e-mail: hgonzalez@delphoslab.cl

productivity, which influences the planning and design of pit limits [2]. It is possible to separate the planning process into levels, according to the characteristics of the decisions made [3]:

– *strategic*: refers to the selection of exploitation methods, mine capacity, processing, and in general to the estimations of mining reserves. The main objective of strategic planning is to synchronize the market with the available resources and the mission of the company
– *tactics*: corresponds to the specification of the processes to be carried out throughout the life of the mine such as long-term production programs and programming models for the use of equipment and processing plants. Tactical or conceptual planning determines the way to achieve the objective previously established by strategic planning. Its result is the mine plan which defines how the resources will be extracted
– *operational*: involves the delivery of the material to its destination (for example, using trucks) or the change of location of a shovel. The operational processes and indexes resulting from the mining plan are included in the operational planning.

The objective of this work is the creation of a methodology to support the development of an allocation plan for loading equipment in an optimal way that allows compliance with a production plan. In this way, a bridge between the levels of tactical planning with the operational can be created. A base production plan from a real mine was used to compare the results obtained.

1.2   Related Work

Over the years, many techniques associated with operations research have been developed to assist in decision-making in mining. Temeng et al. [4] proposed an equipment dispatch system. His work describes a model whose main limitation is the exclusion of short-term production and the location of the shovels. Gurgur et al. [5] proposed a linear optimization problem that provides the location of trucks and shovels to minimize deviations from the progress of the mine provided by strategic planning. However, it only considers the long-term information, leaving aside costs of production and movement of the equipment.

Upadhyay and Askari-Nasab [6] proposed a model that includes both long-term and short-term objectives, as well as movement costs and allocation of loading equipment and trucks. However, it performs this assignment based on the sequencing obtained in a previous stage using a clustering and scheduling algorithm.

Linear optimization applied to the optimization of the mining operation reveals the following:

– the allocation of the shovels has not received enough attention in the literature,
– the models do not present communication between strategic planning and production in the operation,

– the models depend on multiple stages to find a solution,
– the sequencing of the extraction in many cases is an input for the assignment of shovels and trucks.

The model proposed in this paper seeks to incorporate the aforementioned points (single-stage optimization, communication between strategic planning and production, and the sequencing of the extraction as result of the shovel assignment) into the optimization problem to obtain a one-stage solution that is interpreted as planning at the operational scale and which leads to meeting long-term goals.

1.3 Problem Statement

Data from a real mine operation were used to validate the model. The name remains confidential at the request of the suppliers. The optimization problem was addressed using the Python programming language.

The data used included:

– the material movements per period determined by the long-term plan, as well as the destinations associated with each block, without modification
– the pushbacks (without modification) and the sequence of extraction of the blocks conditioned at the level of years as it is considered in the block model with the solution delivered by the optimization problem on a monthly scale
– the extracted mineral was quantified in proportion to the *extracted tonnage* and the *mineral/total tonnage* ratio of each bench
– equipment operational and investment costs as well as equipment characteristics (obtained from catalogs).

2 Methodology

A review of the data obtained from the mine site was performed to determine the mineral depletion throughout the mine life. Since the assignment of loading equipment to the particular workplace is sought, a catalog of equipment was used to obtain data regarding equipment characteristics, costs and capabilities, among others. The construction of the optimization model that determines the allocation of the loading equipment to the production pushbacks over time to minimize production costs was made.

The equipment assignment was made manually as well as using the model to measure the differences. The results obtained using modeling were compared with the manual assignment and the base production plan.

3   Optimization Model

Within the dynamics in which the loading equipment operates in a mining operation, numerous factors that affect productivity were considered:

– mechanical availability
– operational factors
– available operating space
– precedencies between bench of the same and different pushbacks
– feed requirements to the processing plant
– production goals
– cost of production and acquisition of equipment
– productivity of the equipment.

3.1   Variables

The decision variables for the model made according to Eqs. 1 through 6:

$$x_{\text{pbft}} = \text{percentage of period } t \text{ that shovel } p \text{ is in bench } b \text{ of phase } f \tag{1}$$

$$\bar{x}_{\text{pbft}} = \begin{cases} 1, \text{ if the shovel } p \text{ is in bench } b \text{ of phase } f \text{ of period } t, \\ 0 \text{ if not} \end{cases} \tag{2}$$

$$z_{\text{bft}} = \begin{cases} 1, \text{ bench } b \text{ of phase } f \text{ is active in the period } t, \\ 0 \text{ if not} \end{cases} \tag{3}$$

$$\bar{z}_{\text{bft}} = \begin{cases} 1, \text{ bench } b \text{ of phase } f \text{ was extracted in period } t \text{ or later,} \\ 0 \text{ if not} \end{cases} \tag{4}$$

$$w_{\text{pt}} = \begin{cases} 1, \text{ if the shovel } p \text{ is bought in period } t \text{ or earlier,} \\ 0 \text{ if not} \end{cases} \tag{5}$$

$$\bar{w}_{\text{pft}} = \begin{cases} 1, \text{ if the shovel } p \text{ is assigned to phase } f \text{ in period } t, \\ 0 \text{ if not} \end{cases} \tag{6}$$

Equation (1) is the decision variable that quantifies the production associated with each equipment in operation while the variables (2)–(6) are used to regulate the precedencies and assignments of the equipment to the operation.

3.2 Objective Function

The final objective function is given by Eq. (7)

$$\text{min:} \quad \sum_t K_p \cdot w_{pt} \cdot \text{FD}_t + \sum_{p,t,f,b} C_p \cdot x_{pbft} \cdot Q_p \cdot D_p \cdot \text{Fll}_p \cdot \text{FO}_{bf} \cdot T_t \cdot \text{FD}_t \quad (7)$$

The objective function of the model (Eq. 7) seeks to minimize the costs associated with the acquisition of loading equipment (K_p) and the operational cost based on the extracted tonnage (C_p). The tonnage extracted in each period is expressed by the multiplication of the capacity per hour of the equipment (Q_p) by the corresponding operational factors (D_p: mechanical availability, Fll_p: filling factor, and FO_{bf}: utilization), the fraction of the period the equipment is operating (x_{pbft}), and the duration of the period (T_t). The values are discounted in time using the discount factor (FD_t) that corresponds to the duration of the period. In this way, you can use the model with periods of days, weeks or months.

The variables are subject to different restrictions to ensure that the solution obtained represents the operation in the best possible way. In particular, the restrictions indicate that:

– variable (1) cannot exceed the duration of the assigned period;
– the movement of material associated with the variable (1) must meet the productive goal for the end of the total periods;
– the equipment can only be assigned if the variable (5) indicates that the equipment is available;
– to begin work on a new bench all the material of the predecessor benches must be extracted, which is indicated by the variable (4);
– the precedencies are given by the sequence of benches of the same phase and different pushbacks according to operational criteria;
– to assign working time to a bench, the bench must be marked as active according to the variable (3) and with an equipment assigned according to the variable (2);
– in order to assign an equipment to a bench, space must be available for its entry, which is entered as an input for each bench and is updated period by period according to the material extracted in that sector;
– the total extracted mineral must comply with the requirements of the plant;
– there is a limit of assignment of the same equipment to different pushbacks of work in each period.

4 Model Inputs

The model seeks to generate an equipment allocation plan for each month of a year of production. The optimization is applied to a long-term plan (Fig. 1) obtained with the software Whittle, which considers a constant production rate for each period. By

incorporating the model developed at the production bench scale, the tactical plan and the operational plan can be linked. Data associated with the equipment, benches to be extracted within the period of 4 years and operating parameters, specified in Sects. 4.2 and 4.3 were considered.

4.1   Material to Be Extracted

The material to be extracted associated with each bench is entered into the model. The data entered also includes the phase to which it corresponds, the number of the bench (growing with depth), the total tonnage to be extracted, the tonnage of ore present in the bench, and the revenue per ton that presents its extraction.

4.2   Loading Equipment

The model sought to complete the production plan with the total extraction of the material entered in each bench; it made decisions regarding shovel selections to minimize costs. The information required for each equipment was an associated name (P0X), the cost of acquisition, the capacity in tons, the utilization and fill factor in percentage and the operational cost in dollars per hour.

Given the way in which the model was built, it is necessary to express the operational cost of the equipment in USD/hour. To achieve this, the following assumptions will be considered:
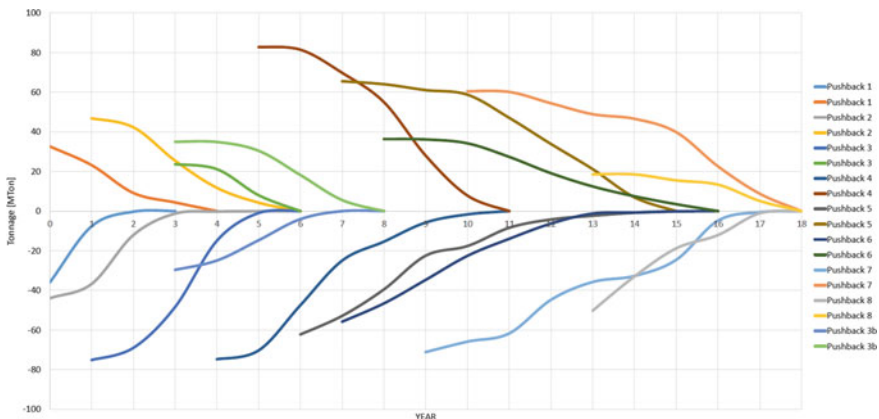
Fig. 1 Graph of depletion of material for the whole life of the mine. In the upper part of the horizontal axis are the mineral tonnages and in the lower the sterile. Year 4 was the basis for the study

– the fleet of trucks allows the blades to be saturated
– each truck will be filled with three buckets of the shovel that loads it.

The first assumption was made to express the productivity of the shovel in relation to itself without depending on the cycle of the transport equipment while the second was done to express productivity directly from the bucket capacity of each shovel. This last assumption is quite strong and works well when the shovels chosen for production do not differ so much in size, but in the case of a considerable difference, the assumption implies that the truck fleet must be different in order for the condition of cargo to be fulfilled.

4.3   General Parameters

Data associated with the mining operation: the ore tonnage requirement for the plant's feeding, the discount rate, the bench height, and the density of the material were incorporated within the model.

5   Results

5.1   Model Simulations

To facilitate the representation and form in which the results are presented, the results referring to the manual allocation of equipment and that obtained with the model are displayed simultaneously. The following scenarios were considered:

– case A: Manual assignment of equipment selecting the lowest cost per ton
– case B: Manual assignment of equipment selecting those with the lowest investment
– case C: Assignment of equipment according to model considering lower investment equipment
– case D: Assignment of equipment according to model
– case E: Assignment of equipment according to model with restriction of area.

Scenario D resulted in the lowest global cost because the model did not have restrictions associated with equipment usage nor with space restrictions. Table 1 shows the equipment assignment and the percentage difference in resulting cost between each exercise with exercise D. Despite both scenarios B and C use the same loading equipment the case C manages to obtain lower costs. This reveals the great impact of the allocation of equipment and the sequence of extraction on costs and how a better strategy for the use of equipment can help reduce the costs of the mine.

Between the cases C and D, it can be seen that by giving the model freedom to choose the equipment to be used, it selects other equipment than equipment chosen

Table 1 Type and quantity of equipment selected for each scenario: the percentage difference in costs obtained in relation to case D

Scenarios	Selected equipment	Δ% to scenario D
A	2 P01–2 P12	+162.2
B	2 P01–2 P04 – P05	+42.4
C	2 P01–2 P04 – P05	+14.3
D	2 P01–2 P02–2 P03	–
E	2 P01–2 P03 – P04	+0.6

manually, thus achieving the production goal in the same way. The difference between case A and B indicate that for the evaluation period of 1 year, the operational cost less relevant than the acquisition cost. This may be reversed when several years of operation are evaluated while the large tonnage to be moved allows the operational cost to become an important part of the total costs.

Figure 2 shows the production plan generated by the assignment of equipment from scenario E. It can be seen that the material movements have a ramp-up during the first periods before stabilization; this is due to the area restrictions imposed on benches. It is also possible to notice variations in the tons of waste and ore extracted from one month to another. This is because production is conceived as the result of a particular equipment assigned to a specific sector and not as a constant flow of tons. In this way, the model manages to capture and better represent what happens in the operation allowing to create more feasible plans.
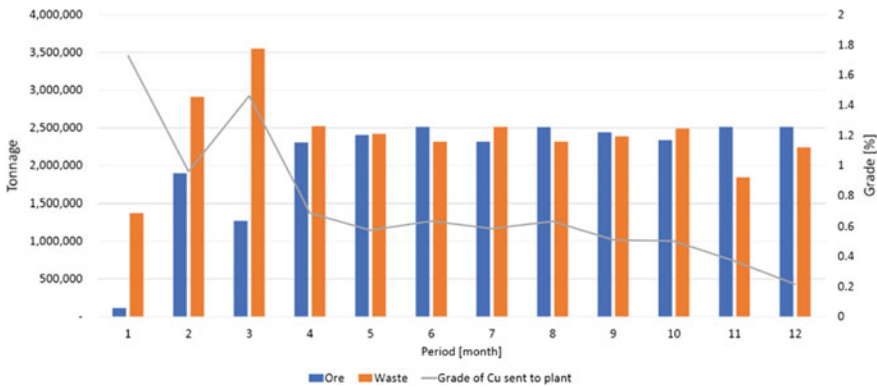
Fig. 2 Production plan for Scenario E

5.2 Scenario E Versus Long-Term Plan

The comparison of the results obtained with Scenario E with the production plan obtained in the long-term planning is shown in Fig. 3, where it can be seen that, for the ore in Pushbacks 2 and 4, the extraction was slower than estimated according to the long-term plan while Phase 1 does it faster after period 4 (the line graph obtained by the model goes below the long-term line). This may mean that when the plan was put into operation, there were problems with the mineral feed to the plant, especially in the first 4 months.

6 Conclusion

The developed methodology allows to obtain an assignment for a fixed fleet of shovels to the workplaces that meets operational and production restrictions for the short and medium terms. It provides a guide for the planner, which saves time and resources. The model also allows to evaluate different fleet investments options, in the case of greenfield operations, based on their productivity in different work sector.

The consideration of the movement capacity associated with real equipment instead of a defined daily movement allows obtaining a plan that is better adjusted to what actually happens in the mining operation, allowing to estimate revenues and costs more accurately as well as determining the vulnerabilities in the plant feed.

The model also delivers an operational plan that complies with the projected production in the long-term plan, serving as a tool capable of incorporating the
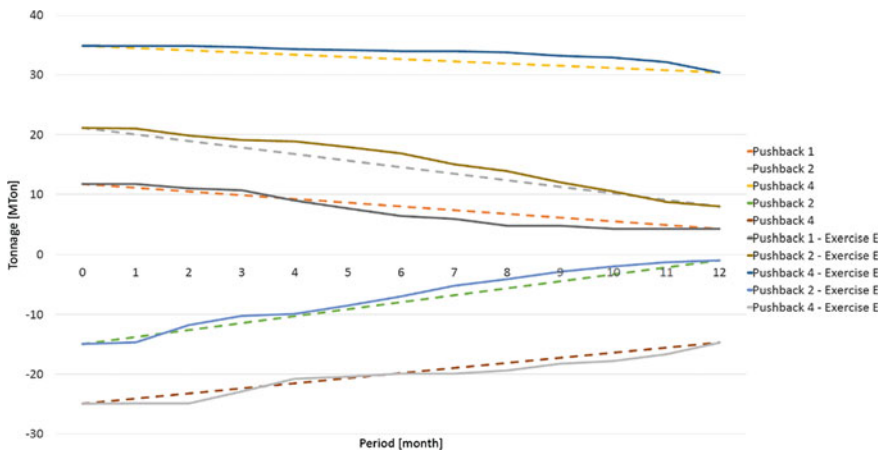
Fig. 3 Material depletion comparison of Scenario E with the initial plan. Base case is represented by dotted line while model by the continuous line. Only selected pushbacks are presented given the difference of order of magnitude between the movements among pushbacks

characteristics of the mining operation and obtaining a sequencing that serves as a bridge between the different levels of planning.

References

1. Le-Feaux, R.A., Vázques, G.B.: Diseño y operaciones de minas a cielo abierto **11**(13), 165–167 (2008)
2. Bozorgebrahimi, H., Hall, E.R., Blackwell, A.G.: Sizing equipment for open pit mining—a review of critical parameters. Min. Technol. **3**, 2–3 (2003)
3. Newman, A.M.: A review of operations research in mine planning. Interfaces 40. INFORMS **3**, 222–245 (2010)
4. Temeng, V.A., Otuonye, F.O., Frendewey, J.O.: Real-time truck dispatching using a transportation algorithm. Int. J. Surf. Min. Reclam. Environ. **11**(4), 203–207 (1997)
5. Gurgur, C., Dagdelen, K., Artittong, S.: Optimization of a real-time multi-period truck dispatching system in mining operations. Int. J. Appl. Decis. Sci. **4**(1), 57–79 (2011)
6. Upadhyay, S.P., Askari-Nasab, H.: Truck-shovel allocation optimization: a goal programming approach. Min. Technol. **125**(2), 82–92 (2016)

A Transportation Problem-Based Stochastic Integer Programming Model to Dispatch Surface Mining Trucks Under Uncertainty

A. M. Afrapoli, M. Tabesh and H. Askari-Nasab

1 Introduction

In surface mining operations, truck dispatching is the process of determining the best assignment of trucks to the right destinations. All thus far, published research has introduced a two-stage decision-making model to solve truck dispatching problem with the exception of one proposed by [1]. The two stages are called upper stage or production optimization stage and lower stage or truck dispatching stage [2]. The set of decisions made in the lower stage is a set of dynamic operational outlines to meet the upper stage targets. Several decision-making models have been developed to address the two sets of decisions.

Researchers have applied different operational research approaches to solve the upper stage problem. White and Olson [3] developed a two-segment linear programming (LP) model that in its first segment, it maximizes shovels' dig rate by minimizing total material handling costs [3]. Then, it determines the optimum flow rate for each path in the mine. They developed the most popular currently available truck dispatching decision maker tool in the market [4] based on their two-segment LP model.

In 1989, a combination of mixed-integer LP and nonlinear programming (NLP) operational research approach was introduced by [5, 6]. The developed model schedules trucks' travel between any source and destination in the mine in two steps. One important advantage of the model developed by [5, 6] is that before implementing

A. M. Afrapoli (✉) · M. Tabesh · H. Askari-Nasab
Mining Optimization Laboratory (MOL), University of Alberta, Edmonton, Canada
e-mail: moradiaf@ualberta.ca

M. Tabesh
e-mail: tabesh@ualberta.ca

H. Askari-Nasab
e-mail: hooman@ualberta.ca

an NLP model to allocate trucks to shovels, it first runs a MILP to assign shovels to the right working faces.

Following that [7] published an LP model that was called transportation model for truck dispatching in mines. The model tries to minimize transportation work required for each path. Implementing the developed LP model, optimum number of trucks to meet the path production requirement is determined.

In the late 1990s, [8] developed a truck allocation model that works based on goal programming approach. With respect to ore grade, shovel dig rate, stripping ratio, and dumping points' capacities, the model maximizes shovel production.

A chance-constrained stochastic approach was applied to the upper stage (truck allocation or production optimization) problem by [9]. The developed model determines optimum number of trucks of a kind to be allocated to a path to meet its production requirement in presence of truck cycle time and its capacity uncertainties.

By adding shovel assignment to the mining faces, [10] developed an LP truck allocation model that is capable of minimizing deviation from the strategic level production requirements. Ta et al. [11] developed a mixed-integer LP model that solves truck allocation problem based on the probability of shovel idle time. The objective of the developed model is to minimize total number of trucks required to meet the production target. In the same year, [12] introduced an availability-based mixed-integer LP model that tries to solve upper stage problem using knapsack problem approach. The developed model maximizes cumulative truck fleet production within a fixed time horizon. Chang et al. [13] developed a mixed-integer LP model to solve truck allocation problem. The model maximizes transportation revenue with respect to priority of shovels. A heuristic algorithm was developed to solve the model for each operation shift. Readers are encouraged to read [2] and [14] for detailed information regarding the approaches and solution methodologies.

Despite all the aforementioned efforts in developing mathematical models to solve the upper stage problem, a limited number of models can be found in the literature that deals with the lower stage truck dispatching problem. White and Olson [3] and Soumis et al. [6] applied assignment problem approach toward making decisions on trucks next destination. Li [7] developed a model that minimizes the relative difference between the actual time that next truck will arrive at a destination and the time that next truck must be in that destination based on upper stage results. Lizotte et al. [15] developed a simulation-based semiautomated model that assigns trucks to the destinations using three different heuristic models. Temeng et al. [16] implemented a transportation-based approach toward dealing with the truck dispatching problem. However, there is a limitation in the abovementioned models. Although most of the input parameters are uncertain and show stochastic behavior, the developed models use deterministic input parameter values. One of the input parameters that is used in many models is truck cycle time. The truck cycle time in a mining operation is subject to fluctuations from its deterministic value due to different factors including road conditions, traffic conditions, intersection blockages, trucks' bunching effects, etc.

The aim of this paper is to minimize the idle time of shovels and trucks through improved dispatch logic that quantifies the impact of empty haulage travel time uncertainty on the haulage cycle time calculations and truck assignments. To achieve the objective of the paper, we present a stochastic integer programming model that makes truck dispatching decisions while considering the uncertainties in truck travel time. The travel time has been selected due to its higher contribution in the material handling cycle time than any other components of a cycle time such as spot time, load time, and dump time. To assess the developed model, we implemented it in an open-pit mine operation simulation and results are presented here.

2 Model Formulation

The model development consists of two main steps. At the first step of the model development, a deterministic model was developed. Then,by implementing the recourse approach [17], we developed a stochastic model based on the model developed in the first step to capture uncertainty in truck travel time.

The model presented in this section is a deterministic model with all its input parameters taking deterministic values. It can also be categorized as a mixed-integer linear programming model based on transportation problem. The objective function of the model, presented in Eq. 1, minimizes the cumulative absolute time difference between the times truck t will reach shovel s after dumping at dump d (tts) and the time shovel s will be available to load the next truck (nas). The second part of the objective function tries to maximize the adjustment factor (AF) encouraging the model to maximize a balanced material delivery to all destinations. AF will be explained later on. Finally, VBN stands for very big number.

$$\min Z = \sum_{t=1}^{T} \sum_{d=1}^{D} \sum_{s=1}^{S} C_{\text{tds}} x_{\text{tds}} + \text{VBN}(mf - AF)$$

$$\forall t \in \{1, \ldots, T\}, \forall d \in \{1, \ldots, D\}, \text{ and } \forall s \in \{1, \ldots, S\} \qquad (1)$$

The objective function coefficient for each of the variables is calculated using Eq. 2

$$
\begin{aligned}
C_{\text{tds}} &= |t_{\text{ts}} - na_s| \\
&= |T(t, 3 + s) - S(4, s)| \\
&= \left| ltt_{\text{td}} + qt_{\text{td}} + dt_{\text{td}} + ett_{\text{tds}} - \sum_{t'=1}^{TT} (tinq_{t's} + tenr_{t's}) \times (st_{t's} + lt_{t's}) \right|
\end{aligned}
$$

$$\forall t \in \{1, \ldots, T\} \ \& \ \forall s \in \{1, \ldots, S\} \ \& \ \forall d \in \{1, \ldots, D\} \qquad (2)$$

where

ltt_{td} loaded travel time from current truck t position to dump d
qt_{td} time truck t must spend in queue at dump d to dump its material
dt_{td} time truck t spends at dump d to back up and dump its material
ett_{ts} time truck t spends to travel empty from the dump location d to shovel s
$tinq_{t's}$ time a truck of type t' that is already in queue must spend in shovel s queue
$tenr_{t's}$ time a truck of type t' must travel from its current position to reach shovel s.
$st_{t's}$ spot time for a truck of type t' at shovel s
$lt_{t's}$ loading time for a truck of type t' at shovel s

Moreover, the decisions need to meet operational constraints such as trucks' and shovels' supply (Eqs. 3 and 4), destination demand constraint (Eq. 5), balancing truck distribution over the paths (Eq. 6), and binary constraints (Eq. 7).

$$\sum_{d=1}^{D}\sum_{s=1}^{S} x_{tds} \leq 1 \ \forall \ t \in \{1, \ldots, T\} \tag{3}$$

$$\sum_{t=1}^{T}\sum_{d=1}^{D} tc_t x_{tds} \leq sc_s \ \forall \ s \in \{1, \ldots, S\} \tag{4}$$

$$\sum_{t=1}^{T}\sum_{s=1}^{S} tc_t x_{tds} \geq AF \times pc_d \ \forall \ d \in \{1, \ldots, D\} \tag{5}$$

$$0 \leq AF \leq mf \tag{6}$$

$$x_{tds} \in \{0, 1\} \ \forall t \in \{1, \ldots, T\}, \ \forall d \in \{1, \ldots, D\}, \ \text{and} \ \forall \ s \in \{1, \ldots, S\} \tag{7}$$

where

x_{tds} binary integer variable to assign truck t to the path connecting shovel s to dump d
tc_t capacity of truck t
sc_s capacity of shovel s
pc_d capacity of dump d (ton)
AF adjustment factor that forces model to evenly distribute extra available trucks among all the possible destinations
mf proportion of the cumulative available trucks' capacity to the cumulative required path flow rate that can be met using the available trucks
pf_{sd} required path flow rate for path from shovel s to dump d based on upper stage decisions
$pmsf_{sd}$ met so far path flow rate for path from shovel s to dump d.

Constraint (3) makes sure that truck t cannot be assigned to more than one shovel. Constraint (4) ensures that summation of nominal capacity of all the trucks assigned to shovel s does not exceed the shovel's nominal digging rate (capacity). AF in constraint (5) is defined as adjustment factor. The adjustment factor is a variable that is forcing the model to evenly distribute the truck fleet capacity between all the destinations and is constrained by mf as in Eq. 6; mf is a matching factor that is

calculated based on cumulative available truck capacity and cumulative path material handling requirement. This factor is equal to 1 when the total truck fleet capacity is less than the required path flow rate and is equal to the proportion of the available truck capacity to the total path requirements when there is extra fleet capacity available. The adjustment factor is constrained by mf in order to uniformly distribute the extra truck fleet capacity among all the needy paths to balance ore and waste production.

The presented model uses expected (deterministic) values for the input parameters. However, most of the parameters affecting the truck dispatching decisions are random variables. In this paper, we formulated our model as a stochastic integer programming model with recourse [17] to capture the uncertainty of one of the major parameters affecting the operation (trucks' empty travel time). Reason to capture uncertainty in trucks' empty travel time is that more than 90% of trucks' cycle time in each cycle is spent in traveling. From that time, about 50% is spent in travel empty. As most of the time a truck needs to be dispatched has already passed some portion of its loaded travel or even completed its loaded travel, the most important parameter where the uncertainty associated with it needs to be captured is empty travel. Thus, the objective function of the stochastic model that captures empty travel time uncertainty is (Eq. 8):

$$
\begin{aligned}
\text{Minimize } Z = & \sum_{t=1}^{T}\sum_{d=1}^{D}\sum_{s=1}^{S} C_{\text{tds}} x_{\text{tds}} \\
& + VBN(1 - AF) \\
& + \frac{1}{nR} \sum_{t=1}^{T}\sum_{d=1}^{D}\sum_{s=1}^{S}\sum_{r=1}^{nR} \bigg| ltt_{\text{td}} + qt_{\text{td}} + dt_{\text{td}} + ett_{\text{tds}}^{r} \\
& - \sum_{t'=1}^{TT} (tinq_{t's} + tenr_{t's}) \times (st_{t's} + lt_{t's}) \bigg| \times x_{\text{tds}}
\end{aligned}
\tag{8}
$$

where

ett_{tds}^{r} time truck t spends to travel empty from the dump location d to shovel s in rth realization

r   is an index referring to a scenario in the stochastic integer model

nR number of realizations implemented to generate random variables for empty travel time from its distribution.

In the developed model, the first two components of the objective function are the same as the deterministic model. The third component is the minimization of the truck or shovel idle time in material handling given the uncertainty in trucks empty travel time. The model is constrained with Eqs. (3)–(7). For each of the realizations r in the stochastic model with nR number of realizations, a random value is being sampled from the fitted distribution of the historical data of the empty truck velocity. The sample is then imported into the model after preprocessing procedure that calculates required travel time and is used during the decision-making procedure.

The developed model was implemented in a simulation study of an iron ore mine and the results of key performance indicators (KPI) were compared against model developed by [3] which is used as the backbone of the operation optimization in [4] fleet management system. There are two small size shovels in the operation serving two active processing plants with an input feed rate requirement of 2300 ton per hour of the operation. Another small shovel alongside with two large ones is digging waste material to meet the stripping ratio requirement.

3   Results

Some key performance indicators (KPI) were chosen to compare the results of implementation of the developed stochastic truck dispatching model against the benchmark truck dispatching model as listed in Table 1.

Results of the simulation of the case study show that the required plant feed rates are met when using the developed model as the dispatching logic while plant feed rates will be short by 5–10% when using the benchmark dispatching logic (Fig. 1).

Using benchmark truck dispatching model, none of the plants are fed with their required hourly feed rate. Plant 1 is on average 12% short on its hourly feed target rate, whereas plant 2 is on average of 8% short. However, by replacing the benchmark truck dispatching model with the stochastic truck dispatching model, both plants' target rate is met. Figure 1 also shows that implementing benchmark truck dispatching, plant 2 is fed 4% more than plant 1. It is due to a critical drawback of the benchmark model. The benchmark model dispatches trucks based on minimum distance between trucks and destinations. However, it does not account for the queue that might happen after a truck reaches to the assigned destination. Thus, if we have multiple destinations similar to what we have in this case study, the benchmark model dispatches trucks to the destinations with the shorter distance. Here in this case study, plant two is located about 400 m closer to the ore shovels than plant one. As a result, plant one is served more by the benchmark model comparing to plant two. This difference in feeding rate is not happening when the benchmark truck dispatching model is replaced by

Table 1 Key performance indicators to assess the developed stochastic model

No.	KPI	Description
1	Plant feed rate (t/hr)	Amount of material delivered to each processing plant in an hour of operation
2	Shovels' utilization (%)	Percentage of shovels' available time being used in the operation
3	Queue length	Number of trucks lining up in front of a resource when a truck reaches there
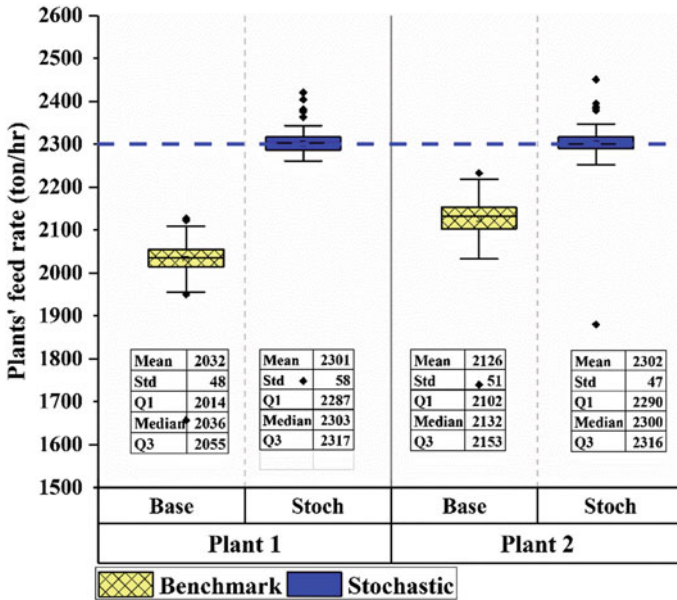
Fig. 1 Ore delivered to processing plants; the horizontal dashed line on 2300 (t/hr) stands for the required plant feed rate for each of the active processing plants in the operation. For each processing plant, the left-hand side box plot (hatched yellow) shows plant feed rate using benchmark model and the right-hand side box plot (blue) shows the plant feed rate using the proposed model

the stochastic truck dispatching model. As one of the advantages of the stochastic model, it does account for all of the possible queueing that will happen when the truck is assigned. Thus, it is capable of feeding the plants equally in a multiplant mining operation.

Another important KPI is the utilization of the shovels as the second most expensive equipment after the processing plant in mining operation. A comparison of shovels' utilization when using the developed and the benchmark dispatching logic is presented in Table 2.

Table 2 Comparison of utilization of active shovels in the operation

Shovel	Utilization (%) (benchmark)		Utilization (%) (stochastic model)		Difference (%)
	Mean	Standard deviation	Mean	Standard deviation	
1	88.9	1.1	96.4	2.9	8
2	84.7	1.2	95.5	3	11
3	97.5	1.7	75.8	2.8	−22
4	96.4	1.4	76.7	2.9	−20
5	99.9	5.1	90.5	2.6	−9

Shovel 1 and Shovel 2 feed the processing plants by extracting ore material and Shovel 3, Shovel 4, and Shovel 5 remove waste materials. Shovels working on the waste mining faces are approximately 10% more utilized than the ore shovels when using the benchmark truck dispatching decision-making model. However, the trend is reversed when using the stochastic model: the ore shovels are utilized more than 90% of their available time whereas the waste shovels are utilized about 80% of their available time. The difference is mainly due to the fact that the benchmark truck dispatching model makes decisions based on the distance between trucks and the shovels and it does not include the time trucks have to spend in the queue at each specific shovel when they reach to that shovel. Though, the stochastic model involves the expected queue time in the decision-making procedure.

There are two possibilities when a truck reaches a loader. Either it encounters a shovel standing idle and waiting for the next truck to load or it meets a shovel that is currently loading a truck and has to enter a queue. In either case, the mine is not working efficiently. In the former, shovel is utilized less than its available time and in the latter, the truck is losing its available time in the queue. Figure 2 represents a graphical and statistical comparison of the histograms of the number of trucks in the queue at shovels when a truck arrives to that shovel between the time
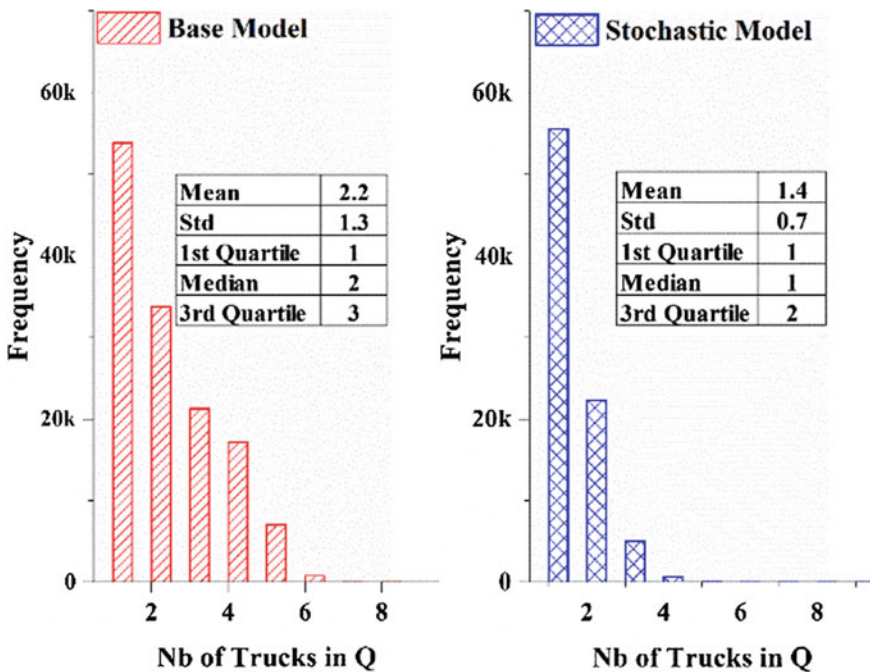
Fig. 2 Histogram of number of trucks waiting in the queue when a truck arrives at a loading point when the truck dispatching decisions are made by the base model (red bars) and the time the truck dispatching decisions are made by the stochastic model (blue bars)

the base decision-making model makes decisions on the truck dispatching problem and the time the base decision-making model is substituted by the stochastic model developed in this study.

Simulation results show that the average number of trucks in queue at shovel when a truck arrives at that shovel decreases by 36% by replacing the benchmark model with the stochastic model. The developed stochastic model also shows a 50% reduction in the median. It means by replacing the base model with the developed model most of the time when a truck reaches to a shovel it encounters with only one truck waiting in the queue instead of 2 which happens in the base model. This consequently results in shorter queue time.

4   Conclusion

Truck dispatching problem in the surface mining operations has been addressed in this paper. Despite uncertainties associated with the governing operational parameters, most of the conducted research in the field thus far has ignored random nature of input parameters. However, in this paper, a stochastic integer programming model was introduced that accounts for the uncertainties associated with truck travel times into the truck dispatching problem-solving procedure. This helps to make more realistic decisions for trucks optimal destinations. The model was developed based on the transportation problem approach. The model was implemented in a simulated case study and results of its implementation were compared against results of implementation of the model developed by [3] which is backbone of [4] as benchmark truck dispatching model from the literature. Results of the comparisons show a promising improvement in all of the measured KPI.

References

1. Hauck, R.F.: A real-time dispatching algorithm for maximizing open-pit mine production under processing and blending requirements. In: Seminar on Scheduling in Mining, Smelting and Metallurgy, pp. 1–10 (1973)
2. Alarie, S., Gamache, M.: Overview of solution strategies used in truck dispatching systems for open pit mines. Int. J. Mining, Reclam. Environ. **16**(1), 59–76 (2002)
3. White, J.W., Olson, J.P.: Computer-based dispatching in mines with concurrent operating objectives. MIN Eng-littlet **38**(11), 1045–1054 (1986)
4. Modular Mining Systems: DISPATCH Fleet Management, [Online]. Available: http://www.modularmining.com/ (2017)
5. Soumis, F., Ethier, J., Elbrond, J.: Truck dispatching in an open pit mine Int. J. Surf. Mining, Reclam. Environ. **3**(2), 115–119 (1989)
6. Soumis, F., Ethier, J., Elbrond, J.: Evaluation of the new truck dispatching in the mount wright mine. In: 21st APCOM Proceedings, pp. 674–682 (1989)
7. Li, Z.: A methodology for the optimum control of shovel and truck operations in open-pit mining. Min. Sci. Technol. **10**(3), 337–340 (1990)

8. Temeng, V.A., Otuonye, F.O., Frendewey, J.O.: A non preemptive goal programming approach to truck dispatching in open pit mines. Miner. Resour. Eng. **7**(2), 59–67 (1998)
9. Ta, C.H., Kresta, J.V., Forbes, J.F., Marquez, H.J.: A stochastic optimization approach to mine truck allocation. Int. J. Surf. Mining, Reclam. Environ. **19**(3), 162–175 (2005)
10. Gurgur, C.Z.: Optimisation of a real-time multi-period truck dispatching system in mining operations. Kadri Dagdelen and Songwut Artittong **4**(1), 57–79 (2011)
11. Ta, C.H., Ingolfsson, A., Doucette, J.: A linear model for surface mining haul truck allocation incorporating shovel idle probabilities. Eur. J. Oper. Res. **231**(3), 770–778 (2013)
12. Mena, R., Zio, E., Kristjanpoller, F., Arata, A.: Availability-based simulation and optimization modeling framework for open-pit mine truck allocation under dynamic constraints. Int. J. Min. Sci. Technol. **23**(1), 113–119 (2013)
13. Chang, Y., Ren, H., Wang, S.: Modelling and optimizing an open-pit truck scheduling problem. Discret. Dyn. Nat. Soc. (2015)
14. Moradi Afrapoli, A., Askari-Nasab, H.: Mining fleet management systems: a review of models and algorithms. Int. J. Mining, Reclam. Environ. (2017)
15. Lizotte, Y., Bonates, E., Leclerc, A.: Analysis of truck dispatching with dynamic heuristic procedures. In: Golosinski, T.S., Srajer, V. (eds.) Proceedings of the International Symposium on Off-Highway Haulage in Surface Mines. Balkema, Rotterdam, pp. 47–55 (1989)
16. Temeng, V.A., Otuonye, F.O., Frendewey, J.O.: Real-time truck dispatching using a transportation algorithm. Int. J. Surf. Mining, Reclam. Environ. **11**(4), 203–207 (1997)
17. Birge, J.R., Louveaux, F.: Introduction to Stochastic Programming, 2nd edn. New York, USA (2011)

A Discrete-Event Simulation for a Truck-Shovel System

E. Y. Baafi and W. Zeng

1 Introduction

The truck-shovel mining method is the most flexible mining method that can be widely applied in open-pit mines. A truck-shovel mining system generally consists of shovels and associated truck fleets. Ore of different qualities and waste are loaded into trucks by shovels and transported from loading sites to ore crushers or waste dumps. The productivity of an operating truck depends on the actual truck payload and the truck cycle time. A single truck cycle includes spotting and loading, hauling loaded, dumping, hauling empty, waiting and incorporates operational delays.

In a truck-shovel system, the complex and dynamic interactions between the variables in the haulage system have determined that analytical methods are not feasible for model development [1]. With simulation, it is possible to evaluate the static, dynamic and stochastic elements of a truck-shovel system, and also offers a management tool to evaluate and compare alternatives for better decision-making [2].

According to the level of modelling detail, there are currently two kinds of simulation approaches to the traffic control problem: the macroscopic and microscopic approaches [3]. The macroscopic approach describes the traffic process via the low-level detailed traffic objects such as the traffic flow and density; while the microscopic involves a high detailed modelling approach, considering the traffic elements, for instance, individual vehicle units, haul routes, the interaction between the vehicle units and the influence of the traffic network on the vehicle units.

Previous work on road transport [4–6] has pointed out that the macroscopic approach is not able to reproduce the individual vehicle movement and to capture the traffic interaction on the haul route networks. Furthermore, Jaoua et al. [7] proved

E. Y. Baafi (✉) · W. Zeng
School of Civil, Mining and Environmental Engineering, University of
Wollongong, Wollongong, Australia
e-mail: ebaafi@uow.edu.au

that with no consideration of the real-time haulage network constraints or traffic congestion and truck interaction, the macroscopic models could bias simulation results [3]. However, most of the previous truck-allocation models [8–13] were developed using the macroscopic approach. The macroscopic traffic models are usually simplistic and tend to ignore factors such as the bunching effect and the truck behaviour at an intersection area.

A discrete-event truck-shovel simulation model, referred to as Truck and Shovel JaamSim Simulator (TSJSim), was developed to evaluate the Key Performance Indicators (KPIs) of truck-shovel mining systems by considering a truck as an individual traffic vehicle unit that dynamically interacts with other trucks in the system as well as other elements of the entire traffic network.

2   Truck-Shovel Model with Arena and FlexSim Software

Arena is a discrete-event simulation software package developed by Rockwell Automation [14]. The framework of Arena mainly consists of blocks called flowchart modules along with data modules, allowing the truck-shovel mining system to be converted to the following operational components: trucks, shovels, routes and queues.

The basic material flow considers the flowing *Entities* to be trucks which travel between the loading sites and dumps without being destroyed or leaving the system. The major mutually connected modules include: the *Truck-allocation* module, which is responsible for assigning trucks under a fixed truck-allocation rule, the *Shovel* and *Dump* modules which model loading and dumping procedures, the *Route* module, which guides trucks to loaders and dumps, the *Priority* module, which manages the intersection passing priority, and the *MTBF/MTTR* module, which is responsible for operational delays that include non-scheduled equipment breakdowns.

In the Arena model, the truck assignments can be specified for each group of *Entities*. After a truck fleet *Resource* is assigned to each group of *Entities*, these *Entities* are sent to the dumps and then return to certain shovels according to the *Sequence* data module. This means that the *Entities* keep circling within the system, and the production data is generated by recording the accumulated the circle times of the *Entities* in the system.

FlexSim is another discrete-event simulation software package developed by FlexSim Software Products, Inc. [15], which provides an object-oriented environment for model development.

In the FlexSim model, the *Flowitems* are generated at the truck loading points and disposed of at the dump sites. The main process is to transport the *Flowitems* (ore and/or waste) with trucks from the loading sites to the dump sites, then send the empty trucks back to the loading sites to repeat the cycle.

Based on the functionality, the truck-shovel simulation model in FlexSim includes the following components: *Truck Dispatcher*, *Truck*, *Loading Zone*, *Dump Zone* and *States Recording* objects. The *Truck Dispatcher* object manages the *Task Sequences* of allocating *Trucks* to *Loading Zones*, initiating the *Loading Zones* to execute the

loading task, allocating the *Trucks* to *Dump Zones*, initiating the *Dump Zones* to execute the dumping task, and then reallocating the *Trucks* to the *Loading Zones*.

3 Limitations of Both Arena and FlexSim

Both Arena and FlexSim DES software are not designed specifically for the truck-shovel mining operation, thus the need for modelling of operational components in the truck-shovel mining system. The truck speed or hauling time is determined by truck configurations, that include truck capacity, truck performance and retarder curves, loading capacity, along with route parameters, such as, grade, rolling resistance and the dynamic traffic conditions that include traffic intersection management and route section speed control. Therefore, a more detailed model that considers the actual operational constraints in the truck-shovel mining system is difficult, if not impossible, to build using only the model units provided by Arena and FlexSim. Furthermore, there are significant limitations with data communications among the various model units in both Arena and FlexSim. The data communication depends on the type of connection between the model units, for example, in FlexSim, the information can only be shared between the two objects if they are connected via *Ports*. However, access to information from all the operating units and the entire traffic environment is necessary for a highly interactive and dynamic truck-shovel mining system, especially when used for the purpose of truck-allocation.

4 Limitations of Commercial Truck-Shovel System Simulation Software

Some commercial simulation software packages that are designed exclusively for a truck-shovel mining system have been found to be not sophisticated enough for the modelling of the dynamic and interactive aspects of a truck-shovel haulage network system. For instance, TALPAC [16] can only model one single loading unit at any one time; Caterpillar's Fleet Production and Cost Analysis (FPC) simulator supports only mean value inputs for the loading and dumping times. RPMGlobal's HAULSIM [17] integrates both the TALPAC equipment database and FlexSim's discrete-event simulation engine. HAULSIM includes multi-loader and truck analysis, full network travel time determination, modelling of congestion and queuing, display of dashboard results and 3D visualisation. However, HAULSIM is a closed-source commercial simulation software which does not allow users to create their own modelling objects. Some important operational aspects, such as the bunching effect and specific traffic management at an intersection, cannot be specified and investigated using the functions provided by HAULSIM.

5 Truck-Shovel System Development Using JaamSim

Java Animation Modelling and Simulation (JaamSim), is a free open-source discrete-event simulation software package developed by Ausenco [18], that allows users to create their own palettes of high-level objects for new applications. New objects can be programmed with 3D graphics along with the *Input Editor* and *Output Viewer* and can be dragged-and-dropped for direct usage. This is the key feature that distinguishes JaamSim from commercial off-the-shelf simulation software packages.

JaamSim offers a highly effective simulation engine and allows users to establish their own high-level modelling objects for complex operating systems. With the aid of JaamSim, the special functionality of the model objects based on the actual truck-shovel operational elements and conditions can be developed, and a flexible and customised truck-shovel mining system model can be built using these objects. The loader, truck, dump, and the traffic environment, such as haul routes, traffic intersections, can all be developed as model objects involving all the necessary operational constraints. The interactions between the objects for example, the interaction between the individual trucks and the interaction between the hauling trucks and the traffic environment, can be specified in detail.
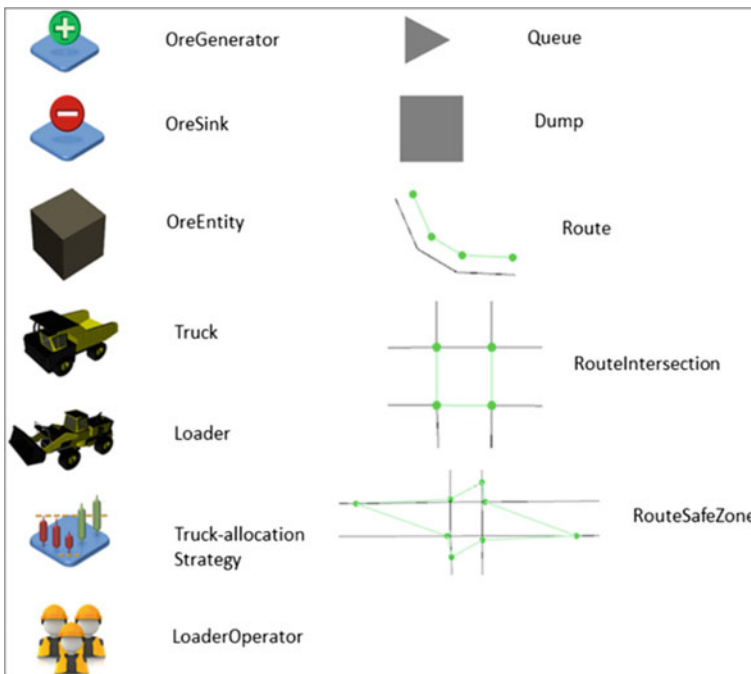
Fig. 1 TSJSim model objects

A flexible Truck-Shovel JaamSim Simulator (TSJSim) was developed for estimating the impact of operational elements on the performance of the truck-shovel system. TSJSim considers the stochastic, dynamic and interactive features of a truck-shovel network system. Twelve new objects shown in Fig. 1 was developed for modelling a typical truck-shovel mining network system.

The main simulation model objects are *OreGenerator*, *OreSink*, *OreEntity*, *Truck*, *Loader*, *Dump*, *Queue*, *Route*, *RouteIntersection*, *RouteSafeZone*, Truck-allocation Strategy and *LoaderOperator*.

The main functionality of each of these model objects is summarised in Table 1.

From a modelling point of view, the truck-shovel mining system was considered as a material handling system in which the material mined (*Entity*) flows through the system, with the trucks hauling this material in the system (between loaders and dumps). The basic logic flow of the truck-shovel system model in TSJSim is shown in Fig. 2.

The *OreEntity* object (material mined) is generated by the *OreGenerator* object, and processed at the *Loader* object, and then transported by the *Truck* object from the *Loader* object to the *Dump* object through the *Route* object. The travelling speed of the *Truck* object is influenced by both the condition of the haul routes and the operational factors of the truck. When the *Truck* object arrives at the *Dump* object, the *OreEntity* object is sent to the *OreSink* object to be disposed of, and the empty *Truck* object is sent back to the *Loader* object, completing a single truck cycle.

In TSJSim, the *Route* object is divided into various segments depending on the combination of route variables which include grade, rolling resistance and traffic infrastructure. Trucks travel along these segments of the hauling route with different mean travelling speeds that are dependent on the particular segment. When bunching occurs, depending on which of the segment(s) both the truck ahead (the slower truck) and the truck behind (the faster truck) are within, three bunching possibilities are considered in TSJSim, these being the three-stage bunching possibility, the two-stage bunching possibility and the safe correction distance possibility [19].
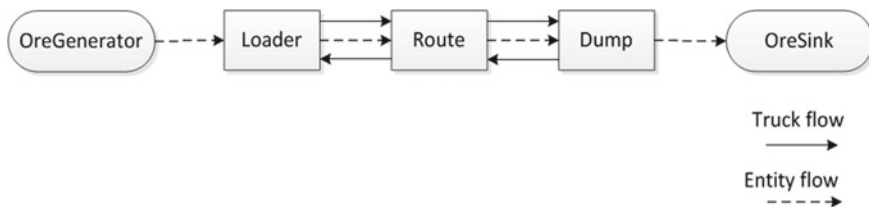
Fig. 2 Flow process chart of the truck-shovel system model in TSJSim

Table 1 Functionality of TSJSim model objects

Model objects	Description	Functionality
OreEntity	Flows through the system as the material is transported by the *Truck*	Properties such as shape, weight, can be assigned
OreGenerator	Generates the *OreEntity* consistently	The first/inter arrival time and the maximum amount of the *OreEntity* can be set
OreSink	Dispose of the *OreEntity*	
Queue	Works as a storage area for the *Truck* at the loading site or dump when the *Loader* or the *Dump* is busy	Collects the information relating to the queuing trucks including the number of queuing trucks and waiting times
Loader	Receives the *OreEntity* from the *OreGenerator*, processes it and sends it to the *Truck* when the *Truck* is ready	1. The loading time and loading amount can be specified according to the capacity of the truck, the bucket capacity of the shovel, the truck spotting time, fill factor, swell factor, material density, and the shovel working cycle time 2. Operators with different skills can be assigned to the *Loader* to reflect the varied performance of the *Loader*
LoaderOperator	Influences the performance of the *Loader*	Working cycle time and working hours for each *LoaderOperator* can be set
Dump	Receives the *OreEntity* from the *Truck*	Dumping time varies according to the size of the *Truck* and the weight assigned to the *OreEntity*
Truck	Transports the *OreEntity* between the *Loader* and the *Dump* on the *Route*	1. The speed of the *Truck* is set by considering the *Truck*'s configurations, such as dimension, weight, capacity, performance and retarder curves, and the *Route*'s condition including rolling resistance and grade 2. The mutual influence of the *Truck* has been considered. The bunching effect resulting from mixed equipment with varied capacities has been considered
Route	The track on which the *Truck* is hauling	The spatial coordinates of the *Route*, the rolling resistance and the coefficient of traction for each segment can be specified
RouteIntersection	The intersection of the routes	By combining the *RouteIntersection* and the *Route*, the traffic network forms

(continued)

Table 1 (continued)

Model objects	Description	Functionality
RouteSafeZone	The abstract area that implements the traffic management rules	1. The priority of the *Route*, namely the main road for production, can be set, so that the trucks hauling on the main road have higher priority for passing through the *RouteSafeZone* area 2. The traffic rules for trucks to pass through the intersection area can also be specified, for instance, the priority for heavy truck
Truck-allocation Strategy	Assigns the *Truck* under certain truck-allocation rules	The truck-allocation rules are: 1. Fixed truck assignment 2. Minimising truck waiting time 3. Minimising truck semi-cycle time 4. Minimising shovel production requirement
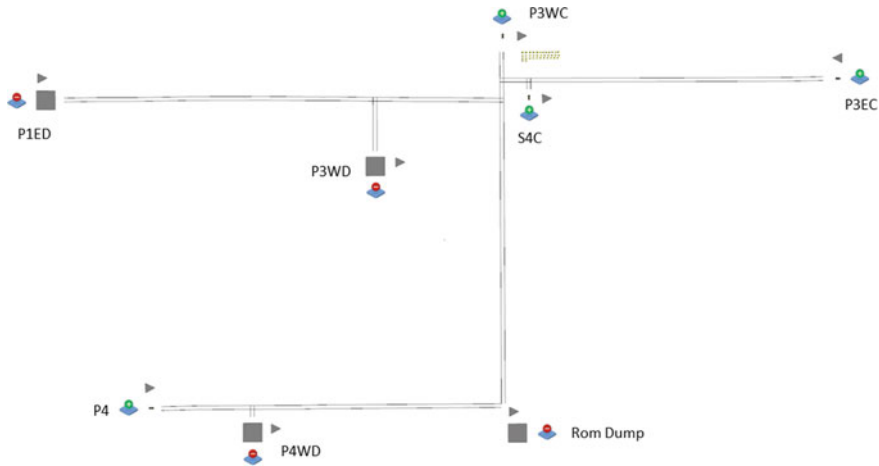
Fig. 3 Active haul routes of Easter Ridge OB23/25 operation

6 A Truck-Shovel Network System Model

The developed TSJSim model was validated using field data collected by [20] at a truck-shovel mining operation in Western Australia. The mining operation known as Easter Ridge OB23/25 consists of four loading sites, namely S4C, P3WC, P3EC and P4, and four dumping sites, namely P1ED, P3WD, P4WD and ROM Dump (Fig. 3). The Liebherr 9250 excavator works at P3WC, two Hitachi 1900BE excavators work at S4C and P3EC and the CAT 993 wheel loader works at P4. Four trucks (CAT 785C) are assigned to route P3WC—ROM Dump; four trucks (CAT 789C) to

Table 2 Truck inputs for CAT 785C and 789C

Truck type	Empty weight (kg)	Capacity (kg)	Length (m)	Width (m)	Height (m)
CAT 785C	102,150	147,330	11.02	6.64	4.98
CAT 789C	135,670	181,845	12.13	7.97	5.69

Table 3 Distributions of loading times

Loader type	Distribution (s)
Liebherr 9250	Normal (122.35, 18.08)
Hitachi 1900BE (loading 785C)	LogNormal (5.19, 0.16)
Hitachi 1900BE (loading 789C)	Normal (250.6, 33.14)
CAT 993 Wheel Loader (loading 785C)	LogNormal (5.73, 0.12)

Table 4 Distributions of dumping times

Truck type	Distribution (s)
CAT 785C	Normal (35.77, 11.02)
CAT 789C	Normal (46.88, 11.97)

route S4C—P1ED; four trucks (CAT 785C) to route P3EC—P3WD; one truck (CAT 785C) to route P4—ROM Dump and one truck (CAT 785C) to P4—P4WD.

The main input parameters associated with trucks are provided in Table 2.

The loading times of the four shovels and the dumping times of the trucks are summarised in Tables 3 and 4, respectively. The bucket capacity of the Liebherr 9250 is 15 m^3 and the capacity of the Hitachi 1900BE and the CAT 993 is 12 m^3.

The assumptions for the model implementation were:

– each truck is assigned to a fixed route (fixed truck-allocation mode)
– the bunching effect is considered
– the simulation model runs for 11 h representing one shift during the simulation run
– the experiment comprises 100 simulation replications.

Table 5 Case 1: Truck-shovel network shift simulation results

Loader	Fleet size	Ave waiting time (s)	Ave cycle time (s)	Truck utilisation (%)	Shovel utilisation (%)	Shovel production (t)	MF
Shovel 1	7	51	867	94	99	51,656	1.04
Shovel 2	8	119	1492	92	99	36,253	1.07
Shovel 3	8	103	1455	93	99	34,005	1.08
Shovel 4	5	87	918	91	99	32,519	1.08

7 Case Study

7.1 Case 1: Over-Trucking to Maximise Production at the Expense of OPEX

If the KPI for the entire truck-shovel network system is tonnes of materials moved, the focus for the operation is to maximise total production across the entire fleet of shovels and trucks. The following two production constraints can be set:

1. The utilisation of each shovel above 95%;
2. The truck utilisation in the range of 90–95%.

Table 5 shows the truck fleets configuration and the associated performance parameters for the entire truck-shovel network system using these production constraints. There are 28 trucks serving the system in which 7 trucks are allocated to Shovel 1, 8 trucks to Shovel 2, 8 trucks to Shovel 3 and 5 trucks to Shovel 4. The match factor for each fleet is close to 1, the balance point which implies that the shovel and the associated trucks are well matched. The production of each shovel in the system is maximised as indicated by the full utilisation of the shovel and also the truck utilisation is controlled. The system production per shift (11 h) is 154,433 t.

Assuming that the cost for a mining dump truck to operate is AU$ 400 per hour and an excavator AU$ 800 per hour [21]. The total queuing time for all the trucks is 83,381 s or 23.16 h, and the total idle time for all the loaders is 1430 s or nearly 0.40 h. In this case, the total OPEX caused by truck queuing and the loader waiting is AU$ 9582 per shift at approximately 6 cents per tonne.

7.2   Case 2: Slightly Under Trucking to Reduce OPEX Savings at the Cost of Production

If the KPI for the truck-shovel network system is to maximise truck utilisation and also the focus of operational planning is to reduce OPEX by slightly under trucking, then the following two production constraints can be imposed:

1. The utilisation of each shovel at around 90%;
2. The truck utilisation above 95%.

   Table 6 shows the simulation results. In this case, the truck fleet size is 24 with 6 trucks assigned to Shovel 1, 7 trucks to Shovel 2, 7 trucks to Shovel 3 and 4 trucks to Shovel 4. As the shovel utilisation decreases, the total shift production is reduced to 138,498 tonnes.

   The total queuing time for all the trucks is reduced to 26,758 s or 7.43 h, with the total idle time for all the loaders increasing to 17,144 s or 4.76 h. The total OPEX caused by truck queuing and loader waiting is AU$ 6783 per shift at approximately 5 cents per tonne. Compared with Case 1, AU$ 2799 per shift (1.3 cent per tonne) is saved from OPEX. In Case 2, the fleet size is reduced to 24. Suppose the capital cost of each saved truck is approximately AU$ 1,650,000 [22] and the serving time of the truck fleet is 20 years, without considering depreciation, the cost saved from CAPEX is AU$ 414 per shift at approximately 0.3 cent per tonne. Therefore, the total cost saved from OPEX and CAPEX, compared with Case 1, is AU$ 3214 per shift at 1.6 cent per tonne.

Table 6   Case 2: Truck-shovel network shift simulation results

Loader	Fleet size	Ave waiting time (s)	Ave cycle time (s)	Truck utilisation (%)	Shovel utilisation (%)	Shovel production (t)	MF
Shovel 1	6	19	835	98	88	46,041	0.89
Shovel 2	7	40	1417	97	92	33,386	0.93
Shovel 3	7	45	1398	97	92	31,068	0.94
Shovel 4	4	24	859	97	85	28,003	0.86

8 Conclusion

This paper presents a developed discrete-event truck-shovel simulation model, referred to as Truck and Shovel JaamSim Simulator (TSJSim), based on a microscopic traffic and truck-allocation approach. The TSJSim simulation model may be used to evaluate the Key Performance Indicators (KPIs) of the truck-shovel mining system in an open-pit mine. TSJSim considers a truck as an individual traffic vehicle unit that dynamically interacts with other trucks in the system as well as other elements of the traffic network. The developed model provides the capability for evaluating the impacts of bunching, intersection traffic management and truck-allocation strategies on a surface mine truck-shovel system. The model can also be used to estimate the optimal truck fleet size for the entire truck-shovel network system.

References

1. Ramani, R. V.: Haulage systems simulation analysis. In: Kennedy, B. A. (ed.) Surface Mining, 2nd edn, pp. 724–739. Society for Mining, Metallurgy, and Exploration, Inc., Littleton, Colorado (1990)
2. Ebrahim, T., John, S., Virginia, I., Danny, T.: Simulation and animation model to boost mining efficiency and enviro-friendly in multi-pit operations. Int. J. Min. Sci. Technol. **25**, 671–674 (2015)
3. Jaoua, A., Riopel, D., Gamache, M.: A framework for realistic microscopic modelling of surface mining transportation systems. Int. J. Min. Reclam. Environ. **23**, 51–75 (2009)
4. Liu, R., Van vliet, D., Watling, D.: Dracula-microscopic, day-to-day dynamic modelling of traffic assignment and simulation. In: Proceedings of the 1995 4th International Conference on Applications of Advanced Technologies in Transportation Engineering, pp. 444–448. ASCE, New York (1996)
5. Larry, E.O., Yunlong, Z., Lei, R., Gene, M.: Street and traffic simulation: traffic flow simulation using CORSIM. In: Proceedings of the 32nd Conference on Winter Simulation, Society for Computer Simulation International, Orlando, FL (2000)
6. Ben-Akiva, M., Cuneo, D., Hasan, M., Jha, M., Yang, Q.: Evaluation of freeway control using a microscopic simulation laboratory. Trans. Res. Part C: Emerg. Technol. **11**, 29–50 (2003)
7. Jaoua, A., Gamache, M., Riopel, D.: Comparaison D'approches De Modélisation De Problèmes Tests Pour Le Pilotage Du Transport, 7ème Conférence Internationale de Modélisation: Optimisation et Simulation des Systèmes MOSIM 08, Paris, France (2008)
8. Alarie, S., Gamache, M.: Overview of solution strategies used in truck dispatching systems for open pit mines. Int. J. Surf. Min. Reclam. Environ. **16**, 59–76 (2002)
9. Lizotte, Y., Bonates, E.: Truck and shovel dispatching rules assessment using simulation. Min. Sci. Technol. **5**, 45–58 (1987)
10. Baafi, E.Y., Ataeepour, M.: Using arena to simulate truck-shovel operation. Min. Resour. Eng. **07**, 253–266 (1998)
11. Hashemi, A.S., Sattarvand, J.: Simulation based investigation of different fleet management paradigms in open pit mines—a case study of Sungun copper mine. Arch. Min. Sci. **60**, 195–208 (2015)
12. Sofranko, M., Wittenberger, G., Skvarekova, E.: Optimisation of technological transport in quarries using application software. Int. J. Min. Miner. Eng. **6**, 1–13 (2015)
13. Que, S., Anani, A., Awuah-Offei, K.: Effect of ignoring input correlation on Truck-Shovel simulation. Int. J. Min. Reclam. Environ. **30**, 405–421 (2016)

14. Rockwell Automation: Arena Simulation Software [Online]. Available: https://www.arenasimulation.com (2017). Accessed 02.05.2018
15. FlexSim Software Products Inc.: FlexSim Simulation Software [Online]. Available: https://www.flexsim.com/ (2018). Accessed 02.05.2018
16. RPMGlobal Holdings Ltd.: Haulage&Loading-TALPAC [Online]. Available: http://www.rpmglobal.com/software/talpac (2018a). Accessed 02.05.2018
17. RPMGlobal Holdings Ltd.: Haulage Simulation-HAULSIM [Online]. Available: http://www.rpmglobal.com/software/haulsim (2018b). Accessed 02.05.2018
18. JaamSim. JaamSim software [Online]. Available: http://jaamsim.com/ (2018). Accessed 02.05.2018
19. Zeng, W., Baafi, E.Y., Walker, D.: A simulation model to study bunching effect of a Truck-Shovel System. Int. J. Min. Reclam. Environ., 1–16 (2017). https://doi.org/10.1080/17480930.2017.1348284
20. Shaw, G.: Proactive Production Estimation and Fleet Management of A Surface Mining Operation. Unpublished BE(Mining) Thesis, University of Wollongong (2012)
21. Nel, S., Kizil, M.S., Knight, P.: Improving Truck-Shovel matching. In: 35th APCOM Symposium—Application of Computers and Operations Research in Minerals Industry, Wollongong. Australasian Institute of Mining and Metallurgy, pp. 381–391 (2012)
22. Machinery Trader: Construction Equipment for Sale [Online]. Sydney, Australia. Available: https://www.machinerytrader.com.au/listings/construction-equipment/for-sale/list/?Mdltxt=785&mdlx=contains&Manu=CATERPILLAR&FullText=CAT+785&byp=1 (2016). Accessed 02.05.2018

Increasing the Productivity of the Transport Fleet by Reducing the Carryback Load

W. Felsch Jr., M. das Graças Silva, C. Arroyo, M. Vinicius Baeta, A. C. Souza, R. Fonseca and A. Curi

1 Introduction

The oscillations in the mining market together with constant changes in the productive process of the companies make it increasingly necessary to apply improvement works that reduce the operational cost and increase the productivity of the organizations.

The transport operation in mining can contribute about 52% of the total production costs, depending on the method of mining adopted and type of ore mined. Therefore, the implementation of an improvement in this step implies a significant impact on the final cost of production [1].

The mine haulage truck selection was based on the following criteria [2]:

– loading tool match required for mining ore and waste,
– availability of capital to and delivery dates,
– productivity rate to achieve the mine plan,
– pit geometry and haulage routes.

In open-pit mining, many parameters can affect the efficiency of the fleet such as [3, 4]:

– mine plan and mine layout
– speed, payload and cycle time
– tire wear and rolling resistance
– age and maintenance of the vehicles

W. Felsch Jr. · M. Vinicius Baeta · A. C. Souza · R. Fonseca
CSN Mineração, Congonhas, Brazil

W. Felsch Jr. · C. Arroyo (✉) · A. Curi
Mining Engineering Department, Federal University of Ouro Preto, Ouro Preto, Brazil
e-mail: carroyo@ufop.edu.br

M. das Graças Silva
Universidade Presidente Antonio Carlos. UNIPAC, Conselheiro Lafaiete, Brazil

– dump site design
– idle time
– engine operating parameters and transmission shift patterns.

   The average load carried has a great impact on the productivity of transport equip-
ment. The retention of material in the trucks' bed is a problem that directly affects the
productive potential of the equipment because it limits the mass transported in each
cycle, besides increasing costs with fuel consumption. These materials tend to accu-
mulate and increase in volume with each loading and unloading performed, which
means that after a few cycles, there is a considerable loss of volume transported.

   This problem known as "Carry Back" is characterized by materials that become
agglutinated in the trucks' bed after unloading the material from the bucket, as shown
in Fig. 1. This retention occurs mainly due to the humidity of the material transported
associated with high alumina and manganese grade.

   High humidity increases the possibility of aggregate particles, resulting in an
increase in the load trapped in the trucks' bed, among other operational factors that
make mining difficult [5].

   The lithotypes that possess the minerals aluminum and manganese have
hydrophilic characteristics, that is, minerals with greater affinities in the absorption
of water, thus making minerals with greater concentration of humidity.

   Aluminum is the most abundant metal element on earth, being the most modern of
common metals, having been isolated in 1825 and introduced to the public in 1855.
Its lack of knowledge over time is due to the fact that, unlike other metallic elements
(copper or iron), it does not occur naturally in its metallic form, always existing in
combination with other elements, mainly oxygen, with which forms an extremely
hard oxide, known as alumina [6].

   The article was developed at the "Casa da Pedra" mine, located in the state of
Minas Gerais, Brazil. The method of mining is open-pit mining, requiring transport
by trucks of both ore and waste. The trucks used in mining have a transportation
capacity of 240 metric tons.

Fig. 1 Examples of carryback load in trucks

There are some solutions in the market aiming to reduce the carryback load, most of them liners made exclusively for truck bed. Among the liners identified, the following stand out: polyethylene-based liners; polyurea-based liners; rubber liners. These liners have several positive and negative aspects in their use. Its viability depends on factors such as type of material transported and dimension of the trucks.

The solution used in the present work consists of the implantation of the technology of heating of the truck floor bed. A comparative analysis was performed between two similar equipment, applied in the same operational conditions, measuring the carryback of both, in two different period. The duration of first period was 7 days, having a requirement that the trucks must be dispatched to the same mining front. The duration of the second period was 30 days, and the trucks were dispatched as if running through normal operation, there were no fixed routes.

Carryback load information is identified through the embedded telemetry system. The concept of telemetry can be defined by the transfer and use of data originated from a network of remote equipment, with the purpose of monitoring, measurement, and control. Communication can be done via fixed network or wireless network.

For the implementation of the monitoring of the equipment through the telemetry, it is necessary that there are specific sensors, correctly installed; persons capable of analyzing parameters and systematic routines of analysis.

To maximize the benefits of using information technology, the mining industry must standardize data formats and protocols for unrestricted data exchange. The adoption of such rules facilitates the provision of real-time data to support managerial decision [7].

2 Objective

The objective of this work is the reduction of operational costs through the increase of productivity and effective use of the haulage fleet. The approach used will be to reduce the volume of carryback load using heated truck bed system. The system disaggregates the material that is hang-up, letting the floor bed without retained material. The reduction of the aggregate material results in the reduction of floor bed cleaning events, generating an increase in the effective use of the haulage fleet.

Secondary objectives include:

– reduction of diesel oil consumption
– agility of material unloading, reducing dumping time
– reduction of the number of occurrences of floor bed cleaning
– extension in the useful life of the beds due to the reduction of the impacts of auxiliary machines performing cleaning.
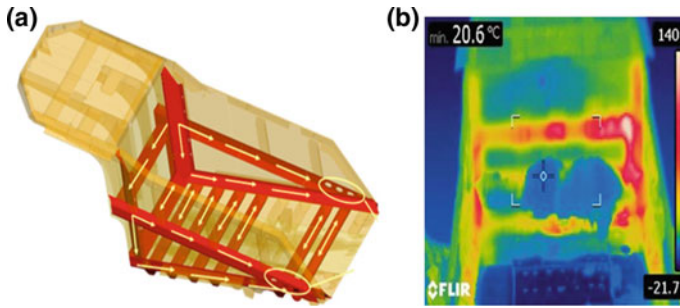
Fig. 2 Illustration of gas impact locations (**a**) and thermal analysis of the active system (**b**)

3 Methodology

The methodology used to reduce the retention of material in the trucks' bed is to use the exhaust gases themselves from the combustion of the diesel engine to heat the internal galleries of the floor bed. Exhaust gases run through the entire bed, until they are exhausted into the atmosphere at the back of it. These gases are not harmful to the useful life of the bed, because they have constant flow, and due to the favorable climate in the region do not condense and do not generate sulfuric acid. The heated bed is designed not to generate backpressure in the engine. With the application of this system of piping and redirection of the gases, the bed will always remain warm and, consequently, the material will not clump [8].

The exhaust system makes a noise as the dump bed is lifted. Noise measurement was performed, resulting in the overall mean of 63.5 dB in the dumping period, which lasts approximately 45 s. The maximum level allowed by Brazilian legislation is 85 dB.

The heating kit will be applied to Caterpillar model 793F trucks with MSDII body (Mine-specific Design). This lightweight body has great use in mining activities around the world [9]. At the "Casa de Pedra" mine, there are 31 trucks in operation, with 8 trucks with MSDII type body. Figure 2a illustrates the locations where the gases impact on the trucks' bed, and Fig. 2b shows the thermal analysis of the active system.

Comparative operational tests were performed with two identical trucks. The equipment used in the test were:

– CM-7924—Caterpillar Model 793F (heated system installed)
– CM-7927—Caterpillar model 793F (without heated system).

As assumptions adopted in the test, the following adjustments were made to the equipment:

– balances and suspensions check
– height and equalization of the adjusted suspensions (10″ in the front suspensions and 8″ in the rear suspensions)

– cleaning the floor bed
– fuel tank full
– allocation of the trucks for loading on the same mining fronts.

The first test was conducted over a period of seven consecutive days, with trucks allocated on the same operational routes through the Intellimine fleet management system. For the second test, the CM-7924 truck was maintained with the heated body system and its results were followed up by another 30 days of operation. The allocations related to this test were dynamic, that is, the optimization algorithm of the Intellimine system was used to direct the equipment to the loading and dumping places.

The type of material transported has great relevance in the test results. High alumina and manganese lithotypes have a property that facilitates the bonding of material in the truck bed along with finer, drier materials. In order to stratify the impact of these materials, a differentiated analysis criterion was proposed. Materials with alumina content above 2% or manganese content above 1% were classified as materials with a high degree of retention impact.

Table 1 shows the list of geological lithotypes contained in the mining.

Figure 3 identifies the lithotypes present in "Casa de Pedra" mine with their respective alumina and manganese content. According to stipulated classification, the lithotypes (CGM, ARG, CEL, IBG, and IBM) were classified as high impact materials in agglutination of transported mass.

The database of the fleet management system (electronic dispatch) was used to store the test data. This information is handled through Structured Query Language (SQL) queries in the Database Management System (DBMS) and displayed through the Report Service (reporting platform integrated with SQL tools and components) [10].

After this treatment, several information is collected, being the most relevant for this work: Haulage mass (t); Average load (t); Number of cycles; material moved lithotype; equipment used for transportation, among others.

Table 1 Geological lithotypes mapped in the "Casa de Pedra" mine

Lithotypes List			
CGM	Ore canga	IBS	Soft siliceous itabirite
ARG	Clay	HBA	Soft hematite
CEL	Colluvium	ICC	Hard carbonated itabirite
IBG	Soft goethite itabirite	HCP	Hard hematite
IBM	Soft manganiferous itabirite	ICS	Hard siliceous itabirite
IBR	Sift high-grade itabirite	RBIB	Soft intrusive basic rock

(%) Global Content - Al / Mn
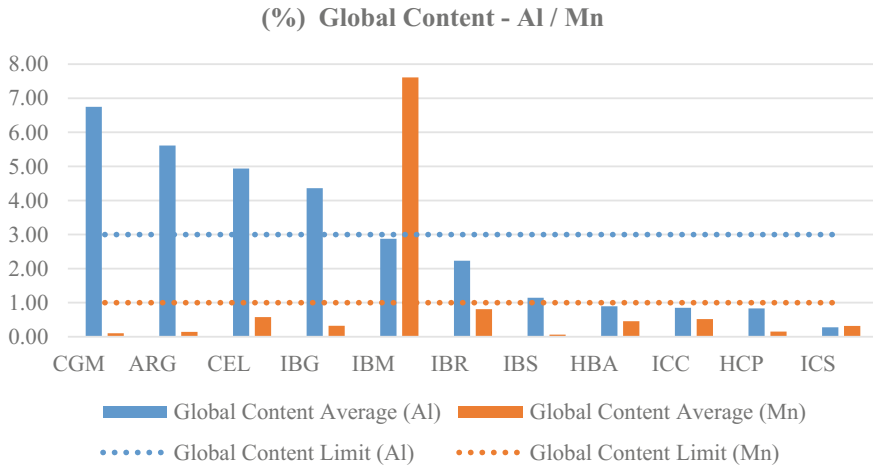
Fig. 3 Average global content of lithotypes related to Alumina and manganese

Table 2 Result of the first operational test for the 7-day operating period

Truck	Number of cycles	Haulage mass (t)	Carryback load (t)	% Carryback load	Average carryback load (t)	% high impact material
CM-7924	142	34.187	117	0.34	0.8	28
CM-7927	247	58.989	1.319	2.24	5.3	34

4 Results

The first operational test carried out (7 days of operation) showed that the truck with the installed system carried 85% less carryback load (volume) compared to the truck that does not have the system. During the test, the CM-7924 truck carried the average carryback load value of 0.8 tons per cycle, while the CM-7927 carried an average value of 5.3 tons per cycle. This information is shown in Table 2. The difference in the number of cycles performed between the equipment was due to corrective maintenance in the CM-7924.

The second test lasted 30 days and generated similar results to the initial test. It was verified that the CM-7924 truck carried 75% lower carryback load compared to CM-7927. The highlight was the identical volume of high impact material transported by trucks through dynamic allocations. The results can be verified in Table 3.

The results of the two test periods are shown in Fig. 4. The CM-7924 truck proved to be more productive in both scenarios.

A secondary analysis was carried out, regarding the carryback load values of each geological lithotype transported. The CM-7924 was more productive in the transport of all types of materials, even in materials more adhered to the bed (lithotypes classified with high impact of agglutination), according to Fig. 5.

Table 3 Result of the second operational test for the 30-day operating period

Truck	Number of cycles	Haulage mass (t)	Carryback load (t)	% Carryback load	Average carryback load (t)	% high impact material
CM-7924	750	211.192	821	0.39	1.1	21
CM-7927	867	223.063	3.846	1.72	4.4	21

Analisys: Carry back (t) X High Impact Material (%)
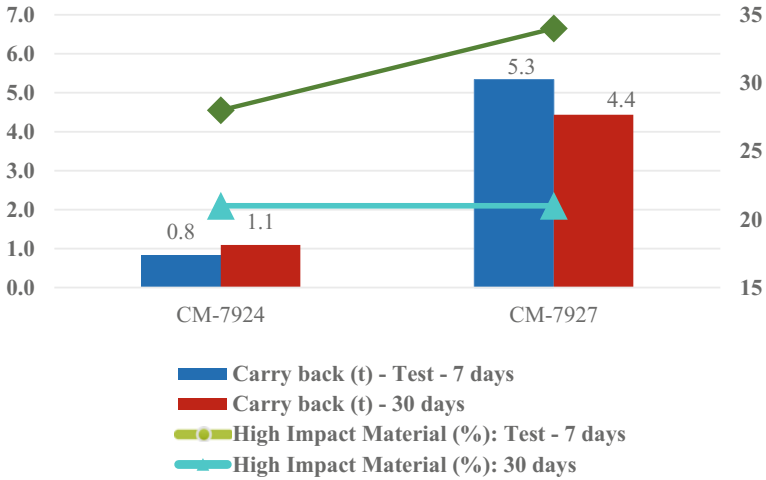
Fig. 4 Consolidated result for carryback and percentage of high impact material

Average Carry back (t) - lithotypes
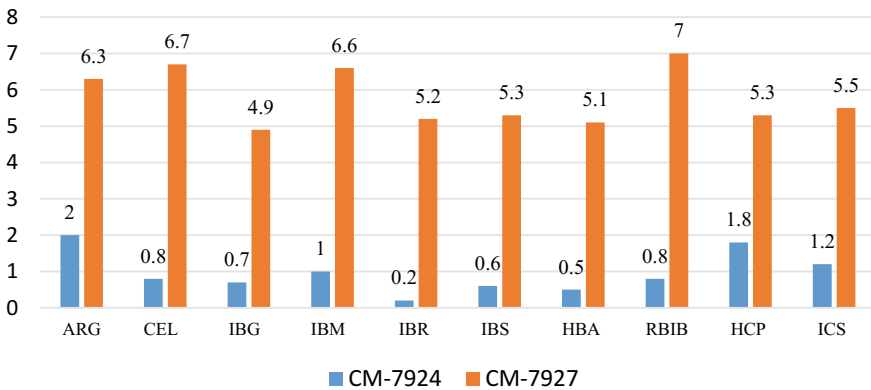
Fig. 5 Average carryback for each lithotype

Gains from reduction of bed floor cleaning and driving to the cleanup site may result in a 0.76% increase in the use of the transportation fleet.

5 Discussion

Production processes are constantly being optimized with the aid of embedded electronics, information technology, and communication systems for real-time information. Remote data transmission technology is a resource of fundamental importance for the mineral sector, since with the economic advance, online communication is an essential factor for strategic decision making and reduction of operational costs.

The accounting of the carryback load through the embedded telemetry system provides the possibility of seeking improvements in the transportation process, with the quantification of the financial gains and viability of the projects.

Material with low-grade minerals retained in truck beds may disintegrate and cause ore contamination as they are dumped to the plants, increasing their dilution.

Several factors can influence the accumulation of carryback load in the floor bed of the trucks of several fleets:

– Rainfall indices
– Type of material loaded and transported
– Dimension of the bed
– Fragmentation index of the material transported
– Type of allocation of the equipment for the loading fronts.

6 Conclusion

Heated bed floor technology was tested on a Caterpillar 793F truck in two distinct periods (7 days and 30 days). The truck tested transported a lower mean carryback volume by 85% on the first test and 75% on the subsequent test compared to other similar sized equipment.

The final result showed that deployment of the technology throughout the transport fleet can result in a 1.8% increase in productivity and 0.76% in the actual use of the equipment.

Among the different geological lithotypes present in the mining, the tests were also favorable to the reduction of the carryback load transported for all types of materials, including those more adherent to the bed (materials classified as high impact).

In addition to improved productivity and fleet utilization, benefits such as increased physical availability of trucks can be identified by extending truck beds lifespan.

The noise emitted by the system does not cause hearing damage to the operators. It can be seen that there is no exposure to levels above 85 dB (maximum level allowed by Brazilian legislation).

References

1. Trueman, E.: In pit crushing: the application and benefits of track mounted crushing equipment. In: Goldfields Mining Expo. Western Austrália. In: National Seminar on New Trends in Cost Effective Iron Ore Mining. Noamundi, Bhar, Índia, 27p (2001)
2. Baloo, D.T.: Equipment selection at Tenke Fungurume Mining. In: Proceedings of Seventeenth International Symposium on Mine Planning and Equipment Selection, Beijing, China, Ed. Univ. Laval/Int. Journal of Mining, Rec. Env., pp. 269–278 (2008)
3. Australian Government: Department of Resources, Energy and Tourism. Analyses of Diesel for Mine Haul and Transport Operations, A Case Study, Australia (2010)
4. Harry, M.J.: Six Sigma Predictability Analysis and Process Characterization. Addison-Wesley Publishing Company, Reading, Massachusetts (1998)
5. Macedo, L., Silva, J., Cintra, M.: Alocação de poços de rebaixamento um estudo de caso no complexo de mineração de Tapira da Vale Fertilizantes. Anais do XVIII Congresso Brasileiro de Águas Subterrâneas. Belo Horizonte/MG, 9p (2014)
6. Mártires, R.: Balanço Mineral Brasileiro, 2001 – Alumínio. Agencia Nacional de Mineração (ANM), (2001). http://www.anm.gov.br/dnpm/paginas/balanco-mineral/arquivos/balanco-mineral-brasileiro2001-aluminio/view. Available to 5 de Março de 2018
7. Knighs, P.F., Daneshmend, L.K.: Open systems standards for computing in the mining industry. CIM Bull. **93**(1042), 89–92 (2000)
8. CSN Mineração: Technical report. "centro de monitoramento de telemetria" (Período: janeiro a Março de 2018)". CSN. Cia Siderúrgica Nacional. Congonhas. Brasil (2018)
9. Caterpillar: Caterpillar Performance Handbook, 47 edn, vol. 2. US Caterpillar Company, Peoria, Illinois, USA (2017)
10. CSN Mineração: Technical report. "Movimentação detalhada" (Período: janeiro a março de 2018)". CSN. Cia Siderúrgica Nacional. Congonhas. Brasil (2018)

Environmental Comparison of Different Transportation Systems—Truck-Shovel and IPCCs—In Open-Pit Mines by System Dynamic Modeling

H. Abbaspour and C. Drebenstedt

1 Introduction

Nowadays, environmental problems of mining activities became an important part such that mine design without considering environmental concerns cannot be acceptable. These environmental concerns are normally defined based on laws that will finally result in a "sustainable design", which not only economic, but also environmental issues are covered [1–4]. The transportation system of any mining project is counted as one of the most crucial sections of the mine that is responsible for a major part of environmental condition in mine sites. Trucks, as the conventional transportation systems in mines, are producing a remarkable amount of emissions and dusts [5–8]. Accordingly, introducing a substitutional transportation system that can reduce these effects is highly in demand. In-Pit Crushing and Conveying (IPCC) systems in which the crusher station is located in the pit and crushed ore or waste transferred to its related destination through the conveyor belt, was introduced in 1956 in Germany [9]. It is used as an alternative to the conventional transportation system (Truck-Shovel system) in surface mining operations [10]. These systems can reduce the environmental effects of transportation, especially by using electricity instead of burning fossil fuels for conveying materials.

Environmental-friendly feature of IPCC systems attracted a few researches to focus on this issue. One of the focusing points was studying the greenhouse gas emission from IPCC systems [11]. The researchers in that study estimated the reduction of greenhouse gas generation by using IPCC systems. Based on a life cycle assessment study, it was shown that using IPCC systems produced 4–22% less greenhouse gases, which the former amount is related to the electricity generated by coal and the latter is electricity generated by natural gas [11]. They also mentioned that this

H. Abbaspour (✉) · C. Drebenstedt
Institute for Mining and Special Civil Engineering, TU Bergakademie
Freiberg, Freiberg, Germany
e-mail: hossein.abbaspour@student.tu-freiberg.de

emission is highly dependent on the transportation distances and annual capacity of the system. In a more or less similar research, the difference of trucks and in-pit crushing and conveying system in the case of using energy and CO_2 emission was investigated [12]. Some other researchers examined the environmental benefits of utilizing conveyor belt against trucks for transferring ore in a gold open-pit mine through the life cycle assessment [13]. They showed that using trucks would result in 300% more potential of acid rain. They also demonstrated that using natural gas instead of coal for producing electricity could reduce the environmental impact by using conveyor belts.

Based on the literature, the concentration was only in the evaluation of just one transportation system, Truck-Shovel or IPCC systems, and a comparison of these systems was not thoroughly investigated. On the other hand, most of these studies are statistical, which do not consider the time during evaluation. Accordingly, this research presents an investigation about the efficiency of different transportation systems in an environmental point of view in a frame of dynamic behavior. Hence, a dynamic model of environmental factors for these systems by system dynamic modeling was built and compared together to choose the one with the highest environmental index.

2 Method

2.1 General Description of System Dynamic Modeling

System Dynamics is a method for modeling, simulating, and analyzing complicated systems to evaluate changes through the time [14]. This method was first developed in the 1950s in order to assist managers to enhance their understanding of the processes. Nowadays, system dynamics is used in all sectors for policy analysis and design. In contrast to statistical modeling, which time has no role in simulation, system dynamics modeling is dealing with the dynamic status of systems, which is the behavior of systems through the time. In system dynamics modeling, the modelers try to recognize the patterns of behavior expressed by important system variables, and then construct a model that can simulate the patterns. When a model has this ability, it can be used as a pilot for testing different scenarios [15]. Generally, there are two different types of system dynamic models: "open systems", which the outputs do not have any effect on their inputs, in contrast with "closed systems" where the outputs can control the inputs. Every system dynamic model consists of constants, auxiliaries, stocks, flows, and feedbacks. They are briefly explained in the following sections.

2.2 Constants and Auxiliaries

All the parameters that form a system dynamic model are divided into two different groups: constants or auxiliaries. Constants are permanently fixed along the system processing, while auxiliaries are defined as an equation among different constants, which might change during system processing [15].

2.3 Stocks and Flows

The main variables in system dynamic are known as stocks and flows. Stocks show results of accumulations over time. Their values are "level", which are also called "states" as they integrally represent the state of the system at any time [16]. Some examples of stock could be number of injuries, fatalities, lost time injuries, accidents, etc. Flows directly flow into and out of the stocks, which lead to changing their levels. They are representative of the "rate of change" in stocks [16]. Emission rate, particulate matter rate, etc., are examples of flows. The unit of the rates must be defined as *quantity/time*. This feature fulfills the possibility of accumulation of the stocks during the time. The graphical representation of stock and flow diagram is as Fig. 1. The general equation of any stock–flow diagram can be described as

$$\frac{d(\text{Stock})}{dt} = \text{Inflow(t)} - \text{Outflow(t)} \tag{1}$$

2.4 Feedback and Feedback Loops

Although stocks and flows are both necessary and sufficient for generating dynamic behavior, they are not the only components of system dynamics. In a more precise description, the stocks and flows in real-world systems, that may get feedback from each other, are part of a feedback loop. These feedback loops could be consisted of different feedbacks and occasionally connected together via nonlinear couplings that often cause counterintuitive behavior [15]. Figure 2 shows a simple stock–flow system with a feedback that connects stock to inflow.

Generally, closed systems are controlled by positive or negative feedback loops. Positive loops depict "self-reinforcing" processes, which an action creates a result

Fig. 1 A schematic view of a simple stock and flow diagram
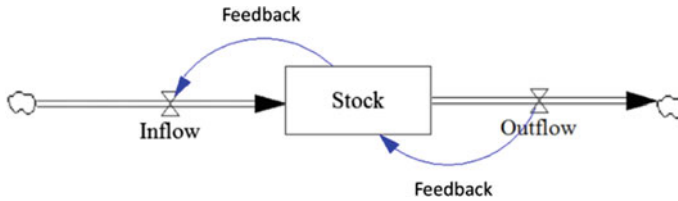
Fig. 2 Feedback loop in a stock–flow diagram

that generates more of the action, and hence more of the result. Positive feedback loop processes make systems unstable and force them to change their current state. Accordingly, they are responsible for the growth or decline of systems [15]. On the other hand, negative feedback loops, define "goal-seeking" processes that generate actions aimed at moving a system toward, or keeping a system in a desired state. In general, negative feedback loop processes stabilize systems, although they may occasionally destabilize them by causing them to oscillate [15].

2.5 The Concept of In-Pit Crushing and Conveying (IPCC) Systems

In Truck-Shovel system in open-pit mines, the material is transferred from inside the pit to the destinations outside, which are crusher station for ore and waste dump for waste. However, in the In-Pit Crushing and Conveying (IPCC) systems, the crusher station is located in the pit and crushed ore or waste transferred to its related destination through the conveyor belt. The idea of using this system was introduced in 1956 in Germany [9]. It was used as an alternative to the conventional transportation system (Truck-Shovel system) in surface mining operations [10]. It generally resolves many deficits of Truck-Shovel system, e.g., reducing operating costs [17] mainly because of the reduction of the labor force and fuel consumption [18]. In addition, in safety point of view, conveyor belts (as one of the important parts of IPCCs) showed lower quantity of accidents, injuries, and fatalities [19]. Despite of these advantages, there are still some particular attitudes to its flexibility [20], reliability, and efficiency [21].

Generally, this system is categorized into four different types: (1) Fixed In-Pit Crushing and Conveying (FIPCC) system, in which the location of the crusher is fixed along the mine's life. Commonly, the position of this type of IPCC systems is near the pit rim or inside, which is not affected by mining operations. (2) Semi-Fixed In-Pit Crushing and Conveying (SFIPCC) system is located in a strategic junction point in the pit and mostly is fed by the mining trucks. Its relocation needs disassembly of the entire crusher station into several parts or multiple modules. (3) Semi-Mobile In-Pit Crushing and Conveying (SMIPCC) system, which is usually located at the operational level. It is possible to be fed through trucks or loaders from

different loading points. (4) Fully Mobile In-Pit Crushing and Conveying (FMIPCC) system, which can continuously change its location and benefit from an integrated transportation mechanism [22].

The common feature of FIPCC, FMIPCC, and SMIPCC is that trucks perform feeding and conveyor belt transfers crushed material outside the pit. In fact, these systems are a combination of two transporting equipment: trucks and conveyor belt. On the other hand, shovels directly feed FMIPCC and the conveyor belt is responsible for transporting crushed material.

3 Modeling in System Dynamic

The primary step in building a system dynamic model is to define its constants and variables, which determine the system behavior. Unlike constants, which are fixed during the simulation, variables including auxiliaries, flows, and stocks can change during simulation. In addition, they interactively influence each other and the whole system.

In spite of this fact that numerous items can be described as influencing factors on environmental condition, however, more relevant and measurable factors in the transportation system are considered. Accordingly, the following items are taken into account for building the system dynamic model and measuring the environmental index of the system:

– total emissions (CO_2, SO_2, and NO_x)
– total particulate matter ($PM_{2.5}$, PM_{10}, and PM_{30})
– total water consumption.

The total emissions, particulate matter, and water consumption comprise the total emissions, particulate matter, and water consumption in trucks and conveyor belt. A general view of the system dynamic built for defining the environmental index of the transportation system of an open-pit mine is shown in Fig. 3. Each part of this model is shown in Figs. 4 through 6, which are total emissions, total particulate matters, and total water consumption, respectively.

3.1 Total Emissions (CO_2, SO_2, and NO_x)

Trucks and conveyor belts are the most important transportation equipments in Truck-Shovel and IPCC systems, respectively, produce different kind of emissions while operating. Trucks and conveyor belts generate emissions through burning fossil fuels and electricity consumption generated from different sources of energy (e.g., coal, oil, peat, and natural gas). This introduces truck as a direct source of emissions and the conveyor belt as an indirect source of emission. The most significant and well-

Fig. 3 System dynamic model for environmental index of transportation system in an open-pit mine

Fig. 4 System dynamic model for total emissions

known emissions are considered as CO_2, SO_2, and NOscattered into the surroundin. Therefore, in this study, these emissions are evaluated.

Emission factor is one of the most important items that determine the quantity of emission; however, it can be different from one place to another [23–25]. Accordingly, one of the main tasks is to determine these factors. In this research, it is assumed that lignite is burnt in the power plant to produce electricity. In addition, the fuel of trucks is considered as diesel. With these assumptions, the related emission factors for CO_2, SO_2, and NO_x are calculated according to Eqs. 3 through 5.

Fig. 5 System dynamic model for total particulate matters
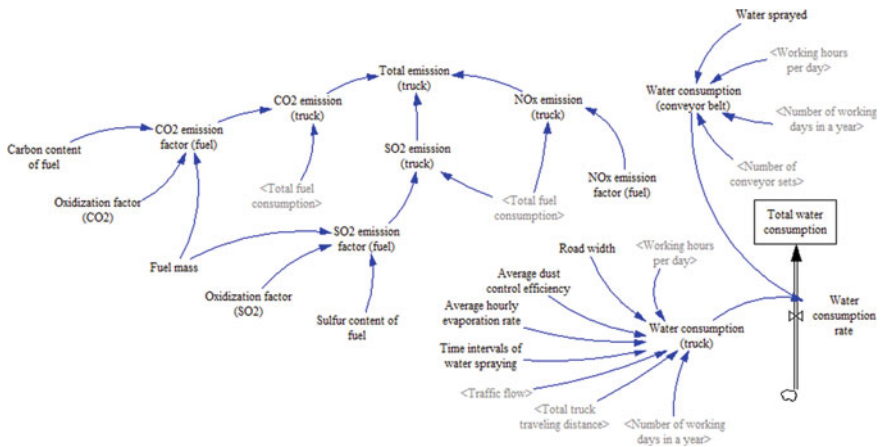
Fig. 6 System dynamic model for total water consumption

Table 1 Emission factors of CO_2, SO_2, and NO_x in conveyor belts

Emission factor	Equation/Quantity	Unit	References
CO_2	0.36	kg/kWh	[29]
SO_2	SO_2 coefficient × Weight percent of sulfur in fuel	kg/t	[30]
NO_x	6.81	kg/t	[30]

3.1.1 Total Emissions of Conveyor Belt

For calculating the emissions from the conveyor belt, it is necessary to quantify the burnt fuel for producing electricity. Therefore, the concepts of heat rate and heat content need to be introduced. Heat rate is the energy consumed by a power plant or an electrical generator to produce one kilowatt-hour (kWh) of electricity [26] while heat content means how much energy will be produced by burning a specific amount of fuel. The former is expressed in Btu/kWh and the latter is defined in Btu/t. Hence, Eq. (2) for calculating the amount of burnt fuel is defined

$$\text{Burnt fuel} = \frac{\text{Heat rate}}{\text{Heat content}} \left(\frac{t}{\text{kWh}} \right) \tag{2}$$

In this model, it is assumed that coal is burnt in power plants for producing electricity. Hence, the quantity of heat rate and heat content would be 10,059 Btu/kWh and 21.258 MBtu/t, respectively [27, 28]. Regarding the emission factors of CO_2, SO_2, and NO_x (Table 1), Eqs. (3), (4), and (5) for the determination of CO_2, SO_2, and NO_x can be defined as

$$\begin{aligned} CO_2 \text{ emission} = {}& CO_2 \text{ emission factor} \times \text{Conveyor power} \\ & \times \text{Number of working days in a year} \\ & \times \text{Working hours per day} \end{aligned} \tag{3}$$

$$\begin{aligned} SO_2 \text{ emission} = {}& \text{Burnt fuel} \times SO_2 \text{ emission factor} \\ & \times \text{Conveyor power} \times \text{Number of working days in a year} \\ & \times \text{Working hours per day} \end{aligned} \tag{4}$$

$$\begin{aligned} NO_x \text{ emission} = {}& \text{Burnt fuel} \times NO_x \text{ emission factor} \\ & \times \text{Conveyor power} \times \text{Number of working days in a year} \\ & \times \text{Working hours per day} \end{aligned} \tag{5}$$

Table 2 Emission factors of CO_2, SO_2, and NO_x in trucks

Emission factor	Quantity	Unit	References
CO_2	2.622	kg/L	[31]
SO_2	2.47×10^{-5}	kg/L	[31]
NO_x	0.034	kg/L	[32]

3.1.2 Total Emissions of Trucks

The emission of trucks is originated from burning fuels in trucks' engines. There-fore, in contrast with the conveyor belt, which indirectly considered as an agent of emission, trucks are directly responsible for emissions and pollution. As the first step for evaluating emissions from trucks, it is required to determine the emission factors of CO_2, SO_2, and NO_x. In the case of CO_2 and SO_2, Eqs. (6) and (7) are introduced based on the content of carbon and sulfur in diesel fuel [31]

$$(44/12) \times \text{Oxidization factor } (CO_2) \times \text{Carbon content of fuel} \times \text{Fuel mass} \quad (6)$$

$$(64/32) \times \text{Oxidization factor } (SO_2) \times \text{Sulfur content of fuel} \times \text{Fuel mass} \quad (7)$$

"44/12" and "64/32" represent the portion of the molecular weight of CO_2 and SO_2 to the molecular weight of carbon and sulfur, respectively. Oxidization factors depict that how much percent of carbon or sulfur are changed to CO_2 and SO_2 after burning, respectively. In fact, in a complete combustion, 100% of carbon and sulfur are burnt. However, in most cases, it is not happening and a percentage of carbon and sulfur remain unburnt. Therefore, the oxidization factors for CO_2 and SO_2 in this study is considered as 99 and 98%. The carbon and sulfur content of fuels are different from one to another. However, for diesel fuel, the carbon and sulfur content of fuels are generally 86% and 15 ppm of the fuel mass, respectively. Fuel mass (diesel mass) is also set as 840 (g/L). Table 2 shows a summary of emission factors of diesel fuel in trucks. By multiplying the emission factors of CO_2, SO_2, and NO_x in total fuel consumption of trucks, their relevant emissions will be determined. The total emissions of the truck will be the sum of the emissions of CO_2, SO_2, and NO_x.

3.2 Total Particulate Matters ($PM_{2.5}$, PM_{10}, and PM_{30})

Particulate Matter (PM) is a definition for a mixture of solid and liquid particles that are scattered into the surrounding air [33]. There are different forms of classification for particulate matter; however, the most famous classification forms are categorizing by their physical size. Particle size is generally based on the aerodynamic diameter [33]. The abbreviation PM_x denotes all particles with a diameter less than x microm-

Table 3 Emission factors of particulate matter in transition points of conveyor belt

PM_x	Quantity (g/t)	References
$PM_{2.5}$	6.5×10^{-6}	[34]
PM_{10}	2.3×10^{-5}	[34]
PM_{30}	7×10^{-5}	[34]

eters (μm). The most common diameter considered in research is $PM_{2.5}$, PM_{10}, and PM_{30}.

In transportation system of a mine, various sources of particulate matters can be recognized. For instance, the transition points between conveyor sets (chutes) and wind erosion in transferring material by conveyor belt and the particulate matters from haul roads and wind erosion in moving material by trucks, are the main sources.

3.2.1 Particulate Matter Generated from the Conveyor Belt

In the crushing process, different factors can affect the emission of particulate matters such as rock type (ore or waste type), feed size and distribution, moisture content, output rate, crusher type, size reduction ratio, and fines content [34]. Different emission factors of particulate matter are provided in any steps of crushing through various references [34]. Since crusher for all the transportation systems is assumed the same, the transition points of conveyor belt (chutes) as the most important source of generating particulate matters are merely considered. These emission factors are shown in Table 3. These quantities can be measured and modified for any project. Equation (8) can be set for calculating the total amount of particulate matter 2.5, 10, and 30 based on the production rate

$$\text{Emission of } (PM_{2.5}, PM_{10}, PM_{30}) = \text{Number of conveyor sets} \times \text{Production per year}$$
$$\times \text{Emission factor } (PM_{2.5}, PM_{10}, PM_{30}) \quad (8)$$

3.2.2 Particulate Matter Generated from Trucks

Generally, in mine site, trucks are moving on roads and ramps that are unpaved. This causes of dust generation in a way that when a truck travel on the road, surface materials are pulverized due to the forces of the trucks' wheel. Consequently, these powder materials lifted and dropped continuously by rolling wheels. In addition, by passing truck, a turbulent is generated behind it, which worsens this situation [35]. As previously described, emission factor is the most important part of calculating the particulate matter. For trucks traveling on unpaved surfaces at industrial sites, the emission factor (9) is defined [35] as

Table 4 The constant of emission factor of particulate matters from trucks in industrial roads (EPA 1995)

Constant	$PM_{2.5}$	PM_{10}	PM_{30}
k (lb/VMT)	0.15	1.5	4.9
A	0.9	0.9	0.7
B	0.45	0.45	0.45

$$\text{Emission factor of PM}_x = k \left(\frac{s}{12} \right)^a \left(\frac{W}{3} \right)^b \tag{9}$$

where s is surface material silt content (%), W is mean vehicle weight (t), k is the emitted particulate matter in pound per vehicle mile traveled[1] (lb/VMT), and a and b are constants (Table 4).

Based on the definition of PM_x, PM_{30} consisted of both PM_{10} and $PM_{2.5}$. Accordingly, the total emission of particulate matter of trucks can be estimated from Eq. (10)

$$\text{Total PM} = \text{Emission factor PM}_{30} \times \text{Number of cycles}$$
$$\times \text{Total truck traveling distance} \times 2 \tag{10}$$

3.3 Total Water Consumption

In the transportation system of a mine, there are different means of water consumption. In trucks and conveyor belts, water is mostly consumed for dust suppression caused by trucks movement and in transition points at conveyor belts. However, there are other sources of water consumption, e.g., the cooling system of trucks and washing. The water consumption in this model is considered as the total water is consumed for particulate matter suppression caused by trucks and conveyor belts.

The control efficiency of spraying water is as Eq. 11 [36]:

$$C = 100 - \left(\frac{0.8 \times p \times d \times t}{i} \right) \tag{11}$$

where p is potential average hourly daytime evaporation rate (mm/h), d is the average hourly daytime traffic rate (vehicles/h), i is the application intensity of water (lit/m^2), and t represents the time between watering applications (h). The goal is to find the water intensity (i) with the assumption of a road width of 30 m. In the model, c, p, and t are set as 75%, 0.28 mm/h, and 0.5 h, respectively. For suppression of dust in transition points of conveyor belt, a rate of 20 L per minute of water sprayed is

---

[1]VMT is calculated by adding up all the miles driven by all the cars and trucks on all the roadways in a region.

considered. Hence, the water needed in conveyor belt in order to suppress the dust is calculated from Eq. (12)

$$\text{Water sprayed(lit/min)} \times \text{Number of working days in a year} \\ \times \text{Working hours per day} \times \text{Number of conveyor sets} \times 60 \qquad (12)$$

3.4 Environmental Index

As it mentioned before, the environmental factors that are used for defining the environmental index of the transportation system are total emissions, total particulate matter, and total water consumption. The relation of the environmental index with each of these factors is inversely proportional, in which the higher emissions, particulate matter, and water consumption resulted in worst environmental situation and the environmental index would be decreased. Accordingly, the Environmental Index (EI) can be defined as Eq. (13)

$$\text{EI} = \frac{10^6}{\text{Total emissions} + \text{Total PMs} + \text{Total water consumption}} \qquad (13)$$

The environment index is defined as 100 at the start of the project and it would be reduced by progressing the project through the years because of the expansion of the transportation system.

4 Results and Discussion

A hypothetical copper mine with a reserve of 700 million tonnes was simulated during its life. Based on Taylor's method [37], the mine's life and annual production calculated by the Eqs. (14) and (15), respectively.

$$T = 0.2(\text{ore reserve})^{0.25} \qquad (14)$$
$$\text{Production per Year} = 5(\text{ore reserve})^{0.75} \qquad (15)$$

Accordingly, the mine's life and production per year of the project were 32.53 years (2049 as the final year of the project) and 21.52 million tonnes, respectively.

Year 2016 is considered as the start of the ore extraction. The model was run for five transportation systems of the Truck-Shovel, FIPCC, SFIPCC, SMIPCC, and FMIPCC. The technical parameters considered in the simulations are represented in Table 5.

Table 5 Technical parameters in dynamic simulation of the model

Parameter	Quantity	Unit
Working days in a year	350	
Working hours per day	22	(h)
FIPCC relocation's year	2030	
Depth of relocation of FIPCC	150	(m)
First year of SFIPCC relocation	2018	
Intervals of relocations of SFIPCC	4	(years)
Depth of relocation of SFIPCC	100	(m)
Last year of SFIPCC relocation	2040	
First year of SMIPCC relocation	2018	
Intervals of relocations of SMIPCC	2	(years)
Depth of relocation of SMIPCC	70	(m)
Last year of SMIPCC relocation	2040	
Average FMIPCC advancement rate in depth	40	(m/year)
Average faces advancement rate in depth	40	(m/year)

4.1 Total Emissions

As it can be seen in Fig. 7, the total emissions (CO_2, SO_2, and NO_x) increase by progressing the project due to increasing the quantity of trucks and conveyors sets. However, the total emissions in FMIPCC system are lower than others along mine's life. It can be interpreted as the lack of trucks in this system, which is one of the most dominant sources of emissions. In addition, it shows that producing electricity in power plant for using in FMIPCC system generates fewer emissions in comparison with its equivalent Truck-Shovel system, which directly uses fuels. In fact, it is more environmentally friendly to use electricity in transportation system even considering that lignite is burnt to generate electricity. In other systems and until 2028, the difference in emission is not considerable; however, afterward SMIPCC and SFIPCC generated more emission.

4.2 Total Particulate Matter

The total particulate matter emitted from FMIPCC system is the lowest and has a considerable difference with others (Fig. 8). As it was expected, the total particulate matter of the Truck-Shovel system is the highest due to the higher number of trucks, which are the most important sources of particulate matters. FIPCC produces the same level of particulate matter until 2031; however, after this year, which relocation
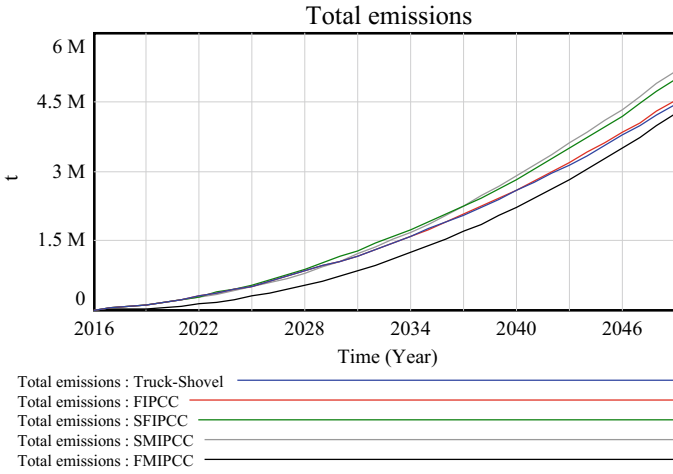
Fig. 7 Total emission from different transportation systems
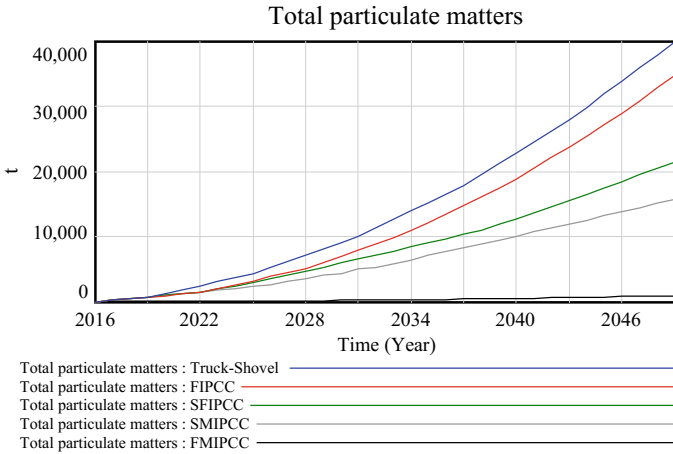
Fig. 8 Total particulate matters emitted from different transportation systems

happens, the number of trucks does not increase anymore and conveyor belt system is inserted. This results in lower particulate matters of FIPCC rather than Truck-Shovel system after 2031. SFIPCC shows the higher amount of particulate matters rather than SMIPCC. This can be explained based on the lower relocations in this system, which results in using more trucks rather than SMIPCC.
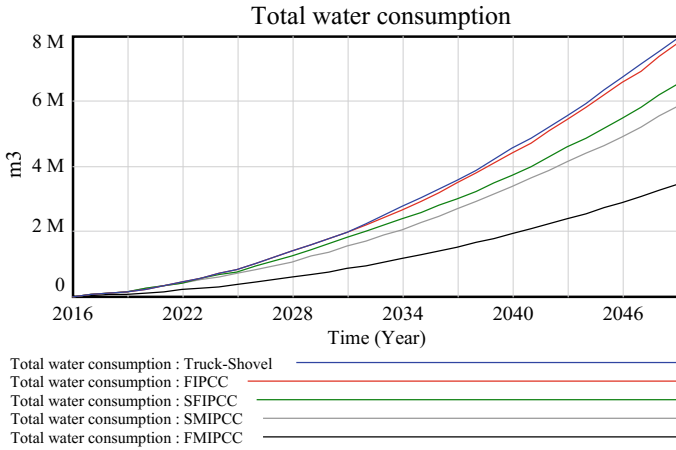
Fig. 9 Total water consumption in different transportation systems
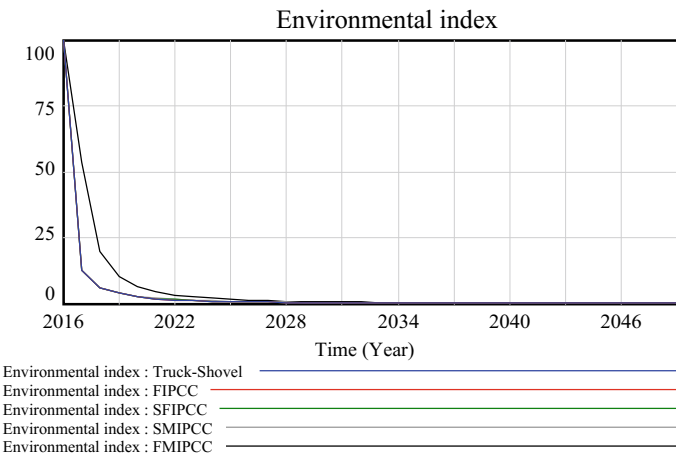
Fig. 10 Environmental index of different transportation systems

4.3 Total Water Consumption

In this study, the total water consumption was considered as the water needed for the dust suppression in the site area. Accordingly, the water consumption of FMIPCC system shows the lowest (Fig. 9) because of not using trucks in this system. On the other hand, dust generated in the conveyor system, especially in transition points (chutes) is considerably lower than dust generated by trucks. Similar to the particulate matter emission, SMIPCC consumes lower water than SFIPCC, FIPCC, and Truck-Shovel systems.

Table 6 Ranking of different transportation systems based on the environmental index

Transportation system	Total emissions ranking lowest (1) to highest (5)	Total particulate matters lowest (1) to highest (5)	Total water consumption lowest (1) to highest (5)	Environmental index best (1) to worst (5) 2016–2019 /2019–2021 /2021–2049
Truck-Shovel	2	5	5	2/4/3
FIPCC	3	4	4	2/4/3
SFIPCC	4	3	3	2/2/2
SMIPCC	5	2	2	2/3/2
FMIPCC	1	1	1	1/1/1

4.4 Environmental Index

According to the environmental factors, which are, the environmental index based on the Eq. (13) would be as Fig. 10. It is clear from Fig. 10, FMIPCC system stands as the first rank with a high difference rather than others. This can be concluded because of the lowest amount of emissions, particulate matters and water consumption in this system. From 2016 to 2019 (Fig. 11a), other transportation systems, i.e., Truck-Shovel, FIPCC, SFIPCC, and SMIPCC, show the same environmental index. However, from 2019 to 2021 (Fig. 11b), SMIPCC is near the FIPCC and SFIPCC systems and from 2021 until the end of the project (Fig. 11c), SMIPCC depicts a better environmental index rather than SFIPCC. Table 6 reports a ranking for different types of transportation systems based on emissions, particulate matters, water consumption, and environmental index.

The following points need to be considered while building and running the model:

1. In spite of numerous environmental factors, which are resulted from mining activities, this model considered the most important factors including emissions, particulate matters, and water consumption.
2. It is possible to add any other environmental factor into the model; however, it is important to recognize its proper location and connection with other variables in the model.
3. The result of the model was based on fixed inputs and obviously can be changed by modelers. However, attention needs to be paid in this case, while the conclusion can be totally affected by taking inputs.
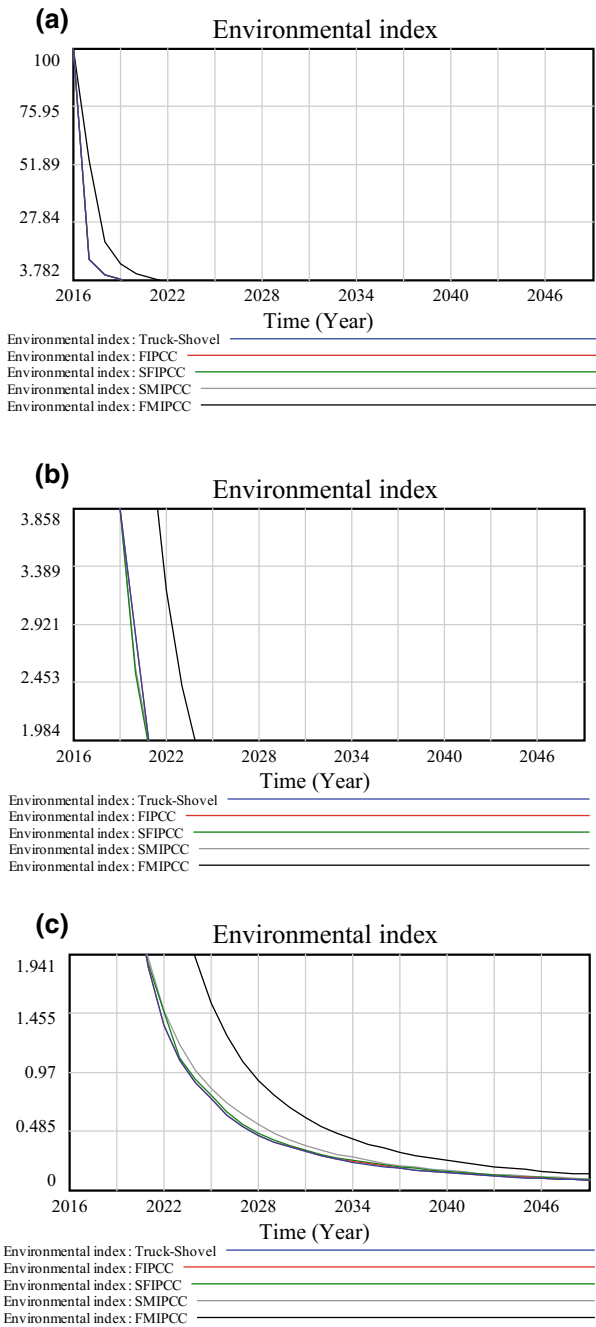
Fig. 11 Environmental index of different transportation systems **a** 2016–2019, **b** 2019–2021, **c** 2021–2049

5 Conclusion

Transportation system of any mining project counted as one of the most significant sources of environmental issues. Accordingly, it is favorable for planners to select the most environmental-friendly transportation system, especially in the case of high sensitivity in environmental concerns. In this paper, five transportation systems, i.e., the Truck-Shovel, FIPCC, SFIPCC, SMIPCC, and FMIPCC systems were introduced. A system dynamics model, based on the environmental factors of total emissions, total particulate matters, and total water consumption, for evaluating the environmental index of these systems was built. This model was able to evaluate the environmental index of each transportation system in the mine's life, which based on them a decision could be made. In all environmental factors, FMIPCC system stood at the first rank with the highest environmental index, which the reason can be interpreted as the lack of trucks, as the most important sources of emissions, particulate matters, and water consumption. On the contrary, the Truck-Shovel system is placed at the fifth rank due to operating trucks in this system.

References

1. Moran, C., Lodhia, S., Kunz, N., Huisingh, D.: Sustainability in mining, minerals and energy: new processes, pathways and human interactions for a cautiously optimistic future. J. Cleaner Prod. **84**, 1–15 (2014)
2. Lodhia, S., Hess, N.: Sustainability in mining, minerals and energy: new processes, pathways and human interactions for a cautiously optimistic future. J. Cleaner Prod. **84**, 43–50 (2014)
3. Gomes, C.M., Kneipp, J.M., Kruglianskas, I., Barbieri da Rosa, L.A., Bichueti, R.S.: Management for sustainability in companies of the mining sector: an analysis of the main factors related with the business performance. J. Cleaner Prod. **84**, 84–93 (2014)
4. Dubiński, J.: Sustainable development of mining mineral resources. J. Sustain. Min. **12**, 1–6 (2013)
5. Kecojevic, V., Komljenovic, D.: Haul truck fuel consumption and CO_2 emission under various engine load conditions. Min. Eng. **12**, 44–48 (2010)
6. Soofastaei, A., Aminossadati, S., Kizil, M., Knights, P.: A comprehensive investigation of loading variance influence on fuel consumption and gas emissions in mine haulage operation. Int. J. Min. Sci. Technol. **26**, 995–1001 (2016)
7. USBM: Cost-effectiveness of Dust Controls Used on Unpaved Mine Haul Roads. United States Bureau of Mines Report, Minneapolis (1983)
8. Soofastaei, A., Aminossadati, S., Kizil, M., Knights, P.: Simulation of payload variance effects on truck bunching to minimise energy consumption and greenhouse gas emissions. In: Coal Operators' Conference, University of Wollongong (2015)
9. Ritter, R., Herzog, A., Drebenstedt, C.: Automated dozer concept aims to cut IPCC downtime. Eng. Min. J., 52–55 (2014)
10. Radlowski, J.K.: In-pit crushing and conveying as an alternative to an all truck system in open pit mines. The University of British Columbia, Cracow, Poland (1988)
11. Norgate, T., Haque, N.: The greenhouse gas impact of IPCC and ore-sorting technologies. Min. Eng., 13–21 (2013)

12. Raaz, V., Mentges, U.: Comparison of energy efficiency and CO_2 emissions for trucks haulage vs in-pit crushing and conveying of materials: calculation methods and case studies. SME Annual Meeting, Denver (2011)
13. Awuah-Offei, K., Checkel, D., Askari-Nasab, H.: Evaluation of belt conveyor and truck haulage systems in an open pit mine using life cycle assessment. CIM Bull. **4** (2009)
14. Pruyt, E.: Small System Dynamics Models for Big Issues. TU Delft Library, Delft, Netherlands (2013)
15. Radzicki, M.J., Taylor, R.A.: Introduction to System Dynamics, A Systems Approach to Understanding Complex Policy Issues. Sustainable Solutions, Inc., USA (1997)
16. Barlas, Y.: System Dynamics. Encyclopedia of Life Support System, Oxford, UK (2009)
17. Terezopoulos, N.: Continuous haulage and in-pit crushing in surface mining. Min. Sci. Technol., 253–263 (1988)
18. Dean, M., Knights, P., Kizil, M.S., Nehring, M.: Selection and planning of fully mobile in-pit crusher and conveyor systems for deep open pit metalliferous applications. AusIMM, 219–225 (2015)
19. Hill, J.: An assessment of the effectiveness of safety interventions in the field of bulk material handling. In: International Materials Handling Conference, Pretoria (2011)
20. McCarthy, B.: Evaluating the lack of flexibility against the benefits of in-pit crushing and conveying. In: Optimizing Mine Operations Conference, Toronto (2013)
21. Dzakpata, I., Knights, P., Kizil, M.S., Nehring, M., Aminossadati, S.M.: Truck and shovel versus in-pit conveyor systems: a comparison of the valuable operating time. In: Coal Operators' Conference, University of Wollongong (2016)
22. Ritter, R.: Contribution to the capacity determination of semi-mobile in-pit crushing and conveying systems. Quality Content of Saxony (qucosa), TU Bergakademie Freiberg (2016)
23. USEPA: Compilation of Air Pollutant Emission Factors, North Carolina. United States Environmental Protection Agency (1995)
24. SPCC: Air Pollution from Coal Mining and Related Developments, Sydney. State Pollution Control Commission (1983)
25. NERDC: Air Pollution from Surface Coal Mining: Volume 2 Emission Factors and Model Refinement. National Energy Research and Demonstration Council (1988)
26. EIA: U.S. Energy Information Administration. 10 May 2017. [Online]. Available: https://www.eia.gov/tools/faqs/faq.php?id=107&t=3
27. EIA: Annual Electric Generator Report. U.S. Energy Information Administration (2015)
28. EIA: Monthly Energy Review. U.S. Energy Information Administration (2017)
29. Quaschning, V.: Regenerative energiesysteme. Carl Hanser, München (2015)
30. Eastern Research Group, Inc.: Uncontrolled Emission Factor Listing for Criteria Air Pollution. Emission Inventory Improvement Program (EIIP), United States Environmental Protection Agency (2001)
31. EPA: Average Carbon Dioxide Emission Resulting from Gasoline and Diesel Fuel. Environmental Protection Agency, Washington (2005)
32. EPA: Compilation of Air Pollutant Emission Factors. Environmental Protection Agency, Ann Arbor (1985)
33. Vallius, M.: Characteristics and sources of fine particulate matter in urban air. The National Public Health Institut, Kuopio (2005)
34. EPA: Crushed Stone Processing and Pulverized Mineral Processing. Compilation of Air Pollutant Emission Factors, North Carolina. U.S. Environmental Protection Agency (1995)
35. EPA: Miscellaneous Sources. Compilation of Air Pollutant Emission Factors, North Carolina. U.S. Environmental Protection Agency (1995)
36. Cowherd, C., Muleski, G.E., Kinsey, J.S.: Control of Open Fugitive Dust Sources. U. S. Environmental Protection Agency, Research Triangle Park, North Carolina (1988)
37. Hustrulid, W., Kuchta, M., Martin, R.: Open Pit Mine Planning and Design. Taylor & Francis Group, Boca Raton, Florida (2013)

Truck-and-Loader Versus Conveyor Belt System: An Environmental and Economic Comparison

C. M. de Almeida, T. de Castro Neves, C. Arroyo and P. Campos

1 Introduction

The oscillation in commodities prices and the significant increase in operating costs have made the mining sector seek to obtain processes that are more and more efficient. In addition, some other factors, such as the relationship with stakeholders and increased environmental and social responsibilities, complement the main motivations for organizations to look into better processes [1–4].

In this scenario, the mapping of an organization's operational processes assists in identifying the stages that most contribute to the high costs of the most inefficient processes [5]. The main mining stages involved in the production of ore in open-pit mines are rock blasting, loading, and transportation, in which the latter can be responsible for 40–60% of the mining costs [3, 6, 7].

The definition of the best transportation method becomes, therefore, fundamental for obtaining the most efficient and cheapest mining process. In addition, environmental and social factors need to be taken into account, since these systems can generate waste, emit gases [8, 9], noise and dust [10], which impacts the residents near the mine, if any, and the environment as a whole.

According to [3], the conventional mining method consists of transportation by trucks that are loaded by loaders or excavators. Lopes also presents the belt conveyor system as an efficient method for transportation of ore into the mine.

C. M. de Almeida · T. de Castro Neves
Samarco, Mariana, Brazil

C. Arroyo (✉)
Mining Engineering Department, Federal University of Ouro Preto, Ouro Preto, Brazil
e-mail: carroyo@ufop.edu.br

P. Campos
Mining Engineering Department, Federal University of Minas Gerais, Belo Horizonte, Brazil

The objective of this study is to carry out a comparison between two ore transportation methods in open-pit mines: conveyor belts and trucks. As to specific objectives, it seeks to point out their main applications, advantages, disadvantages, and differences according to the criteria of environmental and social costs and impacts. The study is relevant for academia and companies, since in addition to filling this knowledge gap, it can also help organizations to understand the different possibilities of ore transportation and its advantages for a possible application.

2 Methodology

The first strand of the research is theoretical, with a qualitative approach, characterized as a literature review, and assesses studies that deal with the proposed themes. The second aspect is empirical, with a quantitative approach, characterized as an experimental research. It is sought, through experimental simulation, to obtain practical results for ore transportation with truck and with belts. It was simulated, then, the equipment design for ore movement per different Average Haulage Distances (AHT), seeking to obtain results for each scenario with both methods. The data will be analyzed according to the main results of this simulation, such as cost and consumption of inputs, waste disposal and manpower required in each scenario.

3 Literature Review

In general, the objective of any mine operation is to mine the ore and have it transported to the processing plant, considering the lowest cost and respecting the environmental, health, safety and social responsibility guidelines [11, 12]. Each open-pit mine is different and should be evaluated and analyzed before determining the most applicable and affordable transportation solution. Due to the high operational costs of trucks, many mining companies tend to seek alternatives that may present lower costs, such as the continuous operation with the use of conveyor belts [13].

3.1 Truck Haulage

Conventional mining with truck haulage, a completely discontinuous system [14], consists of material dismantling, which can be carried out mechanically or with the use of explosives, loading with loaders or excavators and transporting by trucks to the hopper (ore transfer equipment to the belt that will convey the material), crushing or stockpile, in the case of ore, as exemplified in Fig. 1, or to the waste dumps.

In open-pit mines, truck haulage is the classic method and is the most commonly used transportation system in mining operations [3, 14, 16].
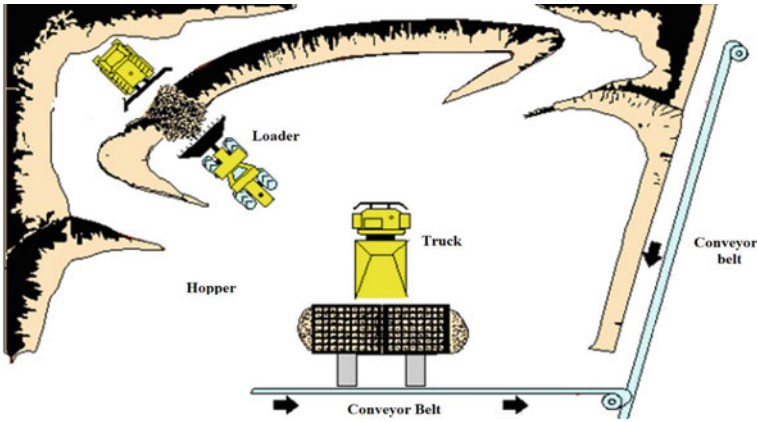
Fig. 1 Schematic layout of conventional mining with truck haulage. Adapted from [15]
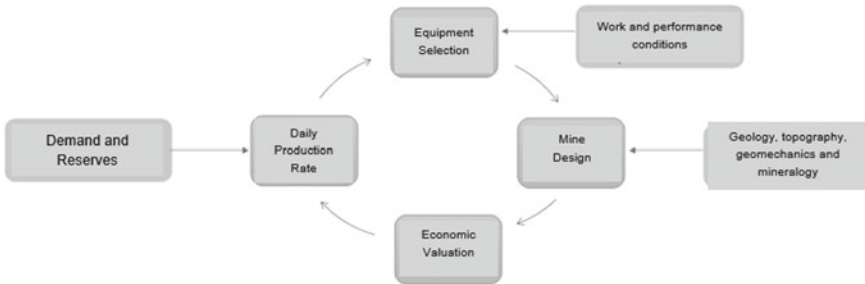
Fig. 2 Equipment selection cycle. Adapted from [17]

Equipment selection is determined by several factors, including the size and characteristics of the deposit, the scale of production, the geometry of the pit, the geology of the deposit and the amount of capital available for investment [3, 17]. Figure 2 shows the interaction of these factors with equipment selection.

According to [18], the selection of equipment size affects the layout and design of the mine and directly influences the operational costs. Figure 3 shows typical mine operating costs.

As shown in Fig. 3, transport-related costs represent approximately 46% of the total mining costs, and about 30–50% refers to the cost of equipment maintenance [3, 16].

The choice of the best transportation system is still related to the advantages and disadvantages of each method along with an economic evaluation, and this is not always the predominant factor [3].

According to [3, 4, 14, 19, 20], the following advantages and disadvantages can be highlighted.
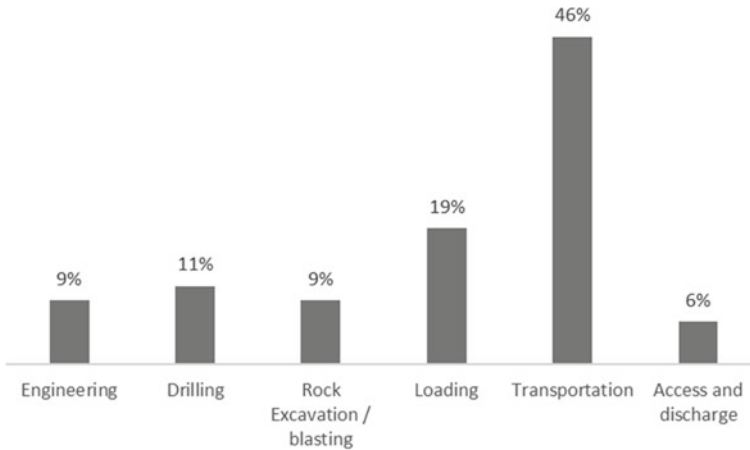
Fig. 3 Total mine cost per stage. Adapted from [17]

3.1.1 Truck Haulage Advantages

– high operational flexibility. The equipment can be easily transferred to other mining fronts according to production sequencing in case of crusher, hopper or even of loading equipment unexpected stoppages;
– applicability of the system to different haulage distances, usually between 100 and 3000 m;
– ability to adapt to all types of material and varied particle size;
– easiness in varying the production rate, increasing the fleet and the percentage of use;
– possibility of contracting additional fleet;
– the need for relatively simple and inexpensive infrastructure;
– well-known system, which makes it easier to hire labor for operation and maintenance;
– reduced assembly and commissioning time, or "start-up", as the equipment arrives preassembled at the operating site;
– the operation of the mining front is not interrupted if one of the trucks is unavailable. It is possible to maintain the activity reducing the production of the mining front until an economic limit of trucks;
– existence of a great variety of models that allows selecting the equipment that best adapts to the conditions of mine operation;
– lower initial investment, when compared with other methods, such as conveyor belts;
– In the case of production expansion, it is easy to increase the number of trucks.

3.1.2 Truck Haulage Disadvantages

– high operating cost, if compared with conveyor belts;
– requires a large amount of labor for operation and maintenance;
– relatively low energy efficiency, with 50% for the displacement of its own weight and 50% for displacement of the load;
– high empty displacement time. On average, 50% of the transport cycle time of the truck is spent returning from the point of discharge to the mining front;
– reduced productivity by increasing haulage distance. The accesses are relatively long due to the slope limitation of the ramps, increasing the total distance to be traveled when increasing the unevenness of the area of the mining front and dumping point;
– in general, the increase in haulage distances implies in the increase of the truck fleet to maintain the required production or in the increase of equipment size;
– high cost of access opening and maintenance, requiring additional equipment for this activity;
– reduced productivity or even operation stoppage in the event of heavy rains and fog that might hinder operator's visibility;
– greater exposure to the risk of operational accidents;
– high lead time of equipment delivery, in case of high commodity prices and high market demand;
– large amount of diesel consumed during operation;
– greater environmental impacts: emission of gases, noise, vibration, generation of particulates;
– requires more time to resume production cycle after operational stoppage;
– higher cost per unit ($/tmn), when compared to transportation by belts;
– need for large support facilities, equipment and maintenance teams to service the truck fleet.

3.2 Conveyor Belt

The continuous belt system [14] consists of material dismantling, which can be carried out mechanically or with the use of explosives, loading with loaders or excavators, which directly feed a loader, and an in-pit crushing system or a loading chute, as exemplified in Fig. 4.

The belt conveyor system consists of the following components [21]:

– conveyor belt—load and transport support
– rollers (load, impact, return, among others)—support, guide, and conform the belt
– drive system (engine, speed reducer, coupling, drums, and safety devices)—belt displacement
– anchoring system—tensioning the belt
– structure.
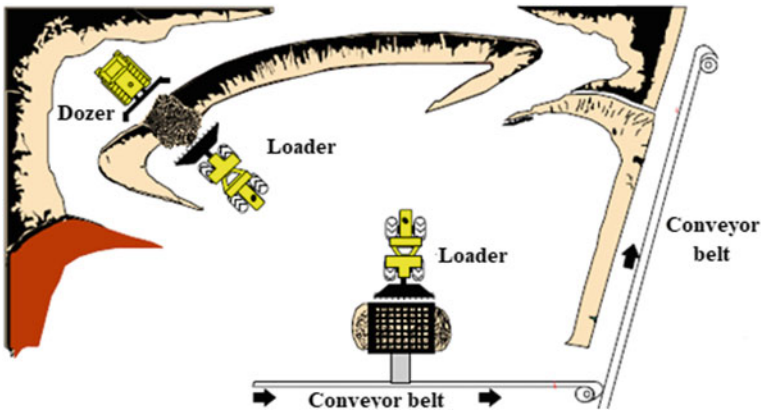
Fig. 4 Schematic layout of a mining operation using conveyor belts. Adapted from [15]

Given the design of the belt profile and desired production, engineering specifies the electromechanical components required according to the constraint of the structural design of the belt, determining then the final nominal capacity of the system.

According to [3, 4, 5, 14, 22], the following advantages and disadvantages can be highlighted.

3.2.1 Conveyor Belt Advantages

– low maintenance cost;
– demand of relatively uniform electric energy, and may even generate energy in descending belts;
– reduced labor for operation and maintenance of the belt system;
– lower operating cost;
– lower environmental impacts, emission of gases, noise and dust;
– less use of fossil fuel;
– the transport capacity is independent of the haulage distance;
– operations are less sensitive to climatic variations;
– greater energy efficiency compared with trucks;
– reduction of construction and maintenance of mine access;
– ability to overcome ramps up to 30° without loss of efficiency;
– lower quantities of equipment involved in the operation, leading to a reduction in the risk factor.

3.2.2   Conveyor Belt Disadvantages

– lower system availability—system availability depends on the individual components that are comprised of the entire system, which are usually connected in series, causing the production to stop when any of the equipment is stopped.
– less flexibility to react to changes in the deposit and in operational requirements;
– higher initial investment cost when compared with truck haulage;
– requires detailed short- and medium-term planning;
– the loader productivity is influenced by the distance from the front to the unloading point on the belt;
– if there is a need to change the mining front, it is necessary to carry out the realignment/extension of the belt system, stopping the production during a certain period of time;
– the life of the loader tires may be compromised due to eventual increases in the transport load; Limited particle size of the system.

4   Discussion

4.1   Method Replacement

When analyzing a mine that already operates with the conventional truck haulage method, there are some peculiarities to perform the system substitution, such as alteration in mining planning and financial evaluation of equipment replacement, as well as changes in mine design and infrastructure. These particularities are often not applicable to a mine that is not yet in operation, that is, it will already be started with the belt conveyor method.

According to [23], the mining plan of a mine that uses the belt system as the main transportation method is more complex when compared to the mines that use trucks. Due to the greater difficulty in changing the position of belts, the mine loses in flexibility, since in conventional truck haulage a change of route to another mining front is considerably simpler.

In addition, when used in a mine with mixed mining method (belts and trucks), the arrival of conveyor belts to the mining fronts influences truck access planning, which makes mining planning even more challenging.

In order to carry out the replacement of the equipment to change the method of material handling, it is important to evaluate factors such as the residual value of the current equipment, implementation cost of the new system, which should contain the costs of alteration in the mining plan, existing accesses, execution of earthmoving projects for the installation of belts, acquisition and installation of new belts, and need for technical training of specific labor.

On the other hand, [4, 23], point out that the number of trucks in a mine is directly linked to the number of operators, maintainers, tire and fuel consumption, which
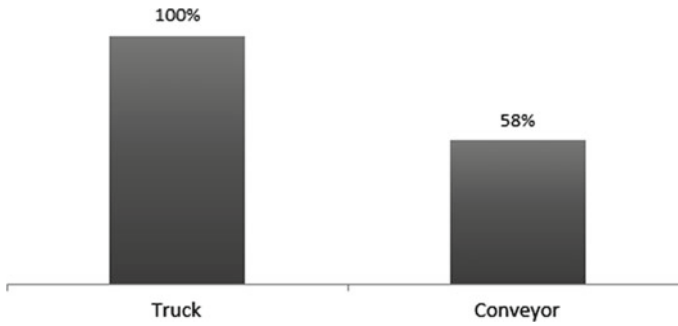
Fig. 5 Truck and conveyor belt operational cost comparison

consequently affects the OPEX. Yet, the operating cost with belts tends to be lower, depending on the individual characteristics of the mine, due to the direct connection with the number of operators and the use of electric energy.

Thus, an economic feasibility study is important, considering the characteristics of implantation for the analysis of indicators such as payback and internal rate of return. It is worth remembering that this study should not be the only determining factor for the implantation of conveyor belts. Environmental and social factors must also be taken into account.

4.2 Operational Cost

When analyzing the operational costs of transportation methods, the costs of wear materials, operational inputs and labor were compared. The wear materials, namely: tire, belt, and soil drilling tools, were calculated according to manufacturers' assumptions and market prices.

For the operational inputs, the specific consumption of each equipment and the market prices were considered. Finally, the labor cost was calculated according to information from the National Employment System (SINE) [24], an agency linked to the Brazilian Ministry of Labor [25]. The positions of machine operator for the mobile equipment and of production operator for the conveyor belts were considered.

Figure 5 shows a comparison of total operational cost. It is possible to observe that, when the wear materials, material supplies, and labor are taken into account, the mining costs using conveyor belts to transport the ore stand for about 58% of the mining costs using trucks to transport the same amount of ore for an average distance of 3 km.

One of the main factors impacting this result is the consumption of supplies, since the unit cost ($/t) of electric energy consumed by conveyor belts is significantly lower than the unit cost of diesel consumed in truck haulage systems. In addition, labor cost also has a significant influence on the cost difference, since conveyor belt systems
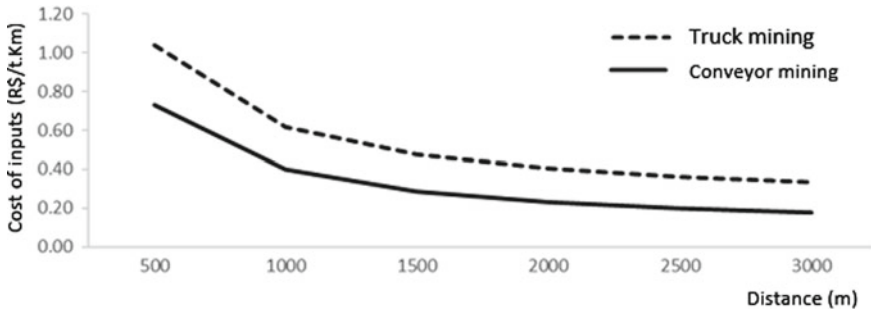
Fig. 6 Conveyor and truck input unit costs

require a lower number of operators when compared to ore transportation by trucks. While truck haulage requires one operator by equipment, in belt conveyor systems a single operator can be responsible for the operation of several belts.

It is important to note that these are only the operating costs and, in this scenario, the maintenance costs of both systems and the installation costs of the belt conveyor system in the front line are not taken into account.

4.3 Input Costs

Figure 6 presents a comparison between input unit costs for truck haulage and belt conveyor systems and their behavior under haulage distance variations.

For the latter one, the electric energy for the operation of the belts and diesel of the loader involved in the operation were considered as inputs, and about 60% of the total input costs in this field refers to the diesel needed by the loader. For truck mining, the considered input was the diesel consumed by the loader and the trucks.

It is possible to notice that the belt system presents significantly lower input costs compared with the truck system, regardless of the haulage distance.

4.4 Equivalent CO_2 Emission

In belts, CO_2 is emitted by two sources: by the combustion of the diesel in loaders and by the belts that use electric energy.

The emission of CO_2 by the belts was calculated according to the emission factor of the National Integration System considering the base year of 2014 [26].

In order to determine the emission of CO_2 by the combustion of diesel in both belt conveyor and truck systems, the CO_2 emission factor for heavy diesel equipment was used [27].
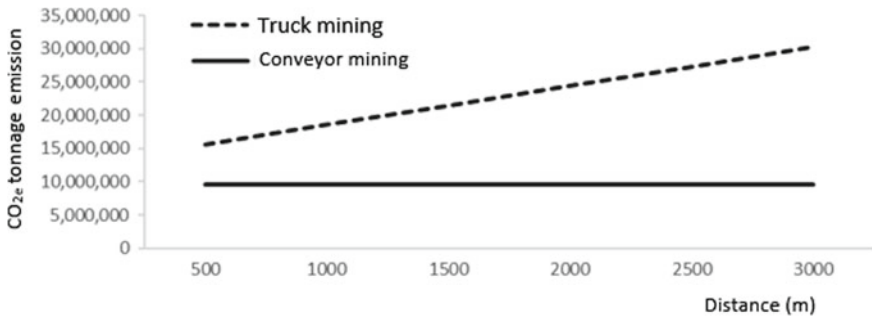
Fig. 7 Conveyor and truck CO_2e emission comparison

Figure 7 presents a comparison of CO_2 emission between the methods according to the increase in haulage distance. It is important to note that the main emission source in the conveyor belt method is the diesel used in the system's feed loader, which represents about 99.99% of the total emission. The additional CO_2 emission as the haulage distance increases is insignificant.

Therefore, it is possible to observe that the greater the haulage distance, the greater the CO_2 emission discrepancy between the methods.

4.5 Waste Generation

Figure 8 presents a comparison between the generation of waste tires and belts, considering an average haulage distance of 3000 m and a simulated transport of 30,000 t. Tire and wheel loader data are based on information from suppliers of these products for mining.

Fig. 8 Conveyor belt and truck waste generation comparison
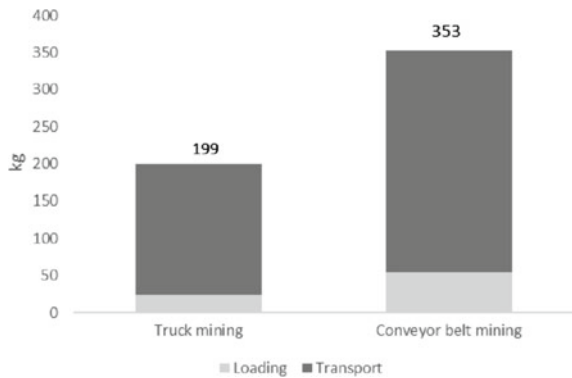
It is possible to conclude that the total waste generated by truck haulage is about 56% less than the total waste generated by the belt conveyor systems.

5   Conclusion

The definition of the best transportation method in a mine should be done through a multicriteria analysis. When carrying out a punctual analysis, observing only some of the criteria, it is possible that the decision is not the best, especially in a medium- and long-term scenario.

In addition to the operational costs, which present a favorable condition for operation with conveyor belts, several other information may be relevant, such as safety factors in the operation, availability of specialized labor, generation of waste, mining flexibility, and cost of equipment acquisition. When taking the last three criteria into account, for example, the use of trucks tends to be the most feasible.

Regarding the quantitative results, belt conveyor systems proved to be favorable in terms of operating costs, input costs and CO_2 emission. Regarding the generation of waste, truck haulage showed greater viability. Several qualitative variables classified as advantages and disadvantages of each method were presented according to the initial research proposal, emphasizing the main applications, advantages, disadvantages, and differences according to environmental and social costs and impacts.

The study presented some limitations, such as the use of theoretical data for the elaboration of scenario simulations and the delimitation of operating costs, disregarding maintenance and installation costs. As a suggestion of future work, the addition of these maintenance and installation costs to the total costs, as well as the use of actual data from companies that use both transportation methods, are recommended.

References

1. Babi, K., Asselin, H., Benzaazoua, M.: Stakeholders' perceptions of sustainable mining in Morocco: a case study of the abandoned Kettara mine. Extr. Ind. Soc. **3**, 185–192 (2013)
2. Freitas, C.A., Almeida, C.M.: Papel da Gestão de Projetos na Inovação: Estudo na Mineração Mundial. Mundo Proj. Manage. Ano **15**(76), PG 56–63 (2017)
3. Lopes, J.R.: Viabilização Técnica e Econômica da Lavra Contínua de Minério de Ferro com Uso de Sistema de Britagem Móvel "In Pit" Auto Propelido. Dissertação de Mestrado, PPGEM-UFOP (2010)
4. Ribeiro, B.: Estudo de Viabilidade Econômica para a Implantação de Correias Transportadoras de ROM de Minério de Ferro. Estado de Minas Gerais. Dissertação PPGEM-UFOP, Estudo de Caso Da Mina Fábrica em Congonhas (2013)
5. Santos, D.C.: Mapeamento de Processos: Estudo Sobre a sua Aplicação como Ferramenta Estratégica para a Análise de Requisitos no Desenvolvimento de Sistemas (2010)
6. Ercelebi, S., Bascetin, A.: Optimization of shovel-truck system for surface mining. J. South. Afr. Inst. Min. Metall. **109**, 433–439 (2009)
7. Pinto, C.L., Dutra, J.I.: Introdução ao Planejamento e Operação de Lavra (2007)

8. Mattos, L.B.R.: A Importância do Setor de Transportes na Emissão de Gases do Efeito Estufa—O Caso do Município do Rio de Janeiro. Tese COPPE/UFRJ (2001)
9. Monteiro, A.G.: Estratégia de Redução de Emissões de Poluentes no Setor de Transportes por meio de Substituição Modal em São Paulo. Tese—COPPE/UFRJ (1998)
10. Cabral, L.N., Pereira, S.S., Alves, T.L.B.: Degradação Ambiental e Implicações para a Saúde Humana: Trabalhadores de uma Pedreira no Município de Campina Grande/PB. Hygeia **8**(15), 104–118 (2012)
11. Bullivant, D.: An Appraisal of the Correct Transport System for a Surface Mine, pp. 189–192. The best of bulk solids handling (1984)
12. Cravol, L.B., Ferreira, F.S.: Sustentabilidade—Uma Reflexão a Respeito do Compromisso das Empresas com o Meio Ambiente. Rev. Hórus **7**(3), 37–55 (2012)
13. Althoff, H.: Cost Reduction by In-Pit Crushing and Conveying, pp. 199–201. The best of bulk solids handling (1985)
14. Jimeno, C., Limeno, E., Alonso, S., Santos, J., Heras, J.: Manual de Arranque, Carga Y Transporte en Mineria a Cielo Aberto. 2ª Edição (1995)
15. Wghleber, V. http://www.ebah.com.br/content/ABAAAAkjEAH/mineracao (2017)
16. Morad, A., Mohammad, M., Sattarvand, J.: Application of reliability-centered maintenance for productivity improvement of open pit mining equipment: case study of Sungun Copper Mine. Central South University Press and Springer-Verlag, Berlin Heidelberg (2014)
17. Bozorgebrahimi, E.: The Evaluation of Haulage Truck Size Effects on Open Pit Mining. Tese—The University of British Columbia (2004)
18. Bozorgebrahimi, E., Hall, R.A., Blackwell, G.: Sizing equipment for open pit mining—a review of critical parameters. Min. Technol. (Trans. Inst. Min. Metall. A) **112**, A171–A179 (2003)
19. Santos, J.: Sandwich Belt High Angle Conveyors—Applications in Open Pit Mining, pp. 139–149. The best of bulk solids handling (2014)
20. Soofastaei, A., Amin, S.M., Kizil, M.S., Knights, P.: Comprehensive investigation of loading variance influence on fuel consumption and gas emissions in mine haulage operation. Int. J. Min. Sci. Technol. (2016)
21. Mercúrio.: Manual Técnico de Correias Transportadoras. Int. J. Min. Sci. Technol. (2016)
22. Kutschera, S.: Planning Aspects for the Application of Continuous Transport Systems Open Pit Mines, pp. 183–187. The best of bulk solids handling (2014)
23. Nehring, M., Knights, P.F., Kizil, M.S., Hay, E.: A comparison of strategic mine planning approaches for in-pit crushing and conveying, and truck/shovel systems. Int. J. Min. Sci. Technol. **28**, 205–214 (2018)
24. Sistema Nacional de Emprego. https://www.sine.com.br/ (2017)
25. Ministério do Trabalho. http://trabalho.gov.br/servicos-do-ministerio/servicos-do-trabalho/para-o-trabalhador/vagas-de-emprego-sine (2017)
26. Sanquetta, C., Maas, G., Sanquetta, F., Sanquett, M., Corte, A.: Emissões de Dióxido de Carbono Associadas ao Consumo de Energia Elétrica no Paraná no Período de 2010–2014. BIOFIX Sci. J. **2**(1), 1–6 (2017)
27. Álvares, J.O., Linke, R.: Metodologia Simplificada de Cálculo das Emissões de Gases do Efeito Estufa de Frotas de Veículos no Brasil. CETESB, São Paulo (2001)

How to Exit Conveyor from an Open-Pit Mine: A Theoretical Approach

M. Pericheh and M. Osanloo

1 Introduction

Recent and ongoing future events force mining operations to be first a nonstop and second a more difficult course of action. The mining operation is required if the quality of life, job creation, and economic growth are to be improved. Nonstop growth in population rate of the world entails a nonstop mining operation. On the other hand, the geological resources discovered near the surface are either elicited or are going to be exhausted. What remains are the reserves located in remote and inaccessible/hardly accessible regions. Hence, the mining operation must be continued in the deeper earth with more stripping. The historical data show that the depths to the top of the mineralized zone discovered during the year 1900–2015 in the world tends to increase and its average reaches over 300 m, while before 1950, most of the deposits were just near the surface [1].

In line with increasing the depth, the average head grade has also been decreased in all base and precious metal deposits [2]. It means that future mining operations would have immense stripping ratios. The most suited and maybe the only type of mining methods which is able to handle these vast amounts of stripping is open-pit mining. Nowadays, a truck-shovel system is used in more than 90% of open-pit mines all around the world [3, 4]. One paramount thing is that trucks are not outstanding in such above-talking deep open-pit mines. Past history of trucks has shown that they can only be economically applied for 2 miles. Hauling cost accounts for more than 50% of the total mining cost [4–6] and it exponentially increases with an increase in haulage length. This sharp rise in the trucking cost would be acceptable for mining companies up to a threshold. This point is exactly where another transportation alternative may work better. In these situations, many open-pit mines have switched

M. Pericheh (✉) · M. Osanloo
Department of Mining and Metallurgical Engineering,
Amirkabir University Technology, Tehran, Iran
e-mail: morteza_pariche@yahoo.com

to in-pit crushing systems around the globe. Crushing inside the pit allows the material to be transportable by conveyors. By this way, a smaller part of material handling requirement in the pit from working faces to the in-pit crusher will continue to be done by trucks and a larger proportion from the in-pit crusher to the final destination by conveyors. Actually, the idea was born in 1956, but not in the same situation as described above [7]. However, the conveyor is an economically superior option. Its operating cost is about one-quarter to one-third of truck cost [8]. Today, more than 447 mines realized large cost savings by installing the in-pit crushing and conveying systems to displace trucks in elevating the material from within the pit [9]. Many researchers talked favorably about the in-pit crushing and conveying (IPCC) systems and have highlighted different aspects of the system to date. In-pit crusher location as the heart of the system optimization has been solved using simulation, heuristics, hub-location model, makov-chain model, dynamic location model, and transportation model [10–16]. Transition time from a pure-truck system to an IPCC system has also considered using heuristics [17, 18]. As well, the two modes of transport (i.e., pure-truck and IPCC) have already compared economically by some researchers [19–23]. One impressively influential thing on the above-mentioned decisions related to how to design the IPCC system has already been unseen or at least overlooked from the academician's standpoint. That is how to exit the conveyor from the pit. The proper exit method selection can drastically bring about a reduction in operating and capital cost of an IPCC. Therefore, it surely affects the economic superiority of IPCC system against the pure-trucking system. The problem was investigated many years ago by [24]. They provided a computer program to compare the tonnage aspects of various layouts of a standard conveyor. The standard conveyors impose extra stripping to the projects because of their flatter slope than common stable pit wall slope. In addition to this option which needs a dedicated ramp slot (DRS), there are three other options named tunnel, high angle conveyor (HAC), and existing ramping system (ERS) by which a conveyor system can exit the open pits. In this paper, these four alternatives were compared economically at different depths. A theoretical approach was conducted to evaluate the alternatives in a hypothetical open-pit mine representing the regular-shaped pits. The break-even points between the systems were also found. The approach presented here can be easily adapted to specific situations at any stage of mine life.

2　Conveyor Exit Schemes

An IPCC system usually involves four different conveyor lines. The first always is placed immediately after crushing plant and feeds the second one which moves the materials inside of the pit up to the third conveyor. The second line usually is a movable bench conveyor which may source ore or waste material from up to three working benches/faces. It has the flexibility to follow the progress of mining and its configuration will change from year to year. The third conveyor line called trunk conveyor is the most important line because it takes the materials out of the pit.

Fig. 1 A general form of existing truck ramping system
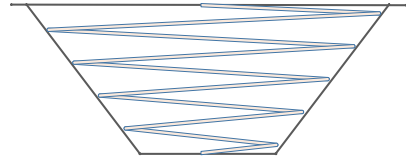
Trunkline moves the raw materials from a lower height level on the in-pit crushing level to an upper height level on the ground. Actually, it does the major part of material handling requirements. The last line conveys the materials overland to the final destination, usually processing plant or waste dump. The main theme of this paper turns around the third conveyor line. There are four ways by which the conveyors from an in-pit crusher can exit the pit:

- via an existing haul road;
- a dedicated (generally steep) conveyor ramp;
- a tunnel (i.e., inclined tunnel);
- high angle conveyors.

Conveyor length, design, and subsequently operating and capital cost are quite different for these alternatives. Besides, tunnel and DRS impose extra excavation and stripping to the project. These extra excavation/stripping cost should be considered during the economic comparison. In the next subsections, the alternatives are described in details and main affecting factors in the effectiveness of either option are discussed. Conveyor length, extra stripping/excavation requirements as the most important factors are argued quantitatively.

2.1 Existing Ramping System

The existing spiral/zig-zag ramping system (ERS) that is usually left in the mine wall may be used to exit the conveyor. These ramps usually have a gradient between 8 and 12%. These ramps are shown inside the pit in Fig. 1. In this case, the length of the conveyor system will increase as the depth increases as in Eq. 1.

$$\text{CL}_{\text{ERS}} = \frac{h}{\sin \alpha} \tag{1}$$

where h is the depth considered to exit the conveyor from which and α is the gradient of the existing ramping system. This alternative is suggested previously to be the best for existing steady-state operations for material handling in horizontally advancing mines [25]. In this case, different conveyor lines with lengths of at most 50 m are linked series and either conveyor line feeds the subsequent line [9]. Therefore, a large number of transfer points would be required in open-pit mining operations, especially where switch-backs are not out of mind.

2.2 Dedicated Ramp Slot

Recommended inclination angles for open-pit mine products vary from 12° to 22° with respective angles of repose from 29° to 44°. This means that typical conveyors will have a gradient of at most 22° [26]. Since conventional conveyors are steeper than truck ramping systems (i.e. 12° − 22°) and usually flatter than optimal mine slope angles, additional excavation like the one shown in Fig. 2 is required to accommodate the conveyors. The concept of conveyor ramp slot has been practiced in the past at Chuquicamata and Carmeaux mines [6]. Figure 2a shows a schematic plan view of a ramp slot which is constructed in the mine wall. Figure 2b also indicates a cross-sectional view of this ramping system as well as the pit limit.

This type of exit method of conveyor imposes the extra cost of waste mining, which should be anticipated before. The first thing to do is getting a sketch of the solid obtained by a conveyor slot (Fig. 3-the middle). The solid is shown in three different cross-sections; the left one for the case if we cut the solid at any y, the right for the case if the solid is cut at any x and the top for when we cut the solid at any z. The line which has a φ degree slope is the path that the conveyor will pass through. In this figure, the angle θ shows the stable wall slope. To obtain the volume of the solid, it is divided into three parts. The left and right hands parts have the same volume each one with a triangle shape in cross-sectional view if they are cut at any y (i.e., parts C), while the inner part has a rectangular shape in cross-section (i.e., part B). Actually, the volume of the solid is equal to the summation of volumes of two same triangle-based pyramids and one rectangular-based wedge. But, we only need the volume of the slot which is colored blue and labeled A in the cross-section perpendicular to the x-axis. The extra volumes which should be diminished from the solid are labeled D and E in the cross-section perpendicular to the z-axis. These extra volumes are actually a part of the pit limit and would be elicited anyway. They involve two same trapezoid-based pyramids and one rectangular-based wedge.

The overall volume of the conveyor slot is calculable from the Eq. 2. It is a function of depth (h), conveyor ramp slope (φ), stable wall slope (θ) and also the minimum width of the conveyor path (m). This minimum dimension includes the width of the conveyor chassis and the minimum space required to maintain the conveyor. In Eq. 2, φ and θ may change from 12° to 22° and from 30° to 50° respectively.

(a)   **(b)**
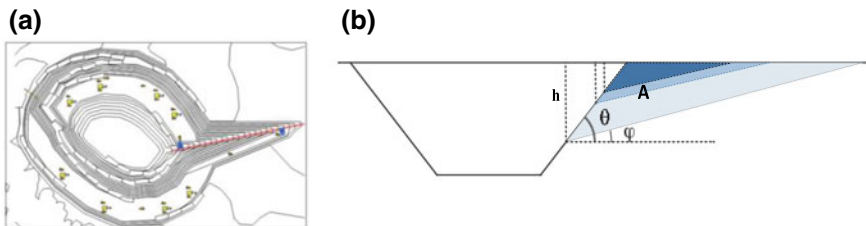
Fig. 2 A general form of dedicated ramp slot, **a** plan view [6], **b** cross-sectional view
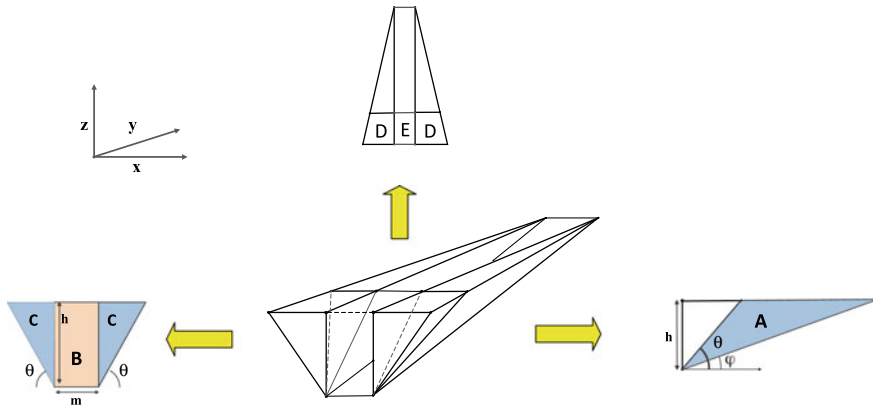
Fig. 3 A 3D sketch of dedicated ramp slots

Fig. 4 DRS volume by depth
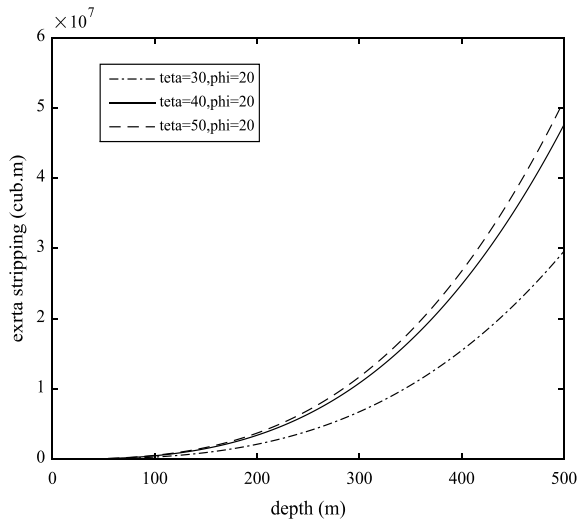
$$V_{\text{DRS}} = \frac{h^3}{3\tan^2\theta}\left(\frac{\tan\theta}{\tan\varphi} - 2 + \frac{\tan\varphi}{\tan\theta}\right) + \frac{mh^2}{3}\left(\frac{1}{\tan\varphi} - \frac{1}{\tan\theta}\right) \qquad (2)$$

Suppose *m* has a 20 m size. As it is shown in Fig. 4, the amount of extra stripping tends to intensively increase by increasing the depth. For instance, for a depth of 500 ms, more than 44 million cubic meter waste removal is needed (φ is 20°, θ is 40°). The volume of the slot is less dependent on *m* and is very sensitive to the three other parameters.

In addition to the extra stripping because of conveyor slot, conveyor length must be identified based on which depth is to be considered for routing the conveyor. In

this case, the conveyor would travel over a $\varphi°$-inclination. As the one previously defined in Eq. 1, the conveyor length would be changed by depth as in Eq. 3.

$$\mathrm{CL_{DRS}} = \frac{h}{\sin \varphi} \tag{3}$$

2.3 Tunnel

Tunnels/inclined tunnels are alternatives which are dominantly applied in underground mining operations. They have also been implemented in surface mining operations where the topography does permit. Actually, they could not be applied in those regions consisting of weak surrounding rocks. Tunnels are only applicable where the topography presents an impediment to the use of the other alternatives. They are technically the last option may be used in most of the cases and give the lowest score among the four [25]. The excavation cost of tunnels/inclined tunnels are very high and may change from 50 to 120 thousand dollars per meter of tunnel length [27]. The conveyor length in a tunnel option can be calculated similarly to that of DRS as in Eq. 4.

$$\mathrm{CL_{TUNNEL}} = \frac{h}{\sin \varphi} \tag{4}$$

2.4 High Angle Conveyor

Characteristics of bulk materials such as density, effective angle of internal friction, lump size and shape are all factors which dictate the maximum incline angle of standard/conventional belt conveyor without having the material roll or slip backward on the belt [28]. HACs are designed to overcome the problem of backsliding. The idea of HACs is based on two principles. The first is the intensification of internal friction angle of material using the sandwich belts and the second is avoiding material backsliding using bucket-shape elevators. Sandwich belt system employs two ordinary rubber belts on top of each other which sandwich the material and provide hugging pressure to the material in order to develop sufficient friction at both material to material and material to belt interface to prevent the material sliding back at the designed conveying angle [29, 30]. While the main disadvantage of the conventional low angle conveyors is to impose extra stripping and tunneling, the HAC, therefore, seems to be the key to IPCC system optimization and reducing this extra cost.

Historical data show that the system has been used to elevate different types of materials, different conveying rates, different conveying angles and heights. The system has already been used for lifting material from 270 m below the surface [30–32]. It is obvious that the system can be easily implemented for deeper pits. As

the pit continues to deepen, the second HAC will be installed at the lower elevation to dump onto the first. This system would be installed over the wall of that part of the pit which is reached to its final limit or it will not be extracted for a long time. Therefore, the conveying angle will be the same angle as the stable wall slope of the region. The conveyor length can be estimated using Eq. 5. The parameters are already defined.

$$\mathrm{CL_{HAC}} = \frac{h}{\sin \theta} \tag{5}$$

3 Theoretical Foundation

The main question is to clarify where (depth) up to which either option may economically be superior over the others. An alternative may involve higher capital while lower operating cost and vice versa. Hence, those alternatives which yield lower net present cost (NPC) during the remaining life of the mine are to be better. In the present paper, the NPC is utilized as a criterion. Equation 6 shows how one can calculate the NPC of an alternative transport system.

$$\mathrm{NPC} = I + I' + \sum_{t=1}^{T} \frac{\mathrm{CF}_t}{(1+e)^t} \tag{6}$$

where both of I and I' are regarded as initial capital expenditure (CAPEX) of the system, I is the owning cost and I' is the extra stripping or tunneling cost, T is the remaining life of the project (from IPCC installation to the end), CF is the yearly cash flow, e is discounted rate and t is the counter of year. In this equation, CF can be calculated using Eq. 7:

$$\mathrm{CF}_t = \mathrm{OP}_t + D_t \tag{7}$$

where OP is annual operating cost and D is yearly depreciation cost of the system. In this study, a straight line method is used for calculating the depreciation (Eq. 8). T' is regarded as the useful life of the conveyor systems, which is usually a number between 20 and 25 years.

$$D_t = \frac{I}{T'} \tag{8}$$

The three first exit schemes (i.e., ERS, DRS, and TUNNEL) use the conventional conveyor systems to handle the material while the last uses a HAC, usually more than 30°-angle. Owning cost and unit operating cost of the conventional and high angle conveyors are quite different. These costs are somehow functions of some more technical and economic factors such as production rate (PR), mine life (T), useful

life of equipment (T'), stable pit wall slope (θ), conveyor ramp slope (φ), slope of existing ramping system of trucks (α), labor (pl) and electricity cost (pe), effective operating hour (hour), stripping (c) and tunneling cost (d) as well as mine depth (h).

3.1 Standard Conveyor Cost Estimation

In order to make a fair economic comparison of the alternatives, the two terms capital and operating costs of both conventional and high angle systems must be predicted based on the above-mentioned technical and economic factors. To this end, a set of data released by [33] was used to predict the price of one-meter standard conveyor. Figure 5 shows the relationship between the owning cost of standard conveyor installation per meter and conveyor throughput.

Equation 9 indicates how one can calculate the capital outlay needed for buying a meter of standard conveyor installation with a given capacity of PR.

$$I_{stc} = 0.375 \times PR + 1641 \tag{9}$$

where: I_{stc} is the owning cost and PR is the production rate in ton per hour. Now, the total owning expenditure can be estimated by multiplying the I_{stc} by the conveyor length (Eqs. 1, 3, and 4). Yearly operating cost (OP) is divided into three categories as power (PC), spare part and maintenance (SMC), and labor (LC) costs. Power cost includes electrical power required to move the belt and material on it. Spare part and maintenance cost also includes conveyor maintenance, lube, and parts as well as infrastructure costs such as chassis maintenance cost. Labor cost also includes
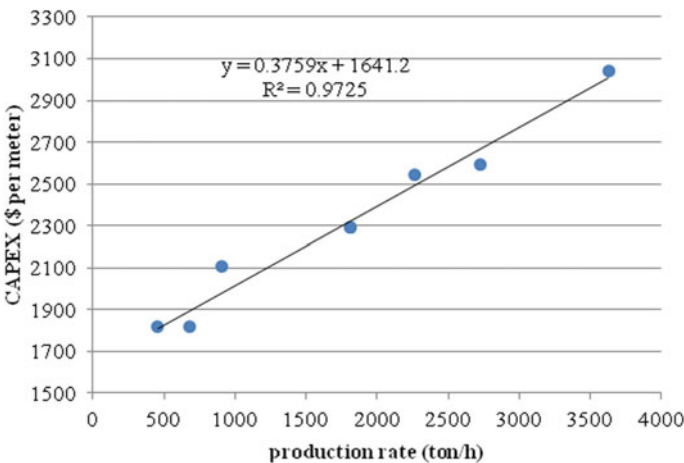
Fig. 5 The relationship between the owning cost of the standard conveyor and their capacity
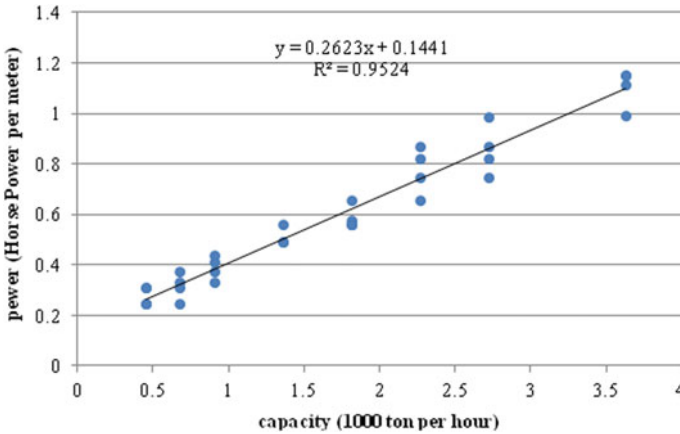
Fig. 6 The relationship between the electrical power required and conveyor throughput

maintenance and control labors. The unit haulage cost for the conveyor is calculated from the Eq. 10:

$$OP = PC + LC + SMC \tag{10}$$

Power (HP) itself is a function of conveying speed, conveyor width and length, friction between belt and idlers/belt and pulleys as well as material density and ambient temperature [28]. Regardless of temperature, friction, and conveyor length, all other factors can be summarized as production rate or the amount of material conveyed per unit of time. Figure 6 shows the correlation between the required powers to move one-meter conveyor and conveying capacity. Equation 11 also reveals the best curve fitted to the data. It is important to note that existing frictions are also implicitly considered in Eq. 11.

$$HP_{stc} = 0.262 \times \left(\frac{PR}{1000} \right) + 0.144 \tag{11}$$

Labor cost is usually considered per length of the conveyor. For example, if three labors per every 500 m of the conveyor are sufficient for all maintenance and control operations, the labor cost can be well estimated considering a given local labor cost. According to [28], a percentage of the total owning cost can be considered as annual spare part and maintenance cost. To conclude, total yearly operating cost (OP) of a conventional conveyor can be estimated using Eq. 12.

$$OP_{stc} = HP_{stc}(PR) \times CL \times hour \times 0.7457 \times pe + \frac{CL}{500}$$
$$\times a \times pl \times 365 \times 3 + I_{stc}(PR) \times CL \times b \tag{12}$$

where CL is the conveyor length which can be calculated using Eqs. 1, 3, and 4, hour is regarded as the effective operating hour of the whole IPCC system, *pe* is the electricity cost ($/kWh), the number 0.7457 is the coefficient to convert horsepower to kilowatt hour, coefficient *a* is the number of labor force for each 500 m length of conveyor, pl is labor price per shift, coefficient *b* is the percentage of total owning cost which is considered as spare part and maintenance costs. The two factors I_{stc} and HP_{stc} are functions of production rate (PR) and should be calculated before, using Eqs. 9 and 11, respectively. In Eq. 12, it is supposed that mine operates in 3 shifts per day.

3.2 High Angle Conveyor Cost Estimation

In order to estimate the capital and operating costs of HAC systems, the data provided by [34] are used. Dos Santos (2002) compared the CAPEX of three high angle conveyors of 45°, 60° and 90° with a conventional 15° conveyor to handle the material for different lifts. The results of this investigation were provided in a relative form to allow simple analyzing of the systems. Indeed, any reader can normalize this cost comparison, according to their own buying and/or selling experience. The relative CAPEX of HACs regardless of their capacity is as in Fig. 7.

To estimate the real CAPEX of high angles beyond the lifting high of 76 m, these relative weights must be predicted first. Therefore, for either conveying angle, a proper curve fitting was done first. Table 1 indicates the prediction functions obtained for different conveying angles.

Where: $K_\theta(h)$ is the relative CAPEX of a HAC of $\theta°$ slope conveying the material from a depth of *h* meter. Linear interpolation technique was used (Eqs. 13 and 14) to predict the relative CAPEX for remaining conveying angles from 22° to 60°. If $22 < \theta < 45$, the relative CAPEX is as

Fig. 7 Relative CAPEXs of HACs compared to a 15° standard conveyor
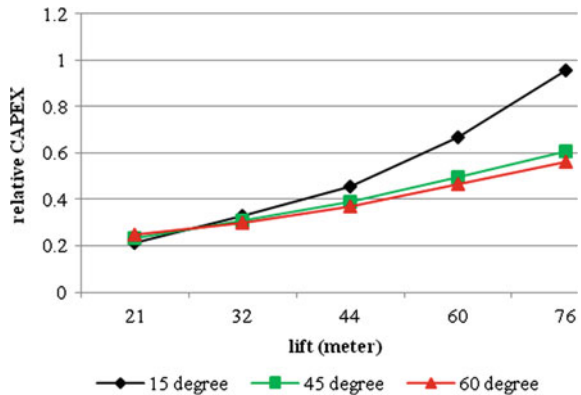
Table 1 The best curve fitted to the relative CAPEX of HACs

Conveying angle	Function	R^2	No of equation
15	$K_{15}(h) = 0.030 \times h^2 - 0.001 \times h + 0.193$	0.998	(13)
45	$K_{45}(h) = 0.093 \times h + 0.126$	0.993	(14)
60	$K_{60}(h) = 0.079 \times h + 0.15$	0.986	(15)

$$K_\theta(h) = \left(\frac{K_{45}(h) - K_{15}(h)}{30} \right)(\theta - 15) + K_{15}(h) \tag{13}$$

If $45 < \theta < 60$, the relative CAPEX is as

$$K_\theta(h) = \left(\frac{K_{60}(h) - K_{45}(h)}{15} \right)(\theta - 45) + K_{45}(h) \tag{14}$$

Considering the CAPEX of the corresponding 15°-conventional conveyor line, the CAPEX of HAC can be properly estimated. Equation 15 guides how the total real capital expenditure of a HAC can be estimated.

$$I_{hac} = I_{stc} \times \frac{h}{\sin(15)} \times \frac{K_\theta(h)}{K_{15}(h)} \tag{15}$$

where I_{hac} is regarded as the total CAPEX of a $\theta°$ high angle conveyor system which moves the materials from a depth of h meter below the surface.

As the same as conventional conveyors, the unit operating cost of a HAC is also a function of the three parts of power, maintenance and spare part as well as labor costs. In order to estimate the power required, a set of 70 data are gathered [30–32]. It is found that there is no meaningful correlation between the total power required and factors such as density, conveying angle and belt speed. Inversely, there was a positive correlation between the power (HP) and the production rate (PR) and also the power (HP) and convening height (h). Thereafter, a multiple linear regression technique was used to predict the power using these parameters. After data processing, we have obtained a prediction function as in Eq. 16.

$$HP_{hac}(PR, h) = -42.526 + 0.129 \times PR + 2.04 \times h \tag{16}$$

The coefficient of determination and standard error were 0.95 and 27.5, respectively. Finally, the yearly operating cost of a HAC system can be estimated using Eq. 17. All parameters are already defined.

$$
\begin{aligned}
OP_{hac} = {} & HP_{hac}(PR, h) \times hour \times 0.7457 \times pe \\
& + \frac{h}{(250 \times \sin(15))} \times a \times pl \times 365 \times 3 + I_{hac} \times b
\end{aligned}
\tag{17}
$$

In Eq. 17, unlike the previous operating cost formula of standard conveyors (Eq. 12), the labor cost is considered in every 250 m of conveyor length. It is supposed that for a given lift, the labor force needed for a HAC is twice that of standard conveyor because of HAC complexities.

4   Finding and Discussion

As described earlier, DRS and tunnel impose extra capital costs to the projects. Also, the two alternatives HAC and ERS usually entail multiple transfer points because of the limited length of conveyor systems. Indeed, in these two cases, multiple conveyor units may be arranged in series with the lower module discharging onto the upper one to achieve the conveyor requirement from deep open pits. The extra discharging cost (f) is also considered in the last part of Eqs. 12 and 17 as a percentage of spare part cost. Furthermore, the commissioning and installing costs must be considered during a true cost comparison. This extra installing cost (k) also is considered as a percentage of the owning cost. The theoretical foundation described in the previous section is coded in MATLAB to analyze the cost of alternative schemes in different depths. The program is verified and debugged several times to assure that it works well and the results are reliable. Besides, the results are compared with several hand-solved examples. The technical and economic data brought in Table 2 are also used in the base case.

As it is shown in Fig. 8, the NPC of three alternatives HAC, ERS, and TUNNEL increase linearly with depth while the NPC of DRS increases exponentially. Actually, it fully follows the behavior of extra stripping by depth (refer to Fig. 4 and Eq. 2). The results show that in the base case, the DRS scheme is the best alternative up to a depth of 140 m while the HAC has the lowest NPC from 140 m onward. The break-even points between DRS-ERS and DRS-TUNNEL are also about 260 and 375 m, respectively.

One may ask how much are the capital costs of the systems for a depth of 100, for example. As stated before, an alternative transport scheme may impose higher capital expenditure while a lower operating cost and vice versa. Figure 9a, b shows the cumulative net present cost of four alternative schemes during the 20 years life of the project for depths of 100 and 200 m, respectively. As shown, the HAC system has lower capital costs than others in both cases. The operating costs of DRS and TUNNEL are the same and this fact has been reflected well in the cumulative net cost of both alternatives. In other words, the slopes of the cumulative net cost of both curves are the same during the time. The pictures also say that the operating cost of the ERS is higher than other schemes. This is mainly because of the longer conveyor length of this alternative.

Table 2 The proposed technical and economic data

Factor type	No.	Factor	Explanation	Value	Unit	Reference
Technical	1	α	Existing ramping slope	10	%	[3]
	2	φ	Conveyor ramp slope	15	Degree	[28]
	3	θ	Stable wall slope	40	Degree	–
	4	PR	Mining rate	5000	Ton/hour	–
	5	T	Remaining mine life	20	Year	–
	6	T'	Useful life of equipment	20	Year	[35]
	7	Hour	Valuable annual operating time	3500	Hour/year	[36]
	8	h	Depth	1–500	Meter	–
Economic	9	c	Cost of stripping	3	$/cub.m	–
	10	d	Tunnel excavation cost	80	$1000/m	[27]
	11	e	Discounted rate	10	%	–
	12	k	% of CAPEX as installation cost	15	–	[35]
	13	b	% of CAPEX as maintenance cost	5	–	[35]
	14	pe	Electricity price	0.07	$/kWh	–
	15	pl	Labor price	300	$/shift	–
	16	m	Width of the conveyor pass	15	Meter	[25]
	17	a	Number of labor required per pieces of conveyor	3	–	[35]
	18	f	% of maintenance cost as extra cost of discharge points	10	–	–
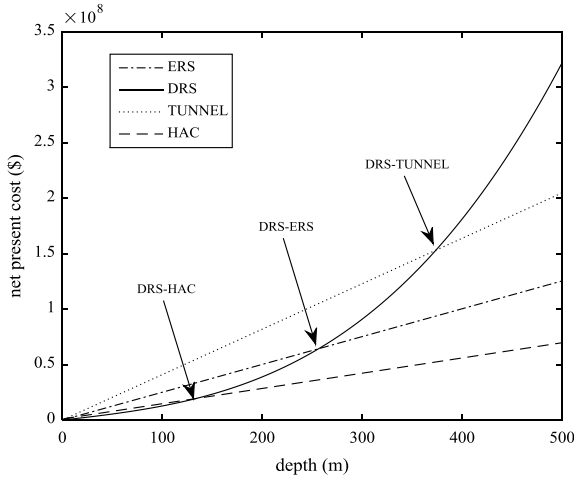
Fig. 8 NPC of alternative schemes by depth
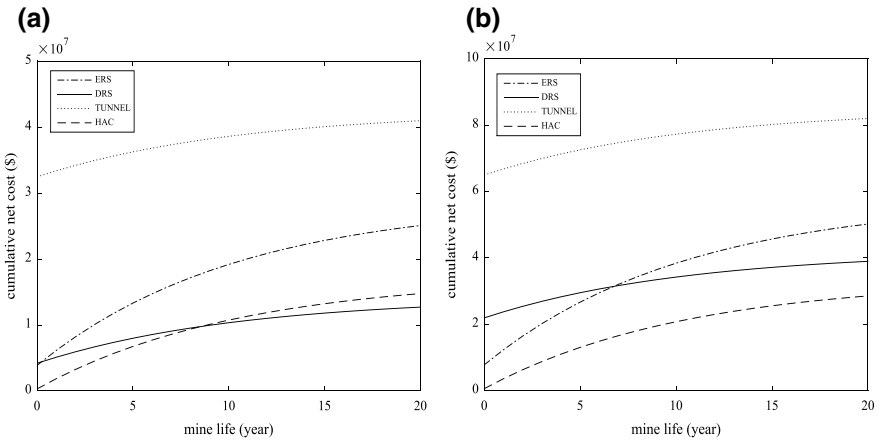
Fig. 9 Cumulative net present cost of alternatives, **a** a depth of 100 m, **b** a depth of 200 m

5 Conclusion

The present paper provides a theoretical basis for determining the capital investment and annual operating costs for four alternative schemes of conveyor exit from within the open-pit mines. Indeed, the basis is developed to allow cost analysis of the alternative schemes for different depths of open-pit mines. The given depth mainly represents where an in-pit crusher unit may be installed. Identifying the domains that either alternative could be economically preferable over other schemes is extremely desirable. Eighteen factors contributing to the problem are detected and their influ-

ences are modeled mathematically. The criterion NPC is chosen to evaluate the alternatives. In the base case, the computational results indicate that a DRS is the best alternative up to 140 m depth. Similarly, the HAC has the highest NPC from 140 m forth.

References

1. Arndt, N.T., Fontboté, L., Hedenquist, J.W., Kesler, S.E., Thompson, J.F.H., Wood, D.G.: Future global mineral resources. Geochem. Perspect. **6**(1), 85 (2017)
2. Mudd, G.M: The Sustainability of Mining in Australia: Key Production Trends and Their Environmental Implications for the Future. Research Report No RR5, Department of Civil Engineering, Monash University and Mineral Policy Institute, Revised—April 2009, ISBN: 978-0-9803199-4-1 (2009)
3. Hartman, H.: Introductory Mining Engineering. Wiley (1987)
4. Czaplicki, J.M.: Shovel-Truck Systems: Modelling. CRC Press, Analysis and Calculations (2008)
5. Zimmermann, E., Kruse, W.: Mobile crushing and conveying in quarries-a chance for better and cheaper production in Institut für Bergbaukunde III der RWTH Aachen. In: 8th International Symposium Continuous Surface Mining (2006)
6. Tutton, D., Streck, W.: The application of in-pit crushing and conveying in large hard rock open pit mines in Niagara-on-the-Lake. In: Mining Magazine Congress (2009)
7. Koehler, F.: In-pit crushing system the future mining option. In: Twelfth International Symposium on Mine Planning and Equipment Selection (2003)
8. Dean, M., Knights, P., Kizil, M.S., Nehring, M.: Selection and planning of fully mobile in-pit crusher and conveyor systems for deep open pit metalliferous applications. In: 3rd International Future Mining Conference. AusIMM (2015)
9. Ritter, R.: Contribution to the capacity determination of semi-mobile in-pit crushing and conveying systems. Ph.D. thesis, Technische Universität Bergakademie Freiberg (2016)
10. Sturgul, J.R.: How to determine the optimum location of in-pit movable crushers. Int. J. Min. Geol. Eng. **5**(2), 143–148 (1987)
11. Abbaspour, H., Drebenstedt, C., Paricheh, M., Ritter, R.: Optimum location and relocation plan of semi-mobile in-pit crushing and conveying systems in open-pit mines by transportation problem. Int. J. Min., Reclam. Environ. (2018)
12. Konak, G., Onur, A.H., Karakus, D.: Selection of the optimum in-pit crusher location for an aggregate producer. J. South Afr. Inst. Min. Metall. **107**(3), 161–166 (2007)
13. Roumpos, C., Partsinevelos, P., Agioutantis, Z., Makantasis, K., Vlachou, A.: The optimal location of the distribution point of the belt conveyor system in continuous surface mining operations. Simul. Model. Pract. Theor. **47**, 19–27 (2014)
14. Rahmanpour, M., Osanloo, M., Adibi, M.: An approach to locate an in pit crusher in open pit mines. Int. J. Eng.-Trans. C: Aspects **27**(9), 1475 (2014)
15. Yarmuch, J., Epstein, R., Cancino, R., Peña, J.C.: Evaluating crusher system location in an open pit mine using Markov chains. Int. J. Min. Reclam. Environ. **31**(1), 24–37 (2017)
16. Paricheh, M., Osanloo, M., Rahmanpour, M.: In-pit crusher location as a dynamic location problem. J. South Afr. Inst. Min. Metall. **117**(6), 599–607 (2017)
17. Changzhi, Y.: In-pit crushing and conveying system and Dexin pit copper haulage optimisation for ore transport. In: Fifth Large Open Pit Mining Conference, November 2003, pp. 49–53. Kalgoorlie, WA (2003)
18. Paricheh, M., Osanloo, M., Rahmanpour, M.: A heuristic approach for in-pit crusher and conveyor system's time and location problem in large open-pit mining. Int. J. Min., Reclam. Environ. 1–21 (2016)

19. van Leyen, H.: Aspects of in-pit crushing, conveying and dump layout. In: Mining Latin America/Minería Latinoamericana, pp. 397–411 (1986)
20. de Werk, M., Ozdemir, B., Ragoub, B., Dunbrack, T., Kumral, M.: Cost analysis of material handling systems in open pit mining: Case study on an iron ore prefeasibility study. Eng. Econ. **62**(4), 369–386 (2016)
21. Terezopoulos, N.G.: Continuous haulage and in-pit crushing in surface mining. Min. Sci. Technol. **7**(3), 253–263 (1988)
22. Sevim, H., Sharma, G.: Comparative economic analysis of transportation systems in surface coal mines. Int. J. Surf. Min. Reclam. Environ. **5**(1), 17–23 (1991)
23. Ribeiro, B.G.C., Sousa, W.T., Luz, J.A.M.: Feasibility project for implementation of conveyor belts in an iron ore mine. Study case: Fabrica Mine in Minas Gerais State, Brazil. Rem: Rev. Escola Minas **69**(1), 79–83 (2016)
24. Lonergan, J., Barua, E.: Computer-assisted layout of in-pit crushing/conveying systems. In: SME-AIME Fall Meeting (1985)
25. Turnbull, D., Cooper, A.: In-pit crushing and conveying (IPCC)–A tried and tested alternative to trucks. In: The AusIMM New Leaders Conference, Brisbane, Queensland (2009)
26. Dos Santos, M.J., Dos Santos, J.A.: High-Angle Conveyor System (2016)
27. Efron, N., Read, M.: Analysing International Tunnel Costs. An Interactive Qualifying Project, Worcester Polythecnic Institute (2012)
28. Conveyor Equipment Manufacturers Association (CEMA): Belt Conveyors for Bulk Materials, Published by the Conveyor Equipment Manufacturers Association, Fifth Edition, ISBN 1-891171-49-6 (2002)
29. Dos Santos, J.A., Frizzell, E.M.: Evolution of Sandwich Belt High-Angle Conveyors. CIM Bull. **576**(855), 51–66 (1983)
30. Dos Santos, J.A.: High Angle Conveying the Vital (missing) Link to IPCC Systems, pp. 44–53. Australian Bulk Handling Review—ABHR, July/August (2013)
31. Dos Santos, J.A., Stanisic, Z.: In-pit crushing and high angle conveying in a Yugoslavian copper mine. Int. J. Surf. Min. Reclam. Environ. **1**(2), 97–104 (1987)
32. Kuchersky, N., Shelepov, V., Gumenik, I., Lozhnikov, A.: Development of inclined conveyor hard rock transportation technology by the cyclical-and-continuous method. In: Proceedings of the 12th International Symposium Continuous Surface Mining-Aachen (2014)
33. InfoMine USA.: Mine Cost Services Mining Model. InfoMine USA (2014)
34. Dos Santos, J.A.: The Cost and Value of High Angle Conveying, p. 51. Port Technology (2012)
35. Mular, A.L., Haibe, D.N. Barratt, D.J.: Mineral Processing Plant Design, Practice and Control: Proceedings. Society for Mining, Metallurgy, and Exploration, Inc. (SME), Littleton, Colorado USA, ISBN 0-87335-223-8 (2002)
36. Dzakpata, I., Knights, P., Kizil, M.S., Nehring, M., Aminossadati, S.M.: Truck and shovel versus in-pit conveyor systems: a comparison of the valuable operating time. In: Coal Operators' Conference, The University of Wollongong, pp. 463–476, 10–12 February (2016)

Bulk Material Volume Evaluation and Tracking in Belt Conveyor Network Based on Data from SCADA

P. Stefaniak, P. Kruczek, P. Śliwiński, N. Gomolla, A. Wyłomańska and R. Zimroz

1 Introduction

The general effectiveness of mine mainly depends on the optimal use of technical and human resources responsible for exploitation and transportation processes of extracted material. As mine expands, the mining infrastructure is becoming ever more complex and optimization task requires much more advanced techniques based on real data analysis. It is important to analyze the availability of the machines in the machinery park. Therefore, it is recommended to support the maintenance tasks in the mine [1–3]. Identification of quantity loading parameters for belt conveying system is crucial for efficient and safe control transportation process as well as to support current mining process and ore enrichment plant. The challenge is to determine volume of ore stream in time and space and develop a model for tracking run-of-mine ore flow within conveying system. In the literature, the subject of identification of loading parameters for belt conveyors is well known. In [4, 5] we can find a few approaches to analyze loading process realized by trucks and load-haul-dump (LHD) machines in discharged points with screens. In [6, 7] a method to track the extracted ore stream compound with the application of process analytic technology tags has been presented. It allows to identify both the quality (ore mass) and quantity

P. Stefaniak (✉) · P. Kruczek · A. Wyłomańska
KGHM Cuprum Ltd, R&D Centre, ul. Sikorskiego 2-8, 53-659 Wroclaw, Poland
e-mail: pkstefaniak@cuprum.wroc.pl

N. Gomolla
DMT GmbH & Co. KG, Am Technologiepark 1, 45307 Essen, Germany

P. Śliwiński
KGHM Polska Miedź, ul. Skłodowska-Curie 48, 59-301 Lubin, Poland

R. Zimroz
Faculty of Geoengineering, Mining and Geology, Wrocław University of Science and Technology, Na Grobli 15, 50-421 Wroclaw, Poland

(lithological composition, Cu content) parameters of copper ore stream hauled from mining faces to dumping points and identify the ore flow in conveyor network. Such solution may be used to optimize enrichment process of run-of-mine copper ore by early customizing operation parameters of processing machines. A similar approach can be found in many different articles [8–10].

The mass of the transported ore in the mine is measured by the scales located on particular belt conveyors. It is worth mentioning that, only the crucial machines are equipped with scales (e.g., before or after the bunker, the last conveyors in the division, etc.). However, in order to track the ore flow through the transportation system it would be beneficial to posses the weight for each conveyor. In this paper, we are studying the relation between the electric current and the weight of the transported ore. It is shown that linear regression can be fitted to this data. Using this model, we are able to estimate the amount of transported ore. This is a powerful tool and the results are promising. The method was tested for three different belt conveyors operating in the underground copper mine.

2 Description of Conveying System

The conveying system, which operates in analyzed copper ore mine, was designed especially for room and pillar technology. It is expected that a huge amount of ore would be transferred from the dumping points to the shaft. Loading of belt conveyors in the production is a cyclic process realized by LHD machines, which transport ore from mining faces. In case, the main haulage belt conveyors are fed continuously from bunkers or preceding conveyors. The belt conveyor transportation system is vast network, which consists of more than 80 conveyors connected in series [11, 12]. Their total engine power exceeds 30,000 kW and annual energy consumption of conveying system represents around 10% of overall mine consumption. Conveyors are spatially distributed in five divisions. The locations of belt conveyors may vary and depend on many different features, namely recently active mining faces or the planned new routes of LHD machines. The total length of conveyors' routes exceeds 50 km. The exemplary scheme of conveyor network is presented in Fig. 1.

The realization of the production plan is a crucial issue in the proper mine operation. It is expected to maximize the amount of excavated and transported ore. Furthermore, some of the belt conveyors have to transport the varying amount of ore. They are mainly located near the production and their load is directly related to the excavation process. It is a challenging task to approximate their load. Therefore, they are typically equipped with the oversized drivetrain, namely their power is too high. The transportation system is fully automated by the SCADA system, which provides operational data from each objects. The detail information about the probable amount of transported ore would be helpful in optimization of the transportation system, its effective control, and energy consumption analysis [13–15].
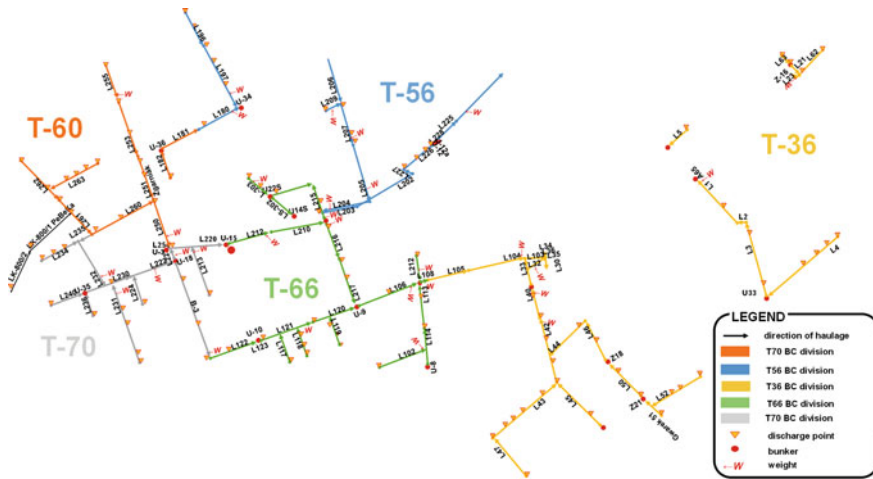
Fig. 1 The conveying system in underground copper ore mine

2.1 SCADA Systems for Belt Conveyors

SCADA systems (Supervisory Control and Data Acquisition) expand functionality of existing control systems. The main tasks of SCADA are: data acquisition, data processing, data storage, reporting and visualization of monitored process, notification about alarm conditions, etc. SCADA systems are able to communicate with PLC controllers. Indeed, they are able to change the control program when the system is operating. SCADA systems provide many informative operational parameters related to efficiency of the production process and technical condition of objects. For instance, SCADA is focused only on raw data acquisition and its visualization. In mining condition, this kind of data is very difficult to analyze because of missing values, external interferences, and complexity of monitored processes. Due to large amount of monitored components, it is expected to develop automatic procedures to analyzed data, prepare decision-making process, and generate reports.

In case of belt conveyors, the following variables are measured:

– electric current consumption for each engine (almost all conveyors), weight of the transported ore (selected conveyors),
– speed belt (conveyors with scale), and
– amount of ore in the bunker in % (all bunkers).

SCADA is a multichannel system with relatively low sampling frequency. The size of datasets turned out to be comparatively big so, it was decided to reduce it by acquiring observations only when the change is bigger than a prior-fixed value. Therefore, data has to be validated and interpolated before the analysis. It was decided to set the time interval equal to 1 s. The electric current signals were interpolated

using the previous value method. On the other hand, the weight measurements were interpolated linearly.

3   Methodology

In theory, it is expected that more load causes the higher electric current consumption. Indeed, in the real data there is a strong linear relation between the weight and electric current. Therefore, it was decided to fit the linear regression. In this section, the methodology is described. First of all, the real data has to be preprocessed. Indeed, we have observed some outliers or weight observations smaller than zero (Fig. 2). The analysis are performed for the cumulative signals. When the conveyor is not working and the electric current consumption is equal to zero, then the ore is not transported.

Therefore, such observations have to be detected and set to 0. Furthermore, sometimes conveyor operates without the external load. In this case, the ore is not transferred and the signal of cumulative weight is constant. Therefore, it was decided to erase the observation with the electric current lower that fixed threshold, when the belt conveyor was operating without the external load. Finally, the linear regression is fitted to the preprocessed data. It is assumed, that the relation between the cumulative electric current ($e = \{e_1, e_2, \ldots, e_n\}$) and cumulative weight ($w = \{w_1, w_2, \ldots, w_n\}$) can be described by Eq. (1):

$$e_i = a * w_i \tag{1}$$
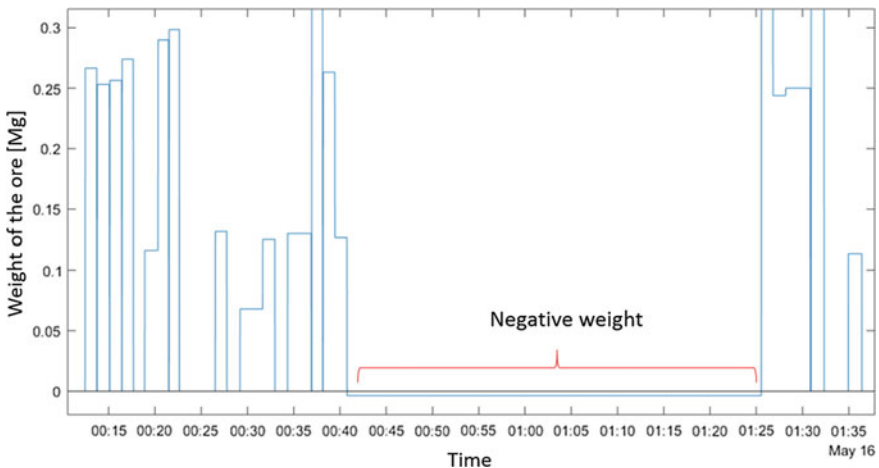
Fig. 2 The exemplary weight signal with negative values resulting from measurement errors

where a is a slope coefficient. It is worth mentioning that, the intercept term is set to 0. Indeed, in the starting point the electric current is zero and it is not transporting the ore. The electric current consumption is a sum of observation for all of the engines. In the analysis, we are considering different types of machines. It is expected that the relation between current and weight depends on many different features, thus, for each machine the coefficient has to be calculated separately. The results of the analysis are verified using the well-known statistics. First, the coefficient of determination is calculated as

$$R^2 = \frac{\sum_i^n (\hat{w}_i - \bar{w})^2}{\sum_i^n (w_i - \bar{w})^2}. \tag{2}$$

where $\hat{w}_i$ is estimated weight, and $\bar{w}$ is mean value. The mean absolute percentage error for n samples is also derived:

$$\text{MAPE} = \frac{100\%}{n} \sum_i^n \left| \frac{w_i - \hat{w}_i}{w_i} \right|. \tag{3}$$

Finally, the total absolute percentage error (TAPE) was also calculated for total sum of transported ore in given period:

$$\text{TAPE} = \frac{\left| \sum_i^n \hat{w}_i - \sum_i^n w_i \right|}{\sum_i^n w_i} * 100\%. \tag{4}$$

4 Real Data Analysis

The proposed model was tested by fitting it to real data obtained from the belt conveyor located in the underground mine. The data recorded for 5 days (July 17–21) is analyzed. The model is build only for first three days (training sample). Then it is validated on the days, which were not taken into account in the model building stage (testing sample). In Fig. 3 raw electric current and weight data for time horizon 17–19 July is presented. In Fig. 4 the comparison of preprocessed data and the raw one is presented.

Indeed, in the preprocessed data the linear dependency is stronger. Therefore, before further analysis the data processing has to be applied. In the next step, the linear regression was fitted to the data. The results are presented in Fig. 5. This model explains properly the relation between these signals. The coefficient of determination is equal to $R^2 = 0.99974$ and the slope parameter is $a = 0.0019691$. In order to verify the model properties the cumulative estimated weight is compared with the real observation (Fig. 6). The fitted model is appropriate and estimated weight using linear regression is almost equal to the real one. The MAPE is equal to 3.6%.
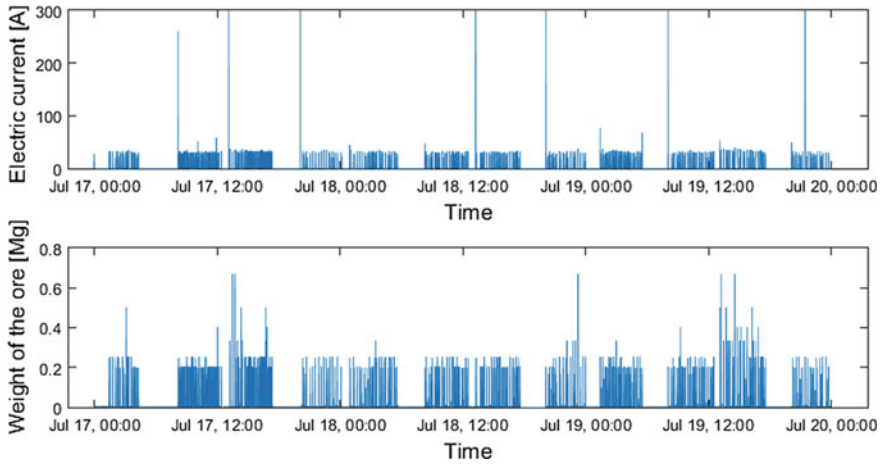
Fig. 3 The electric current for one engine and weight of the ore with respect to time
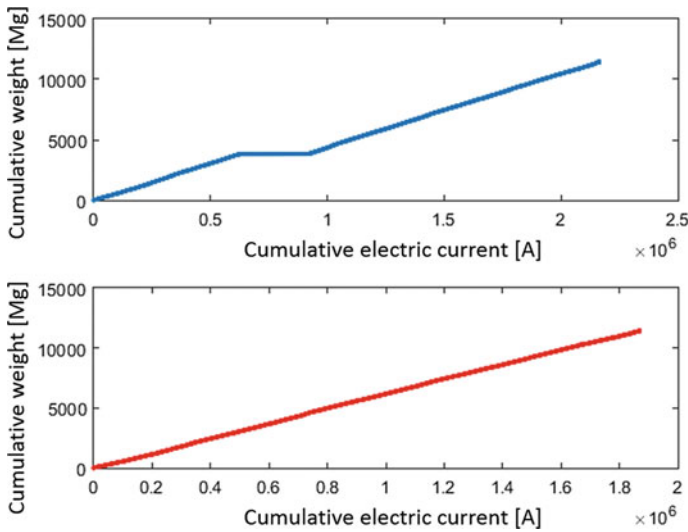
Fig. 4 The relation between the cumulative electric current and cumulative weight, raw observations (top), the preprocessed data (bottom)

Furthermore, the TAPE during this period is just 0.8%. Finally, the differences per one hour between the real and estimated weight signals are illustrated (Fig. 7). Moreover, the obtained errors are also presented. One can observe that the errors are small and most of the observations are similar. On the other hand, it can be illustrated that the proposed preprocessing significantly boost the results. In Fig. 8, the estimated weight for the raw data is presented.
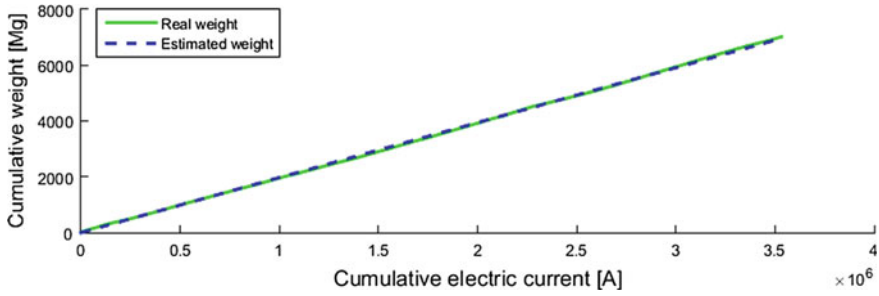
Fig. 5 Fitted linear regression to the cumulative electric current and cumulative weight. The coefficient of determination is equal to $R^2 = 0.99974$
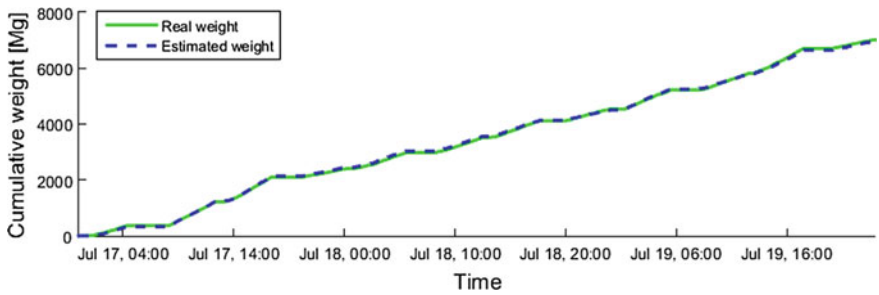
Fig. 6 Comparison of estimated and real cumulative weight
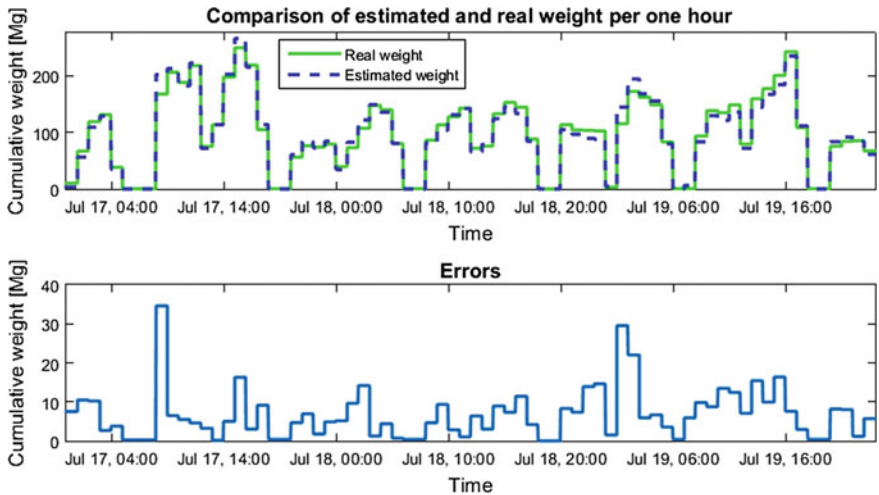
Fig. 7 Comparison of estimated and real weight per one hour

One can observe that the results are worse, comparing to the preprocessed data (Fig. 6). Furthermore, the MAPE is equal to 31%. Therefore, the errors are much
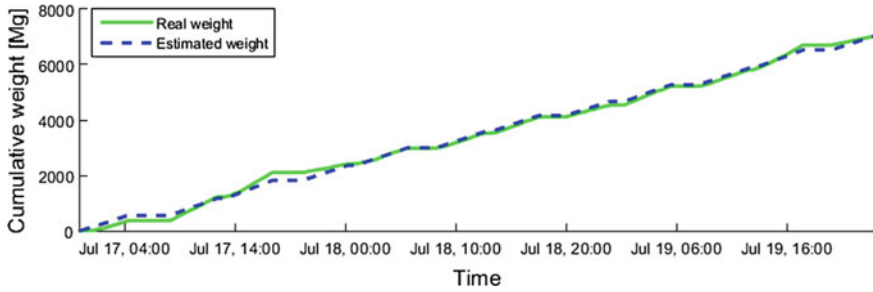
Fig. 8 Comparison of estimated and real cumulative weight for the raw data (without preprocessing)
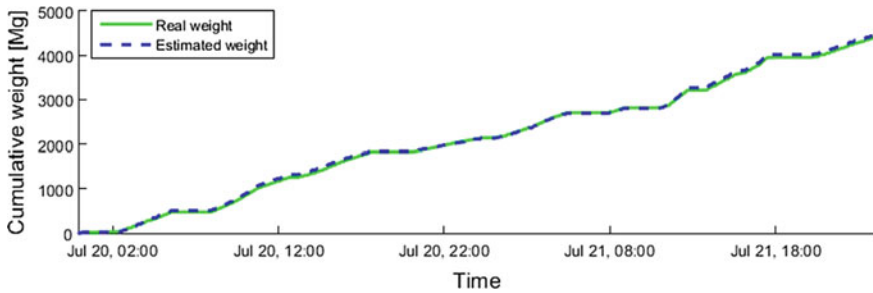
Fig. 9 The out-of-sample test for estimated weight

Table 1 The out-of-sample results for different belt conveyors

Machine	R^2	TAPE (%)	MAPE (%)
1	0.99	1.1	2.7
2	0.987	6.5	6
3	0.998	0.36	6.4

higher and the proposed approach improves the estimation. Finally, the out-of sample test is performed. The estimated model is fitted to the data, which was not taken into account during the training process. It is a crucial step in the proper model validation. The estimated weight is presented in Fig. 9. The MAPE is equal to 2.7%, $R^2 = 0.9991$ and the TAPE for the whole out-of sample is equal to 1.1%. According to the result, the weight can be estimated using the linear regression. The differences per one hour between the real and estimated weight signals for out-of sample test are illustrated in Fig. 10 (top). Moreover, the obtained errors are also presented. The results are promising and the errors are relatively small (Fig. 10 bottom).

This method was also applied for two different belt conveyors (machine 1 was presented above). The results for the out-of sample test are presented in Table 1. One can observe that the proposed method is appropriate also for another belt conveyor. The errors are small, and the estimated weight properly approximate the real signal.
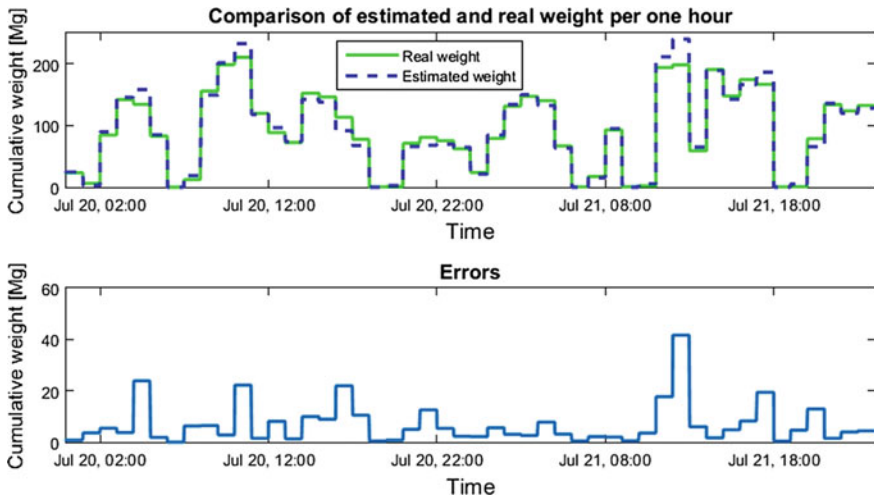
Fig. 10 Comparison of estimated and real weight per one hour for out-of-sample test

5 The Cloud System Implementation

Nowadays, there is a need to develop the cyber-physical software system for mine maintenance. Indeed, this kind of the tool would significantly improve the management process. Many different variables are measured in the mine. They would be transferred to the cloud storage and processed there. Such approach can significantly reduce the computation time and gives an accessibility for the data for many different users. Maintenance system would consist of many different components for the condition monitoring or effectiveness analysis. For instance, the presented algorithm for the weight estimation can be implemented in such system. The appropriate information about the ore volume transported by the conveying system could be used for visualization of the ore stream process. Furthermore, it would be possible to build the model for what-if strategies and perform the simulation of the ore flow through the belt conveyors system.

6 Conclusions

In this paper, the relation between the electric current and weight of the transported ore for the belt conveyor was analyzed. It was proposed to apply linear regression. In the first step, the data has to be properly preprocessed. It was described that the model without preprocessing has worse results. The obtained results ensure that, the weight can be properly estimated using the electric current. This method can be used to validate the real observation from the scale. Furthermore, in the mine only crucial

conveyors are equipped with the scale. In such situation, this method can be applied to approximate the mass of the transported ore. It would help to track the ore flow through the belt conveyor transportation system.

References

1. Galar, D., Gustafson, A., Martínez, B.V.T., Berges, L.: Maintenance decision making based on different types of data fusion. In: Eksploatacja i Niezawodnosc-Maintenance and Reliability, vol. 14, pp. 135–144. Polish Maintenance Society (2012)
2. Lodewijks, G.: Strategies for automated maintenance of belt conveyor systems. Bulk Solids Handling **24**, 16–22 (2004)
3. Stefaniak, P.K., Wyłomańska, A., Obuchowski, J., Zimroz, R.: Procedures for decision thresholds finding in maintenance management of belt conveyor system—statistical modeling of diagnostic data. In: Proceedings of the 12th International Symposium Continuous Surface Mining-Aachen 2014, pp. 391–402. Springer (2015)
4. Stefaniak, P., Zimroz, R., Obuchowski, J., Sliwiński, P., Andrzejewski, M.: An effectiveness indicator for a mining loader based on the pressure signal measured at a bucket's hydraulic cylinder. Procedia Earth Planet. Sci. **15**, 797–805 (2015)
5. Kruczek, P., Polak, M., Wyłomańska, A., Kawalec, W., Zimroz, R.: Application of compound poisson process for modelling of ore flow in a belt conveyor system with cyclic loading. Int. J. Min. Reclam. Environ 1–16 (2017)
6. Jurdziak, L., Kaszuba, D., Kawalec, W., Król, R.: Idea of identification of copper ore with the use of process analyser technology sensors. In: IOP Conference Series: Earth and Environmental Science, vol. 44, pp. 20–37. IOP Publishing (2016)
7. Jurdziak, L., Kawalec, W., Król, R.: Study on tracking the mined ore com-pound with the use of process analytic technology tags. In: International Conference on Intelligent Systems in Production Engineering and Maintenance, pp. 418–427. Springer (2017)
8. Jansen, W., Morrison, R., Wortley, M., Rivett, T.: Tracer-based mine-mill ore tracking via process hold-ups at Northparkes mine. In: Tenth Mill Operators' Conference, Adelaide, SA (2009)
9. Rabe, J., Fouche, P., O'Neill, K.: Development of a RF tracer for use in the mining and minerals processing industry. In: The Third Southern African Conference on Base Metals (2005)
10. Wortley, M., Nozawa, E., Riihioja, K.: Metso smarttag–the next generation and beyond. In: 35th APCOM Symposium, pp. 24–30. Wollongong (2011)
11. Stefaniak, P., Wodecki, J., Zimroz, R.: Maintenance management of mining belt conveyor system based on data fusion and advanced analytics. In: International Congress on Technical Diagnostic, pp. 465–476. Springer (2016)
12. Stefaniak, P., Zimroz, R., Bartelmus, W., Hardygóra, M.: Computerised decision-making support system based on data fusion for machinery system's management and maintenance. Appl. Mech. Mater. **683**, 108–113 (2014)
13. Zhang, S., Xia, X.: Optimal control of operation efficiency of belt conveyor systems. Appl. Energy **87**, 1929–1937 (2010)
14. Zhang, S., Xia, X.: Modeling and energy efficiency optimization of belt conveyors. Appl. Energy **88**, 3061–3071 (2011)
15. Ján Jr., K.: Energy calculation model of an outgoing conveyor with application of a transfer chute with the damping plate. Mech. Sci. **7**, 167 (2016)

Haul Productivity Optimization: An Assessment of the Optimal Road Grade

V. F. Navarro Torres, J. Ayres, P. L. A. Carmo and C. G. L. Silveira

1 Introduction

When it comes to the management of mine haul routes, there are still few references on the subject, most research studies and tests developed in isolated work initiatives [1]. The accesses for material handling in the mines have not yet evolved to the extent that they have reached a fully satisfactory level given the importance they have in the production process.

In the context of Civil Engineering, the study on haul roads is much more developed, both in its conception and in its realization. Due to the peculiarities of the mining operations, the mine roads have their own characteristics, which lead to the need for different analyzes in relation to road pavements. Some parameters that compose the study of the mine haulage ways have some similarity with those established for the vicinal roads of ground, however, they must also be worked so that they are applicable to the reality of the mining.

Mining haul costs represent about 50–60% of the total open-pit mining operations [2] hence an effective methodology to decrease the mentioned costs is very significant and urgently needed in the majority of the mines.

V. F. Navarro Torres (✉) · C. G. L. Silveira
Instituto Tecnológico Vale (ITV), Ouro Preto, Brazil
e-mail: vidal.torres@itv.org

C. G. L. Silveira
e-mail: leandro.silveira@itv.org

J. Ayres · P. L. A. Carmo
Vale S.A, Itabira, Brazil
e-mail: jane.ayres@vale.com

P. L. A. Carmo
e-mail: andre.carmo@vale.com

In most mining problems, the solution involves several simultaneously concurrent goals that are often conflicting. In this way, one must look for tools that return efficient solutions. Therefore, optimization techniques, which involve the minimization or maximization of a set of objectives satisfying a set of constraints, become important allies of the professional to solve the problem.

There are several software on the market such as What's Best®, Gurobi®, Lingo®, Simplex®, GLPK®, among others that work as solvers, that is, solvers to find optimal solutions to not-so-trivial problems. However, decision-making must be carried out by the professional, establishing the objectives and imposing the constraints of such a problem in order to obtain the optimal solution in fact [3].

In the mining literature, the use of simulation and optimization methods to maximize the productivity of mine operations has been explored since the 1960s. The complexity involved in constructing a model and the time required for it are the main obstacles to the development of applicable models and their application in the mining industry [4].

Several studies involving optimization in open-pit mining are available in the literature, such as [5] who used optimization techniques applied to ore blending in Itabira and [6]. However, there are no studies, even in a practical approach, that optimize the mine access grade.

Regarding the main publications on mathematical modeling in general, the study developed by [7] highlights, which proposes a method of estimation and management of the productivity of mining from multiple regressions based on operational data of the mine. The proposed methodology, considering the reference data, presented a high coefficient of determination, about 98%. The base variables considered was: the hourly productivity, fixed times and variable times of the transport cycle, distance traveled, and average load of the trucks. However, such work does not contemplate a productivity assessment with regard to trucks, haul routes, and other related variables, nor does it perform optimization evaluations of geometric parameters such as the grade.

In this context, this study proposes an innovative approach to optimize the main haul road grades in a large-scale iron open-pit mine, located in Quadrilátero Ferrífero, Brazil. This research proposes an optimization mathematical model and presents the results of a geometric evaluation using a mining planning software.

2 Mathematical Models to Assess Haul Productivity

Four haul routes of the mining complex under study were selected based on their relevance in terms of haul distance and haul productivity. These stretches represented high-flow truck paths and a direct impact on the mine's operational strategy. Moreover, the CAT 793 truck model was selected for analysis because it represents the largest fleet of trucks in the mining complex in question. Then, each route was evaluated to determine the optimum grade in terms of ore release and productivity, which could have productivity gains.

Then, the current hourly productivity of Caterpillar trucks 793D, P_t original, per section of the accesses and then the average productivity, was calculated using the Eq. (1) proposed by [8] for the studied routes. This calculation was carried out with the purpose of obtaining the current productivity in the transport for later comparison with the optimized production.

$$P_{t \text{ original}} = \frac{60 * C_e * \rho_{re} * E_t * F_t}{T_m + T_q + T_d + T_e + \frac{1}{16.67}\left[\frac{d_i}{v_i} + \frac{d_v}{v_v}\right]} \tag{1}$$

where: P_t: haul productivity (t/h); C_e: off-road truck bucket capacity (m³); ρ_{re}: swollen ore or waste density (t/m³); E_t: efficiency; F_t: filling bucket factor; T_m: maneuver time; queue time (min); T_q: loading time (min); T_d: dumping time (min); T_e: queue time (min); d_i: loaded traveled distance (m); d_v: empty traveled distance; v_i: loaded truck speed (km/h); v_v: loaded truck speed (km/h).

To create the objective function, and thus maximizing the productivity corresponding to the optimum value of the road grade, it was necessary to express productivity as a function of the grade. Thus, with the aid of Fig. 1, Eq. (3) was defined.

$$d_i, d_v = \sqrt{x^2 + h^2} \tag{2}$$

where x: is the projected ramp length (m); h: is the height that truck must overcome when hauling (kg/t); d_v: empty traveled distance (m), and d_i: loaded traveled distance (m)—ramp new length after optimization.

The parameter x can be expressed as a function of the grade, i and height, h as shown in Eq. (4). The empty and loaded traveled distance were expressed as a function of the grade, i corresponding to the round travel of the truck, substituting Eq. (3) in (2), thus obtaining Eq. (4).

$$x = \frac{h}{i} \tag{3}$$

$$d_i, d_v \text{ optimization} = \sqrt{\left(\frac{h}{i}\right)^2 + h^2} \tag{4}$$

Fig. 1 Schematic representation of mine ramps
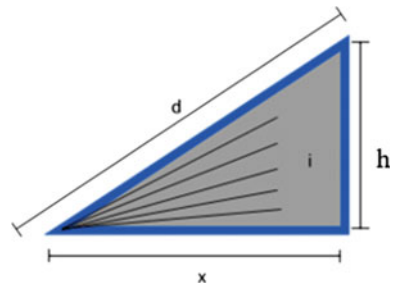
Replacing Eq. (4) in (1), the general mathematical model of productivity as a function of the grade, P_t optimization, (Eq. 5), was obtained considering a payload of 240 tonnes and a fixed time considered constant and equal to 6.8 min, since these variables are not influenced by the haul routes.

$$P_{t \text{ optimization}} = \frac{1}{n} * \sum_{j,k=1}^{n} \frac{60 * 240}{6.8 + \frac{1}{16.67} * \left[\frac{\sqrt{\left(\frac{h_j}{i_j}\right)^2 + h^2}}{v_{i,j}} + \frac{\sqrt{\left(\frac{h_k}{i_k}\right)^2 + h^2}}{v_{v,k}} \right]} \qquad (5)$$

With the above-mentioned model, the Lindo® What's Best tool was used in the solver mode of nonlinear programming to determine the optimal variation of the road grades, that is, the grade value corresponding to the maximum productivity for each access studied. Therefore, the objective function was expressed as Eq. (6).

$$\text{Max } P_{t \text{ optimiztion}} = \frac{1}{n} * \sum_{j,k=1}^{n} \frac{60 * 240}{6.8 + \frac{1}{16.67} * \left[\frac{\sqrt{\left(\frac{h_j}{i_j}\right)^2 + h^2}}{v_{i,j}} + \frac{\sqrt{\left(\frac{h_k}{i_k}\right)^2 + h^2}}{v_{v,k}} \right]} \qquad (6)$$

Subject to constraints:

$$-0.17 \leq i_{j,k} \leq 0.17 \quad \forall j, k \in Z_+^* \qquad (7)$$

$$v_{i,j} > 0 \quad \forall k \in Z_+^* \qquad (8)$$

$$v_{v,k} > 0 \quad \forall k \in Z_+^* \qquad (9)$$

$$h_j = C_j \quad C_j \in IR_+^* \qquad (10)$$

$$h_k = C_k \quad C_k \in IR_+^* \qquad (11)$$

where n: is the number of record points of speed, grade and height of ramp; j, k: is the grade in the point j of loaded travel or k of empty travel; $v_{i,j}$: is the speed in the point j of loaded travel or k of empty travel (km/h); $v_{v,k}$: is the speed in the point k of empty travel (km/h).

The constraint (7) refers to the maximum and minimum grade variation that should obey the maximum and minimum traction capacity for performance issues of the 793D trucks, 17 and -17%, according to [9] Restrictions (8) and (9) refer to the nonnegativity conditions of the round-trip velocities, respectively. The constraints (10) and (11) are, in fact, the definitions of the height values of the accesses that vary from point to point of measurement in the accesses.

For practical application in the mines, in addition to the above-mentioned restrictions, the following premise was taken into consideration: the grade variation could occur only in parts of the route sections, therefore, only parts of the routes were included in the study. The main routes were considered in the same conformation

Table 1 Parameters from a large-scale iron mine, located in Brazil, used in the model

Parameter	Unit	Route A	Route B	Route C	Route D
P_t	t/h	646.32	352.84	331.58	1128.07
C_e	m^3	91.18	91.18	91.18	91.18
ρ_{re}	t/m^3	2.63	2.63	2.63	2.63
E_t	%	100.00	100.00	100.00	100.00
F_t	%	100.00	100.00	100.00	100.00
T_t	min	22.28	40.81	43.43	12.77
T_q	min	3.50	3.50	3.50	3.50
T_v	min	15.48	34.01	36.63	5.97
d	km	2.28	6.18	5.41	0.74
v_i	km/h	12.39	18.17	12.54	12.88
v_v	km/h	30.66	27.20	30.14	17.39
T_d	min	0.90	0.90	0.90	0.90
T_e	min	2.40	2.40	2.40	2.40

and position in function of the geometric limitation for reallocation and thus still maintain the connection between open pits and mining regions.

After obtaining the results of the optimal grade values, it was possible to calculate the new length (distance to be covered) of the routes. Thus, in the optimizations that showed opportunities of productivity gain of haul off-road trucks, the geometric evaluation of the proposal was carried out using the Vulcan® 8.2 software to measure the applicability of the proposed scenarios and their respective impacts on the open pit and consequently, on the stripping ratio and on the ore release.

3 Results and Discussion

3.1 Optimization

Table 1 shows a summary of the calculation parameters and average productivity obtained in each route. It is important to emphasize that the efficiency and the filling bucket factor of the truck were considered equals to a hundred percent.

Note: P_t: haul productivity (t/h); C_e: off-road truck bucket capacity (m^3); ρ_{re}: swollen ore or waste density (t/m^3); E_t: efficiency; F_t: filling bucket factor; T_m: maneuver time; queue time (min); T_q: loading time (min); T_d: dumping time (min); T_e: queue time (min); d_i: loaded traveled distance (m); d_v: empty traveled distance; v_i: loaded truck speed (km/h); v_v: empty truck speed (km/h).

With the hourly productivity of the Caterpillar 793 D off-road trucks practiced in the routes, the next step was to optimize the productivity to determine the optimal

grade value, considering the aforementioned premises and restrictions. Table 2 shows the obtained results in the optimization for each route, comparing with the original scenario, that is, without optimization.

Note: P_t original and optimized: are the haul productivity before and after the optimization, respectively (t/h); d original and optimized: are the ramps distance before and after the optimization, respectively (km), Vmed original and optimized are the average speed before and after the optimization, respectively (km/h); T_t original and optimized are the average speed before and after the optimization, respectively (min).

3.2 Geometrical Assessment of Optimal Haul Road Grade

From the optimization scenarios, the haul road grades that showed opportunities for gain in off-road truck productivity, the geometric evaluation was carried out to measure the applicability of the proposed grades and their impacts on the pit geometry and, consequently, on the stripping ratio.

Therefore, the geometries of the aforementioned paths were changed and the ramps were configured for the optimized grades using the Maptek Vulcan® 8.2 software, as shown in Figs. 2 and 3.

The mass of the original geometries and the mass differences encountered in the revised geometries are presented in Table 3.

Table 2 Comparison between optimized and original scenario

Parameter	Unit	Route A	Route B	Route C	Route D
Original grade	%	8.3	8.1	8.5	8.8
Optimized grade	%	9.2	8.9	8.7	9.6
Variation	%	+10.8	+9.9	+2.4	+9.1
P_t original	t/h	646.32	352.84	331.58	1128.07
P_t optimized	t/h	651.40	357.84	322.13	1148.47
Variation	%	+0.8	+1.4	−2.9	+1.8
d original	km	2.28	6.18	5.41	0.74
d optimized	km	2.24	6.10	5.33	0.72
Variation	%	−16	−1.2	−1.4	−1.7
Vmed original	km/h	21.52	22.68	21.34	15.13
Vmed optimized	km/h	17.56	21.89	21.44	15.11
Variation	%	−18.40	−3.52	+0.45	−0.13
T_t original	min	22.28	40.81	43.43	12.77
T_t optimized	min	22.11	40.24	43.43	12.54
Variation	%	−0.8	−1.4	+0.0	−1.8

Table 3 Comparison between optimized and original scenario

Route	Grade	Ore (10^3 t)	Waste (10^3 t)	Total mass (10^3 t)	Stripping ratio
A, B	G orig.	34.810	89.190	124.000	2.56
	G otim.	910	2.670	3.580	2.93
Var (%)		+2.6	+3.0	+2.9	+14.5
D	G orig.	28.080	5.960	34.040	0.21
	G otim.	2.230	500	2.730	0.22
Var (%)		+7.9	+9.1	+8.1	+6

The change in geometry with the new ramp grades on routes A and B increased the ore release by 2.6%, with a mass increase of 910,000 t. This ore has a waste associated stripping ratio of 2.93, which is greater than stripping ratio of the pit, which is 2.56. There was an increase of waste mass of 2,670,000 t.
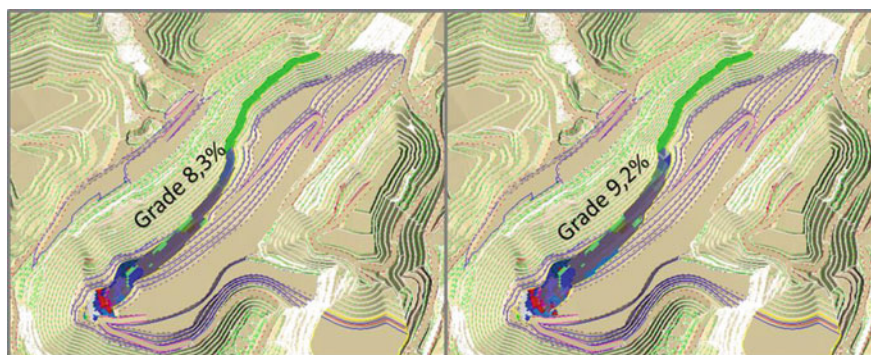
Fig. 2 Review of the ramps geometry in the routes A and B. On the left, path in the original grade: on the right, path according to optimization
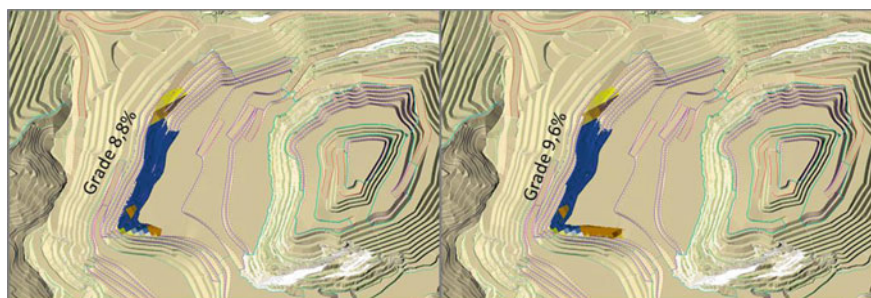
Fig. 3 Review of the ramps geometry in the route D. On the left, path in the original grade: on the right, path according to optimization

In route *D*, the geometry change increased the ore release by 7.9%, adding 2,230,000 t of mass to the ore of the original geometry. The stripping ratio presented a slight increase, but remained close to the pit levels, which is 0.21.

Therefore, the long-term mining planning must evaluate according to its premises of ore and waste movement whether the proposed grade alteration implementation of especially in routes A and B, is viable. In the case of the route D, the proposed grade appears to be plausible for application, since ore liberation occurs without major impact on the stripping ratio.

4 Conclusion

The assessment performed in this work showed that haul road grades are relevant geometric parameters and deserve attention in determining the pit geometry. The models developed to optimize haul road grades are an important complement for the analysis of the productivity and costs. Integrated models for quantifying productivity and costs are extremely important tools to maximize productivity and thus minimize the costs of hauling ore or waste in open-pit mining.

The study have shown that there are opportunities to maximize the hourly productivity of off-road trucks with small variations of haul road grades, as shown by determining the optimal values. Although increasing the traveled time, decreased the total distance traveled, generating a positive effect in the total cycle time of the off-road truck. For each 1% on average of grade change, the gain of productivity gain was about 7%.

The optimization using the models developed for Caterpillar 793C truck shows an excellent result and with great potential for practical application in the open-pit mining operations. In view of the obtained results, its pilot application in open-pit mines is extremely important.

References

1. Vale: Manual de estradas de mina (Interno) [Guidelines for mine haul road design], pp. 12–13 (2011)
2. Ercelebi, S.G., Bascetin, A.: Optimization of shovel-truck system for surface mining. J. South Afr. Inst. Min. Metall. **109**, 433–439 (2009)
3. Arroyo, J.E.C.: Heurísticas e metaheurísticas para otimização combinatória multi-objetivo, p. 180. Unicamp, Heuristics and metaheuristics for combinatory oprtimization. Tese de Doutorado (2002)
4. Brandão, R., Tomi, G.: Metodologia para estimativa e gestão da produtividade de lavra. Methodology to estimate and manage mining productivity. R. Esc. Minas **64**(1), 77–83 (2011)

5. Moraes, E.F.: Um modelo de programação matemática para otimizar a composição de lotes de minério de ferro da mina Cauê da CVRD. A mathematical programming model to optimize the composition of iron ore lots at the Cauê mine of CVRD Dissertação de Mestrado: Programa de Pós-Graduação em Engenharia Mineral da Universidade Federal de Ouro Preto, 78p (2005)
6. Pantuza Júnior, G.: Métodos de otimização e simulação multiobjectivos aplicado ao problema de planejamento operacional de lavra em minas a céu aberto [Multiobjective optimization and simulation methods applied to the problem of operational planing in open pit mines] Dissertação de Mestrado: Programa de Pós-Graduação em Engenharia Mineral da Universidade Federal de Ouro Preto, 75p (2005)
7. Rodovalho, E.C., Tomi, G.: Reducing environmental impacts via improved tyre wear management. J. Clean. Prod. **142**, 1419–1427 (2017)
8. Navarro Torres, V.F.: Minimização efetiva dos custos de lavra a céu aberto [Open pit mine costs effective minimization], 47p. Instituto Tecnológico Vale (2016)
9. Caterpillar: Caterpillar Performance Handbook, vol. 46, p. 2378 (2016)

Part VI
Waste Disposal

Sensitivity Analysis of Mechanical and Geometrical Properties of Fly Ash Stabilized Overburden Dumps Using Mathematical Simulations

T. Gupta, M. Jamal, M. Yellishetty and T. N. Singh

1 Introduction

It is without a doubt that modern surface mining operations provide the highest production and productivity figures among all other mining methods. From coal for firing the power plants to hematite for iron and steel, maximum productions are seen from the large-scale opencast mines throughout the world. For instance, major coal producing nations like India and Australia have a much higher percentage of production from surface mining operations as compared to underground mining. The share of coal produced from surface mining operations in India increased from 87% in 2008 to 93% in 2017 [1]. A similar rise is seen for Australia, Colombia, and the USA [2]. Increasing production demands and technological advancements have also led to a multifold increase in the production of other important minerals which can be mined today at substantially lower grades [3, 4]. These advancements have made mining at higher stripping ratios economic, thus allowing the removal of higher quantities of overburden during mining operations [5–10].

Storing these increasingly large amounts of overburden inside the mining premises has always been a logistical and economic challenge in a surface mining operations. The overburden material is traditionally stored either inside or outside the active mining area based on the mining methodology, forming internal and external dumps, respectively. Since there is always a dearth of land available for mining activities, these dumps must be made higher and steeper in order to store more material in a

T. Gupta
IITB-Monash Research Academy, IIT Bombay, Powai 40076, Mumbai, India

M. Jamal · M. Yellishetty (✉)
Resources Engineering, Monash University, Clayton 3800, Australia
e-mail: mohan.yellishetty@monash.edu

T. N. Singh
Department of Earth Sciences, IIT Bombay, Mumbai 400076, India

limited area. This increase in the geometrical dimensions such as height and slope angle of overburden dumps can result in destabilization of dump slopes which can be catastrophic for the mining operation and can result in the loss of life and property [11–14].

Thus, it becomes necessary to introduce artificial stabilization measures to make sure these dumps remain stable for a safer mining operation and simultaneously hold large volumes of overburden material. Among the many methods of dump stabilization such as mechanical stabilization [15–19], chemical stabilization [20–23], and biological stabilization [24–26]. One of the latest methods is to stabilize the dump slopes using fly ash composite layers. Gupta et al. 2015 [27] have established this method as a highly feasible, environmentally safe, and economic, stabilization method for dump slopes which can not only stabilize the present slopes but also considerably enhance the dump's capacity [27, 28]. Their studies made use of an indigenously developed fly ash composite that was layered in overburden dumps, thus improving its stability (Fig. 1). The thickness of composite layers that could give maximum stability was optimized (and termed as critical layer thickness) according to the dump geometry and material properties of the composite and overburden material, using the factor of safety (FOS) as the deciding factor [27].

To extend the fly ash composite stabilization model and to make it universally applicable, an extensive analysis was performed to predict the optimized fly ash composite thickness for any geometry of overburden dump, and for any type of overburden and fly ash composite material. All these factors affected the stability of the dump slopes to a certain extent and it was important to understand the effect of each individual parameter on the overall slope stability and the optimized composite thickness for designing a stabilized dump slope.
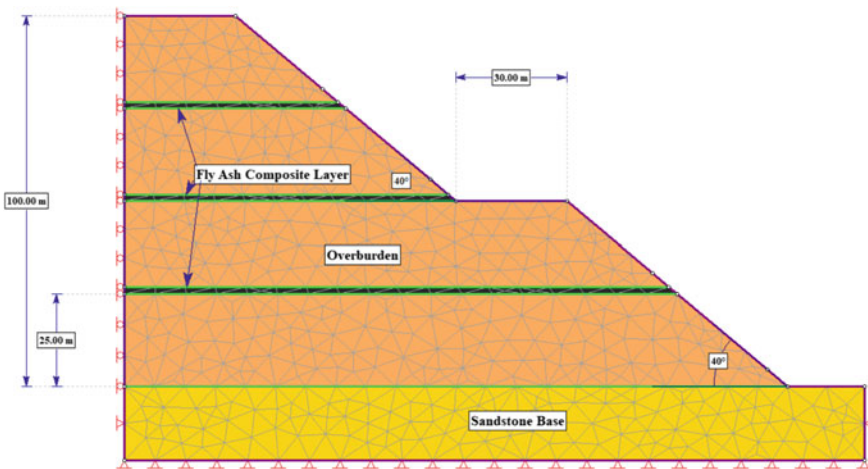
Fig. 1 Stabilization model of overburden dump by fly ash composite layers

This paper discusses the sensitivity of the FOS and the optimized critical layer thickness on the design parameters and the material properties of the overburden dump. The work of Gupta et al. [27] was progressed to analyze the FOS and critical layer thickness while varying the design parameters and material properties of overburden dumps including dump height, bench slope, berm width, number of composite layers, cohesion, internal angle of friction, and unit weights of the composite and overburden material. Simulation models of the dump slopes were generated and solved using the finite element method (FEM) and the limit equilibrium method (LEM) for all the parametric variations and the sensitivity analysis was performed for each of them. This paper acts as a preliminary research for further universalizing the fly ash layered composite stabilization model.

2 Materials and Methods

The stabilization composite used was a fly ash based construction material which was optimized by a series of laboratory experiments to get maximum compressive strength and other structural properties [27, 29]. The base constituents of the composite included fly ash, overburden material (as aggregate), and clinker (as an external source of lime). The mechanical properties of the optimized composite were obtained from Gupta et al. [27], and are provided in Table 1. Later research has also proven that better mechanical properties can be obtained in case slacked lime is used in place of clinker. This also makes the composite a cement-free and economic concreting material.

The methodology followed for this research is an extension of Gupta et al. 2015 [27]. A dump slope was simulated with an original height of 100 m, consisting of two benches staggered along the berm to decrease the overall slope. The dump was stabilized by horizontal composite layers separated equally along the dump height (Fig. 1). Stability of these dumps was computed using Finite Element (FEM) and Limit Equilibrium (LEM) models for mathematical simulations. While the FEM is based on dividing the geometry into nodes and elements and analyzing the FOS by strength reduction technique, the LEM takes use of the critical failure circles and initiation points to calculate the FOS (Fig. 2a, b). Since both techniques are unique and applicable to slope stability analysis, the model providing the least FOS for each simulation was considered for the evaluation of results.

Table 1 Material properties of the optimized fly ash composite and overburden material

Material property	Fly ash composite	Overburden material
Cohesion (kPa)	4800	85
Internal angle of friction (°)	38	38
Unit weight (kN/m^3)	19.8	20.5
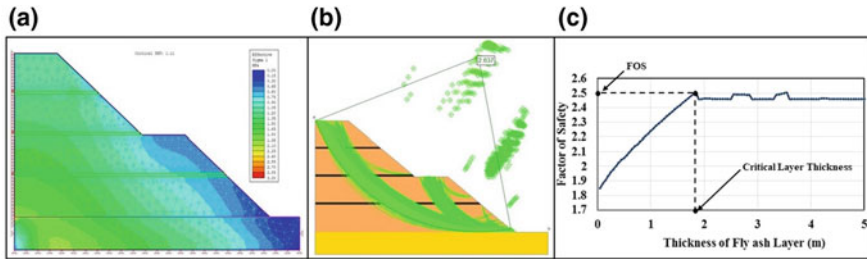
Fig. 2 Stability analysis performed using **a** FEM, and **b** LEM. **c** An example for determining critical layer thickness due to the plateauing effect of the FOS with an increase in composite layer thickness

For calculating the critical layer thickness that provides the maximum FOS in the given dump design, models with varying layer thickness were simulated and analyzed for FOS. The thickness of composite layers was evaluated from 0.05 to 5 m, with a variation of 0.05 m, making 100 individual simulation models for each dump design. It was observed that in most dump designs, the FOS initially increased and then plateaued with an increase in composite layer thickness (Fig. 2c). The plateauing of FOS signified that any further increase in composite layer thickness would not add to the stability of dump slope. Thus, the thickness of fly ash composite layer at which the FOS plateaued was taken as the critical layer thickness for that dump design.

To find the critical layer thickness for varying dump designs and to see the effect of design and material parameters on critical layer thickness and FOS, different dump design models were simulated. Each dump design was analyzed for its critical layer thickness as described above. Ten parameters including those of dump geometry and material properties were varied to calculate critical layer thickness for each case. The geometrical parameters (the dump height, slope angle, berm width, and number of stabilization layers) were varied so as to cover a wide variety of dump designs prevalent in surface mining operations today. The material properties of overburden were varied to simulate a broad range of materials that can be present in different mining scenarios. Since the properties of fly ash composite are based on nature of constituents used [30], the variations in its material properties were performed accordingly. The variations are summarized in Table 2. A total of 406 distinct dump designs were analyzed for their critical layer thickness and FOS, resulting in a total of 40,600 simulations conducted for this study (Fig. 3).

Sensitivity analysis was carried out on one at a time (OAT) approach, where a single parameter was varied while others were kept at some constant base values. This method of sensitivity analysis gave sensitivities of FOS and critical layer thickness on individual parameters, thus giving their independent impact quantifications. Though the OAT approach does not consider the interdependence of parameters, it can be considered suitable for the present type of study [13, 31].

The quantification of sensitivities was performed by calculating the sensitivity index for individual parameters. Sensitivity index (SI) is a dimensionless index that

Table 2 Variation studied and simulated in geometrical and material parameters

S. no.	Parameter	Original value (X_0)	Range (X_1–X_2)	Intervals	Total design models
1	Dump height (m)	100	50–200	5	30
2	Slope angle (°)	40	20–80	2	30
3	Berm width (m)	30	2–60	2	29
4	Number of fly ash composite layers	3	1–6	1	6
5	Fly ash composite cohesion (kPa)	4800	3840–6000	43.20	50
6	Fly ash composite Internal angle of friction (°)	38	30.4–47.5	0.34	50
7	Fly ash composite unit weight (kN/m^3)	19.8	15.84–24.75	0.38	50
8	Overburden cohesion (kPa)	85	68.00–106.25	0.77	50
9	Overburden internal angle of friction (°)	38	30.40–47.5	0.34	50
10	Overburden unit weight (kN/m^3)	20.5	16.4–25.625	0.19	50
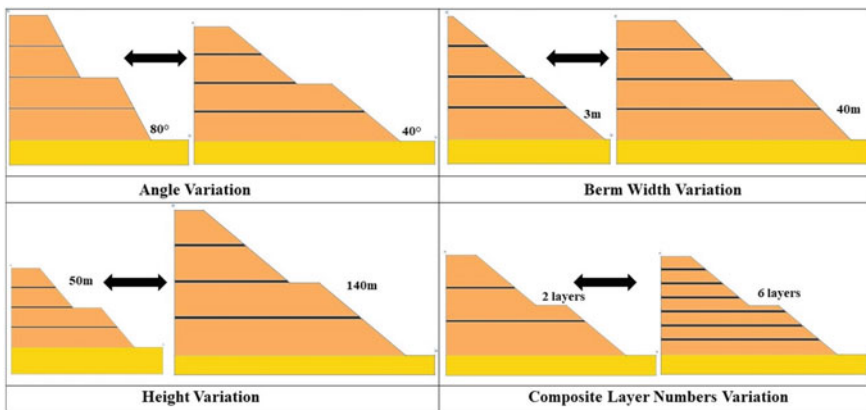
Fig. 3 Some of the simulated dump designs due to geometrical parametric variations

was evaluated by the Eqs. 1 and 2. A higher absolute value of SI will indicate the greater sensitivity of that parameter [32]. SI can be broadly categorized into four groups; Very high sensitivity (SI > 1.0), High sensitivity (SI = 0.2–1.0), Medium sensitivity (SI = 0.05–0.2), and Low sensitivity (SI < 0.05) [32].

Fig. 4 Calculation of sensitivity index during OAT analysis [13]

$$SI = \frac{(Y_2 - Y_1)/Y_o}{(X_2 - X_1)/X_o}$$
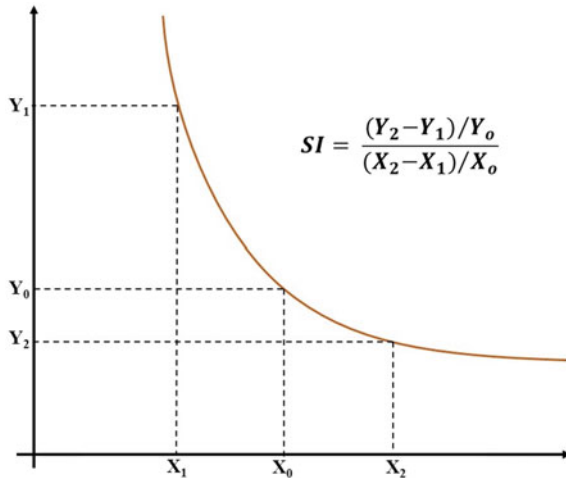
$$SI = \frac{Y_2 - Y_1/Y_0}{X_2 - Y_1/X_0} \qquad (1)$$

$$X_2 - X_0 = X_0 - X_1 = \Delta X \qquad (2)$$

Here SI is the dimensionless sensitivity index, Y_0 is the initial output of the critical fly ash thickness, X_0 is the initial input value of the parameter, ΔX is the parametric variation in the analysis, and Y_1, Y_2 are the outputs for X_1, X_2, as per Eqs. 1 and 2 and Fig. 4.

3 Results and Discussion

The SI of each parameter was calculated for FOS as well as critical layer thickness. The sensitivity plots for each of these parameters are presented in Figs. 5, 6, 7 and 8, and the sensitivity indices are summarized in Table 3.

The FOS for the dump slope decreased with increase in the slope angle and the dump height, while it was seen to marginally increase with an increase in the berm width of the overburden dump (Fig. 5). These results were expected as the effective stress on the slope increased in case of an increase in height and slope angle. Since the effective slope decreases by an increase in the berm width, the FOS increase with an increase in berm width. The FOS exhibits a linear increase with an increase in number of composite layers used for stabilization.

Using the trends of the FOS obtained here, the SI was calculated. It was observed that the FOS exhibited a high sensitivity toward the dump height, slope angle, and the number of composite layers (Table 3), all having SI > 0.4. However, the FOS was
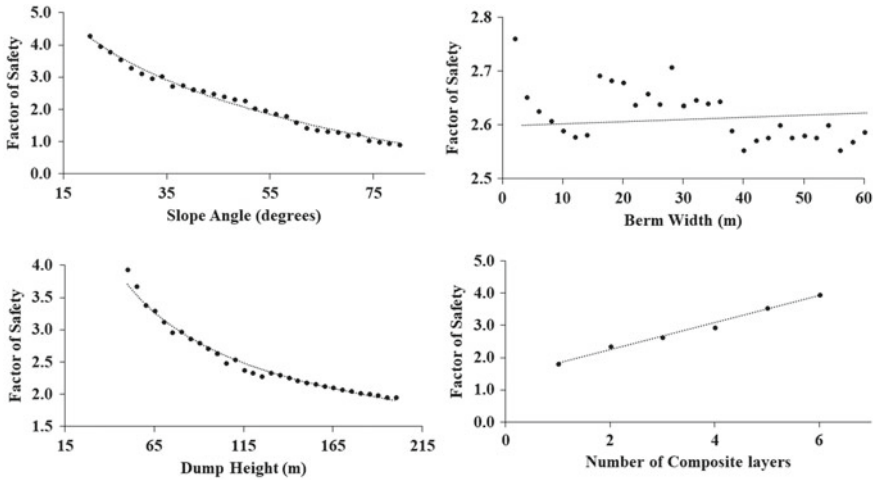
Fig. 5 Sensitivity plots of FOS for geometrical parameters of dump slope
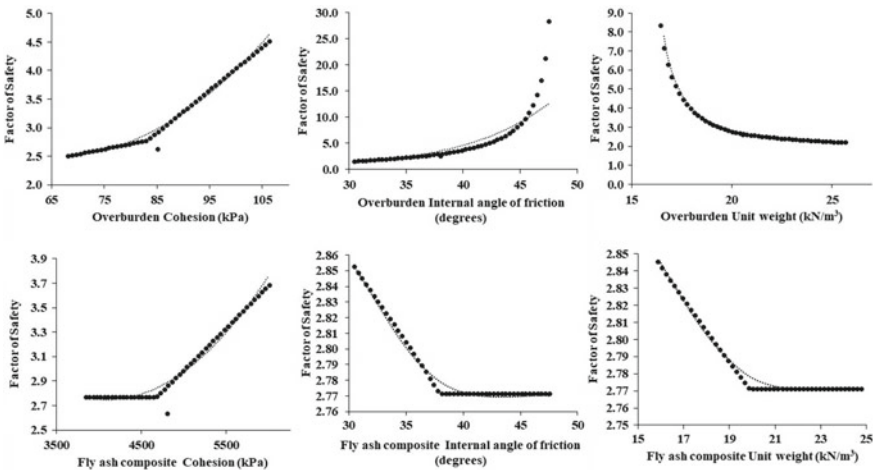
Fig. 6 Sensitivity plots of FOS for material parameters of dump slope

least sensitive towards berm width, with a SI of 0.02, indicating that although there was an increase in FOS due to increase in berm width, it was not substantial.

With respect to material properties, the FOS was seen to substantially increase with an increase in the cohesion and internal angle of friction of overburden material (Fig. 6). These trends clearly suggest the increase in strength of overburden material, resulting in the increase in the factor of safety. The FOS shows a decreasing trend with the increase in the unit weight of overburden due to increasing stresses applied due to larger weight (Fig. 6).
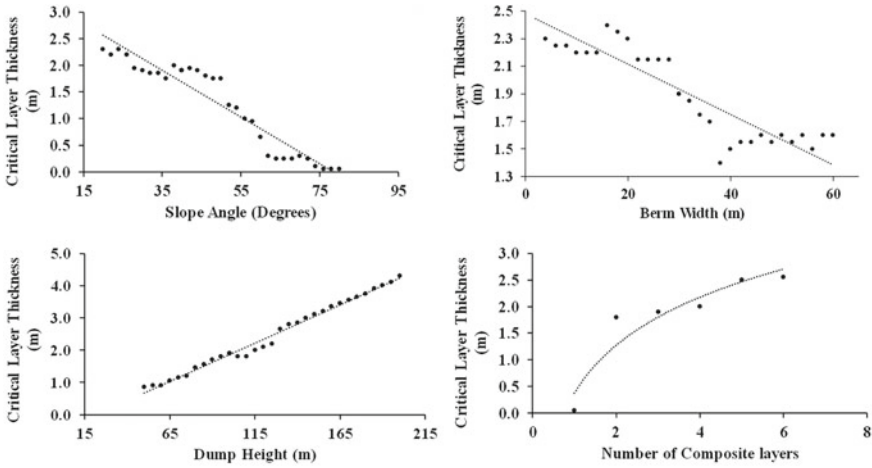
Fig. 7 Sensitivity plots of critical layer thickens for geometrical parameters of dump slope
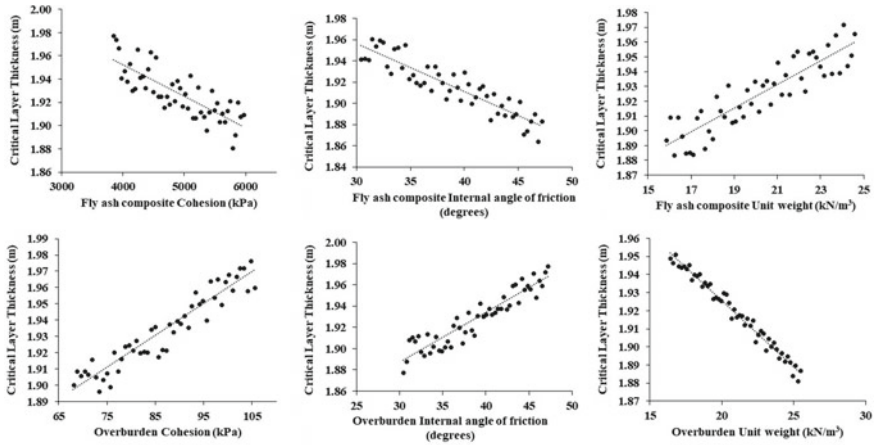
Fig. 8 Sensitivity plots of critical layer thickens for material parameters of dump slope

For fly ash composite, the FOS exhibited prominent horizontal sections (constant values) in some parts of sensitivity curves. This was due to the fact that beyond a certain value of material properties of the composite, the failure started to occur just in the overburden region of dump slope. This can be seen in Fig. 2b where some failure circles pass only through the overburden material. Since after this point of 'failure shift', the dump failure becomes independent of the fly ash composite layers, any change in material property of the composite would not change the overall FOS.

FOS was found to have very high sensitivities towards all the material properties of overburden, and the cohesion of fly ash composite. However, it was observed to be

Table 3 Sensitivity index of all varied parameters for critical layer thickness and FOS

S. no.	Parameter	Sensitivity index for critical layer thickness	Sensitivity index for factor of safety
1	Slope angle (°)	−0.90	−0.83
2	Dump height (m)	1.25	−0.46
3	Berm width (m)	−0.29	0.02
4	Number of fly ash composite layers	0.74	0.47
5	Fly ash composite cohesion (kPa)	−0.08	1.27
6	Fly ash composite internal angle of friction (°)	−0.09	−0.15
7	Fly ash composite unit weight (kN/m^3)	0.09	−0.14
8	Overburden cohesion (kPa)	0.09	1.69
9	Overburden internal angle of friction (°)	0.10	9.56
10	Overburden unit weight (kN/m^3)	−0.08	−2.98

less sensitive toward the internal angle of friction and unit weight of the composite (Table 3).

The critical layer thickness of fly ash composite was observed to increase with an increase in the dump height, indicating the requirement of a thicker stabilization layer for higher dumps. However, with increase in the slope angle of dump, the critical layer thickness was seen to decrease (Fig. 7). This was because as the dump slope angle increased, greater amount of material remained unsupported on the bench top and edges (Fig. 3). Therefore, the stage of failure shift occurs at a lower thickness value beyond which no additional stabilization occurs with a further increase in composite layer thickness. Thus, with an increase in slope angle the critical layer thickness decreases. On similar lines, in case of an increase in the number of composite layers, there is a reduction of the effective unsupported overburden which can fail independently. This ensures that thicker composite layers can be designed without overburden failing independently. Thus, the critical layer thickness increase with an increase in the number of composite layer and offers greater stabilization (Fig. 7).

The sensitivity of critical layer thickness was higher for all the geometrical parameters, with SI > 0.29. It also had very high sensitivity towards dump height, with a sensitivity index of 1.25. This indicates that geometrical parameters play a critical role in designing an effective stabilization plan.

In terms of the variation in material properties, critical layer thickness was seen to decrease with increase in cohesion and the internal angle of friction of the composite, while it increased with increase in the unit weight (Fig. 8). This is an indication of the requirement of the lower thickness of composite layer for effective stabilization of dump, when the strength of composite is higher. A composite with higher unit weight will require a greater thickness of composite for best stabilization.

When the strength of overburden material increases either through an increase in cohesion or its internal angle of friction, the independent failure of overburden at bench edges is reduced. This prolongs the stage of failure shift allowing a higher thickness of fly ash composite layer with better stabilization opportunity. This is reflected in Fig. 8, where critical layer thickness increased with an increase in cohesion and internal angle of friction of overburden. Conversely, a denser overburden will become more unstable, thus the critical layer thickness was seen to decrease with the increase in unit weight of overburden (Fig. 8).

In contrast to the FOS, the critical layer thickness exhibited medium to low sensitivity toward all the material properties of composite and overburden with $SI < 0.1$ for all cases (Table 3). This indicates that although there is an effect of material properties on the required layer thickness for maximum optimization, the effect is not consequential for major design aspect.

4   Conclusion

This study establishes the criticality of the dump geometry on the stabilization planning of a dump slope. The thickness of fly ash composite that provides maximum stabilization in an overburden can be effectively increased till the failure happens only in the unsupported overburden material. This thickness was largely affected by the dump's height, slope angle, number of composite layers, and the berm width, as was indicated by the higher values of sensitivity index. The Factor of Safety of the dump, however, was more dependent on the material properties of overburden and to some extent on the geometry of the dump slope.

This study also establishes some limiting cases for this stabilization method where no thickness of fly ash composite proves sufficient for complete stabilization. A cross-reference between the critical layer thickness and the associated factor of safety will be crucial for designing an effective stabilization plan.

The results from this analysis are important checkpoints that will pave steps for universalizing this economic, environmentally safe, and effective stabilization method. Further studies will make use of statistical and artificial intelligence (AI) based analysis tools to generate a design toolbox that will help mining and civil engineers throughout to world to not only stabilize the dump slopes but also enhance dump's capacity to achieve the requirement of sustainable but economic mining.

References

1. GOI_PCS: Provisional Coal Statistics 16–17, C. C. s. Organisation (Editor), Ministry of Coal, Government of India, Kolkata (2017)
2. Fuginski, Z.: Underground Coal Mining—Global Picture and Brief Overview. Colombai Clean Power, Colombai (2012)

3. MOC: Annual Report 2016–17. Annual Report, M. o. Coal (Editor), Ministry of Coal, Government of India, New Delhi (2017)
4. Sehgal, A., Tongia, R.: Coal Requirement in 2020: A Bottom-Up Analysis (2016)
5. IEA: Coal Information 2017. Coal Information, I. E. Agency (Editor), International Energy Agency (2017)
6. AEU: Australian Energy Update 2017. Australian Energy Update, E. S. a. A. Section (Editor), Department of Environment and Energy, Australian Government, Canberra (2017)
7. MSOPI: Energy Statistics 2017. Energy Statistics, C. S. Office (Editor), Ministry of Statistics and Programme Implementation, Government of India, New Delhi (2017)
8. Da Gama, C.D.: Easy profit maximization method for open-pit mining. J. Rock Mech. Geotech. Eng. **5**, 350–353 (2013)
9. Falkie, T.V., Porter, E.: Economic surface mining of multiple seams. In: Application of Computer Methods in the Mineral Industry Proceeding (1973)
10. Ziling, S., Yundong, M.: A new method to confirm the economic and reasonable stripping ratio of surface coal mine. In: Second International Conference on Computational Intelligence and Natural Computing (CINC) IEEE, pp. 47–52 (2010)
11. Bowman, P., Gilchrist, H.: Waste dump instability and its operational impact for a canadian plains lignite mine. In: Proceedings of the International Symposium on Stability in Coal Mining, pp. 381–394. Vancouver, British Colombia, Canada (1978)
12. Kainthola, A., Verma, D., Gupte, S., Singh, T.: A coal mine dump stability analysis—a case study. Geomaterials **1** (2011)
13. Rai, R., Kalita, S., Gupta, T., Shrivastva, B.: Sensitivity analysis of internal dragline dump stability: finite element analysis. Geotech. Geol. Eng. **30**(6), 1397–1404 (2012)
14. GOI: Update on ECL Rajmahal Coal Mine Accident. M. o. C. Government of India (Editor) (2016) http://pib.nic.in
15. Lersow, M.: Deep soil compaction as a method of ground improvement and to stabilization of wastes and slopes with danger of liquefaction, determining the modulus of deformation and shear strength parameters of loose rock. Waste Manag **21**, 161–174 (2001)
16. Clegg, B.: Kneading Compaction. Aust. Road Res. (1964)
17. Olufowobj, I., Ogundoju, A., Michael, B., Aderinlewo, O.: Clay soil stabilisation using powdered glass. J. Eng. Sci. Technol. **9**(5), 541–558 (2014)
18. Li, Q., Li, Y., Dasgupta, G., Song, D., Qiao, L., Wang, L., Dong, J.: Analysis of the blasting compaction on gravel soil. J. Chem. **2015**, 1–9 (2015)
19. Geosimpro: Static Weight Compaction (2017)
20. Maaitah, O.N.: Soil stabilization by chemical agent. Geotech. Geol. Eng. **30**(6), 1345–1356 (2012)
21. Onyejekwe, S., Ghataora, G.S.: Soil stabilization using proprietary liquid chemical stabilizers: sulphonated oil and a polymer. Bull. Eng. Geol. Env. **74**(2), 651–665 (2014)
22. Hamzah, H.N., Al Bakri Abdullah, M.M., Yong, H.C., Zainol, M.R.R.A., Hussin, K.: Review of soil stabilization techniques: geopolymerization method one of the new technique. Key Eng. Mater. **660**, 298–304 (2015)
23. Karatai, T.R., Kaluli, J.W., Kabubo, C., Thiong'o, G.: Soil stabilization using rice husk ash and natural lime as an alternative to cutting and filling in road construction. J. Constr. Eng. Manage. **04016127** (2016)
24. Nguyen, L.: Fibre Reinforced Clay. U. r. g. u. s. a. Carpeting (Editor), CRICOS, UTS Newsroom (2014)
25. Calderwood, T.: Why is hydroseeding better than traditional methods of growing lawns. RadioYu (2016)
26. Shahram, P., Afshin, A., Bujang, B.K.H., Nuno, C., Fasihnikoutalab, M.H.: Application of alkali-activated agro-waste reinforced with wollastonite fibers in soil stabilization. J. Mater. Civil Eng. **29**(2) (2017)
27. Gupta, T., Yellishetty, M., Singh,T.: Optimization of Ash Content in Overburden Dumps: A Numerical Approach, pp. 997–1004. Mine Planning and Equipment selection (MPES-2015), The South African Institute of Mining and Metallurgy (2015)

28. Gupta, T., Singh, T.: Geo-hydrological stability analysis of fly ash stabilised overburden dump slopes in opencast coal mines using finite element analysis. Int. J. Adv. Sci. Eng. Info. Technol. **8**(2), 405–410 (2018)

29. Gupta, T.: Fly Ash Utilisation in Haul Road Construction in Open Cast Coal Mines: A Geo-Environmental and Hydrogeological Investigation, vol. 211. Department of Earth Sciences (IITB), Department of Civil Engineering (Monash University) PhD, Indian Institute of Technology Bombay, IIT Bombay (2018)

30. Niranjan and Radhakrishnan: An experimental investigation on fal-g paste. Int. Adv. Res. J. Sci. Eng. Technol. **2**(3), 41–49 (2015)

31. Gupta, T., Rai, R., Jaiswal, A., Shrivastva, B.: Sensitivity analysis of coal rib stability for internal mine dump in opencast mine by finite element modelling. Geotech. Geol. Eng. **32**(3), 705–712 (2014)

32. Lenhart, T., Eckhardt, K., Fohrer, N., Frede, H.-G.: Comparison of two different approaches of sensitivity analysis. Phys. Chem. Earth, Parts A/B/C **27**(9–10), 645–654 (2002)

Part VII
Rock Mechanics and Geotechnical Applications

Three-Dimensional Integral Modeling of Large Open-Pit Slopes: An Innovative Stability Analysis

G. F. Napa-García, V. F. Navarro Torres, I. R. Trópia, R. B. Capelli and T. R. Câmara

1 Introduction

The stability of the slopes excavated by the mining activities in surface is of key importance when dealing with large-scale projects because failure events may lead to large financial loses and delays, safety issues and even to the complete interruption of an entire mining project. In this context, the knowledge of the mechanical behavior of the geotechnical environment before the new conditions imposed by the mining activity is fundamental. All of the information necessary to represent this behavior must be contained in the geotechnical model for the mine planning. The geotechnical model of an open–pit mine is constituted essentially by four parts: geology, structural, geomechanics, and hydrogeology. The assertiveness of the material spatial distribution as well as their geotechnical properties are fundamental for the quality, accuracy and safety problems prediction. However, the large amount of uncertainty sources turns this a colossal task. In this sense, any kind of reduction of

G. F. Napa-García (✉) · V. F. Navarro Torres
Instituto Tecnológico Vale, Mining, Belém, Brazil
e-mail: gian.garcia@itv.org

V. F. Navarro Torres
e-mail: vidal.torres@itv.org

I. R. Trópia · T. R. Câmara
Vale S.A, Rio de Janeiro, Brazil
e-mail: isabela.tropia@vale.com

T. R. Câmara
e-mail: tais.camara@vale.com

R. B. Capelli
NUGEO, Universidade Federal de Ouro Preto, Ouro Preto, Brazil
e-mail: renatabzc@gmail.com

371

the uncertainty in the components of the geotechnical model improves the safety of the project by means of reducing the geotechnical risk.

The open-pit slope design should minimize risks to personnel and equipment, maximize ore recovery and minimize waste volume to maximize the profits. For the case of geotechnical analyses, two-dimensional models of slope stability are usually employed. Two-dimensional slope stability methods are mostly used due to their simplicity; however, they consider some simplifying assumptions to reduce the three-dimensional reality to a two-dimensional representation, and so, the accuracy of the estimation of the factor of safety will vary according to each case as much as 30% [1]. Limit equilibrium is typically used for analyzing standard problems and numerical method codes are occasionally used in few more complicated cases.

Open-pit iron ore mines have been reaching greater depths, with some slopes having more than 300 m height. With the increasing pit depths and slopes heights, there is a growing concern that stability analyses should be based on assumptions closer to the geometric, geological and geomechanical reality of the deposit. The three-dimensional models can contribute greatly to solve this problem.

According to [1], the three-dimensional analysis becomes important in cases where the geometry of the deposit is so complex that it is difficult to select a typical two-dimensional section to analyze. A 3D analysis may be necessary when the geometry of the slope and slip surface varies significantly in the lateral direction, the material properties are highly inhomogeneous or anisotropic, amongst other complicating factors.

The majority of the works of stability analysis strongly suggests that the 2D factor of safety is conservative when compared to the 3D factor of safety. Three-dimensional analysis is more realistic in being able to account properly for the slope geometry, leading to a better understanding of the fundamental nature of slope failure mechanisms [2]. Thus, this paper presents a geotechnical safety modeling routine that incorporates information from the geological model and uses this basis to build up automatically the geotechnical model using geological, structural, geomechanical and hydrogeological data. The study case of a large iron ore mine located in the Iron Quadrangle in Brazil is presented to show some results obtained using the routine.

2   Methodology

The geological block model constructed for any deposit can also bring together different rock mass characteristics. This block model contains geological and geometrical information such as the lithotype and the spatial distribution of lithologies in absolute coordinates. In addition, other information such as the Geological Strength Index (GSI), typical structural sectors, and the presence of faults were added to the existing information in order to complement the data needed to create the model. The following attributes were exported in order to create an enhanced geological block model:

- IJK Indexes
- block centroids coordinates (XC, YC, ZC)
- cell size—Cartesian dimensions of the block (XINC, YINC, ZINC)
- rock type (3 character alias)
- fault indicator (0 when false, 1 when true)
- origin coordinates (XMORIG, YMORIG, ZMORIG)
- number of blocks in the original prototype (NX, NY, NZ)
- GSI.

This enhanced geological model is the first keystone of the modeling routine presented following.

The three-dimensional numerical modeling was carried out in a software based on finite differences—FLAC3D [3]—because this code is adequate to solve the majority of the problems related to geotechnical engineering. FLAC3D simulates the three-dimensional behavior of structures constructed in soil, rock or other possible materials subject to plastic flow when their limits in terms of rupture are reached. The available programming environment is unique and called FISH [3]. Also, FLAC3D incorporated a Python console in its version 6.0 as well as a FLAC3D library to handle the model variables from the Python console. Python language is commonly used in scientific computing because of its excellent support for scientific and numerical programming solutions. The FLAC3D geotechnical model was implemented combining FISH and Python programming.

2.1 Numerical Grid

The routine to build up the geotechnical block model consists in constructing the FLAC3D grid file using an external routine written in Python, including all the characteristics mentioned above grouping zones according to similar characteristics when possible. The reading process creates a list of zone objects by filling in and calculating the attributes. The enhanced block model must be in text format such as .csv, .txt or another one keeping the order listed above. Finally, the grid file is loaded into FLAC3D.

2.2 GSI Representation

Once the GSI values read from the enhanced block model, they are saved using a Python array to be used later. The GSI array is loaded after the grid has been created in FLAC3D since the GSI of each block is free to be different.

2.3 Hydrogeology

The local hydrogeological behavior can be represented by a full conductivity tensor flow analysis or a phreatic/hydrostatic pore-pressure generation. In the case of the full tensor analysis, the conductivity is calculated using the structural information relative to sectors and geometric/hydraulic properties of the joints in each lithotype and sector. Otherwise, pore-pressures are simply calculated based on a phreatic surface.

2.4 Geomechanics

The geomechanical behavior of the rock mass can be represented using three failure criteria coexisting in the same model: generalized Hoek–Brown (HB), Mohr—Coulomb (MC), and Ubiquitous-Joint (UJ). An input file containing the mechanical parameters of the intact rock and foliations, as well as the corresponding failure criterion must be provided in text format. The structural sector is also taken into account to define the dominant orientation of the foliated lithotypes. The input parameters of the three models are calculated in Python for each block and saved in the FLAC3D model. A disturbance factor $D = 0.7$ was considered to represent the probable reduction in physical properties of faulted materials (HB and UB) and reduced parameter was used for MC materials as well. A short description of the failure criteria used in this model is explained following.

2.4.1 Failure Criteria

The Generalized Hoek–Brown criterion is an empirical failure criterion, which establishes the strength of rock according to major and minor principal stresses. It was used as the basis of the geomechanical model. However, it is known that this criterion is isotropic and, hence, it is not able to represent the anisotropic behavior imposed by the presence of structural geological features such as foliations. The geological mapping showed the presence of foliations in some lithotypes of the study site. The ubiquitous-joint model was adopted, in order to consider this type of feature.

Hoek et al. [4] showed the generalized Hoek–Brown criterion [5], in terms of major and minor principal stresses σ'_1 and σ'_3,

$$\sigma'_1 = \sigma'_3 + \sigma_{ci}\left(m_b\frac{\sigma'_3}{\sigma_{ci}} + s\right)^a \tag{1}$$

where σ_{ci} is the uniaxial compressive strength (UCS) of the intact rock material.

$$m_b = m_i \exp\left(\frac{GSI - 100}{28 - 14D}\right) \tag{2}$$

$$s = \exp\left(\frac{\text{GSI} - 100}{9 - 3D}\right) \tag{3}$$

$$a = \frac{1}{2} + \frac{1}{6}\left(e^{-\text{GSI}/15} - e^{-20/3}\right) \tag{4}$$

where m_i is a material constant for the intact rock, GSI (the Geological Strength Index) relates the failure criterion to geological observations in the field, and D is a "disturbance factor" which depends upon the degree of disturbance to which the rock mass has been subjected by blast damage and/or stress relaxation ($D = 0$, for high quality blasting and $D = 1$, for poor quality blasting).

The ubiquitous-joint model available in the FLAC3D is based on the Mohr—Coulomb isotropic model, except for the weakness planes orientation. The presence of weakness planes is considered with another Mohr–Coulomb criterion (with lower resistance) superposed to the isotropic material, which occurs only for a predetermined orientation.

Using the equivalence between the generalized Hoek–Brown model and the Mohr–Coulomb model it is possible to use the ubiquitous-joint model. To obtain the equivalence, the range of working stresses must be previously known. In practice, the maximum value of σ_3', $\sigma_{3\text{max}}'$ is estimated as, in the case of slopes:

$$\frac{\sigma_{3\text{max}}'}{\sigma_{\text{cm}}'} = 0.72\left(\frac{\sigma_{\text{cm}}'}{\gamma H}\right)^{-0.91} \tag{5}$$

where H is the slope height, γ is the rock mass specific weight and σ_{cm}' the rock mass strength.

With the defined stress range, it is possible to estimate the parameters of the Mohr–Coulomb model:

$$\phi' = \text{sen}^{-1}\left[\frac{6am_b\left(s + m_b\sigma_{3n}'\right)^{a-1}}{2(1 + a)(2 + a) + 6am_b\left(s + m_b\sigma_{3n}'\right)^{a-1}}\right] \tag{6}$$

$$c' = \frac{\sigma_{ci}\left[(1 + 2a)s + (1 - a)m_b\sigma_{3n}'\right]\left(s + m_b\sigma_{3n}'\right)^{a-1}}{(1 + a)(2 + a)\sqrt{1 + 6am_b\left(s + m_b\sigma_{3n}'\right)^{a-1}/[(1 + a)(2 + a)]}} \tag{7}$$

where $\sigma_{3n}' = \sigma_{3\text{max}}'/\sigma_{ci}$

The shear strength of rock discontinuities, foliations, and fractures was interpreted based on the Barton-Bandis model [6]. In these models, three strength parameters are necessary: the basic friction angle of the failure surface (ϕ_b), the joint roughness coefficient (JRC) and the joint wall compressive strength (JCS). In general, the strength parameters of the discontinuities were retroanalyzed based on the parameters described in the geological survey: Joint roughness number (Jr) and Joint alteration number (Ja).

The basic friction angle of the failure surface was obtained through the direct shear test, when possible. For the other situations, the friction angle was adopted in a manner compatible with the intact rock. The JCS was obtained as the uniaxial compression strength reduced by the value of the corresponding joint alteration number. The spacing of the discontinuities in the same family (S) was quantified based on the measurements made during the geological survey in the case of fractures. For foliations, the spacing was disregarded because its presence will be considered as ubiquitous.

2.5 *Slope Stability Analysis*

Once the slope model is created stresses are geostatically initialized and then the equilibrium is solved to find the in-situ stresses. Lateral earth pressure coefficient is considered during the geostatic initialization. Next, the mining process is simulated by removing the corresponding zones using a progressive stiffness/weight reduction. After the excavation, the factor of safety is calculated using the Shear Strength Reduction method.

3 Case Study: Large-Scale Iron Ore Mine

The methodology described was considered for the stability analysis of an iron deposit located in the Iron Quadrangle, south-central of Minas Gerais state in Brazil. The structural features of the deposit show a complex pattern of planar and linear elements which may be referred to at least three events of deformation. The iron bodies and their country rocks have a deformed structural type with a lithological anisotropy recognized as foliation.

From the bottom to the top, the local stratigraphy can be simply described as the basement mainly composed by gneiss rock in fault contact with meta volcanic-sediments (schists). Above those sediments, a younger sequence of quartzite, schists and itabirites (iron formation) constitute the largest part of the mine slopes and are identified as the Supergrup Minas formation.

The geomechanical quality of the rock mass was considered through the Geological Strength Index—GSI. The GSI was evaluated and classified in 821 points corresponding to 83 drill holes (georeferenced). Figure 1 shows the spatial distribution of the samples in the deposit.

These data were used to interpolate the GSI by using the Inverse distance weighting method. The interpolation was carried out on the regular mesh of the prototype block model, with $50 \times 50 \times 10$ m dimensions. Each sub-block within the original block (even IJK) inherited the GSI from the block. The result of this process is shown in Fig. 2.
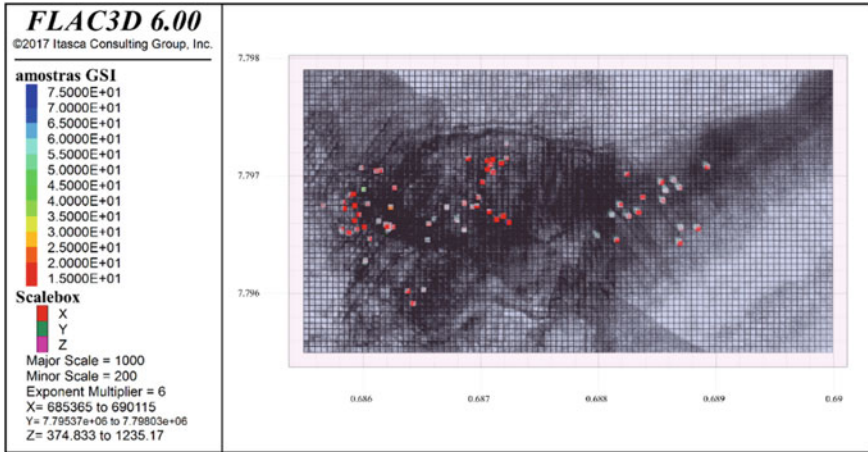
Fig. 1 Spatial distribution of GSI samples [7]
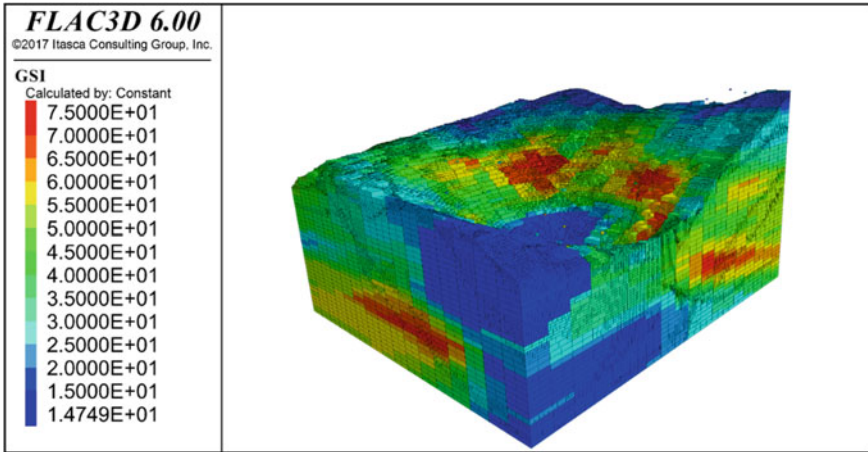
Fig. 2 Spatial distribution of the interpolated GSI in the pit [7]

The analysis resulted in surface displacements with a great concentration in the northeast wall and a floor heave of the order of 100 mm. Additionally, it can be observed that there is a displacement concentration in the region of the fault outcrop. Section A was sampled to show the behavior of the most critical region of the pit, the northeast wall (Fig. 3). In this region, the slope present 250 m height and 40° global inclination. In general, the displacements are below 100 mm of magnitude and below 20 mm in the horizontal direction, except of the middle region of the slope where it can be observed horizontal movements of more than 200 and 350 mm of magnitude.

The stress–strain ratio (SSR) indicates the presence of two regions of considerable concentration at the top of the slope and at the middle region of the slope height
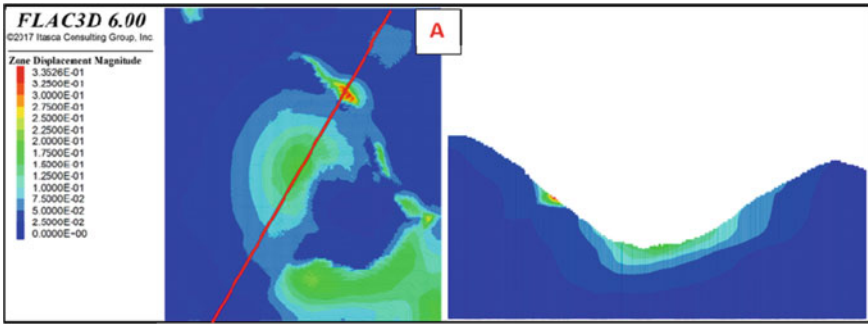
Fig. 3 Displacements of surface in the final pit, section A [7]
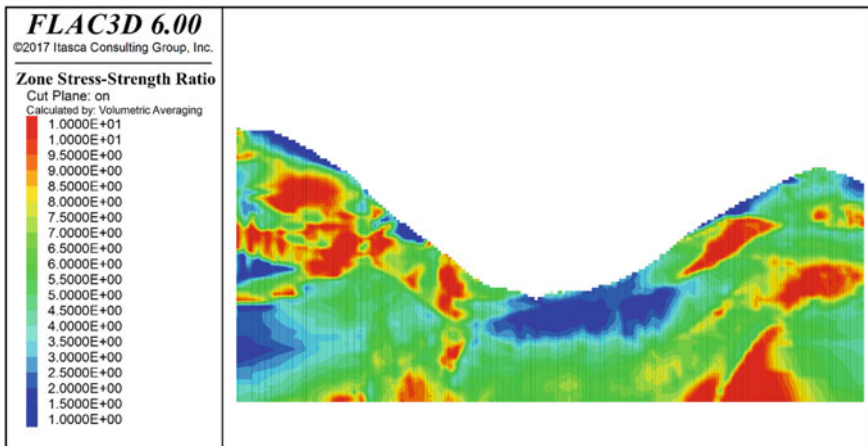
Fig. 4 SSR in the final pit [7]

(Fig. 4). The concentration region near the top is located in friable quartzites and the intermediate region is found in the friable shale as an extension of about 40 m.

The main result of the safety analysis in this study is the factor of safety (FS). The current method consists in projecting the pit slopes by evaluating the factor of safety and to compare this result with a minimum predefined factor. This minimum value is commonly adopted from values used in practical operations. Table 1 summarizes the typical values of factor of safety and probability of failure used as acceptance criteria in the mining industry [8].

In the case of safety evaluations using three-dimensional numerical models, there are still no direct comparison values in the literature. It should be remembered that the typical recommendations are based on two-dimensional analyses, which provide values of factor of safety intrinsically different from those obtained through three-dimensional analyses [1, 9, 10].

Table 1 Typical FS and probability of failure (Pf) acceptance criteria values

Slope scale	Consequences of failure	Acceptance criteria		
		FS min	FS min	Pf max
		Static	Dynamic	P[FS < 1] (%)
Bench	Low-high	1.1	NA	25–50
Inter-ramp	Low	1.15–1.2	1.00	25
	Medium	1.2	1.00	20
	High	1.2–1.3	1.10	10
Overall	Low	1.2–1.3	1.00	15–20
	Medium	1.3	1.05	10
	High	1.3–1.5	1.10	5

Source [8]

However, the values showed in Table 1 were taken as a reference only for comparison purposes. More accurate three-dimensional security analyses should have as a basis of comparison the target probabilities of failure (presented in the same table), however, this type of analysis is not the scope of this study.

The final open-pit studied presented an overall safety factor of 1.78, with the main occurrence in the northeast slope. This behavior might be originated by the presence of the fault, which cuts the wall pit and contributes for the presence of low resistance materials outcropping in the northeast wall. However, it should be noted that these results correspond to a deep mechanisms and do not exclude the occurrence of small surface events such as thin planar landslides, buckling or falling blocks that were not represented in this analysis.

Finally, the computational routine presented along this paper is advantageous when compared to the typical manual procedure because, first, it is fast at building up complex models automatically, and, second, it is capable of being controllable by an external routine, e.g., to perform sensitivity, calibration, or probabilistic analyses. However, one of the main problems is the programming interface which may seem complicated for practitioners. In this sense, the ongoing improvements are focused on improving the input interface. Additionally, incorporation of damage and self—calibration are being implemented to improve the representativeness of the models as well as hybrid limit equilibrium to fasten the safety calculations.

4 Conclusions

Geological models are usually constructed in a three-dimensional way using information obtained through sample drilling and interpreted according to the local geology. These models contain information of ore grades and contaminants and are also capa-

ble of incorporating geotechnical data. However, regarding geomechanical models, 3D models are hardly used, being replaced by simplified models.

In the present study, it was demonstrated how it is possible to take advantage of the information available in geological block models and core data to reconstruct, generate and analyze the three-dimensional behavior of the geomechanical stability of slopes of open-pit mines. The 3D-modeling method developed for this study case proved to be accurate, systematic and fully reproducible. The incorporation of the IPython console into FLAC3D has reduced the computational effort in terms of the construction and execution of the geotechnical model.

The use of 3D models supports the automatic identification of the most problematic regions and can enable decision-makers to take corrective measures, to evaluate the areas that need more systematic monitoring and even to propose some change in the final slope angle, for a better economic use of the reserve.

References

1. Albataineh, N.: Slope Stability Analysis Using 2D and 3D Methods. University of Akron (2006)
2. Griffiths, D.V., Marquez, R.M.: Three-dimensional slope stability analysis by elasto-plastic finite elements. Geotechnique **57**(6), 537–546 (2007). https://doi.org/10.1680/geot.2007.57.6. 537
3. Itasca Consulting Group INC.: FLAC3D (Fast Lagrangian Analysis of Continua in 3 Dimensions) (2012)
4. Hoek, E., Carranza-Torres, C., Corkum, B.: Hoek-Brown failure criterion—2002 Edition. In: Proceedings of NARMS-Tac, pp. 267–273 (2002)
5. Hoek, E.: Strength of jointed rock masses. Geotechnique **23**, 187–223 (1983). https://doi.org/ 10.1680/geot.1983.33.3.187
6. Barton, N., Bandis, S.: Review of predictive capabilities of JRC-JCS model in engineering practice. In: Barton, N., Stephansson, O. (eds.) International Symposium on Rock Joints, Loen, pp. 603–610 (1990)
7. Torres, V.F.N., Napa-García, G.F., Trópia, I.R., Capelli, R.B.: Análises numéricas integradas ao monitoramento hidrogeotécnico para avaliação da estabilidade de taludes em cavas: relatório final do projeto Análises numéricas integradas ao monitoramento hidrogeotécnico para avaliação da estabilidade de taludes em cavas. Ouro Preto, MG: Instituto Tecnológico Vale (2018). https://doi.org/10.29223/prod.tec.itv.mi.2018.10.torres
8. Read, J., Stacey, P.: Guidelines for Open Pit Slope Design. CSIRO Publishing/CRC Press, Collingwood (2009)
9. Lu, H., Xu, L., Fredlund, M., Fredlund, D.: Comparison of 3D finite element slope stability with 3D limit equilibrium analysis. In: Proceedings of the 18th International Conference on Soil Mechanics and Geotechnical Engineering, p. 4, Paris, France: ISSMGE (2013)
10. Chen, Z., Mi, H., Zhang, F. and Wang, X.: A simplified method for 3D slope stability analysis. Can Geotech. J. (2003)

Collocated Ground Deformation and Pore Pressure Measurements in Open Pit Mines: Laboratory Testing and Analysis of Wireless Sensing Platform

E. Widzyk-Capehart, A. Barberán, M. J. Briceño, C. Navarro, P. M. V. Nguyen, C. Opazo and S. Steffen

1 Introduction

In the design of open pit mines, the geomechanical properties of the rock mass are one of the critical sources of uncertainty, which affect the stability of slopes with results that can be catastrophic: the design can drastically influence mining production and its economic viability [1]. Therefore, there are multiple challenges when assessing subsurface deformations and variation in pore pressure within the rock mass mainly because there are a limited number of devices that can be installed inside the boreholes. In addition, the correlation of displacement data with pore pressure, especially in low-permeability environments, is complex the respective sensors are installed in separate drill holes.

Rigorous monitoring of surface and subsurface to determine the displacement is one of the ways to have a general assessment of the behavior of the slopes, allowing for the protection of personnel and equipment, maintaining safer operating conditions; early notifications of potentially unstable areas; provision of geotechnical information to analyze any slope instability mechanism that may be developed, allowing the development of appropriate corrective action plans leading to the improvement of future slope design as well as evaluating the performance of the slope design implemented.

E. Widzyk-Capehart · P. M. V. Nguyen
Advanced Mining Technology Center (AMTC), University of Chile, Santiago, Chile

A. Barberán · C. Navarro (✉) · C. Opazo
CSIRO Chile International Centre of Excellence, Santiago, Chile
e-mail: canavarr.ing@gmail.com

M. J. Briceño
Independent Consultant, Santiago, Chile

S. Steffen
Elexon Electronics, Brendale, Australia

The surface slope displacement monitoring instruments are quite sophisticated with automatic wireline extensometers, universal EDM stations, 3D digital photogrammetry and laser scanning and ground-based and satellite-based radars. All of them can provide us with a real-time 3D record of any surface movement that may occur around the walls of the pit [2]. However, in-ground movement monitoring instruments are less sophisticated. Typically, they include shear strips and/or time domain reflectometers (TDR), extensometers, and inclinometers placed in boreholes to locate the propagation of subsurface movement after evidence of subsurface deformation has been detected [3]. Less typically, they are placed where it is expected that the surface instruments cannot detect movement, sometimes being able to detect deformation in real time as it propagates to the surface. Most of the time, subsurface sensors are adapted from civil engineering applications to mining; often they do not work well in some areas because the deformation to which they are subjected, affects their casing, restricting the internal movement of the sensor or even causing breakage of communication cables, as is the case with inclinometers and Shape Accelerometer Array (SAA) [4].

To address the disadvantages of today's ground instrumentation, the use of wireless sensor technology with multiple detection capabilities, providing more robust system without dependence on cable connection for the transmission of data to the surface, possibility to combine measurements of different variables within a single unit, capability to install an array of sensors in a single hole, ease of installation.

In this article, the latest developments of the monitoring platform that combines the measurement of deformations and pore pressure with the wireless transmission of data in real time are described.

2   Enhanced Networked Smart Markers (ENSM)

The Enhanced Networked Smart Markers (ENSM) are electronic devices developed by Elexon Electronics, which represent the evolution of their previous technology, the Smart Markers (SM). The current ENSMs (Fig. 1) are equipped with an accelerometer and a magnetometer, to measure the inclination (ENSM Tilt) or, additionally, with a piezometer (ENSM Pore-pressure). The device includes radio transceivers (Green) that operate on battery, incorporating a plastic housing (Yellow) of 34.5 cm long and 6.35 cm in diameter, filled with epoxy material, and protections (White and blue) for radio transceivers and battery to improve the resistance of the product to blasting [5–7].

2.1   Deformation Measurements

The main deformation measuring device in open pit mines is an inclinometer, which measures the rock movement with respect to the vertical axis through a gravity

Fig. 1 Prototype of new ENSM adapted to the NSM case [8]

sensing transducer [9, 10]. Deformation measurement within the ENSM platform is accomplished using a three-axis MEMS accelerometer and magnetometer. The magnetometer provides three orthogonal channels of magnetic field measurement, while each of the channels provides an orientation to the movement detected by the accelerometer. The data obtained from the three axes accelerometer readings allow to determine horizontal and vertical displacements in the position of the marker.

2.2 Pore Pressure

Reductions in groundwater pressure increase the effective tension in the rock mass and, as a consequence, increase the shear strength. In some cases, the dehydration of the rock mass is the only way to increase its resistance, therefore reducing the probability of slope failure [11]. The precise characterization of the vertical distribution of pore pressure requires in situ pressure measurements at different depths and is particularly important if vertical gradients are relevant, such as in open pit mines and in operations with active depressurization programs.

At present, geotechnical engineering uses several types of piezometers to measure pore pressure, among which, stand out the vibrating rope piezometers, which predominate in open pit mines, which are installed in boreholes that are filled with grouting and bentonite by the total injection method, process that undergoes these sensors, during this process of "grouting" (and before setting) to load pressures can increase depending on the depth of the well and the density of the grout; The head pressure (pressure head) exerted by the grout is higher than the pressure of the head of an equivalent water column, mainly due to the density of the grout, therefore, the sensor must withstand a wide range of pressures while maintaining the accuracy of the measurement after installation [12].

The pore pressure measurement within the ENSM is accomplished using the TTF-1 pressure transducer, manufactured by the German company Wika [13], which has been selected for its precision and ability to withstand overpressures. This sensor

must be protected against blockage and mechanical damage while allowing the flow of water. Therefore, a 48 μm steel mesh has been installed, which allows the passage of water but not of the slurry, providing protection to the sensor without the water pressure measurements being altered. The initial results of the laboratory testing of the pore pressure sensor were reported in [8, 12].

3 ENSM Testing and Results

A series of tests were carried out at the Elexon's laboratories in Brisbane, Australia and at the Advanced Center for Mining Technology (AMTC) of the University of Chile in Santiago de Chile.

3.1 Inclinometer Testing

Three different test configurations (angles) were carried out in the laboratory to analyze the accuracy of the inclinometers. The antenna remained fixed at one end, at the other end was the marker raised to different heights with respect to the fixed point (0, 15 and 30 cm). For each position, the readings of the accelerometer (Ax, Ay, Az) and the magnetometer (Bx, By, Bz) were recorded. Figure 2 shows the accelerometer readings and Fig. 3 shows the magnetometer readings on the three axes. The first position (0 cm) is shown in first 7 samples (1–7), the second position (15 cm) in 3 samples (8–10), and third position (30 cm) in 30 samples (11–30).
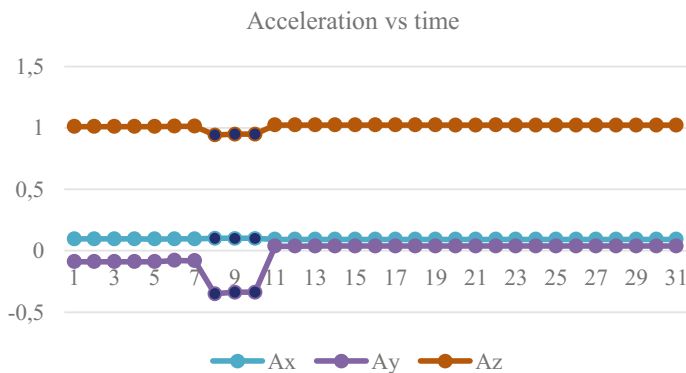
Fig. 2 Accelerometer readings (linear gravity vector) over time (iteration)
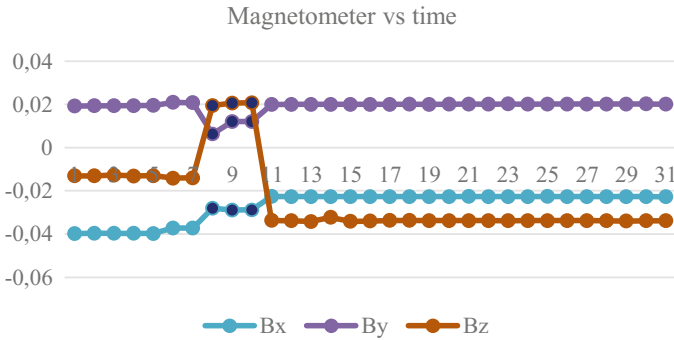
Fig. 3 Magnetometer readings (gauss magnetic vector) over time (iteration)

3.2 Tilt Sensor Testing

The test set-up involved a small slab of granite rock (stone kitchen bench material), with 14 ENSM devices glued to it. The rock was suspended on springs in an insulated and thermally regulated chamber specifically made for this test. The thermal chamber kept the devices at a constant $36° \pm 0.5°$ temperature.

With MEMs devices, the accelerometer readings vary with temperature. However, the temperature in the ground deeper than a few meters tends to be quite constant at approx. $\pm 0.5°$ difference, which will thus ensure stability of the readings at greater depths.

Each data point in Figs. 4 and 5 represents a reading taken from an ENSM device. The sensor dataset recorded by each device consists of three-axis acceleration readings, three-axis magnetometer reading, and temperature. The three-axis accelerometer readings were combined into the devices' roll and pitch values. Figures 4 and 5 show that the sensors are recording highly correlated changes in tilt direction and extent. This recorded movement is due to the floor of the building's tilt-slab concrete deforming. There are variations between various devices readings. Some of the variations are attributed to the effect that changing temperature has on the accelerometer. Some of it can be interpreted as noise. The error in the readings is approximately a quarter of the amount that concrete laboratory floor is moving. The error is $\pm 0.05°$ which translates into approx. 2.5 mm over a 3 m length (or submillimeter over 1 m). The resolution of the sensor is about 1 mm over a 3 m length (Fig. 4). The temperature in the chamber is being varied by ± 0.5 °C (Fig. 5). The analysis of the data suggests that approximately 50% of the errors are caused by the variation in temperature. At this stage, the error is constant over time; the readings are not diverging as time goes on.
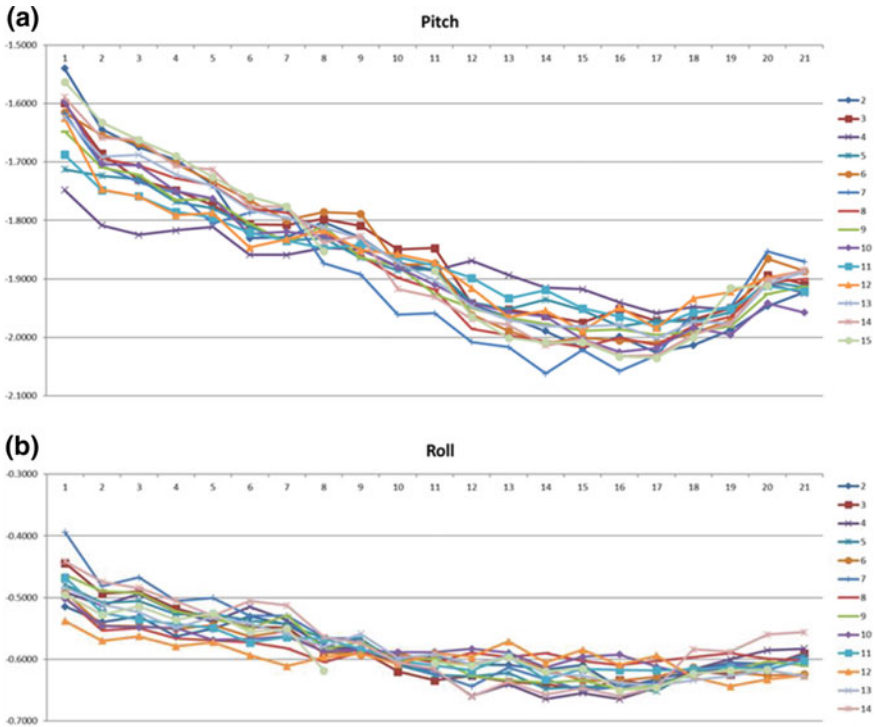
Fig. 4 Pitch (**a**) and roll (**b**) values (angles) versus time (days)
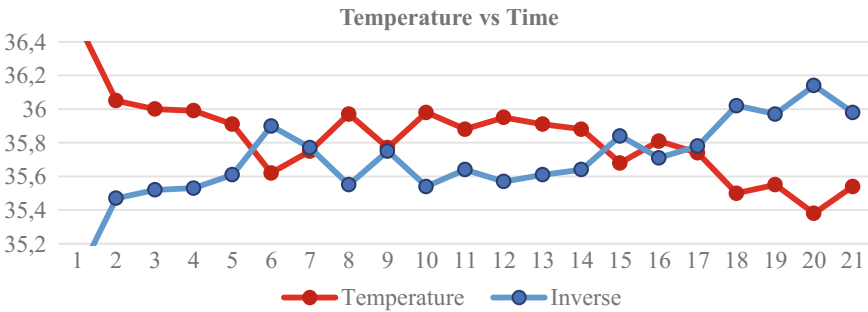
Fig. 5 Temperature in the test chamber (Celsius) versus time (days)

3.3 Pore Pressure Measurement

One of the key factors that could affect the correct measurements of pore pressure is the permeability of the grout and the time lag until the sensor is exposed to the water pressure present in the rock. The grout permeability can be up to two or three orders of magnitude greater than the permeability of the rock, which reaches

10^{-6} to 10^{-8} cm/s. This range is controlled by the water/cement ratio. The time lag depends on the type of sensor, the volume of water required to record the variation of the recorded pressures, the grout permeability, the formation of air bubbles during installation and the degree of the grout saturation.

3.3.1 Grouting Properties

For the installation of the ENSM in the borehole, grouting mixture is used to fix the sensors in place. In Chile, pozzolanic cement instead of Portland cement is generally used to create the grout [14, 15]. Therefore, tests were carried out to examine the possible differences between the grouts with different cements; Pozzolanic cement and SuperGel-X CETCO. In addition, calcium bentonite or sodium bentonite can be used as sodium bentonite absorbs more water than calcium bentonite [15].

The result of the test to determine the influence of the type of bentonite on the grout behavior showed both types of grout behaved similarly during the setting and curing process, despite the differences in viscosity observed during processing, confirming that the type of bentonite does not influence the behavior of the grout [8].

3.3.2 Permeability and Saturation

The permeability and saturation test was carried out to determine the permeability and saturation degree of the bentonite cement grout, which is to be used in the field installation of the ENSM markers. In addition, possible variation in the curing time of the mixture and whether the permeability was within the parameters reported by [14] and [15] was also tested. The hypothesis was formulated that the use of pozzolanic cement could lead to a decrease in permeability as compared to Portland cement used internationally.

A flexible wall permeameter was used in triaxial equipment, at variable load, to measure the permeability (K) [16]. Three samples of grout were prepared and analyzed, the first at 7 days of curing, the second at 14 days and the third at 28 days (Fig. 6a).

All samples were tested at an effective pressure of 10 kPa. The corresponding sample at 14 days was also tested at 32.98 and 163 kPa effective chamber pressure of the permeameter (Fig. 6b). To allow the free flow of the grout during the field tests, the grout component proportions used were "water: cement: bentonite" in relation "2.5: 1: 0.25" (modified after [14]).

The degree of saturation is calculated according to Eq. 1:

$$S = V_w / V_v \tag{1}$$

where: V_w: volume of water and V_v is the volume of voids; V_v: was obtained indirectly from the specific gravity of the particles (Eq. 2)
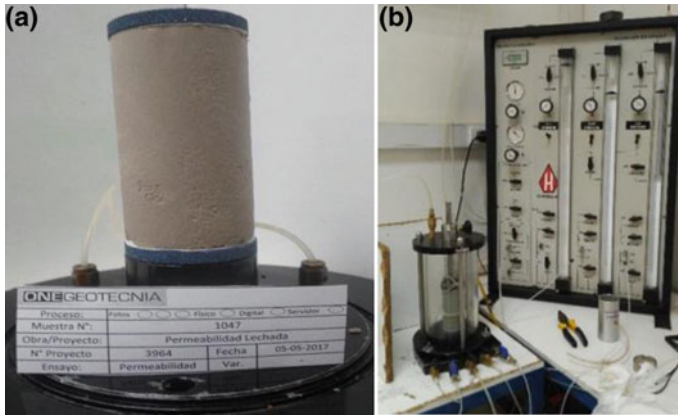
Fig. 6 Grouting sample: **a** at 14 days of curing; **b** in a flexible wall permeameter

$$G_s = \gamma_s / \gamma_w \tag{2}$$

where: γ_s: volume of solids and γ_w: volume of water.

The unit weight of the sample was calculated as (Eq. 3):

$$\gamma = W_s / V_s \tag{3}$$

where: W_s: weight of solids and V_s: volume of solids.

The natural moisture of the sample was calculated as (Eq. 4):

$$\omega = W_w / W_s \tag{4}$$

where: W_w: weight of water and W_s: weight of solids.

The tests were performed according to the Chilean Standards [17, 18]. The permeability values obtained are shown in Table 1.

Figure 7 shows the results of permeability tests over time (7, 14 and 28 days with pressure of effective chamber of 10 kPa) and pressure (10, 32, 98 and 163 kPa). The permeability values are of the order of magnitude of 10–6 to 10–8 cm/s. The results show that the permeability increases by two orders of magnitude from 7 to 14 days of curing time. However, from 14 to 28 days of curing, the permeability is maintained within 10^{-6} m/s. The results show an expected increase in permeability

Table 1 Results of permeability

Sample (days)	Permeability (cm/s)
7	6×10^{-8}
14	2×10^{-6}
28	5×10^{-6}
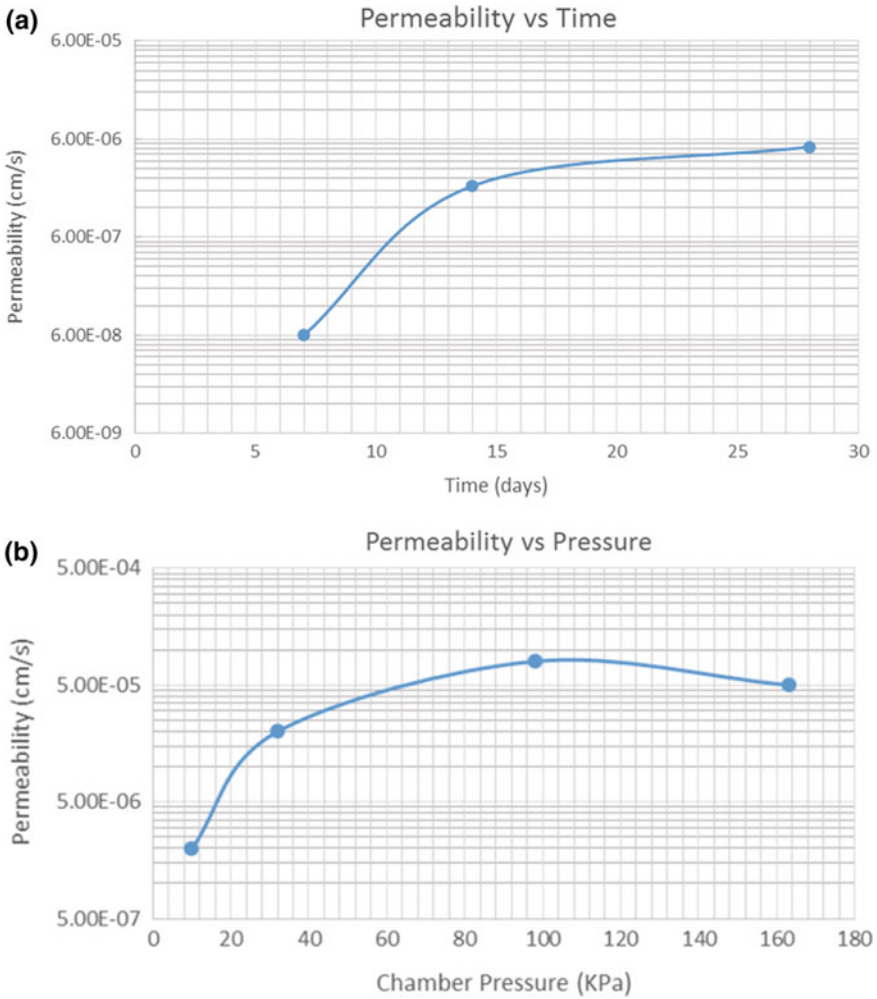
Fig. 7 Permeability of the grout: **a** over time; **b** over chamber pressure

up to 14 days of curing; however, the expected linear behavior is not observable from day 14 onwards (Fig. 7a).

The effect of increase in pressure also shows a different behavior as the permeability increases with the pressure increase of 10–32 kPa. However, when reaching pressures in the range of 98–163 kPa, the permeability decreases (Fig. 7b).

Therefore, although the observed permeability values are within the order of magnitude, the influence of the pressure increase on the permeability does not match the results presented by [17] in the full pressure scale. As the tests were performed in accordance with Chilean standards, the results are unexpected in the highest range

of pressures and more investigations are being carried out to determine the source of this discrepancy.

4 Conclusions

The results of the tests carried out for the grout showed that the type of bentonite does not influence the curing process of the grout. However, the results of the permeability tests showed mixed results; while the permeability values were within the order of magnitude, the evolution of the permeability with respect to the curing time of the slurry and the pressure to which it was subjected, showed differences with the expected results as described in the literature.

The tilt sensor tests show that the error seems to be reasonably constant over time; the readings continue to ensure consistency in the results as time goes on, while simulating the field conditions in the laboratory and improvements are made to the processing algorithms to ensure the acquisition and processing of data in real time during testing of field. Finally, the sensors were calibrated to consider the variable of temperature change in the environment.

Additional tests are being carried out to analyze the response times of the pore pressure sensors based on the analysis of the grout test results of the new detection platform to determine: (1) the time elapsed between the installations of the sensors until the hydrostatic pressure of the medium begins to be measured. It is assumed that the duration of these tests is conditioned by the behavior of the slurry and is expected to be at least 28 days and (2) the response time after stabilization, that is, the time between a pressure disturbance in the mean and time that the sensor records the disturbance. This time depends on the volume of the water to be moved from the medium to the measuring chamber and the ease of the associated water to flow. Low response times are expected from minutes to hours.

References

1. Wyllie, D.C., Mah, C.W.: Movement monitoring. In: Wyllie, D.C., Mah, C.W. (eds.) Rock Slope Engineering, 4th edn. Spon Press, New York (2004)
2. Cook, D.: Robotic total stations and remote data capture: challenges in construction. Geotech. News **24**(3), 42–45 (2006)
3. Bayoumi, A.: On the evaluation of settlement measurements using borehole extensometers. Geotech. Geol. Eng. **29**(1), 75–90 (2011)

4. Dowding, C.H., O'Connor, K.M.: Comparison of TDR and inclinometers for slope monitoring. ASCE Geotech. Spec. Tech. Publ. **106**, 80–90 (2000)
5. Elexon Mining.: Networked Smart Marker System. Available at: http://www.elexonmining.com/networked-smart-markers-2. Accessed 1 Nov 2015
6. Whiteman, D.S.: The smart marker system—a new tool for measuring underground ore body flow in block and sub-level mines. In: 2nd International Symposium on Block and Sublevel Caving, pp. 603–622, Perth, Australia (2010)
7. Widzyk-Capehart, E., Hölck, C., Fredes, O., Pedemonte, I., Steffen, S.: Implementation of Novel Subsurface Deformation Sensing Device for Open Pit Slope Stability Monitoring—The Networked Smart Markers System, MPES 2015 (2015)
8. Widzyk-Capehart, E., Gonzalez, N., Pedemonte, I., Sanchez, E., Steffen, S.: Towards real-time, wireless in-ground simultaneous monitoring of rock deformation and pore pressure in open pit mines. MPES **2017**, 7 (2017)
9. Widzyk-Capehart, E., Hölck, C., Fredes, O., Sánchez, E., Pedemonte, I., Marciniak, M., Floría, E., Poulson, J., Steffen, S.: Emerging developments of the Networked Smart Markers System Towards an Integrated Monitoring Platform. Minin (2016)
10. Holck, C.: Open pit geomechanics and mine planning integration: design and economic assessment of a subsurface slope deformation monitoring campaign. M.Sc. Thesis, University of Chile (2016)
11. Beale, G., Price, M., Waterhouse, J.: Framework: assessing water in slope stability. In: Beale, G., Read, J. (eds.) Guidelines for Evaluating Water in Pit Slope Stability, pp. 19–64. CSIRO Publishing, Collingwood (2013)
12. Sánchez, E., Widzyk-Capehart, E., Poulson, J., Ortuño, F., Fredes, O., Steffen, S.: Slope stability management: coupling deformation measurements with pore pressure data using novel Networked smart markers platform. Water Min. (2016)
13. WIKA: Transductor de presión OEM. Available at: http://www.wika.cl/ti_1_es_es.WIKA. Accessed on 1 Sept 2015
14. Mikkelsen, P.E., Green, G.E.: Piezometers in fully grouted boreholes. In: Myrvoll (ed.) Field Measurements in Geomechanics, pp. 545–553. Lisse: Swets & Amp; Zeitlinger (2003)
15. Contreras, I.A., Grosser, A.T., VerStrate, R.H.: The use of the fully-grouted method for piezometer installation. Geotech. News **26**, 30–37 (2008)
16. ASTM D5084.: Standard Test Methods for Measurement of Hydraulic Conductivity of Saturated Porous Materials Using a Flexible Wall Permeameter. American Standard Testing Materials
17. NCh. 1515 of. 1979.: Determinación de la Humedad. Instituto Nacional de Normalización INN (1979)
18. NCh. 1532 of. 1980.: Densidad de Partículas Sólidas. Instituto Nacional de Normalización INN (1980)

Determination of the Crown Pillar Thickness Between Open Pit and Underground for Coal Mining

P. M. V. Nguyen, E. Widzyk-Capehart and Z. Niedbalski

1 Introduction

Nowadays, consideration of making a transition from OP to UG is strongly increasing for the biggest open pit mines worldwide. The main reasons for this transition are unprofitable OP operation, inability of maintaining stability of high open pit slopes, increased environmental impacts of further OP development and social expectations to reduce noise, dust, and nuisance [1]. In OP-UG transition project, the crown pillar located under the pit bottom must be considered before starting a UG operation. The main role of crown pillar is to maintain stability of both the open pit slopes and the underground workings simultaneously for a certain period of time. The crown pillar with adequate thickness will minimize detrimental interference between the two working areas while maximizing ore recovery. Determining the most adequate thickness of a crown pillar in the combined OP-UG mining method is one of the most challenging problems faced by mining engineers today [2]. Limited studies have been undertaken over the years to determine the crown pillar thickness with the majority of cases focused on metalliferous ore deposits [3]. To-date, OP-UG transition cases have been recorded for coal mining in several countries including Russia, Australia, China, and Vietnam [4, 5]. The main question is: what is the equivalent crown pillar thickness for OP-UG transition cases in coal mining?

In this paper, an approach for determining the pillar thickness is based on the prevention of water inrush into UG workings from nearby OP mine. The numerical

P. M. V. Nguyen (✉) · E. Widzyk-Capehart
Advance Mining Technology Center (AMTC), University of Chile, Santiago, Chile
e-mail: nguyen.pmv@amtc.uchile.cl

E. Widzyk-Capehart
e-mail: Eleonora.widzykcapehart@amtc.uchile.cl

Z. Niedbalski
AGH University of Science and Technology, Kraków, Poland

modelling was carried out using finite difference software FLAC to define the crown pillar thickness for coal mine with selected variables including rock mass properties and depth of coal seam deposition. In addition, guidelines are presented for determination of crown pillar thickness between Open Pit and Underground mines for coal mining.

2   Determination of Crown Pillar Thickness in OP-UG Transition—An Overview

An initial design chart for crown pillar thickness was developed by plotting thickness to span, (t/S), ratios for stable and failure cases against rock quality assessed using both the geomechanical Rock Mass Rating (RMR) and NGI-Q values. Carter and Miller [6] proposed the following formula (Eq. 1):

$$\frac{t}{S} = 1.55 Q^{-0.62} \tag{1}$$

where: t—crown pillar thickness, m; S—crown pillar span, m; and Q—Barton's quality index of the rock mass.

Bakhtavar et al. [2] presented crown pillar thickness as a function of the most effective variables: stope span (S), stope height (h), cohesion strength (C), RMR (Bieniawski's quality index of the rock mass) and specific weight of rock (γ) (Eq. 2):

$$t = \frac{13.22 \cdot C^{0.03} \cdot S^{0.41} \cdot h^{0.56}}{\gamma^{0.03} \cdot \mathrm{RMR}^{0.66}} \tag{2}$$

Flores [7] raised a number of questions of a geotechnical nature or involving geotechnical considerations with respect to the OP-UG transition project. A series of parametric two-dimensional numerical stress analyses of crown pillar stability were carried out for a range of open pit and underground geometries, stress fields, and rock mass characteristics. Based on the results of these analyses, a series of design charts were developed, which provide an estimate of minimum permissible crown pillar thickness for simultaneous open pit and underground operation (Fig. 1).

3   A New Approach to Determine Crown Pillar Thickness for Coal Mining

UG coal mining, such as longwall mining of coal seams, may cause movements of overburden strata and mining-induced fractures [8]. Surface water can penetrate through the discontinuous zones and rush into the underground workings. Water inrush is one of the most serious geological hazards in underground engineering, causing equipment damage, project delays, and casualties [9–11]. In case of OP-UG transition, the possibility of water inrush from the pit bottom or from the watered rock
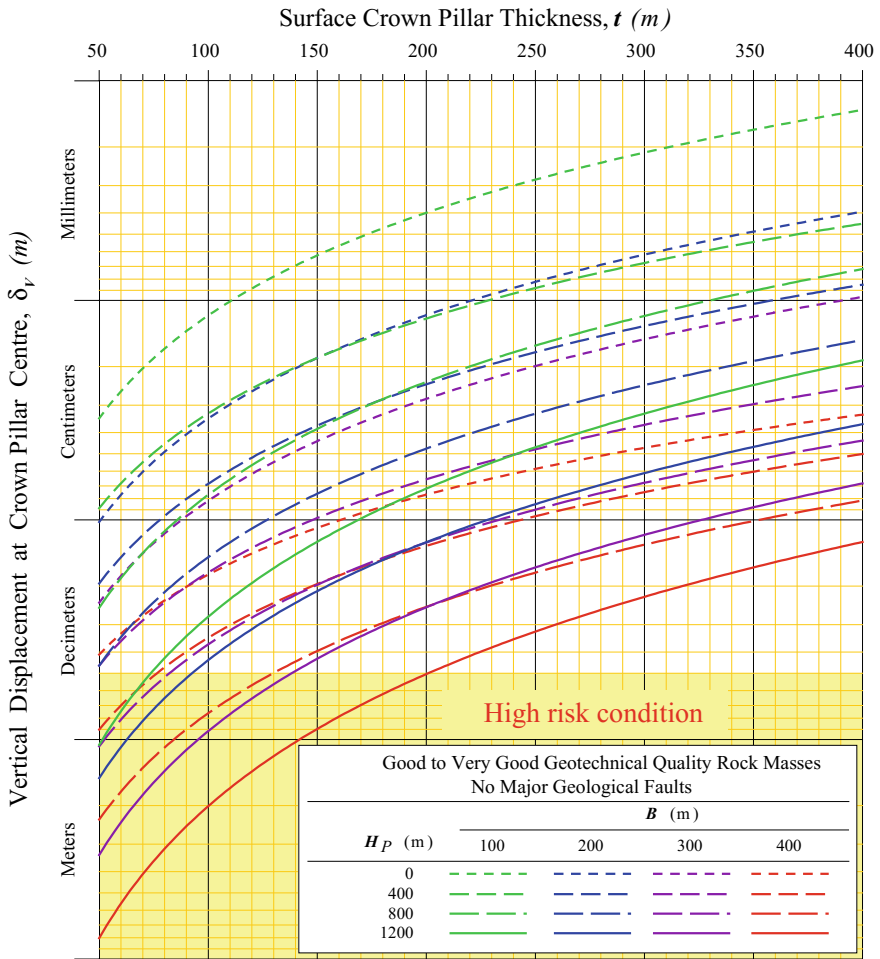
Fig. 1 An example of design chart for a surface crown pillar in a transition from open pit to underground mining by caving [7]

layers located above the coal seam through crown pillar to underground workings should be considered.

The well-designed crown pillar with the equivalent thickness should prevent the water inrush and maintain stability and continuity of both OP and UG operations. The behaviour of the rock mass that forms the crown pillar can be assessed with selected variables, such as thickness of coal seam, rock mass properties, and depth of coal seam deposition. The calculations can be performed using the FLAC2D program based on the Finite Difference Method [12]. In FLAC2D, one of many indicators that can be used to assess the state of the numerical model is plasticity indicator. It determines the possibility of failure of individual rock mass points as a result

of tensile or shear stresses. Moreover, display of displacements, velocity vectors, stresses, strains, and other variables can be made, if necessary.

4   Numerical Modelling

Numerical model undertaken in this study included the pit floor, where water may be accumulated, and three mining-induced zones (caved zone, fractured zone, and sagging zone). It was assumed that the shape of caved zone and fractured zone were rectangular (Fig. 2). A coal seam of 3–4 m thickness is, generally, observed to provide normal working height for efficient extraction and is suitable for the most conventional mining methods [13–15]. The coal seam of 4 m thickness was selected for numerical modelling.

Many works have been carried out to determine the geometry of caved zone and fractured zone [8, 16, 17]. In this study, the heights of the caved zone h_{cz} and the fractured zone h_{fz} were calculated according to [16]. The h_{cz} and h_{fz} mechanical properties differ depending on type of rock mass and strongly affect the shape of the surface deformation. The heights are defined by Eqs. 3 and 4:

$$h_{cz} = \frac{100g}{c_1 g + c_2} \tag{3}$$

$$h_{fz} = \frac{100g}{c_3 g + c_4} \tag{4}$$
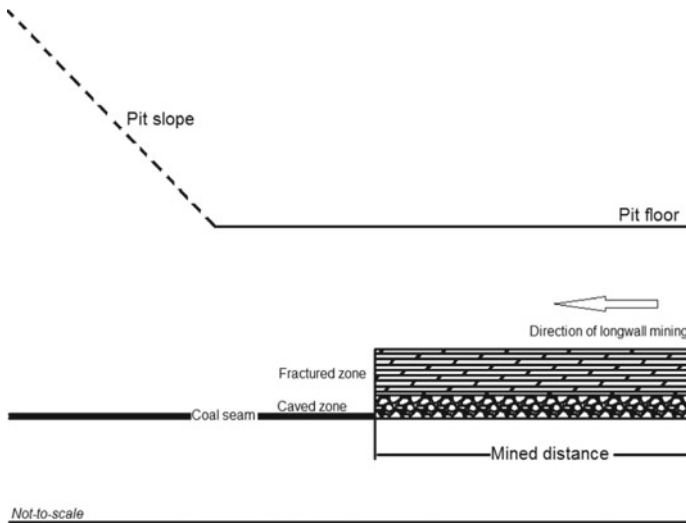
Fig. 2 Two-dimensional numerical model and location of rock layers

Table 1 Coefficients for average height of caved zone and fractured zone [16]

Strata lithology	Coefficients			
	c_1	c_2	c_3	c_4
Strong and hard	2.1	16	1.2	2
Medium strong	4.7	19	1.6	3.6
Soft and weak	6.2	32	3.1	5

Table 2 Heights of caved zone and fractured zone due to rock mass class with the coal seam thickness of 4 m

	Soft and weak	Medium strong	Strong and hard
Height of caved zone, m	7	11	16
Height of fractured zone, m	23	40	59
Sum of failure zone height	30	51	75

where h_{cz}—height of caved zone, m; h_{fz}—height of fractured zone, m; g—thickness of coal seam, m; c_1, c_2, c_3, c_4—constant coefficients dependent on compressive strength (Table 1).

The heights of caved zone and fractured zone calculated based on Eqs. 3 and 4 are presented in Table 2.

The rock mass was assumed to be homogeneous and isotropic, with mechanical properties defined according to the Hoek–Brown criterion and recommendations of [18]. The mechanical properties of the rock masses are summarized in Table 3.

Since there is no access to the caved zone nor the fractured zone, finding equivalent mechanical properties able to express the heterogeneity of those materials is very difficult.

4.1 Caved Zone

Various studies have been conducted to assess the equivalent mechanical properties of caved zone [19–21]. The elastic modulus within the caved zone can be calculated based on functions (Eqs. 5 and 6) proposed by [20]:

$$E_{cz} = \frac{10.39 \cdot \sigma_c^{1.042}}{BF^{7.7}} \tag{5}$$

$$BF = \frac{c_1 g + c_2}{100} + 1 \tag{6}$$

where σ_c—the compressive strength of the intact rock; BF—the bulking factor of caved zone; c_1, c_2 and g are defined in Eq. 3.

According to Eqs. 5 and 6, the bulking factor and the elastic modulus within the caved zone calculated according to rock mass classes are shown in Table 4.

Table 3 Typical mechanical properties of the various rock mass classes [18]

Parameter	Rock mass class		
	Soft and weak (very poor quality)	Medium strong (average quality)	Strong and hard (very good quality)
Hoek–Brown criterion			
Intact rock strength, σ_{ci} (MPa)	20	80	150
Hoek–Brown constant, m_i	8	12	25
Geological strength index, GSI	30	50	75
Mohr–Coulomb fit			
Friction angle, θ (deg)	24	33	46
Cohesive strength, c (MPa)	0.55	3.5	13
Rock mass compressive strength, σ_{cm} (MPa)	1.7	13	64.8
Rock mass tensile strength, σ_{tm} (MPa)	0.01	0.15	0.9
Deformation modulus, E_m (GPa)	1.4	9	42
Poisson's ratio, ϑ	0.3	0.25	0.2
Dilation angle, α (deg.)	0	4	11.5
Post-peak characteristics			
Friction angle, θ_p (deg.)	–	–	38
Cohesive strength, c_p (MPa)	–	–	0
Deformation modulus, E_{mp} (GPa)	1.4	5	10

Table 4 The calculated bulking factor of caved zone

	Soft and weak	Medium strong	Strong and hard
The bulking factor	1.568	1.378	1.244
Elastic modulus, MPa	7.4	84.6	358

Table 5 Estimations of the post-peak characteristics of rock mass

Rock mass class	Post-peak strength guidelines [18]
Strong and hard	Rock mass behaves in an elastic-brittle manner. All strength lost at failure. It can be assumed to behave as a material with a friction angle of approximately 38° and zero cohesive strength and tensile strength
Medium strong	Assume strain softening, loss of tensile strength retains shear strength. It can be assumed to behave as a material with a friction angle of approximately 30°, zero tensile strength and cohesive strength is reduced to about 50% of initial rock mass
Soft and weak	Rock mass behaves in an elastic-perfectly plastic manner. This means that it continues to deform at a constant stress level and that no volume change is associated with this ongoing failure. All strengths are retained the same as initial rock mass

It was assumed that caved zone behaved as heavily broken rock mass with zero tensile strength, zero cohesive strength, Poisson's ratio of 0.4, and a friction angle of 20–35° [22].

4.2 Fractured Zone

The behaviour of fractured zone adopted as the post-peak behaviour of rock mass is shown in Table 5.

All numerical calculations for each rock type (strong, medium and weak) were carried out according to the elastic-plastic model of Mohr–Coulomb using the finite difference code FLAC2D. The initial model was solved as an elastic model to obtain the initial stress conditions. Then, the vectors and speeds of displacements were zeroed. The next step was assigning the "null" model to the zone corresponding to the caved zone and the fractured zone and re-assigning the Mohr–Coulomb model with equivalent parameters to those zones and modelling the conditions again. The boundaries were chosen as; the model bottom is fixed, two sides of model are roller, and the top surface is set free (Fig. 3).

As discuss in Sect. 3, the plasticity indicator was used to assess the possibility of water inrush from pit floor into the underground workings below. The calculation variants were as follows:

– for strong/hard rock and medium strong rock, calculations were carried out for coal seam deposition of 100, 150, 200 and 250 m because the sum of heights of caved zone and fractured zone was greater than 50
– for soft and week rock, calculations were carried out for coal seam deposition of 50, 100 and 150 m. Coal seam deposition of 200 m would be tested if necessary.
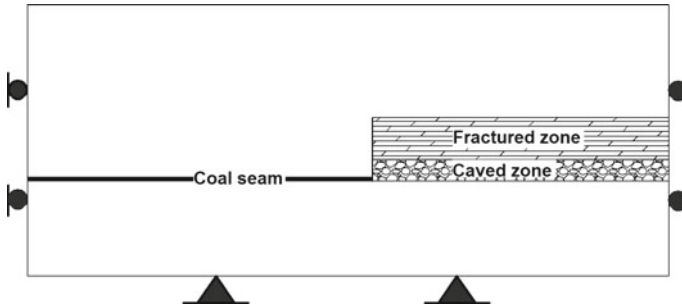
Fig. 3 Numerical model and boundary conditions

5 Results and Analysis

An assessment of the possibility of water inrush based on the plasticity indicator for strong and hard rock is shown in Fig. 4. For coal seam deposition of 100 m, tensile failure reaches to the surface of pit floor and connects to shear failure, creating a directly joint 'pit floor—UG workings'. It means water can easily penetrate through those failures into the underground workings. The risk of water inrush is extremely high (Fig. 4a). For coal seam deposition of 150 m, there is no connection between tensile failure and shear failure. However, the distances between those failures are low (up to 20 m). The possibility of water inrush is still high, especially in the rainy season (Fig. 4b). In case of coal seam deposition of 200 m, the distances between those failure zones are about 60 m horizontally and 30 m vertically (Fig. 4c), whereas, for coal seam deposition of 250 m, the distances between those failure zones are increased over 100 m horizontally and close to 60 m vertically (Fig. 4d).

The plasticity indicator shows that the possibility of water inrush is low in case of 250 m coal seam deposition for strong and hard rock. It means the crown pillar of 250 m is considered sufficient to prevent water inrush for UG operation. After carrying out the same analysis for medium-strong rock and soft and weak rock, the following results were obtained:

– for medium-strong rock, the crown pillar of 150 m was considered sufficient to prevent water inrush for UG operation below
– for soft and weak rock, the crown pillar of 100 m was considered sufficient to prevent water inrush for UG operation below.

6 Conclusions

Modelling rock mass behaviour in forming crown pillar in OP-UG transition is a difficult task due to the complexity of mining-induced failure zones; the caved and fractured zones (geometry and mechanical properties). For the specific geological

(a)
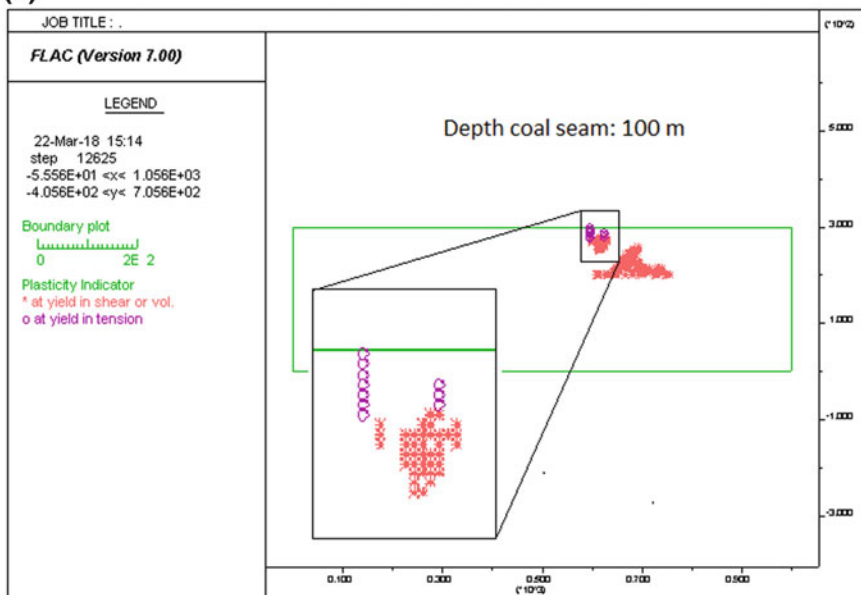
(b)
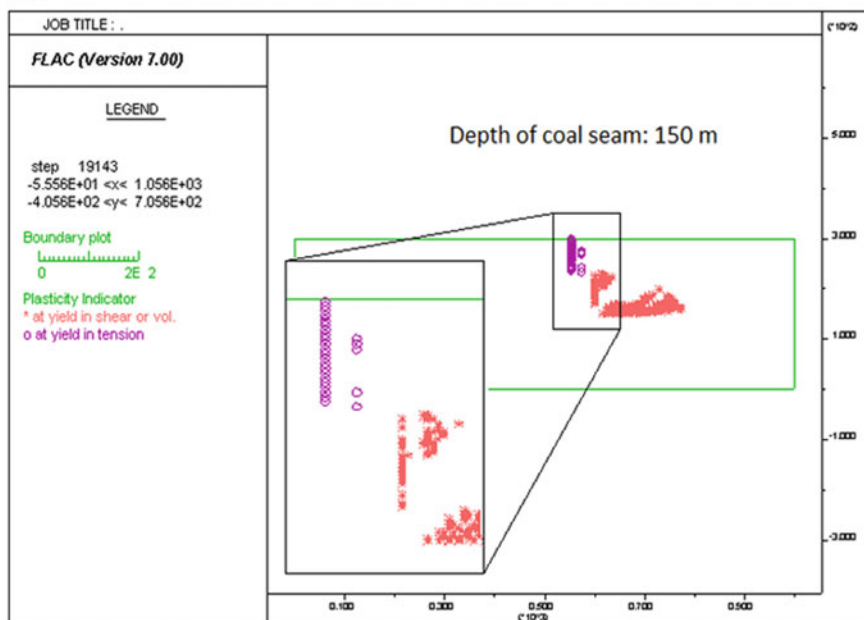
Fig. 4 Plasticity indicator for strong and hard rock with different coal seam depositions

(c)
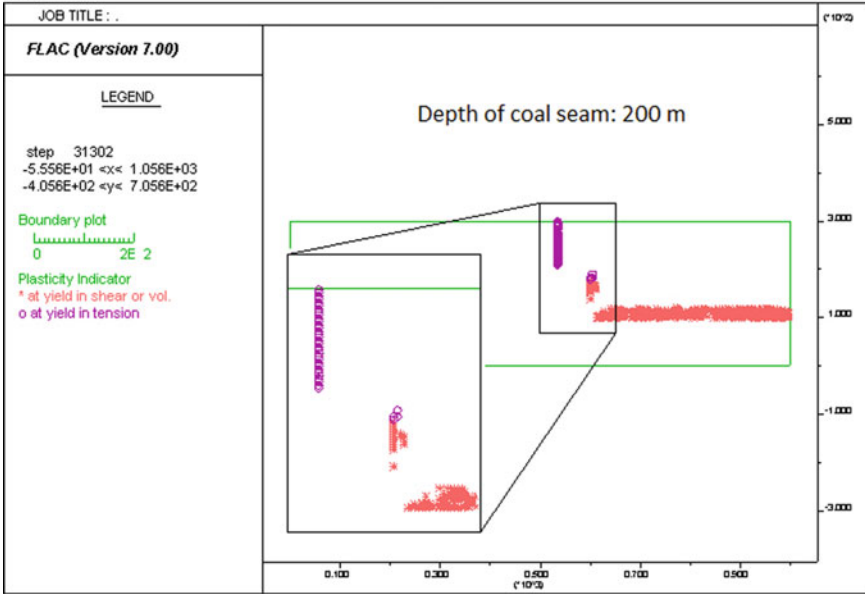
(d)
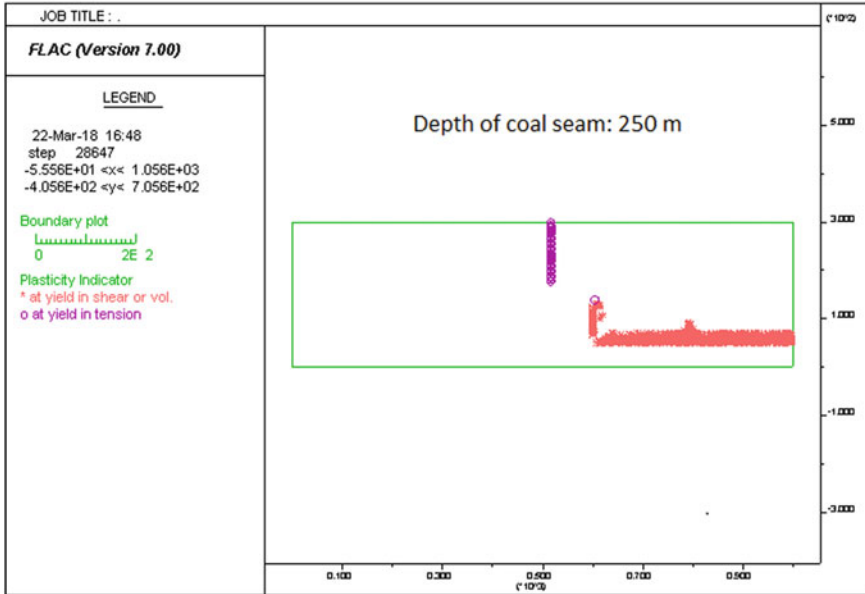
Fig. 4 (continued)

and mining conditions of realistic OP-UG case, those issues should be considered before carrying out analysis to obtain higher accuracy of results.

In this study, the determination of crown pillar thickness for coal mining based on preventing water inrush has been performed successfully. The obtained results indicate that for the longwall mining operation with coal seam of 4 m, crown pillar thickness in the range of 100–250 m can be considered sufficient to prevent water inrush from pit floor into the UG workings: the stronger and more brittle rock the thicker the crown pillar required.

The results of this research could be used by coal mining engineers as a first approximation towards the design of the crown pillar thickness, due to specific assumptions used in the studies.

Some practical activities for risk management in OP-UG transition case to prevent water inrush are recommended: preparing high capacity of surface water drainage, especially in rainy season; installing in-ground monitoring system to detect the range of possible failures inside the rock mass forming crown pillar; carrying out the up-to-date numerical analysis during the advance of underground operation.

References

1. Brown, E.T.: Block Caving Geomechanicse, 2nd edn. JKMRC, Brisbane, Australia (2007)
2. Bakhtavar, E., Oraee, K., Shahriar, K.: Detemination of the optimum crown pillar thickness between open pit and block caving. In: Proceedings of the 29th International Conference on Ground Control in Mining, pp. 325–332 (2010)
3. Nguyen, P.M.V.: Optimization of crown pillar in transition from open pit to underground for coal basin Quang Ninh Vietnam (in Polish). Ph.D. Thesis, AGH University of Science and Technology, Cracow, Poland (2017)
4. Nguyen, P.M.V., Niedbalski, Z.: Numerical modeling of open pit (OP) to underground (UG) transition in coal mining. Stud. Geotechnica Mech 35–48 (2016)
5. Ordin, A.A., Vasilev, I.V.: Optimized depth of transition from open pit to underground coal mining. J. Min. Sci. 696–706 (2014)
6. Carter, T.G., Miller, R.I.: Crown pillar risk assessment planning aid for cost—effective mine closure remediation. Trans. Inst. Min. Met. A41–A57 (1995)
7. Flores, G.E.: Rock mass response to Transition from open pit to underground cave mining. Ph.D. Thesis, University of Queensland, Brisbane (2005)
8. Peng, S.S., Chaing, H.S.: Longwall Mining. Wiley, New York (1984)
9. Qiuan, Q., Lin, P.: Safety risk management of underground engineering in China: progress, challenges and strategies. J. Rock Mech. Geotech. Eng. 423–442 (2016)
10. Li, S., Liu, B., Nie, L., Liu, Z., Tian, M., Wang, S., Su, M., Guo, Q.: Detecting and monitoring of water inrush in tunnels and coal mines using direct current resistivity method: a review. J. Rock Mech. Geotech. Eng. 469–478 (2015)
11. Odintsev, V.N., Miletenko, N.A.: Water inrush in mines as a consequence of spontaneous hydrofracture. J. Min. Sci. 423–434 (2015)
12. Itasca Consulting Group Inc.: FLAC (2-Dimensional Finite Difference Code), Version 7.0. Minneapolis. (www.itascacg.com) (2013)
13. Kumar, R., Singh, A.K., Mishra, A.K., Singh, R.: Underground mining of thick coal seams. Int. J. Min. Sci. Technol. 885–896 (2015)
14. Singh, R.D.: Principles and Practices of Modern Coal Mining, 1st edn. New Age International Ltd., Publishers, New Delhi, India (1997)

15. Ghose, A.K.: Underground methods of extraction of thick coal seams—a global survey. Min. Sci. Technol. 17–32 (1984)
16. Bai, M., Kendorski, F., Van Roosendaal, D.: Chinese and North American high-extraction underground coal mining strata behavior and water protection experience and guidelines. In: The 14th International Conference on Ground Control in Mining, Morgantown (1995)
17. Shabanimashcool, M., Charlie, C.L.: Numerical modelling of longwall mining and stability analysis of the gates in a coal mine. Int. J. Rock Mech. Min. Sci. **51**, 24–34 (2012)
18. Hoek, E., Brown, T.: Practical estimates of rock mass strength. Int. J. Rock Mech. Min. Sci. 1165–1186 (1997)
19. Yavuz, H.: An estimation method for cover pressure re-establishment distance and pressure distribution in the goaf of longwall coal mines. Int. J. Rock Mech. Min. Sci. **41**, 193–205 (2004)
20. Tajdus, K.: New method for determining the elastic parameters of rock mass layers in the region of underground mining influence. Int. J. Rock Mech. Min. Sci. **46**, 1296–1305 (2009)
21. Cheng, Y., Wang, J., Xie, G., Wei, W.: Three-dimensional analysis of coal barrier pillars in tailgate area adjacent to the fully mechanized top caving mining face. Int. J. Rock Mech. Min. Sci. **47**, 1372–1383 (2010)
22. Barton, N., Kjærnsli, B.: Shear strength of rockfill. J. Geotech. Eng. Div. 873–891 (1981)

Identifying Geochemical Anomalies Associated with Cu–Mo Epithermal Mineralization Using PCA and Concentration–Area Fractal Modeling in the Heris Belt, East Azarbaijan (IRAN)

M. Safari, M. Manouchehryniya and M. Barikany

1 Introduction

Due to the diversity of lithology and epigenetic activity, the study area is of great importance for exploration. The area is morphologically composed of Cenozoic and Cretaceous rock formations in a rugged, high northern boundary to the eroded rocky units of Miocene, located in the central and southern ranges. The geological significance of this region is due to the volcanic zone of Urmia—dokhtar in the southwestern part of the region and Sahand tectonomagnetic activities. Intrusive masses are generally diorite, which causes extreme and extensive alteration in Eocene igneous rocks in the study area which is the main source of copper and molybdenum mineralization in the region [1]. On the other hand, in the northwest of this region, there are arsenic deposits in the veins and veins of the realgar and orpiment in the region, which is secondary and extends beyond the boundaries of fractures and faults in this area [2].

In exploratory surveys on a regional scale that is used to explore secondary halos of possible deposits, a large area is usually first covered by geochemical exploration. This operation leads to the discovery of apparent anomalies in the secondary environments (drainage sediments). Due to the fact that in geochemical methods each element is directly measured, attention is not paid to its phase of formation (supergene or hypogene), hence the secondary halos discovered cannot always represent mineralization. Therefore, to distinguish real anomalies that are related to the phenomena

M. Safari (✉)
Department of Geology, Payame Noor University, Tehran, Iran
e-mail: Mb.safari@yahoo.com

M. Manouchehryniya
Department of Geology, Damghan University, Damghan, Iran

M. Barikany
Department of Geology, Kashan University, Kashan, Iran

Table 1 Bulk device sensitivity limit ICP-MS [5]

No.	Elements	Detection	No.	Elements	Detection	No.	Elements	Detection
1	Ag	0.02	14	La	30	27	U	0.5
2	As	1	15	Li	5	28	V	20
3	Au	0.0003	16	Mn	30	29	W	0.5
4	B	5	17	Mo	0.4	30	Y	5
5	Ba	50	18	Nb	5	31	Zn	10
6	Be	0.5	19	Ni	2	32	Zr	10
7	Bi	0.1	20	P	100	33	SiO_2	0.10%
8	Cd	0.05	21	Pb	2	34	Al_2O_3	0.10%
9	Co	1	22	Sb	0.1	35	TFe_2O_3	0.05%
10	Cr	15	23	Sn	1	36	MgO	0.05%
11	Cu	1	24	Sr	5	37	CaO	0.05%
12	F	100	25	Th	4	38	Na_2O	0.05%
13	Hg	0.0005	26	Ti	100	39	K_2O	0.05%

of mineralization and have significant epigenetic components, other elements that are usually related to rock formation (spherical component) should be controlled. Creating a geochemical level based on the concentration of sediment elements is not a trivial method. At present, contrary to the lithogeochemical data, the concentration of elements in the sediment of the stream does not represent the variable field space and in the second, the results are related to a specific catchment area [3]. Continuous basin methods including weighted moving average, inverse weighted distance, and kriging are useful methods that are based on Earth science statistics and considering interpolation parameters including variance, amplitude, and spatial scale and with the help of variograms.

On the other hand, discontinuous basins can be preferred because of the fact that in some areas the use of a moving average does not provide the inverted and spatial correlation of samples at regional scales [4] (Table 1).

In this study, 168 samples of drainage sediments were collected from an area of ″650 km^2 and analyzed by chemical spectrometry of 32 elements using the ICP-MS method (Fig. 1). In this paper, about the elements of copper, molybdenum, arsenic, and antimony were studied. In Table 2, the sensitivity limit of the various elements is given by the ICP-MS method. (Detection limit is on P.P.M and Percentage) In Fig. 2, the dispersion of sampled samples with a density of 2.5 km^2 is shown in the study area.

Univariate methods and classic geostatistic by use of frequency histogram, box plot, QQ plot, and multivariate methods including principal components analysis, cluster analysis, and multifractal models by geographic information systems (GIS) has expanded considerably in recent years to analyze geochemical data [4, 6, 7, 8, 9, 10]. Univariate and multivariate processing methods based on the frequency distribution or correlation of geochemical data may be effective to solve some of the
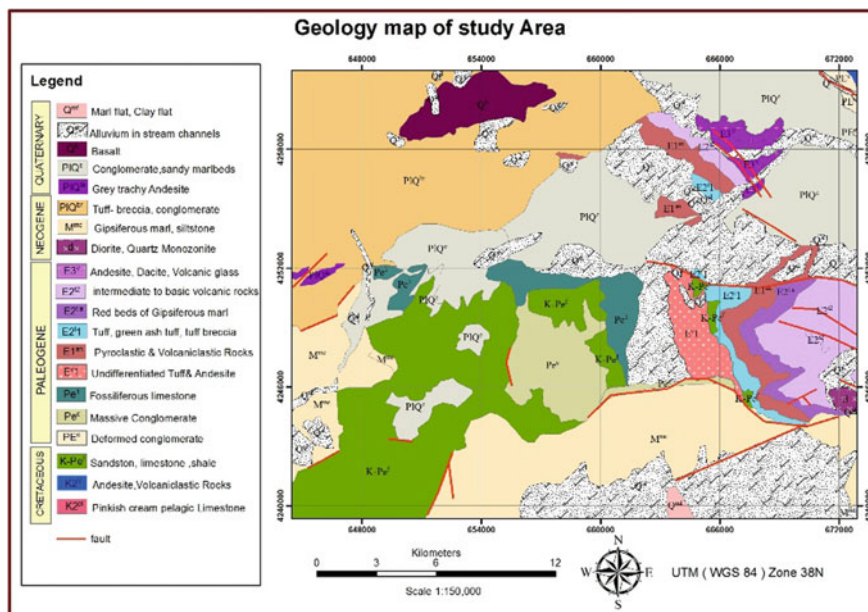
Fig. 1 Geological map of the study area (adapted from sheet 1:100,000 geology geodesy, province of Azerbaijan, Iran)

problems in the frequency domain, but cause limitations in the spatial domain due to the inherent correlation of geochemical data multifractal methods, especially the

Table 2 Statistical components of geochemical data of channel sediments (p.p.m)

		As	Cu	Mo	Sb
No. of samples		168	168	168	168
Mean		30.198	53.879	2.030	1.404
Median		18.000	48.200	1.900	1.100
Mode		8.9	37.8	1.8	.8
Std. deviation		31.8744	22.5759	.7497	1.5354
Variance		1015.978	509.671	.562	2.357
Skewness		3.325	1.588	1.213	6.264
Range		248.4	156.4	4.5	14.1
Minimum		5.6	18.6	.7	.2
Maximum		254.0	175.0	5.2	14.3
Percentiles	5	7.790	26.525	1.200	.400
	25	12.200	38.800	1.500	.700
	75	35.100	65.400	2.400	1.700
	95	90.105	95.630	3.555	2.655
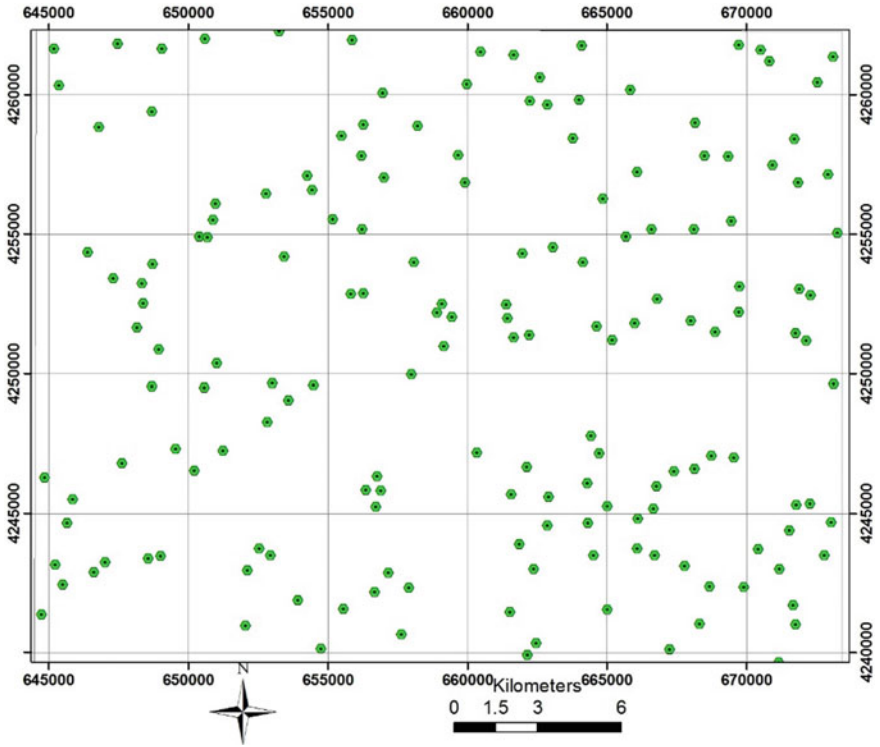
Fig. 2 Layout map of stream samples with a 2.5 km^2 sampling rate

C–A method, have a special look at both frequency and location components and are a powerful tool for the study and analysis of complex geochemical communities and can even identify weak anomalies in a strong geochemical field [8]. In this paper, a combination of C–A, PCA methods to identify copper anomalies in the Harris ore deposit has been investigated.

2 Method

2.1 MIDW Method

The inverse distance weighting (IDW) method is one of the most popular interpolation methods, based on the assumption that neighboring values are more involved than distant points [11]. The strength of this method is that the results are intuitive and its application and interpretation is easy, but its disadvantage is that the weight of the values is only based on the location and the data variance is not affected [9]. But

in the MIDW method, much of this problem has been highlighted, and this method has proven itself as a powerful tool for exploratory data studies [9] and geochemical analysis. A common drawback of moving average interpolation techniques such as IDW is that the non-consideration of the local properties of data. In contrast, multifractal inverse distance weighting (MIDW) incorporates local singularity into the basic model of moving average interpolation.

2.2 PCA Method

Basically, PCA implies performing a linear transformation of the original coordinate axes of the data (multispectral vector space), into a new vector space where the axes are uncorrelated. Mathematically, this means that the covariance matrix in the new system is diagonal, having all elements equal to zero, except the first diagonal, where the elements (i.e., the variances of the data in the transformed coordinates) are in decreasing order. These variances of the data in the transformed multispectral vector space (or principal components) are the eigen values of the covariance matrix [12].

This method is the most valid method in multivariate analysis, which is a useful tool for combining dependent variables and extraction of a variable, and, consequently, reducing the volume of data based on covariance and degree of correlation of variables [13]. The main components of the analysis are the following:

1. The largest spectral information quantity of a multivariate image is introduced in a small number of main component variables, which results in a smaller number of lesser mineralization variables for studying data, which reduces the space required by the computer and increases the processing speed.
2. You can use this fan to intensify special features. In other words, using the selection of sample surfaces on a particular phenomenon, one can show the desired phenomena to the desired level and increase its resolution from phenomena and field values.
3. Analysis of the main components is a valuable method for creating a series of non-correlated images from a series of highly correlated data. Using this property, you can separate the different categories in a series of data.

2.2.1 Fractal Methods

In fractal geometry, each form and its complexity are represented in the form of numbers, as in Euclidean geometry, the concepts of angle, length, area and one to three-dimensional spaces are used. In fractal geometry, there are fractal symmetries that are usually not correct integers, and are called fractals, which can be used to express the complexity of a form.

The study of [14] was among the first papers to address the importance of fractal models used for geochemical landscape studies and to predict their profound

impact on geochemical exploration. [8] proposed the concentration–area fractal model (C–A), which represents the first important advancement in fractal/multifractal modeling of geochemical data [15] and is a fundamental technique used frequently for modeling geochemical anomalies [8]. The spectrum–area fractal model (S–A), introduced by [6] as a version of the C–A model in the frequency domain, can separate overlapping populations using more than one cutoff value. Based on Mandelbrot's radial-density law, by replacing density with concentration, [16] proposed the concentration–distance (C–D) fractal model, which is used for discriminating geochemical anomalies from the background. [6] reviewed the fractal/multifractal methods used to model geochemical data in his book Geochemical Anomaly and Mineral Prospectivity Mapping in GIS and demonstrated the advantages of these models. [17] extended the C–A fractal model to 3D and developed the concentration–volume (C–V) fractal model to identify various zones of mineralization. These models have been acknowledged widely as powerful tools for identifying anomalies as well as for determining geochemical baseline in environmental studies.

The general form of the model is shown in Eq. (1), where $A(\rho)$ denotes the area with concentration values greater than the contour value ρ, v represents the threshold, and $a1$ and $a2$ are characteristic exponents. The area $A(\rho)$ for a specified ρ is equal to the cell area multiplied by the number of cells with pixel values greater than ρ. The changes in slope between straight-line segments on a log–log plot and the corresponding values of ρ are used as cutoff (threshold) values to separate pixel values into components that represent different causal factors. In this study, we use the C–A fractal model to separate pixels with different cosine values and to determine the threshold value between different populations.

$$A(\rho \leq v)\infty\rho - a1; \ \ A(\rho \geq v)\infty\rho - a2 \tag{1}$$

3 Results and Discussion

The range studied in the Harris index is between 38°, 15° to 38°, and 30° North, and 46°, 40° to 46°, and 55° North. The intrusive masses from the Cretaceous to Miocene, which are generally located in the east and center of the study area, play a major role in the mineralogy of the region. The area is tectonically divided into three regions: the first zone is in the southwest and the boundary between Marl and Gypsum Neogene units and the second zone in the northeast is located on the boundary between the penetrative units of dacite and Andesite Palaeogenic and the third zone in the east and southeast The boundaries of the Tuff Palaeogenic units are located and all three regions have a different geochemical pattern in terms of background and anomalies [18]. The main fault directions in the region are E–W direction, which is a diverse variety of copper mineralization in the control area, which is generally located near the semi-acid penetrating Contacts and carbonate rocks.
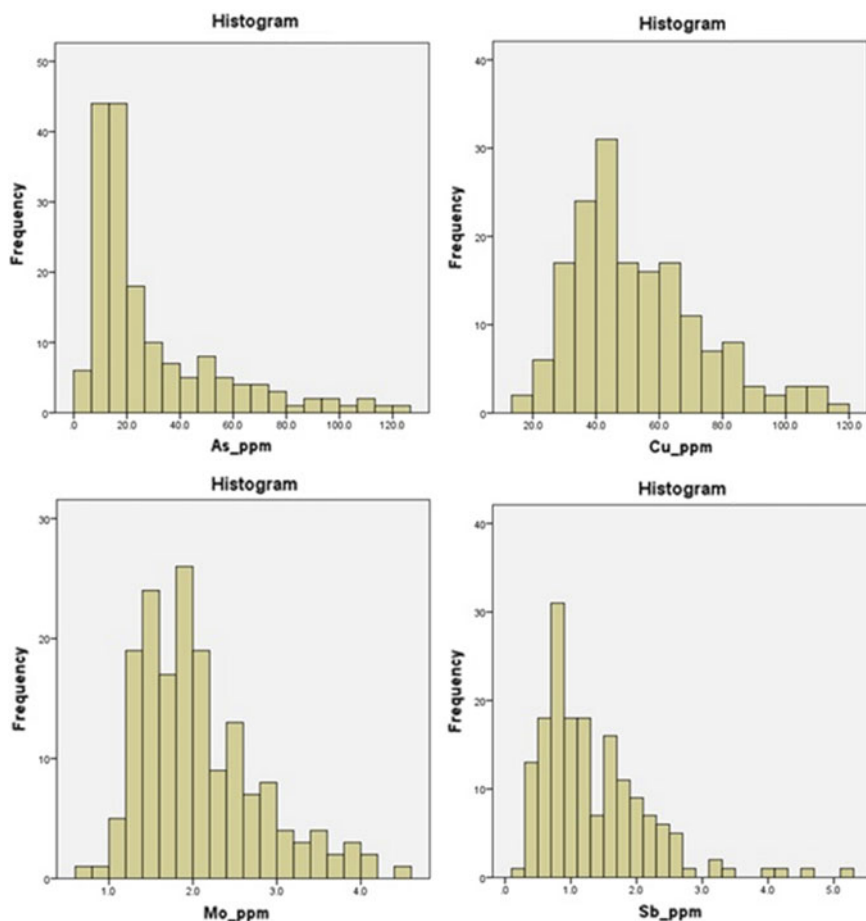
Fig. 3 The histogram of the frequency of normal data in the desired range

Based on the results of the analysis of the stream samples (Fig. 2), only As, Cu, Mo, Sb elements were selected to examine the mineralization of the epithermal type and to control the geochemical migration of copper in comparison with molybdenum [19].

The statistical parameters (Table 2) indicate the abnormal distribution of the data for the desired elements in the first step, you need to normalize the data that is displayed in Figs. 3, 4, and 5 include of histograms of the dispersion and Q-Q Plots of elements after normalization.

Table 3 shows the analysis of the main components and Fig. 6 shows the Pearson correlation graph of the elements in the studied range. As it comes from the values of the main components, these values obtained from the correlation matrix and for the reduction of the number of variables and the extraction of several non-correlated
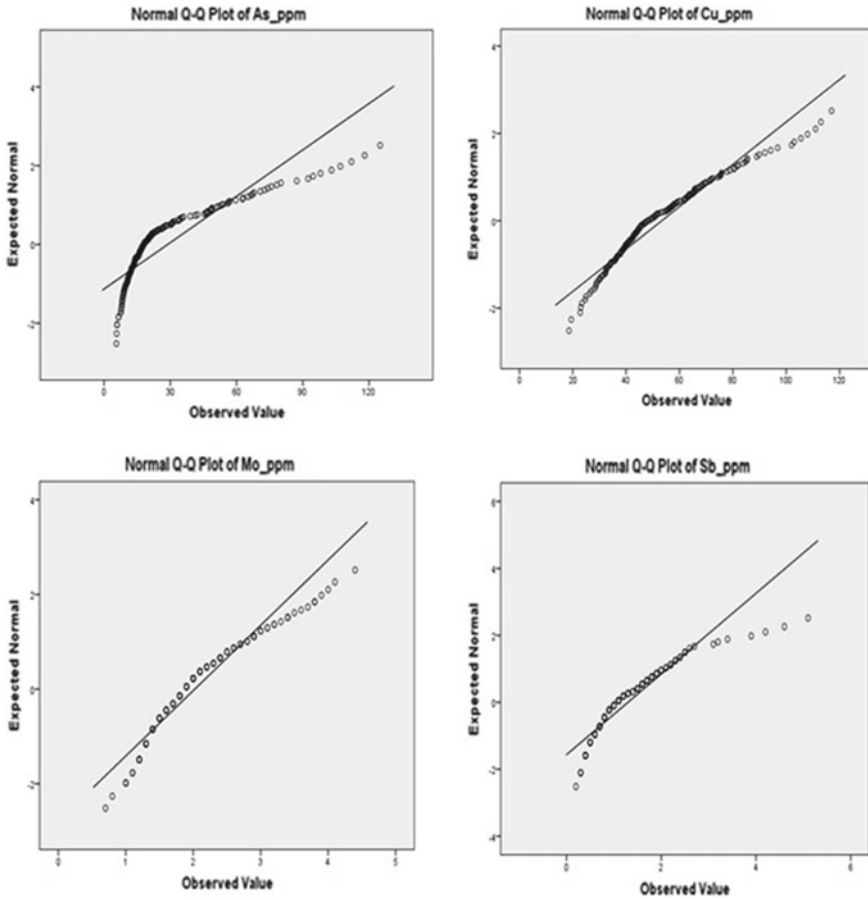
Fig. 4 *Q-Q* plans for normal data in the desired range

variables [20], including the highest data variance with our Eigen value values, are between -0.6 and 0.9, which is the first component Which contains 56% of the total variance of multivariate data, which, as it is known, shows the second component with a significant correlation between copper and molybdenum dispersion and their dependence on the presence of arsenic and antimony, which after applying the CA fractal method in the region And the formation of cohesive logarithmic graphs of the area, managed to separate the various geochemical communities and Removing field values and local thresholds from data (Fig. 7).

As shown in Fig. 6, the copper element shows a significant correlation with zinc and manganese and anomaly with molybdenum, and, on the other hand, indicates a spatial correlation between the antimony and arsenic, which indicates the mineralization of epithermal copper in the region.

(a)

(b)

(c)

(d)
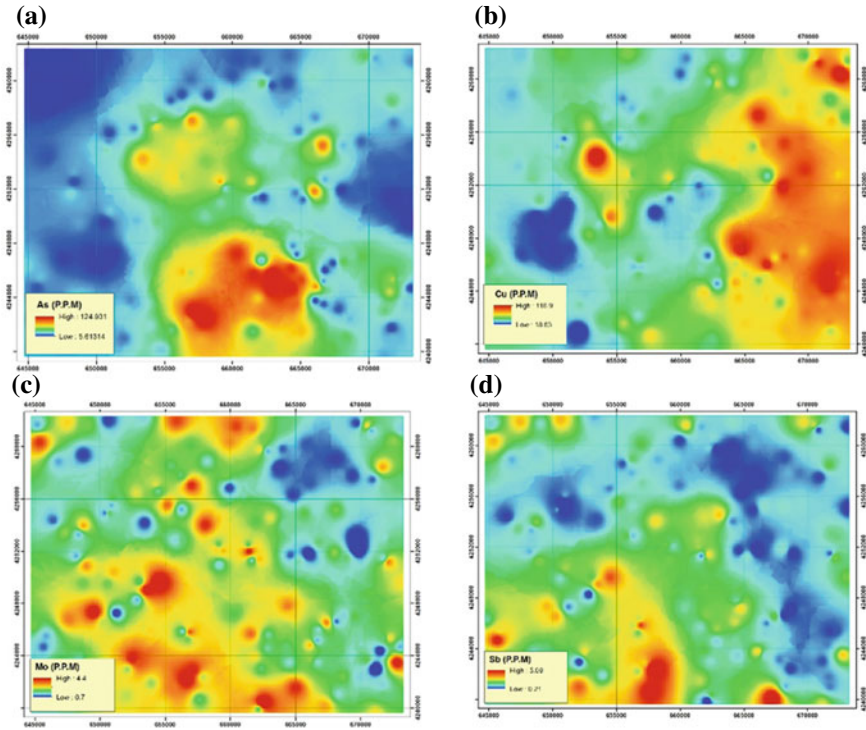
Fig. 5 The single-valued Raster maps show the distribution of the MIDW trace elements in the GIS software. **a** As, **b** Cu, **c** Mo, **d** Sb

Table 3 Analysis of main components of geochemical data of channel sediments (As, Cu, Mo, Sb)

Eigenvalues and eigenvectors					
	As	Cu	Mo	Sb	Percent
PCI	−0.26	0.7	0.63	−0.18	56.5
PC2	0.29	0.71	−0.61	0.17	23
PC3	−0.32	0.007	0.11	0.93	14.5
PC4	0.85	−0.024	0.45	0.24	6

4   Conclusions

The studies have shown the ability and power of the fractal method and the role of it in the separation of geochemical communities and the stages of the enrichment of the elements. Definitely, the combination of the results with geological evidence can provide a much better view of the stages of mineralization of each element and its secondary dispersion. The multivariate anomaly map implies the existence of anomalies in line with SW–NE which is in line with the Eocene intrusive masses and faults of the region with the same direction that has created a suitable environment

	As_…	Be_…	Bi_…	Co_…	Cr_…	Cu_…	Mn…	Mo…	Ni_…	Pb_…	Sb_…	Se_…	Sn_…	Sr_…	Zn_…
As_…															
Be_…	0.19														
Bi_…	0.03	0.04													
Co_…	0.06	-0.08	0.13												
Cr_…	-0.11	0.08	-0.23	-0.12											
Cu_…	0.11	0.18	-0.15	0.08	0.01										
Mn…	0.03	0.07	-0.19	0.10	0.11	0.61									
Mo…	0.11	0.02	0.25	0.13	0.00	-0.25	-0.20								
Ni_…	-0.03	0.18	0.09	0.00	0.11	-0.45	-0.44	0.19							
Pb_…	0.30	0.38	-0.02	0.05	0.09	0.18	0.43	-0.07	0.11						
Sb_…	0.09	0.05	0.32	-0.12	0.04	-0.23	-0.29	0.55	0.22	-0.13					
Se_…	0.04	0.01	0.21	-0.10	-0.07	-0.01	-0.05	0.12	0.05	-0.01	0.29				
Sn_…	-0.01	0.00	-0.04	0.01	0.39	-0.10	-0.06	0.25	0.04	-0.07	0.17	0.02			
Sr_…	0.23	0.32	0.02	0.08	0.01	-0.12	0.17	0.06	0.13	0.28	-0.02	-0.07	-0.04		
Zn_…	0.20	0.20	-0.15	0.03	0.20	0.59	0.67	-0.11	-0.33	0.38	-0.08	-0.03	0.00	0.02	

Color Coding (signficance 0.950)
- very strong
- strong
- moderate
- weak
- very weak
- null

Fig. 6 Correlation table of geochemical data of channel sediments (Pearson)

for the formation of epithermal deposits in the region. The identified anomalies of Sb, Mo, As, and Cu in the center and north of the region require more exploratory studies, especially geophysics, with methods such as IP-RS, and on the other hand, in the western part, the presence of anomalies indicates the Cretaceous linguistics of the region. These studies show that Harris index has a high potential for exploration of epithelial deposits. In this paper, a single-variable and multivariate CA fractal model is presented to reveal copper anomalies, which suggests that the new models derived from the combination of CA and PCA fractal methods are useful tools for identifying geochemical anomalies, which, while investigating the spatial correlation of elements, It has the ability to distinguish between different anomalies and is used extensively in field exploration.
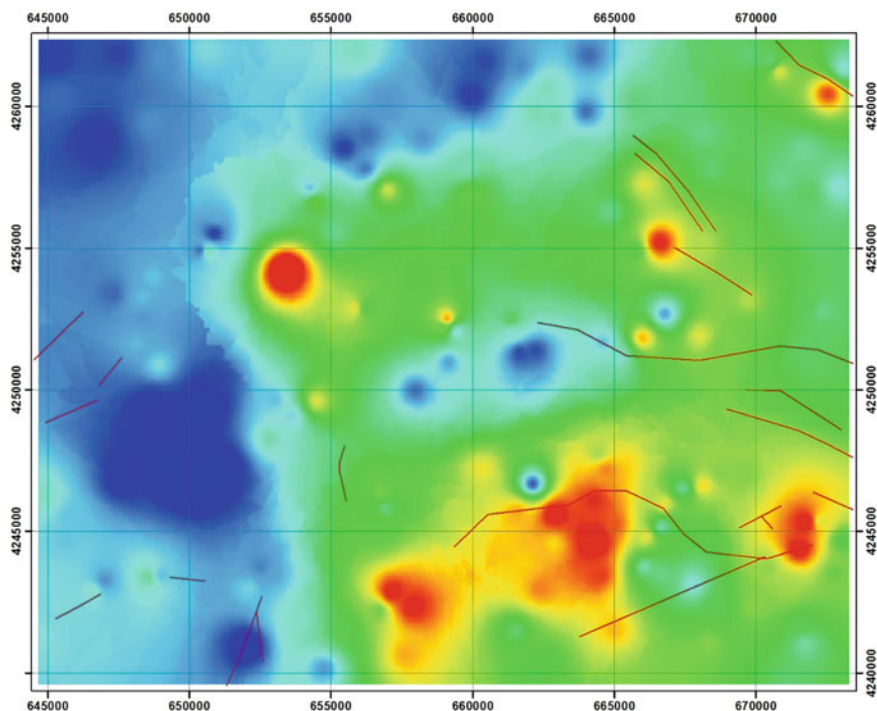
Fig. 7 *C–A* fractal map on the second principal component with main faults location

References

1. Asadiyan, A.: Geology Map 1:100,000 Tabriz. Geological Survey and Mineral Exploration of IRAN (1972)
2. Mostafa, P.N.: Economic geology studies on genesis of arsenic reserves in Waleon region. Master's thesis, Tabriz University (2001)
3. Ludington, S., Castor, S.B., Budahn, J.R., Flynn, K.S.: Geochemical analyses of geologic materials from areas of critical environmental concern, Clark and Nye Counties. U.S. Geological Survey Open-File Report 05-1450, Nevada. http://pubs.usgs.gov/of/2005/1450/ (2006)
4. Carranza, E.J.M.: Geochemical Anomaly and Mineral Prospectivity Mapping in GIS. Handbook of Exploration and Environmental Geochemistry, vol. 11. Elsevier, Amsterdam (2008)
5. Wang, X., Xie, X., Zhang, B., Hou, Q.: Geochemical probe into China's continentalcrust. Acta Geoscientica Sinica **32**, 65–83 (2011) (in Chinese with English abstract)
6. Carranza, E.J.M.: Mapping of anomalies in continuous and discrete fields of stream sediment geochemical landscapes. Geochem. Explor. Environ. Anal. **10**, 171–178 (2009)
7. Carranza, E.J.M.: Catchment basin modeling of stream sediment anomalies revisited: incorporation of EDA and fractal analysis. Geochem. Explor. Environ. Anal. **10**, 365–381 (2010)
8. Cheng, Q., Agterberg, F.P., Ballantyne, S.B.: The separation of geochemical anomalies from background by fractal methods. J. Geochem. Explora. **51**, 109–130 (1994)
9. Cheng, Q.: Modeling local scaling properties for multiscale mapping. Vadose Zone J. **7**, 55–523 (2008)
10. Grunsky, E.C.: The interpretation of geochemical survey data. Geochem. Explor. Environ. Anal. **10**, 27–74

11. Lima, A., De Vivo, B., Cicchella, D., Cortini, M., Albanese, S.: Multifractal IDW interpolation and fractal filtering method in environmental studies: an application on regional stream sediments of (Italy), Campania region. Appl. Geochem. **18**, 1853–1865 (2003)
12. Cheng, Q., Bonham-Carter, G.F., Wang, W., Zhang, S., Li, W., Xia, Q.: A spatially weighted principal component analysis for multi-element geochemical data for mapping locations of felsic intrusions in the Gejiu mineral district of Yunnan, China. Comput. Geosci. **5**, 662–669 (2011)
13. Jolliffe, I.T.: Principal Component Analysis, 2nd edn., p. 487. Springer, New York (2002)
14. Bölviken, B., Stokke, P.R., Feder, J., Jössang, T.: The fractal nature of geochemical landscapes. J. Geochem. Explor. **43**, 91–109 (1992)
15. Zuo, R., Carranza, E.J.M., Cheng, Q.: Fractal/multifractal modelling of geochemical exploration data. J. Geochem. Explor. **122**, 1–3 (2012)
16. Li, C., Ma, T., Shi, J.: Application of a fractal method relating concentrations and distances for separation of geochemical anomalies from background. J. Geochem. Explor. **77**, 167–175 (2003)
17. Afzal, P., Fadakar, A.Y., Khakzad, A., Moarefvand, P., Rashidnejad, O.N.: Delineation of mineralization zones in porphyry Cu deposits by fractal concentration–volume modeling. J. Geochem. Explor. **18**, 220–232 (2011)
18. Rafiee, A.: Seperating geochemical anomalies in stream sediment media by applying combination of fractal concentration-area model and multivariate analysis (Case study, Jebal-e-Barez 1:100000 Sheet, Iran). In: 20th World Mining Congress Proceeding National Geosciences Database of Iran, pp. 461–470 (2005)
19. Pourmafi, M., Kohansal, R., Ghorbani, M., Khalatbari, M., Omrani, J.: Petrology and Petrogenesis of Pillow Lavas in the Ferwood Area, Northeast of Iran (2015)
20. Cheng, Q., Agterberg, F.P.: Singularity analysis of ore-mineral and toxic trace elements in stream sediments. Comput. Geosci. **35**(2), 234–244 (2009)

Numerical Simulations of Geomechanical State of Rock Mass Prior to Seismic Events Occurrence—Case Study from a Polish Copper Mine Aided by FEM 3D Approach

W. M. Pytel, P. P. Mertuszka, T. Jones and H. Paprocki

1 Introduction

The Lower Silesian Copper District is located in south-west part of Poland and this is one of the most important mining areas in Europe, extracting over 30 million tons of copper ore per year. Copper ore is excavated in three underground mines belonging to KGHM: the Lubin, Polkowice-Sieroszowice and Rudna mines. The stratoidal deposit is characterised by variable thickness (from 0.4 to 26 m), small inclination (approximately 4°), and varying lithological profile. The room-and-pillar mining system is a dominant technology utilized in underground copper mines in Poland. This mining method is well suited to the hardness of the local rock and is proven to be highly adaptable and suitable to the local mining and geological conditions [1].

With the increasing depth of exploitation and higher variability of rock-mass characteristics within roof strata, it was observed that increasing stress created more difficulties in the mining process [2]. The biggest risk to the mining operations is created by high-energy tremors with hypocenters located within the main roof strata, about 40–200 m above the excavated copper ore body. They are extremely difficult to both predict and to analyse due to their short duration and unpredictable time of occurrence [3]. The strongest tremors, reaching seismic energy levels over 10^9 J, can be considered as small earthquakes and are quite often associated with rockbursts. Due to the dynamic nature of the rock mass failure, some of these rockbursts can cover the working areas, becoming a hazard to both crew and equipment safety.

W. M. Pytel · P. P. Mertuszka (✉)
KGHM CUPRUM Ltd. Research & Development Centre, Wrocław, Poland
e-mail: pmertuszka@cuprum.wroc.pl

T. Jones
Luossavaara-Kiirunavaara AB, Malmberget, Sweden

H. Paprocki
KGHM Polska Miedź S.A., Lubin, Poland

The aim of the paper was to determine the overall stress/deformation states within the considered mining panel immediately prior to selected historic seismic events and subsequently to judge how the progress of mining could affect the occurrence of instability in the roof strata. The geomechanical problem solution and results visualization were based on the NEi/NASTRAN computer program code utilizing 3D finite elements method.

2 Seismicity Within the Considered Mining Panel

The XIII/4 mining panel is located in the central part of the Lubin—Małomice mining area, about 3 km to the east of the L-I and L-II shafts on the depth between 728 and 785 m beneath the surface. The form of the deposit is classified as stratoidal and single-level. The ore bed includes grey Rotliegend sandstones and copper-bearing lower-Zechstein shales. The deposit is extended in the NW–SE direction and declines about 3° in the NE direction.

The specific geologic structure of the overburden, which is typical in KGHM's copper mines, favours the occurrence of strong seismic events. The material of the strata is mostly characterised by high strength and low deformability. From the geomechanical point of view, the occurrence of dynamic events is caused by high stress-strain levels within the material surrounding mine workings, leading to a low value of the bearing capacity margin. This means that even a slight additional load in the form of adverse stress changes—according to the accepted strength hypothesis—may lead to instability in a certain area of the workings.

Experiences gained from previous observations lead to the conclusion that the seismicity level depends on the progress of mining in a particular panel, and on the geologic and mining conditions. This is why seismicity varies over the years. Figure 1 shows the seismic activity in the all KGHM mines starting from 1990. Tremors with the seismic energy lower than 10^3 J were omitted.

Based on Fig. 1, one may conclude that the number of tremors has generally increased in the past years. General trend of number of events could be approximated
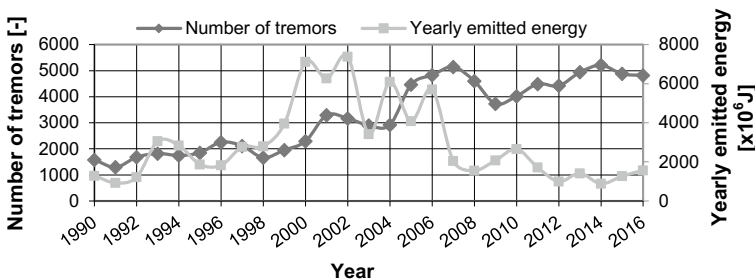
Fig. 1 Number and energy of tremors recorded between 1990 and 2016 in KGHM mines

by linear function with the relatively high coefficient of determination $R^2 = 0.8586$. The total annual energy emission from mining-induced tremors increased extremely between 1990 and 2000 when seismic energy reached the peak value. High level of seismic activity remained stable over the next 2 years and then decreased significantly. This situation stabilised in 2007. The seismic activity level has remained relatively low and stable from 2007 until 2016.

The subject of the case of study, the XIII/4 mining panel, is one of the panels in the Lubin mine. The deposit within this mine is characterised by the frequent occurrence of tectonic discontinuities within the orebody, which can create difficulty during mining operations, even leading to abandonment in some cases.

The inventory of the seismic events from the Lubin mine between 2007 and 2016 (see Fig. 2) indicates that significant fluctuation can be observed in practically all energy classes, especially in the case of events with the seismic energy greater than 10^6 J. When considering exclusively tremors with the energy greater than 10^7 J, sudden increase of the number of tremors of this energy class may be observed.

However, when considering the relationship between the event count and the total energy released in each energy class, one may conclude that most of energy comes from large events with energy magnitudes greater than 10^6 J. It should be also noted, that the total energy of tremors is inversely proportional to frequency of events occurrence. The differences between the energy released in any two subsequent years varied significantly, from 12% up to 343%. This is the best example of how dynamic events' occurrence is unpredictable.

The seismic activity in this panel has remained at a very high level from the beginning of mining works in this area. The frequency of tremor occurrence and quarterly released energy increased almost linearly since 2014. The XIII/4 mining panel was active in the light of seismic activity, both spontaneous and blasting-induced, which allows the determination of the relationship between the stress/deformation states within the analysed mining panel both prior to and after a specific seismic event. Based on this relationship it is possible to judge how the progress of mining could affect the likelihood of the occurrence of instability in the rock mass.

	2007	2008	2009	2010	2011	2012	2013	2014	2015	2016
E3J	725	511	256	272	441	561	569	539	331	380
E4J	509	378	166	206	236	272	253	225	152	224
E5J	202	114	61	88	120	104	69	129	121	164
E6J	25	15	8	28	29	31	28	32	17	39
E7J	2	4	1	4	8	4	12	2	13	11
E8J	0	0	0	1	0	0	0	0	1	0
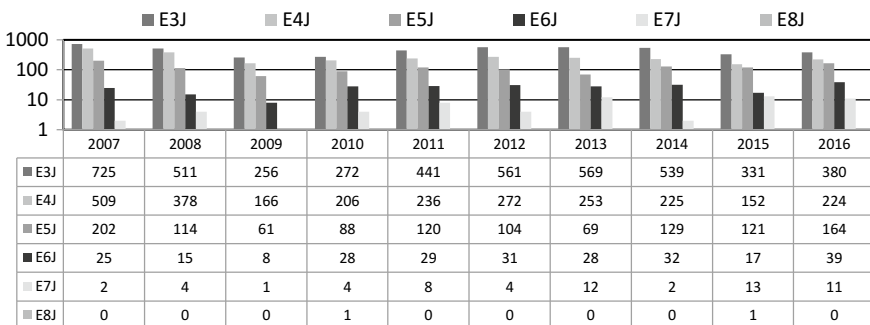
Fig. 2 Number of seismic events of the particular energy classes recorded within the Lubin mine between 2007 and 2016
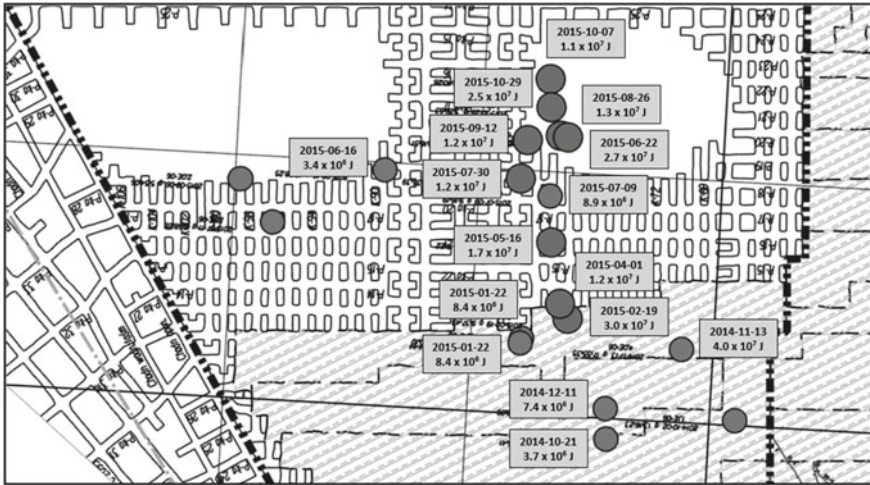
Fig. 3 Locations of high-energy tremors within XIII/4 mining panel between 2014 and 2015

From a geometric point of view, the locations of almost all recorded high-energy tremors were determined to be in a single, straight line (Fig. 3). This indicates, that the mining-geological conditions encountered on the right side of the contact between undisturbed rock mass and the excavated workings were the main source of the geomechanical type of instabilities.

3   Geomechanical Analysis Based on FEM Modelling

Twenty tremors with an energy level of 10^7 J occurred between February 2015 and November 2016 within the considered mining panel, 10 of which caused serious damage to the mine workings. For the purpose of the presented paper, three cases of tremors of which full documentation was available, were examined. Computer simulations were performed using a numerical model based on the geometry of the mine workings at the time when the following seismic events occurred (Fig. 4)

– June 22, 2015—seismic energy of $E_s = 2.7 \times 10^7$ J with excavations' geometry described later as 'Event 1'
– May 11, 2016—seismic energy of $E_s = 1.9 \times 10^7$ J with excavations' geometry described later as 'Event 2'
– November 3, 2016—seismic energy of $E_s = 7.6 \times 10^6$ J with excavations' geometry described later as 'Event 3'.

Geomechanical problem solution and results visualization were based on the NEi/NASTRAN computer program code utilizing FEM in three dimensions [4]. It was assumed that all of the materials reveal linear elastic characteristics, except for

Event 1

District: **G-2**
Mining panel: **XIII/4**
Energy: **2,7 x 10^7 J**
Date: **22.06.2015**
Time: **6:16**
Depth: **- 587 m**

Event 2

District: **G-2**
Mining panel: **XIII/4**
Energy: **1,9 x 10^7 J**
Date: **11.05.2016**
Time: **6:01**
Depth: **- 594 m**

Event 3

District: **G-2**
Mining panel: **XIII/4**
Energy: **7,6 x 10^6 J**
Date: **3.11.2016**
Time: **1:59**
Depth: **- 585 m**

location of event ■ damaged area ▢ closing pillar ▨ mined out area
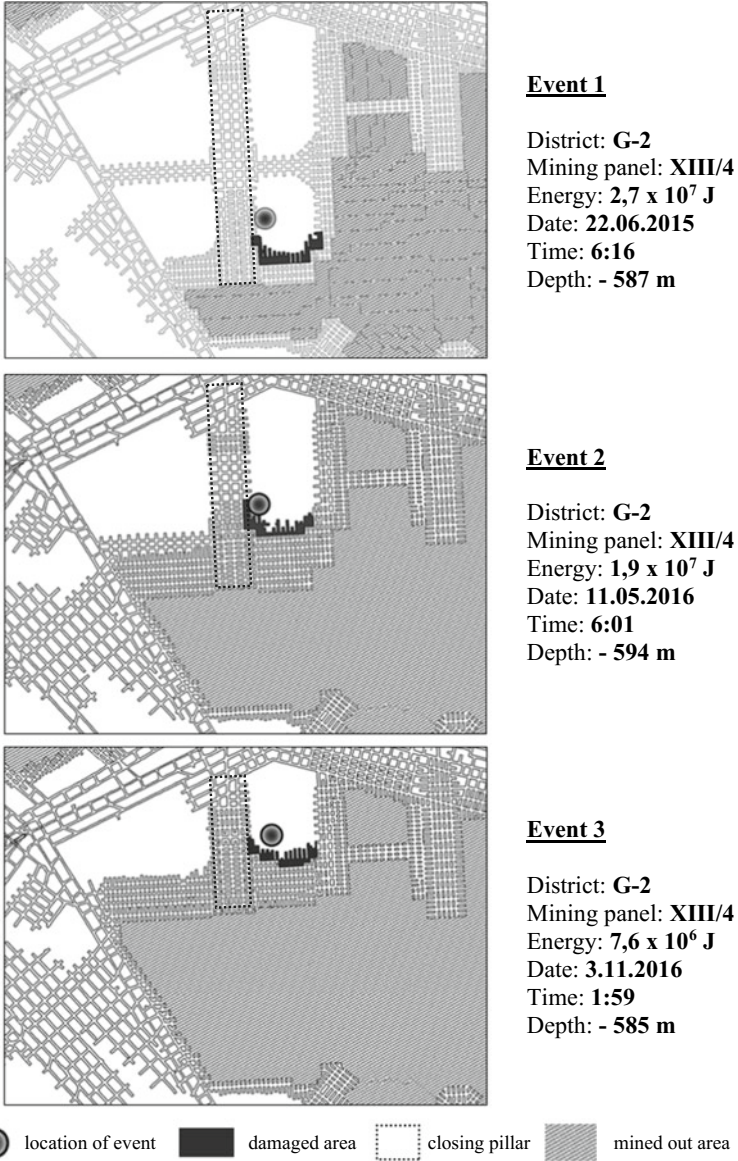
Fig. 4 Location of the considered seismic events with the geometry of mining drifts

rocks comprised within pillars which exhibit elastoplastic behaviour with strain softening [5]. The boundary conditions of the entire numerical models were described by displacement-based relationships. A non-linear calculation procedure was applied, including an adaptive phase (elastic solutions with successive modification of over-

loaded pillars and an iterative procedure for selection of pillars for which the vertical load σ_z was greater than the critical value σ_p, and subsequently using a constant residual load σ_r instead of such pillars) and a final phase (verification of safety factors within the roof layers). The displacement boundary conditions were formulated as follows: no vertical displacements of the bottom layer in the model and no movements in the direction perpendicular to the lateral walls. The external load was divided into the following two groups: the self-weight load of the tertiary and quaternary formations and the self-weight load of the other rocks represented by material characteristics, including the density (gravitation).

As a basic physical model for the problem, the multi-plate overburden model has been accepted. It was assumed that the overburden strata consists of several homogeneous rock plates reflecting the real lithology in the area and that the technological and remnant pillars work effectively within a post-critical phase (elastic-plastic with strain softening behaviour) [6, 7]. To illustrate the effect of mining face geometry, the XIII/4 mining district has been modelled in 3D FEM code. A mining system with roof deflection was assumed. The averaged geological data over the considered area and the estimated rock mass parameters are given in Table 1.

where: σ_{cm} and σ_{tm} are compression and tension strengths for rock mass, assessed according to Hoek approach [8].

Numerical experiments permitted the determination of the overall stress/deformation states which were later used for quantitative characterization of the actual level of safety, using the indicator called safety factor, related to

Table 1 Geological data in the vicinity of considered area

Rock type	Thickness (m)	σ_c σ_{cm} (MPa)	σ_t σ_{tm} (MPa)	E_s $E^{(r)}$ (MPa)	Poisson's ratio (ν)	Level
Clayey shale	12.2	22.5 1.56	1.7 0.006	13,500 3375	0.18	Roof strata
Anhydrite	136.8	88.5 17.1	6.25 0.21	55,500 13,875	0.18	
Limestone	13.8	174.0 92.1	9.9 1.3	52,500 13,125	0.24	
Dolomite II	10.8	119.3 37.0	8.2 0.49	57,100 14,275	0.24	
Dolomite I	9.2	146.7 61.4	9.9 0.85	51,400 12,850	0.24	
Copper ore	2.8	40	2.7	13,000 6500	0.17	Extraction range
White sandstone	10	34.4	1.9	11,600 5800	0.17	Floor strata
Quartz sandstone	290	17.9	0.9	5100 2550	0.13	

different failure criterions. In this paper, safety factor F_{HB} spatial distribution has been calculated utilizing the Hoek–Brown theory (see [6])

$$\sigma_1 = \sigma_3 + \sqrt{A\sigma_3 + B^2} \tag{1}$$

Or

$$\tau_m = \frac{1}{8}\left[-A \mp \sqrt{A^2 + 16(A\sigma_m + B^2)}\right] \tag{2}$$

Safety factor may be then presented as follows:

$$F_{HB} = \frac{\frac{1}{8}\left[-A \mp \sqrt{A^2 + 16(A\sigma_m + B^2)}\right]}{\tau_m} \tag{3}$$

where
$A = \frac{R_c^2 - R_r^2}{R_r}, B = R_c;$
σ_p—average value of principal stresses;
τ_m—maximum shear stress in specific location of the rock mass.

The values of safety factor smaller than 1 indicate the likely occurrence of instability in the rock mass. The selected results of calculations are shown in Figs. 5, 6 and 7 as contours of safety factor at 5.2 m (dolomite I), 9.7 m (dolomite I), 14.7 m (dolomite II), 20.1 m (dolomite II), 26.25 m (limestones), 33.15 m (limestones) above the roof strata for considered events.

From the presented geomechanical analysis, one may conclude that safety factors will reach the lowest value at levels closer to the excavation, especially in mined-out areas (roof fall hazard). Furthermore, it was found that in all three considered cases, safety factor values $F_{HB} \ll 1$ are located both in mined-out zones as well as in working areas. The lowest values of safety factors were calculated in the vicinity of so-called *closing pillar* in the immediate roof strata within Dolomite I and Dolomite II, i.e. 2.8–22.8 m above the floor level of the excavations. In addition, all recorded high-energy seismic events were developed within that height range.

With respect to geometry, in general, a series of high-energy tremors occurred on the right side of the mining front. As the mining front progressed, they were observed at relatively regular time-space intervals, almost in one straight line. This suggests, that they were caused by the geometry of the rock mass shaped in the form of a sharp corner directed to yielded pillars.

The results of calculations coincide with the actual conditions, i.e. the indicated areas of increased risk of instability coincide with the actual range of damages around the workings. The determined area of possible instability occurrence contained the location of all considered high-energy tremors.
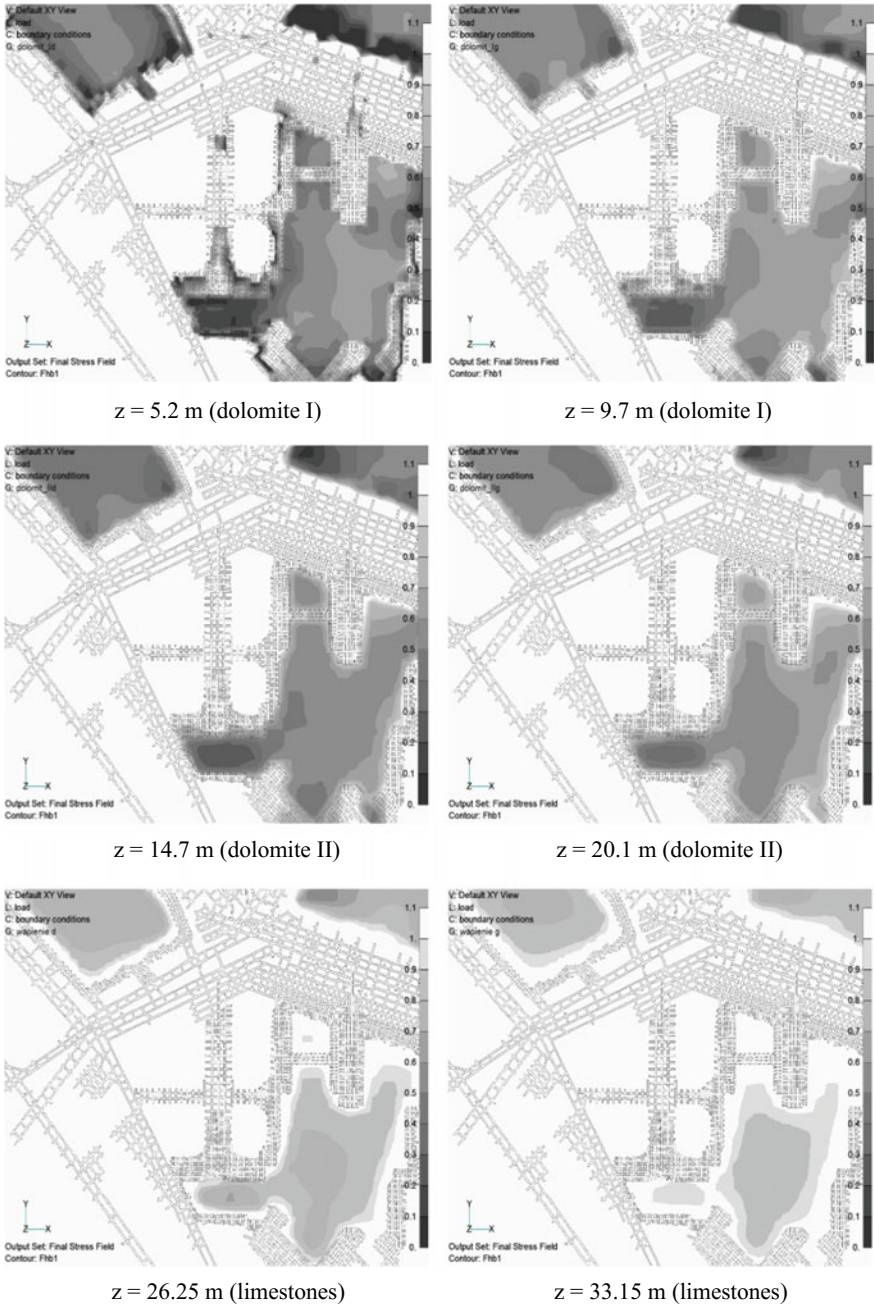
z = 5.2 m (dolomite I)   z = 9.7 m (dolomite I)

z = 14.7 m (dolomite II)   z = 20.1 m (dolomite II)

z = 26.25 m (limestones)   z = 33.15 m (limestones)

Fig. 5 Contours of calculated values of safety factor in the roof strata (event 1)
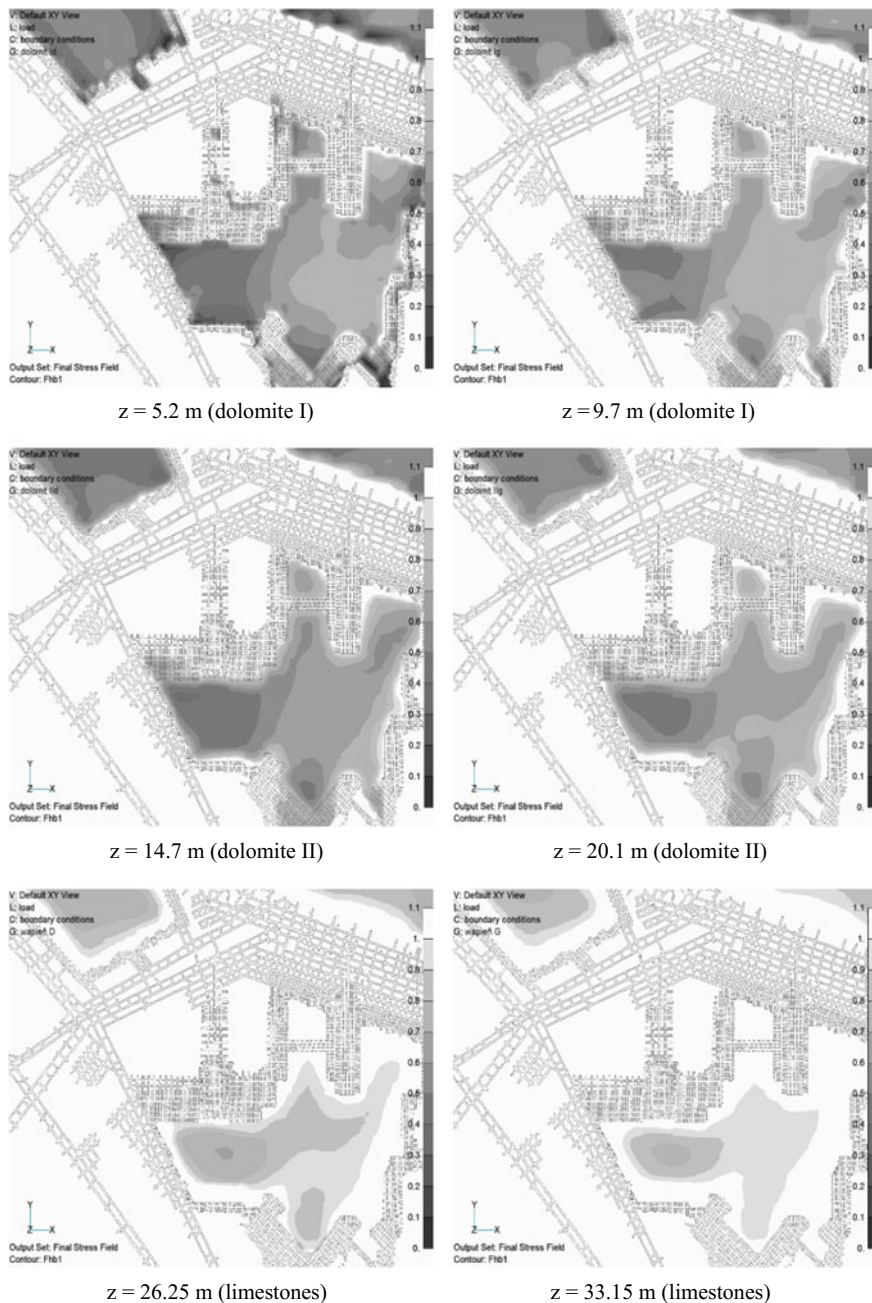
z = 5.2 m (dolomite I)   z = 9.7 m (dolomite I)

z = 14.7 m (dolomite II)   z = 20.1 m (dolomite II)

z = 26.25 m (limestones)   z = 33.15 m (limestones)

Fig. 6 Contours of calculated values of safety factor in the roof strata (event II)

z = 5.2 m (dolomite I)

z = 9.7 m (dolomite I)

z = 14.7 m (dolomite II)

z = 20.1 m (dolomite II)

z = 26.25 m (limestones)

z = 33.15 m (limestones)
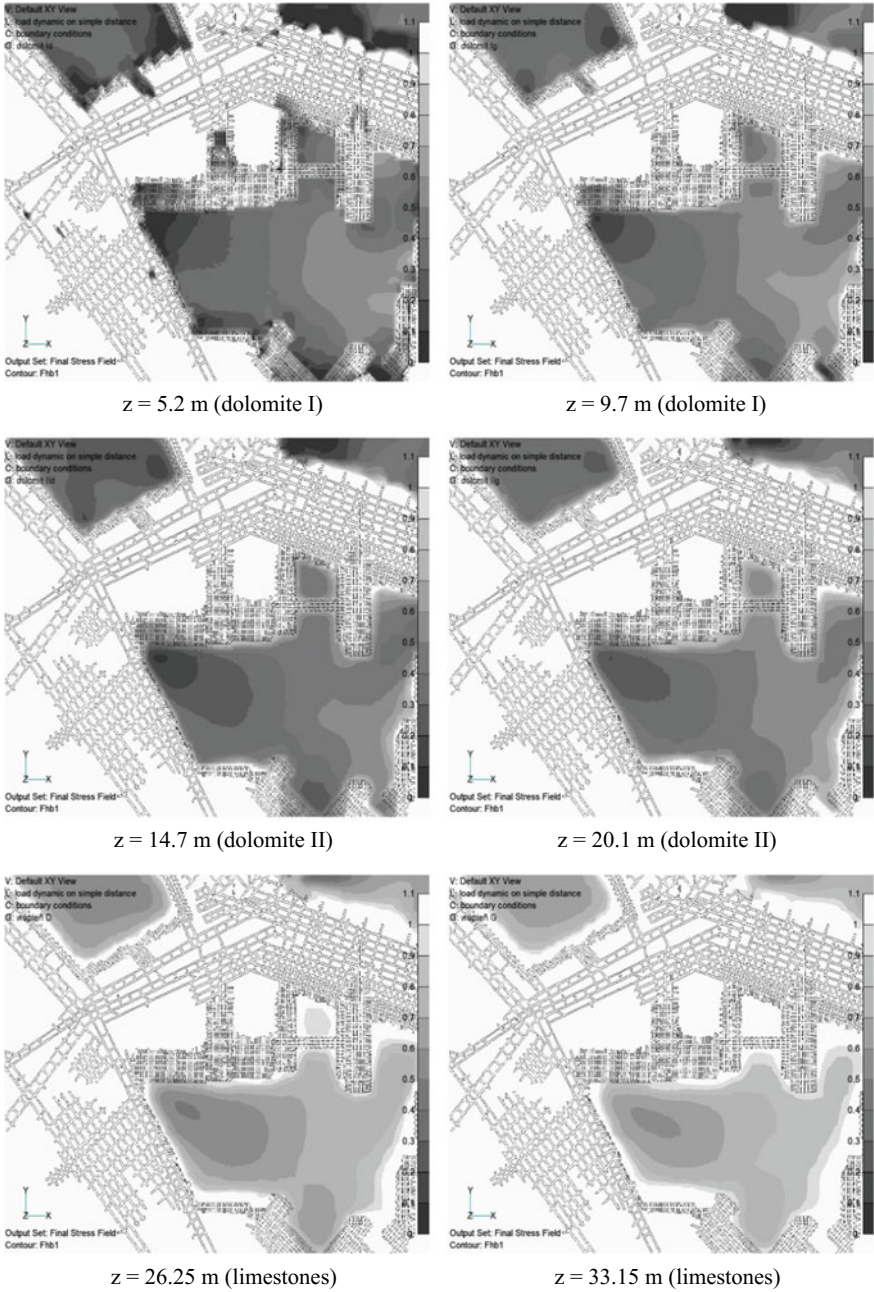
Fig. 7 Contours of calculated values of safety factor in the roof strata (event III)

4   Conclusions

The presented numerical models, based on the classic finite element method, is a very efficient 3D tool to identify areas of the main roof strata in underground mines that are weak/prone to potential seismicity and rock bursting. The numerical models were validated based on locations of known stress relief events. The knowledge about the areas in which the safety margins indicate that an instability event occurrence very likely makes it possible to verify the results obtained using the developed numerical model. The applied numerical methods have revealed themselves to be very effective in the verification of the 'primary' conditions, i.e. stress and deformations within the analysed area of the rock mass.

According to the above-presented analysis, one may conclude that the precise identification of overstressed areas is possible using these numerical tools. This method may be applied as a routine procedure while assessing rock mass behaviour, and possibly in the future as a rockburst prevention method as well.

References

1. NEi/Nastran (Version 9.2) [Computer Software]. Noran Engineering, Inc, Westminster, CA
2. Pytel, W.: Rock mass—mine workings interaction model for polish copper mine conditions. Int. J. Rock Mech. Min. Sci. **40**(4), 497–526 (2003)
3. Orlecka-Sikora, B., Pytel, W.: Integration of geomechanical and geophysical analysis methods for the prediction of seismic events in underground mining. In: Kwaśniewski, M., Łydżba, D. (eds.) Rock Mechanics for Resources, Energy and Environment, pp. 751–756. Taylor & Francis Group, London (2013)
4. Pytel, W., Pałac-Walko, B.: Geomechanical safety assessment for transverse isotropic rock mass subjected to deep mining operations. Can. Geotech. J. **52**, 1477–1489 (2015)
5. Hoek, E.: Practical rock engineering. Retrieved from https://www.rocscience.com (2007)
6. Pariseau, W.G.: Design Analysis in Rock Mechanics. Taylor and Francis, UK (2012)
7. Butra, J., Dębkowski, R., Szpak, M.: Room and pillar mining systems for polish copper orebodies. In: Proceedings of the 23rd International Symposium on Mine Planning & Equipment Selection, Johannesburg, South Africa, pp. 657–668 (2015)
8. Drzewiecki, J.: Zoning of foci of seismic tremors in division G-23, KGHM Polska Miedź S.A. J. Sustain. Min. **16**(2), 31–37 (2017)

Seismic Hazard Prediction Using Passive Seismic Tomography in Polkowice-Sieroszowice Copper Ore Mine, SW Poland

A. B. Gogolewska and D. Smolak

1 Introduction

Since the very beginning of exploitation in 1970s, seismic shocks and their effects, namely, rock bursts, have constituted the most dangerous threat to miners and equipment in underground mines excavating copper ore in the southwest part of Poland. Three copper ore mines, Polkowice-Sieroszowice mining plant, Rudna mining plant and Lubin mining plant, which belong to the KGHM Polish Copper JSC, have been using special exploitation technology to provide work safety. Therefore, such technology should include rock burst prevention methods and techniques which would recognize the hazard and monitor seismicity, mitigate, reduce or prevent the threat and finally control their effects. Miners, scientists, and industrial experts have been working on rock bursts mechanisms and technologies to improve the prevention and its effectiveness for about 50 years [2]. Prediction of the exact place, time, and strength of seismic events has always been of the utmost importance to mining operations. To-date, several preventive techniques and methods have been implemented to monitor the seismic threat in the mines; however, only one of them, i.e., the passive seismic tomography, can predict, to a certain extent, the occurrence of seismic events. Such tomography was previously applied to determine the interior structure of the Earth with the use of the velocity of P and S waves produced by earthquakes [6]. This calculation method was adapted in underground mines to recognize the places of accumulated strain, stress, and potential energy, where P wave velocity should be high and seismic anomalies positive and substantial [1, 5, 7]. Calculation of these parameters involves spontaneous (i.e. mining-induced) seismic events recorded by

A. B. Gogolewska (✉) · D. Smolak
Faculty of GeoEngineering, Mining, and Geology, Wrocław University
of Science and Technology, Wroclaw, Poland
e-mail: anna.gogolewska@pwr.edu.pl

D. Smolak
e-mail: smolakdaria@wp.pl

429

mine seismological network. To verify whether the passive seismic tomography is reliable enough to predict seismic hazard accurately, the number, energy, and location of spontaneous shocks and rock bursts were analyzed. Spontaneous seismic events which occurred in several subsequent weeks after tomographic calculations were taken into account. The location of high and low-velocity zones as well as anomaly zones was depicted in relation to the coordinates of tremors and rock bursts. One mining division in the Polkowice-Sieroszowice mine was investigated. The implementation of the seismic tomography in the division took place in 2006. The analysis of the results of tomographic calculations embraced the period of 2007–2016 years. The paper describes the methodology used for assessing the effectiveness of seismic hazard prediction. Verification encompassed 17 tomographic results with the majority correctly and accurately forecasting the location of hazardous zones.

2   Research Site and Methodology Description

The study covered the G-54 mining division of the Polkowice-Sieroszowice mine, which is located in south-western Poland, in the northern part of Lower Silesia. The mine excavates copper and silver ores within four mining areas: Sieroszowice I, Polkowice II, Radwanice Wschód (East Radwanice), and part of the Głogów Głęboki-Przemysłowy area (Deep-Industrial Glogow area) (Fig. 1). These deposits are accessible through 10 shafts with depths of 703–1219 m and exploited by 11 mining divisions and 27 exploitation fields (i.e. mine sections). The deposit depth varies from 530 to 1120 m and the exploitation thickness changes from 1.8 to 3.9 m. The prime method of operation is a one-step room-and-pillar system with roof deflection. The mine is exposed to water, gas, heat, and seismic hazards as well as to rock bursts, which pose the greatest challenge for mine services [2, 3].

2.1   Rock Burst Hazard and Prevention

Rock burst hazard in the G-54 division has always been significant. The risk factors include high strength parameters of rocks and their capacity to accumulate energy. Complicated tectonics and substantial depth of the deposit as well as the geometry of exploitation fields and gobs affect the size of the threat which is reduced by yielding the seam at the stage of deposit cutting or by group blasting works which provoke (induce) tremors (i.e., shooting-induced tremors). Such works entail blasting simultaneously as many mining faces as possible to distress rock mass and, thus decrease its seismicity [2, 3].

The seismic hazard cannot be completely eliminated. However, it is possible to partially limit it or minimize its effects by introducing preventive measures, which involves assessing the rock mass condition, combating, mitigating or limiting the hazard and evaluating the effectiveness of preventive actions. Evaluation of rock mass

Fig. 1 Location of mining areas of the Polkowice-Sieroszowice mine, Rudna mine and Lubin mine (*OG stands for mining area*)

state plays a crucial role in the threat recognition. In the Polkowice-Sieroszowice mine, the assessment and monitoring of the rock burst hazard employ mine seismology, the geological recognition, the measurements of the rock mass pressure and the underground observations. Moreover, the mine uses analytical methods, passive seismic tomography, convergence measurements, and observations of the seismoacoustic activity induced with group blasting [2, 3]. To combat the rock burst hazard, both passive and active methods are used. The former entail activities taken at the design stage (the appropriate choice of operating parameters), the organizational methods, which include limiting employees' presence in vulnerable zones and technological ones, such as strengthening the housing. The latter involves, for example, group blasting works (maximizing the number of faces shot concurrently), distressing shooting or torpedo shooting in the surrounding rocks [2].

2.2 Passive Seismic Tomography

Mine seismological networks collect information on seismic activity induced by mining operations. These data enable not only to determine epicenter location and energy of a shock but also to examine structure and properties of the rock mass through which seismic waves propagate. The seismic tomography is a non-invasive method of the object structure investigation and consists in calculating seismic wave parameters and their spatial distribution. Usually the longitudinal P wave's travel time, velocity and amplitude are measured to study the object interior [5]. In mines, the active and

the passive tomographies are adapted. The former uses human-induced vibrations triggered by mechanical impact or explosives and the latter observes mining-induced seismic activity registered by mine seismological networks. P wave velocity usually increases with increasing stress, which may be caused by clamping the gaps and pores in rocks. Thus, analyzing the velocity of seismic waves, it is possible to forecast changes of seismic hazard. Moreover, relocation of shocks with the tomographic calculations allows precise determination of their position without the in situ testing [1].

The foci of strong shocks frequently occur in areas of substantial P wave velocity and the high gradient of velocity field changes while the zones with poor seismicity are characterized by the low P wave velocity field [6]. Due to the dynamic variability of such fields, mainly in exploitation areas, they should be analyzed cyclically, following the directions of their changes in relation to the development of operational fronts [7]. The spatial distribution of the wave velocity and seismic anomaly, allows identification of seismic hazard zones and monitoring their variability in time and space [2].

2.3 Research Methodology and Data

To assess the effectiveness of the passive seismic tomography in predicting seismic hazard, the archival results of tomographic examinations and the seismic activity of the G-54 mining division in the years 2007–2016 were investigated. The key term here constitutes the word forecast, which is understood as the prediction of the place, time and strength of the seismic event, thus these three parameters were examined. The accuracy of predicting stress distribution in the rock mass by means of seismic wave velocity and seismic anomaly obtained from tomographic calculations was evaluated. The archival tomographic documentation obtained from the Mine Rock Burst Department was used to describe zones of the elevated and lowered wave velocity and seismic anomaly. The archival calculations made for a given time period related to shocks that took place in the previous calculation period, usually in two or three previous months. Comparing subsequent images of wave velocity fields in moving time windows, one can follow changes in the location of particular potentially hazardous zones. The tomographic method helps one forecast a potential seismic risk within a specified time and space, based on empirical data [4].

The interpretation of calculation results employs the rule saying that the areas with increased wave velocity in relation to the average one (averaged in a given area) are the zones of the highly strained rock mass, whereas, in places with a high-velocity gradient the release of accumulated elastic energy is extremely probable [4].

The compliance of the passive tomography results with the actual situation in the mining excavations was checked by reference to the location of the shocks that occurred in the period (after tomographic examinations) for which the prognosis was prepared. The spontaneous shocks, which occurred within 8 weeks after the day of tomographic calculations, were marked on the map. The location of the zones, the

maximum, minimum and average velocities as well as seismic anomalies were given (contours on maps).

The tomographic results allowed one to identify and verify the predicted location of the areas of the potentially highest seismic hazard. In the years 2007–2015, 22 passive tomographic tests were conducted. Since the epicenter coordinates of some shocks were not specified, only epicenter-related ones were used for the analysis. Moreover, the year 2010 (five measurements) was omitted as the mine and seismic tomography used different coordinate systems during that year. Consequently, the analysis embraced 17 tomography results. The location, number, and energy of registered spontaneous shocks were analyzed in relation to the location of seismic hazard zones predicted by seismic tomography. High and low-velocity zones of longitudinal wave as well as positive and negative seismic anomalies were investigated and described.

3 Seismic Activity in the G-54 Mining Division

Seismic activity was depicted by the number of shocks and rock bursts in particular years. The effectiveness of prediction was analyzed with the use of spontaneous shocks and rock bursts, i.e., mining-induced events (not induced deliberately). The seismic events with the energy $E \geq 10^3$ J ($E3$) were considered as shocks and those with energy $E \geq 10^5$ J ($E5$) as high-energy ones.

In years 2007–2016, there were 1544 shocks, including 245 of high-energy. In 2011 and 2012, the most shocks occurred, 331 and 300, respectively. The most high-energy events occurred in 2010 and 2013, 39 and 37, respectively. Whereas, the least number of events occurred in 2016 and 2008, 34 and 42, respectively (Fig. 2). There were 791 shocks with $E3$ energy, 598 with $E4$ energy, 186 with $E5$ energy, 44 with $E6$ energy, and 15 with $E7$ energy (Fig. 3). It can be concluded that the seismic activity was high.

The number of spontaneous and provoked shocks is presented in Fig. 4. There were 1544 seismic shocks including 1066 spontaneous ones. The lowest proportion

Fig. 2 The number of high-energy and low-energy seismic shocks in the G-54 mining division in years 2007–2016
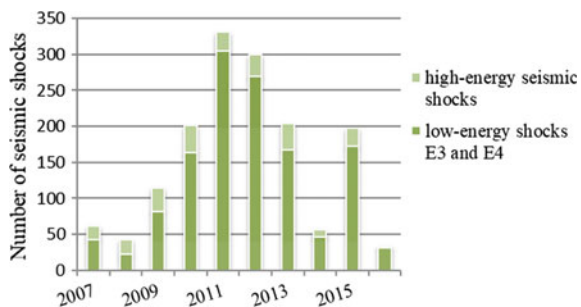
Fig. 3 The number of shocks related to particular energy classes in the G-54 mining division in years 2007–2016
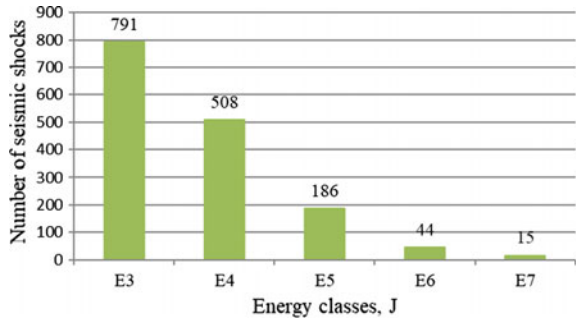
Fig. 4 The number of spontaneous (mining-induced) and provoked (shooting-induced) shocks in the G-54 mining division in years 2007–2016
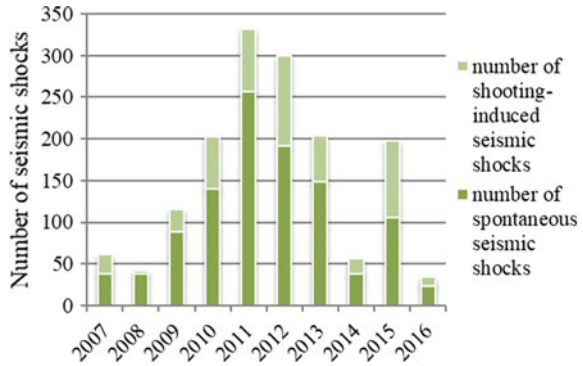
Fig. 5 The number of rock bursts in relation to spontaneous ones in the G-54 mining division in years 2007–2016
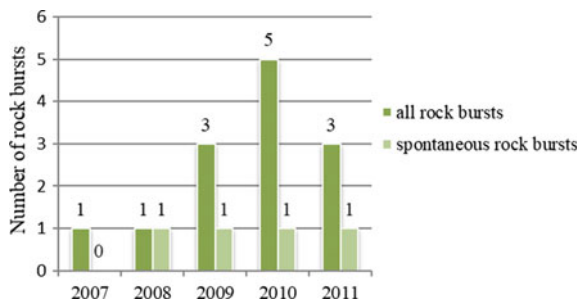
of spontaneous shocks of 53% occurred in 2015 and the highest of 90% was observed in 2008. On average 69% of spontaneous tremors were attributed to one year.

The rock bursts took place in years 2007–2011. During 5 years, there were 13 seismic events, 9 provoked, and 4 spontaneous rock bursts. In 2007, there was one provoked and no spontaneous rock bursts. The highest proportion of spontaneous rock bursts of 100% was in 2008. In 2009, there were two provoked and one spontaneous rock bursts. The greatest number of rock bursts was in 2010, five events, including one spontaneous. Two provoked and one spontaneous rock bursts occurred in 2011 (Fig. 5). The energy of 80% spontaneous rock bursts was of the order of 10^7 J and that of 20% events-of 10^5 J (Fig. 6).

Fig. 6 Energy of
spontaneous rock bursts in
the G-54 mining division in
2007–2016 period
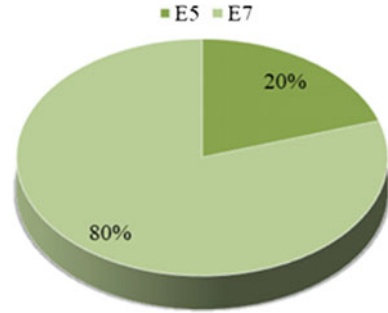
4 Effectiveness of Seismic Hazard Prediction

In 2007, in the G-54 mining division, only one study forecasting seismic activity with the use of passive seismic tomography was performed and four high-velocity zones were established and only one of them recorded shocks (exactly three). Practically, all shocks took place outside these areas. The location of 60% of observed seismic events coincided with the location of calculated high-velocity zones (Table 1). In 2009, most shocks were registered within the high-velocity zones. Unfortunately, a strong spontaneous shock of 1.6×10^7 J, resulting in a rock burst, did not occur in any of the calculated high-velocity zones. The percentage of shocks that occurred in these zones was 72%. In 2011, spontaneous shocks occurred within the determined high-velocity zones which were located along the exploitation front or near the deposit cutting and gobs. The most seismic events took place in these areas. In July, the zone of low wave velocity was distinguished where eight shocks with total energy of 1.3×10^6 J occurred. Furthermore, in November a high-energy spontaneous shock with energy of 10^7 J which resulted in a rock burst, was recorded outside the calculated high-velocity zones. The location of seismic shocks was predicted with 72% accuracy. In 2012, virtually all seismic shocks that were recorded in the zones determined by tomography referred to the most active part of the deposit. In the April survey, attention was paid to the low-velocity zone where three seismic events with a total energy of 3.4×10^4 J occurred. The effectiveness of seismic activity prediction amounted to 85%. In 2013, two tomographic examinations were performed. The high-velocity zones were located far from the places where most seismic events took place. The compatibility of the location of shocks and high-velocity zones reached 66%. In 2014, one passive tomography test was carried out. Eleven seismic spontaneous shocks occurred within three of five high-velocity zones. The shocks that took place in the zones accounted for 69% of all shocks. In 2015, two tomographic examinations were performed. Ten of forty-five shocks occurred in high-velocity zones located in areas distinguished by the highest seismic activity. In July, attention was paid to the zone of low velocities where seven seismic events with total energy of 1.9×10^5 J occurred. Therefore, the effectiveness of seismic activity prediction reached only 22% (Table 1).

Table 1 The number of spontaneous seismic shocks which occurred in high-velocity zones determined with passive seismic tomography in the G-54 mining division in 2007–2015 period

Year	Number of shocks	Number of seismic shocks in high-velocity zones	Prediction effectiveness (%)
2007	5	3	60
2009	71	51	72
2011	172	124	72
2012	164	139	85
2013	53	35	66
2014	16	11	69
2015	45	10	22
Total	526	375	71

The lowest percentage of accurately predicted shock location occurred in 2015 (22%). The prediction effectiveness in the remaining years reached more than 50% with the highest value of 85% in 2012. In years 2007–2015 the average effectiveness of seismic hazard prediction amounted to 71%.

5 Seismic Wave Velocity, Seismic Anomalies and Seismic Activity

An attempt was made to discern the relationship between seismic activity and the seismic anomaly as well as the seismic wave velocity within the zones of high seismic hazard predicted with tomography. The connection between this velocity and the number of shocks appearing in the predicted high-velocity zones was examined. The largest number of seismic shocks was observed in zones with a wave velocity of 6800 m/s. The high velocity of 6100–6800 m/s was obtained in the years 2007–2011. In the following subsequent years, these velocities did not exceed 6000 m/s, which could be caused by gradual deterioration of roof conditions or operations in the near-fault zone and disturbances in the continuity of roof layers. Therefore, all shocks recorded in the zones with velocity less than or equal to 6000 m/s occurred in years 2012–2016. In this period, the most shocks were noted in the zones where the maximum wave velocity was 5800 m/s, and slightly fewer in the zones with a velocity of 5700 m/s. In low-speed zones with velocity of 4600–5500 m/s, the number of shocks was much lower. The correlation coefficient, which amounted to 0.3, indicated a weak direct proportional relationship between the number of shocks and the maximum wave velocity.

Most seismic shocks occurred for the seismic anomaly greater than or equal to 10%, thus in places where the wave velocity was 10% higher than the average velocity in a given area. The most shocks occurred for the anomaly equal to 13 and 11%.

The occurrence of shocks in zones with the significant negative anomaly of -9 and -11% was considered unfavorable. These anomalies characterized the seismic wave low-velocity zones, where seismic events and their effects should not occur. The correlation coefficient was 0.53 and indicated a proportional relationship between the number of shocks and the seismic anomaly. The only apparent relationship was the occurrence of 95% of all shocks in zones with a positive seismic anomaly.

The relationship between the total energy of shocks and the maximum velocity of the seismic wave in the high-velocity zones was ambiguous: neither growing nor decreasing trend was noticed. The largest total energy of 1.0×10^9 J occurred at the wave velocity of 6800 m/s. Huge energies of over 1×10^8 J were also observed for the wave velocity range of 5600–6000 m/s; the smallest energy, however, for the velocity of 6200 m/s. The correlation coefficient was 0.33, which indicated a weak proportional relationship between the energy of shocks and the wave velocity in the forecast zones.

The largest total energies of 1×10^8 J were observed for the seismic anomaly of 11, 14, and 10%; the smallest ones concerned the anomaly of -12%. It was noticed that huge energy was associated with a positive anomaly. The notable exception, however, was the anomaly of -5% for which the energy was of the order of 10^7 J. Such a situation was a consequence of single shocks with huge energy. The correlation coefficient reached 0.44 and indicated a proportional relationship between the energy of shocks and the seismic anomaly in the predicted zones of elevated wave velocities.

6 Conclusions

It was found that the effectiveness of passive seismic tomography in predicting seismic hazard was relatively satisfactory, although not sufficient. More than half of the shocks were located within zones of predicted high seismic activities (high seismic longitudinal wave velocities and huge positive seismic anomalies). The significant number of shocks occurred in the vicinity of the calculated zones. Most of the rock bursts occurred in the high-velocity and positive seismic anomaly areas. Unfortunately, sometimes in the zones with the lowest negative seismic anomaly and wave velocity a large number of tremors, huge total energy, and rock bursts were noticed. The lowest annual efficiency of seismic hazard forecasting reached 22%, the highest one amounted to 85% and, in most years, the accuracy of the forecast was greater than 50%. Poor direct proportional relationship was established between the number of shocks and the maximum wave velocity as well as between the energy of shocks and the wave velocity in the predicted zones of elevated velocity. The direct proportional dependence was established between the number of shocks and the seismic anomaly as well as between the energy of shocks and the seismic anomaly in the predicted zones of elevated velocities. In the zones of positive seismic anomaly, 95% of shocks took place.

Forecasting of seismic hazard with passive seismic tomography is currently the only way, though not totally perfect, to predict, to a certain extent, the location of

sites with a potentially high seismic hazard. The analysis of the state of the rock mass and the seismic hazard should be deepened in relation to the parameters calculated by the passive seismic tomography.

References

1. Bańka, P.: Passive Seismic Tomography—Selected Problems. Silesian University of Science and Technology, Gliwice (2009) (in Polish)
2. Butra, J.: Exploitation of Copper Ore Deposit in Rock-Burst and Caving Hazards, Poland, KGHM Cuprum, pp. 154–298. Research-Development Centre, Wrocław (2010) (in Polish)
3. KGHM Polish Copper JSC: Mining Assets of KGHM Polish Copper JSC in Legnica. Glogow Copper District, Lubin (2012) (in Polish)
4. KGHM Polish Copper JSC Polkowice-Sieroszowice Mine: Data and Information from Rock Burst Department, Kaźmierzów (2007–2016) (in Polish)
5. Lurka, A.: Selected Theoretical and Practical Issues of Passive Tomography in Underground Mining, vol. 879. Research Studies of Main Institute of Mining Engineering, Katowice (2009) (in Polish)
6. Maxwell, S.C., Young, R.P.: Application of seismic tomography to induced seismicity investigations. In: Proceeding of Eurock '94, Balkema, Rotterdam (1994)
7. Mutke, G.: Assessment of rock-burst hazard in underground mines taking into account vibration parameters near the shock centers—experiences from polish mines. AGH Min. Geoeng. Q. (3/1), 439–450 (2007) (in Polish)

Modeling Permeability Filtration in Outburst Zones

R. Khojayev, R. Gabaidullin, S. Asainov and I. Filatov

1 Introduction

The process of penetration of gases through porous media has been a subject of numerous studies for more than two centuries. Theory of gases and liquids motion in a porous medium was developed by Darcy, Dupuit, Masket, Collins, Zhukovskiy, Numerov, Polubarinova-Kochina, Schelkachev and others [1–5].

Mathematical analysis of filtration is largely based on the law that was experimentally discovered by the French engineer Darcy in 1856 [6]. This law states the relations of the proportionality of filtration rate of rate (volume of a penetrant floating across the given cross-sectional area of porous media per given period of time) and the pressure gradient projected on the normal to such cross-section plane.

Let v be filtration velocity vector, k—«permeability factor», in units of area, μ—gas viscosity and p—pressure. Then, the Darcy law may be written as [6]:

$$\overline{v} = -\frac{k}{\mu} \cdot \overline{\nabla} p;$$
$$\overline{\nabla} = \overline{i} \cdot \frac{\partial}{\partial x} + \overline{j} \cdot \frac{\partial}{\partial y} + \overline{k} \cdot \frac{\partial}{\partial z} \tag{1}$$

A commonly used permeability factor unit is millidarcy (1 mD $= 10^{-11}$ cm^2). Coal stratums adjacent to mine openings usually show a permeability factor of 10^{-13}–10^{-15} cm^2.

Heavy pressure gradient reproduced in laboratories sometimes better coincide with a more complicated equation (generalized Darcy law for turbulent flow):

R. Khojayev (✉) · R. Gabaidullin · S. Asainov · I. Filatov
GeoMark Research Centre LLP, Karaganda, Kazakhstan
e-mail: director@nicgeomark.kz

$$-\overline{\nabla}p = \frac{\mu}{k} \cdot \overline{v} + \frac{\rho \cdot v}{L} \cdot \overline{v} \qquad (2)$$

where: p—specific density and L—macro-roughness factor, in units of length.

When heavy gradient pressure is present in certain structure soil matrices, then Eq. 2 or even more complicated equations showing dependency of pressure gradient on filtration rate yield more accurate results. If Eqs. 1 or 2 are linked to the equation of gas mass conservation law, the result would present the differential equation defining pressure field and filtration rates field [7].

Numerous calculated flotation rates of oil, water and gases in permeable soils in various conditions fit actually measured rates perfectly, which confirms that Darcy law or its generalization is a stable foundation for theory of filtration [6].

2   Analytical Part

As seen from the short summary given above the most acceptable is a binomial law of airflow.

$$h = R_\mathrm{T} \cdot Q^2 + r \cdot Q \qquad (3)$$

where h—pressure drop at the area of consideration, Pa; R_T—airflow resistance of turbulent flow region, N/s^2 m^8; r—airflow resistance of laminar flow region, N/s m^4; Q—air flow rate through the channel, m^3/s.

The values r and R_T are represented by characteristics of the coal bed and physics of fluid body [8]:

$$r = \frac{\mu}{k_{x,y,z}} \cdot \frac{l_{x,y,z}}{F_\varphi} \qquad (4)$$

$$R_\mathrm{T} = \frac{\rho}{L} \cdot \frac{l_{x,y,z}}{F_\varphi^2} \qquad (5)$$

where μ—dynamic factor of air viscosity, kg/s m; $k_{x,y,z}$—permeability factor, m^2; $l_{x,y,z}$—air filtration distance, m; F_f —filtration area, m^2; p—air density, kg/m^3; L—macroporosity factor, m.

In filtration researches, the porous media is considered as a network of interconnected voids of type specific to structure and texture of the media. The total volume of voids in a given soil comprises of individual voids of varying size and shape. Filtration is a process of flowing of a liquid media or gas through the system of interconnected voids. It shall be noted that penetrating media only fills certain amount of voids, called filtrating (effective) volume, rather than all voids. Effective porosity of soils, whether in relation to gases or liquids, varies widely and depends on numerous

factors. For coals, the effective porosity of voids through which gases diffuse and filtrate is 2–5% of the total volume of coal [9].

The forces of interaction of soil matrix and liquid or gas during filtration is presented as a body force [7]. Various models of permeable media are used in research of gas dynamics in coal-rock bodies. Cubic, spherical, disk-shaped, tubular and rod-shaped models are used for creation of structure of material. The review of these models may be found in [10, 11]. Permeability of media is one of the most important characteristics for the process of filtration. There are numerous theories stating dependency of geometrical structure of porous media on its permeability [12], which, in its turn, depends with effective porosity on a power-law relation.

Virgin coal is anisotropic and is subject to elastoplastic deformation. Due to compression forces, porosity and permeability of virgin coal drop according to exponential law as stratum depth increases [9]. The situation is further complicated by disturbed, fissured coal matter in face space. Thus, to achieve our purpose, we have developed and proposed a mathematical quasi-model of face space suitable for inclusion into general model of mine ventilation network.

Before proceeding to modeling of the object, it is necessary to follow up to the matter of structure of virgin coal.

As already said [13], there are two main points of view, one of which sees coal as colloid system while the other deems it a media of macromolecular structure.

Let's get to the details of the former point of view, recognizing coal as colloid system. According to this point of view, coal is recognized the three-dimensional domain of contacting molecular units—micelles—connected with each other in certain points. Micelles consist of a large number of repeated structural elements. Therefore, the process of carbonification is a change of specific content of substances with different degree of polymerization accompanied by increase of quasi-ordered regions (growth of carbon meshes, decrease of length of side chains and the like) and decrease of content of amorphous matter.

Hypothesis [14], that is the simplest one and, accordingly, the most acceptable one to the extent it corresponds with observation data, suggests that micelles' shape is close to a sphere and their size distribution is close to adopted equivalent value. Change of physical features as carbonification degree increases is explained by ongoing packing of these spheres. Fig. 1 shows the process itself. Micelles deform as elastic spheres, which, once being packed in their spherical shape, further undergo compression. The theory of destruction of spherical segment is the most appreciated and correlates with the loss of coal matter during chemical reaction of carbonification. Using the micellar model, r—radius of micelle, xr—segment height and d—diameter of the largest sphere is able to be packed without destruction of package structure.

The following dependencies of particular interest may be developed form calculations performed by authors of [14]:

Porosity P

$$P = 1 - \frac{\pi \cdot \left(1 - 9 \cdot x^2 - 3 \cdot x^3\right)}{3\sqrt{2} \cdot (1 - x)^3}, \tag{6}$$
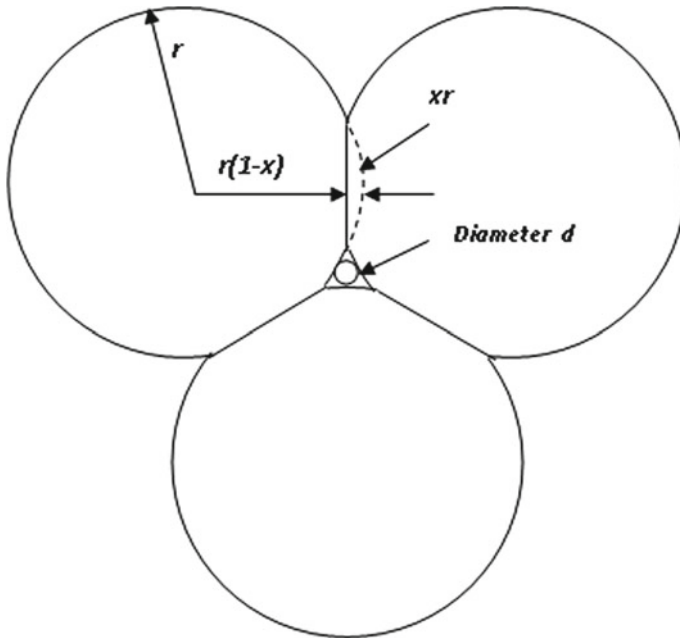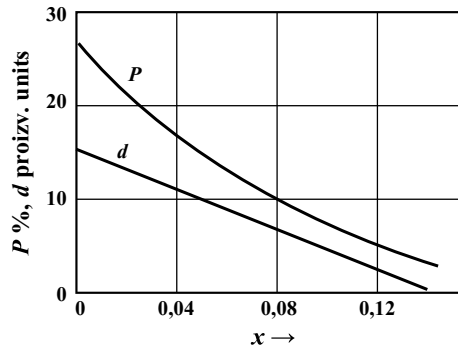
Fig. 1 Model of micellar structure of coal matter

Fig. 2 Dependence of P and d on compression

according to which the variation range is 26–0%; diameter d of the largest sphere able to fit packed structure

$$d = \frac{4}{\sqrt{3}} \cdot r \cdot (1 - x) - 2 \cdot r. \tag{7}$$

The authors calculated ratio of variables P and d and their dependence on x (Fig. 2).

Table 1 Porosity of coals of Karaganda coal basin

Coal layer designation	Porosity (cm^3/cm^3)	Coal rank
K_2	0.030	$III–IV_1$
K_3	0.029	III_3
K_7	0.046	$III_2–III_3$
K_{10}	0.079	$III_2–III_3$
K_{12}	0.082	$III_2–III_3$
K_{13}	0.056	$III_1–III_3$
K_{14}	0.061	$III_2–IV_1$
K_{18}	0.025	IV_1
D_6	0.040	$III_1–III_3$

According to findings [15], porosity of Karaganda Coal Basin coal matter varies from 0.025 to 0.082 (cm^3/cm^3) and depends on coal layer designation and coal rank (Refer to Table 1 for a summary).

Our theoretical and field research in the sphere of mines and coal beds, where outbursts are possible generally, confirm results of [15]. However, the diversity of structural elements and their arrangement in coal is a reason of presence of different size voids, which also shall be seen as structural elements of coal matter [16]; and it shall be noted that porosity in disturbed coal matter may be significantly higher than the upper limit of the range specified above.

Knowledge of distribution of voids according to their size is of particular importance in matters related to permeability and total specific internal surface area of coal matter. It is known that matters of equal porosity may have permeability variations of up to 10^4 [17] times because permeability depends on the shape and size of channels that connect individual voids.

Researchers of Skochinskiy Mining Institute have for many years been conducting researches of differential porosity of coals by impregnating samples with mercury at pressures from 2.5 to 1500 kg/cm^2. This allows obtaining information of voids with the radius from 3 μm to 50 Å.

Undisturbed coal is a monodisperse medium where more than the half of void volume is presented by micropores, and content of intermediary pores is circa 30–40%; the pore size distribution curve show single peak at micropore region. Disturbed coal (including the matter constituting face space of a mine opening) shows significant increase of sub-macropores, while the volume of individual micropores and intermediary sized pores preserves, and the share of intermediary pores decreases to 20%; the pore size distribution curve show another peak at sub-macropore region, which means that disturbed coal is a bidisperse matter (Fig. 3).
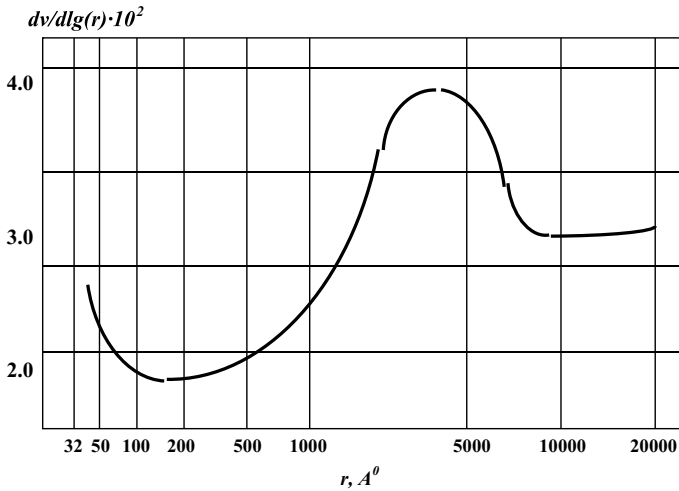
Fig. 3 Distribution of voids according to their radii in disturbed coal matter

3 Conclusions

Performed analysis revealed the average value of a pore to be used in our quasi-model of 10^4–10^5 Å, which means that filtration is of a slow, laminar type [18]. By backward transformation, the values of micellar radii (circa 10^6 Å) were determined and, consequently, diameter values required to calculate permeability and macro-roughness of the coal constituting walls of face space are being modeled.

Values of permeability and macro-roughness obtained by the use of proposed model correlate with experimental and theoretical values (permeability coefficient circa $1.5 \div 4.5 \times 10^{-14}$) [19], which confirms the applicability of quasi-model for practical use in calculations [20, 21].

References

1. Barenblatt, G.I., Entov, V.M., Ryzhikh, V.M.: Theory of the Nonstationary Filtration of Liquids and Gases, p. 208. Nedra, Moscow (1972)
2. Collins, R.: Flow of Liquids Through Porous Materials, 349 p. Mir, Moscow (1964)
3. Numerov, S.N.: To one method of calculating non-linear filtering. Problems of Applied Mathematics and Geometric Modeling, pp 27–32 (1969)
4. Polubarinova-Cochina, P.Ya.: Theory of Groundwater Movement, p 664. Nauka, Moscow (1977)
5. Shchelkachev, V.N., Lapuk, B.B.: Underground Hydraulics, p. 524. Gostoptekhizdat, Moscow (1949)
6. Aravin, V.I.: Full-Scale Filtration Research. Energia, Moscow (1969)
7. Khristianovich, S.A.: On the fundamentals of the theory of filtration. Phys. Tech. Probl. Min. **5**, 3–18 (1989)

8. Grashchenkov, N.F., Petrosyan, A.E., Frolov, M.A., and others.: In: Ushakova, K.Z. (ed.) Mine Ventilation: Directory: Handbook, p. 440. Nedra, Moscow (1988)
9. Ayruni, A.T.: Basics of Preliminary Degassing of Coal Seams at Great Depths, p. 79. Nauka, Moscow (1970)
10. Verigin N.N.: Methods for Determining the Filtration Properties of Rocks, p. 178. Gosstroyizdat, Moscow (1962)
11. Tarasov, B.G.: Forecast of Gas Content of Excavations and Degassing of Mines, p. 208. Nedra, Moscow (1973)
12. Sheidegger, A.E.: Physics of Fluid Flow Through Porous Media, p. 250. Gostoptekhizdat, Moscow (1960)
13. Rzhevsky, V.V., Novik, G.Ya.: Fundamentals of Rock Physics. Nedra, Moscow (1978)
14. Chemistry of Solid Fuel: Collection II, p. 436, translation from Eng. Ed. Karavaeva, N.M., Moscow (1951)
15. Ermekov, M.A., Ortenberg, E.S., Kalyakina, T.N.: Methane capacity of coals and coal bed methane formation of the Karaganda basin. Aerogasdynamics and aeration of coal mines. In: Proceedings of the VSTNI, vol. 19, pp. 11–15 (1973)
16. Veselovsky. V.S.: The Chemical Nature of Fossil Fuels. Publishing House of the USSR Academy of Sciences, Moscow (1955)
17. Engelhardt, V.M.: The Pore Space of Sedimentary Rocks. Nedra, Moscow (1964)
18. Khodot, V.V., Yanovskaya, F., et al.: Physicochemistry of Gas-Dynamic Phenomena in Mines. Collective Monograph, p. 140. Science, Moscow (1972)
19. Akimbekov, A.K.: Managing methane emissions in coal mine development by reducing the gas permeability of the adjacent mountain range, p. 288. Doctoral thesis, Almaty (1996)
20. Akimbekov, A.K., Emelin, P.V.: On the features of modeling gas permeability and porosity of coals of broken structure. Bull. KazNTU Alma-Ata **1**, 3–6 (2007)
21. Emelin, P.V., Khojayev, R.R., Koketayev, A.I.: Estimation of the adequacy of the quasi-analog model of the worked-out space on the basis of contour measurements of filtration flows. Ind. Kaz. **3**(42), 78–80 (2007)

Part VIII
Maintenance and Production Management for Mines and Mining Systems

Predictive Maintenance of Mining Machines—Problem of Non-Gaussian Noise

G. Żak, A. Wyłomańska and R. Zimroz

1 Introduction

Local damage detection in mining machines has been recently one of the most important fields in modern condition monitoring, [1]. It is due to the fact that efficient detection of the developing damage can lead to the significant reduction of the cost in the company.

Authors deal with the main task, namely, type of the noise present in the signal. Vibration signal can be divided into three main components:

– deterministic component,
– fault-related component (impulsive, cyclic), and
– background noise.

Of course, fault-related component will only appear when there is a fault in the machine. First, the deterministic component is considered, which is related to the kinematics of the machine. It has the highest energy from all of the mentioned components and is usually placed in the lower frequency bands. Its energy has the ability to mask the fault and, thus, it is often the object of interest to suppress this component. Generally speaking, deterministic components are signals produced by gear meshing and shaft unbalance. For instance, in case of the faulty gear (chipped or cracked tooth), the meshing will change. Everytime when the faulty tooth will be in contact with another tooth, impulse will be produced. Similarly, when there is crack in the outer or inner race, rolling element will produce impulsive behavior.

G. Żak · R. Zimroz
Diagnostics and Vibro-Acoustics Science Laboratory, Wroclaw
University of Science and Technology, Wroclaw, Poland

A. Wyłomańska (✉)
Faculty of Pure and Applied Mathematics, Hugo Steinhaus Center, Wroclaw
University of Science and Technology, Wroclaw, Poland
e-mail: agnieszka.wylomanska@pwr.edu.pl

Recent years have shown that this task is intensely investigated. [2, 3] researched the cyclo-stationary methods with modifications presented in [4, 5], while genetic algorithms for optimization of filtering are found in [6].

This paper uses methodology based on the stable distribution modeling of the time–frequency decomposed signal. Namely, for each of the extracted time series from the decomposition, authors estimate heavy-tailed dependency measures called codifference, covariation, and fractional lower order covariance. In this case, combined vectors of dependency form new lag–frequency representation, which can be analyzed in similar way as cyclostationarity maps for the detection of cyclicity in data. It is useful when the distribution of the noise is non-Gaussian [7, 8]. The remainder of the paper provides a methodology, the description of the investigated object, and the application of the methods toward real-world signal.

2 Methodology

Authors in their research have developed an approach, which is based on the analysis of the time–frequency decomposed signal. One of the most popular approaches in the literature is via Short-Time Fourier transform (STFT). This transform is defined in Eq. 1 [9]:

$$\text{STFT}(t, f) = \sum_{k=1}^{n} x[k]w(t - k)e^{\frac{2j\pi fk}{n}},$$ (1)

where $w(t - k)$ is the shifting window and $x[k]$ is the discrete signal ($i = 1, 2, …, n$). Its graphical representation, namely, spectrogram, is defined in Eq. 2.

$$\text{spec}(t, f) = |\text{STFT}(t, f)|^2.$$ (2)

In the analysis, authors use time series extracted from the absolute value of the STFT (to analyze real-valued data) called sub-signals. Sub-signals in the analysis are defined in Eq. 3.

$$S_i = |\text{STFT}(t, f_i)|, \quad i = 1, 2, \ldots, M,$$ (3)

where each f_i is given frequency bin and M is equal to $\lfloor \text{nfft} \rfloor + 1$.

Knowledge of the structure of the signal allows one to distinguish as mentioned its major components. These components can be divided into deterministic one related to the type of the work performed by the machine, and random noise which can have Gaussian or non-Gaussian distribution depending on the type of the work or events occurring in nearby environment of the machine and impulsive component present when there is a fault. Impulsive data can be modeled with the application of the non-

Gaussian distributions. One of the most interesting distributions is called α-stable distribution. This distribution is defined via its characteristic function in Eq. 4 [10]:

$$
Ee^{itX} = \begin{cases} \exp\{-\sigma^\alpha |t|^\alpha \left(1 - i\beta\,\mathrm{sgn}(t)\tan\left(\frac{\pi\alpha}{2}\right)\right) + i\mu t\}, & \alpha \neq 1 \\ \exp\{-\sigma |t|(1 + i\beta\frac{2}{\pi}\mathrm{sgn}(t)\ln(|t|)) + i\mu t\}, & \alpha = 1 \end{cases}, \quad (4)
$$

In Eq. 4, parameter α is responsible for the description of how impulsive data are. If it is equal to 2, then distribution reduces to the Gaussian one. It can be considered as a measure of impulsivity. Other parameters, namely, β, σ, and μ, are responsible for skewness, scale, and shift, respectively.

On the other hand, modeling of the heavy-tailed data comes with the disadvantage. One cannot use classical measures of the dependency. These measures are based on the assumption of finite second moment. In the above distribution, under the condition that $\alpha < 2$, there is no finite second moment. Therefore, it is necessary to introduce alternative measures of dependency.

First of these measures is called codifference. It is defined in Eq. 5 [2]:

$$
\mathrm{CD}(k) = \sqrt{\frac{n-k}{n}} \{\ln(\rho(0, -1; k)) + \ln(\rho(1, 0; k)) - \ln(\rho(1, -1; k))\}, \quad (5)
$$

where ρ is an empirical characteristic function for vector of observations $x_1, x_2, \ldots, x_n$ and it is defined in Eq. 6.

$$
\rho(u, v; k) = \begin{cases} (n-k)^{-1} \sum_{t=1}^{n-k} \exp(i(ux_{t+k} + vx_t)), & k \geq 0 \\ (n+k)^{-1} \sum_{t=1}^{n+k} \exp(i(ux_{t-k} + vx_t)), & k < 0 \end{cases}. \quad (6)
$$

Second of the considered measures is called covariation and is defined in Eq. 7:

$$
\mathrm{CV}(k) = \frac{\sum_{i=l}^{r} x_i s_{i-k}}{\sum_{i=1}^{n} |x_i|}, \quad (7)
$$

where: $l = \max(1, 1 + k)$, $r = \min(n, n + k)$, and $s_i = \mathrm{sgn}(x_i)$. However, these measures required for the data to have stability parameter higher than unity.

Last of the proposed measures is called fractional lower order covariance and it is calculated via Eq. 8 [11].

$$
R_{xx}(k) = \frac{\sum_{i=L_1+L_2}^{L_2} |x_i|^A |x_{i+k}|^B \mathrm{sgn}(x_i x_{i+k})}{L_2 - L_1}, \quad (8)
$$

where: $L_2 = \min(n, n - k)$, $L_1 = \max(0, -k)$, $0 \leq A, B \leq \alpha/2$. This measure is a generalization of the standard covariance and was developed for the analysis of the

Table 1 Bearing frequencies

Notation	Description	Value/unit
n_i	Rotational speed of the inner ring	180 RPM
n_e	Rotational speed of the outer ring	0 RPM
F_i	Rotational frequency of the inner ring	3 Hz
F_e	Rotational frequency of the outer ring	0 Hz
F_c	Rotational frequency of the rolling element and cage assembly	1.3 Hz
F_r	Rotational frequency of a rolling element about its own axis	10.6 Hz
F_{ip}	Over-rolling frequency of one point on the inner ring	30.7 Hz
F_{ep}	Over-rolling frequency of one point on the outer ring	23.3 Hz
F_{rp}	Over-rolling frequency of one point on a rolling element	21.1 Hz

heavy-tailed data. In particular cases, for specific values of parameters *A* and *B,* it can reduce to covariation or covariance. All of the proposed measures have been applied by authors to the vibration signals acquired on the copper ore crusher. Due to the regime of work performed by this machine, such signal has non-Gaussian noise and one needs to incorporate methods that detect both impulsivity and cyclicity.

3 Investigated Object

Authors in their analysis have used vibration signal from the copper ore crusher in the mineral processing plant [8]. In this type of the machine, a non-Gaussian noise is a result of ore falling down the chute of the machine and hitting internal walls. Therefore, there are multiple non-cyclic impulsive events. Thus, it is difficult to process such data with methods that are only based on the impulsivity detection. Table 1 shows characteristic frequencies. Signal was acquired with the sampling frequency equal to 25 kHz and its duration is equal to 10 s. In Fig. 1, authors show outlook of the copper ore crusher. The analyzed machine has fault on inner race of the bearing.

4 Results

In Fig. 2, top panel authors have shown time waveform of the analyzed vibration signal. It can be seen that type of the work performed by the machine produces
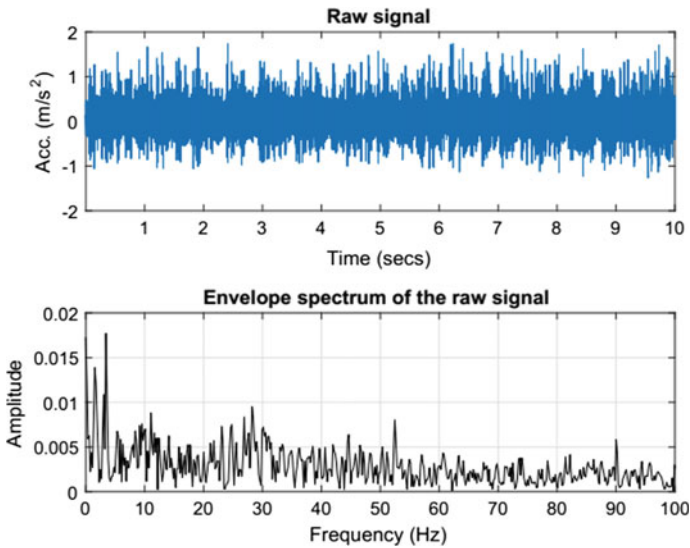
Fig. 1 Copper ore crusher

Fig. 2 Time waveform and envelope spectrum

multiple impulsive events. These events can easily disturb the effectiveness of most of modern algorithms used in local damage detection. Similarly, in an envelope spectrum, one cannot see characteristic frequency equal to 30 Hz (local damage on the bearing's inner race).
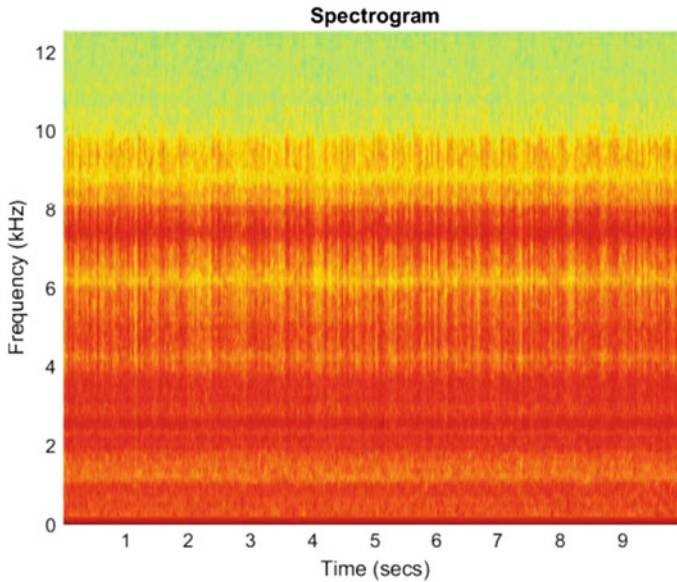
Fig. 3 Spectrogram of the signal

In Fig. 3, there is shown a spectrogram which is graphical representation of the STFT. It can be seen that impulsive noise has high energy and effectively makes it difficult to detect informative frequency band or indicators of local damage.

Applying each of the dependency measures to time–frequency decomposed signal, namely, to absolute value of time series extracted from this representation allows to track changes in the cyclicity.

In Fig. 4, authors show graphical representation of the codifference dependency map. It can be seen that there are cyclical changes in that which can be related to the impulsive component related to the fault. In Fig. 5, there is map of the covariation measure. Similarly, there are indicators of cyclicity; however, in this case, they are only visible in lower frequencies.

Last of the proposed dependency measures combines advantages of previous ones. Applying FLOC measure (see Fig. 6) to the vibration signal proved to be effective. However, to further enhance visibility of indicators, authors used local maxima method [12] (Fig. 7).

Proposed enhancement provides easy to notice vertical lines which indicate that there is a presence of cyclic, impulsive component. To identify this component, one can calculate distance (in lags) between these lines and translate this value into time. Inverse of this value will provide frequency with which these indicators occur. Another approach is similar to this when one analyzes autocorrelation graph. However, one needs to previously integrate matrix representation. Such integration is shown in Fig. 8. Calculating distance between peaks allows to determine that
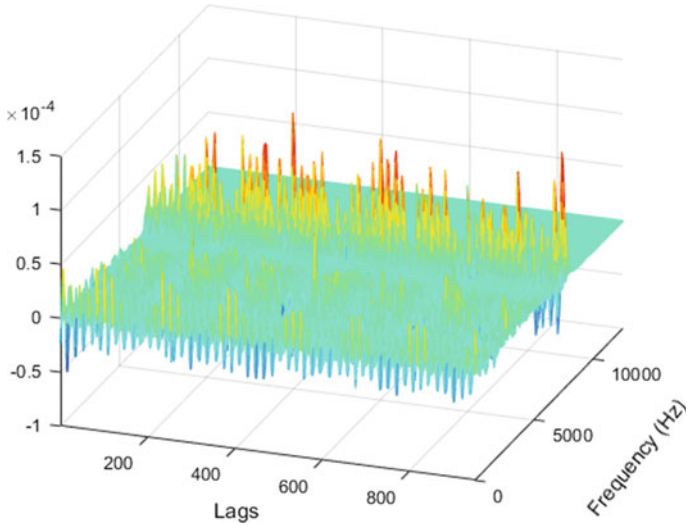
Fig. 4 Codifference map of the signal
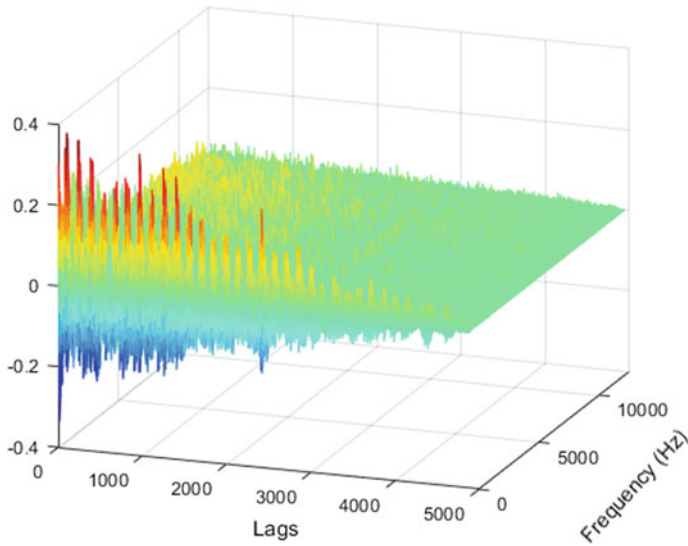
Fig. 5 Covariation map of the signal

occurrence of the fault indicators is spaced with 0.0336 s. This translates onto 30 Hz that is equal to frequency of fault.
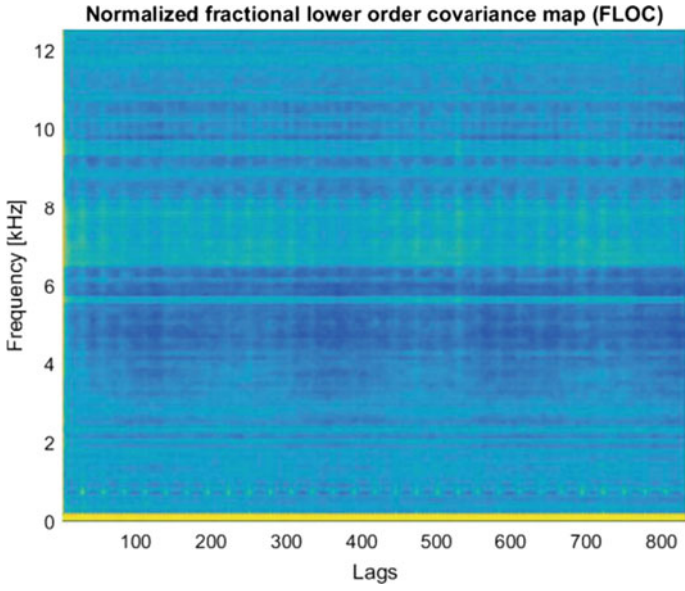
Fig. 6 Normalized FLOC dependency map
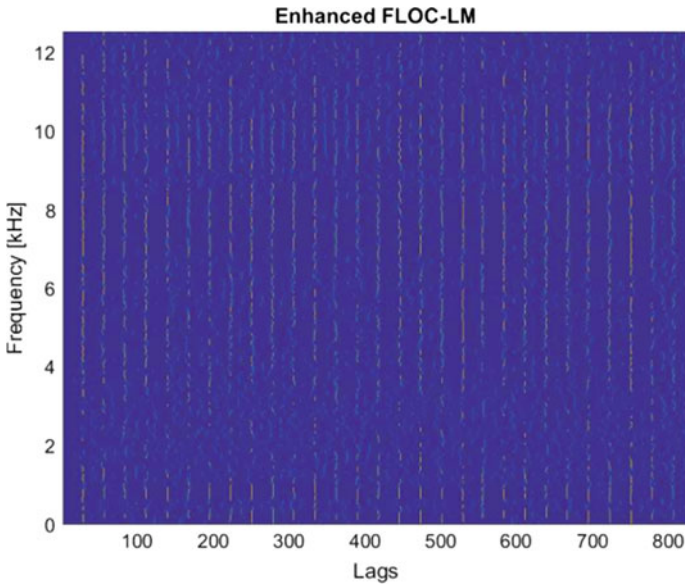
Fig. 7 Enhanced normalized FLOC dependency map
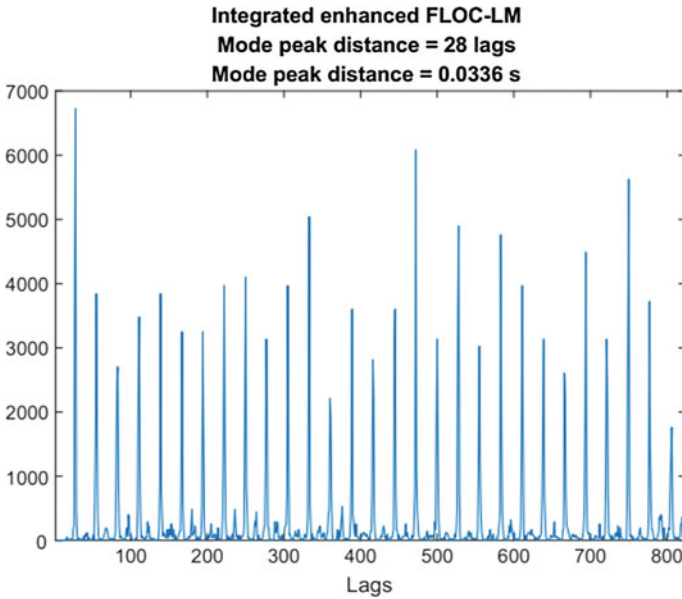
Fig. 8 Integrated enhanced normalized FLOC dependency map

5 Conclusions

In this paper, authors have summarized recently developed methods for local damage detection in the presence of non-Gaussian noise. Methods are based on the time–frequency decomposition of vibration data with usage of short-time Fourier transform. Such transform allows for the efficient energy flow tracking. However, in case of the non-Gaussian noise, these non-cyclic impulsive events make it difficult to analyze data. Thus, one needs to transform data into domain where one can investigate both cyclicity and impulsivity of the signal. Such domain could be lag–frequency one. Authors have shown that application of the heavy-tailed distribution-based dependency measures is effective in analysis of the vibration signals with non-Gaussian noise. These measures do not depend on the assumption of finite second moment and thus are more flexible in application toward industrial data. Authors have shown that application of these methods toward vibration data from the copper ore crusher is effective with ability of local damage detection in the presence of non-Gaussian noise.

References

1. Antoni, J.: The infogram: entropic evidence of the signature of repetitive transients. Mech. Syst. Signal Process. **74**, 73–94 (2016)
2. Rosadi, D.: Testing for independence in heavy-tailed time series using the codifference function. Comput. Stat. Data Anal. **53**(12), 4516–4529 (2009)
3. Antoni, J.: Cyclostationarity by examples. Mech. Syst. Signal Process. **23**(4), 987–1036 (2009)
4. Barszcz, T., Jabłoński, A.: A novel method for the optimal band selection for vibration signal demodulation and comparison with the kurtogram. Mech. Syst. Signal Process. **25**(1), 431–451 (2011)
5. Kruczek, P., et al.: Cyclic sources extraction from complex multiple-component vibration signal via periodically time varying filter. Appl. Acoust. **126**, 170–181 (2017)
6. Wodecki, J., Michalak, A., Zimroz, R.: Optimal filter design with progressive genetic algorithm for local damage detection in rolling bearings. Mech. Syst. Signal Process. **102**, 102–116 (2018)
7. Żak, G., Wyłomańska, A., Zimroz, R.: Local damage detection method based on distribution distances applied to time-frequency map of vibration signal. IEEE Trans. Ind. Appl. (2018). https://doi.org/10.1109/tia.2018.2828787
8. Wyłomańska, A., Zimroz, R., Janczura, J., Obuchowski, J.: Impulsive noise cancellation method for copper ore crusher vibration signals enhancement. IEEE Trans. Industr. Electron. **63**(9), 5612–5621 (2016)
9. Samorodnitsky, G., Taqqu, M.: Stable Non-Gaussian Random Processes. Chapman and Hall, New York (1994)
10. Ma, X., Nikias, C.L.: Joint estimation of time delay an frequency delay in impulsive noise using fractional lower order statistics. IEEE Trans. Sig. Process. **44**(11), 2669–2687 (1996)
11. Allen, J.: Short term spectral analysis, synthesis, and modification by discrete fourier transform. IEEE Trans. Acoust. Speech Signal Process. **25**(3), 235–238 (1977)
12. Obuchowski, J., Wyłomańska, A., Zimroz, R.: The local maxima method for enhancement of time-frequency map and its application to local damage detection in rotating machines. Mech. Syst. Signal Process. **46**(2), 389–405 (2014)

Predictive Maintenance of Mining Machines Using Advanced Data Analysis System Based on the Cloud Technology

P. Kruczek, N. Gomolla, J. Hebda-Sobkowicz, A. Michalak, P. Śliwiński, J. Wodecki, P. Stefaniak, A. Wyłomańska and R. Zimroz

1 Introduction

The mine production depends on the proper operation of the mining machines. Therefore, it is crucial to maintain them. The maintenance process is especially challenging in case of a vast mining transportation system as it consists of many components. In the literature, several methods for maintenance of the transportation system can be found [1–3]. For instance, in breakdown maintenance, machines operate until a failure occurs and can be used for equipment, which is not crucial to the industrial process. In this approach, detection of broken components is undertaken and the repairs are made. It is suggested to have another machine on standby in case there is a need for quick replacement. Another method is the planned preventive maintenance. In this approach, the machine is serviced after a priori fixed operational time. In this case, the condition of the equipment is not taken into account and, thus, healthy components are also replaced during the maintenance shutdown. This can generate unnecessary cost.

As the durability of the machine depends on many variables, the repair time for each component cannot be fixed in advance. Therefore, the most appropriate is a predictive maintenance [4–6]. This method provides the continuous information about

P. Kruczek (✉) · A. Michalak · J. Wodecki · P. Stefaniak · A. Wyłomańska
KGHM Cuprum Ltd, R&D Centre, Sikorskiego 2-8, 53-659 Wroclaw, Poland
e-mail: pkruczek@cuprum.wroc.pl

N. Gomolla
DMT GmbH & Co. KG, Am Technologiepark 1, 45307 Essen, Germany

P. Śliwiński
KGHM Polska Miedź, Skłodowska-Curie 48, 59-301 Lubin, Poland

J. Hebda-Sobkowicz · R. Zimroz
Faculty of Geoengineering, Mining and Geology, Wrocław University
of Science and Technology, Na Grobli 15, 50-421 Wrocław, Poland

the condition of the analysed machine and, therefore, the degradation process is observed and the repair can be planned for the most suitable period. Currently, this approach is becoming very popular in the industry application with the advancements in monitoring systems both in online and periodic acquisition forms. Today, predictive maintenance focuses on the use of data fusion to analyse data acquired simultaneously from various machines in real time. For maintenance and management purposes, it is necessary to propose such set of indicators calculated from measured time series that will enable complete and objective evaluation of objects in technical, economic and organization terms as well as estimation of their residual lifetime. On industrial scale, this type of analysis takes the form of Big Data solution. Therefore, the appropriate data analysis techniques have to be applied for data analysis.

A highly efficient cloud technology, which is based on many objects linked together into the powerful system, has been selected for the analysis. This approach is becoming popular in the industry [7, 8] and proposes to become a large-scale condition monitoring system suitable for different types of machines. Indeed, each group of machines requires their own methods and algorithms for condition monitoring.

In this paper, the most important features of the cloud technology are presented followed by examples of its application to predictive maintenance of underground transportation systems.

2 Cloud Technology—Main Features

The requirements for the predictive maintenance system for the mine are very demanding. Indeed, the environmental conditions are very harsh and mines are very complex systems consisting of many components. For instance, each type of machine needs special methods for diagnostics. In the first step, the typical workflow of the system has to be described (Fig. 1). The flow begins with an object related to the analysed industrial process (e.g. processing of the ore or the transportation of the ore) with the aim to improve such process and make it more efficient. To achieve this goal, some phenomena and quantities should be measured and acquired and, therefore, the analysed object should be equipped with proper sensors to record data. An example of such sensor might be temperatures of driving a system, a conveyor scale, an electric current consumed by electric engines of conveyors, RFID tags carrying information regarding the ore composition, vibrations of machines, pressure of the hydraulic system or fuel consumption. Subsequently, the acquired measurements are remotely transferred to the database and advanced analyses are performed. The use of data mining techniques to extract important information about the industrial processes can be made. Using such analysis, appropriate models of a process can be designed and fitted. The obtained results might be visualized in a simple and transparent way. Results would provide information about the system and give a possibility to find the steps of the industrial processes which might be improved. The variables that might be changed in order to improve performance are called 'control
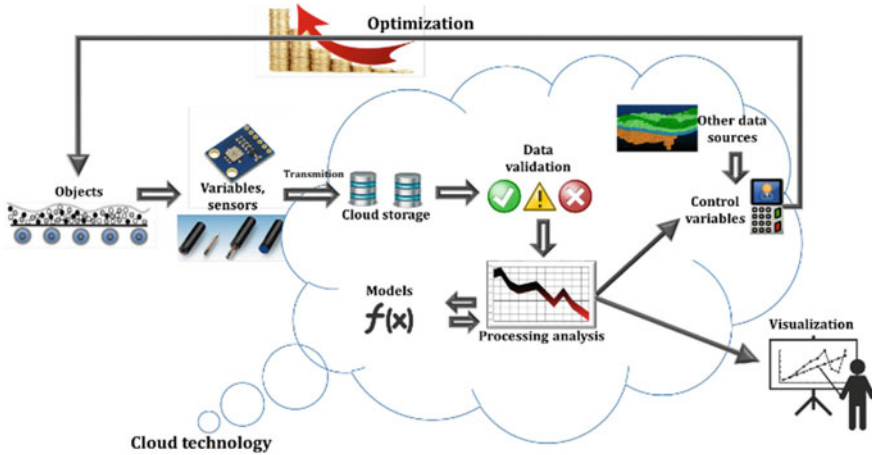
Fig. 1 The proposed system workflow

variables'. One can achieve optimization of the processes by an optimal control procedure. It can have a direct effect on the analysed object or the whole system. As a result, the improved and more efficient industrial process could be obtained.

The predictive maintenance system has to fulfil several important assumptions, including

– Compatibility. The system has to be compatible with all different types of machines and parts of infrastructure in the mine. Typically, mines consist of many different groups of machines, namely, one can consider belt conveyors, LHD machines, road headers, hoisting machines, etc. Indeed, for each type, appropriate models have to be proposed and introduced. Various phenomena are measured on the machines. For instance, in the case of belt conveyor, the temperature or electric current consumption is informative. On the other hand, for LHD machine, we are measuring fuel consumption or temperatures of engines. Therefore, one can observe that it is impossible to develop one branch of algorithms suitable for all types of machines. Therefore, a system should consist of several separated diagnostic parts to be compatible with a wide range of machines and components
– Robustness. The realization of the production plan is crucial in the proper mine operation. Therefore, the diagnostic algorithms cannot suffer any drawbacks and properly diagnose the condition of the machine. Furthermore, the environmental conditions are very harsh, and thus the appropriate sensors and systems have to be used
– Reliability and resistance to dust, humidity and other environmental elements: The complexity of the mine influences the amount of acquired data. In this case, vast datasets are considered, which contain various types of information. Certainly, this feature has to be taken into account.

Nowadays, the methods for analysing enormous data are becoming popular and deeply studied. The Big Data approach for data analysis is of high interest. A cloud approach was proposed to analyse data from various complex transportation systems. The computations are calculated online, and cloud computing approach is applied due to high volume of the data and complexity of algorithms. Cloud is a type of data storage warehouse, which can be accessed online. Physically, the data is stored on multiple servers, which are managed by their owners. Moreover, the servers are linked within a specific network. Typically, storage clouds consist of hundreds of inexpensive elements, which together add up to powerful storage and computing machines. The users pay to rent storage capacity. There are many different ways to access the cloud service, which depends on the particular cloud technology.

2.1 Data Processing

The cloud technology can reduce the cost of the data storage and increase the speed of the computation, if only the particular task can be parallelized. By using the clusters of the cloud, the analysis might be performed on huge datasets. Cloud computing gives a possibility to apply popular data mining techniques for large data using the Big Data techniques. The proposed system should deal with different types of data. Moreover, the data formats might be different for each sensor, e.g. .csv, .txt, .dat, etc. In cloud storage phase, the data is extracted and prepared for the statistical analysis. Moreover, the data might be converted to a specific file format in order to reduce the storage used by the raw files. The correctness of the data has to be validated, and the missing data has to be detected. The data is often acquired on unequal time intervals, and thus the data should be aggregated into equal time intervals. Additionally, the data from different sources should be unified. Such procedures enable the application of data fusion. Clearly, the two main stages can be specified. The first is the IT stage, which is the methodology of acquiring and storing the data while the second is the statistical stage, in which all the preprocessing and data analysing methods are implemented. Indeed, in the statistical stage, all the methods introduced in previous stages of the project have to be implemented in appropriate software, available through the cloud. The storage system architecture has to be properly designed.

2.2 Application of Cloud Technology

At this stage, we test some data mining and machine learning techniques. Our goal is to propose the models for the industrial process in order to optimize them. Obviously, the transportation system in the underground mine is highly complex process, which consists of many different elements. Thus, a lot of different models can be created. Cloud technology gives an opportunity to fit a lot of them and examine their performance. Finally, it is really important to provide the user-friendly application.
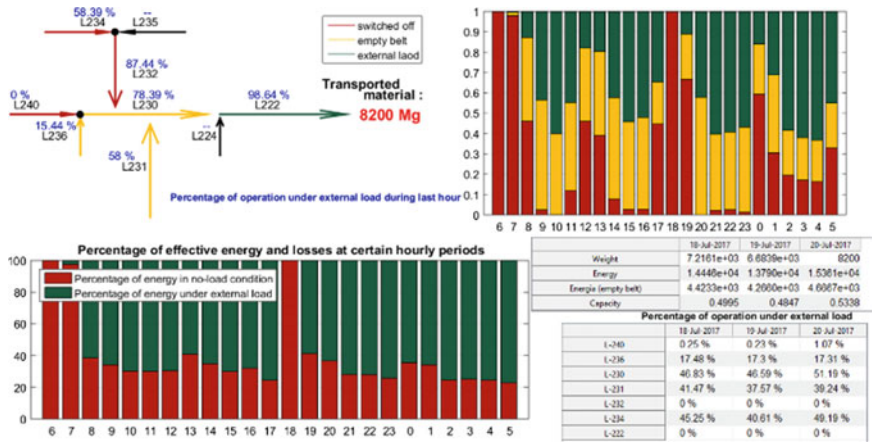
Fig. 2 Belt conveyor effectiveness analysis

Even though it would be based on advanced algorithms, the provided maintenance information has to be clear and easy to understand for all of the users. Furthermore, it is expected that this system can be used by different employees (e.g. machine operators, manager or dispatcher). Therefore, many various features should be introduced there.

3 Case Studies

In this section, case studies of the application of cloud technology are presented based on the authors' experience with the data from mining industry [9–12].

3.1 Belt Conveyors

Belt conveyors play an important role in the ore transportation system in the mine. They are used to transport the ore to the shaft. Therefore, their reliability is crucial for proper operation of the mine. It is, thus, important to use these machines in an effective way. The proper management of the belt conveyor system could influence the electric energy consumption. Thus, the appropriate tools for their effectiveness analysis are needed. In Fig. 2, the effectiveness analysis for belt conveyors is presented. The data obtained includes the weight of the transported ore provided by the scale installed on the particular belt conveyors; this information provided the amount of transported ore. Furthermore, for each belt conveyor, the operational time with external load was calculated. We are able to quantify the amount of inefficient working time.

Another important topic related to the belt conveyors is the ore tracking. In the mine, several different types of rocks can be excavated. The processing (crushing, milling and floatation) of the ore depends on its type. Therefore, there is a possibility to improve the percentage recovery of the minerals. The tracking process can be performed with RFID tags. This kind of approach has already been implemented in several mines [13, 14]. It is important to provide the appropriate system and technology for RFID tags to obtain the highly efficient method for ore tracking. Indeed, it is necessary to build the durable pellets, which are able to survive in the harsh mine conditions. Tags can be used to identify the ore portion, which is transported by particular LHD machine and dropped on the belt conveyor. Therefore, it is proposed to put them into the ore in the dumping point. Each tag possesses their unique number. Then they are read automatically by the gate reader after they are hoisted by a skip into the surface. It is worth mentioning that the preliminary test of such technology in the underground copper mine has been performed as a part of the European project [15]. Authors analyse the expected read rate and tested the writing and reading equipment. After obtaining the satisfactory and promising results, the future studies are planned.

In order to meet the mine industry expectations, the condition monitoring of the parts of transportation system should be performed. Nowadays, many informative features related to the industrial process can be monitored and according to technological opportunity, huge amounts of data can be analysed. There is a need to develop an online fault detection tool for the entire transportation system. In case of the structure, where conveyors are connected in series, the breakdown of one machine influences the whole system. Many different components of the belt conveyor can be diagnosed. One of the crucial parts is the belt, which is often damaged. Another critical component is a drivetrain, which consists of electric motors, pulleys, shafts and gearboxes. In order to perform the condition monitoring of the machine, the appropriate informative phenomena should be measured. Undoubtedly, the belt conveyors installed in the underground mine are working in the harsh conditions. One of the most informative data for damage detection is the vibration of the drive unit, measured by accelerometer [16, 17]. In case of the damage, the impulsive signal is generated. Using appropriate signal processing methods, the fault can be detected. Another informative sensor is a thermometer measuring the temperature of the gearbox or other part of the conveyor. Indeed, the temperature of the damage component should rise, what can be detected employing appropriate data mining techniques. The ammeter can be used to measure the electric current consumption of each engine. This information is also useful in case of condition monitoring. Finally, the rotational speed of the gearbox's shaft is measured. The aforementioned sensors are parts of the condition monitoring systems which are often installed on the belt conveyors. Sensors gather the huge amount of different data about industrial process. Clearly, it is beneficial to collect as much informative data as it is possible. Therefore, it has to be applied to the cloud storage approach.

An example of the damage detection for belt conveyors is shown in Fig. 3, which depicts the electric current consumption and temperature of the drivetrain for the belt conveyor. In the analysed period, the machine was broken and then it was repaired.
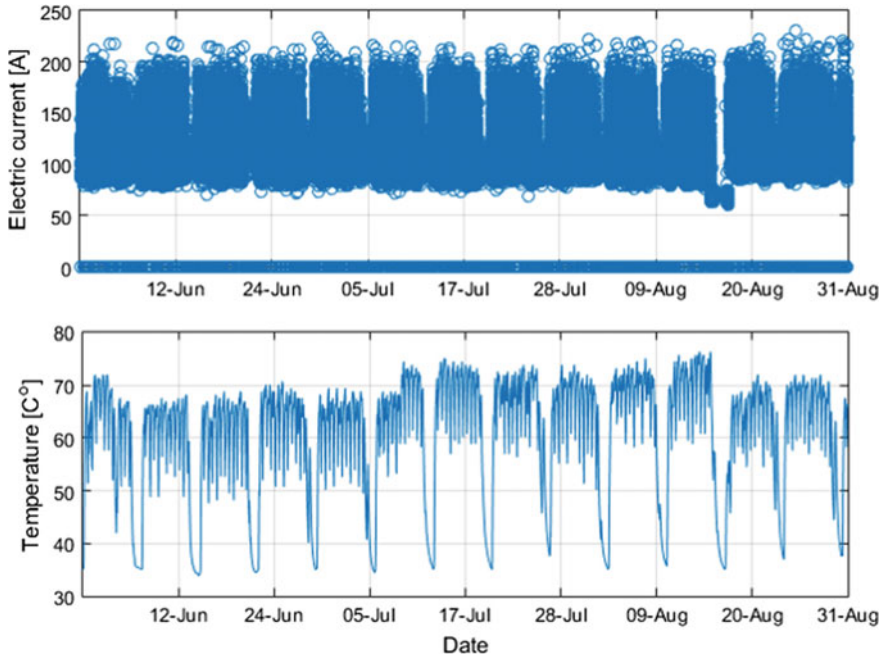
Fig. 3 The electric current and temperature recorded on the belt conveyor

The relation between the electric current and the temperature was analysed using the regression analysis. This method enabled automatic diagnoses of the period when the machine was damaged and set the threshold for the anomaly values (Fig. 4).

3.2 Load–Haul–Dump Machines

LHD machines play a crucial role in the mine. They are a part of the transportation system and are responsible for the delivery of the ore from the mining face to the dumping point. For LHD machines, there are many different variables, which are measured online. Indeed, there are measurements related to combustion engine, hydraulic of working system, drivetrain transmission, drilling, etc. In the case of the LHD machines, the acquired dataset is even bigger than for belt conveyors. For this type of machine, many variables can be informative. The gathered measurements can be used to generate different types of information. First of all, let us mention about the condition monitoring. For LHD machines, the huge investments have to be done, and thus it is expected to extend their lifetime with proper maintenance. On the other hand, we would like to omit the unnecessary repairs. Therefore, the predictive maintenance should be applied. In Fig. 5, the schematic data analysis for LHD machine is presented. The most sufficient way to detect the failure is to perform long-term
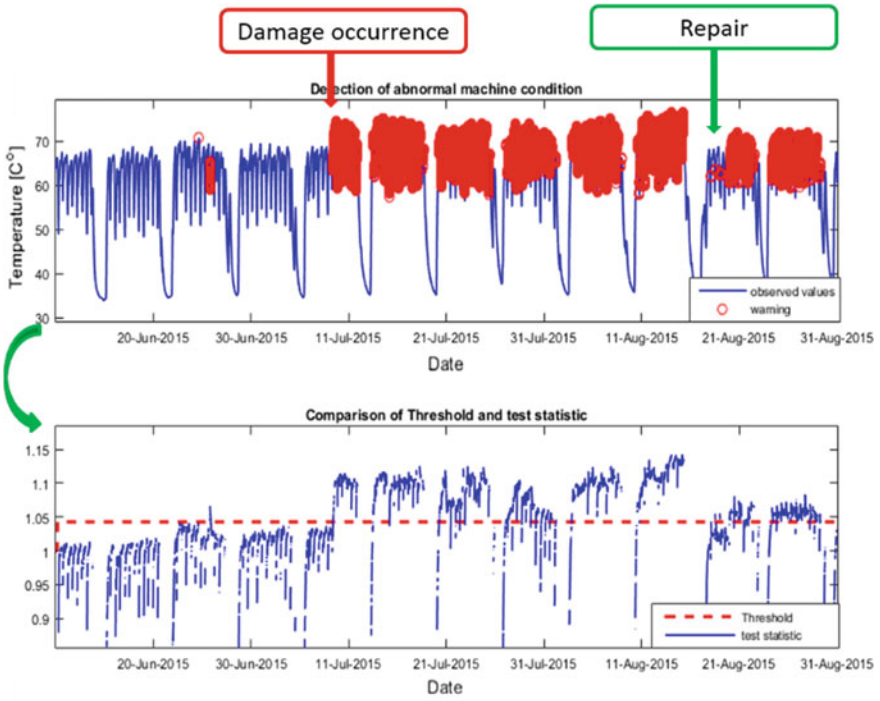
Fig. 4 The automatized indication of the damage in the belt conveyor drivetrain
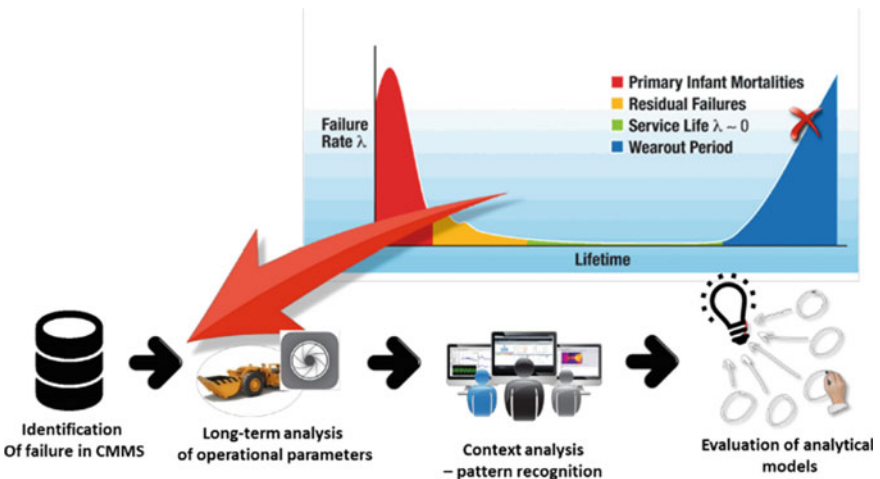
Fig. 5 Data analysis for LHD machine

analysis of operational parameters. The context analysis should be performed and the analytical model is evaluated.

As the example, we would like to illustrate one method applied to the problem of damage detection. In Fig. 6, the temperature of engine coolant is presented. The
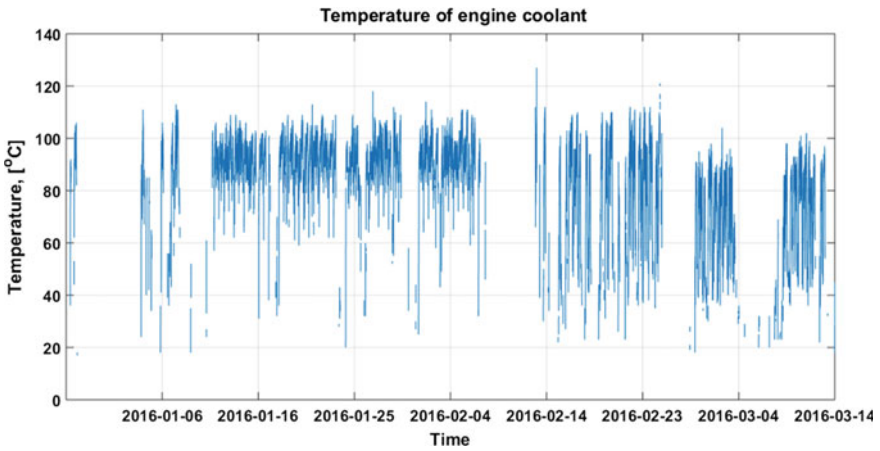
Fig. 6 Temperature of engine coolant
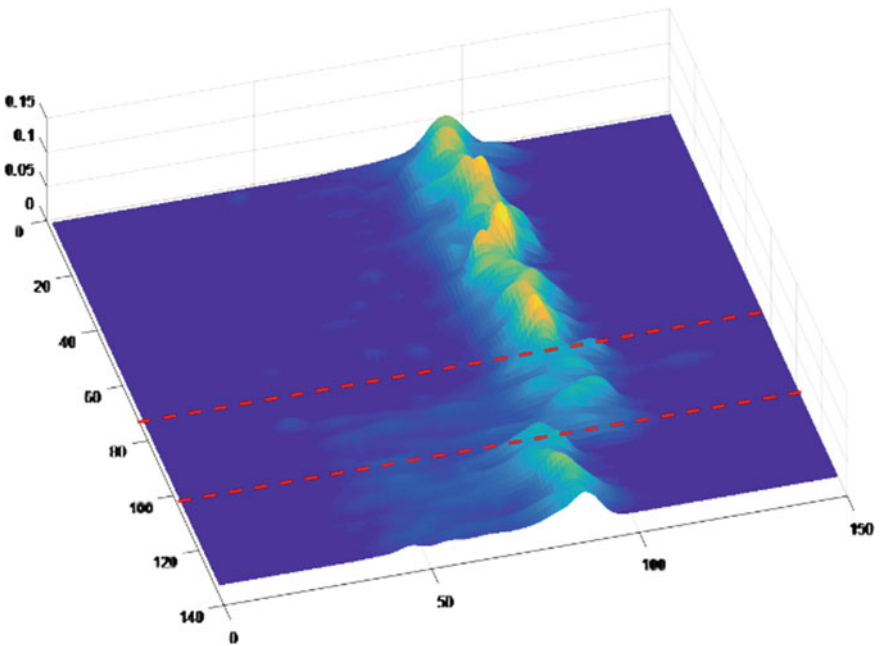
Fig. 7 Probability density function map for temperature data from particular shift [18]

signal was measured on machine operating in the underground mine. The analysed data contain the period before the damage occurs, when the machine was broken and after its repair. In this case, the main interest in the indication of machine condition changes. Therefore, algorithms that automatically detect the damage period and repair were proposed. First of all, the data was preprocessed; the heat map after the processing is presented in Fig. 7. Red lines mark the automatically indicated period, when the machine was broken [18].

The proposed system can also be used for the effectiveness analysis of the LHD machines. Indeed, the signals measured on the machine can be used to evaluate the operation of the machine. The example presented relates the number of cycles performed by the LHD machine. Figure 8 shows that the pressure signal measured at upper chamber of bucket's hydraulics can be used to separate different regimes of machine operation [19]. We are able to distinguish between the operation with empty and loaded bucket.
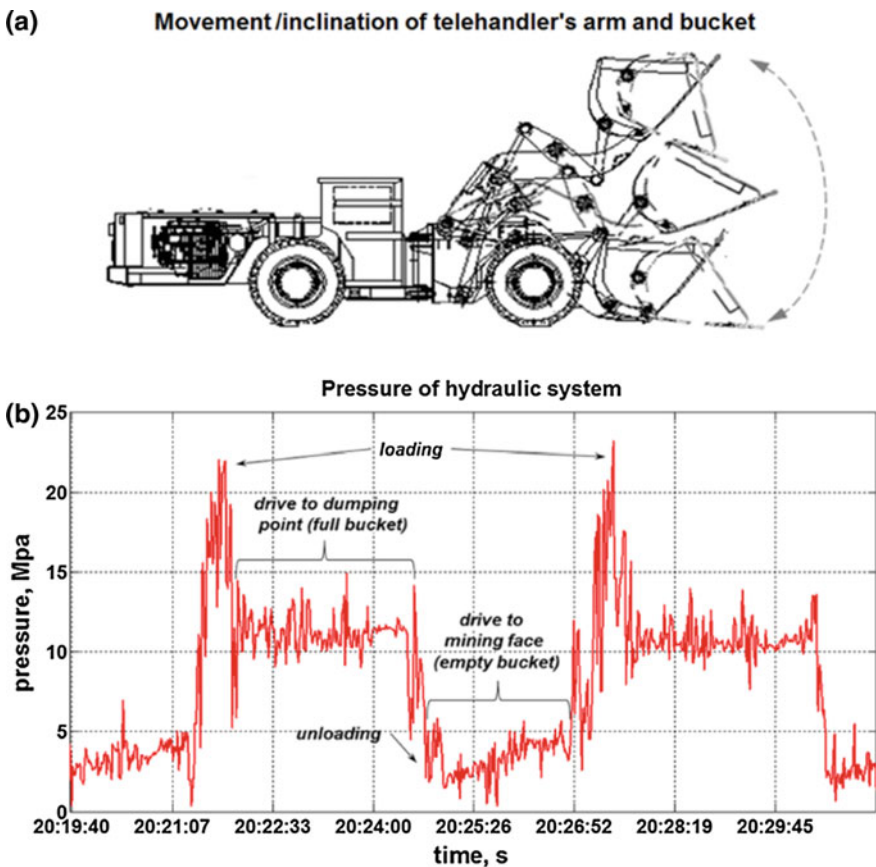
Fig. 8 The pressure signal measured at upper chamber of bucket's hydraulic cylinder [19]

4 Conclusions

The belt conveyors and LHD described in previous sections are one of the most important case studies in the mine. However, one can indicate another important mining machines. For instance, one of the most challenging issues is related to the roadheader. These types of machines are working in the varying operational conditions. The signals recorded are highly influenced by the excavation process. The most crucial component of this machine is the cutting unit. The system for condition monitoring of the cutting unit is now developed in the European project (realized by KGHM CUPRUM in consortium). It is worth mentioning that it is also expected to propose the algorithms for data analysis acquired on mining crushers and mills. Such methods could inform about their condition or evaluate their effectiveness. In case of mining machines, the data analysis is a challenging task. For instance, operational load of the crusher is varying and the related signals contain many impulses [20].

Predictive maintenance is becoming a popular method in the mine industry. The appropriate methods could improve the effectiveness of the operation and reliability of the mining machines. It will provide a possibility to plan the repair of the machine in the optimal period and will extend the lifetime of the machines. Therefore, the novel data analysis system is in development. The main assumptions for such system are its robustness and easy adaptation to many different types of machines. It is worth mentioning that the datasets acquired in the mine are enormous. Thus, the highly efficient algorithm and data analysis methods have to be applied. It is proposed to use the cloud technology. In this approach, the data is easily accessible and the cloud computing methods can be used to process the data. In the article, the main features of the system were described. Furthermore, we illustrated some important use cases (belt conveyors, LHD machines) with possible solution for condition monitoring and effectiveness analysis. The novel system can significantly influence the operation of the mine and we strongly believe that it can boost the mining industry. It is expected that mines in the future will become more atomized. It is expected that the cloud computing technologies for data fusion can highly boost mine production in the coming years. It is proposed to apply highly efficient cloud technology for data mining and analysis.

References

1. Jardine, A., Banjevic, D., Wiseman, M., Buck, S., Joseph, T.: Optimizing a mine haul truck wheel motors' condition monitoring program. Use of proportional hazards modeling. J. Qual. Maintenance Eng. **7**, 286–302 (2001)
2. Zimroz, R., Wodecki, J., Król, R., Andrzejewski, M., Sliwinski, P., Stefaniak, P.: Self-propelled mining machine monitoring system—data validation, processing and analysis. In Mine Planning and Equipment Selection, pp. 1285–1294. Springer, Cham (2014)

3. Moczulski, W., Szulim, R.: On case-based control of dynamic industrial processes with the use of fuzzy representation. Eng. Appl. Artif. Intell. **17**, 371–381 (2004)
4. Mobley, R.K.: An Introduction to Predictive Maintenance. Butterworth-Heinemann, Oxford (2002)
5. Scheffer, C., Girdhar, P.: Practical Machinery Vibration Analysis and Predictive Maintenance. Elsevier, Amsterdam (2004)
6. Garcia, M.C., Sanz-Bobi, M.A., del Pico, J.: SIMAP intelligent system for predictive maintenance: application to the health condition monitoring of a wind turbine gearbox. Comput. Ind. **57**, 552–568 (2006)
7. Ercan, T.: Effective use of cloud computing in educational institutions. Procedia Soc. Behav. Sci. **2**, 938–942 (2010)
8. Chen, M., Zhang, Y., Li, Y., Hassan, M.M., Alamri, A.: AIWAC, Affective interaction through wearable computing and cloud technology. IEEE Wireless Commun. **22**, 20–27 (2015)
9. Wyłomańska, A., Zimroz, R., Janczura, J., Obuchowski, J.: Impulsive noise cancellation method for copper ore crusher vibration signals enhancement. IEEE Trans. Ind. Electron. **63**, 5612–5621 (2016)
10. Makowski, R., Zimroz, R.: New techniques of local damage detection in machinery based on stochastic modelling using adaptive Schur filter. Appl. Acoust. **77**, 130–137 (2014)
11. Wodecki, J., Michalak, A., Zimroz, R.: Optimal filter design with progressive genetic algorithm for local damage detection in rolling bearings. Mech. Syst. Signal Process. **102**, 102–116 (2018)
12. Kruczek, P., Polak, M., Wyłomańska, A., Kawalec, W., Zimroz, R.: Application of compound Poisson process for modelling of ore flow in a belt conveyor system with cyclic loading. Int. J. Min. Reclam. Environ. 1–16 (2017). https://doi.org/10.1080/17480930.2017.1388335
13. Jansen, W., Morrison, R., Wortley, M., Rivett, T.: Tracer-based mine-mill ore tracking via process hold-ups at Northparkes mine. In: Tenth Mill Operators' Conference, Adelaide, SA (2009)
14. Rabe, J., Fouche, P., O'Neill, K.: Development of a RF tracer for use in the mining and minerals processing industry. In: The Third Southern African Conference on Base Metals (2005)
15. DISIRE Integrated Process Control Based on Distributed In-Situ Sensors into Raw Material and Energy Feedstock (2015–2017). https://www.spire2030.eu/disire
16. Kruczek, P., Obuchowski, J., Wylomanska, A., Zimroz, R.: Cyclic sources extraction from complex multiple-component vibration signal via periodically time varying filter. Appl. Acoust. **126**, 170–181 (2017)
17. Wodecki, J., Zdunek, R., Wyłomańska, A., Zimroz, R.: Local fault detection of rolling element bearing components by spectrogram clustering with semi-binary NMF. Diagnostyka **18**, 3–8 (2017)
18. Wodecki, J., Stefaniak, P., Michalak, A., Wyłomańska, A., Zimroz, R.: Technical condition change detection using Anderson–Darling statistic approach for LHD machines—engine overheating problem. Int. J. Min. Reclam. Environ. 1–9 (2017). https://doi.org/10.1080/17480930.2017.1388336
19. Stefaniak, P., Zimroz, R., Obuchowski, J., Sliwinski, P., Andrzejewski, M.: An effectiveness indicator for a mining loader based on the pressure signal measured at a bucket's hydraulic cylinder. Procedia Earth Planet Sci **15**, 797–805 (2015)
20. Obuchowski, J., Zimroz, R., Wylomanska, A.: Identification of cyclic components in presence of non-Gaussian noise—application to crusher bearings damage detection. J. VibroEng. **17**, 1242–1252 (2015)

Condition Monitoring for LHD Machines Operating in Underground Mine—Analysis of Long-Term Diagnostic Data

A. Michalak, P. Śliwiński, T. Kaniewski, J. Wodecki, P. Stefaniak, A. Wyłomańska and R. Zimroz

1 Introduction

In mining sector, maintenance is one of the most critical issues from the viewpoint of economic performance. As stated by [1], total maintenance costs in typical mining company constitute about 30–65% of all operation costs. Furthermore, maintenance together with safety and performance has the most significant impact on final productivity effectiveness. Even a single stoppage of one machine over time affects production which negatively affects total performance of the mine. Therefore, general trend can be observed toward finding methods which ensure decrease of maintenance costs and production losses. Increasing awareness of the advantages of predictive maintenance and condition monitoring is nowadays observed among global mining companies.

In this article, a load–haul–dump (LHD) machine is investigated using underground copper ore mine with room-and-pillar mining system. LHD is the main asset used in production process. Its task consists of extracting ore from active mining faces and loading of trucks or conveyor through dumping into discharge point with screen. LHD operates in very harsh mining conditions (high temperature, dust, salinity, humidity) and high time-varying load [2]. Despite their special design to withstand these difficult operating conditions, the total lifetime of LHDs is relatively short [2, 3]. In Poland, for example, LHDs in production process are used no longer than a couple of years. The most unreliable subsys-

A. Michalak (✉) · J. Wodecki · P. Stefaniak · A. Wyłomańska · R. Zimroz
KGHM Cuprum Ltd, R & D Centre, ul. Sikorskiego 2-8, 53-659 Wroclaw, Poland
e-mail: amichalak@cuprum.wroc.pl

P. Śliwiński
KGHM Polska Miedź, ul. M. Skłodowskiej-Curie 48, 59-301 Lubin, Poland

T. Kaniewski
KGHM Polska Miedź, O/ZG Lubin, ul. M. Skłodowskiej-Curie 188, 59-301 Lubin, Polska

tems are the engine and the hydraulics [4]. For this reason, monitoring system for tracking its asset performance and health as well as production performance has been developed [5–8]. Onboard monitoring system acquires various operational parameters of LHD in real time, e.g., production (drive speed, number of haulage cycle, ore weight in bucket, etc.) and operational data (torque/rotational speed of engine, temperatures/pressures of subsystems, CPU errors, etc.). Their integration and context analysis provide complete assessment in terms of technical, economic, and organizational aspects, and lead to detect irregularities in the haulage process and point to their causes [6, 9, 10]. One of the most common LHD-related issues is overheating that very often causes production interruption.

In this paper, the long-term operational data from LHD machine operating in underground mine is analyzed. The main problem is to find the moment when analyzed signals change their statistics, which corresponds to change in the technical condition [11, 12]. In typical condition monitoring system, solution of this task is based on determining a fixed limit value and indicating the moment of exceeding this value. Unfortunately, such approach is ineffective if it is applied to real data from LHD machine. Due to many various factors related to harsh operating factors, this solution is unreliable.

1.1 Copper Ore Mine

The Lubin mine is the oldest of Polish underground copper ore mines. Its construction began on January 1, 1960 and the first ton of copper ore was extracted 8 years later. Today, the mine covers an area of 158.2 km^2 and is divided into three regions: Eastern, central, and western. The current volume of annual production (in 2014) was estimated at 67.687 Gg of copper and 348 Mg of silver. Small amounts of nickel, cobalt, and molybdenum are also extracted. There are seven shafts located on four shaft sites and used for different purposes (materials and personnel transport, ore transport, spare shaft). Mining technology is based on room-and-pillar systems. The output is separated from the unmined ore deposit mainly by using the blasting technique. Copper ore is transported from mining faces to a dumping point by haul trucks or LHD machines [10], which is subsequently moved by belt conveyors to the shaft. From the shaft, skip hoists transport copper ore to the ground surface, where the ore is crushed and enriched. The extracted ore has a relatively low concentration of copper, 1.28% on average. In the Lubin-Malomice deposit, there are also deposits of high grades of silver in geological resources amounting to 55 g/Mg. The dominant lithological type of copper ore is sandstone rock (70%).

1.2   LHD Machine

Load–haul–dump machines (LHD) are currently most used assets in cyclic transport of underground mines with room-and-pillar system. Their transportation role consists of delivering ore from active mining faces to dumping points with screens. Their operation in production area may be divided into three stages. First, LHD loads blasted ore in mining face using bucket. Next step comes down to transport it to discharging point where material is dumped onto conveyor belt. Finally, machine returns to the mining faces with empty bucket. Each of these subprocesses often differs from cycle to cycle and, consequently, takes up more or less time depending on operating conditions in production area. Depending on length of haulage route, LHD machine may work alone or may operate in various configurations with haul truck. Second mode is realized if length of haulage route is longer than a value predefined for the mine. They are designed to operate in harsh mining condition (high temperature, dust, salinity, humidity) and high time-varying load. Difficult operating condition of LHDs is the main reason for their relatively short total lifetime (Fig. 1).

The economic feasibility of the LHDs is crucial in order to minimize the LHD-related expenses originating in large part from the outcomes of unexpected stoppages of operation (production losses, repair costs, etc.). Hence, those machines are carefully monitored using diagnostic data acquisition. For the type of machines regarded in this paper, every one of LHDs generates 37 separate variables of data sampled every second.

Taking into consideration records spanning several years, the amount of raw data provided for analysis is very large and difficult to handle. However, there are some difficulties with data completeness that can belong to one of several main categories, often present in industrial systems:

– local data gaps: relatively short continuous pieces of missing data, either with or without time record present at that segment;
– empty data structures: entire variables present but without any data inside data structure;
– various variable contents: different number of variables present for different machines;
– varying variable content: for a single machine data from different time periods contains different number of variables;
– unrealistic values: singular samples or segments of consecutive samples taking unreal values and have to be disregarded in the validation process;
– unrealistic behaviors: example: temperature fluctuating around 90 °C with one sample in between equal to 30 °C—impossible for the engine to cool down and heat up that quickly, but the value itself is realistic.

From the "analysis and interpretation" viewpoint, the difficulties are centered around:

– interpretation uncertainty: some of detected anomalies do not originate from the instantaneous or progressing fault, but rather from repair or other planned action;
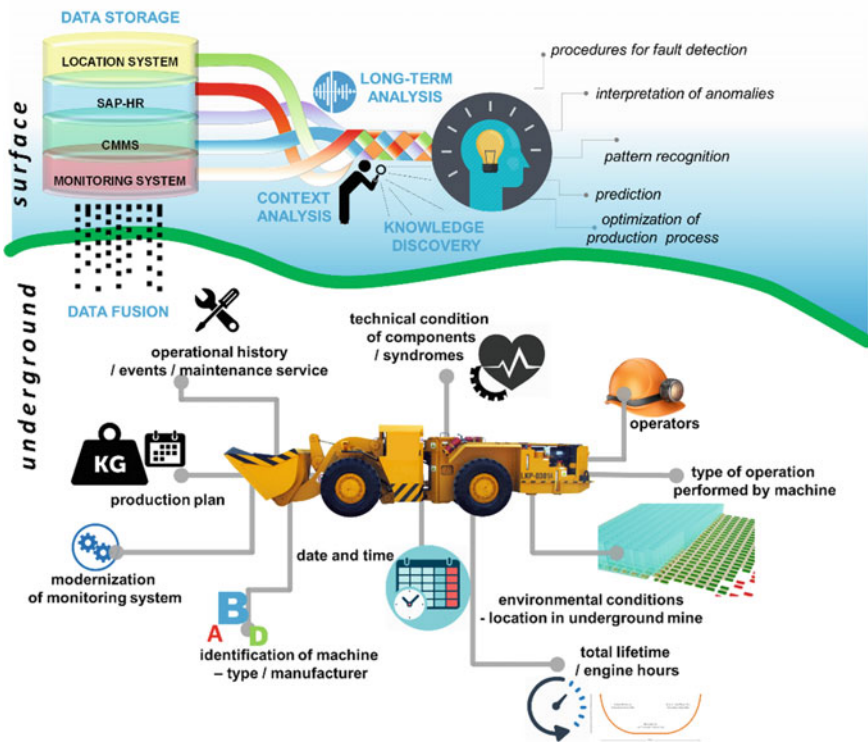
Fig. 1 Data presence regarding load–haul–dump machine

– interpretation selectivity: some of detected anomalies are present in only small percentage of expected variables;
– domain usability: all data exists in time domain, which is not optimal representation for searching anomalies.

2 Methodology

Proposed methodology contains several steps. First, the two-dimensional distribution-based map is calculated based on which the relevant variables for further analysis are selected. Next, the mean in a one-day window is calculated based on time series data. As a final step, the linear regression model is proposed in order to trend analysis in data.

2.1 Distribution-Based Exploratory Assessment

To perform exploratory evaluation of raw data, authors propose to use two-dimensional distribution-based map. Such representation allows to observe distribution-related progression, often invisible on time series plot. It is constructed as an assembly of histograms generated for nonoverlapping data ranges. Histograms are calculated using parameterization for bin width suitable for nonstationary and heavy-tailed data [13]:

$$\text{Bin width} = 2\frac{\text{IQR}(x)}{\sqrt[3]{n}},$$ (1)

where $\text{IQR}(x)$ is the interquartile range of data and n is a number of observations of x. Each histogram is normalized with respect to density integral for the distribution to scale consistently across the entire map. Therefore,

$$\text{hist}_n = \frac{\text{hist}_n}{\sum \text{hist}_n},$$ (2)

where hist_n stands for nth histogram from the map. The input data vectors are characterized with low relative data occurrence within histogram bins due to normalization. Hence, it is proposed to present the map in logarithmic scale for better visibility.

2.2 Regression

To observe the trend line, linear regression was applied. Regression analysis is a statistical technique that allows modeling the relationship between two or more variables. One-dimensional linear regression model was defined according to Eq. 3:

$$y = ax + b$$ (3)

where a is a regression coefficient and b is constant. Analyzed data contained outliers. There are two ways to improve the results of the models obtained. It is possible to remove outliers from data or use robust statistical methods. In this case, the criterion used for determining outliers was specified as $x < q0.25\,(x)$, where x is the data. The identified outliers were removed from the analysis. Subsequently, linear regression was applied using modified data.

3   Results

Figure 2 shows the selected variables acquired by built-in data acquisition system. Data comes from the period between December 1, 2015 and February 12, 2018. Data sampling period was equal to 1 s, which provided over 50 million observations per single variable. The critical values for each variable were marked with a red line.

3.1   Time Series Visual Assessment

The selected variables are plotted as time series in Fig. 2. In variables corresponding with engine temperature (ENGCOOLT and ENGOILT, which is temperature of engine coolant and temperature of engine oil, respectively), we can observe a linear trend in segments of data. Based on ENGHOURS, we have the information when the engine is working and when engine-related maintenance tasks were performed (e.g., engine replacement). In case of such task, the value of this variable is reset to 0.

On the other hand, sudden change in the variable SPEED (instantaneous vehicle speed) was observed around July 2017. However, it is not related to any changing technical condition. From the CMMS system, the information was obtained that the speed sensor was replaced; hence, different values can be observed.

3.2   Data Distribution Assessment

As the first attempt of exploratory evaluation, selected variables were transformed into two-dimensional map described in Sect. 2.1. Comparing ENGOILP (Fig. 2) with ENGOILP (Fig. 3) shows that using this new representation it is possible to observe sudden increase in data concentration within the main range of sample occurrence.

The analysis showed sudden or progressing effects, e.g., monotonic trends and changes in data distribution. In order to follow those clues, it was necessary to aggregate or otherwise downsize the sample data to smaller, more manageable form. This has been achieved by calculating sample mean of the data in one-day window (see Fig. 4). This way it became possible to perform further analysis.

3.3   Trend Analysis

Monotonic or piecewise monotonic trends were investigated, since they can be an important indication of the effects of progress in terms of technical condition of the machine. For this investigation, temperature of engine coolant (ENGCOOLT) was
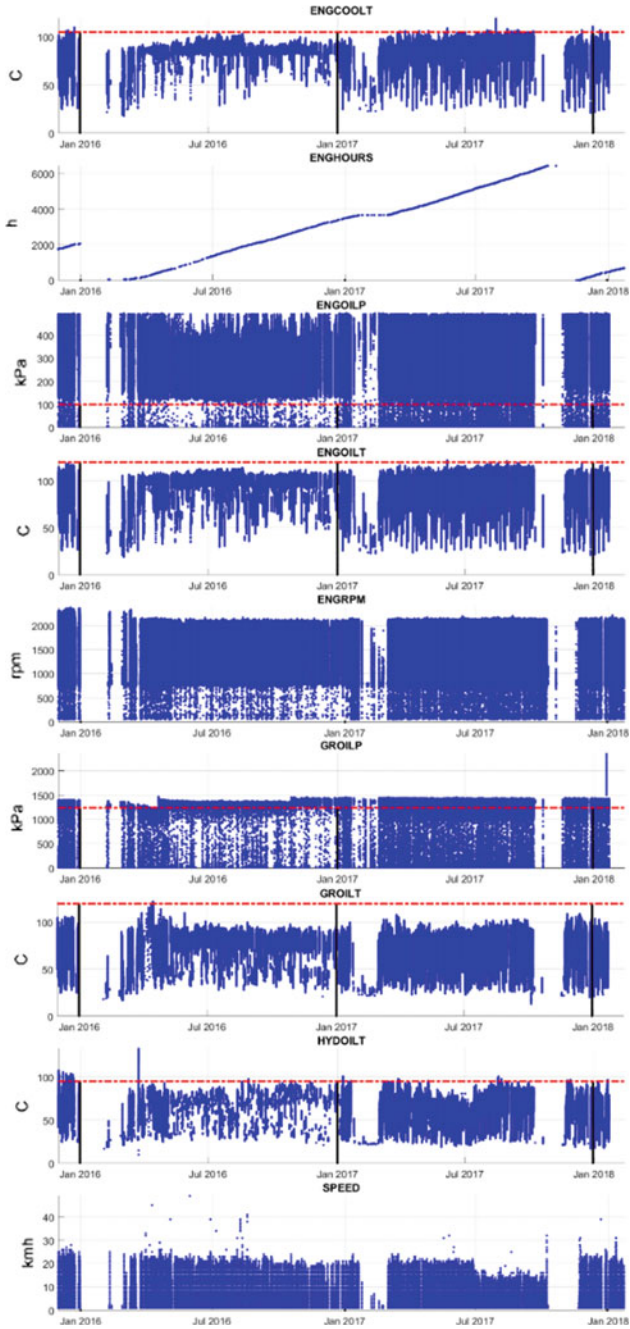
Fig. 2 Time series representation of selected variables
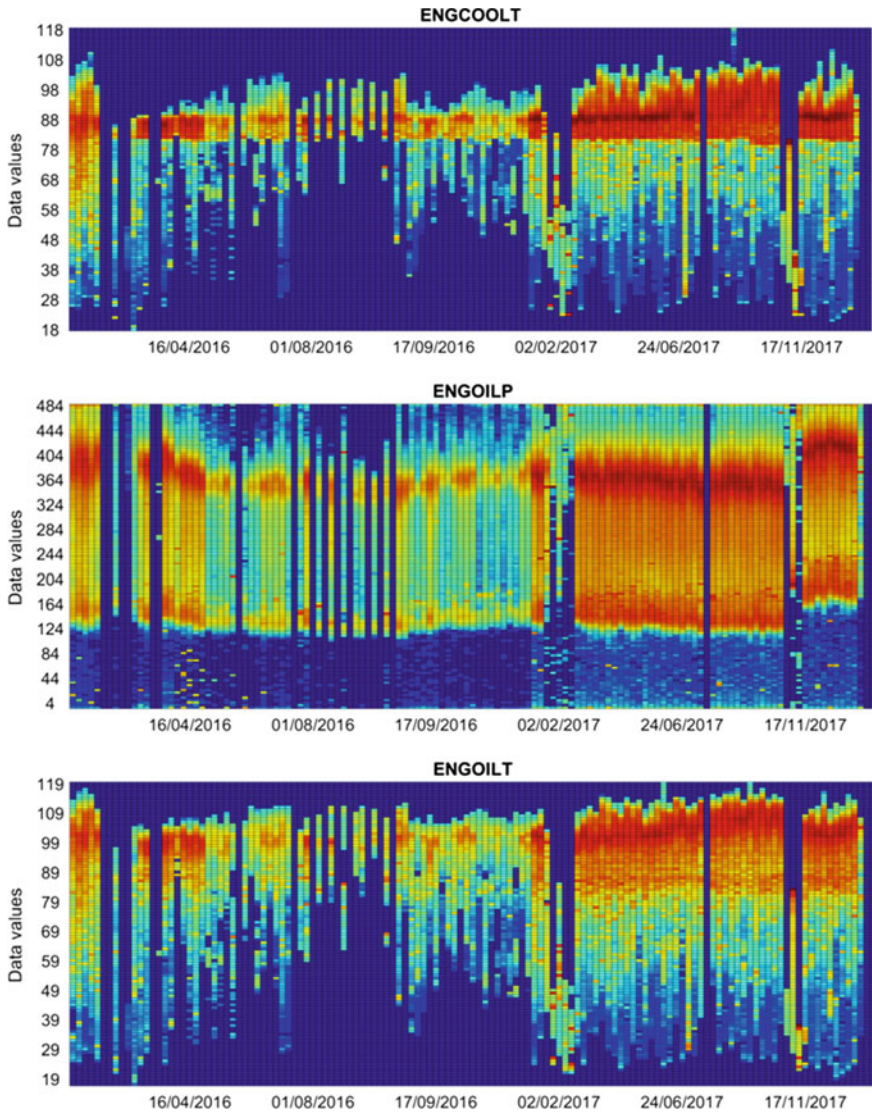
Fig. 3 Distribution-based representation of selected variables

selected as it follows piecewise monotonic increase (Fig. 2, top panel); yet, in Fig. 3 (top panel), the main distribution mode remains stable around 88° C. Piecewise linear trends were calculated based on averaged daily data. Figure 4 presents the average daily data with a linear trend (red line).

Although the trends were observed between March 22 and August 22, 2016, the regression coefficient is less than 0. Therefore, it was necessary to remove outliers
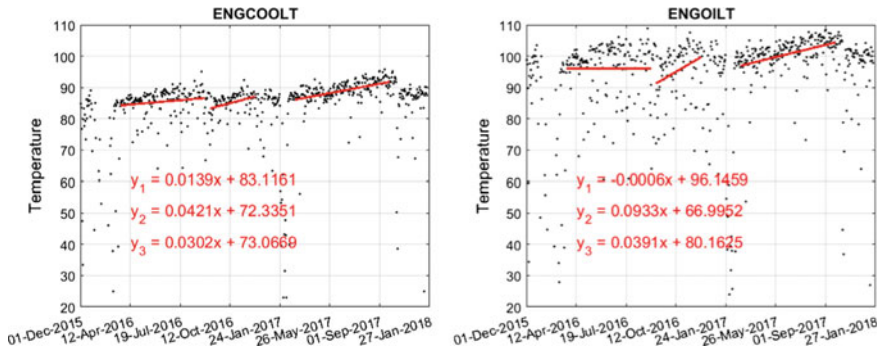
Fig. 4 Averaged daily data with linear regression
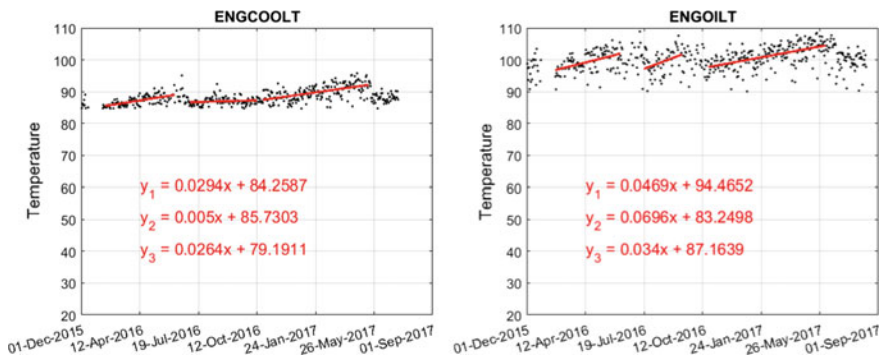
Fig. 5 Averaged daily data with linear regression, after outliers have been removed

and to estimate the regression parameters again (see Fig. 5). At points between described segments, visible decrease of values is observed, which was due to the fact that the maintenance crew cleaned the radiator of the machine's cooling system, which caused overall temperatures to drop. The end of third part corresponds to the decrease to zero value in ENGHOURS variable and increase value in ENGOILP (see Figs. 2 and 3). In addition, information from CMMS shows that in October 2017 there was a problem with the engine reported.

4 Conclusions

Monitoring systems for LHD machines are acquiring huge amount of data. Many different kinds of variables are measured (e.g., temperatures, pressure, or operational parameters). Furthermore, with the sampling frequency equal to 1 s, these data cannot be easily analyzed, let alone visualized. There is a need for some statistical tools to process the data and illustrate it in more informative way.

This paper was focused on visualizing the need for broad context analysis for such large, complex dataset, and the relation between the variables should be taken into account. To indicate the abnormality in the data, it was proposed to fit the linear regression. This tool was useful for tracking the degradation process of the machine. In this paper, several examples were illustrated. Indeed, the anomaly was detected and identified as related to the repair of the machine. However, in the future study, more sophisticated methods will be proposed.

References

1. Cutifani, M., Quinn, B., Gurgenci, H.: Increased equipment reliability, safety and availability without necessarily increasing the cost of maintenance. In: Mining Technology Conference, Freemantle, WA, pp. 10–11 (1996)
2. Gustafson, A., Schunnesson, H., Galar, D., Kumar, U.: The influence of the operating environment on manual and automated load-haul-dump machines: a fault tree analysis. Int. J. Min. Reclam. Environ. **27**, 75–87 (2013)
3. Kumar, U.: Reliability analysis of load-haul-dump machines. Ph.D. thesis, Luleå Tekniska Universitet (1990)
4. Król, R., Zimroz, R., Stolarczyk, Ł.: Failure analysis of hydraulic systems used in mining machines operating in copper ore mine kghm polska miedz sa. Min. Sci. **128**, 127 (2009)
5. Stefaniak, P., Zimroz, R., Obuchowski, J., Sliwinski, P., Andrzejewski, M.: An effectiveness indicator for a mining loader based on the pressure signal measured at a Bucket's hydraulic cylinder. Procedia Earth Planet Sci. **15**, 797–805 (2015)
6. Zimroz, R., Wodecki, J., Król, R., Andrzejewski, M., Sliwinski, P., Stefaniak, P.: Self-propelled mining machine monitoring system—data validation, processing and analysis. In: Mine Planning and Equipment Selection, pp. 1285–1294. Springer, Berlin (2014)
7. Gustafson, A., Lipsett, M., Schunnesson, H., Galar, D., Kumar, U.: Development of a Markov model for production performance optimisation. Application for semi-automatic and manual LHD machines in underground mines. Int. J. Min. Reclam. Environ. **28**, 342–355 (2014)
8. Gustafson, A., Schunnesson, H., Galar, D., Kumar, U.: Production and maintenance performance analysis: manual versus semi-automatic LHDs. J. Qual. Maintenance Eng. **19**, 74–78 (2013)
9. Laukka, A., Saari, J., Ruuska, J., Juuso, E., Lahdelma, S.: Condition-based monitoring for underground mobile machines. Int. J. Ind. Syst. Eng. **23**, 74–89 (2016)
10. Wodecki, J., Stefaniak, P., Śliwiński, P., Zimroz, R.: Multidimensional data segmentation based on blind source separation and statistical analysis. In: Advances in Condition Monitoring of Machinery in Non-Stationary Operations, pp. 353–360. Springer, Berlin (2018)
11. Sawicki, M., Zimroz, R., Wyłomańska, A., Obuchowski, J., Stefaniak, P., Żak, G.: An automatic procedure for multidimensional temperature signal analysis of a SCADA system with application to belt conveyor components. Procedia Earth Planet Sci. **15**, 781–790 (2015)
12. Wodecki, J., Stefaniak, P., Michalak, A., Wyłomańska, A., Zimroz, R.: Technical condition change detection using Anderson–Darling statistic approach for LHD machines engine overheating problem. Int. J. Min. Reclam. Environ. 1–9 (2017)
13. Freedman, D., Diaconis, P.: On the histogram as a density estimator: L2 theory. Zeitschrift für Wahrscheinlichkeitstheorie und Verwandte Gebiete **57**, 453–476 (1981)

Enhanced K-Nearest Neighbors Method Application in Case of Draglines Reliability Analysis

A. Taghizadeh Vahed, B. Ghodrati and H. Hossienie

1 Introduction

Draglines are major production equipment in surface strip mining operation. High productivity with minimum operating cost is the major goal with a reliable dragline. Thanks to new technologies and innovations, new mining machineries are more reliable than the previous one; however, the harsh mining environment does not allow the mining machineries to be as available as it is expected. Lack of proper services, maintenance, and investigation may increase the rate of failures and unavailability [1]. In this condition, the harsh environment causes unexpected breakdowns for a dragline and failure of its components as well. A failure takes place in a subsystem of a dragline that stops the whole machine operation. Therefore, prediction of failure time and failure mode in advance based on the historical data of machine assists the maintenance crews and managers to carry out the proactive actions, which eventually enhance the reliability and increase the availability of the machine.

Reliability of mining machineries has to be seriously considered, so mines can have predictive/preventive maintenance plans which carry out the maintenance program on time, which assure the availability of machineries. In order to conduct the preventive maintenance, it is vital to make an appropriate maintenance plan. In this case, predictive maintenance reveals its functionality. In the predictive maintenance, there is need to get more information and knowledge from historical data, which represents the previous status of machine such as (i) Time to Failure (TTF), (ii) Time Between Failures (TBF), (iii) Time to Repair (TTR), (iv) Time Between Repairs

A. Taghizadeh Vahed · B. Ghodrati (✉)
Division of Operation and Maintenance Engineering, Lulea University
of Technology, Luleå, Sweden
e-mail: Behzad@ltu.se

H. Hossienie
Department of Mining Engineering, Isfahan University
of Technology, Isfahan, Iran

481

(TBF), and (v) maintenance actions. Considering the historical data, it is possible to extract a pattern(s), which is called data mining procedure. Thus, extracted pattern that includes more information and knowledge will be utilized to better proactive maintenance. In conventional method, mines conduct periodic maintenance that is based on a specific period of time or amount of machine use [2, 3]. In the mentioned method, regular inspection, repair, and replacement of parts are done in specific time which is defined by the manufacturer. Therefore, the benefit of preventive maintenance is the reduced probability of equipment breakdowns and extension of equipment life [4]. On the other hand, the disadvantage of preventive maintenance is the need to interrupt production at scheduled intervals to perform the maintenance action [4]. Therefore, based on the machine condition monitoring data and its historical data, there is possibility to plan appropriate proactive maintenance. In order to make a better plan for maintenance, different types of methodologies have been utilized such as (i) Failure Mode, Effect and Criticality Analysis (FMECA), (ii) Fault Tree Analysis (FTA), (iii) Markovian Analysis (MA), and (iv) Reliability Block Diagram (RBD). Since all the named methodologies are based on the conventional linear algebra and statistical algorithms, the application of them in a domain with high volume and variety of data is impractical [5]. However, to the best of the authors' knowledge, machine learning methodologies can be applied in the historical dataset of the dragline in order to make a predictive maintenance model. The machine learning techniques are widely used in order to not only figure out the pattern(s) but also develop a predictive model. Machine learning algorithms can be utilized for fault diagnostics, fault prediction, and prognostics actions. Machine learning gives an extra hand to system health monitoring which contains (i) a set of activities performed on a system to maintain it in operable condition, (ii) maintenance data management systems, and (iii) online reliability estimation by components' degradation signal processing [6]. Therefore, machine learning methodologies can be applied in the mining industry in order to enhance the proactive maintenance. The best practice in the mining industry is based on the application of classical methodologies of reliability analysis, which measure the key performance indicators [7–12]. In the previous studies, TBF and TBR have been applied; however, more data give more chance for making better predictive model and represents more information about status of a machine.

In this study, the machine learning methodology, which is K-Nearest Neighbor (KNN) in order to make a predictor model (i.e., called predictor) for failure type prediction is used. However, based on our previous studies [13, 14], it has been recognized that the machine learning methodologies require some more practice in order to make an appropriate predictor in the case of tuned parameters and hyperparameters as well. Therefore, for enhancing the previous predictor, which was created by KNN, Genetic Algorithms (GAs) were combined with, and better result was obtained. KNNs prone to fall in the local minimum which decrease the predictor's efficiency; therefore, GAs algorithm handles the mentioned issue, and directs the parameter tuning in the way which is close to global minimum. The remaining part of this paper is divided as follows: Sect. 2 represents the background information of machine learning and the utilized methodologies; Sect. 3 includes general infor-

mation about the dragline and how enhanced-KK was implemented; and finally, in Sect. 4, conclusion and some comments are represented.

2 Methods

In this paper, machine learning techniques and algorithms have been applied regards to make a predictor/classifier. A classifier assists to make a prediction for an unlabeled vector of input. Indeed, in the topic of machine learning, there are two major subjects which are widely used: (i) supervised learning and (ii) unsupervised learning. In fact, supervised learning is called classification or regression, but unsupervised learning is called clustering. In unsupervised learning, the predictive model is going to make an algorithm based on a dataset, which does not have any label in its output data. On the other hand, supervised learning methodology uses the datasets which output data has label. Clustering and classification are also called unlabeled and labeled, respectively. The modeling procedure starts by dividing a dataset into two groups: training dataset and testing dataset. In this study, based on the best of the authors' knowledge, 70% of the dataset is used for training and remaining for testing one.

In this study, due to labeled output, a supervised learning methodology is used. KNN was utilized that is known as supervised learning when data analyzer is faced with labeled output data (the historical dataset of the dragline has labeled output, which is classifying problem).

2.1 Supervised Learning Methodology: KNN

The used methodology in this study, KNN, gets a set of n data point in d-dimensional space R^d and an integer k, and the problem is to determine a set of k points in R^d, called centers, so as to minimize the squared distance from each data point to its nearest center [15]. K-nearest neighbors algorithm finds a partition such that squared error between the empirical mean of a cluster and the points in the cluster is minimized. If μ_x be the mean of the cluster c_k, then the squared error between μ_k and the points n cluster c_k is defined as

$$J(c_k) = \sum_{x_i} \left\| x_i - \mu_k^2 \right\|. \tag{1}$$

The main goal of KNN is to minimize the sum of the squared error over all k cluster, which is defined in this study. One way to overcome the local minima is to run the KNN algorithm, for a given K, with multiple different initial partitions and choose the partition with the smallest squared error.

KNN is one of the most popular algorithms for pattern recognition. However, KNN has some limitations such as (i) computationally expensive due to utilizing all the training instants for classification, (ii) KNN's performance is dependent to the training dataset, and (iii) the data in any training dataset does not have any difference with each other. In this case, for handling the limitation of KNN and improve it, Genetic Algorithms (GAs) can be used.

2.2   Genetic Algorithms

Evolutionary computing started by adapting ideas from biological theory into computer science. Genetic algorithms are most popular technique in evolutionary computing system. Evolutionary algorithms are used in the problems for optimization such as (i) machine intelligence, (ii) traveling salesperson problem, (iii) expert system, (iv) medicine, (v) engineering application, and (vi) wired and wireless communication systems. Genetic algorithms are implemented for searching in complex, large, and multidimensional landscapes, which represents near-optimal solutions for objective or fitness function for the optimization issues.

GA encoded the parameters in the search space to form strings (i.e., called chromosomes). As a sequence, the collection of chromosomes creates population. First, a random population is created, which represents different points in the search space. An objective and fitness function is associated with each string that shows the degree of goodness of string. Regarding the survival of the fittest, a few of the strings are selected and each is assigned a number of copies that go into the mating pool. Some operation takes place on the population, for instance, crossover and mutation, which yields new generation of strings. Selection process based on crossover or mutation is continued until the termination threshold is satisfied.

Based on applied genetic operators, the local maximum fitness value is calculated and is compared with the global maximum. In this stage, if the local maximum is bigger than global one, then the global maximum is replaced with the local maximum, and the next iteration takes a place. Algorithm is developed according to the following steps:

1. Number of samples are selected which the training set is going to generate an initial population.
2. Distance between training instance in each chromosome and testing instance is evaluated.
3. Highest fitness value is selected and assigned as global maximum.

   a. For $i = 1$ to L
      i. Reproduction,
      ii. Crossover operator,
      iii. Mutation and new population,
      iv. Calculate the local maximum,
      v. If local maximum > global maximum,

        1. Global maximum $=$ local maximum

  b. Repeat

4. Final result: the chromosome which contains global maximum has the optimum KNN, and it is labeled as classification result.

The mentioned methodology was utilized in this study.

3 Case Study

In this study, enhanced KNN implemented on a dataset, which was formed based on captured data from a dragline that currently is operating in a coal mine. The utilized methods that are categorized as the classification algorithms have 1 feature and 1303 observations. Six different failure types were identified in the dataset. Table 1 presents the causes of dragline failures and failure numbers associated with each type. The input data are Time to Failure (TTF), and the output data are called types of failures. Table 2 shows the sample datasets used as input for the algorithm.

    Overburden stripping task is carried out by the draglines which are widely used in opencast coal mine. In this case, not only reliability but also availability of draglines has great effect on overall production rate of the mine. In order to increase the availability of the dragline, it is vital to focus on its major subsystem such as (i) hoisting, (ii) walking, and (iii) swing. A draglines subsystem failure causes production losses which is around one million dollar per day [16]. In order to increase the availability of a dragline, predictive maintenance can be very suitable and beneficial. Therefore, based on the historical data of the dragline's failures, a predictive maintenance model

Table 1 Causes and number of dragline failures

ID of failure type	Failure type	Failure number
1	Mechanical failure	945
2	Electrical failure	276
3	Energy-related failure	53
4	Major revision	5
5	Maintenance	14
6	Power cut	7

Table 2 Sample dataset

Mean time to failure (h)	ID of failure type
1.6597	1
3.5625	1
14.4167	2
5.5625	6
0.5938	1

Fig. 1 Methodology
flowchart
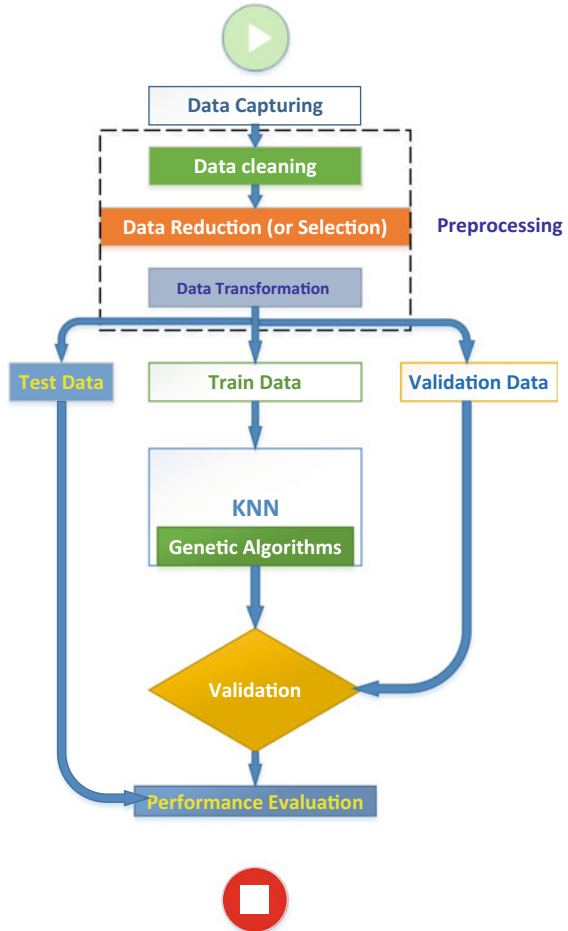
has been developed. As mentioned before, first the dataset is divided into three parts:
training dataset, validation dataset, and testing dataset, and then the enhanced KNN is
fed by training data. Due to labeled output in the training dataset, the enhanced KNN
in this study is used as classifier. In order to evaluate the accuracy of the developed
model, the testing dataset was fed to it, so the accuracy of 82% has been reached
(Fig. 1). The accuracy for the classifying the failure type in previous studies [13, 14]
was at most 72% which had been reached by the conventional method of KNN.

4   Conclusions

Draglines play a major role in the opencast mines particularly in the coal mines. In this case, availability and reliability of dragline are a vital issue that should be considered. Draglines' breakdowns lead to high operation cost (i.e., direct and indirect costs). In order to increase the dragline reliability and its availability as well, predictive maintenance strategies have to be taken into account. In this study, predictive maintenance strategy has been applied, which was tried to predict accurate failure mode in order to carry out preventive maintenance actions. Historical failure data of the dragline which is currently working in a coal mine was obtained and used for making a classifier function (i.e., the mentioned classifier can be applied for unlabeled input which predicts the failure mode). Some preprocessing tasks were carried out on the dataset, and the dataset was divided into two parts: training dataset and testing dataset. Finally, hybridized KNN (i.e., KNN has been combined with GAs) applied on the dragline's dataset, which has represented higher accuracy in contrast to other methodologies used by the author on the same dataset. Accuracy of the enhanced KNN model is 82%, which is 10% more than conventional model of KNN, which has the accuracy of 72%. As a result, a better predictor leads to regulation of better proactive maintenance strategy, so planning and scheduling of the preventive maintenance will be shaped in an appropriate manner.

References

1. Ebeling, C.E.: An Introduction to Reliability and Maintainability Engineering. Waveland Press Inc, Long Grove (2010)
2. Gits, C.: Design of maintenance concepts. Int. J. Prod. Econ. **24**(3), 217–226 (1992)
3. Herbaty, F.: Handbook of Maintenance Management Cost Effective Practices, 2nd edn. Noyes Publications, Park Ridge, NJ (1990)
4. Swanson, L.: Linking maintenance strategies to performance. Int. J. Prod. Econ. **70**, 237–244 (2001)
5. Taghizadeh Vahed, A., Demirel, N.: Application of machine learning for dragline failure prediction. In: The first International Innovative Mining Symposium (2017)
6. Dindarloo, S.R., Siami-Irdemoosa, E.: Data mining in mining engineering: results of classification and clustering of shovels failures data. Int. J. Min. Reclam. Environ. **31**(2), 105–118 (2017)
7. Vagenas, N., Runciman, N., Clément, R.S.: A methodology for maintenance analysis of mining equipment. Int. J. Surf. Min. Reclam. Environ. **11**, 33–40 (1997)
8. Samanta, B., Sarkar, B., Mukherjee, S.K.: Reliability analysis of shovel machines used in an open cast coal mine. Miner. Res. Eng. **10**, 219–231 (2001)
9. Samanta, B., Sarkar, B., Mukherjee, S.K.: Reliability assessment of hydraulic shovel system using fault trees, Institution of mining and metallurgy. Trans. A Min. Technol. **111**, A129–A135 (2002)
10. Roy, S.K., Bhattacharyya, M.M., Naikan, V.N.A.: Maintainability and reliability analysis of a fleet of shovels. Institution of mining and metallurgy. Trans. A. Min. Technol. **110**, A163–A171 (2001)
11. Hall, R.A., Daneshmend, L.K.: Reliability and maintainability models for mobile underground haulage equipment. CIM Bull. **96**, 159–165 (2013)

12. Yuriy, G., Vayenas, N.: Discrete-event simulation of mine equipment systems combined with a reliability assessment model based on genetic algorithms. Int. J. Min. Reclam. Environ. **22**, 70–83 (2008)
13. Taghizadeh Vahed, A. Demirel, N.: Classification of draglines failure type using multilayer perceptron and radial basis function. In: 25th International Mining Congress and Exhibition of Turkey, (2017)
14. Taghizadeh Vahed, A., Demirel, N.: Classification of draglines failure types by K-nearest neighbor algorithm. In: 26th International Symposium on Mine Planning and Equipment Selection (2017)
15. Kanungo, T., Mount, D.M., Netanyahu, N.S., Piatko, C.D., Silverman, R., Wu, A.Y.: An efficient k-means clustering algorithms: analysis and implementation. IEEE Trans. Pattern Anal. Mach. Intell. **24**, 881–892 (2002)
16. Townson, P.G., Murthy, D.N., Gurgenci, H.: Optimization of dragline load. In: Blischke, E.W., Murthy, D.N. (eds.) Case Studies in Reliability and Maintenance, Wiley, USA (2003)

Effect of Spare Parts Policy on Equipment Production Loss in Mining

O. Gölbaşı

1   Introduction

Maintenance cost is the most controllable operating cost in mining which requires an extensive and detailed implementation plan that ensures mining equipment to be operated with an intended efficiency and availability. However, it is generally challenging to apply the best maintenance practices in mines since many uncertainties and dependencies in the equipment mechanisms exist. In this regard, there is a common fault in the mining industry that decisions on the maintenance-related tasks are generally taken subjectively, and without any quantitative and up-to-date validation.

Spare parts inventory management is the integral part of any maintenance policy, and provides a financial balance between *in-stock* and *out-of-stock* status of spare parts. It is a must that an spare part policy should organize the procurement times of different spare part types by considering various dynamic factors such as, component failure frequencies, component criticalities, acquisition periods, potential suppliers and their locations, and classification of spare part orders. It is general in mining companies that the first batch of the required spare parts is ordered and kept available at the site prior to commissioning. Then, a specific policy on the procurement of spare parts is set for the following of operations. This procurement process may consider (i) the minimum allowable limits for spare part amounts in the inventory, (ii) regular ordering periods, (iii) irregular ordering periods, or (iv) combination of these policies. In mining, spare part policies should be specific to the equipment fleet operated in the mine, their operating and maintenance conditions, and risk appetite of the company. In this basis, any improper policy scope may lead to production losses due to unavailability of spare part when needed for maintenance. On the other hand, overstocking may cause a capital cost flow with a high rate, storage space problems, and deformed or corroded products on the shelves in

O. Gölbaşı (✉)
Department of Mining Engineering, Middle East Technical University, Ankara, Turkey
e-mail: golbasi@metu.edu.tr

time. Therefore, an optimal balance needs to be set in such a way that any additional production disruption due to unavailability of spare parts should be prevented while overstocking is minimized.

In the literature, studies on spare parts management generally focus on the policies in initial procurement, normal operation, and end-of-life phases via maximizing spare part availabilities or minimizing economic costs [1]. Sub-steps of these studies are mainly on the classification of spare parts for a proper supply system design, forecasting quantity and procurement time of orders or both of them. Although the academic researches on spare part classification and forecasting are extensively observed in the other production industries, it is quite surprising that there are very limited number of studies which evaluate the effect of spare part policies on the operations in mining. In this sense, Qarahasanlou et al. [2] applied a spare part prediction methodology for dump truck tires by including different covariates such as models of trucks, axle locations, tire technical specifications, rainfall amounts, and temperature values; Ghodrati and Kumar [3] considered operator skills, maintenance crew skills, hydraulic oil quality, climatic conditions, and physical environment as covariates when evaluating the effect of these factors to the decision on spare parts provision of wheel loader hydraulic brake systems; and Ghodrati et al. [4] performed an event tree analysis considering risk assessment to reveal the effect of changeable operating environment to spare parts decisions. They applied the methodology for the hydraulic pump of brake system of a loader fleet in an iron mine. Louit et al. [5] considered different repair rates and cost factors which include capital cost, storage cost, stock-out cost, and repair cost to find out an optimal repairable spare parts inventory policy. An application was carried out for a dozer fleet of coal mine. Martinez et al. [6] developed a joint optimization model of spare part inventory level and insurance policy with a coverage of production loss due to *out-of-stock* conditions. The proposed model was applied to mining hydraulic shovels in an open-pit copper mine. Zhang et al. [7] developed a (R, S) spare parts model for an inventory sharing strategy of multiple mines where R and S refer to the inventory review period and the order-up-to levels of spare parts, respectively.

It was observed from the literature that correlation between a spare parts policy in place and equipment availability has not been well discussed. This study presents a simulation algorithm that is capable of measuring the effect of a spare part policy to production loss. This algorithm first randomizes operating and maintenance behaviors of the system. Then, a spare part policy that simultaneously monitors the spare parts stock level is adapted into the algorithm. Decisions on the procurements and estimation of *out-of-stock* durations are evaluated in a timeline with small time increments. An application was also performed for a dragline by using site-specific data on failures, maintenance activities, spare parts stock levels, and reordering limits.

2 Spare Part Policy Model

2.1 Assumptions

The model intends to simulate the spare part policy as realistic as possible to reveal the availability drops in case that any unexpected downtime due to spare part acquisition takes place. However, it should be noted that many uncertainty factors appear in mining operations. Therefore, the simulation was performed under the following assumptions:

– Functional dependencies between system components were assumed to be series. It means that any component downtime stops the whole system.
– The system was assumed to be operated consistently except for the scheduled halts and corrective maintenance downtimes during operation hours.
– There is not any limitation on the number of maintenance crew, their task allocation, and their competencies. Therefore, no delay due to incompatibility of maintenance crew organization was assumed.
– Spare part acquisition time between spare part inventory and maintenance points was already included into repair time function. Only additional delay when performing any of preventive and corrective maintenance is the duration when a spare part is required but it is still in a delivery process.
– Minimum number of spare parts in inventory is applied as a policy at the mine site. It means that when the numbers of spare parts drop to specific numbers, a procurement process is started for restocking of the related spare parts.
– The model is simulated separately for the current spare part restocking policy and a perfect spare part policy. The word *perfect* means that the number of orders and their trigger points, i.e. the minimum number of spare parts in the inventory which initiate procurement, are properly constituted, and spare parts are always available in the inventory when needed for any maintenance.
– Uptime/downtime characterization of system components and the scheduled breaks were kept identical for both simulations. Only difference between the cases is the application of a site-specific spare part policy.

2.2 Simulation Algorithm

The developed simulation is the integration of various phases such as (1) randomizing uptime and downtime behavior of system with Monte Carlo, (2) inclusion of real-time points of the scheduled halts to the model which realizes scheduled stops, (3) setting the model into a calendar timeline, (4) evaluating *in-stock* and *out-of-stock* conditions for each spare part after the relevant maintenance activities, and (5) estimating the delays in PM, i.e., preventive maintenance, and CM, i.e., corrective maintenance, due

to any *out-of-stock* condition. The study algorithm which evaluates the additional production halts as a negative side of the applied policy can be seen in Fig. 1.

The algorithm uses the variables and constants given as follows:

i	ID of component
j	ID of downtime due to *out-of-stock* status
k	Dummy variable
t	Current simulation time
t_t	Target simulation time
Δt	Time increment
S_i	Stock level of component i at time t
D_i	Minimum number of component i in the stock which triggers reordering
TD_i	Time between reordering and *in-stock* points of component i (Monte Carlo)
TR_i	Exact *in-stock* time point of the ordered component i in timeline
O_i	Number of reordered component i
CD_{ij}	j the downtime due to *out-of-stock* status of component i
SD	Total system downtime due to *out-of-stock* status

3 Case Study

A case study was performed to examine the effectiveness of algorithm. Parameters to randomize system downtime and uptime behaviors, and unit production loss values were retrieved from a study by [8]. The target system is a dragline with a bucket capacity of 30 m^3. Weekly inspection breaks and short breaks during shift hours were taken as scheduled system halts. Following assumptions were considered in the case study:

– System components have their initial stock levels and are reordered at the specific amount limits. It means that whenever the number of spare parts for component i drops to a specific number, reordering process is triggered to acquire a specific number of spare parts.
– Although 30 different components were considered in the system defined by [8], spare part policy is introduced to only 13 of them since the others could not be split into the lowermost elements due to the lack of enough information. Therefore, the current case study will consider the effect of spare part policies of 13 components to the overall system downtime.
– Target simulation time, t_t, is taken as 17,532 h. Number of simulation is defined as 1000.
– Same system is simulated with and without a spare parts policy. By this way, the case without spare parts policy determines the system availability for the case that spare parts are always available in the inventory when necessary. This case type is called *perfect spare part policy* in the study.
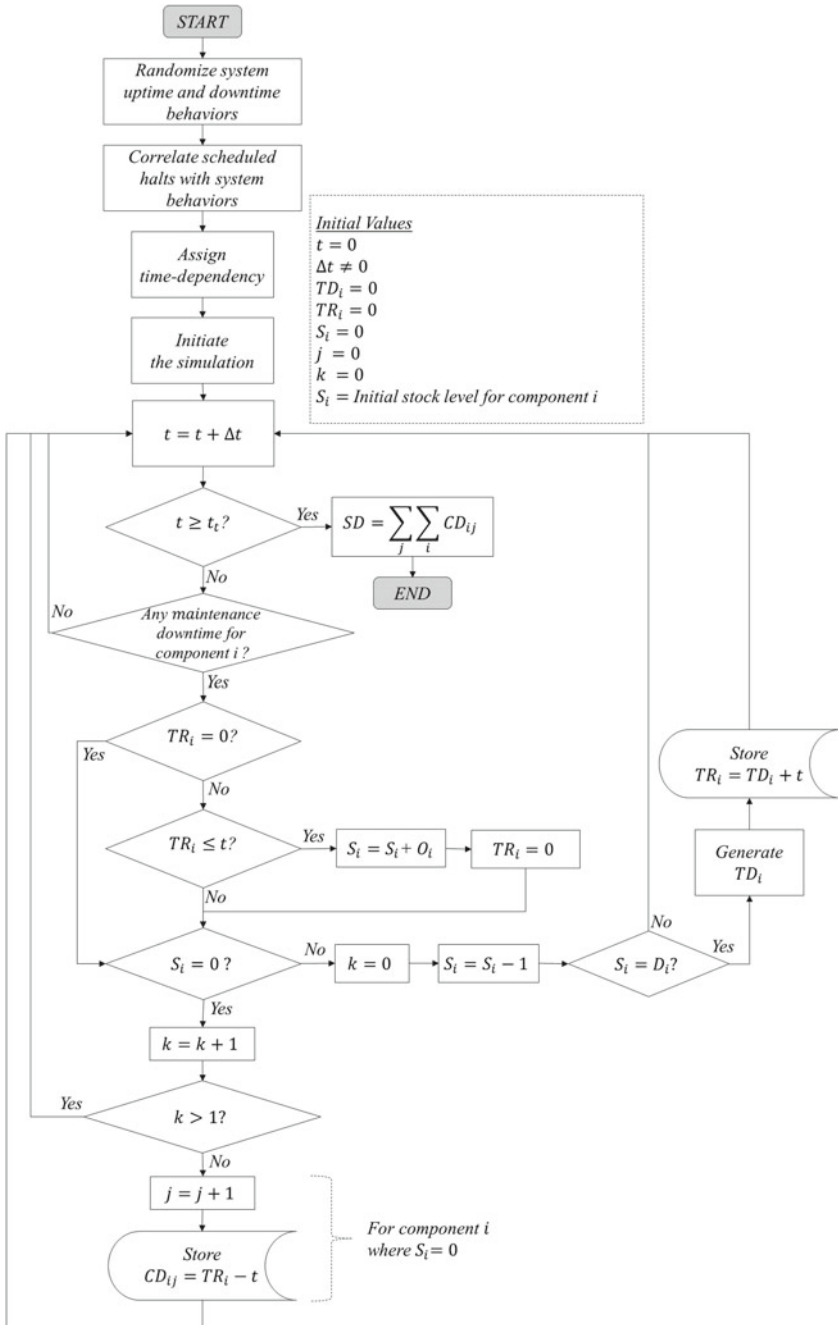
Fig. 1 The study algorithm which investigates the contribution of *out-of-stock* status of the component *i* to the overall system downtime
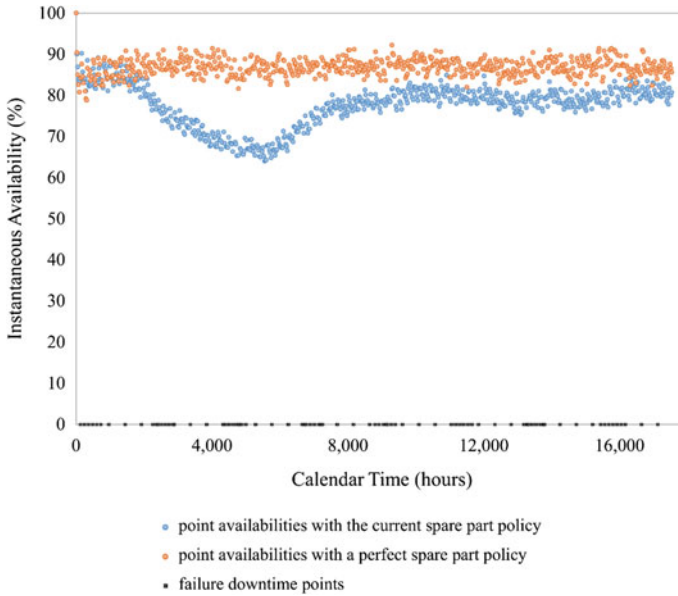
Fig. 2 Instantaneous availability values of two cases for $t_t = 17,532$ h (2 years)

Simulation results for these two different cases can be seen in Figs. 2 and 3. Figure 2 illustrates instantaneous availability values for a period of 17,532 h where the average availabilities of draglines for the given period are shown in Fig. 3.

The results revealed that an increase of 8.34% can be obtained in the system availability if a more appropriate spare parts policy is applied at the mine site. In addition, Table 1 shows the initial stock level, reordering trigger number, average stock number of spare parts in the inventory for 17,532 h, and spare parts used for maintenance in the defined period. Reordering trigger numbers are the minimum numbers of spare parts in the inventory which initiate reordering process. Besides, these numbers and reordered numbers are the same for this case. The component codes given in the table can be examined in [8]. It should be noted that simulation results may variate if the other components, maintenance crew policy, different administration delays, or any other operational factor are included in the algorithm.
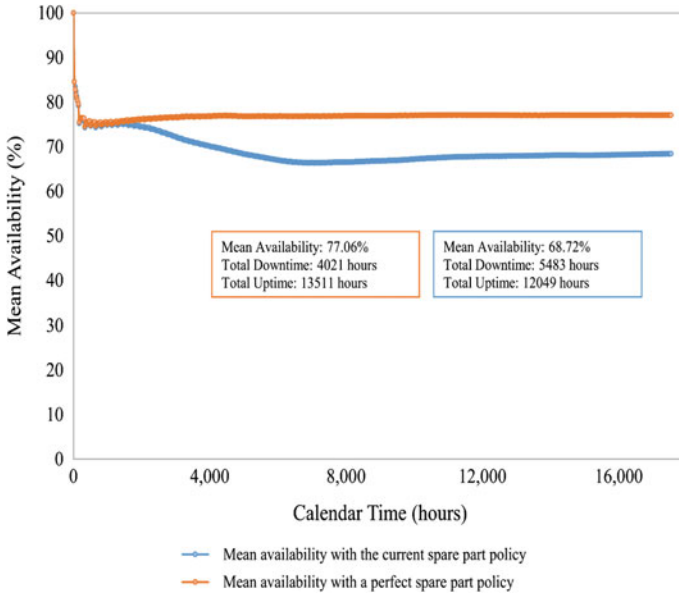
Fig. 3 Mean availability values of two cases for $t_t = 17,532$ h (2 years)

Table 1 Spare parts statistics of the simulation

Components	Initial stock	Trigger number	Average stock in inventory	Items used
BU3	10	5	10	16
BU4	24	12	21	18
BU5	14	7	12	11
BU2	4	2	3	1
DR6	4	2	3	2
DR2	8	4	7	14
DR3	4	2	3	9
DR1	4	2	2	14
HO1	4	2	3	7
HO2	4	2	3	4
RI2	8	4	6	4
RI5	4	2	3	3
RI1	8	4	7	2

4   Conclusion

Mining equipment operate in demanding working environments with changeable production amounts and operating conditions. Deterioration rates of equipment components in time and the resultant maintenance activities are highly specific to equipment themselves. Therefore, monitoring and analyzing of failures, forecasting and prioritization of spare part provisions, and periodic reviewing of uptime and downtime behaviors of equipment are required to be performed to determine up-to-date spare parts policies. Otherwise, it is very likely that improper policies do not ensure spare parts to be in place when they are required for maintenance activities. This condition may lead to a drop in equipment availability and production loss to a large extent. In this sense, this study presents an algorithm that can be utilized to measure effectiveness of applied spare parts policies in terms of availability. The developed algorithm was applied to a dragline. Initial stock levels, reorder limits, and reorder amounts were introduced as algorithm inputs. The system was allowed to act randomly for spare part decisions. At the end of the simulation, it was seen that the accumulated unavailability conditions of spare parts in maintenance times caused a total system availability drop by 8.34% for a period of 17,532 h.

References

1. Hu, Q., Boylan, J.E., Chen, H., Labib, A.: OR in spare parts management: a review. Eur. J. Oper. Res. **266**(2), 395–414 (2018)
2. Qarahasanlou, A.N., Barabadi, A., Ataei, M., Einian, V.: Spare part requirement prediction under different maintenance strategies. Int. J. Min. Reclam. Environ. 1–14 (2017)
3. Ghodrati, B., Kumar, U.: Operating environment-based spare parts forecasting and logistics: a case study. Int. J. Logistics: Res. Appl. **8**(2), 95–105 (2005)
4. Ghodrati, B., Akersten, P., Kumar, U.: Spare parts estimation and risk assessment conducted at choghart iron ore mine. J. Qual. Maintenance Eng. **13**(4), 353–363 (2007)
5. Louit, D., Pascual, R., Jardine, A.: Dynamic optimization model for mining equipment repair by using the spare-Parts inventory. J. Min. Sci. **46**(4), 394–403 (2010)
6. Martínez, A., Pascual, R., Maturana, S.: A methodology for integrated critical spare parts and insurance management. Appl. Stoch. Models Bus. Ind. **32**, 90–98 (2016)
7. Zhang, Q., Lv, X., Shi, J.: Research on inventory sharing model of frequent mining machinery maintenance spare parts. In: Proceedings of 12th IEEE Conference on Industrial Electronics and Applications, 1224–1229, IEEE, Siem Reap (2017)
8. Gölbaşı, O., Demirel, N.: A cost-effective simulation algorithm for inspection interval optimization: an application to mining equipment. Comput. Ind. Eng. **113**, 525–540 (2017)

Why Should Inspection Robots be used in Deep Underground Mines?

R. Zimroz, M. Hutter, M. Mistry, P. Stefaniak, K. Walas and J. Wodecki

1 Introduction

Mining has very long history, in some sense (mechanical processing of minerals) could be dated even in around thousands B.C. Acquiring raw materials has been usually risky and dangerous. Unfortunately, due to a rapid development of modern technologies, as well as globalization, easy-to-mine resources have been already exploited. Socio-environmental awareness also should be considered as serious problem for the mining industry that is frequently presented as "dirty" one. However, space, automotive, IT, etc., technologies require specific raw materials (for example, rare earth). So, deep underground mines impose new challenges for mining industry when searching for new hardly accessible deposits. These challenges are related to

R. Zimroz · P. Stefaniak · J. Wodecki (✉)
KGHM Cuprum Ltd, Research and Development Centre, ul.Sikorskiego 2-8, 53-659 Wroclaw, Poland
e-mail: jwodecki@cuprum.wroc.pl

R. Zimroz
e-mail: rzimroz@cuprum.wroc.pl

P. Stefaniak
e-mail: pkstefaniak@cuprum.wroc.pl

M. Hutter
Robotics Systems Laboratory, ETH Zurich, 8092 Zurich, Switzerland
e-mail: mahutter@ethz.ch

M. Mistry
School of Informatics, University of Edinburgh, 10 Crichton Street, Edinburgh EH8 9AB, UK
e-mail: mmistry@inf.ed.ac.uk

K. Walas
Institute of Control and Information,Engineering, Poznan University of Technology, ul.Piotrowo 3A, Poznan, Wielkopolska, Poland
e-mail: Krzysztof.Walas@put.poznan.pl

locations of deposits, their geometry (thin layers), and harsh environment (dust, temperature, and humidity) including natural hazards (gas emission, water, and seismic events). Even nowadays, miners are allowed to work during shorter (6 h only) shifts. It is expected that this period will be shortened in incoming years. More demanding conditions in the mine focus activities of companies and research institutions toward introducing robots to the mines. There are many successful examples of autonomous machines operated in the mine, robotized processes, and some support from UAVs in open-cast mines. Unfortunately, applications of robotics in an underground mine are still limited [3, 6, 9]. In this paper, we will introduce recently launched project THING, supported by H2020 EU programme that is devoted to the usage of the autonomous four-legged robot ANYmal for inspection of infrastructure in deep copper ore mine. To be more precise, we will discuss how to support daily maintenance procedures for belt conveyors.

In the paper, we will discuss in general development of robotics in mining, analyze inspection robots used in mining industry, and related areas that could be at least in theory easily adapted to the mining industry, and finally briefly present ANYmal, highlight main research tasks from a robotic perspective, and discuss possible inspection missions for belt conveyor maintenance.

1.1 Robotics in Mining—A Review

Robotics has been recognized as future for mining decades ago [1, 2, 4, 22]. Similarly, to other branches of industry a serious resistance from employee unions has been noticed. However, due to mentioned safety demands, more and more harsh conditions and increasing production and effectiveness of mining companies' automation, recent robotics applications are growing in the mining industry.

Robotic solutions could be divided into several groups as follows:

– Inspection robots (tunnels, infrastructure, pipe systems, and slopes) [6, 9, 10, 12, 14, 15, 20, 21, 31],
– Rescue robots (roof collapse accidents) [7, 8, 18, 29],
– Robotics for main technological processes (drilling, autonomous transport, defragmentation of oversized lumps, etc.) [4, 5, 26, 27],
– Robotics for auxiliary technological processes (mapping, exploration) [11, 16, 17, 19, 24, 30], and
– Others [6, 9].

1.2 Robots for Inspection: Mining and Close-to-Mining Applications

Mines are usually located on a large area. In case of underground mine (considered mostly in this paper), our object should be visualized as a complex system with varying in time geometry and environment. According to mining regulations, there is a need to monitor processes, a condition of mining cavities (chambers, tunnels, etc.), geotechnical, electric, and mechanical infrastructure. Unfortunately, this classification is very simplified. Miners should take care of everything during their work underground. Due to a scale of the problem and dynamic development of mine, most of the inspection tasks are performed by miners. For critical stationary elements, there are specialized monitoring systems. Unfortunately, due to cost and technical constraints, it is probably impossible to cover by monitoring systems the whole mine area (3000 km of underground roads). An idea of supporting miners using robots seems to be very promising. In this paper, we propose an inspection robotic system for maintenance of belt conveyors. The advanced legged robotic system developed by ETH will be the basis in the project.

2 Maintenance of Belt Conveyors

Belt conveyor (BC) is an element of a transportation system in the mine. BC is used for transport of copper ore from dumping points to shafts responsible for vertical transport. From mining faces to mentioned dumping points, ore is provided by mobile LHD machines (loaders or trucks).

There is a variety of conveyor design in sense of length (short could have dozens of meters while long might have more than several kilometers), power, and configuration of driving system (one up to four engines for driving station, drives could be installed in different locations to "distribute" stress in belts), structure of belt support, etc. (Fig. 1). In any case, there is a need to monitor and/or inspect the condition of conveyor components and its proper operation [25]. For some components of conveyor, online monitoring (measurement system) is available (current consumption for each electric motor, the temperature of bearings in motor, gearbox, and pulley, etc.) [23]. However, due to spatial nature of conveyor network structure, number of components, number of external factors that could influence process and machine, and finally specific philosophy is applied in machine maintenance in which a human-assisted inspection plays a crucial role. According to general and internal regulations, each conveyor should be inspected every day; sometimes it should be done several times [23, 28].

Introduction of inspection robots can be beneficial on several levels of abstraction. Firstly, elimination of human error can allow to significantly reduce the number of accidents occurring during the inspection. Since robot will not do anything beyond what it is told to do, it is expected to eliminate all situations induced by irresponsible human behavior. Secondly, assessment of environmental conditions (concentration
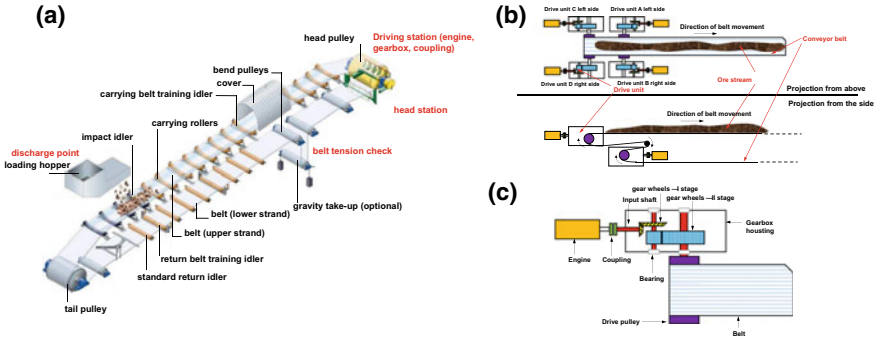
Fig. 1 **a** General structure of belt conveyor, **b** head station with drive units, **c** key elements of a single drive unit

of dangerous gases, air temperature pressure, etc.) can prevent introducing workers to mine areas harmful from the environmental point of view. Thirdly, some inspection tasks (e.g., thermography of the conveyor infrastructure) can improve safety by providing alarming information in a reliable way, which can reduce the impact of hypothetical fire by creating a possibility of sending firefighting crew soon enough. Besides that a worker responsible for such inspection can instead be occupied with other tasks, so the overall effectiveness of this worker would be increased, or at least better focused.

3 ANYmal for Belt Conveyor Inspections

A consortium of University of Edinburgh, ETH Zurich, University of Pisa, University of Oxford, University of Poznan, KGHM Cuprum R&D Center, and two spin-off companies QBROBOTICS SRL and ANYbotics AG has been successfully applied for H2020 research project focused on "THING subTerranean Haptic INvestiGator." It was agreed that basis for the project will be the legged robotic system ANYmal developed by ETH Zurich and ANYbotics AG. Our ambitions are related to support maintenance staff using ANYmal for inspection of belt conveyor system. There are also several key research challenges related to the purely robotic field (perception, control, path planning, adaptive feet, etc.); however, they will be discussed in appropriate journals devoted to robotics. In this paper, we want to discuss an application part of the project, focused on the definition of needs, mission planning, and inspection data processing (online for quick evaluation of situation and critical events detection and offline for long-term analysis out of robotic platform) [12].

Fig. 2 ANYmal legged robot used in the project (ANYbotics) [12]

3.1 ANYmal—Advanced Legged Robotic System

ANYmal is a quadrupedal robot designed for autonomous operation in challenging environments (Fig. 2). Driven by special compliant and precisely torque controllable actuators, the system is capable of dynamic running and high-mobile climbing. Thanks to incorporated laser sensors and cameras, the robot can perceive its environment to continuously create maps and accurately localize. Based on this information, it can autonomously plan its navigation path and carefully select footholds while walking. Driven by its first real-world application, namely, industrial inspection of oil and gas sites, ANYmal carries batteries for more than 2 h autonomy and different sensory equipment such as optical and thermal cameras, microphones, gas-detection sensors, and active lighting. With this payload, the machine weighs less than 35 kg, and hence can be easily transported and deployed by a single operator [12].

3.2 Belt Conveyor Drive Unit Maintenance Problem

Vibration-based gearbox diagnostics is a well-established technique for gearbox condition assessment. In considered mine, it bases on vibration and input shaft rotational speed measurements using portable "Diag Manager" system developed by Wroclaw University of Technology [28]. The preliminary result could be received after 60 s of measurement, for long-term maintenance management purposes measurement and diagnostic features are stored in the GIS-based database system and they are used for reporting. DAQ system is a four-channel measurement system developed using Lab-VIEW and National Instrument DAQ components. To measure acceleration, three sensors are mounted on gearbox housing using magnets (Fig. 3). Speed measurement is used to evaluate load condition of the conveyor drive. Diag Manager system
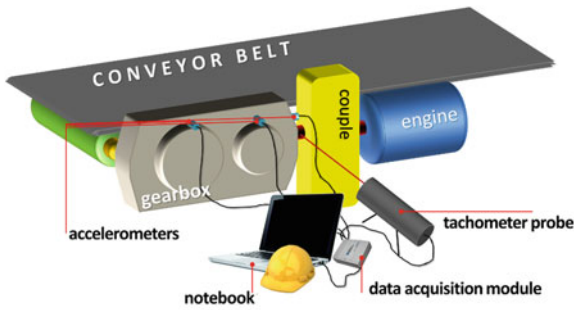
Fig. 3 Maintenance inspection for conveyor gearbox—vibration measurement using Diag Manager system

detects local damages as well as using simple energy-based spectral features it could evaluate operational wear of gearbox. Due to reach history (already it operates several years) and a number of objects covered by the system, we were able to specify warning and alarm thresholds (validated by visual inspection of gear inside).

3.3 Diagnostic Missions

To provide holistic view regarding conveyor condition and operation there are several internal requests announced by higher management responsible for transport. Although they are formalized; however, for robotic inspection they could be redefined. Figure 4 presents graphically what should be done by maintenance staff. Among others, it might cover the following:

1. Vibro-diagnostics of conveyor gearbox.
2. Infrared thermography of conveyor gearbox.
3. General inspection for belt conveyor—image analysis.
4. General inspection for fire protection system for belt conveyor—image/noise analysis.
5. General inspection for belt conveyor—smoke detection.
6. General inspection for belt conveyor—infrared thermography.
7. General inspection for mining corridor—image analysis.
8. General inspection for mining corridor—atmospheric quality assessment.

"Algorithmization" of inspection tasks might be challenging as well. In general, the person responsible for inspection of conveyor should make a decision whether a machine could continue operation, and such decision is based on experience and
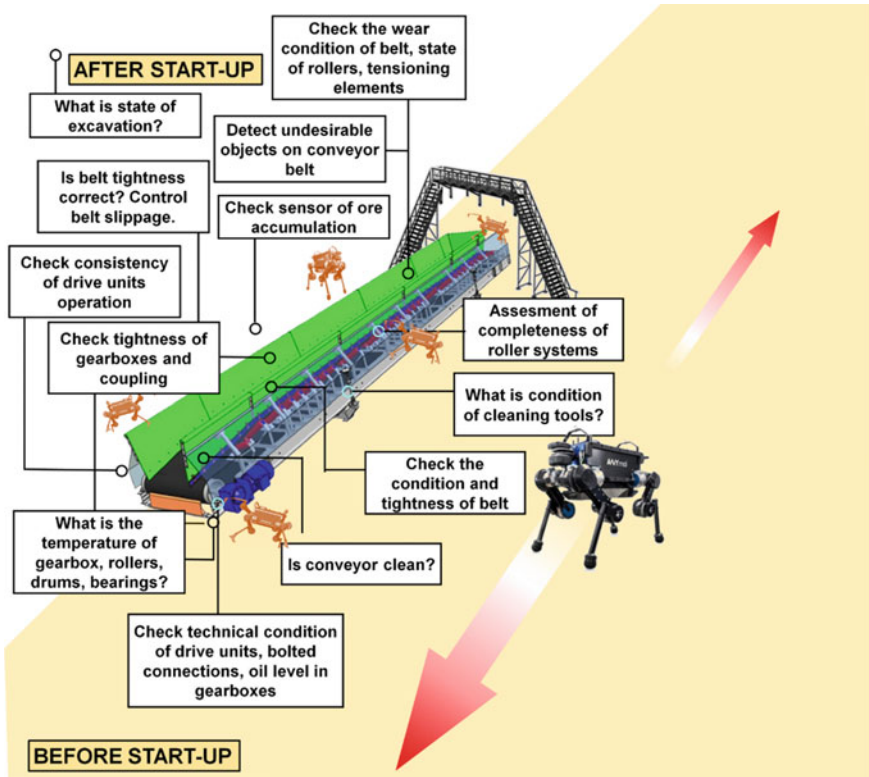
Fig. 4 Inspection missions with ANYmal robot for belt conveyor

deep understanding of the physical object. Using pattern recognition language, they search for the anomaly. However, "normal" case would be very difficult to define formally.

3.4 Diagnostic Mission Example: Haptic Vibration-Based Diagnostics of Gearbox

An idea of this exemplary mission is simply based on repeating the same procedure as defined in the section above. The robot should arrive to drive station, identify the object to diagnose, identify the appropriate place on the gearbox housing, and "touch" it to acquire vibration. In fact, this is what intuitively miners are doing on regular basis—they "touch" housing to "feel" vibration level, temperature, etc. After measurement, robot should perform preliminary analysis (simply check amplitudes of vibration) and store data for offline advanced processing (as Diag Manager system

Fig. 5 The general algorithm for gearbox inspection missions with ANYmal robot
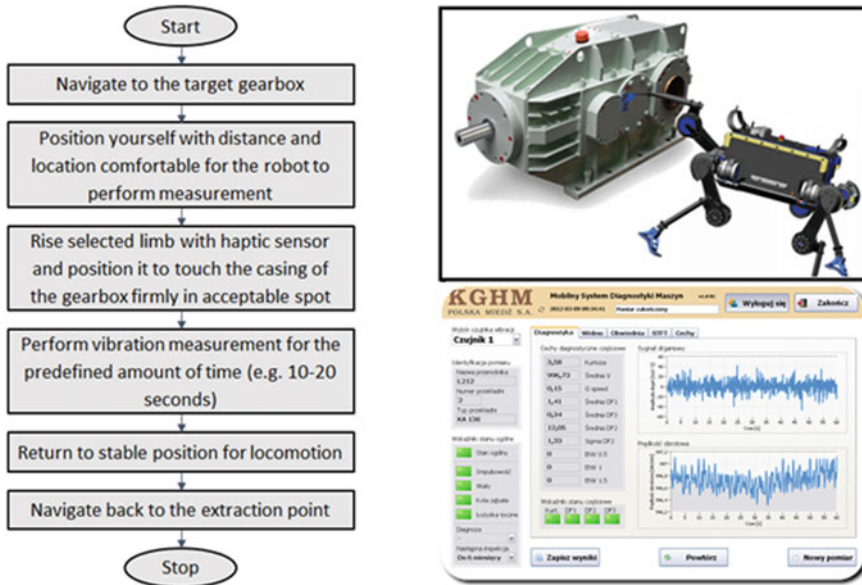
is doing). Figure 5 presents general algorithm for this mission, rough visualization of measurement, and example of the user interface from Diag Manager—the data processing part could be the same for robot-based mission.

3.5 Challenges for Inspection Robot

Although ANYmal robot is a great example of a very advanced robotic system developed for oil and gas industry [12], there are still many challenges when considering its use for belt conveyor inspection. (Note that THING is ICT, robotic-oriented research project; however, we minimize these aspects in this paper as they will be considered in other publications.)

Several keys already identified issues that need to be solved during the project from diagnostic/maintenance perspective which are as follows (Fig. 6):

– Harsh conditions in the mine: There is a lot of dust and low visibility.
– Floor surface in the mine: Water, rock lumps, etc.
– Harsh environment: Dust, humidity, uneven ground surface, and standing water.
– Navigation accessibility: Tight spaces.
– Hardware design and placement: Gearbox type, location, and accessibility.
– Contact accessibility: Safety structures, hardware casings, and rotary elements casings.

Fig. 6 Graphical examples of harsh environment and other constraints

– Tachometric sensor—rotational speed measurement—may not be possible using a robot, speed should be recovered from the vibration signal.
– The access to some parts of the machine is difficult or impossible.
– Correct sensor placement is crucial.

4   Conclusions

This paper discusses several important issues under the umbrella of the question asked in the title: what could be done by inspection robot, how to transform our wishes into algorithms and robotic system, what to measure and how to exploit data acquired by the inspection robot, and finally how robot applications would modify safety, efficiency, etc. of mining processes in deep underground mine. This discussion is introductory material, the project "THING: subTerranean Haptic INvestiGator" technically started in January 2018. Our ambitions are to have an inspection robot to support maintenance of belt conveyor system in deep (>1200 m) mine. Nowadays, such inspections are done by maintenance staff, unfortunately, according to Central Mining Authority [13] reports, accidents happen every year during operation of conveyors. We have presented an idea of an adaptation of ANYmal platform developed by ETH Zurich and ANYbotics AG to form an inspection robot for belt conveyor inspection and maintenance. We have defined examples of inspection/diagnostic missions and some constraints and critical issues have been identified. Illustrations of harsh environment in considered mine have been presented too.

References

1. Anisi, D.A., Gunnar, J., Lillehagen, T., and Skourup, C.: Robot automation in oil and gas facilities: indoor and onsite demonstrations. In: 2010 IEEE/RSJ International Conference on Intelligent Robots and Systems (IROS), 4729–4734 (2010)
2. Bharathi, B., and Samuel, B. S.: Design and construction of rescue robot and pipeline inspection using zigbee. Int. J. Sci. Eng. Res, **1** (2013)
3. Corke P., et al.: Mining robotics. In: Siciliano B., Khatib O. (eds) Springer Handbook of Robotics, Springer, Berlin, 1127–1150 (2008)
4. Ge, F., Moore, W., Antolovich, M., and Gao, J.: Robot learning by a mining tunnel inspection robot. In: 2012 9th International Conference on Ubiquitous Robots and Ambient Intelligence (URAI), IEEE, 200–204, (2012)
5. Green, J., and Vogt, D.: A robot miner for low grade narrow tabular ore bodies: the potential and the challenge. Presented at 3rd Robotics and Mechatronics Symposium, (2009)
6. Green, J., Bosscha, P., Candy, L., Hlophe, K., Coetzee, S. and Brink, S.: Can a robot improve mine safety? Presented at CAD/CAM, Robotics and Factories of the Future, (2010)
7. Green, J.: Mine rescue robots requirements outcomes from an industry workshop. In: IEEE Robotics and Mechatronics Conference (RobMech), **6**, 111–116 (2013)
8. Green, J.: Mine rescue robots requirements outcomes from an industry workshop. In: IEEE. Robotics and Mechatronics Conference (RobMech), 111–116 (2013)
9. Green, J.: Robots in mining. In: CSIR 3rd Biennial Conference: Science Real and Relevant, Pretoria, South Africa, **9** (2010)
10. Green, J.: Underground mining robot: a csir project. In: 2012 IEEE International Symposium on Safety, Security, and Rescue Robotics (SSRR),.IEEE, 1–6 (2012, Nov)

11. Grehl, S., Sastuba, M., Donner, M., Ferber, M., Schreiter, F., Mischo, H., & Jung, B.: Towards virtualization of underground mines using mobile robots–from 3D scans to virtual mines. In: Proceedings 23rd International Symposium on Mine Planning and Equipment Selection, 711–722 (2015)
12. http://www.rsl.ethz.ch/robots-media/anymal.html
13. http://www.wug.gov.pl/bhp/statystyki_wypadkow
14. Jiang, B., et al.: Autonomous robotic monitoring of underground cable systems. In: ICAR'05. Proceedings of the 12th International Conference on Advanced Robotics, IEEE, 673–679 (2005)
15. Kasprzyczak, L., Trenczek, S., Cader, M.: Robot for monitoring hazardous environments as a mechatronic product. J. Autom. Mob. Robot. Intel. Syst. **6**, 57–64 (2012)
16. Maity, A., Majumder, S., and Ray, D. N.: Amphibian subterranean robot for mine exploration. In: IEEE International Conference on Robotics, Biomimetics, and Intelligent Computational Systems (ROBIONETICS), IEEE, 242–246 (2013)
17. Morris, A., Silver, D., Ferguson, D., & Thayer, S.: Towards topological exploration of abandoned mines. In: Proceedings of the 2005 IEEE International Conference on Robotics and Automation, ICRA 2005, IEEE, 2117–2123 (2005)
18. Murphy, R. R., Kravitz, J., Stover, S. L., & Shoureshi, R.: Mobile robots in mine rescue and recovery. IEEE Robotics & Automation Magazine, **16**(2) (2009)
19. Nüchter, A., Elseberg, J., Borrmann, D.: Irma3D—an intelligent robot for mapping applications. IFAC Proceedings Volumes. **46**(29), 119–124 (2013)
20. Ray, Dip N., et al.: Sub-terranean robot: a challenge for the Indian coal mines. Online J. Electron. Electr. Eng, **2**(2), 217–222 (2009)
21. Reddy, T.K., & Krishna, G.B.S.: Hazardous gas detecting rescue robot in coal mines. In: Proceedings of IRF International Conference, Chennai, India, 978–93, 13th April-2014
22. Roh, S.G., Ryew, S., Yang, J.H., & Choi, H.R.: Actively steerable in-pipe inspection robots for underground urban gas pipelines. In: Proceedings of the 2001 ICRA IEEE International Conference on Robotics and Automation, IEEE, **1**, 761–766 (2001)
23. Sawicki, M., et al.: An automatic procedure for multidimensional temperature signal analysis of a SCADA system with application to belt conveyor components. Procedia Earth and Planetary Science **15**, 781–790 (2015)
24. Silver, D., et al.: Scan matching for flooded subterranean voids. In: IEEE Conference on Robotics, Automation and Mechatronics, 2004, IEEE, **1**, 422–427 (2004)
25. Stefaniak, P., Wodecki, J., & Zimroz, R.: Maintenance management of mining belt conveyor system based on data fusion and advanced analytics. In: International Congress on Technical Diagnostic, Springer, Cham, 465–476 (2016, Sept)
26. Stefaniak, P., Wodecki, J., Jakubiak, J., & Zimroz, R.: Development of test rig for robotization of mining technological processes–oversized rock breaking process case. In: IOP Conference Series: Earth and Environmental Science, **95**(4) (2017)
27. Stefaniak, P., et al.: Preliminary research on possibilities of drilling process robotization. In: IOP Conference Series: Earth and Environmental Science, IOP Publishing, **95**(4) (2017)
28. Stefaniak, P., et al.: Computerised decision-making support system based on data fusion for machinery system's management and maintenance. Appl. Mech. Mater. **683**, 108–113 (2014)
29. Subhan, M.A., et al.: Study of unmanned vehicle (Robot) for coal mines. Int. J. Innovative Res. Adv. Eng. **1**(10), 116–119 (2014)
30. Thrun, S., et al.: Autonomous exploration and mapping of abandoned mines. IEEE Robot. Autom. Mag. **11**(4), 79–91 (2004)
31. Yinka-Banjo, C., et al.: Autonomous multi-robot behaviours for safety inspection under the constraints of underground mine terrains. Ubiquit. Comput. Commun. J. **7**(5), 1316 (2012)

Underground Track Design, Construction and Maintenance

S. M. Rupprecht

1 Introduction

Mining presents many challenges to the mining engineer, one of which is the logistics, which should support mining operations quickly and efficiently. Underground haulage is important in the efficient operation of an underground mine as it represents 15% of the total operating costs and is the main artery of the mining operation removing rock, supplying material to and transporting personnel to and from the working face. As mining progresses deeper and further from the shaft, the role of logistics becomes increasingly important if production targets are to be achieved. Underground transportation must be seen as a process requiring an integrated approach, incorporating personnel, material and rock and should consider the particular requirements of the transportation system as a whole.

In South Africa, rail haulage is the principal transportation method and will remain a significant factor in future underground mining operations. The mining engineer must be proficient in the use of railbound transportation systems in order that the lowest cost transportation system is selected and designed. Mine layouts and schedules must be efficiently planned and equipped combined with a culture to move personnel, material and rock safely, quickly and efficiently. This paper that follows [1, 2], reviews underground track design, construction and maintenance and provides mine planners and young mining engineers guidelines in the safe and efficient installation of underground tracks.

Figure 1 depicts poor track conditions as commonly observed underground. The space between tracks is filled with spilled material causing the wheels of the train to operate on dirt rather than run on the actual rail. Timber sprags are also used to secure the rail in position.

S. M. Rupprecht (✉)
University of Johannesburg, Johannesburg, South Africa
e-mail: stevenr@uj.ac.za

Fig. 1 Typical underground track conditions. Note the timber sprags supporting the rail against the sidewall and the material between the tracks

2 Track Construction

As an introduction to track construction, it is important to understand the track gauge used underground and why it was selected over the larger railway gauge commonly used on surface. Since narrow gauge railways are usually built with smaller radius curves and smaller structure gauges, they can be substantially cheaper to build, equip and operate than standard gauge or broad gauge railways, particularly, in mountainous or difficult terrain. The lower costs of narrow gauge railways mean they are often built to serve industries and communities where the traffic potential would not justify the cost of building a standard or broad gauge line. Narrow gauge railways also have specialised use in mines and other environments where a very small structure gauge makes a very small loading gauge necessary.

The earliest recorded railway is shown in the De Re Metallica of 1556, which shows a mine in Bohemia with a railway gauge of approximately 2 ft. (610 mm). During the sixteenth century, railways were mainly restricted to hand-pushed narrow gauge lines in mines throughout Europe. During the seventeenth century, mine railways were extended to provide transportation above ground. These lines were industrial, connecting mines with nearby transportation points, usually canals or other waterways. These railways were usually built to the same narrow gauge as the mine railways from which they developed.

Table 1 Rail sizes and associated dimensions

Sizes	Dimensions in mm					
Kg/m	A	B	C	D	E	F
10	63.5	19.5	10.3	35.0	6.0	63.5
15	76.2	25.4	13.1	41.3	7.5	76.2
22	95.3	31.4	15.5	50.0	10.0	95.3
30	109.5	34.9	17.5	57.2	11.5	109.5
40	127.0	40.5	19.5	63.5	14.0	127.0
48	150.0	43.0	25.0	68.0	14.0	127.0
57	165.0	47.5	26.5	70.0	16.0	140.0

In contrast, standard gauge or broad gauge railways generally have a greater haulage capacity and allow greater speeds than narrow gauge systems. Standard gauge railways are based on Roman road widths which used two horses to draw a cart, thereby establishing the distance between the two tracks.

Track construction plays an important role in terms of the duty of the haulage, the speed of the locomotion and the overall operating costs of trackbound transportation. Track structure could be divided into the following components:

– Bottom formation,
– Ballast,
– Sleepers and sleeper fastenings,
– Rail and fishplates.

Track components play an important role in track construction; the use of any inferior component will negatively impact on the overall competency of the track construction as the overall strength of the system is interdependent to the weakest link.

2.1 Rail

Rails are available in different sizes based on a weight per metre basis, typically 22, 30 and 48 kg/m rails are used underground. As shown in Table 1, the various dimensions of the rail outlined in Fig. 2 change according to the overall change in mass per metre. Figure 3 illustrates a typical track construction.

2.2 Sleepers

The selection of the sleeper must take into account the axle load to be carried, sleeper spacing, the life of the haulage and environmental conditions. Concrete sleepers are

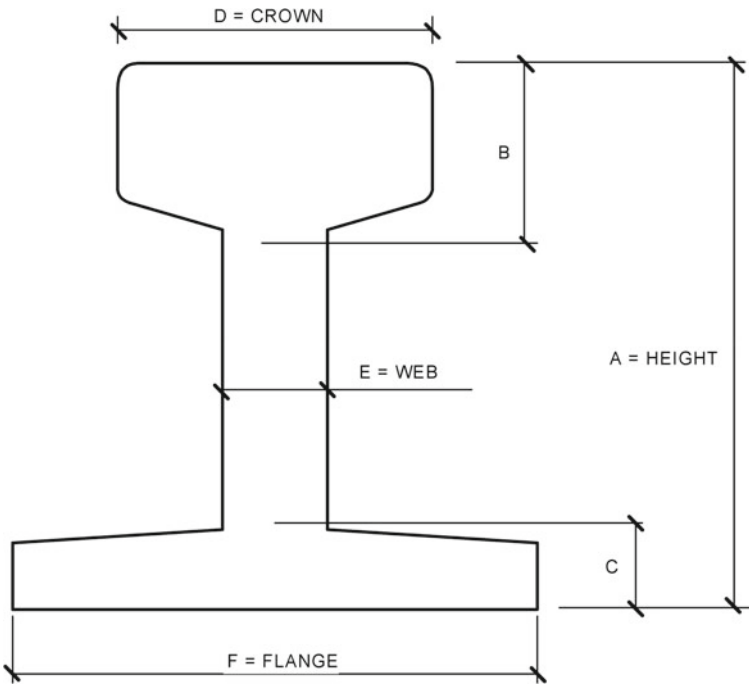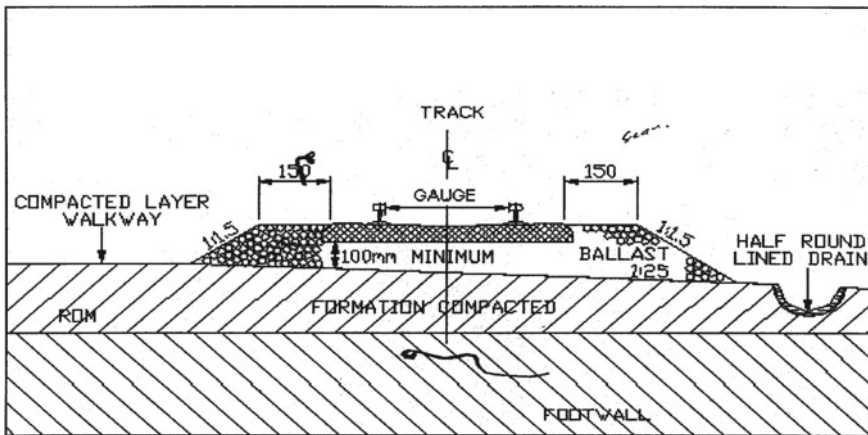**Fig. 2** Basic cross-sectional detail of a rail

Fig. 3 Conventional track construction

preferred for heavy axle loads, high-stability track, wet conditions and low mainte-
nance requirements. Good quality wooden sleepers are becoming increasingly expen-
sive and are not always available. Steel sleepers can be used in dry environments and
in temporary track such as jump sets in development ends.

Table 2 Recommended sleeper spacing based on a 9.1 m rail length

Gauge (mm)	Number of sleepers based on rail length	Spacing (mm)
610	13	730
762	16	580
914	16	580

The spacing of the sleepers is measured centre to centre between consecutive sleepers. The rail profile used and the maximum axle load applied by the rolling stock determine the sleeper spacing. The lighter the rail profile and/or the heavier the axle load, the closer the spacing. Reducing the sleeper spacing can increase the carrying capacity. The relationship between the number of sleepers, spacing and rail gauge for various standard rail profiles is given in Table 2.

2.3 Wooden Sleepers

Timber or wood is suitable for sleepers and although they are lighter and less susceptible to derailment damage, they are becoming more expensive due to the increasing scarcity of suitable hardwoods. Only good quality sleepers that are well seasoned and free from defects, such as loose knots, should be used for rail support as defective timber may affect the strength of the sleeper. Sleepers should be straight, cut square at the ends and have their top and bottom faces parallel to each other.

The standard size of a sleeper is 200 mm wide and 100 mm thick. The minimum length should be equal to the rail gauge plus an additional 600 mm for overlap. Longer and wider sleepers may be used to spread the load further where local circumstances require it. For example, where there is a damp, soft clay floor or where ballast is of inferior stone.

To cater for the wet or damp floor conditions found in mines, timber sleepers should be seasoned and be treated with a mixture of creosote and synthol waxy oil. Timber sleepers provide a wide base which, when properly supported by ballast, distributes the vertical load and offers good friction between sleeper and ballast, thus keeping the track in position horizontally.

2.4 Concrete Sleepers

Concrete sleepers were first introduced in the mining industry for narrow gauge track in 1965. The introduction first came about, as timber in South Africa is not well suited for use as sleepers, which resulted in that most timber sleepers used in South Africa had to be imported. Concrete sleepers were introduced to reduce costs as well as

adding the additional benefit of being more environmentally friendly compared to wooden sleepers and the associated concerns of deforestation.

Concrete sleepers offer further advantages in that concrete does not burn and does not deteriorate under typical wet mining conditions. Concrete sleepers have a long life provided that they are installed correctly and the track installation is to a high standard. The increase in train payloads (axel loads) and higher speeds make concrete sleepers ideal. Disadvantages of concrete sleepers include the weight of sleepers, the fact that they require proper ballast, they fracture with severe ground movement and are easily broken in the course of derailments. This last point is a major concern as a derailed hopper or car can be pulled many metres in attempt to re-rail the hopper or car often causing major damage to the concrete sleepers.

The 10-tonne heavy-duty concrete sleeper should be considered whenever any one of the following criteria is met:

– Axle load of full hoppers exceeds 5 tonnes,
– Maximum speed of train exceeds 16 km/h,
– Gross annual tonnage of the haulage exceeds 500,000 tonnes,
– Life expectancy of the haulage exceeds 5 years.

The benefits of the 10-tonne sleeper are as follows:

– Longer sleeper life,
– More stable track,
– Greatly reduced maintenance of the track,
– Gauge widening possible on curves.

2.5 Steel Sleepers

Steel sleepers, complete with rail fasteners, are a convenient alternative to timber sleepers, except where high speeds or heavy loads are proposed. Steel sleepers are light in mass, less susceptible to derailment damage and require lower ballasting profiles. They are convenient to install, maintain and transfer from one location to another. Due to their shape and size, they tend to settle into the ballast far more quickly than timber sleepers. Generally, they do not have the same resistance to lateral movement as timber sleepers. Steel sleepers are available in 30 kg/m (light duty) and 40 kg/m (heavy duty) profiles.

Steel sleepers are prone to bending where the mine tunnel floor can move, and in this respect, they need to be of suitable strength for the ground conditions envisaged. Mine engineers must be aware of the corrosive environment when considering the type of steel used in manufacture.

2.6   Rail Fasteners

There are two main types of fasteners used underground to fasten the web of the rail against the sleeper. Dog spikes are normally used with wooden sleepers while Pandrol clips are associated with concrete sleepers. Whether rail spikes or Pandrol clips are used it is essential to ensure that all fasteners are used on both sides of the rail flange. Failure to do so reduces the clamping force, and thereby the stability of the track structure.

2.7   Dog Spikes

Dog spikes are the simplest means of fastening rails to timber sleepers; the dog spike is hammered into a pre-drilled hole in the sleeper. A major negative aspect of the dog spike is that the clamping force is reduced over time and vibration. It is recommended that dog spikes are checked on a regular basis to ensure that the dog spike is maintaining its clamping force. Therefore, dog spikes are not recommended for use with heavy-duty rail or haulages.

2.8   Pandrol Clips

The Pandrol spring clip as its name implies is a clip that is pulled onto the sleeper and is able to maintain a constant clamping force under conditions of vibration. Pandrol clips are reuseable and easy to install.

2.9   Rail Fastenings on Steel Sleepers

Steel sleepers can either be secured with screw-type rail fastenings or may have boltless Pandrol clip rail fastenings where the clip retainer is welded onto the upper surface of the sleeper. These retainers also provide a shoulder for locating the rail and setting the gauge.

2.10   Ballast

Proper ballasting is essential to ensure good quality track. Ballast fulfils several purposes, such as transferring the load to the roadway floor, holding the sleepers in place, allowing water to drain and permitting the regrading of track.
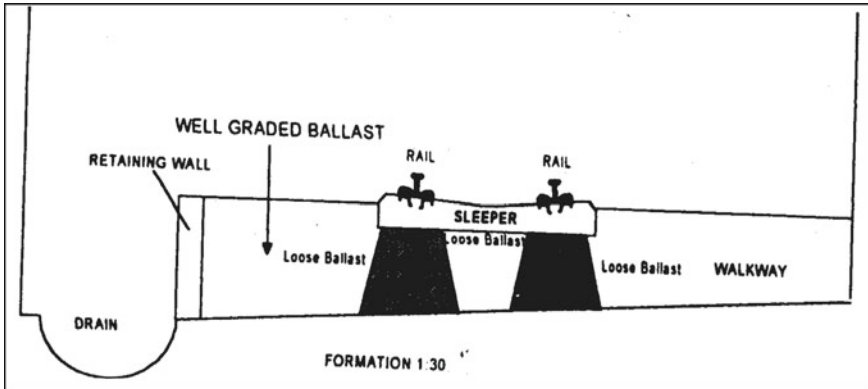
Fig. 4 Ballast and retaining wall

Ballast should be hard, and must be of well-graded size between 20 mm and 35 mm and should not contain fines as these fill the interstices and cause ballast to lose resilience. Ballast sized below 20 mm has poor cyclic load-bearing capability, while ballast greater than 40 mm is difficult to work with and does not allow accurate regrading of the track. Ballast should not crumble under load or wet conditions and should bind together as a mass when laid, yet still retains its open structure to allow for the drainage of water.

Importantly, ballast material should be based on an acceptable specification for the job rather than on the convenience of supply. Run-of-mine waste stone is only suitable as ballast where the railtrack is subjected to light-duty use. It should not be used for ballasting high-speed or heavy-load railtrack. Track built into concrete is not recommended because it does not allow adjustment following floor movement in a mine haulage.

The amount of ballasting required varies according to the type of sleeper and standard of installation but should never be less than 100 mm thick at any point beneath the sleeper. Figure 4 depicts track ballast with a retaining wall to assist with separating underground water from the ballast.

2.11 FishPlates

Fishplates (Fig. 5) are the most common method of joining rails used in underground railtrack. For maximum joint rigidity, fishplates need to be fixed by at least four bolts. The bolts must be installed with spring washers or self-locking nuts. Fishplate bolts must always be installed with the nuts on the inside of the track. This facilitates daily inspections where the tightness of bolts must be checked. Fouling contact with the wheel flanges will only occur in exceptional circumstances of wheel or rail wear.

The following is recommended to improve the performance of a fish-plated joint:
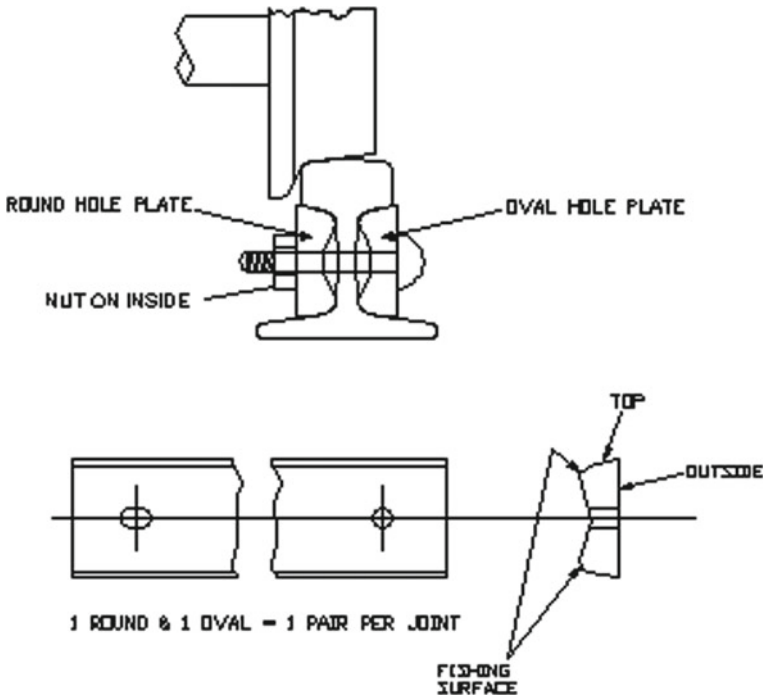
Fig. 5 Fishplate detail

Table 3 Torque for fishplate bolts

Bolt diameter (mm)	Torque (Nm)
12	47
16	118
20	225
22	325
24	395

– Carbon steel or case-hardened fishplates should be used.
– Holes should be drilled and not punched with the nominal size of holes which is 26 mm for 30 and 40 kg/m rails.
– Fish bolts must be tightened to a torque of 340 Nm (See Table 3).
– Spring washers must be fitted under each nut or self-locking nuts must be used.
– The practice of bending the fishplates and not the rails through a curve is not permitted. Bent fishplates are subjected to high lateral forces that ultimately lead to failure of the joint.
– Junction of fishplates must be used for all joints where the rail size changes, i.e. 22 kg/m rail connecting onto 30 kg/m rail in a switch.

2.12   Welding of Rail Joints

In the underground environment, temperatures do not vary more than a few degrees, and therefore it is an ideal environment for continuous rail. A fishplate joint can be replaced by either thermit welding or copper block welding. Welded joints have the following characteristics:

– The rail ends in a joint are perfectly matched when ground correctly.
– There is no dynamic wheel impact, and therefore no deformation of the track which allows for a smoother and quieter ride.
– Sleeper spacing is not affected by the joints, and therefore fewer sleepers required.
– Improved life of rolling stock wheels, bearings and axles.
– No maintenance is required specifically for the joint, and therefore reduced maintenance effort, cost and risk of derailment.
– Track bonding is not required in electrified sections (reduced maintenance).
– High initial cost of welding is recovered in reduced maintenance and derailment costs.

2.13   Thermit Welding

Thermit welding is the preferred method of welding rail joints. It is a specialised exothermic process where molten metal is tapped from a crucible mounted above the pre-heated rail ends. The molten metal is tapped into a mould placed around the rail ends. The moulds are removed, the excess material is removed and the joint is ground down with a grindstone to form an even and smooth surface on the crown and inside running surface.

2.14   Copper Block Welding

For copper block welding, an arc welding process is performed either completely in the gap between the rails or partially on the crown and foot of the rail. Copper blocks are used to contain the flow of metal in the profile of the rail during the welding process. The rail ends are ground out to form a 'vee', which is then filled during welding. This type of welding is susceptible to flaws and is not recommended in high-risk areas such as high-speed haulages and shift haulages.

2.15 Huck-bolted FishPlates

A Huck-bolted fishplate joint that is correctly installed is a viable alternative to a welded joint. The manufacturer's procedures must be strictly followed to ensure that a competent joint that will not work loose is achieved. The following points are important:

– Rail ends must be square, correctly aligned and free of scale, corrosion, oil or dirt.
– High-carbon steel or case-hardened fishplates that have been cut and drilled must be used and not the mild steel cropped and punched type. The drilling must be reduced to 20 mm diameter holes and the centre holes must be closer together by ± 4 mm (to facilitate butting of rail ends).
– The double driving method must be used during installation to ensure even pull up of the fishplates

Maintenance, whether performed by mine personnel or by contractors, must be done on a continuous basis. A maintenance schedule should be drawn up for haulages, which includes daily, weekly and monthly examinations. The personnel required for haulage maintenance should be based on realistic productivity targets. One worker per 2 km of track is appropriate for haulages that are shotcreted and where trackwork is initially installed to a high-quality standard. In addition, some form of quantity and quality surveying should be done to monitor track installation and maintenance.
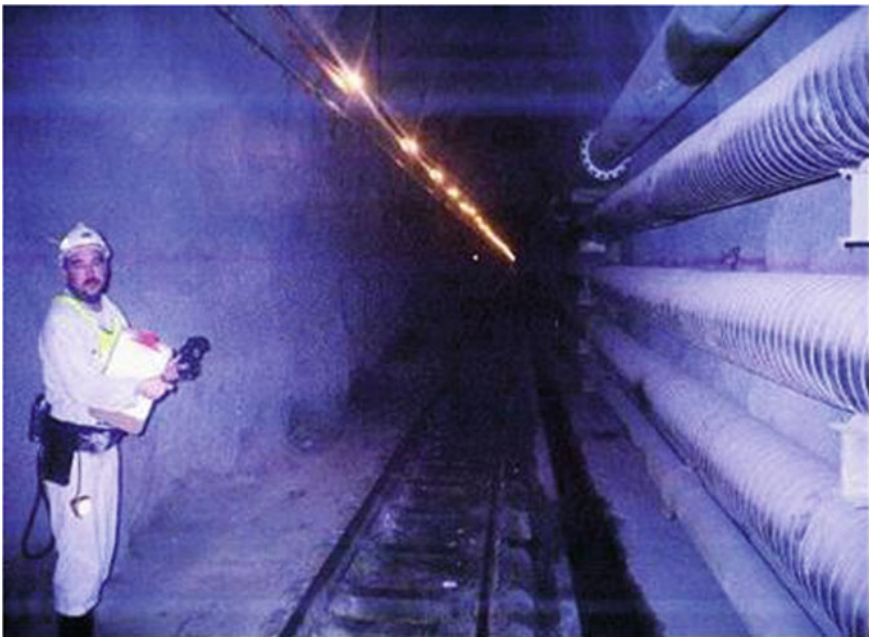

Fig. 6 A well-constructed haulage

3 Conclusions

Traditionally, transport has been viewed as a series of independent activities; however, this is not conducive to an efficient transportation system. A culture to move personnel, material and rock safely, quickly and efficiently must be created and this requires a mindset change. It is intended that this document must be used by mine designers and planners as guide during the design process, which should facilitate efficient underground transportation systems through well-constructed haulages as shown in Fig. 6. Although much of the work presented here is based on underground mining in South Africa, many of the good practice criteria presented here are generic in nature and would be equally applicable to all mining operations served by vertical shafts.

References

1. Rupprecht, S.M.: Best practices for personnel, material and rock in ultra deep gold mines of the Witwatersrand basin, PhD Thesis, University of Natal, South Africa (2003)
2. Rupprecht, S.M.: Guidelines for horizontal transportation, Kalgoorlie Australia. In: Proceedings in the 12th International Symposium on Mine Planning and Equipment Selection, Australasian Institute of Mining and Metallurgy (2003)

Part IX
Research and Development to Improve Health and Safety in Mines

Sustainability Assessment of Angouran Lead and Zinc Mining Complex

M. Heidari and M. Osanloo

1 Introduction

Mining is the principal activity in the path of gaining economic wealth and technological and social advances. Having the mineral deposits being extracted from the surface or underground, societies can have access to different sources of raw materials in order to use them as inputs for their growth and to enrich the quality of life for their present and future generations. However, like most activities, mining has various advantages and disadvantages while it has great influence on the economy of a country or region, it can disturb other potentials such as agronomy, livestock, fishery, forestry, etc. as mining disturbs the environment and surface/underground waters. This fact has been an argument between miners and environmentalists for many years since 1987, when the concept of green mining and sustainability became a global term. The most commonly accepted description was provided by Earth Summit, held in 1992 in Rio de Janeiro. According to this report, the goal of sustainability is to "meet the needs of the present generation without compromising the ability of future generations to meet their own needs." With this definition, every mining company is obliged to consider all stakeholders of the project, which is not only the shareholders of the business, but the society and government, who are influenced by the project. With this approach, the mine owners have to consider the influence of their activities on the environment and society. Surface mining is the most important cause in decomposing the arrangement of soil horizons, so-called overburden, which must be taken before access to the mineral, reducing the soil fertility potential, and changing the topographic conditions of the earth surface [1].

Using most of the minerals resources, while they are considered as nonrenewable resources, deposits are facing the end life, and this question arises of how future generation will provide their needs? [1]. In this regard, many evaluations have been

M. Heidari (✉) · M. Osanloo
Mining Engineering, Amirkabir University of Technology, Tehran, Iran
e-mail: mehrnoosh.heydarii@gmail.com

made in scientific papers on the sustainability of mineral projects as well as various mines in Iran have been investigated. One of the most effective researches in this area is the environmental impact assessment of open-pit mining in Iran by Monjezi et al. [2]. In this study, the Folchi method is used to study the mining impacts on the environmental components of the mining area [3]. There are also several studies evaluating the sustainability and environmental impact assessment available in literature [4–14]. As [13] presented two mining plans in Sungun copper mine in a research project entitled "mine design selection considering sustainable development", one based on maximizing the maximum NPV of the mine and the other for maximizing lifetime of the mine, using the Folchi method to determine which plan will gain more credits in the direction of sustainable development. According to this study, considering sustainable mining will be the key factor in the future of mining to have the least damage to the environment and the greatest profits for future generations [15].

The present study aims to investigate sustainability of Angouran lead and zinc mining complex in Iran. This mine's community is facing several problems due to mining activities in the region for more than 30 years. For this purpose, the social and environmental problems due to mining activities have been studied and their importance and effects are discussed. Next sustainability of the project is assessed using graph theory of DEMATEL. Finally, conclusions are offered in order to prevent further destructions in the region.

2 Methodology of the Study

2.1 Decision-Making Trial and Evaluation Laboratory (DEMATEL) Technique

DEMATEL is an **MCDM** method based upon graph theory, showing a directional and hierarchical structure. Furthermore, DEMATEL establishes the interrelations of criteria and ascertains the vital criteria to signify the effectiveness of all factors [16]. This method has been applied in many situations such as safety problems [17], e-learning [18], supply chain management [19], business process management [20], and risk assessment [21]. In order to implement this method, the following steps must be carried out [22].

First, it is necessary to identify the main components and their impacting factors. For this purpose, the brainstorm method and reviewing the literature can be used. Then, a square matrix with the effective factors put in rows and columns is prepared. Formerly, the experts are questioned to score the direct influence exerted by each factor on the others according to an integer scale ranging from 0 as the lowest influence to 4 as the most influence exerted. The element of comparison matrix is noted by $x_{ij}^{(k)}$, which shows the direct influence of factor (i) on factor (j), given by expert (k). In next step, the average matrix is calculated, which is the average of

pairwise comparison matrix, denoted by A. The (i, j) element of matrix A is a_{ij}, which is calculated as follows:

$$a_{ij} = \frac{1}{h} \sum_{k=1}^{h} x_{ij}^k \tag{1}$$

where h is the number of experts.

The initial direct influence matrix D is calculated by normalizing matrix A, which can be gained from Eqs. (2) and (3).

$$D = A/s \tag{2}$$

where s is a calculated as

$$s = \max\left(\max_{1 \le i \le n} \sum_{j=1}^{n} a_{ij}, \max_{1 \le j \le n} \sum_{i=1}^{n} a_{ij} \right) \tag{3}$$

Next, the total relation matrix T, which shows the total indirect and direct relations, is calculated as follows:

$$T = \sum_{m=1}^{\infty} D^i = D(1 - D)^{-1} \tag{4}$$

By letting t_{ij} to be the (i, j) element of matrix T, the sum of the i-th row and the sum of the j-th column, r_i and c_j, are obtained, respectively, as follows:

$$[r_i]_{n \times 1} = \left(\sum_{j=1}^{n} t_{ij} \right)_{n \times 1} \tag{5}$$

$$[c_j]_{n \times 1} = \left(\sum_{i=1}^{n} t_{ij} \right)_{n \times 1} \tag{6}$$

where r_i represents the total direct and indirect influences of factor i on the other factors and c_j denotes the sum of the direct and indirect influences received by factor j from the other factors. Therefore, when $j = i$, $(ci + r_i)$ provides an index of the strength of influences given and received; in other words, $(c_i + r_i)$ shows the degree that factor i plays in the problem. If $(c_i - r_i)$ is positive, then factor i affects the other factors, and if $(c_i - r_i)$ is negative, then factor i is influenced by the other factors.

Fig. 1 Angouran open-pit mine in Iran (M. Heydari 01/11/2017)

2.2 Angouran Lead and Zinc Complex

Iran has over 220 million tons of proven zinc and lead ore reserves. In 2009, with approximately 165,000 tons of production, Iran ranked first in the Middle East and 15th in the world in terms of zinc and lead production. Angouran lead and zinc mine is one of the eldest mines of Iran (Fig. 1). The annual production capacity of lead and zinc of the mine is 700,000 tons [23].

The mine is near QalehJouk Sadat village and Angouran region. This causes serious damages and threats to these villages from mine activities, such as destruction of the pastures, forests, and agricultural regions water, since contaminated surface water from the mine flows toward the agricultural regions and parts of the fruit gardens (Fig. 2). Pollution of livestock drinking water happens due to dust, which is induced by mining, especially during mine explosions, since the wind flow in this area is one way and from the mine overlooking the village due to the climatic conditions of the village. Blast waves cause cracks in the surrounded area, homes, and livestock stables as well as dust from blasting operations contaminating all fodder, legumes, and seeds. According to the HSE report of the company, the average noise level is 100 dB near crushers, which is 15 dB higher than standard level [23]. It should be noted that these villages are deprived of the minimum welfare issues, such as roads, internet, educational institutes, and ideal residential houses, despite the location of the largest lead and zinc mine of the country in their region.
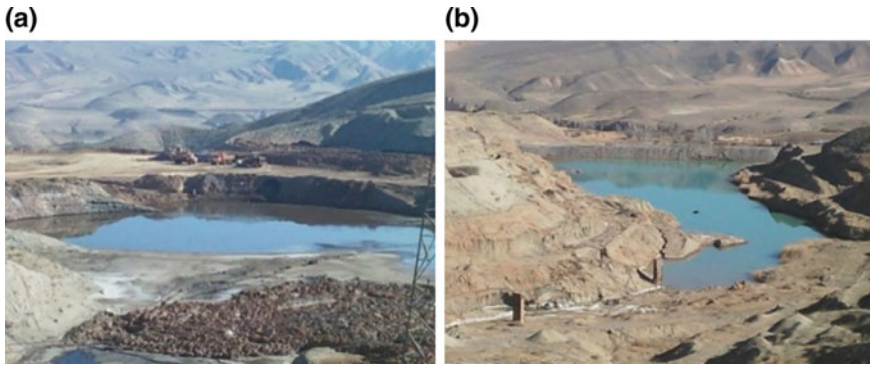
Fig. 2 **a** Leaching plant tailing dam, **b** floatation tailing dam (M. Heydari 01/11/2017)

3 Implementation of the Framework

There are 347 mining segments related to sustainability indicators advocated by earlier studies [24]. The certain indicators must be technically capable of assessing the determined alternatives in terms of the sustainability criteria [25]. Regarding this, 13 indicators are selected for environmental, 11 for social, and 6 for economic assessment. Selection of these factors is based on previous studies mentioned in the literature and personal judgment of the author due to field investigations of the Angouran mine site. Figure 3 shows the hierarchy of the selected parameters in this project. For implementation of the DEMATEL method to assess sustainability in Angouran mine, questionnaires were designed in order to collect the necessary data. Finally, 16 questionnaires were received.

Matrix A was calculated for each sustainability parameter in Table 1. This matrix shows the initial direct effects that a factor exerts and receives from the other factors. Afterward, vectors of (r), (c), $(r - c)$, and $(r + c)$ were calculated for components, and the results obtained were tabulated in Table 1. As previously described, vector (r) indicates the total exert influence on the others, (c) is a vector that shows the total influence received from the others, $(r - c)$ is relation, and $(r + c)$ is impact.

4 Results and Discussion

DEMATEL method is selected for this study from various available MCDM methods due to its advantages and capabilities. Since the number of parameters is high and the cause and effect relation between them is complicated, this method was selected since it finds the relationship between the parameters, identify the most important influencing parameter and the most receiving one among the others. This approach

Table 1 Results of total relationship matrix for sustainability parameters

	Impacting factors	r	c	$r + c$	$r - c$
Environmental factors	C1 Destruction of forests and postures	1.063	1.455	2.519	−0.392
	C2 Exposition of the mining area	0.686	1.259	1.945	−0.573
	C3 Pollution of surface water	1.008	1.020	2.028	−0.011
	C4 Pollution of underground water	0.746	1.023	1.769	−0.277
	C5 Traffic increase in the area	0.956	0.151	1.107	0.804
	C6 Air pollution	0.804	0.737	1.541	0.067
	C7 Fly rock	0.500	0.265	0.765	0.236
	C8 Ground vibration	0.684	0.243	0.927	0.440
	C9 Noise pollution	0.145	0.360	0.505	−0.215
	C10 Soil pollution	1.037	1.111	2.148	−0.074
	C11 Waste dump and tailing-dam-induced pollution	1.003	0.786	1.789	0.217
	C12 Subsidence	0.910	0.815	1.724	0.095
	C13 Ecosystem destruction (flora and fauna)	1.063	1.380	2.442	−0.317
Economic factors	Ec 1 Final price	1.652	1.000	2.652	0.541
	Ec 2 Capital costs	1.706	1.112	2.818	0.594
	Ec 3 Operating costs	1.478	1.231	2.708	0.247

Table 1 (continued)

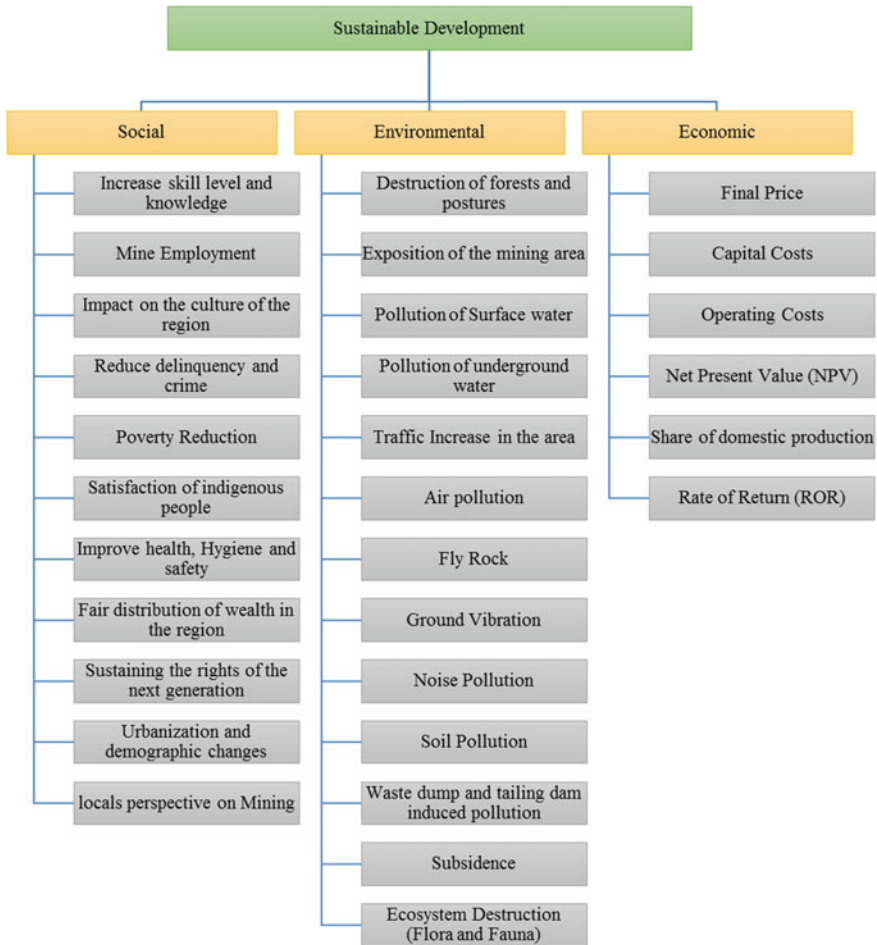|	Impacting factors	r	c	$r + c$	$r - c$
	Ec 4 Net present value (NPV)	0.635	1.232	1.866	−0.597
	Ec 5 Share of domestic production	1.059	1.199	2.257	−0.140
	Ec 6 Rate of return (ROR)	0.768	1.525	2.292	−0.757
Social factors	S1 Employment	1.511	1.079	2.590	0.431
	S2 Increase skill level and knowledge	1.421	1.185	2.606	0.236
	S3 Impact on the culture of the region	1.358	1.530	2.888	−0.172
	S4 Sustaining the rights of the next generation	0.835	1.013	1.848	−0.178
	S5 Fair distribution of wealth in the region	1.227	0.735	1.962	0.492
	S6 Improve health, hygiene, and safety	1.059	1.178	2.236	−0.119
	S7 Locals perspective on mining	0.933	1.124	2.057	−0.191
	S8 Urbanization and demographic changes	1.259	1.092	2.352	0.167
	S9 Satisfaction of indigenous people	0.818	1.350	2.168	−0.532
	S10 Poverty reduction	1.273	1.252	2.525	0.020
	S11 Reduce delinquency and crime	1.201	1.355	2.556	−0.155

Fig. 3 Sustainable development parameters related to each factor

helps the decision-makers to find the impacting factors and solve the issues in the project. Table 1 shows the results for SD components shown in Fig. 3.

Mining activities influence the environment in different ways in the area that the mine is located. When a mining area concerns with the environmental problems, it causes social troubles, loss of life, people immigration, and unemployment. These are examples of the effects of the environmental component. Using the values resulted from DEMATEL technique, Figs. 4, 5, and 6 are generated. According to Fig. 4, forest and ecosystem destruction have the most exerted influence among the impacting factors with the largest (r) value of 1.063, whereas noise is the least total exerted influence with the smallest (r) value of 0.145. Destruction of forests causes land disturbance, air pollution, and soil erosion (of heavy metals) that results in water
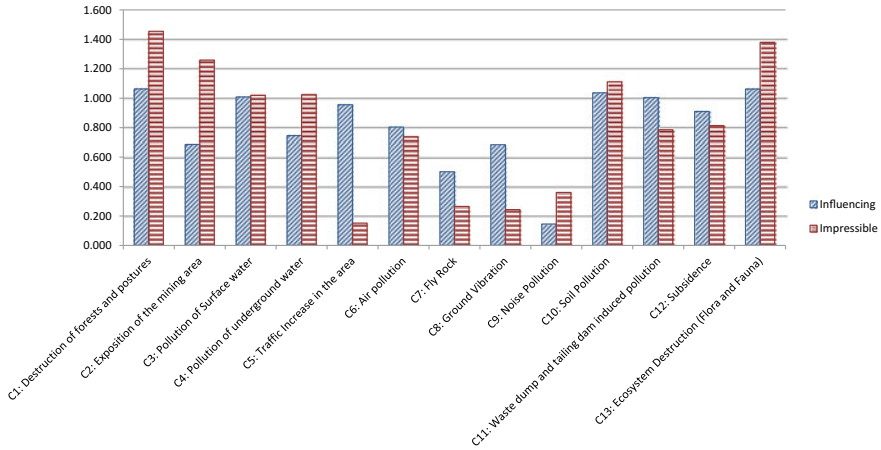
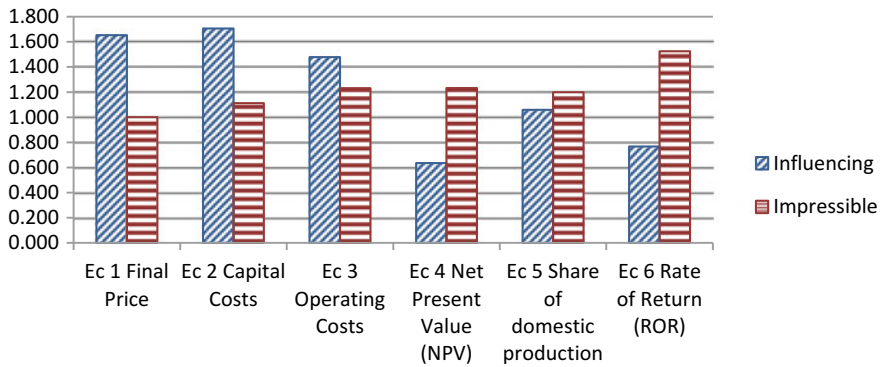**Fig. 4** Total applied and received influence of environmental factors

Fig. 5 Total applied and received influence of economic factors

pollution. On the other hand, it is quite natural that noise is the least total exerted influence factor since it does not increase or decrease any impacting factors. The total exerted influence and total received influence values of air pollution, surface water pollution, soil pollution, and subsidence are close to each other due to inter-relationships among them. In other words, these parameters have influence on each other, which is logical due to their nature and is the reason for their close values in the calculations.

Among economic factors (Fig. 5), capital cost and final price have the most impact values of 1.706 and 1.652. Hence, these factors are the most important among the impacting factors, whereas NPV criterion has the least impact with the value of 0.635, and is the least impacting factor. When the capital costs increase or decrease, other economic impacting factors will be changed. For instance, when production machinery number or bulk volume increases, the operating costs and share in domes-
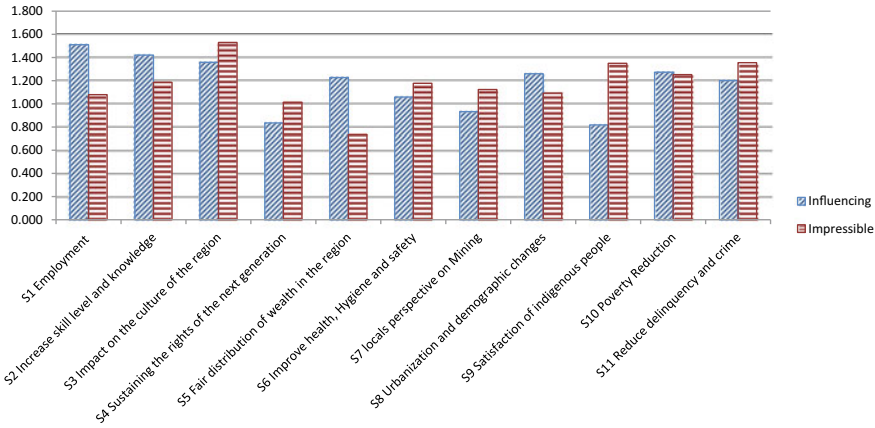
Fig. 6 Total applied and received influence of social factors

tic production will also increase. On the other hand, rate of return, NPV, and share of domestic production must have necessary conditions for selection as influencing economic factors. These parameters are receiving influence from many affecting factors in the project. According to the problems of price estimation, it is quite natural that this impacting factor has the lowest total received influence.

According to Fig. 6, the employment of local workforce has the highest total exerted influence among the impacting factors with the largest (r) value of 1.511, whereas satisfaction of indigenous people has the lowest total exerted influence with the smallest (r) value of 0.818. Culture in every town is in direct relation with resident people and employment structure in that town. It is quite natural that employment of local workforce has the highest total exerted influence. On the other hand, since satisfaction of indigenous people is determined based on many other factors, it has the least total exerted influence relative to other impacting factors.

The results obtained show that impact on the regional culture and crime decrease has the most total received influence impacting factors, whereas fair distribution of wealth in the region is the least total received influence. This can be explained by the fact that the distribution of wealth gained by the company has been spent by the mine owner's tact and government policies. The region does not have proper infrastructures like roads, communication facilities, or health centers like hospitals.

5 Conclusions

This study evaluates the importance of sustainable development factors for Angouran lead and zinc mining complex using DEMATEL technique. This technique was selected as it not only calculates the importance of parameters but also represents the causal relations between them. Consequently, the main advantage of DEMA-

TEL methods is that the project owners can constantly improve project performance from both short-term and long-term perspectives. For this purpose, 30 important parameters of sustainability in Angouran region were investigated through field visits and literature. These parameters were categorized under three components of SD. Angouran region is an environmentally protected area, and this fact is being neglected by the mine owners. Therefore, it is out of doubt that forest protection and ecosystem have the highest impact on sustainability of the region, which is gained as a result of this study. Among economic factors, capital cost and final price are the most important among the impacting factors, since they have the highest influence on the feasibility of the mining project. In social factors, employment of local workforce has the most total exerted influence among the impacting factors. Culture and community in every town are in direct relation with resident people and employment structure in that town. It is quite natural that employment of local workforce has the highest total exerted influence. Taking into account the results of the study, mine planners and project owners recognize the negative impacts of their activities on the region in all three aspects of environment, economy, and society. Therefore, they are able to change their policies in this mine and implement some corrective actions and local optimization methods in areas where there is a state of emergency, to reduce the destructive effects of mining on the region.

References

1. Dubiński, J.: Sustainable development of mining mineral resources. J. Sustain. Min. 1–6 (2013)
2. Monjezi, M., Shahriar, K., Samini namin, F.: Environmental impact assessment of open pit mining in Iran. Environ. Geol. 205–216 (2009)
3. Osanloo, M.: Mine Reclamation (In Persian), 2nd edn. AmirKabir University of Technology Publishing Center, Tehran (2007)
4. Jeswiet, J.: Including towards sustainable mining in evaluating mining impacts. In: Procedia CIRP, 494–499 (2017)
5. Gastauer, M., ReisSilva, J., Caldeira Junior, C.F., JunioRamos, S.: Mine land rehabilitation: modern ecological approaches for more sustainable mining. J. Cleaner Prod. **172**, 1409–1422 (2018)
6. Bini, L., Bellucci, M., Giunta, F.: Integrating sustainability in business model disclosure: evidence from the UK mining industry. J. Cleaner Prod. **171**, 1161–1170 (2018)
7. Ranängen, H., Lindman, Å.: A path towards sustainability for the Nordic mining industry. J. Clean. Prod. **151**, 43–52 (2017)
8. Tiainen, H.: Contemplating governance for social sustainability in mining in Greenland. Resources Policy **49**, 282–289 (2016)
9. Moradi, G., Osanloo, M.: Prioritizing Sustainable Development Criteria Affecting Open Pit Mine Design: A Mathematical Model. Procedia Earth and Planetary Science **15**, 813–820 (2015)
10. Soltanmohammadi, H., Osanloo M., Aghajani Bazzazi, A.: An analytical approach with a reliable logic and a ranking policy for post-mining land-use determination. Land Use Policy **27**(2), 364–372 (2010)
11. Zeng, L., Wang, B., Fan, L., Wu, J.: Analyzing sustainability of Chinese mining cities using an association rule mining approach. Resources Policy **49**, 394–404 (2016)
12. Gu, J.-D.: Mining, pollution and site remediation. Int. Biodeterior. Biodegradation (2018)

13. Rahmanpour, M., Osanloo, M.: A decision support system for determination of a sustainable pit limit. J. Clean. Prod. **141**, 1249–1258 (2017)
14. Espinoza, R.D., Rojo, J.: Towards sustainable mining (Part I): valuing investment opportunities in the mining sector. Resour. Policy **52**, 7–18 (2017)
15. Osanloo, M., Rahmanpour, M.: Mine design selection considering sustainable development, Springer International Publishing, 151–163 (2014)
16. Tsai, S.B., Chien, M.F., Xue, Y., Li, L., Chen, Q.: Using the fuzzy DEMATEL to determine environmental performance: a case of printed circuit board industry in Taiwan. Plos One 129–153 (2015)
17. Liou, J.J., Yen, L., Tzeng, G.H.: Building an effective safety management system for airlines. Air Transp. Manage. 20–26 (2008)
18. Tzeng, G.H., Chiang, C.H., Li, C.W.: Evaluating intertwined effects in e-learning programs: a novel hybrid MCDM model based on factor analysis and DEMATEL. Expert Syst. Appl. 1028–1044 (2007)
19. Chang, B., Chang, C.-W., Wu, C.-H.: Fuzzy DEMATEL method for developing supplier selection criteria. Expert Syst. Appl. **38**, 1850–1858 (2011)
20. Bai, C., Sarkis, J.: A grey-based DEMATEL model for evaluating business process management critical success factors. Int. J. Prod. Econ. 281–292 (2013)
21. Mentes, A., Akyildiz, H., Yetkin, M., Turkoglu, N.: A FSA based fuzzy DEMATEL approach for risk assessment of cargo ships at coasts and open seas of Turkey. Saf. Sci. **79**, 1–10 (2015)
22. Lee, H.S., Tzeng, G.H., Yeih, W., Wang, Y.J., Yang, S.C.: Revised DEMATEL: resolving the infeasibility of DEMATEL. Appl. Math. Model. 6746–6757 (2013)
23. Angouran Lead and Zinc Mining Complex report (2017)
24. Yaylaci, E.D., Duzgun, H.S.: Indicator-based sustainability assessment for the mining sector plans: case of Afsin-Elbistan Coal Basin. Int. J. Coal Geol. **165**, 190–200 (2016)
25. Yaylacı, E.D., Düzgün, S.H.: Evaluating the mine plan alternatives with respect to bottom-up and top-down sustainability criteria. J. Clean. Prod. **167**, 837–849 (2017)

Safety Towards Zero Harm in the South African Platinum Sector

B. Genc, T. Mlangena and M. Onifade

1 Introduction

The South African mining industry is one of the largest industries in the country. The mining industry also remains one of the government's strategic tools for the economic freedom of its people as well as playing a role in the socio-economic development objectives such as provision of skills and employment [1].

Historically, the industry was infamous for the high fatality rates. In 2003, the industry stakeholders set a milestone towards combating the high fatality rates. The milestone was termed 'Zero Harm' and the target was to decrease injuries and fatalities by 20% year-on-year, eventually attaining zero injuries and fatalities. The date to review the industry's performance was set as 2013.

This paper analyses the improvements made by the industry and the factors that contribute to the successes and failures of the 'Zero Harm' initiative in the Platinum Group Metals (PGM) sector in South Africa.

2 Fatalities in the South African Mining Industry

The standard for reporting safety rates is per working hours [2]. The number of working hours to choose from is at the discretion of the company. However, this was not the case in the past when the companies used to record the fatality rates per 1000 men, which did not allow to benchmark companies against each other adequately [3].

The employees' safety was not a priority for management in the twentieth century [4]. In the PGM and gold sectors, the fatality rate in 1995 was 0.58 and 1.27 per million

B. Genc (✉) · T. Mlangena · M. Onifade
University of the Witwatersrand, Johannesburg, South Africa
e-mail: bekir.genc@wits.ac.za

hours worked, respectively [5]. Although commissions launched to investigate the causes and possible remedial solutions, safety records did not compare or come close to international standards. In 2003, the mining industry fatality rate for the United States of America, Canada and Australia combined versus South Africa was 0.07 and 0.3 per million man-hours worked, respectively [6].

The main causes of fatalities in the PGM sector are fall of ground incidents, accidents caused by transport or moving machinery and explosions [7]. The accident/incident theory states that being fallible and taking risks are part of the human condition. However, concentrating on the individual is one-sided. There are other fundamental aspects of undertaking substandard activities that should be considered such as situational and behavioural factors [8]. There are factors for and against the improvement of safety performance. The factors that are for safety improvements include continuing efforts to improve safety performance, improved defences, accident investigation/reporting, behaviour-based safety, internal/external auditing and safety management systems. Factors that are against improved safety are creeping entropy, Murphy's law, normalisation, routinisation and intrinsic hazards [8]. For effective policymaking and implementation, companies should take into cognisance both categories of contributing factors.

3   Selected Companies

The companies selected for the analysis are a good representation of the PGM sector as they are the top five PGM producers in the country, accounting for 97% [9] of the total PGM production in 2010 and 56% [10] of the world PGM production in 2011. The companies that were selected are as follows:

– Anglo American Platinum Limited,
– Lonmin Plc,
– Impala Platinum Holdings (Implats),
– Sibanye Platinum Division and
– Northam Platinum.

The data analysed is from 2005 to 2016. This period was chosen as it gives a good overall outline of the PGM sector. That is, evaluation can be done 2 years after the milestone was set, through the 2008–2009 financial crisis, through the 2012–2014 labour unrest and dispute in the PGM industry, for 2013 when the 10-year period ended and years preceding the 10-year deadline to observe if companies remained steadfast on the goal. The study is limited to fatality rates and is presented per million man-hours worked.
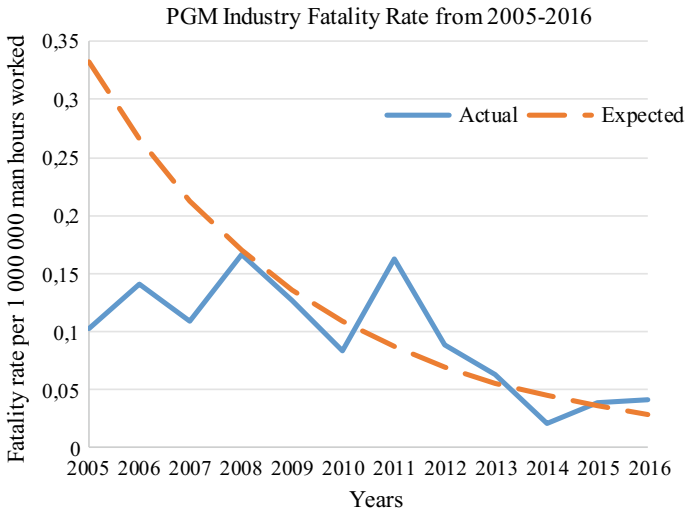
Fig. 1 Fatality rate for the PGM sector 2005–2016 [11–30]

4 Discussion and Analysis

4.1 Overall PGM Sector

The fatality rate improved by 59.6% from 2005 to 2016 (Fig. 1). For most of the years, the sector was performing within the expected targets. The sector recorded its highest fatality rate since 2005 in 2008 and recorded its lowest rate in 2014. From the expected target, although the fatality rate increased in 2008, it was still well below the target for that year. What is of concern is what happened in 2011 when the fatality rate spiked. The major causes of the fatalities were falls of ground, explosives as well as moving machinery.

In 2011, the PGM sector was recovering from the 2008–2009 global recession when the platinum price and production decreased [31]. The suggested reason for the increase in fatality rate is that employees overlooked safety standards. In 2014, the platinum sector experienced the longest platinum wage strike recorded [32]. This strike took place in the Rustenburg area, North West and mostly affected Anglo Platinum, Implats and Lonmin. The strike lasted 5 months. This means that for 2014, the employees' exposure time to underground workings was minimal. Consequently, the likelihood of workers incurring a fatality was reduced. It follows that specifically for the PGM sector, the fatality rates recorded were aided by the months that workers spent on strike and the time employees spent retraining after the lengthy strike.

Moreover, from 2012, there has been a decrease in the number of people employed in the PGM industry. The decline was still prevalent in 2016. A sharp decline is noted in the platinum price from the year 2014. The declining price of platinum forced

Fig. 2 Fatality rates for Anglo American Platinum Limited 2005–2016 [11–15]

operations to evaluate finances resulting in cost reductions by decreasing employment [33]. These retrenchments are still a reality in the PGM sector. Retrenchments imply there will be fewer labourers employed for underground work. Consequently, the fatality rates will decrease as the reduction in the number of workers takes place.

4.2 Anglo American Platinum Limited

Anglo American Platinum has operations across the Bushveld Complex, exploiting both the Merensky and UG2 reef. The reefs are extracted using underground mechanised, conventional and hybrid methods but Mogalakwena mine is using open pit operations.

Although Anglo Platinum did not reach the intended target of zero harm, there has been a steady decline in the fatality rate in the company as shown in Fig. 2.

What is interesting to note with Anglo Platinum is that the company grouped both the open pit and underground operations when reporting the fatality rates. This is misleading as the actual fatality rate is diluted. Underground operations and surface operations are inherently different, thus the risk one is exposed to is different.

Safety initiatives used by Anglo Platinum focused on behavioural, technical and labour solutions to combat the high fatality rates. However, these initiatives have not aided in achieving the 'Zero Harm' target.
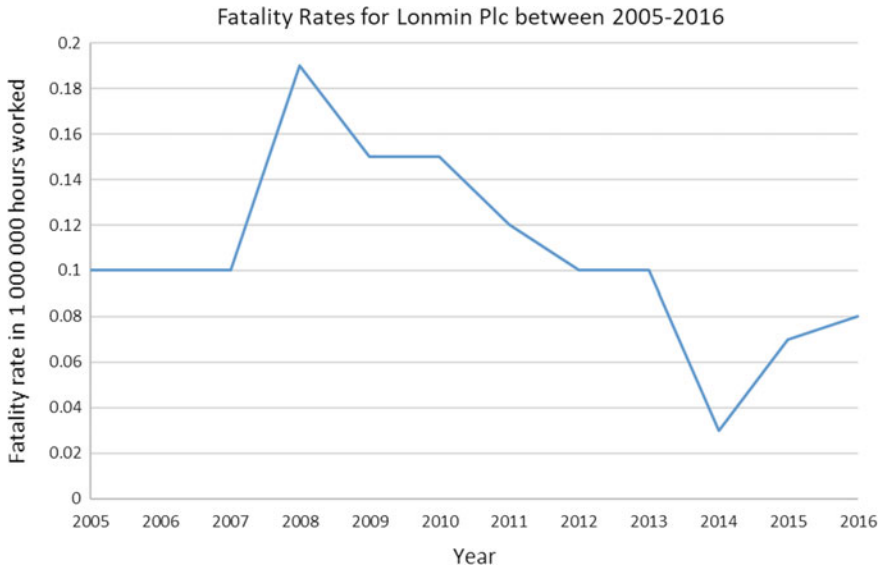
Fig. 3 Fatality Rates for Lonmin Plc 2005–2016 [24–27]

4.3 Lonmin Plc

Lonmin has operations of the western limb of the Bushveld Complex and exploits the Merensky and UG2 reefs using conventional mining methods. Lonmin attempted to mechanise their operations; however, the venture was unsuccessful due to the technical constraints associated with the geological conditions [34].

Lonmin Plc has had quite an interesting journey in the 'Zero Harm' initiative. The company has made a recovery 20% from the 2005 rates. The fatality rate in 2005 was 0.01 and 0.08 in 2016 as shown in Fig. 3. Lonmin Plc has no particular trend. This shows inconsistency in the company's approach to safety. These inconsistencies reflect on the company's organisational culture and behaviours used with regards to safety practices.

Lonmin's safety initiative focused on a strategy to strengthen leadership and accountability, improve the incident analysis process, incident closeout time and review and manage all critical and high-level risks and full implementation of the fatal risk protocols [25]. These initiatives should be reviewed as they have not produced the intended results of decreasing by 20% year-on-year.
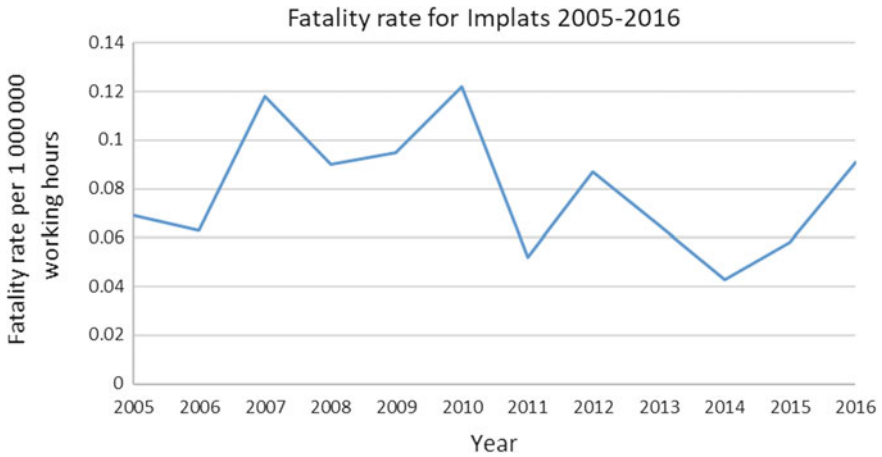
Fig. 4 Fatality rates for Implats from 2005–2016 [20–23]

4.4 Implats

Implats has operations in the Marikana region, on the western limb of the Bushveld Complex. The other operations of Implats are located in the Great Dyke of Zimbabwe, where geology and PGM grades are similar to that of the Bushveld Complex [35].

Implats had a raise of 30% from 2005 to 2016 in fatalities, as shown in Fig. 4. This went in the opposite direction to the vision of the mining industry. There is no visible trend for Implats, which shows many inconsistencies. In 2008, the company reported that the key areas in which the employees were struggling were the compliance with the safety procedures. The organisational culture seems to be a problem.

After a thorough analysis of the company's integrated reports, the manner of reporting has made it difficult to determine the reasons why the milestone was not achieved in 2013 and to identify potential sources for best practice. However, from the CEO's review, it was assumed that it is the lack of compliance to safety standards. The reports did not give any indications of the safety initiatives used in attaining the 'Zero Harm' vision. An on-site investigation would be necessary to understand the reasons for the poor safety performance as well as the initiatives used to combat the safety problem.

4.5 Sibanye Platinum Division

The Sibanye Platinum Division has operations situated on the western limb of the Bushveld Complex and exploiting both the Merensky and UG2 reef.
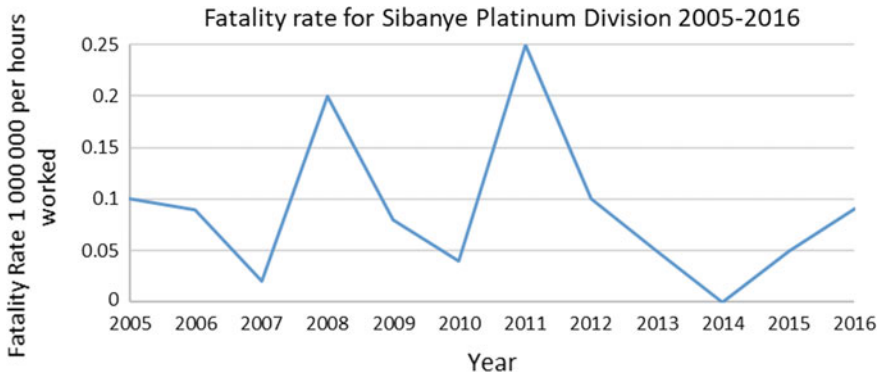
Fig. 5 Fatality rate for Sibanye Platinum Division [16–19]

The data preceding 2015 was obtained from Aquarius Platinum mine integrated report as Sibanye Platinum acquired these from the aforementioned mine. Figure 5 shows that in 2011 when the company reached its highest fatality rate since 2005, they understood that change is needed to be done.

The company implemented a new safety system. The company understood that the main cause of the fatalities increase was due to the attitudes and behaviour of the employees rather than the inherent dangers of mining. They set to make a change. An integrated safety system was introduced [18]. This initiative was implemented in four steps; planning, implementing, monitoring and measurement, and management review. The distinguishing feature of the safety plan laid out by Aquarius Mine was that a behaviour-based approach was implemented. This was unprecedented in the South African mining sector. The company also had an 'I commit to comply' initiative in which employees committed to complying with the safety standards. The results show how companies can begin shifting the organisational culture.

4.6 Northam Platinum

Northam Platinum has operations on the western limb of the Bushveld Complex and exploits the Merensky and the UG2 reef using mechanised mining methods. Figure 6 shows that Northam Platinum Limited had a reduction of the fatality rates by 100%. This is the best safety performance for the companies analysed. Northam Platinum seemed inconsistent; however, as from 2011, there was a decrease until the company reached zero harm, albeit a year after the intended goal date.

Safety initiatives used by Northam were as follows:

– the 'back to basics' approach, which involved enforcing the basic procedures for safety,
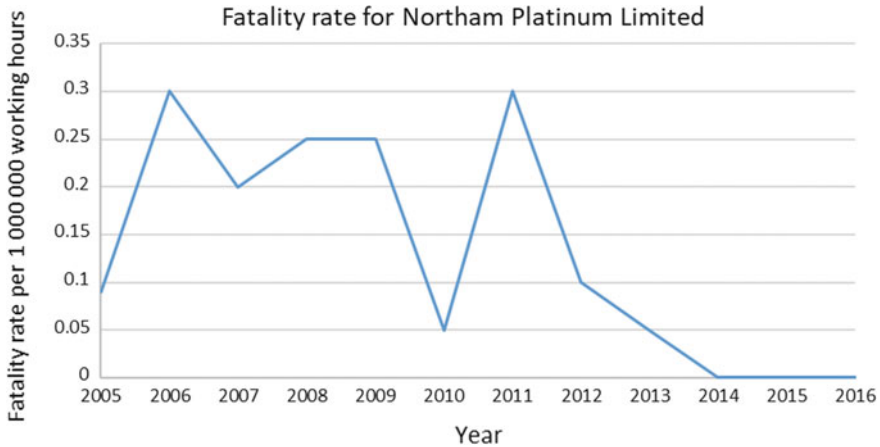
Fig. 6 Fatality rate of Northam Platinum Limited from 2005 to 2016 [28–30]

– 'crack squads' to monitor and remediate through appropriate coaching in the work-
  place,
– the 'shared care' notion, which aimed to instil a shared duty of care amongst
  employees at all levels in the company.

Northam Platinum attributes the majority of its success to the mechanisation
mining method as it is safer than the conventional method due to less people being
exposed to the face.

5   Conclusion

The platinum sector has failed to meet the intended milestone of zero harm. The
trend was a reduction in the reported fatality rates, albeit there has been an increase
in fatality rates in 2015 and 2016. Companies still report fall of ground, transport
and machinery as well as explosives as being the main causes of fatalities.

The best performing company overall was Northam Platinum; not only has
Northam Platinum decreased the number of fatalities each year but it has also man-
aged to reach the 'Zero Harm' target for the operations managed, although it was
reached after the 10-year period set by in the 'Zero Harm' initiative. Anglo Platinum
showed the most improvement amongst the other companies while Implats was the
least improved company and furthest from the target of a 20% decrease year-on-year
and 'Zero Harm' vision.

From the analysis of results, it can be deduced that, with the exception of Sibanye
and Northam Platinum, the companies' organisational culture have poor standard.
The challenges faced by the companies seem to be similar. There is a notion of
non-compliance to safety procedures by the employees. The policies placed much

emphasis on the right procedures being followed but very little on the behavioural and mindset attitudes; only Sibanye and Northam focused their safety initiatives on the latter. It is thus concluded that focusing on the behavioural aspects of the employees is a potential source for best practice; not only will 'shared care' and 'back to basics' aid in reducing the fatalities but will also improve the companies' organisational culture.

References

1. Genc, B.: Where is platinum heading? In: Third International Platinum Conference 'Platinum in Transformation', South Africa, 401–406 (2008)
2. Nosa: Nosa HSE Qualifying Criteria and Classification of Incidents. https://www.nosa.co.za/downloads/AUDP11_10_2015.pdf (2015). Accessed 3 May 2017
3. Ekevall, E., Gillespie, B., Riege, L.: Improving Safety Performance in the Australian Mining Industry Through Enhanced Reporting. PricewaterhouseCoopers, Brisbane (2008)
4. Simons, H.J.: Death in South African Mines. University of Cape Town (1960)
5. South African Colliery Managers: South Africa Mine Statistics. Available at: http://www.sacollierymanagers.org.za/June2004_Att.pdf (2004). Accessed 22 June 2017
6. Hermanus, M., Coulson, N., Pillay, N.: Mine Occupational Safety and Health Leading Practice Adoption System (MOSH) examined—the promise and pitfalls of this employer-led initiative to improve health and safety in South African Mines. J. S. Afr. Inst. Min. Metall. **115**(08), 717–726 (2015)
7. Leger, J.P.: Trends and causes of fatalities in South African mines. University of the Witwatersrand, Johannesburg (1991)
8. Gutierrez, A.M.J.: Theory of Accident Causation, 5th edn. Occupational Safety and Health, Washington (2010)
9. Genc, B., Stacey, T.: Towards benchmarking of safety performance in the platinum sector. In: Fifth International Platinum Conference, South Africa, 123–142 (2012)
10. International Platinum Group Metals Association: (PGMs), The primary production of platinum group metals. International Platinum Group Metals Association, Munich (2013)
11. Anglo American Platinum Limited: Integrated Annual Report. Anglo American Platinum Limited, Johannesburg (2004)
12. Anglo American Platinum Limited: Integrated Annual Report. Anglo American Platinum Limited, Johannesburg (2006)
13. Anglo American Platinum Limited: Sustainable Development Report 2007. Anglo American Platinum Limited, Johannesburg (2007)
14. Anglo American Platinum Limited: Integrated Annual Report. Anglo American Platinum Limited, Johannesburg (2013)
15. Anglo American Platinum Limited: Ore reserves and Mineral Resources Report 2016. Anglo American Platinum Limited, Johannesburg (2016)
16. Aquarius Platinum Limited South Africa: Annual Integrated Report (2006)
17. Aquarius Platinum Limited South Africa: Annual Integrated Report (2010)
18. Aquarius Platinum Limited South Africa: Annual Integrated Report (2011)
19. Sibanye: Annual Integrated Report (2016)
20. Impala Platinum Holdings: Annual Integrated Report. Impala Platinum Holdings (2003)
21. Impala Platinum Holdings: Annual Integrated Report. Impala Platinum Holdings (2006)
22. Impala Platinum Holdings: Annual Integrated Report. Impala Platinum Holdings (2010)
23. Impala Platinum Holdings: Annual Integrated Report. Impala Platinum Holdings (2016)
24. Lonmin Plc: Lonmin Annual Report. Lonmin Plc, London (2004)
25. Lonmin Plc.: Sustainability Report. Lonmin Plc, London (2007)

26. Lonmin Plc: Lonmin Annual Report. Lonmin Plc, London (2010)
27. Lonmin Plc.: Lonmin Annual Report. Lonmin Plc, London (2016)
28. Northam Platinum Limited: Annual Integrated Report. Northam Platinum Limited (2006)
29. Northam Platinum Limited: Annual Integrated Report. Northam Platinum Limited (2010)
30. Northam Platinum Limited: Annual Integrated Report. Northam Platinum Limited (2016)
31. Chamber of Mines of South Africa: Facts and Figures. Chamber of Mines of South Africa, Johannesburg (2016)
32. Saho: Marikana Massacre 16 August 2012. [Online]. Available at: http://www.sahistory.org.za/article/2014-south-african-platinum-strike-longest-wage-strike-south-africa (2014). Accessed 3 August 2017
33. Morrison, L.: PGM Explorer Notifies Union of Retrenchments. [Online] Available at: http://m.miningweekly.com/article/pgm-explorer-notifies-union-of-retrenchments-2009-01-30 (2009). Accessed 9 August 2017
34. Webber, G., Berg, A.A.V.D., Roux, G.L., Hudson, J.: Review of Mechanization Within Lonmin. The Southern African Institute of Mining and Metallurgy, Johannesburg (2010)
35. Cawthorn, G.R.: The platinum group element deposits of the bushveld complex in South Africa. Platin. Met. Rev. **54**(4), 205–215 (2010)

A Move to a 12-Hour Working Shift—The Benefits and Concerns

S. M. Rupprecht

1 Introduction

Traditionally, the South African mining industry has worked an 8-hour 22-minute (8 h 22 min) 11-shift fortnight work cycle. In the later twentieth century, there was a discussion to move to full calendar operations but this never gained full acceptance by the industry. However, over time working faces have moved deeper and further from the shaft as depicted in an isometric view of a layout for a deep-level mine (Fig. 1). Based on recent reviews of working shift cycle times currently encountered by the South African mining industry, it would appear that the current 8-h 20-min (500 min) shift may not support a daily conformant blast. Not only are the shift times adversely affected by the times required to travel to and from the stope but also productivity is often negatively impacted by the age of the infrastructure (low compressed air pressure, poor track conditions) combined with hot working conditions and often stopes are having wet bulb temperatures above 30 °C.

A recent time study [1] conducted on a South African operation (Table 1 and Fig. 2) indicates that some workers are working longer than the stipulated 45-h work week, e.g. 8 h 20 m per day, that is, set by the Basic Conditions of Employment Act, 1997 (ACT 75 of 1997).

Table 1 The estimated hours worked in an underground platinum [1]

Legal hours	Stope A	Stope B	Stope C	Stope D	Stope E
08:20/shift	10:37S	08:40	10:56	13:01	09:33
45:00/week	52:07	43:30	54:45	65:12	47:50

S. M. Rupprecht (✉)
Department of Mining Engineering and Mine Survey,
University of Johannesburg, Johannesburg, South Africa
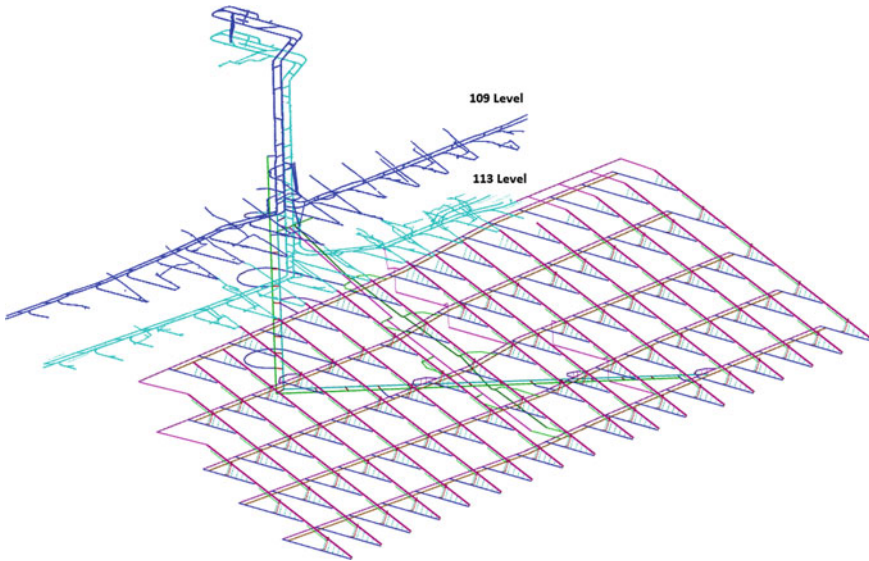e-mail: stevenr@uj.ac.za

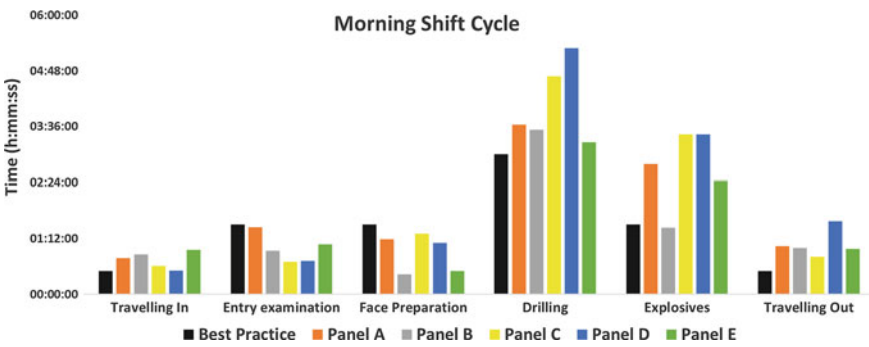**Fig. 1** Isometric view of a deep-level gold mine layout

Fig. 2 Activities of morning shift time compared to best practice [1]

Figure 2 provides information where the working cycle is above the 'best practice'. Notably, travelling to and from the stope face takes longer than prescribed with drilling and charging up taking much longer than scheduled.

2 Mining Cycle

As mining operations progress deeper with working place located as far as 7 km from the shaft, the available time to conduct stoping activities is shrunk due to the
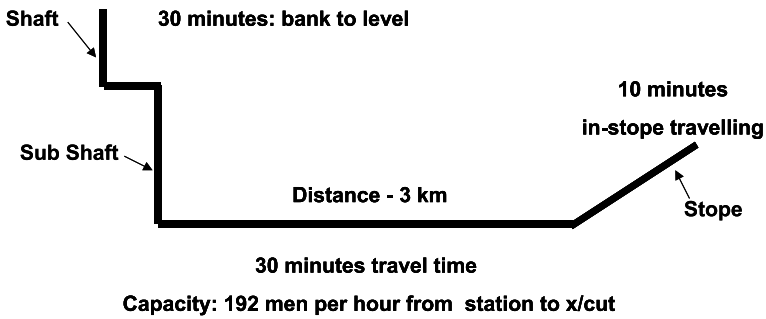
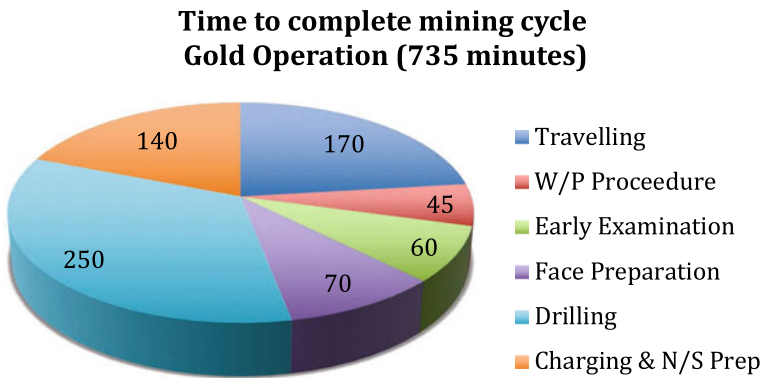**Fig. 3** Travelling time to working face [2]

Fig. 4 Time to complete mining cycle in a South African gold operation

time required to travel to and from surface. For shallow or near-surface underground mines, this time may only account for 1–2 h of the shift period (Fig. 3).

For deeper operations, travel times through vertical/tertiary shaft systems combined with horizontal transportation may account for 3 h (Fig. 4) of the shift period. The face time is further reduced when one considers other legal requirements associated with the South African mining industry; legal obligations such as safety meetings at the waiting place, early safety examinations and the addition of face roof bolting and safety nets for narrow vein stoping. Over 12 h (735 min) may be required to complete a daily blast over a 30 min panel in a gold mine.

Based on the findings of Nelwamondo et al., and the above cycle time, it is clear that to achieve a daily panel blast some workers may be required to work in more than 8 h 20 min. Therefore, there is a real need for the South African gold mining industry to review its current shift time.

Currently, the South African mining industry is researching ways to improve mining productivity. Concerns such as shaft scheduling, horizontal transportation, drilling and blasting, and stope cleaning have been identified with the hopes to reduce the required cycle time requirements to complete a daily blast.

3 Motivation to Change to a 12-Hour Shift

It is clear that the current mining cycle can support a daily panel blast within the allotted 8 h 20 min (500 min) period. Although the introduction of new technology, such as electro-hydraulic rock drilling, may reduce a particular section of the mining cycle, holistically, the message is clear that modifications to the current mining cycle are required.

It is recommended that the South African gold sector investigate the introduction of more extended shifts, thereby ensuring a conformant daily blast. This would result in a change of the work shift from an 11-shift fortnight to 4-day/3-day fortnight cycle or something similar. Notably, this would require a mindset change from labour and management and would require serious negotiations with unions. Although some see negotiations with unions as a considerable hurdle, there are many benefits that should convince labour to welcome this change. Positive spin-offs of adopting a 12-h shift is (1) the ability for labourers to get 3 or 4 days off in the week to relax or conduct personal business and (2) the 12-h shift change will require additional workers to complete a 4-day on 3-day off (week 1) and 3-day on 4-day off (week 2) work cycles. Under these circumstances, unauthorised absenteeism should reduce, as workers will have sufficient time to conduct personal business and overcome fatigue while working full calendar.

Importantly, a change to a 12-h shift can only work if daily quality blasts are achieved, i.e. face advances in the order of 20 min or more would be required, to make the change economically viable.

Many mining operations over the world operate on a 12-h shift basis, and the effect of this mining shift cycle has been investigated. According to Moore-Ede et al. [3], some of the concerns raised over the working of a 12-h shift are as follows:

– Increased work time in a harsh mining environment, where operating temperatures are well above the perceived acceptable temperature of 28 degrees.
– When one considers that workers must travel to and from their homes to get to work, a worker could spend 14 h away from home resulting that workdays leave little time for activities other than work, meals and sleep with no spare time for social time during workdays.

Countering the above-stated concerns are the following highlighted benefits of a 12-h shift:

– Sufficient time is provided for work teams to complete the necessary tasks to obtain a safe daily quality blast.
– Currently, absenteeism is a problem as mineworkers struggle to find sufficient time to handle issues that require their physical presence.
– As some workers are already working extended shifts—workers time will be officially recognised thus enabling a worker to rest 3 to 4 days per week.
– The longer shift supports one-miner one-panel which reduces the face length and ventilation requirements of a mine when compared to providing a miner with two panels (double face length requirements and ventilation requirements).

– Achieving a daily blast—promoted by the additional time provided to complete all activities to achieve a daily blast—equates that all the work leading to a blast, i.e. travelling, entry procedure, support, etc. all result in attaining a blast.

4 Concerns

Unlike other operations, many South African gold mines operate at extreme depths with several operations working below 3000 mbs. At these depths, virgin rock temperatures can be in the region of 56.2 °C with stope environmental conditions reaching in the region of 32 °C.

Ventilation is a costly component to mining for gold mines. Not only concerning the money spent to operate fans or providing cooling but also there are safety and productivity correlations when wet bulb temperatures are above 30.5 °C. According to Smith [4], an increase in the injury rate was recorded from 16.3 incidents to 41.8 incidents per 1000 employees per annum and productivity (tonnes/worker/month) decreased by 40% with the increase in the wet bulb temperature.

According to Brake et al. [5], 'a large number of safety injuries and incidents where persons work in heat may be caused by mental and physical decrements as a consequence of poor hydration'. With many deep mining stopes operating in temperatures above 30 °C, the question is raised if stope workers can work extended periods in these hot and humid conditions. This is the research that will need to be conducted before 12 shifts can be implemented. Mitigating strategies will also need to be considered, such as cooling garments or schedule breaks in cool rooms based on temperature and type of work.

It is clear, even for 8-h 20-min shifts, the deep-level gold operations must reduce their in-stope temperatures to approximately 28.5 °C or below. This will be even more critical if a 12-h shift is adopted. Under these lower temperatures, workers should be able to work longer shifts. However, it will still be a good idea to make provisions to combat worker fatigue and heat exhaustion.

5 Conclusion

The 12-h shift is used worldwide but is not commonly used in South Africa, as the 8-h 20-min 11-shift fortnight cycle is the standard and preferred work shift. However, as gold mining operations migrate deeper and further from the shaft and additional task have been introduced into the mining cycle, it is becoming difficult for stope crews to complete the blasting cycle within a single shift. This results in workers either extending their working shifts or a lost blast to occur. Therefore, it has become necessary for the mining industry to consider moving to a 12-h shift to complete a conformant daily blast. Mine management, labour and government must be open minded regarding the proposed shift change. There are both benefits and

concerns regarding the proposed shift change, in which providing more free time and increasing employment are perceived benefits, and concerns are the fear of not achieving the perceived increase in production and the requirement to reduce stope temperatures. The South African gold mining industry must investigate the viability to move to 12-h shifts, and therefore must engage with both labour and government as well as conduct research to establish the feasibility of the proposed shift change.

References

1. Nelwamondo, P., Mpanza, M., Rupprecht, S.: The influence of work pressure on worker attitudes towards health and safety in a platinum mining stope. In: Society of Mining Professors 6th Regional Conference Johannesburg, 12–14 March 2018 The Southern African Institute of Mining and Metallurgy, (2018)
2. Rupprecht, S.M., Williams, S.B.: Audit and review of current man transport systems. Deepmine Task 12.1.1, CSIR Division of Mining Technology, Johannesburg (2000)
3. Moore-Ede, M., Davis, W., and Sirois, W.: Advantages and disadvantages of twelve-hour shifts: a balanced perspective. Circadian Inf. Limited Partnership (2007)
4. Smith, O.: The effects of a cooler underground environment on safety and labour productivity on President Steyn Mine: In Gill A.J., et al. (ed) Proc. Mine Safety and Health Congress, Johannesburg Chamber of Mines of South Africa (Mine Safety Division), pp. 105 –112 (1988)
5. Brake, R., Donoghue, M., Bates, G.: Management of heat stress in a hot, humid, underground environment. Saf. Sci. Monit. (1999)

Part X
Mineral Processing

Optimizing the Rougher Flotation Process of Copper Ore

I. Derpich and V. Monardes

1 Introduction

Mining is one of Chile's priority economic sectors, accounting for 9% of GDP; however, there is a low level of technology adoption in decision-making in the mining company, which results in low production efficiency [1]. Mining production costs are divided into operating costs (mine costs + processing costs + transport costs), plus financial and depreciation costs. The natural factors in mining productivity are the ore grade to which, the higher the law, the higher the productivity, and vice versa. The natural factors in mining labor productivity are the hardness of the mineral, the sterile mineral-to-copper ratio, the availability of water, environmental, and health aspects. The costs of the process of obtaining copper concentrate represent 77% of the total cost. One ton of copper concentrate is sold at US $ 6090, from which the following cost structure can be derived [1]. Given that the price of the concentrate is an exogenous variable that cannot be influenced, companies should focus on the cost of production and especially on operational costs. The average operational cost of the copper mining industry in Chile reached a value of 225 c/lb in 2015, it was 4.4% greater than 216 c/lb in 2014. By bringing operational costs to a form of cash cost according to Chilean Copper Corporation (COCHILCO), the average value of the country reached 174 c/lb in 2015, 9.2% higher than the price in 2014. On the other hand, in 2016 the operational cost was 225 c/lb. When comparing these prices with international data, it is concluded that the country is 28% above the world average, with 75% of world production at a cost lower than the Chilean average [1]. For this

I. Derpich
Industrial Department—OPTILAB, University of Santiago of Chile, Santiago, Chile

V. Monardes (✉)
Industrial Department, University of Antofagasta, Antofagasta, Chile
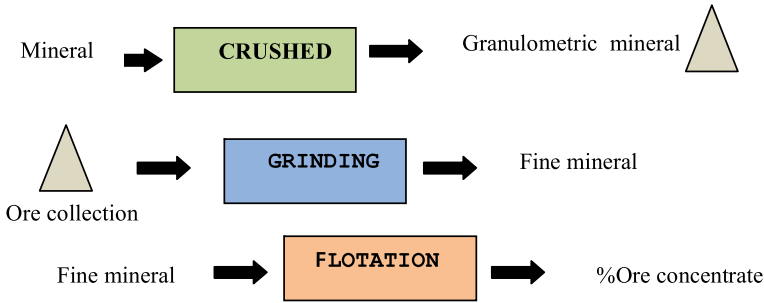e-mail: vinka.monardes@uantof.cl

Fig. 1 Diagram of the process of obtaining copper concentrate from sulfur

reason, it is a key that Chilean companies refine their production processes in order to optimize copper production processes.

This paper focuses on optimizing the parameters of the copper ore flotation process, which is the most expensive in obtaining copper concentrate, in order to improve the copper grade, corresponding to the fine copper law in the copper concentrate and metallurgical recovery, in order to obtain more final tons of fine copper, in the concentrate. The improvement of the ore and the metallurgical recovery also reduce the total cost of operation per unit, due to a lower cost of the concentrate by dividing the total cost by a higher production. In addition, there are aspects related to the raw material that enters the process, such as the ore grade and the hardness of the incoming rock. In these aspects are the mixed technical concepts of process structure, such as crushing, grinding, and flotation circuits (see Fig. 1); and chemical aspects such as the reagents used, the concentrations, and quantities processed. This also depends on the administration and decision-making of the process. For example, it is interesting to know in the flotation process that the combination of reagents for a given grade of ore in the raw material produces the maximum copper ore grade in the final concentrate and, in the same way, it is sought to determine how the maximum amount of copper can be obtained during metallurgical recovery.

1.1 The Flotation Process

Flotation with foam is one of the most important and widespread concentration methods, which is based on exploitation of the differential properties of valuable minerals and gangue, also known as wettability [2]. The flotation circuit generally involves a number of stages or subcircuits. Each subcircuit consists of several cells of connected tanks where the flotation process is carried out. Before the actual flotation process, the mineral particles reach the stirred tank (conditioner) and mix with water and reagents that make the valuable minerals within the flotation paste hydrophobic. When air bubbles are introduced into the pulp, hydrophobic mineral particles join and rise to the surface of the water, forming foam. The foam is collected from the

surface as the mineral-rich concentrate, while the remaining pulp becomes the feed to the next cell or flotation section, or the circuit is discarded as tailings. In the conditioner, the collectors, foamers, and pH modifiers are mixed well. The rougher stage produces a final concentrate of 26% copper. Final relave with a law of 0.13% copper and final concentrate of the mill with a 16% copper grade. The tail of the rougher cells feeds the scavenger cells (see Fig. 2).

The industrial sector is more interested in new technologies due to the new economic and environmental challenges as well as the question of the exhaustion of high-grade deposits. Models and optimization techniques arise naturally when dealing with the problem of the design of optimal flotation circuits. According to [3], all known optimization approaches can be classified into four general groups: mathematical methods based on techniques without integer variables, methods based on mathematical techniques with integer variables, heuristic methods, and evolutionary methods based on genetic algorithms. The first group includes mainly some initial approaches based on Linear Programming (LP), techniques based on Markov chains, dynamic programming [4] as well as simple methods of nonlinear optimization, direct search, random search, reduced gradient procedures, etc. [5]. It should be noted that such optimization techniques are usually heuristic, whose convergence rates and the quality of the solution found cannot be confirmed theoretically. In addition, they are
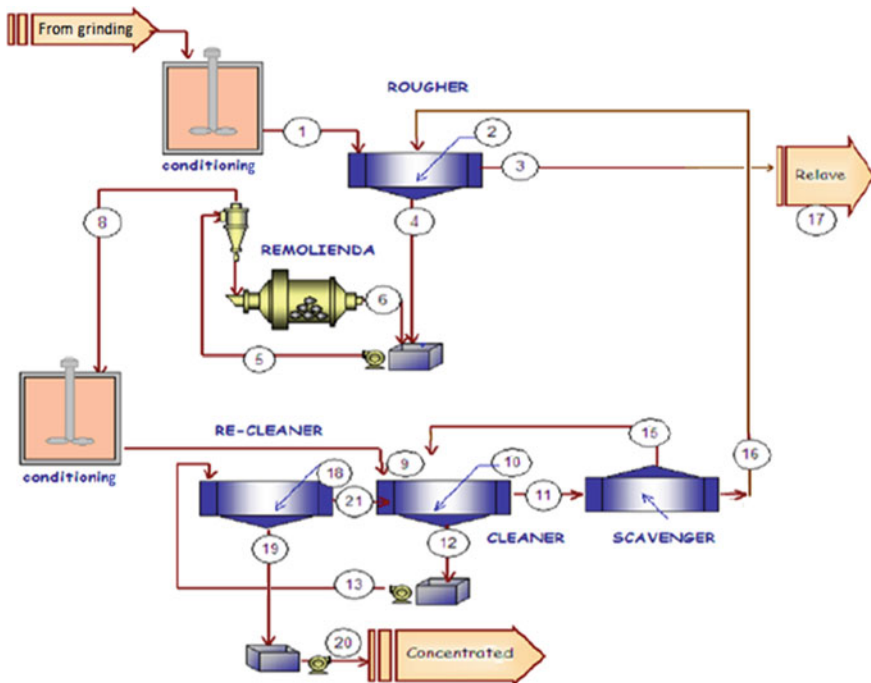

Fig. 2 Flotation process diagram

often more sensitive to the choice of starting points. On the other hand, the objective function often contains some nonlinear terms (for example, reflect economies of scale for the capital costs of the process units) that make the optimization problem not convex. In this case, any conventional optimization method, by gradient algorithms, has not been shown to converge to the global optimum and, therefore cannot be directly applied. Other authors consider statistical techniques, for example, response surface methodology, combined with convex commercial software solvers to optimize a flotation process [6–8]. Finally, there are genetic algorithms and basic metaheuristic approaches to optimize the design and performance of the flotation circuit. In [9] the genetic algorithms of non-dominated selection with the operator of the modified jump gene are developed with the objective of optimizing the performance of the foam flotation circuits. The authors address several variants of a single objective (for example, maximizing recovery according to the desired level of concentration) and multi-objective optimization problems (up to four criteria) and affirm that the approach developed is successful in finding optimal global solutions (Pareto).

However, as mentioned in [3], although the genetic algorithms allowed the authors to obtain solutions that are better in comparison with the "traditional" methods, there is no exact argument that the solutions found are the global optimum. Other implementations of genetic algorithms for the optimization of the flotation circuit design include a process-oriented variant that takes into account some technological limitations in order to simplify the configuration of the circuit [10], a genetic combined with modeling of pulp and foam phase in each flotation cell [11], a multi-objective genetic algorithm to determine an optimal circuit configuration for a coal washing plant with respect to two performance indices [12]. Other studies address evolutionary algorithms combined with careful experimental design techniques and regression analysis to optimize a flotation process and determine its best performance. For example, [13] studied the column flotation of an igneous apatite mineral and considered three independent variables (collector dose, depressant dosage, and airflow rate) that affect four responses: P_2O_5, Fe_2O_3, SiO_2, and recovery of P_2O_5. It must be taken into account that the main disadvantage of the algorithms of multi-objective evolution is their inability to guarantee the Pareto optimality of the solutions found. It is only known that none of the generated solutions dominates the others. As mentioned, most design optimization approaches for current flotation and performance circuits are based on commercial solvers and evolutionary algorithms that converge too slowly or cannot guarantee global optimality, especially when the corresponding optimization problem is not convex. In addition, the real problems involve multiple objective functions that must be optimized simultaneously and, as far as we know, almost all the solution methods developed are metaheuristic or involve adding multiple objectives in a single one that often does not provide a good approximation to the set of optimal values of Pareto.

1.2 Optimization Models in Mineral Processing

Metallurgically, it becomes complex to take the process under control according to the optimal expected in the feeding of the process. In addition, it should be added that because the desired separation cannot be achieved in a single stage, several coupled stages are used, which are called flotation circuit. The behavior of the whole process, therefore, depends on the configuration of the circuit and the chemical and physical structure nature of the treated pulp [14].

One of the first attempts to use deterministic techniques of global optimization and multi-objective optimization to improve the performance and efficiency of the flotation process, based on mathematical programming to solve a problem with bi-objective applied. It was developed by [15], supported by the base of studies [16, 17] and others. In general, the flotation process is controlled by operators who make their decisions according to the experience obtained in the field, obtaining in some cases deficient performance, which translates into a decrease in the profitability of concentrate production.

2 A Practical Case

In this section, we carry out a case study to maximize the ore grade in the copper concentrate and determine the best operating conditions (for example, reagent dosages) of the flotation process in a mineral processing plant in Chile.

Our methodology consisted of a linear regression type study for the estimation of the copper law on one side and metallurgical recovery on the other. We searched for the variables that affect the copper law and metallurgical recovery. However, only relationships between these variables and the fine copper law were found at the end of the copper concentration process. The built model is a simple model of six explanatory variables, which responds to a first look at the problem; however, the results obtained are consistent with the reality of the process and is a good tool for estimating tons of fine copper in the concentrate copper made.

2.1 Identification Problem and Model Formulation

To model the copper ore flotation process, an analysis was made on the factors that affect the results of the process. We choose the following seven factors as independent variables. Table 1 shows the values of the case of a condition.

where
x_1 is the addition of type 1 collection agent (in grams per ton),
x_2 is the addition of type 2 collection agent (in grams per ton),
x_3 is the consumption of foaming agent (in grams per ton),

x_4 is the content of 74 μ of grain class in the hydrocyclone overflow (in % mass),
x_5 is the total copper grade in the feed, in % mass, and
x_6 is the total content of oxidized copper in the feed (in % mass).

Let Y_i be the metallurgical recovery of lot i and x_i corresponds to each of the independent variables in Table 1.

$$Y_i = \alpha_1 \, x_1 + \alpha_2 \, x_2 + \alpha_3 \, x_3 + \alpha_4 \, x_4 + \alpha_5 \, x_5 + \alpha_6 \, x_6 \tag{1}$$

The intercept is zero, because the adjustment led to the regression line passing through the zero value. It must be borne in mind that, although we study a specific flotation process for copper ores, its oxidized degree can vary within a range. Therefore, the range of copper grades in the feed was also chosen as independent variables

Table 1 Predictive variables of the tons of fine copper in percentage evaluated at the point of the process

	Variables	Minimum	Maximum	Unity	Coefficients	Values
1	Addition of primary collecting agent	15	30	gr/ton	22.5	0.658
2	Addition of secondary collector agent	3.75	7.5	gr/ton	5.625	0.699
3	Consumption of foaming agent	25	35	gr/ton	7.5	0.97
4	Content of 74 microns class of grain in the overflow of hydrocy-clones	23	25	%	24	0.13
5	Copper law at the entrance	0.7	1	%	1%	0.629
6	Total oxidized copper content at the entrance	0.02	0.04		0.03	0.847
Average						29.16
Metallurgical recovery						90%
Ton Cu in the ore concentrate						26.25

for its study. The regression coefficients were obtained from a study experiment for the copper ore at the end of the process. Regarding metallurgical recovery, this was assumed in 90% according to what was declared by the company. In the data of Table 1, only the prediction of the fine copper ore in the copper concentrate has been considered, due to the lack of data that relate variables x_1 to x_6 with metallurgical recovery values. This means that the linear regression model implicit in Table 1 does not show the process in all its technical complexity. This also implies that not all the values of the variables x_i can be represented in the regression equation.

2.2 Discussion of the Results

One of the first attempts to use deterministic techniques of global and multi-objective optimization to improve the performance and efficiency of the flotation process, based on mathematical programming to solve a problem with bi-objective applied, was dabbled by [15], relying on its base of studies in some authors like [16, 17]. In general, the flotation process is controlled by operators who make their decisions according to the experience obtained in the field, obtaining in some cases deficient performance, which translates into a decrease in the profitability of concentrate production, with this model can be oriented in the management of the ranges of various parameters, in order to obtain an estimate of the copper law on the one hand and metallurgical recovery on the other.

Table 1 shows the coefficients of linear regression that predicts the behavior of the percentage of recovered copper concentrate variables. The parameters that were significant are the six shown in Table 1. It should be noted that the law variables of copper concentrate and metallurgical recovery influence the tons of fine copper as follows: Fine copper ton = % entry copper grade *% metallurgical recovery * tons of ore processed.

We also developed a regression model similar to that estimated for the copper concentrate law, for metallurgical recovery, but no statistically significant values were obtained. Therefore, to estimate the final tons of fine copper, a recovery of 90% was assumed, which is the figure declared by the company in which this work was done.

Our methodology is simple to use, based on linear regression for the estimation of the copper law on the one hand and metallurgical recovery, so that operators can familiarize without inconvenience. This built model responds to a first look at the problem; however, the results obtained are consistent with the reality of the process within the mining company and is a good tool for estimating tons of final copper in the concentrate.

It is known that the behavior of the global flotation process depends on the configuration of the circuit and the chemical and physical structure nature of the treated pulp [14]. This point is important to highlight, since the conditions found are particular to the mining company. So it should be made clear that the results obtained are only valid for this particular process.

3   Conclusions

The relationship found between the variables of the process and the copper law showed a linear relationship. This was done using a linear regression model. The data used to establish this linear model cannot be published for reasons of confidentiality. The data was adjusted so that the model has zero intercept. The regression obtained does not allow to represent all the values of the independent variables fully, which may be due to the fact that this linear model leaves out other variables, such as metallurgical recovery among others.

Due to the diversity of the geological aspects between the copper ore deposit, which implies different structures between the chemical and physical conditions of these, in addition to various configurations that make up the flotation cells between concentrate plants, it is interesting to replicate this study in other mining plants, in order to verify if the quotients of the parameters and the model are confirmed for other characteristics.

References

1. Cochilco: Mercado, tendencias, demanda, productos y usos, registro de propiedad intelectual número 285490
2. Moimane, T.M., Corin, K.C., Wiese, J.G.: Investigation of the interactive effects of the reagent suite in froth flotation of a merensky ore. Miner. Eng. **96**, 39–45 (2016)
3. Méndez, D.A., Gálvez, E.D., Cisternas, L.A.: State of the art in the conceptual design of flotation circuits. Int. J. Miner. Process. **90**, 1–15 (2009)
4. Maldonado, S., Richard Weber, R.: A wrapper method for feature selection using support vector machines. Inf. Sci. **179**, 2208–2217 (2009)
5. Yingling, J.: Parameter and configuration optimization of flotation circuits, part II. A new approach. Int. J. Miner. Process. **38**, 41–66 (1993)
6. Azizi, A.: Optimization of rougher flotation parameters of the sarcheshmeh copper ore using a statistical technique. J. Dispersion Sci. Technol. **36**, 1066–1072 (2015)
7. Aslan, N., Fidan, R.: Optimization of Pb flotation using statistical technique and quadratic programming. Sep. Purif. Technol. **62**, 160–165 (2008)
8. Rath, S., Sahoo, H., Das, B.: Optimization of flotation variables for the recovery of hematite particles from BHQ ore. Int. J. Miner. Metall. Mater. **20**, 605–611 (2013)
9. Guria, Ch., Varma, M., Mehrotra, S.P., Gupta, S.K.: Simultaneous optimization of the performance of flotation circuits and their simplification using the jumping gene adaptations of genetic algorithm. Int. J. Miner. Process. **77**, 165–185 (2005)
10. Ghobadi, P., Yahyaei, M., Banis, S.: Optimization of the performance of flotation circuits using a genetic algorithm oriented by process-based rules. Int. J. Miner. Process. **98**, 174–181 (2011)
11. Hu, W., Hadler, K., Neethling, S.J., Cilliers, J.J.: Determining flotation circuit layout using genetic algorithms with pulp and froth models. Chem. Eng. Sci. **102**, 32–41 (2013)
12. Pirouzan, D., Yahyaei, M., Banisi, S.: Pareto based optimization of flotation cells configuration using an oriented genetic algorithm. Int. J. Min. Process. **126**, 107–116 (2014)

13. Barrozo, M., Lobato, F.: Multi-objective optimization of column flotation of an igneous phosphate ore. Int. J. Miner. Process. **146**, 82–89 (2016)
14. Jamett, N., Cisternas, L., Vielma, J.P.: Solution strategies to the stochastic design of mineral flotation plants. Chem. Eng. Sci. **134**, 850–860 (2015)
15. Gruzdeva, T., Ushakov, A., Enkhbat, R.: A biobjective DC programming approach to optimization of rougher flotation process. Comput. Chem. Eng. **108**, 349–359 (2018)
16. Enkhbat, R., Gruzdeva, T., Barkova, M.: D.C. programming approach for solving an applied ore-processing problema. Am. Inst. Math. Sci. **14**(2), 613–623 (2018)
17. Strekalovsky, A.: On local search in d.c. optimization problems. Appl. Math. Comput. **255**, 73–83 (2015)

Modification of High Water Content Sediment for Rare Earth Mining in Deep Sea by Surfactants Agents

T. Funatsu, T. Sakiyama, A. Hamanaka, T. Sasaoka, H. Shimada and K. Takahashi

1 Introduction

In recent years, the demand for rare mineral resources has grown and a lot of investigations have been conducted to discover new ore deposits all over the world. As a result, it was discovered that abundant rare-earth element-rich mud exists on the deep-sea floor in Japanese Exclusive Economic Zone (EEZ) [1, 2]. However, it is required to evaluate the deformation behavior of rare-earth element-rich mud in seabed mining because it will cause suspension and topographic variation [3]. For this reason, it is important to control the deformation behavior of rare-earth element-rich mud in order to evaluate environmental impact in seabed mining. In the previous study, [4] reported that the deformation behavior of the mined seabed sediments is classified based on the ratio of water content and liquid limit as shown in Table 1. Therefore, if the liquid limit of the sediment can be varied by adding materials such as surfactant agents, the deformation behavior of the sediment can be controlled in order to obtain more suitable behavior for mining. This paper discussed the deformation behavior of seabed sediment by adding several different types of surfactant agents and measure the liquid limit and viscosity to evaluate the effectiveness.

T. Funatsu (✉)
Green Asia Education Center, Kyushu University, Fukuoka, Japan
e-mail: funatsu@mine.kyushu-u.ac.jp

T. Sakiyama · A. Hamanaka · T. Sasaoka · H. Shimada
Faculty of Engineering, Kyushu University, Fukuoka, Japan

K. Takahashi
Ube Industries. Ltd, Yamaguchi, Japan

Table 1 Classified table of deformation behavior of simulated soil
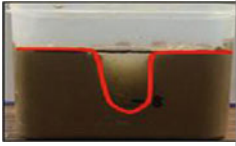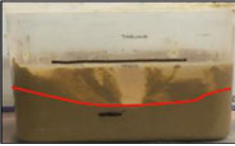
W_C/W_L	<1.3 (sharp)	1.3 ~ 1.6 (cone-shape)	>1.6 (circular arc)
Deformation behavior			

Table 2 Property of sample of rare-earth element-rich mud [3]

	A-1	A-2	A-3	A-4	B	C
Density (g/cm^3)	2.850	2.831	2.792	2.792	2.833	2.821
Liquid limit (%)	116.3	111.1	98.7	105.4	117.1	109.8
Water content (%)	124.1	138.9	156.3	140.3	128.8	146.1

2 Sample Preparation and Test Method

2.1 Properties of Seabed Sediment and Simulated Sediment Sample Preparation

Rare-earth element-rich mud is classified as clay on soil classification. However, liquid limit and water content of rare-earth element-rich mud are different depending on the place and it is expected that these differences change the deformation behavior of rare-earth element-rich mud on suction mining. The geotechnical properties of rare-earth rich mud are shown in Table 2. The simulated sediment samples which had liquid limit and water content ware prepared and used in laboratory test. Those soil samples were prepared by blending two types of bentonite clay in different mixing ratios. Liquid limit and water content of the sample are 120 and 130%, respectively.

2.2 Liquid Limit Test

Liquid limit tests were conducted according to test method for liquid limit and plastic limit of soils (JIS A 1205:2009). Soil sample is put in a brass dish with the thickness of 1 cm and cut a groove in the sample in the cup. Turn the handle of the device at a rate of two drops per second. Count the number of blows until the two halves of the soil sample come in contact along a distance of 1.5 cm. Adding or evaporating water to collect the data.

Fig. 1 B-type viscometer

2.3 Viscosity Measurement

Viscosity of the sample was measured by B-type viscometer shown in Fig. 1. One cycle of changing the rotational speed is in the order of 0.3, 0.6, 1.5, 3.0, 6.0, 12, 30, 60, 30, 12, 6.0, 3.0, 1.5, 0.6, and 0.3 rpm. The cycle is repeated for a total of four times. The interval of each speed is 30 s. The viscosity of the first 0.3 rpm in the first cycle was calculated as the viscosity at the time of the structural failure of the simulated sediments.

2.4 Type of Surfactants

The flowability of the particles suspended in the liquid generally depends on the dispersion and aggregation of the suspended particles. When a strong attractive force is generated between the particles and strongly aggregated primary aggregates or secondary aggregates due to the weak attraction formed, the water restrained between the particles increases and the free water involved in the fluidity decreases and the fluidity decreases. On the other hand, when a strong repulsive force acts on the particles, the particles are dispersed, restrained water is reduced, and fluidity is improved. In order to enhance the water reducing the effect, it is necessary to increase the dispersibility of the particles, and a stable dispersion force is required.

Therefore, the following surfactant agents are used in this study and they are classified as three groups:

1. Dispersant

   Low molecular weight polycarboxylic acid ethers,
   High molecular weight polycarboxylic acid ethers, and
   Alkyl ammonium salt.

2. Water retention agent

   Hydroxypropylmethylcellulose,
   Water-absorbing polymer.

3. Thickener

   Hydroxyethyl cellulose,
   Alkyl ammonium salt, alkyl aryl sulfonate blend, and
   Polyacrylamide.

3   Result and Discussion

Figure 2 shows the relationship between the liquid limit and the addition rate. When water retention agents were added, the liquid limit is increased, whereas dispersant type agents tend to reduce the liquid limit. For the thickener type agents, the specific trend was not observed. Further, when the hydroxyethyl cellulose and the water-absorbing surfactant were added, a larger effect of increasing the liquid limit was obtained as compared with other surfactants. On the other hand, the alkyl ammonium salt, and the alkyl ammonium salt and alkyl sulfonate blend were used, the liquid limit is decreased significantly.

The viscosity test was conducted on each sample under the same conditions. Figure 3 shows the relationship between the viscosity and the addition rate of each surfactant. As shown in the figure, when the water-absorbent polymer and hydroxyethyl cellulose were added, the viscosity is increased more than the other surfactants. In addition, when the alkyl ammonium salt, and the alkyl ammonium salt and alkyl sulfonate blend surfactants were added, the viscosity is decreased more greatly than other surfactants.

Figure 4 shows the relationship between the ratio of water content to liquid limit (W_C/W_L) and the addition rate of each surfactant. As the water content is fixed, the trend of the variation of the ratio is similar to the trend of liquid limit variation.

From the above results, in the modification of the suction behavior of the simulated sediment, we can select the most suitable surfactant agents.
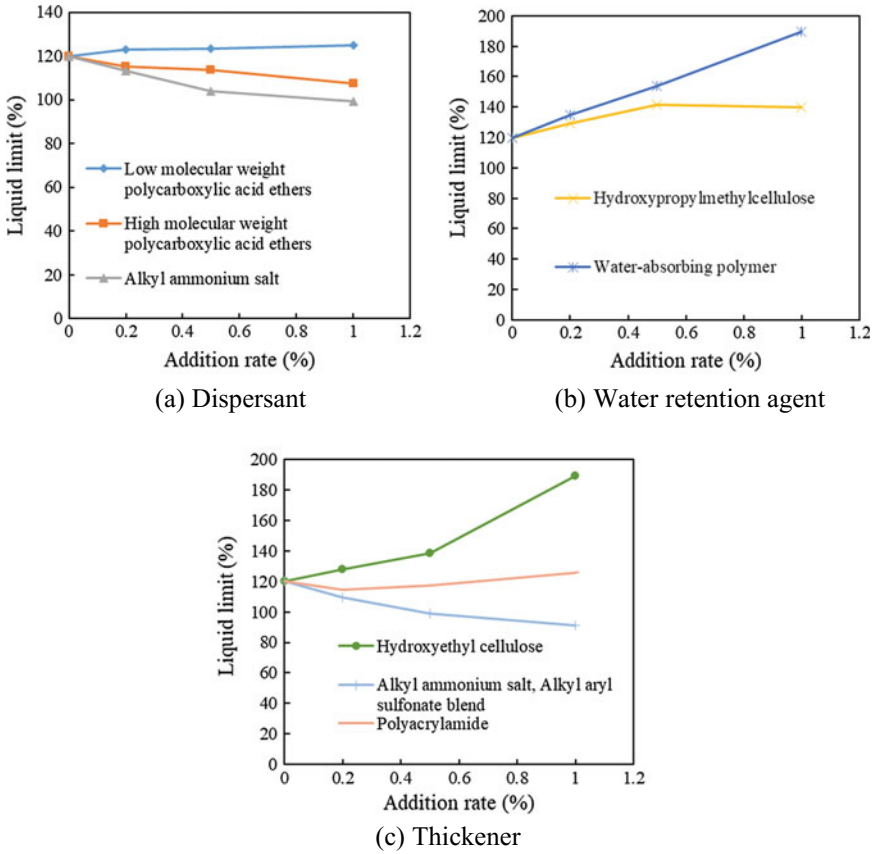
(a) Dispersant

(b) Water retention agent

(c) Thickener

Fig. 2 Relationship between liquid limit and addition rate of each surfactant **a** dispersant, **b** water retention agent, and **c** thickener

For example, if we want to modify the behavior from a circular arc structure to a cone-shaped one, it is considered that the water-absorbing polymer and hydroxyethyl cellulose are applicable. When we want to modify the behavior from a sharp structure to a cone-shaped one, it is preferable to use an anionic–cationic surfactant and a cationic surfactant.
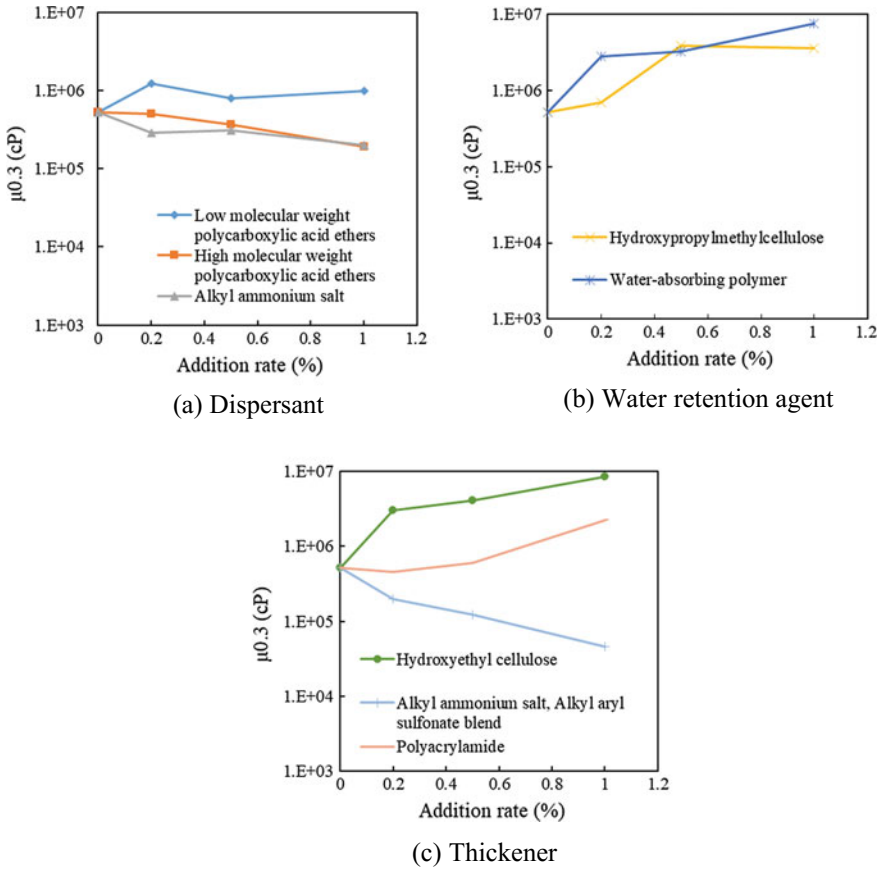
(a) Dispersant

(b) Water retention agent

(c) Thickener

Fig. 3 Relationship between viscosity and addition rate of each surfactant **a** dispersant, **b** water retention agent, and **c** thickener

4 Conclusion

In order to investigate the modification method of rare-earth sediment fluidity, a series of laboratory experiments were conducted. We selected eight different surfactants which can be divided into three types. They are dispersant type, water retention type, and thickener type. We carried out liquid limit tests and viscosity measurement of the sediment mixed with the agents. It is found that the water-absorbing polymer increases the liquid limit and viscosity, whereas anionic/cationic surfactant decreases the liquid limit and viscosity. It is possible to control the sediment behavior by adding suitable surfactants.
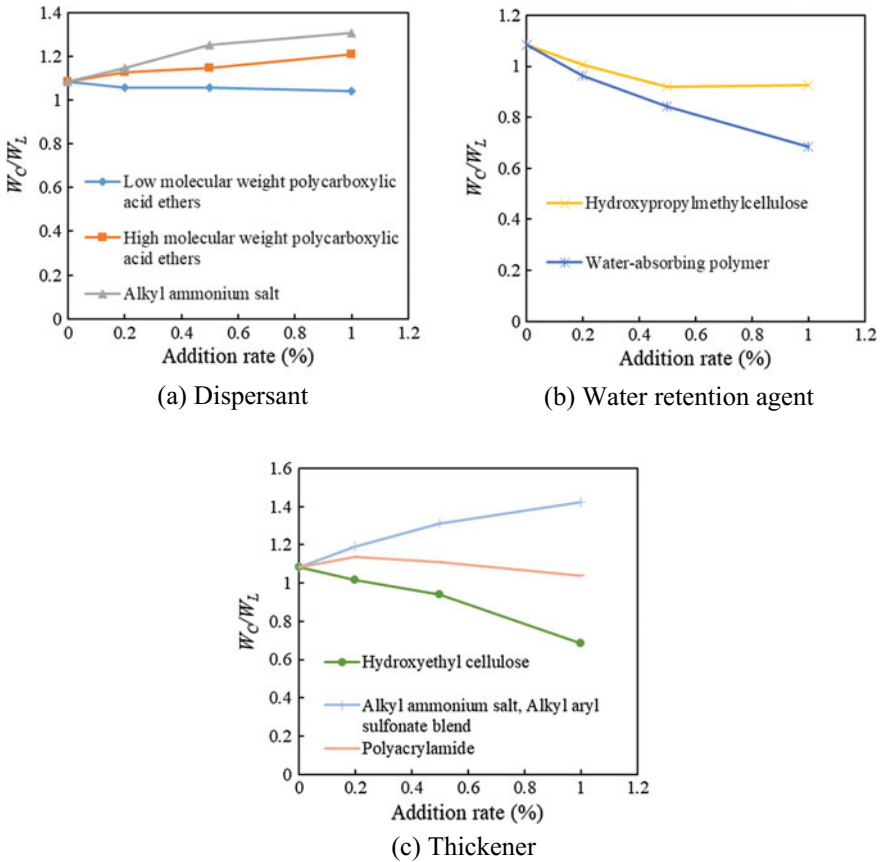
Fig. 4 Relationship between the ratio of water content to liquid limit (W_C/W_L) and addition rate of each surfactant **a** dispersant, **b** water retention agent, and **c** thickener

References

1. Hiraki, K.: Trends in metal resource development and strategies for resource security, surface science for resource issues 114–115 (2014)
2. Kato, Y.: Taiheiyou no Reaasudei ga Nihon wo sukuu, Tokyo, PHP interface press, 167–180 (in Japanese) (2012)
3. Ministry of the Environment: Report of Technology Assessment of Environmental Impact, 223–228 (2011)
4. Tagami, T., Sakiyama, T., Funatsu, T., Hamanaka, A., Sasaoka, T., Shimada, H., Takahashi, T.: Study on deformation behavior of rare-earth elements-rich mud and applicability of sealing materials in seabed mining. In: Proceedings International Symposium on Earth Science and Technology, 161–164 (2017)